Université de la Réunion
Faculté des sciences et technologies
École doctorale 542 :
« sciences, technologies et santé » (STS)
section CNU 68

Transfert et réactivité de contaminants majeurs et traces dans les sols volcaniques et tropicaux de l'île de la Réunion

Document de synthèse
pour l'habilitation à diriger des recherches

Frédéric FEDER
CIRAD, UPR « recyclage et risque »
Station de la Bretagne,
BP 20, 97408 Saint-Denis Messagerie CEDEX 9,
île de la Réunion

Sommaire

RÉSUMÉ

Les interactions entre la solution du sol et la phase solide sont au coeur de l'évolution des sols. Mes recherches ont consisté à étudier cette solution du sol notamment *in situ* au sein de sols hydromorphes dans un premier temps, puis dans les sols volcaniques et tropicaux de l'île de la Réunion.
Le recyclage des produits résiduaires organiques (PRO) en agriculture présente de multiples bénéfices mais peut également apporter des contaminants de diverses natures. Ceux-ci peuvent se dégrader intégralement, s'accumuler dans les sols, être prélevés par les cultures ou être lixiviés vers le sous-sol. Mes travaux ont essentiellement porté sur les nitrates et les éléments traces métalliques (ETM). Afin de quantifier les transferts de ces polluants dans les sols et d'en comprendre les déterminants, ma démarche a été de mettre en place des expérimentations à plusieurs échelles spatiales (au laboratoire en colonnes de sol et en plein champ), puis à utiliser ces résultats dans des modèles de simulation afin de mettre en évidence les processus géochimiques en jeu et de simuler des impacts à long terme pour les ETM ou à l'échelle régionale pour les nitrates.
Lors de l'épandage d'un lisier de porc riche en azote sous forme organique et ammoniacal, les nitrates sont essentiellement produits par nitrification avant d'être lixiviés, mais plus tardivement que les autres anions, notamment les chlorures initialement présents dans le lisier. Ainsi, pour deux grands types de sols de la Réunion (un cambisol andique et un nitisol), les transferts de nitrates sont ralentis du fait d'une capacité d'échange anionique, mais ils entrent en compétition avec les chlorures pour l'adsorption sur les charges, variables avec le pH, de ces sols. Néanmoins, ils demeurent disponibles pour les cultures plus longtemps, permettant une gestion agronomique des apports de PRO et réduisant les risques de transferts vers le sous-sol. À l'échelle du territoire de l'ouest de la Réunion, les zones les plus vulnérables aux transferts de nitrates ont été identifié grâce aux caractéristiques des sols et à l'élaboration d'un indice de vulnérabilité.
La mobilité des ETM a été mesurée en colonne de sol ainsi qu'en conditions réelles sur le terrain. Les ETM présentent un comportement très différent des nitrates puisqu'ils n'ont jamais montré de transfert au-delà des vingt premiers centimètres de sols. La problématique de contamination des nappes phréatiques ne se pose donc pas pour ces éléments. En revanche, nous avons utilisé un modèle empirique réalisant des bilans « entrée / sortie » pour quantifier l'accumulation à long terme des ETM dans les couches superficielles. Ce modèle a été validé pour un sol sur lequel quatorze cycles de cultures maraîchères ont été menés. Un rapide dépassement des seuils réglementaires pour le zinc a été mis en évidence.

Mon projet de recherche s'articule autour de l'utilisation de deux sites expérimentaux, lourdement instrumentés, pour comprendre la dynamique des grands cycles biogéo-

chimiques après apports de PRO, mais également pour quantifier les flux de deux types de contaminants, les ETM et les composés traces organiques, dans les différents compartiments de l'agro-écosystème et ce, sur le long terme.
Le premier site est celui du SOERE PRO de la Réunion. Il a été mis en place en 2013 sur la station du CIRAD à La Mare. Des boues de STEP, des lisiers de porc et des litières de volailles sont apportés sur une culture de canne à sucre. Le second site est celui de la station de l'ISRA (institut sénégalais de recherche agricole) à Sangalkam où des boues de STEP, des litières de volaille et des digestats de méthanisation sont apportés sur des cultures maraîchères. Dans ces deux situations, les flux d'eau et de solutés sont mesurés continuellement, les lixiviats, le sol et les cultures sont régulièrement échantillonnés. L'objectif est d'identifier les déterminants de la mobilité des contaminants entre les compartiments et de quantifier ces transferts. Par ailleurs, sur le site de la Réunion, les flux de CO_2 et de N_2O sont également mesurés plusieurs fois par jour afin d'améliorer le bouclage des cycles des éléments majeurs.
Sur le site de Sangalkam, l'influence des PRO sur la qualité nutritionnelle des cultures maraîchères et sur la résistance aux bio-agresseurs et aux ravageurs sera évaluée. Par ailleurs, nous déterminerons un niveau d'intensification *durable* optimal préservant la qualité des sols et n'impactant pas négativement les autres compartiments de l'écosystème, dont les cultures.
L'acquisition de données de référence et le suivi sur le long terme des contaminants sont des étapes indispensables pour renseigner et utiliser des modèles permettant d'évaluer leur devenir et de prédire les éventuels risques associés.

AVANT-PROPOS

Au cours de ma formation initiale en géologie à l'université de Rennes, quelles qu'aient été les disciplines enseignées (paléontologie, volcanisme, sédimentologie, etc.), j'ai tout de suite été fasciné par cet aller-retour incessant, mais nécessaire, entre les observations de terrain et leurs fondements théoriques. Au fur et à mesure, mes centres d'intérêts en sciences de la terre se sont rapprochés de la surface jusqu'à sa couche la plus superficielle, le sol. Cette fine couche, qui m'a tant embêtée pour trouver un affleurement rocheux pendant mes stages de cartographie, était enseignée par Guilhem Bourrié alors détaché de l'INRA comme professeur à l'université de Rennes 1. Or, mon second centre d'intérêt étant la géochimie, il m'a proposé de m'orienter après la maitrise vers le DEA national de science du sol. Dans le contexte tempéré des sols hydromorphes de Bretagne et des processus d'oxydo-réduction qui s'y développe, j'ai donc réalisé mon stage, en 1998, puis ma thèse, soutenue en 2001, sous la direction de Guilhem Bourrié et de Fabienne Trolard, au laboratoire de science du sol de l'INRA de Rennes dans un premier temps. Ces derniers ayant été appelés pour développer l'unité « géochimie des sols et des eaux » à Aix-en-Provence, j'ai donc terminé d'écrire ma thèse là-bas, en 2001, dans un second temps. Entre temps, durant les mois de février et mars 2000, au court d'un séjour en Amazonie, j'ai découvert la dynamique du fer dans les sols ferrugineux tropicaux avec Emmanuel Fritsch, chercheur à l'IRD ; un signe précurseur peut-être.
J'ai ensuite été recruté au CIRAD et affecté à la Réunion, en août 2001, en tant que « biogéochimiste » pour travailler sur le recyclage des déchets organiques en contexte tropical. Armé de mon bagage de géochimiste, je me suis progressivement intéressé aux interactions entre la solution du sol et la phase solide ; les sols tropicaux et surtout les sols volcaniques présentant des caractéristiques géochimiques et minéralogiques si particulières et nouvelles pour moi. Pour cela, j'ai commencé à travailler sur les transferts de solutés aux échelles de la colonne de sol puis de la parcelle. Cette période (2001–2011) à la Réunion fut exaltante, mais après dix années, j'ai saisi l'opportunité de rebondir avec une nouvelle affectation au Sénégal. Si la problématique du recyclage agricole des déchets organiques est constante, le contexte agro-pédologique du maraîchage en milieu périurbain est tout autre.

Au cours de ce parcours, j'ai travaillé avec de nombreux chercheurs, ingénieurs et techniciens, en particulier ceux de mon unité de recherche, j'ai encadré de nombreux stagiaires et j'ai participé à l'encadrement de plusieurs doctorants. Que toutes ces personnes soient ici remerciées pour leurs collaborations, leurs échanges et leurs interactions.

Enfin, je dédie ce mémoire et tout le fruit de mon travail à ma petite famille, Carole, Édouard et Charles, sans lesquels je ne serais pas aussi heureux aujourd'hui.

PREMIÈRE PARTIE :
PRÉSENTATION DU CANDIDAT

CHAPITRE 1

CURRICULUM VITÆ

1.1 État civil

Frédéric FEDER,
né le 26 septembre 1972 à Nancy (France), marié, deux enfants.
Coordonnées professionnelles actuelles :
LEMSAT (IRD–ISRA–UCAD), campus de Bel-Air, route des hydrocarbures, BP 1386, 18524 Dakar, Sénégal.
Téléphone : +221 33 849 33 17 ; adresse email : frederic.feder@cirad.fr

1.2 Études, diplômes et parcours professionnel

1991 – 1994 : DEUG A de « science et structure de la matière », mention physique, chimie et science de la terre (PCST), université de Rennes I.

1994 – 1996 : licence et maîtrise de « science de la terre » (mentions assez bien), université de Rennes I.

1996 – 1997 : diplôme de « dynamique de l'eau et télédétection » (mention assez bien) délivré par le CNED de Rennes et le laboratoire COSTEL.

1997 – 1998 : DEA (master 2) national de « science du sol » (mention assez bien), diplôme co-habilité ENSAR, INA-PG, ENSAM et université H. Poincaré (Nancy I).

1998 – 2001 : thèse de doctorat intitulée « dynamique des processus d'oxydo-réduction dans les sols hydromorphes. Monitoring *in situ* de la solution du sol et des phases solides ferrifères. ». Université d'Aix-Marseille III.
Bourse de doctorat financée par le ministère de l'éducation nationale et de la recherche. Doctorat réalisé au laboratoire de science du sol de l'INRA de Rennes et à l'unité de recherche « géochimie des sols et des eaux » de l'INRA à Aix-en-Provence sous la direction de G. Bourrié et F. Trolard.

2001 – aujoud'hui : chercheur en science du sol dans l'unité « recyclage et risque » du CIRAD (centre de coopération internationale en recherche agronomique pour le développement), département PERSYST (performances des systèmes de production et de transformation tropicaux) :

- septembre 2001 – octobre 2011 : affecté à la Réunion (CIRAD, station de la Bretagne) ;
- depuis novembre 2011 : affecté au Sénégal (LMI IESOL, Dakar).

1.3 Formations complémentaires

1. Formation à l'étude et à la modélisation des transferts d'eau : Montpellier, cinq jours, septembre 2002.
2. Formation en statistiques spatiales : Montpellier, cinq jours, mars 2004.
3. Formation en statistique sous SAS et R : Saint-Denis, cinq jours, avril 2005.
4. Formation à R : Saint-Denis, cinq jours, mai 2005.
5. Formation à l'utilisation des centrales d'acquisition Campbell : Saint-Denis, trois jours, septembre 2005.
6. Formation aux SIG : Saint-Denis, trois jours, avril 2007.
7. Formation à la rédaction scientifique en anglais : Saint-Denis, quatre jours, septembre 2007.
8. Formation aux transferts d'eau et solutés à l'aide des logiciels HYDRUS, PHREEQC et HP1 : Montpellier, cinq jours, septembre 2008.
9. Formation à l'utilisation du logiciel ARCGIS : Saint-Denis, cinq jours, avril 2009.
10. Formation à la programmation en CRBASIC et au matériel Campbell : Paris, deux jours, février 2013.
11. Formation à la pratique de l'anglais : Saint-Denis, 27 heures, de février à juin 2010.
12. Formation à la pratique de l'anglais : par téléphone, quinze heures, de avril à septembre 2013.
13. Formation aux suivis et aux mesures de gaz *in situ* : Paris, deux jours, octobre 2015.

1.4 Distinction et prix

Au cours de la 19^{e} réunion des sciences de la terre (RST) à Nantes en juin 2002, j'ai reçu le prix HAÜY-LACROIX 2002 décerné par la société française de minéralogie et de cristallographie (SFMC) pour mon travail de thèse.

1.5 Affiliation à des sociétés savantes

Je suis membre de l'association française pour l'étude des sols (AFES) depuis 1997. J'ai été élu quatre fois au conseil d'administration (2001–2004, 2005–2008, 2009–2012 et 2013–2016) et j'ai été vice-président pendant deux ans (2006–2007). Je participe aux activités scientifiques et administratives de cette société savante, la seule existante dans ma discipline. J'ai été rédacteur de la lettre trimestrielle de l'AFES de 2003 à 2012.
Depuis 2012, je coordonne avec Ch. Walter la réalisation de webinaires pour l'AFES. Ce sont des vidéo-conférences diffusées en direct sur internet sur différents thèmes relatifs au sol et à la recherche en science du sol (https://vimeo.com/channels/webinairesafes).

CHAPITRE 2

LISTE DES PUBLICATIONS ET DES TRAVAUX

2.1 Articles

2.1.1 Articles dans les revues à facteurs d'impact

1. Feder, F., Bourrié, G. and Trolard, F. 1998. *In situ* continuous monitoring of soil solution chemistry. *Mineralogical magazine*, 62A, 441-442.
2. Bourrié, G., Trolard, F., Refait, Ph. and Feder, F. 2004. A solid solution model for Fe(II)-Fe(III)-Mg green rust "Fougerite": structural and geochemical constraints. *Clays and Clay Minerals*, 52(3), 382-394.
   http://dx.doi.org/10.1346/CCMN.2004.0520313
3. Feder, F., Trolard, F., Klingelhöfer, G. and Bourrié, G. 2005. *In situ* Mössbauer spectroscopy: Evidence for green rust (fougerite) in a gleysol and its mineralogical transformations with time and depth. *Geochimica et Cosmochimica Acta*, 69(18), 4463-4483.
   http://dx.doi.org/10.1016/j.gca.2005.03.042
4. Trolard, F., Bourrié, G., Abdelmoula, M., Refait, Ph. and Feder, F. 2007. Fougerite, a New Mineral of the Pyroaurite-Iowaite Group: Description and Crystal Structure. *Clays and Clay Minerals*, 55(3), 323-334.
   http://dx.doi.org/10.1346/CCMN.2007.0550308
5. Feder, F. and Findeling, A. 2007. Retention and leaching of nitrate and chloride in an andic soil after pig manure amendment. *European Journal of Soil Science*, 58(2), 393-404.
   http://dx.doi.org/10.1111/j.1365-2389.2006.00885.x
6. Payet, N., Findeling, A., Chopart, J.-L., Feder, F., Nicolini, E., Saint Macary, H. and Vauclin, M. 2009. Modelling the fate of nitrogen following pig slurry application on a tropical cropped acid soil on the island of Réunion (France). *Agriculture, Ecosystems & Environment*, 134(3-4), 218-233.
   http://dx.doi.org/10.1016/j.agee.2009.07.004
7. Legros, S., Doelsch, E., Feder, F., Moussard, G. D., Sansoulet, J., Gaudet, J.-P., Rigaud, S., Basile-Doelsch, I., Saint Macary, H. and Bottero, J. Y. 2013. Fate and behaviour of Cu and Zn from pig slurry spreading in a tropical water-soil-plant system. *Agriculture, Ecosystems & Environment*, 164, 70-79.
   http://dx.doi.org/10.1016/j.agee.2012.09.008
8. Alary, K., Babre, D., Caner, L., Feder, F., Szwarc, M., Naudan, M. and Bourgeon, G. 2013. Pretreatment of Soil Samples Rich in Short-Range-Order Minerals Before

Particle-Size Analysis by the Pipette Method. *Pedosphere*, 23(1), 20-28. http://dx.doi.org/10.1016/S1002-0160(12)60076-9

9. Feder, F. 2013. Soil map update: Procedure and problems encountered for the island of Réunion. *Catena*, 110, 215-224. http://dx.doi.org/10.1016/j.catena.2013.06.019
10. Wassenaar, T., Doelsch, E., Feder, F., Guerrin, F., Paillat, J.-M., Thuriès, L. and Saint Macary, H. 2014. Returning Organic Residues to Agricultural Land (RORAL) — Fuelling the Follow -the- Technology approach. *Agricultural Systems*, 124, 60-69. http://dx.doi.org/10.1016/j.agsy.2013.10.007
11. Feder, F., Bochu, V., Findeling, A. and Doelsch, E. 2015. Repeated pig manure applications modify nitrate and chloride competition and fluxes in a Nitisol. *Science of the Total Environment*, 511, 238–248. http://dx.doi.org/10.1016/j.scitotenv.2014.12.059
12. Hodomihou, R. N., Feder, F., Masse, D., Agbossou, K. E., Amadji, G. L., Ndour-Badiane, Y. et Doelsch, E. *Diagnostic de contamination des agrosystèmes périurbains de Dakar par les éléments traces métalliques.* Biotechnologie, Agronomie, Société et Environnement, vol. 20, n° 3. septembre 2016.

2.1.2 Articles dans les revues à comité de lecture sans facteurs d'impact

1. Feder, F. et Bourgeon G. 2009. Mise à jour de la carte des sols de la Réunion : démarche suivie et problèmes rencontrés. *Étude et gestion des sols*, 16(2), 85-99.
2. Doelsch, E., Basile-Doelsch, I., Bottero, J. Y., Cazevieille, P., Chevassus-Rosset, Cl., Feder, F., Garnier, J.-M., Gaudet, J.-P., Legros, S., Levard, Cl., Masion, A., Moussard, G. D., Rose, J. et Saint Macary, H. 2011. Recyclage agricole des déchets organiques dans les sols tropicaux (île de la Réunion) : quel impact sur les transferts d'éléments traces métalliques? *Étude et gestion des sols*, 18(3), 175-186.
3. Lahbib-Burchard, T., Wassenaar, T., Doelsch, E., Feder, F. et Bravin, M. 2012. Prédiction de l'accumulation à long-terme des éléments traces métalliques dans les sols en contexte de recyclage agricole de produits résiduaires organiques en milieu tropical : validation d'un modèle par mesures *in situ*. *Bulletin du groupe francophone humidimétrie et tranferts en milieux poreux* (58) : 185-192.
4. Hodomihou, N. R., Feder, F., Doelsch, E., Agbossou, E. K., Amadji, G. L., Ndour-Badiane, Y., Cazevieille, P., Chevassus-Rosset, C. et Masse, D. 2015. Caractérisation des risques de contamination des agrosystèmes périurbains de Dakar par les éléments traces métalliques. *Agronomie Africaine*, 27(1), 69-82.

2.1.3 Articles soumis ou en préparation

1. Feder, F., Finizola, A., Crovisier, M. and Payet, N. Monitoring of water fluxes by SP and TDR in the unsaturated vadoze zone during an intense cyclone. En préparation.
2. Rakotoarisoa, J. *et al.* Paramètres chimiques du transfert des nitrates dans les sols de l'essai « Système de cultures du riz pluvial » à Andranomanelatraha (Hauts plateaux malgaches – région d'Antsirabé) En préparation.
3. Hodomihou, R. N., Feder, F., Agbossou, K. E., Amadji, G. L. et Doelsch, E. Assessment of metals speciation in soils and organic wastes used as fertilizers in the suburban agricultural area of Dakar, Senegal. En préparation.
4. Diallo, F., Feder, F. *et al.* Effets des apports réguliers de matière organique sur le rendement de la culture de laitue sur les Arénosols et les Fluvisols de la zone des Niayes. En préparation.

5. Ntoma-Diallo, R., Feder, F., Masse, D., Diome, F., Akpo, L. E. Long-term effects of intensive and repeated inputs of organic matter on the evolution of market gardeners soils in the region of Dakar, Senegal. En préparation.

2.2 Actes de colloques

2.2.1 Communications orales

1. Feder, F., Trolard, F., Bourrié, G., Klingelhöfer, G. et Génin J.-M. R. 1999. Utilisation *in situ* de la spectrométrie Mössbauer pour la caractérisation des oxydes de fer dans les sols hydromorphes. *Journées « jeunes chercheurs »*, association française pour l'étude du sol (AFES), Paris, France, 1999/11/18.
2. Klingelhöfer, G., Trolard, F., Bourrié, G., Feder, F. and Génin, J.-M. R. 1999. The monitoring of iron mineralogy and oxidation states by Mössbauer spectroscopy in the field; the Green Rust mineral in hydromorphic soils. *American Geophysical Union, Fall Meeting*, San Francisco, USA, 1999/12/13-17.
3. Bourrié, G., Berthelin, J., Génin, J.-M. R., Trolard, F., Klingelhöfer, G., Abdelmoula, M., Appenzeller, B., Benali, O., Bernhardt, B., Block, J.C., Ehrhardt, J.-J., Feder, F., Géhin, A., Gury, M., Herbillon, A., Jeanroy, E., Jorand, F., Ona-Nguema, G., Refait, Ph. et Stemmler, S. 2000. Rôle des processus biogéochimiques sur les transformations minéralogiques des oxydes de fer dans les sols hydromorphes. *Les composés lamellaires*, réunion de la société française de minéralogie et de cristallographie et du groupe français des argiles, Porquerolles, France, 2000/10/09-11.
4. Bourrié, G., Trolard, F., Refait, Ph. and Feder, F. 2002. A solid solution model for FeII–FeIII–Mg green rust (fougerite) : structural and geochemical constraints. *17th World Congress of Soil Science*, Bangkok, Thailande, 2002/08/14-20.
5. Feder, F., Klingelhoefer, G., Trolard, F. and Bourrié, G. 2002. *In situ* Mössbauer spectroscopy and soil solution monitoring to follow spatial and temporal iron dynamics. *17th World Congress of Soil Science*, Bangkok, Thailande, 2002/08/14-20.
6. Feder, F. and Chabalier, P.-F. 2002. Agricultural valorisation of organic waste in Réunion island: andosols characteristics. *Volcanic soils: Properties, Processes and Land Use.* COST Action 622 (Soil Resources of European Volcanic Systems), Budapest, Hungary, 2002/09/18-22.
7. Feder, F., Gosme, M., Chabalier, P.-F., Saint Macary, H., Doelsch, E. et Isautier, J. 2004. Recyclage de déchets par la canne à sucre : essais avec des vinasses de distillerie. *Rencontres internationales pluridisciplinaires, la canne, une passion à partager. Perspectives de développement de la canne à sucre en milieu insulaire : approches technico-économiques, sociales, culturelles.* Congrès de la STASM, Piton Saint-Leu, la Réunion, 2002/10/02-05.
8. Feder, F., Gosme, M. et Saint Macary, H. 2004. Recyclage de déchets par la canne à sucre : essais avec des vinasses de distillerie. *Méthodes d'évaluation de l'impact agronomique et environnemental du recyclage agricole des déchets agro-industriels*, séminaire de restitution des travaux de l'ATP 2001-10, Montpellier, France, 2004/07/01-02.
9. Feder, F. et Findeling, A. 2004. Flux d'eau et de soluté dans un andosol des Colimaçons après un apport de lisier : expérimentation en colonnes de sol. *Méthodes d'évaluation de l'impact agronomique et environnemental du recyclage agricole des déchets agro-industriels*, séminaire de restitution des travaux de l'ATP 2001-10, Montpellier, France, 2004/07/01-02.
10. Feder, F., Findeling, A., Saint Macary, H. et Payet, N. 2004. Mise en place de deux sites expérimentaux pour l'étude de la valorisation agronomique des déchets à l'île de

la Réunion. *Méthodes d'évaluation de l'impact agronomique et environnemental du recyclage agricole des déchets agro-industriels*, séminaire de restitution des travaux de l'ATP 2001-10, Montpellier, France, 2004/07/01-02.

11. Feder, F. and Findeling, A. 2004. Solute and water fluxes in andisol fertilized with pig manure: soil columns experimentation. *In : Volcanic soil resources in Europe*. Rala Report, n° 214, Oskarsson, H., (ed.) and Arnalds, O. (ed.). COST Action 622, Final Meeting, Akureyri-Egilsstadir, Iceland, 2004/06/04-08.
12. Feder, F. and Findeling, A. 2004. Physical and chemical transformations and solutes transfer in andisol under pig manure spreading. *Eurosoil 2004*, Freiburg im Breisgau, Germany, 2004/09/04-12.
13. Doelsch, E., Saint Macary, H., Feder, F., Moussard, G. D., Findeling, A., Chevassus-Rosset, Cl., Cazevieille, P., Basile-Doelsch, I., Bottero J. Y., Garnier, J.-M., Masion, A., Rose, J., Moustier, S. et Gaudet, J.-P. 2006. Recyclage agricole des déchets organiques dans les sols tropicaux (île de la Réunion) : quel impact sur les transferts d'éléments traces métalliques ? *De la recherche sur les sols à la décision publique : journées d'échanges et de prospective*, MEEDDAT, ADEME,, 2006/11/21-22.
14. Sansoulet, J., Feder, F., Simunek, J., Bochu, V., Findeling, A. and Doelsch, E. 2008. Transport of reactive anions and cations in a volcanic soil : Experiments and modelling. ECSSS, EUROSOIL *2008. Soil, Society, Environment*, Vienna, Austria, 2008/08/25-29.
15. Feder, F., Bochu, V., Doelsch, E., Findeling, A. and Sansoulet, J. 2008. Retention and leaching of nitrate after nitrification of pig manure on variable charge soil (Nitisol). *In :* ECSSS, EUROSOIL *2008. Soil, Society, Environment*, Vienna, Austria, 2008/08/25-29.
16. Doelsch, E., Basile-Doelsch, I., Bottero, J. Y., Cazevieille, P., Chevassus-Rosset, Cl., Feder, F., Garnier, J.-M., Gaudet, J.-P., Legros, S., Levard, Cl., Masion, A., Moussard, G. D., Moustier, S., Rose, J. et Saint Macary, H. 2008. Recyclage agricole des déchets organiques dans les sols tropicaux (île de La Réunion) : quel impact sur les transferts d'éléments traces métalliques ? *Les matières organiques du sol : rôles, risques et enjeux.* Colloque de restitution du programme GESSOL 2, MEEDDAT, ADEME, p 17-22, Paris, 2008/12/04.
17. Legros, S., Doelsch, E., Chaurand, P., Masion, A., Rose, J., Feder, F., Sansoulet, J., Gaudet, J.-P., Proux, O., Hazemann, J.-L., Briois, V., Saint Macary, H. et Bottero, J. Y. 2009. Évaluation de l'impact environnemental de l'épandage de lisier de porc par une approche multi-échelle. *In : actes du séminaire* RESMO *2009 « séminaire matières organiques et environnement »*, INRA.
18. Lahbib-Burchard, T., Wassenaar, T., Doelsch, E., Feder, F. et Bravin, M. N. 2012. Prédiction de l'accumulation à long-terme des éléments traces métalliques dans les sols en contexte de recyclage agricole de produits résiduaires organiques en milieu tropical : validation d'un modèle par mesures *in situ. 50 ans de l'Orgeval et 37es journées du GFHN.*
19. Thuriès, L., Moussard, G. D., Gauvin, M.-C., Feder, F., Doelsch, E. and Legier, P. 2013. Organic status of tropical soils predicted by near infrared spectroscopy: Réunion Island as a case study. *In :* NIR *2013. Proceedings of 16th International Conference on Near Infrared Spectroscopy: Picking up good vibrations*, La Grande-Motte, France, 2013/06/02-07.
20. Oustrière, N., Lahbib-Burchard, T., Doelsch, E., Feder, F., Wassenaar, T. and Bravin, M. N. 2013. Predictive modelling of the long-term accumulation of trace metals in tropical soils amended with organic wastes – field trial validation. *15^{e} conférence internationale* RAMIRAN *: recyclage des résidus organiques pour l'agriculture : de la*

gestion des déchets aux services écosystémiques, Versailles, France, 2013/06/03-05.

21. Hodomihou, N. R., Feder, F., Agbossou, K. E., Masse, D., Ndour-Badiane, Y., Cazevieille, P., Chevassus-Rosset, Cl., Montès, M., Marger, J.-L. and Doelsch, E. 2013. Negative externalities of intensive use of organic wastes on two tropical soils in the context of urban agriculture in the region of Dakar. *15^e conférence internationale* RAMIRAN *: recyclage des résidus organiques pour l'agriculture : de la gestion des déchets aux services écosystémiques*, Versailles, France, 2013/06/03-05.
22. Hodomihou, N. R., Feder, F., Agbossou, E. K., Doelsch, E., Amadji, G. L., NDour-Badiane, Y., Cazevieille, P., Chevassus-Rosset, Cl. et Masse, D. 2014. Caractérisation des risques de contamination de deux sols tropicaux par les éléments traces métalliques en contexte de recyclage des produits résiduaires organiques. *12^es journées d'étude des sols : le sol en héritage*, Le Bourget-du-Lac, France, 2014/06/30-07/04.
23. Hodomihou, N. R., Feder, F., Agbossou, E. K., Doelsch, E., Amadji, G. L., NDour-Badiane, Y., Cazevieille, P., Chevassus-Rosset, Cl. et Masse, D. 2014. Caractérisation des risques de contamination des agrosystèmes périurbains de Dakar par les éléments traces métalliques. *4^e semaine scientifique agricole de l'Afrique de l'Ouest et du centre et 11^e assemblée générale du* CORAF-WECARD, Niamey, Niger, 2014/06/16-20.
24. Feder, F. and Sansoulet, J. 2014. Impact study on the application of vinasse to cambisol and vertic luvisol in Ethiopia. *20^th World Congress of Soil Science*, Jeju, Corée du Sud, 2014/06/08-13.
25. Feder, F., Diallo, F., Ndour Badiane, Y., Ndiaye-Cissé M. F., Ndienor, M. et Masse, D. 2016. Suivi *in situ* et en continu des flux d'eau et de contaminants après apports de produits résiduaires organiques sous cultures maraichères. 6^e conférence internationale de métrologie, Dakar (Sénégal) 2016-03-21/2016-03-24.

2.2.2 Communications posters

1. Feder, F., Bourrié, G. et Trolard, F. 1999. Mesures en continu et *in situ* des paramètres de la solution du sol. Réunion de la direction scientifique « Environnement Forêt et Agriculture », INRA/EFA, Évian, France, 1999/02.
2. Klingelhöfer, G., Trolard, F., Bernhardt, B., Bourrié, G., Feder, F. and Génin, J.-M. R. 1999. The monitoring of iron mineralogy and oxidation states by Mössbauer spectroscopy in the field ; the green rust mineral in hydromorphic soils. *International conference on applications of Mössbauer effect*, Garmisch-Partenkirchen, Germany, 1999/08/30-09/03.
3. Feder, F., Klingelhöfer, G., Trolard, F., Bernhardt, B., Bourrié, G. et Génin J.-M. R. 2000. Suivi *in situ* par spectrométrie Mössbauer de la dynamique des oxydes de fer dans un sol hydromorphe. *6^es journées nationales d'étude des sols*, Nancy, France, 2000/04/25-28.
4. Payet, N., Saint Macary, H., Feder, F., Findeling, A., Nicolini, E. and Vauclin, M. 2004. Assessment of nitrate leaching following pig manure application at the surface of an andisol in La Réunion island. *Joint Earth Sciences Meeting*, Strasbourg, France, 2004/09/20-25.
5. Feder, F., Sevagamy, V., Saint Macary, H. et Chabalier, P.-F. 2004. Création de dispositifs expérimentaux pérennes de suivi *in situ* des risques environnementaux liés au recyclage et à la valorisation agronomiques des déchets et effluents agro-industriels et urbains. *Rencontres internationales pluridisciplinaires, la canne, une passion à partager. Perspectives de développement de la canne à sucre en milieu insulaire : approches technico-économiques, sociales, culturelles.* Congrès de la STASM, Piton Saint-Leu, la Réunion, 2002/10/02-05.

6. Basile Doelsch, I., de Junet, A., Boucherle, A., Legros, S., Bottero, J. Y., Rose, J., Masion, A., Borschneck, D., Moustier, S., Brun, T., Balesdent, J., Marol, C., Derrien, D., Derenne, S., Templier, J., Saint Macary, H. et Feder, F. 2005. Les complexes organo-minéraux du sol : rôle sur la dynamique de séquestration du carbone. *Colloque de Restitution du Programme* ECCO–PNBC, Toulouse, France, 2005/12/05-07.
7. Dudal, Y., Soobadar, A., Doelsch, E., Feder, F., Findeling, A., Salpéteur, L., Benoît, P., Houot, S. et Boudenne, J.L. 2006. Nature et suivi dans les sols des MOD d'origine anthropique à l'aide de la spectroscopie de fluorescence. *Les matières organiques en France. État de l'art et prospectives*, Paris, France. INRA, CNRS, IHSS, INSU, Carqueiranne, France, 2006/01/22-24.
8. Feder, F., Olivier, R., Alary, K. and Bourgeon, G. 2006. Characterisation Of a Soil Catena on the Western Slope of The Piton Des Neiges Volcano (la Réunion). *18th World Congress of Soil Science*, Philadelphia, Pennsylvania, USA, 2006/07/09-15.
9. Doelsch, E., Feder, F., Findeling, A., Dudal, Y. and Saint Macary, H. 2006. Assessing the Risk of Soilborne Heavy Metals Leaching in an Andosol after Sewage Sludge Spreading. *18th World Congress of Soil Science*, Philadelphia, Pennsylvania, USA, 2006/07/09-15.
10. Bourrié, G., Trolard, F. et Feder, F. 2007. Critères d'identification de la fougérite dans les sols hydromorphes et nature de l'anion compensateur. *9es journées nationales d'études des sols*, Angers, France, 2007/04/03-05.
11. Feder, F., Robin, J.-G. et Bourgeon, G. 2008. Cartographie de la vulnérabilité des aquifères de l'ouest de l'île de la Réunion au transfert de polluants / Cartography of groundwater vulnerability to polluants transfer in Western part of La Reunion Island. IWRA, *13^{e} congrès mondial de l'eau*, Montpellier, France, 2008/09/01-04.
12. Feder, F. and Bourgeon, G. 2010. Updating the soil map of Réunion island: methodology and problems to be overcome. *19th World Congress of Soil Science*, Brisbane, Australia, 2010/08/01-06.
13. Michaud, A., Mercier, V., Rampon, J.-N., Morvan, T., Burban, M., Montenach, D., Hammel, F., Sappin Didier, V., Watteau, F., Feder, F., Paillat, J.-M., Masse, D., Hien, E., Bacheley, H. and Houot, S. 2013. SOERE PRO: Long term field experiment network for research on the recycling of organic matters issued of wastes in agriculture. *15^{e} conférence internationale* RAMIRAN *: recyclage des résidus organiques pour l'agriculture : de la gestion des déchets aux services écosystémiques*, Versailles, France, 2013/06/03-05.
14. Feder, F., Finizola, A., Crovisier, M. and Payet, N. 2014. Monitoring of water fluxes by self-potential and TDR probes in the unsaturated vadoze zone during an intense cyclone. *20th World Congress of Soil Science*, Jeju, Corée du Sud, 2014/06/08-13.
15. Feder, F., Diallo, F., Ntoma, R., Masse, D., Diome, F. and Akpo, L. E. 2015. Repeated inputs of organic matter in the long term protect soils from global changes. CSA *2015. Building tomorrow's research agenda and bridging the science-policy gap.* CIRAD, INRA, IRD, Agropolis International, Wageningen UR, CGIAR, UCDAVIS, FAO, Agreenium, GFAR, Montpellier, France, 2015/03/16-18.
16. Masse, D., Ndour-Badiane, Y., Hien, E., Akpo, L. E., Diatta, S., Bilgo, A., Hien, V., Diédhiou, I., Ndiaye-Cissé, M. F., Tall Diouf, L., Ndienor, M., Founoune Mboup, H., Feder, F., Médoc, J.-M., Lardy, L., Assigbetse, K. and Cournac, L. 2015. Ecological intensification for a climate smart agriculture: applications from Senegal and Burkina Faso. CSA *2015. Building tomorrow's research agenda and bridging the science-policy gap.* CIRAD, INRA, IRD, Agropolis International, Wageningen UR, CGIAR, UCDAVIS, FAO, Agreenium, GFAR, Montpellier, France, 2015/03/16-18.
17. Diouf, A., Eick, M. and Feder, F. 2015. Effect of Organic Amendments on the Heavy

Metal Distribution in Market Gardens in Senegal. ASA, CSSA, SSSA, ESA, Joint Annual Meeting, Minneapolis, MN, November 15-18, 2015.

18. Houot, S., Bourdat-Deschamps, M., Ferhi, S., Bernet, N., Mercier, V., Montenach, D., Feder, F., Moussard, G. D. and Patureau, D. Repeated applications of organic waste products in field conditions hardly impact pharmaceutical concentrations in soil and soil leachates. 1st International Conference on Risk Assessment of Pharmaceuticals in the Environment – ICRAPHE, 8-9 septembre 2016, Paris (75).

2.3 Ouvrages

2.3.1 Mémoires et thèse

1. Feder, F. 1996. *Cartographie géologique de l'île de Jersey.* Rapport de stage de terrain de maîtrise de science de la terre. Géoscience Rennes, 55 pages + annexes.
2. Feder, F. 1998. *Suivi en continu de la dynamique de la solution du sol dans les sols hydromorphes. Les équilibres rédox et les conditions de stabilité des rouilles vertes dans le milieu naturel.* Mémoire du DEA national de science du sol, 23 p.
3. Feder, F. 2001. *Dynamique des processus d'oxydo-réduction dans les sols hydromorphes. Monitoring in situ de la solution du sol et des phases solides ferrifères.* Thèse de l'université de Aix-Marseille III, 199 p.

2.3.2 Chapitre d'ouvrage

1. Barbet-Massin, V., Bourgault, G., Feder, F., Girard, M., Hardouin, E., Hébert, A., Macé, F., Nedellec, J.-L., Ponet, J. et Ramsamy, Y. 2010. Aménagement et interventions foncières. *In : Guide des bonnes pratiques agricoles à la Réunion.* Saint-Denis : Ziberlin O., DAF (éd.), 14-61.

2.4 Rapports technique et expertises

1. Feder, F. 2003. Rapport intermédiaire 2002-2003 de la convention avec la société Isautier. Saint-Denis, la Réunion : CIRAD-CA, 13 p.
2. Feder, F. et Saint Macary, H. 2004. Épandage des vinasses de la distillerie Isautier. Rapport final 2002-2003. 19 p.
3. Feder, F. et Saint Macary, H. 2005. Étude expérimentale de l'épandage des vinasses de distillerie sur la canne à sucre : rapport final de la convention CIRAD–Isautier. Montpellier : CIRAD-CA, 70 p.
4. Basile-Doelsch, I., Bottero, J. Y., Cazevieille, P., Chevassus-Rosset, Cl., Doelsch, E., Feder, F., Findeling, A., Garnier, J.-M., Gaudet, J.-P., Legros, S., Levard, C., Masion, A., Moussard, G., Moustier, S., Rose, J. et Saint Macary, H. 2005. Recyclage agricole des déchets organiques dans les sols tropicaux (île de la Réunion) : quel impact sur les transferts d'éléments traces métalliques ? Montpellier : CIRAD-CA, 87 p.
5. Doelsch, E., Feder, F., Findeling, A. et Dudal, Y. 2005. Éléments traces métalliques : impact de l'épandage d'une boue d'épuration sur la mobilité et la spéciation des ETM d'un andosol. Saint-Denis, la Réunion : CIRAD-CA, 103 p.
6. Frissant, N. et Feder, F. 2005. Étude de la zone non saturée sur le site de La Mare, Commune de Sainte-Marie. Phase 2. Rapport intermédiaire.
   Rapport BRGM/RP-54419-FR. 41 pages, 6 tableaux, 6 illustrations.
7. Ladouche, B., Frissant, N., Mouvet, Ch., Feder, F. et Petit, V. 2006. Étude de la zone non saturé sur le site de La Mare, commune de Sainte-Marie (la Réunion). Phase 2. Rapport BRGM/RP-54419-FR. 95 pages, 8 tableaux, 46 illustrations.

8. Basile-Doelsch, I., Bottero, J. Y., Cazevieille, P., Chevassus-Rosset, Cl., Doelsch, E., Feder, F., Findeling, A., Garnier, J.-M., Gaudet, J.-P., Legros, S., Levard, Cl., Masion, A., Moussard, G. D., Moustier, S., Rose, J. et Saint Macary, H. 2006. Recyclage agricole des déchets organiques dans les sols tropicaux (île de la Réunion) : quel impact sur les transferts d'éléments traces métalliques ? Rapport de la convention ADEME-CIRAD n° 0475C0013. CIRAD, département PERSYST, 122 p.
9. Feder, F., Robin, J.-G. et Bourgeon, G. 2007. Évaluation des risques de transfert des polluants à travers les sols. *Rapport final à la convention de recherche entre la* DIREN *et le* CIRAD. CIRAD, département PERSYST, 49 p.
10. Feder, F. and Sansoulet J. 2007. Impact study on the application of vinasse to soils in Metahara, Ethiopia. *Final report*, 7 december 2007. Confidentiel. CIRAD, département PERSYST, 24 p.
11. Feder, F., Robin, J.-G. et Bourgeon, G. 2008. Évaluation des risques liés au transfert des polluants à travers les sols et vers les nappes. *Rapport final de la convention de recherche entre le ministère de l'Outre-mer et le* CIRAD. CIRAD, département PERSYST, 75 p.
12. Feder, F. et Morel, J. 2011. Projet Run Innovation II. *Rapport final de l'expérimentation sur le lisier (site de Saint-Joseph, la Réunion).* Confidentiel. CIRAD, département PERSYST, 55 p.
13. Feder, F. Bièque, S. et Condom, N. 2012. Étude complémentaire portant sur l'impact de l'utilisation des eaux épurées sur les sols et le développement des végétaux. Projet de Reuse de la STEP du Grand Prado. *Rapport intermédiaire au 15 mai 2012 de la convention Cirad-Cinor-La Créole.* CIRAD, département PERSYST, 90 p.
14. Farinet, J.-L. et Feder, F. 2014. Étude et dimensionnement d'une unité pilote de compostage à la CSS, Richard Toll, Sénégal. *Rapport confidentiel*, mars 2014, CIRAD, département PERSYST, 31 p.
15. Feder, F. 2015. Étude complémentaire portant sur l'impact de l'utilisation des eaux épurées sur les sols et le développement des végétaux. Projet de Reuse de la STEP du Grand Prado. *Rapport final de la convention* CIRAD-CINOR-*La Créole.* CIRAD, département PERSYST, 145 p.

2.5 Chapitres de rapport

1. Feder, F., Saint Macary, H., Gosme, M., Chabalier, P.-F. et Doelsch, E. 2002. Étude expérimentale de l'épandage des vinasses sur la canne à sucre. Vinasses de la distillerie Isautier, Saint Pierre de la Réunion. *In : rapport d'exécution 2001-2002*, Saint-Denis, la Réunion, CIRAD-CA, 11 p.
2. Saint Macary, H., Chabalier, P.-F., Boyer, J., Feder, F., Payet, N., Bernard, H. et Doelsch, E. 2003. Agriculture durable, environnement et forêt. Risque environnemental, gestion agronomique, recyclage des déchets (REGARD). *In : rapport annuel 2002 du* CIRAD *Réunion*, Saint-Denis, la Réunion, p. 34-40.
3. Saint Macary H., Chabalier P.-F., Medoc J.-M., Feder F., Bernard H. et Doelsch E. 2004. Agriculture durable, environnement et forêt – Risque environnemental, gestion agronomique, recyclage des déchets (REGARD). *In : rapport annuel 2003* CIRAD *Réunion.* De Taffin, G. (éd.), Saint-Denis, la Réunion, p. 34-38.
4. Saint Macary H., Payet N., Feder F., Doelsch E., Chabalier P.-F., Medoc J.-M. et Guerrin F. 2005. Agriculture durable, environnement et forêt – Risque environnemental, gestion agricole, recyclage des déchets (REGARD). *In : rapport annuel 2004* CIRAD *Réunion.* De Taffin, G. (éd.), Saint-Denis, la Réunion, p. 47-51.

5. Feder F., Saint Macary H., Doelsch E., Medoc J.-M., Guerrin F. 2006. Agriculture durable, environnement et forêt – Risque environnemental, gestion agricole, recyclage des déchets (Regard). *In : rapport annuel 2005 du* Cirad *à la Réunion.* Gay, J.-P. (éd.), Saint-Denis, la Réunion, p. 45-52.
6. Feder F., Saint Macary H. et Chopart J.-L. 2007. Comportement des nitrates dans les sols et pratiques agricoles respectueuses de l'environnement. *In : le* Cirad *à la Réunion en 2006.* Gay, J.-P. (éd.), Saint-Denis, la Réunion, p. 6-8.

2.6 Supports de formation

1. Saint Macary, H., Findeling, A., Feder, F. et Payet, N. 2008. Risque environnemental : cas des nitrates à la Réunion. Montpellier : Cirad, diaporama (44 vues).
2. Saint Macary, H., Findeling, A., Feder, F. et Payet, N. 2010. Cours n° 6 : évaluation environnementale : 6.2 Illustration par le cas des nitrates à la Réunion. Rennes : Uved-Cirad, diaporama (42 vues).
3. Saint Macary, H., Findeling, A., Feder, F. et Doelsch, E. 2010. Cours n° 6 : évaluation environnementale : 6.1 Risques agro-environnementaux liés aux matières organiques. Rennes : Uved-Cirad, diaporama (26 vues).
4. Saint Macary,, H., Feder, F. et Payet, N. 2012. Risques agro-environnementaux liés aux matières organiques. Illustration par le cas des nitrates à la Réunion : session 6. Gestion des risques environnementaux. *In : séminaire « Enjeux et conditions de la mobilisation de la matière organique issue des déchets (ménagers et organiques) dans les pays du Sud. Impacts agronomiques et environnementaux ».* Cirad, Prasac, Ademe, diaporama (40 vues), Douala, Cameroun, 2011/09/12-16.
5. Saint Macary, H., Findeling, A., Doelsch, E. et Feder, F. 2012. Risques agro-environnementaux liés aux matières organiques : session 6. Gestion des risques environnementaux. *In : séminaire « Enjeux et conditions de la mobilisation de la matière organique issue des déchets (ménagers et organiques) dans les pays du Sud. Impacts agronomiques et environnementaux ».* Cirad, Prasac, Ademe, diaporama (23 vues), Douala, Cameroun, 2011/09/12-16.
6. Doelsch, E., Saint Macary, H., Feder, F., Moussard, G. D., Chevassus-Rosset, Cl., Cazevieille, P., Bravin, M., Thuriès, L., Basile, I., Bottero, J. Y., Garnier, J.-M., Masion, A., Rose, J., Moustier, S., Gaudet, J.-P., Legros, S., Levard, Cl., Collin, Bl., Guigues, S., Van de Kerchove, V., Payet, N., Garnier, J.-N., Bracco, I., Badat, F. et Navarro, O. 2012. Contexte régional et enjeux agronomiques et environnementaux du recyclage en agriculture des boues à la Réunion : session 6. Gestion des risques environnementaux. *In : séminaire « Enjeux et conditions de la mobilisation de la matière organique issue des déchets (ménagers et organiques) dans les pays du Sud. Impacts agronomiques et environnementaux ».* Cirad, Prasac, Ademe, diaporama (14 vues), Douala, Cameroun, 2011/09/12-16.

2.7 Articles de presse et autre

À plusieurs reprises, j'ai été interviewé par des journalistes de la presse écrite et audio-visuelle de la Réunion. Je retiendrais les articles suivants :

- *Le grand paradoxe des sols réunionnais.* Deux pleines pages dans le *Journal de la Réunion*, supplément *De Natura* du 29/05/2009.
- *Une diversité inouïe sur une petite île.* Un tiers de page dans Agronews, n° 2 de 11/2009.

TABLEAU 2.1 – *Données bibliométriques synthétiques extraites du Web of Science^{TM} au 5 juin 2016.*

Nombre de publication de rang A	12
Nombre de publication dans des revues à comité de lecture sans facteur d'impact	4
Nombre total de publication dans des revues à comité de lecture	16
Nombre de publications comme premier ou second auteur	8
Nombre de citations total	153
Nombre de citations pour l'article le plus cité	58
Facteur H	6

- *Station d'épuration du Grand-Prado : Que faire des boues et des eaux épurées ?* Trois quart de page dans *Le Quotidien* du 31/01/2011.
- *Utiliser les eaux épurées pour irriguer les champs.* Un quart de page dans Agronews, n° 4, 05/2011.

2.8 Données bibliométriques synthétiques

Les tableaux 2.1 et 2.2 présentent les données synthétiques extraites du Web of Science^{TM} à la date du 5 juin 2016. Pour la moitié de ces publications, je suis premier ou deuxième auteur. Les autres situations reflètent principalement ma participation à des travaux de thèse pour lesquels je n'étais pas l'encadrant principal. Je suis auteur ou co-auteur de huit articles au cours des cinq dernières années (de 2012 à 2016 inclut), soit en moyenne 1,6 article par an.
Sur les douze articles de rang A, huit font partis du premier quartile dans leur domaine et deux articles du deuxième quartile ; la majorité des articles sont donc publiés dans les meilleurs revues de leur domaine. Les domaines de publication sont nombreux (7) mais restent regroupés autour de la science du sol et de ses disciplines connexes.

TABLEAU 2.2 – *Données bibliométriques synthétiques. Les facteurs d'impact et les quartiles sont ceux de l'année de publication.*

Article	Année	Journal	Facteur d'impact	Rang	Quartile de la revue dans son domaine
Hodomihou *et al.*	2016	*Biotechnologie, Agronomie, Société et Environnement.*	0,46 *	63/81 215/223	Q4 Agronomy Q4 Environmental sciences
Feder *et al.*	2015	*Science of the Total Environment*	4,1 *	18/221	Q1 Environmental sciences
Wassenaar *et al.*	2014	*Agricultural Systems*	2,91	3/56	Q1 Agriculture, multidisciplinary
Feder	2013	*Catena*	2,48	6/34	Q1 Soil science
Alary *et al.*	2013	*Pedosphere*	1,38	20/34	Q3 Soil science
Legros *et al.*	2013	*Agriculture, Ecosystems & Environment*	3,20	1/56 38/216	Q1 Agriculture, multidisciplinary Q1 Environmental sciences
Payet *et al.*	2009	*Agriculture, Ecosystems & Environment*	3,13	1/45 29/181	Q1 Agriculture, multidisciplinary Q1 Environmental sciences
Feder and Findeling	2007	*European Journal of Soil Science*	2,73	2/30	Q1 Soil science
Trolard *et al.*	2007	*Clays and Clay Minerals*	1,37	7/25 10/30	Q2 Mineralogy Q2 Soil science
Feder *et al.*	2005	*Geochimica et Cosmochimica Acta*	3,90	3/55	Q1 Geochemistry and geophysics
Bourrié *et al.*	2004	*Clays and Clay Minerals*	1,12	13/55 11/23	Q1 Water resources Q2 Mineralogy
Feder *et al.*	1998	*Mineralogical magazine*	0,83	11/23	Q2 Mineralogy

* Facteur d'impact de l'année 2014.

CHAPITRE 3

ADMINISTRATION ET ANIMATION DE LA RECHERCHE

3.1 Administration de la recherche

3.1.1 Participation à des projets déposés

1. *Organo-mineral interactions : nanoscale mechanisms for carbon sequestration in soils (NanoSoilC).* Projet coordonné par I. Basile-Doelsch (INRA, UR géochimie des sols et des eaux). Financement demandé à l'agence nationale de la recherche (France) dans l'appel d'offre Défi 1 (2016) ; le budget prévisionnel du projet est de 650 k€.

3.1.2 Coordonnateur principal de projets en cours

1. 2013–2030 : *Système d'observation et d'expérimentation sur le long terme pour la recherche en environnement consacré aux produits résiduaires organiques à la Réunion* (SOERE PRO RÉUNION). Projet coordonné par F. Feder et J.-M. Paillat (CIRAD, UR recyclage et risques) et financé par Veolia Eau, l'État et l'Europe (convention 11114D974000051) et AllEnvi ; le budget annuel du projet est de 330 k€.
2. 2016–2018 : *Intense Maraîchage.* Projet coordonné par F. Feder avec S. Simon et financé par le métaprogramme GloFoodS « Transitions pour la sécurité alimentaire mondiale » ; le budget du projet est de 35 k€.

3.1.3 Coordonnateur d'une tâche ou d'une action de projets en cours

1. 2013–2016 : *Externalités négatives de l'intensification des sols cultivés en milieu péri-urbain : méthodes et outils d'évaluation et pratiques alternatives.* Projet n° 03.GRN.05 coordonné par E. Hien (université de Ouagadougou) et financé par le CORAF/WECARD dans le cadre de l'appel à propositions de notes conceptuelles de projets « Recherche et développement sur la gestion des ressources naturelles » ; le budget du projet est de 485 k€.
2. 2016–2017 : *Mise en œuvre du volet « recherche scientifique » du programme national de biogaz domestique au Sénégal.* Projet coordonné par S. Legros et financé par le programme national de biogaz domestique au Sénégal ; le budget du projet est de 30 k€.
3. 2016–2019 : *Diagnosis of waste treatments for contaminant fates in the environment (Digestate).* Projet coordonné par E. Doelsch (CIRAD, UR recyclage et risques) et financé par l'agence nationale de la recherche ; le budget du projet est de 690 k€.

3.1.4 Coordonnateur principal de projets terminés

1. *Biogéochimie des sols en interaction avec l'apport de déchets.* Projet coordonné par F. Feder (CIRAD, UR recyclage et risques) et financé par le CIRAD, la région Réunion et le FEOGA (2002–2006) ; le budget annuel du projet était de 50 k€.
2. *Évaluation des risques liés au transfert des polluants à travers les sols et vers les nappes.* Projet coordonné par F. Feder (CIRAD, UR recyclage et risques) et financé par le ministère de l'outre-mer et la Diren Réunion (2006–2009) ; le budget du projet était de 105 k€.
3. *Création et pilotage de systèmes de cultures adaptés aux risques environnementaux.* Projet coordonné par F. Feder (CIRAD, UR recyclage et risques) et financé par le CIRAD, la région Réunion et le FEADER (2008–2011) ; le budget annuel du projet était de 50 k€.
4. *Étude complémentaire portant sur l'impact de l'utilisation des eaux épurées sur les sols et le développement des végétaux.* Projet coordonné par F. Feder (CIRAD, UR recyclage et risques) et financé par la CINOR (2010–2014) ; le budget du projet était de 285 k€.

3.1.5 Coordonnateur d'une tâche ou d'une action de projets terminés

1. *Méthodes d'évaluation de l'impact agronomique et environnemental du recyclage agricole des déchets agro-industriels. Contribution à la mise au point d'outils d'aide au suivi et à la planification des épandages d'effluents par l'étude des mécanismes biogéochimiques affectant la mobilité et la disponibilité des solutés dans les sols.* Projet coordonné par H. Saint Macary et S. Marlet (CIRAD, UR recyclage et risques et UMR G-eau) et financé par le Cirad dans le cadre de l'action thématique programmée ATP 2000/10 (2001–2004) ; le budget du projet était de 1095 k€.
2. *Recyclage agricole des déchets organiques dans les sols tropicaux : quel impact sur les transferts d'éléments traces métalliques (île de la Réunion) ?* Projet coordonné par E. Doelsch (CIRAD, UR recyclage et risques) et financé par l'ADEME dans le cadre du programme Gessol2 (2004–2008) ; le budget du projet était de 110 k€.
3. *Étude de la zone non saturée sur le site de La Mare.* Projet coordonné par M. Moulin (BRGM, la Réunion), financé par le conseil général et la DIREN Réunion (2004–2006) ; le budget du projet était de 10 k€.
4. *Les complexes organo-minéraux du sol : rôle sur la dynamique de séquestration du carbone.* Projet coordonné par I. Basile-Doelsch (université de Aix-Marseille III) et financé par le programme national ACI–FNS « ECCO (écosphère continentale : processus et modélisation) » (2004–2007).
5. *Run Innovation II.* Projet coordonné par Phytorem® et financé par la région Réunion, le fonds unique interministériel (2007–2010) ; le budget du projet était de 1300 k€.
6. *Intensification écologique des systèmes de production agricoles par le recyclage des déchets (Isard).* Projet coordonné par H. Saint Macary (CIRAD, UR recyclage et risques) et financé par l'agence nationale de la recherche (France) dans le cadre de l'appel à projet Systerra 2008 (2009–2012) ; le budget du projet était de 960 k€.
7. *Gestion intégrée des résidus organiques par la valorisation agronomique à la Réunion (Girovar).* Projet coordonné par T. Wassenaar (CIRAD, UR recyclage et risques) et financé par le ministère de l'alimentation, de l'agriculture et de la pêche dans le cadre de l'appel à projet CAS-DAR 2010 (2010–2014) ; le budget du projet était de 287 k€.
8. *Création d'un résau d'essais au champ pour l'étude de la valeur agronomique et des impacts environnementaux et sanitaires des produits résiduaires organiques recyclés*

en agriculture (Réseau Pro). Projet coordonné par l'association de coordination technique agricole (Acta) et financé par le ministère de l'alimentation, de l'agriculture et de la pêche dans le cadre de l'appel à projet CAS-DAR 2010 (2010–2014) ; le budget du projet était de 500 k€.

3.1.6 Expertises publiques et privés

1. *Agronomical impact of vinasse spreading in irrigated soils.* Expertise réalisée par F. Feder et J. Sansoulet (CIRAD, UR recyclage et risques) et financée par Sucre austral (2007, montant 12 k€).
2. *Étude de la faisabilité des rejets de l'installation de traitement des lixiviats de l'installation de stockage des déchets non dangereux de la Civis.* Tierce expertise du CIRAD réalisée par F. Feder (CIRAD, UR recyclage et risques) et financée par la CIVIS (2010, montant 5 k€).
3. *Effluents porcins aux Seychelles.* En 2011, j'ai intégralement construit le montage financier, partenarial et scientifique de cette expertise réalisée en 2012 par mon collègue J.-L. Farinet en collaboration avec deux experts de la DAAF et de la FRCA (fédération régionale des coopératives agricoles). Le montant total du projet est de 39 k€ financé par le fonds de coopération régional (FCR) et le programme opérationnel européen de coopération territorial (POCT).
4. *Étude et dimensionnement d'une unité pilote de compostage à la compagnie sucrière du Sénégal, Richard Toll, Sénégal.* Expertise réalisée par J.-L. Farinet et F. Feder (CIRAD, UR recyclage et risques) et financée par la compagnie sucrière du Sénégal (2014, montant 9 k€).
5. *Étude de l'utilisation d'eaux usées épurées pour l'irrigation de cultures ou d'espaces verts à la Réunion.* Projet réalisé par M. Bravin, E. Doelsch et F. Feder (CIRAD, UR recyclage et risques) et financé par l'office de l'eau de la Réunion (2015) ; le budget du projet était de 16 k€.

3.2 Animation de la recherche

3.2.1 Responsabilités, management

De 2004 à 2011, j'ai été le responsable d'un technicien basé sur la station du CIRAD de la Bretagne et, de 2007 à 2011, j'ai également été le responsable scientifique de quatre à cinq techniciens basés sur la station du CIRAD des Colimaçons. Ces encadrements scientifiques consistaient à planifier, coordonner et organiser leurs activités puis à réaliser le suivi et la bonne réalisation de ces activités. De plus, j'assurais intégralement la responsabilité administrative de ces techniciens : gestion au quotidien des congés, des missions, des formations et gestion annuelle de leur parcours professionnel (entretien annuel obligatoire, perspectives d'évolution de carrière, etc.).
De 2009 à 2011, j'ai assuré les fonctions d'animation scientifique et administrative du programme PILMO regroupant les membres de l'unité de recherche basés à la Réunion (6 chercheurs, plusieurs doctorants et VCAT et 7 techniciens). Au niveau scientifique, cette tâche consistait à coordonner les synthèses des travaux de recherche de l'équipe et à les restituer semestriellement auprès de la direction régionale du CIRAD Réunion et des partenaires financeurs (État, conseil régional de la Réunion, département de la Réunion, autres partenaires scientifiques institutionnels et privés, etc.).
De 2009 à 2011, j'ai été membre du comité éditorial d'Agronews (le magazine semestriel du CIRAD Réunion). À ce titre, je sollicitais des auteurs, je participais aux choix des articles et je participais aux corrections aux différentes étapes de la réalisation du magazine.

3.2.2 Partenariats

Partenariats construits à la Réunion

Les partenariats que j'ai initié et développé ou entretenu au cours de mon parcours professionnel à la Réunion sont les suivants :

- le laboratoire Géosciences Réunion (université de la Réunion) ;
- l'UR Aïda (CIRAD);
- le BRGM de la Réunion ;
- les UMR LTHE (laboratoire d'étude des transferts en hydrologie et environnement), ECO&SOL, ECOSYS (anciennement UMR EGC) et CEREGE (centre européen de recherche et d'enseignement des géosciences de l'environnement) ;
- les sociétés Phytorem, Ecofilæ et Veolia Eau (Réunion).

Partenariats construits au Sénégal

Les partenariats que j'ai initié et développé ou entretenu au cours de mon parcours professionnel au Sénégal sont les suivants :

- le laboratoire national de recherches sur les productions végétales (LNRPV) de l'ISRA (institut sénégalais de recherche agricole) ;
- le centre pour le développement de l'horticulture (CDH) de l'ISRA (institut sénégalais de recherche agricole) ;
- la faculté des sciences et techniques de l'université Cheikh Anta Diop de Dakar ;
- l'UR Hortsys (CIRAD) ;
- l'UFR SVT de l'université de Ouagadougou ;
- le laboratoire d'hydraulique et de maitrise de l'eau (LHME) de l'université d'Abomey-Calavi ;
- le programme national biogaz domestique du Sénégal (PNB-SN) du ministère de l'énergie et du développement des énergies renouvelables du Sénégal.

3.2.3 Participation aux réflexions scientifiques interne et externe

Depuis 2012, je suis co-responsable des animations scientifiques de l'unité « recyclage et risques », avec mon collègue T. Wassenaar. Notre tâche consiste à élaborer une stratégie annuelle, à rechercher des intervenants extérieurs et à organiser et animer tous les mois ces animations scientifiques. Les objectifs recherchés sont multiples, mais il s'agit principalement de créer une dynamique d'équipe autour de nos thèmes intégrateurs, de s'informer et d'échanger avec la communauté scientifique, voire d'imaginer et faire germer nos futurs projets de recherche intégrateurs.

3.2.4 Évaluation d'articles scientifiques

Depuis 2001, j'ai relu et évalué 17 articles pour les journaux suivants : Journal of Environmental Management (5), Journal of Arid Environment (2), Plant and Soil (2), Soil Research (continuing Australian Journal of Soil Research) (1), European Journal of Soil Science (1), African Journal of Agricultural Research (1), Journal of Geochemical Exploration (1), Geochemistry: Exploration, Environment, Analysis (1), Archives of Agronomy and Soil Science (1), Polish Journal of Environmental Studies (1) et Vertigo, revue des sciences de l'environnement (1).

3.2.5 Évaluation de projets scientifiques

Depuis 2012, je suis membre du comité de sélection des projets proposés au fonds d'impulsion pour la recherche scientifique et technique (FIRST) du ministère de l'enseignement supérieur de la recherche du Sénégal. Je suis membre de deux commissions (agriculture et environnement). Tout les ans, j'évalue une trentaine de dossiers scientifiques au sein de chacune de ces commissions.
Depuis 2014, je participe, au nom du CIRAD, au comité de sélection des bourses de thèse et de post-doctorat du service de coopération et d'action culturelle (SCAC) de l'ambassade de France à Dakar. Pour la session de 2015, j'ai évalué et commenté près de 150 dossiers.

CHAPITRE 4

ACTIVITÉS D'ENCADREMENT ET DE FORMATION

4.1 Activités d'encadrement

4.1.1 Encadrements principal de thèses

1. Diallo, F. : *Impacts à long terme du recyclage des matières organiques en maraîchage.* Université Cheikh Anta Diop de Dakar. Thèse commencée le 1er janvier 2016.
2. Hodomihou, R. N. : *Comment concilier l'intensification de l'agriculture périurbaine à l'aide d'intrants organiques et la préservation durable des agrosystèmes tropicaux ?* Soutenance prévue au second semestre 2016 à l'université d'Abomey-Calavi (Bénin).
3. Diallo-Ntoma, R. : *Effets à long terme d'apports intensifs et répétés de matières organiques sur l'évolution des sols maraîchers de la région de Dakar (Sénégal).* Soutenance prévue au premier semestre 2017 à l'université Cheikh Anta Diop de Dakar.

4.1.2 Référent scientifique de thèse pour une partie des activités de recherche

1. Bernard, H. (2004) : *Évaluation des risques de transfert d'herbicides dans les sols tropicaux de l'ouest de l'île de la Réunion.* Thèse de doctorat de l'université de Poitiers. Dans le cadre de cette thèse, j'ai appuyé le doctorant dans l'élaboration de ses protocoles de suivis et dans la mise en place de son expérimentation sur le terrain (La Saline, antenne d'irrigation 4).
2. Payet, N. (2005) : *Impact des apports de lisier sur un sol cultivé de la Réunion : étude expérimentale et modélisation des flux d'eau et de nitrate dans la zone non saturée.* Thèse de doctorat de l'université de la Réunion.
   Dans le cadre de cette thèse, j'ai participé avec le doctorant à la conception et la mise en place de son expérimentation sur le terrain (station des Colimaçons) puis à l'analyse et l'interprétation de ses résultats. Les références Feder *et al.* (2004), Payet *et al.* (2004, 2009) reflètent ce travail.
3. Legros, S. (2008) : *Évaluation multi-échelle de l'impact environnemental de l'épandage de lisier de porc sur un sol tropical (île de la Réunion) : spéciation et modélisation du comportement du cuivre et du zinc.* Thèse de doctorat de l'université de la Réunion. Dans le cadre de cette thèse, j'ai appuyé le doctorant pour la conception et la mise en place de son expérimentation sur le terrain (station des Colimaçons) puis à l'analyse et l'interprétation de ses résultats. L'article Legros *et al.* (2013) reflète ce travail.
4. Rabetokotany, N. (2013) : *Matières organiques issues de l'élevage et de la ville en milieu tropical : apports de la spectrométrie proche infra-rouge (*Spir*) pour orienter*

leurs usages agronomiques et/ou énergétiques. Thèse de doctorat de l'université de la Réunion et de l'université d'Antananarivo.
Dans le cadre de cette thèse, j'ai appuyé la doctorante pour l'élaboration d'un outil de hiérarchisation et de classification des propriétés des matières organiques.

4.1.3 Participations à des comités de pilotage de doctorats

1. Pautremat, N. : *Conséquences du recyclage agricole de déchets agro-industriels liquides et fermentescibles sur la mobilité de métaux préexistants dans le sol (Fe, Mn, Cr, Ni) ; interactions entre transfert, microbiologie et réactivité géochimique abiotique.* Université d'Avignon et des Pays de Vaucluse.
2. Bernard, H. : *Évaluation des risques de transfert d'herbicides dans les sols tropicaux de l'ouest de l'île de la Réunion.* Université de Poitiers.
3. Payet, N. : *Impact des apports de lisier sur un sol cultivé de la Réunion : étude expérimentale et modélisation des flux d'eau et de nitrate dans la zone non saturée.* Université de la Réunion.
4. Legros, S. : *Évaluation multi-échelle de l'impact environnemental de l'épandage de lisier de porc sur un sol tropical (île de la Réunion) : spéciation et modélisation du comportement du cuivre et du zinc.* Université de la Réunion.
5. Perrin, A. : *Évaluation environnementale des systèmes agricoles urbains en Afrique de l'Ouest : Implications de la diversité des pratiques et de la variabilité des émissions d'azote dans l'analyse du cycle de vie de la tomate au Bénin.* Université de Montpellier.
6. Rabetokotany, N. : *Matières organiques issues de l'élevage et de la ville en milieu tropical : apports de la spectrométrie proche infra-rouge (*SPIR*) pour orienter leurs usages agronomiques et/ou énergétiques.* Universités de la Réunion et d'Antananarivo.
7. Nobile, C. : *Spéciation et phytodisponibilité du phosphore dans les sols tropicaux amendés en* PRO. Université de la Réunion.

4.1.4 Encadrements de stages

1. Sevagamy, V. (2002) : *Caractérisation et aménagement de parcelles destinées à l'évaluation du risque environnemental des pratiques agricoles.* Mémoire du DESS « études d'impacts environnementaux ». Université Montesquieu, Bordeaux IV, 106 p.
2. Gosme, M. (2002) : *Agro-épuration des vinasses de distillerie sur l'île de la Réunion.* Rapport de stage de deuxième année d'ingénieur, ENSAR, Rennes, France, 83 p.
3. Calichiama, L. (2003) : *Transformations physico-chimiques et transfert de solutés dans un andosol liés à l'épandage d'un déchet organique.* Rapport de stage d'ingénieur-maître, IUP « environnement », département « environnement technologies et sociétés », 66 p.
4. Levrel, G. (2004) : *Dynamique et spécialisation des éléments traces métalliques (*ETM*) dans un sol volcanique tropical après épandage de boue de* STEP. Mémoire du DEA national de sciences du sol. Université H. Poincaré, Nancy I.
5. Olivier R. (2005) : *Étude d'une toposéquence dans l'île de la Réunion.* Rapport de stage de troisième année. INH, Angers, France, 31 p.
6. Bochu, V. (2006) : *Impacts de l'épandage d'un lisier de porc sur un Nitisol de l'île de la Réunion.* Mémoire de fin d'étude de l'école supérieure d'agriculture d'Angers, France.

7. Blondel, A. (2007) : *Caractérisation hydro-géochimique des différents types d'eaux dans les sols volcaniques de la Réunion.* Mémoire de deuxième année de master recherche « transfert-sol-aquifère », université d'Avignon.
8. Oliviero, A. (2009) : *Suivi des nitrates dans des sols à capacité d'échange anionique.* Mémoire de fin d'études ingénieur de l'ENESAD, spécialité agriculture, 45 p.
9. Vessière, H. (2010) : *La valorisation de la matière organique sur l'ouest de la Réunion : caractérisation des pratiques de fertilisation et hiérarchisation des risques de lixiviation des nitrates.* Mémoire de fin d'études de l'ISTOM, 121 p.
10. Roux, L. (2010) : *Caractérisation des sols par* SPIR *(spectrométrie proche infrarouge), suivi de la matière organique et des* ETM *dans les sols à la Réunion et comparaison de différents itinéraires techniques.* Mémoire de fin d'études d'école d'ingénieur de Purpan, 177 p.
11. Bièque, S. (2011) : *Impacts de l'utilisation d'eau usée épurée sur le sol et le développement de végétaux.* Mémoire de deuxième année pour le diplôme d'ingénieur AgroParisTech, 43 p.
12. Ashenafi, M. S. (2013) : *Adaptation d'un logiciel de pilotage de l'irrigation à la réutilisation des eaux usées.* Mémoire de deuxième année de master STIC et santé, spécialité « bioinformatique, connaissances, données », université de Montpellier II.
13. Diallo, F. (2013) : *Évaluation des risques de contamination des sols et des ressources en eau souterraine par les éléments traces métalliques dans les systèmes intensifs de production agricole périurbains recourant massivement aux produits résiduaires organiques dans la région de Dakar (Sénégal).* Mémoire de première année du master « gestion durable des agro-écosystèmes horticoles », faculté des sciences et techniques, université Cheikh Anta Diop de Dakar, 17 p.
14. Thiam, M. (2013) : *Modèle de transport de solutés dans les sols avec évaluations des risques environnementaux.* Mémoire de master 2 de l'institut africain des sciences mathématiques (AIMS), Sénégal, 75 p.
15. Diallo, F. (2015) : *Arrières effets de la fertilisation organique des sols ferrugineux tropicaux dans la zone des Niayes sur les rendements des cultures maraichères.* Mémoire de deuxième année du master « gestion durable des agro-écosystèmes horticoles », université Cheikh Anta Diop de Dakar, faculté des sciences et techniques, 65 p.

4.1.5 Encadrements scientifiques directs de VCAT et de VSC

1. Robin, J.-G. (24 mois) : dans le cadre du projet d'évaluation des transferts de nitrates vers les nappes que j'ai coordonné, réalisation des prélèvements pédologiques, compilation des informations et synthèse cartographique.
2. Morel, J. (24 mois) : dans le cadre du projet RunInnovationII, suivi de l'expérimentation d'apports de lisiers de porc en bambouseraie à Saint-Joseph.
3. Simon, E. (20 mois) : dans le cadre du projet SOERE PRO RÉUNION, suivi de l'échantillonnage, gestion de l'instrumentation.

4.2 Activités de formation

C'est au cours de ma thèse qu'il m'a été offert l'opportunité de gouter à l'enseignement à travers des travaux pratiques en géologie à l'université de Bretagne occidentale. Par la suite, une fois au CIRAD, j'ai réalisé plusieurs modules d'enseignements à l'université de la Réunion et à l'université Cheikh Anta Diop de Dakar dans le domaine de la science du sol.

4.2.1 Université de Bretagne occidentale

En 1999 et 2000, j'ai élaboré et réalisé des travaux pratiques en géologie à l'université de Bretagne occidentale dans la licence de biologie coordonnée par L. Dabouineau. Au cours de ces travaux pratiques, j'ai enseigné aux étudiants comment décrire, caractériser et identifier des roches volcaniques, sédimentaires et métamorphiques. J'ai réalisé dix séances de travaux pratiques de trois heures.

4.2.2 Université de la Réunion

De 2005 à 2008, j'ai réalisé des enseignements en science du sol en licence et en maitrise de biologie végétale : annuellement, trois cours magistraux de deux heures.
De 2001 à 2010, j'ai réalisé ponctuellement des enseignements au BTSA « gestion de l'irrigation » du lycée agricole de Saint-Paul.
En 2010, j'ai réalisé un enseignement au sein de la licence professionnelle « agriculture et développement durable » : deux cours magistraux de quatre heures.

4.2.3 Université Cheikh Anta Diop de Dakar

Depuis 2012, je suis responsable d'un module d'enseignement en science du sol au sein du master GEDAH « gestion durable des agro-écosystèmes horticoles » de la faculté des sciences et techniques de l'université Cheikh Anta Diop de Dakar au Sénégal. Je réalise environ seize heures de cours magistraux annuellement auprès des premières et deuxièmes années de ce master. En outre, je réalise un cours d'introduction à la science du sol (de quatre à huit heures annuellement) dans les masters AFECA (« agroforesterie, écologie et adaptation ») et BIOVEM (« biotechnologies végétales et microbiennes ») de l'université Cheikh Anta Diop de Dakar.

4.2.4 Autres formations dispensées

En 2010, j'ai réalisé une formation (huit heures) pour les agents de l'ONF de la Réunion. Il s'agissait de donner des bases en science du sol, d'expliquer la genèse et les propriétés des sols de la Réunion et d'apporter des réponses aux problèmes auxquels les agents de l'ONF avaient été confrontés.
En 2015, avec mes collègues du CIRAD à la Réunion, j'ai participé à la réalisation d'une formation sur plusieurs jours pour les agents de la DAAF de la Réunion (2015). J'ai intégralement réalisé trois modules :

- potentialité et fertilité des sols et rôle de la matière organique (une heure) ;
- pertes par érosion et lixiviation-lessivage (deux heures) ;
- présentation des expérimentations sur la station de La Mare (trois heures).

DEUXIÈME PARTIE : MÉMOIRE DES TRAVAUX DE RECHERCHE

CHAPITRE 5

ÉVOLUTION DES OXYDES DE FER ET DE LA GÉOCHIMIE DES EAUX DANS LES SOLS HYDROMORPHES

Au cours de mon stage de DEA en science du sol à Rennes, j'ai étudié la dynamique de la géochimie de la solution du sol dans les sols hydromorphes en Bretagne. En effet, près de 20 % de la superficie de la Bretagne présente des sols soumis à l'hydromorphie. De plus, leurs positions dans les paysages, souvent à l'interface avec le réseau hydrographique, exacerbe leur importance environnementale. Or, l'intensification des systèmes de production agricole et la forte concentration des élevages induisent des excédents en matières organiques structurels en Bretagne difficiles à résorber. La compréhension des processus géochimiques qui se déroulent dans les sols hydromorphes est donc primordiale pour comprendre les transformations des matières organiques et pour évaluer les impacts de leur recyclage.
J'ai poursuivi cette thématique durant ma thèse en la complétant par un suivi de l'évolution de la minéralogie des oxydes de fer caractéristiques de ces milieux. La modélisation des équilibres thermodynamiques de ces phases minérales avec la solution du sol m'apparait comme un aboutissement dans la compréhension de ces dynamiques géochimiques. Avec le recul, je réalise que j'ai ainsi baigné, dès mes débuts, dans l'instrumentation et le suivi des paramètres du sol. Ce chapitre présente donc mes premiers travaux de recherche, encadrés par G. Bourrié et F. Trolard de l'INRA, et qui ont donné lieu à quatre publications à facteur d'impact (Feder *et al.*, 1998 ; Bourrié *et al.*, 2004 ; Feder *et al.*, 2005 ; Trolard *et al.*, 2007), cinq communications orales (Feder *et al.*, 1999b ; Klingelhöfer *et al.*, 1999a ; Bourrié *et al.*, 2000 ; Feder *et al.*, 2002 ; Bourrié *et al.*, 2002) et quatre communications sous formes de poster (Feder *et al.*, 1999a, 2000 ; Klingelhöfer *et al.*, 1999b ; Bourrié *et al.*, 2007).

5.1 Les processus d'oxydo-réduction dans les sols hydromorphes

5.1.1 Éléments de contexte

Les zones humides sont des écosystèmes reconnus pour leur intérêt écologique, du fait de leur diversité floristique et faunistique, mais également pour les services écosystémiques indéniables et nombreux qu'elles rendent ; elles font l'objet de la convention internationale de Ramsar (1971) dont la mission est leur conservation et leur utilisation rationnelle. En effet, les zones humides jouent notamment un rôle clef sur les plans hydrologiques et bio-géochimiques parce qu'elles sont à l'interface avec le réseau hydrographique. Les sols hydromorphes sont caractéristiques de ces zones humides et accumulent souvent la matière organique qui se dégrade lentement du fait de l'engorgement en eau et donc de la faible

diffusion de l'oxygène. Les tourbières représentent un terme ultime de cette accumulation de matières organiques. Lorsque les teneurs en matières organiques métabolisables sont suffisantes, l'oxygène dissous est consommé par les micro-organismes aérobies puis anaérobies facultatifs suivis par les micro-organismes anaérobies stricts. En effet, les réactions d'oxydo-réduction sont fondamentales dans la nature parce qu'elles sont la source d'énergie de tous les êtres vivants, qu'ils soient autotrophes ou hétérotrophes. Selon la séquence classiquement acceptée, les nitrates, le manganèse, le fer et les sulfates sont successivement utilisé comme accepteurs finaux d'électrons. Une fois les nitrates consommés, le fer devient l'élément le plus impliqués dans les processus d'oxydo-réduction qui se développent dans les sols hydromorphes car le manganèse présente habituellement de faibles concentrations dans les sols tempérés. Ces processus d'oxydo-réduction complexes sont donc à l'origine du potentiel épurateur des sols hydromorphes vis-à-vis des nitrates et des composés xénobiotiques essentiellement.
Cependant, les processus d'oxydo-réduction demeurent peu étudiés dans les écosystèmes. Non pas qu'ils soient anecdotiques, mais principalement du fait de la difficulté de mesurer et d'interpréter correctement le potentiel d'oxydo-réduction, d'une part et de préserver rigoureusement des conditions représentatives du milieu d'autre part. En effet, tous les couples d'oxydo-réduction ne sont pas susceptibles d'imposer un potentiel à une électrode à cathode métallique ; les couples où le fer intervient possèdent cette capacité vis-à-vis des électrodes de platine. De plus, plusieurs couples d'oxydo-réduction peuvent intervenir conjointement et rendent l'interprétation et la signification du potentiel mesuré, par rapport au potentiel de Nernst utilisé comme référence, délicate.

5.1.2 Objectifs de la thèse

L'objectif général de ma thèse était de comprendre la dynamique des processus d'oxydo-réduction *in situ* dans un sol hydromorphe ainsi que les équilibres thermodynamiques entre les phases minérales et la solution du sol. Pour cela, nous avions décliné en plusieurs objectifs spécifiques le déroulement de mon travail.
Ainsi, le premier objectif spécifique de ma thèse a été de mesurer les conditions géochimiques de la solution du sol et son suivi dans le temps. Bien que cela puisse paraitre trivial, il a fallu imaginer, concevoir et mettre en place un dispositif pérenne et automatisé qui perturbe le moins possible le milieu et qui ne modifie pas les conditions d'oxydo-réduction lors de l'analyse *in situ* ou de prélèvement ponctuels. Le second objectif spécifique a été de caractériser les phases minéralogiques ferrifères *in situ* et leurs transformations dans le temps lors des modifications des conditions hydro-géochimiques suivies par ailleurs. Enfin, le troisième objectif spécifique a été de déterminer si certaines phases ferrifères spécifiques à ces milieux étaient à l'équilibre avec la solution du sol et contrôlaient la dynamique du fer en solution.

5.1.3 Les minéraux ferrifères dans les sols hydromorphes

Deux groupes de minéraux ferrifères, fondamentalement différents, coexistent dans les sols hydromorphes. Les minéraux silicatés, généralement argileux, proviennent essentiellement du substrat rocheux par altération hydrolytique ou simple micro-division. Ces minéraux ne sont pas spécifiques des sols hydromorphes mais ils sont une source de fer et potentiellement un puit. En effet, Stucki *et al.* (1984), Fanning *et al.* (1989), Komadel *et al.* (1995) et Drits & Manceau (2000) ont montré que ces minéraux étaient sensibles aux processus d'oxydo-réduction de part la modification du degré d'oxydation du fer structural. Par ailleurs, parmi les oxydes et oxy-hydroxydes de fer, les plus communs dans les sols hydromorphes sont les rouilles vertes (Feder *et al.*, 2005), la gœthite, la lépidocrocite et, dans une moindre mesure, la ferrihydrite (Cornell & Schwertmann, 1996). Contrairement aux

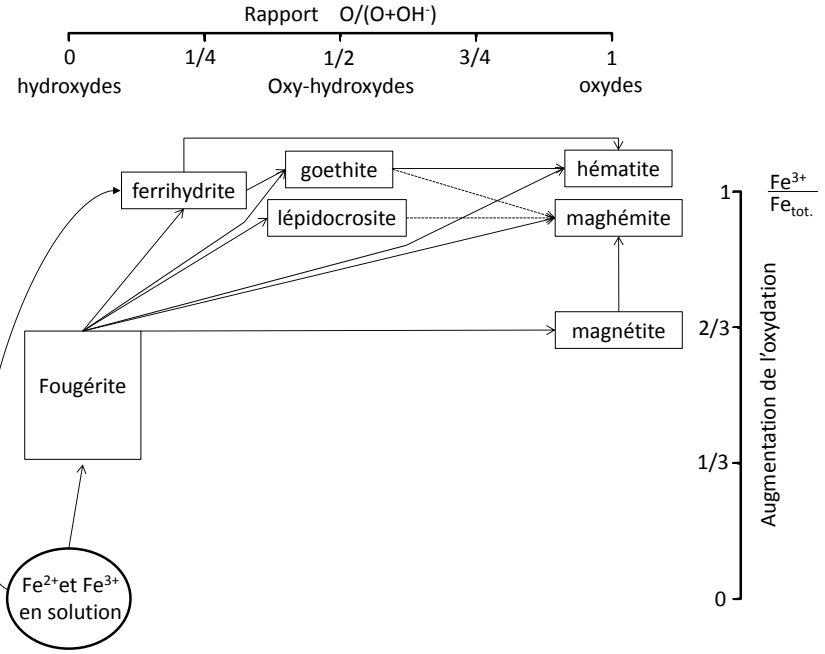

FIGURE 5.1 – *Schéma de formation des oxydes de fer. En abscisse, de gauche à droite le ratio molaire $O/(O + OH^-)$ augmente. En ordonnée, le ratio molaire $Fe^{3+}/Fe_{tot.}$ augmente de bas en haut; d'après Trolard* et al. *(2007).*

minéraux silicatés primaires, ces espèces sont labiles en milieu réducteur et se dissolvent en libérant du fer Fe^{2+}. La mobilité du cation Fe^{2+} est comparable à celle des alcalins ou des alcalino-terreux et le fer Fe^{2+} peut être, ainsi, aisément transporté et redistribué dans le paysage si le système est ouvert. Lorsque les conditions physico-chimiques sont oxydantes, ces minéraux ferrifères peuvent précipiter.
La figure 5.1 montre que la fougérite, minéral de la famille des rouilles vertes, est le précurseur des autres oxydes de fer rencontrés dans les sols hydromorphes (Cornell & Schwertmann, 1996 ; Trolard *et al.*, 2007). La fougérite est un hydroxyde lamellaire mixte de fer Fe^{2+} et de fer Fe^{3+} appartenant au groupe structural des pyroaurites (Bourrié *et al.*, 2004). Schématiquement, les rouilles vertes sont des feuillets hydroxydes du type de la brucite $Mg(OH)_2$ mais composés de fer Fe^{2+} et de fer Fe^{3+} à la place du magnésium. Entre ces feuillets chargés positivement du fait de charges supplémentaires induites par la présence de fer Fe^{3+}, des anions sont intercalés pour compenser ces charges. La formule structurale est idéalement :

$$[\mathrm{Fe}^{2+}_{1-x}\ \mathrm{Fe}^{3+}_{x}\ (\mathrm{OH})_2]^{x+}\ [(\tfrac{x}{\mathrm{n}})\mathrm{A}^{\mathrm{n}-},\ \mathrm{m\,H_2O}]^{x-}$$

où $x = \mathrm{Fe}^{3+}/\mathrm{Fe}_{\mathrm{tot.}}$ et $\mathrm{A}^{\mathrm{n}-}$ est un anion en position interfoliaire.
L'existence de rouilles vertes naturelles dans les sols a été démontrée, pour la première fois, à l'aide des spectrométries Mössbauer mais aussi Raman, au cours des études réalisées à Fougères sur le sol hydromorphe sous forêt étudié ici (Trolard *et al.*, 1997). L'occurrence de ce minéral naturel dans les sols est désormais prouvée sur différents types de matériaux parentaux (par exemple sur schiste et sur granite en Bretagne) ainsi que dans des conditions environnementales variées.

TABLEAU 5.1 – *Caractéristiques pédologiques du sol de Fougères.*

horizon	$Si_{tot.}$	$Fe_{tot.}$	$Al_{tot.}$	C	pH_{eau}	pH_{KCl}	A	LF	LG	S
		$mmol.kg^{-1}$					$g.kg^{-1}$			
0 – 15 cm : horizon holo-organique	13897	209	824	6227	4,4	3,7	76	365	451	108
15 – 50 cm : horizon rédoxique	13636	210	830	2896	4,3	3,6	121	270	505	105
50 – 80 cm : horizon réductique	12707	324	961	386	4,6	3,7	144	195	366	294
80 cm et plus : arène granitique réductique	10926	623	1690	462	5	3,9	108	190	141	560

A = argiles ($< 2\mu$m) ; LF = limons fins (2–20 μm) ; LG = limons grossiers (20–50 μm) ; S = sables (50–2000 μm).

5.2 Site d'instrumentation et méthodes de mesure

5.2.1 Le site expérimental de Fougères

Le hêtre, exploité en futaie, est l'essence dominante de la forêt domaniale de Fougères qui s'étend sur environ 1 500 hectares à 50 km au nord-est de Rennes. Le climat est océanique, la pluviométrie moyenne annuelle est de 900 mm tandis que les températures moyennes oscillent entre 5 et 18°C. Le site expérimental est situé sur le versant nord-est d'une vaste butte entaillée de talwegs rayonnants. Les sols se développent sur une arène granitique sablo-limoneuse surmontée d'une couverture limoneuse d'origine éolienne héritée de la dernière glaciation (tableau 5.1). D'amont en aval de ce versant, les sols bruns acides faiblement lessivés évoluent vers des sols dégradés à structure glossique formant ainsi une séquence d'alocrisols et de rédoxisols.

5.2.2 Instrumentation et suivi *in situ*

L'instrumentation mise en place sur le terrain est constitué d'un spectromètre Mössbauer miniaturisé pour caractériser les oxydes de fer, d'une sonde multiparamétrique destinée à l'acquisition de la physico-chimie de la solution du sol et d'un système de prélèvement de cette solution pour analyse chimique (figure 5.2).

Le spectromètre Mössbauer Mimos II

Le spectromètre Mössbauer que nous avons utilisé a été miniaturisé et développé pour la NASA et l'agence spatiale européenne. Il était donc initialement destiné aux missions spatiales vers la planète Mars et il a été spécifiquement adapté aux conditions et à l'environnement terrestre (Klingelhöfer *et al.*, 1999a). Pour utiliser le spectromètre sur le terrain, nous avons mis au point un dispositif destiné à recevoir et protéger le spectromètre. Trois parties forment ce dispositif :

- Un tube en PVC d'un diamètre de 20 cm, d'une longueur totale de 2 mètres aux trois quarts enfoncé verticalement dans le sol. Il est percé sur toute sa longueur de fenêtres en plexiglas au travers desquelles des spectres peuvent être acquis. Le spectromètre est placé sur une plateforme que l'on déplace dans le tube le long d'un guide et d'une tige filetée afin de le positionner précisément en face d'une des fenêtres pour acquérir un spectre Mössbauer du sol situé juste derrière au contact.
- Le tube est surmonté d'un boîtier étanche qui contient la carte d'acquisition des données à laquelle le spectromètre est relié. La programmation, le paramétrage et

la récupération des données se font en connectant un ordinateur portable sur cette carte électronique via un logiciel dédié.

– Les batteries sont placées dans un autre boîtier étanche placé au pied de ce dispositif.

Afin d'acquérir un spectre de qualité suffisante, le spectromètre Mössbauer est positionné à une profondeur donnée pendant 3 à 4 jours. Deux fois par semaine, il est déplacé afin d'acquérir un nouveau spectre à une autre profondeur d'intérêt, notamment dans la zone de battement de la nappe.

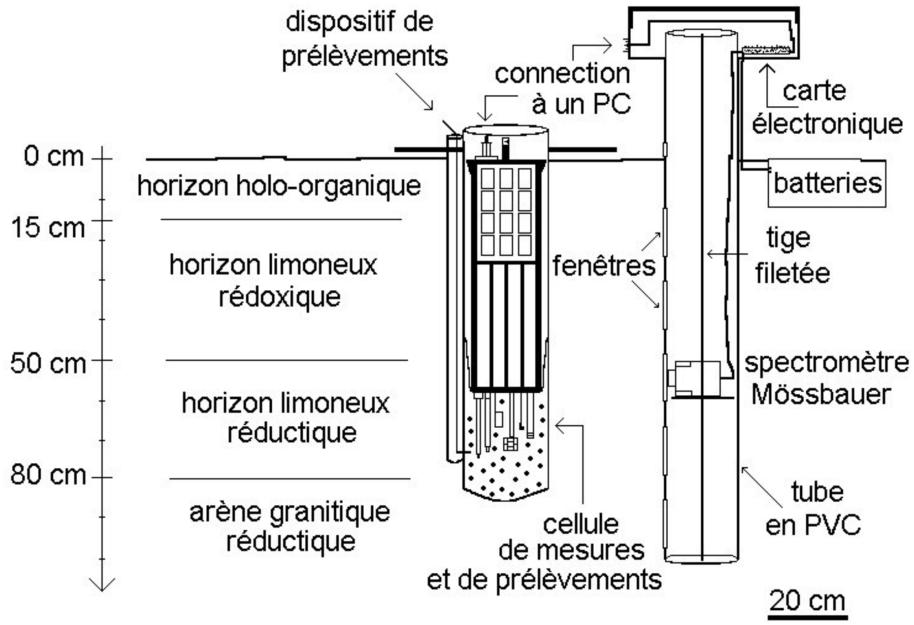

FIGURE 5.2 – *Schéma du dispositif expérimental incluant le spectromètre Mössbauer et la sonde multiparamétrique en fonction de la profondeur des horizons pédologiques. La distance réelle entre les deux instruments est d'environ 1 mètre.*

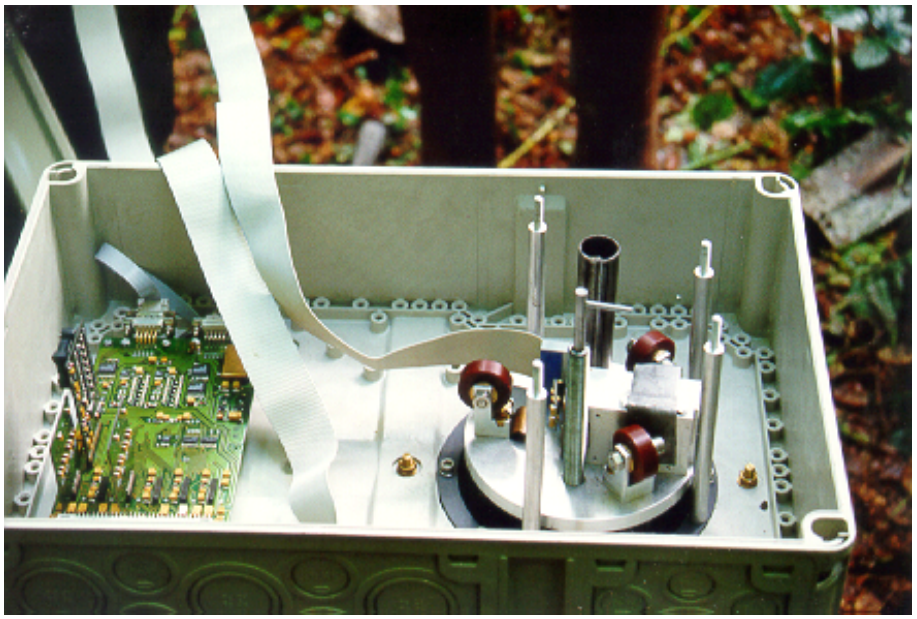

FIGURE 5.3 – *Sur la droite, le spectromètre Mössbauer miniaturisé est présenté sur son chariot en haut du tube en* PVC. *Il peut être descendu dans le tube et reste relié à la carte d'acquisition (à gauche) par un câble plat.*

Suivi de la géochimie des eaux

La sonde de mesure multiparamètrique se compose d'un cylindre en acier inoxydable de 80 cm de longueur pour 10 cm de diamètre. Originellement dédiée aux campagnes océanographiques, nous l'avons insérée dans un tube en PVC afin de protéger les électrodes et de créer une enceinte où sont réalisées les mesures et où sont faits les prélèvements de la solution du sol. Les capteurs suivants sont installés sur la face inférieure :

- une électrode pH combinée, avec système de référence XEROLYT® de Ingold ;
- une électrode rédox en platine combinée avec un système de référence XEROLYT® de Ingold et une électrode de référence Ag/AgCl ;
- une cellule de mesure de la conductivité électrique constituée de sept électrodes en titane disposées symétriquement dans un cylindre creux en céramique ;
- un capteur polarographique de type Clark pour mesurer l'oxygène dissous ;
- un capteur de température formé d'une résistance en platine protégée dans un tube perforé en acier inoxydable ;
- un transducteur de pression constitué par un produit piézorésistant alimenté par un courant constant.

Un agitateur est placé au milieu de ces capteurs ; il se programme pour être déclenché avant et pendant chaque série de mesure. Les fréquences d'acquisition et d'enregistrement des données sont programmables à l'aide d'un logiciel dédié.
Un dispositif complémentaire situé sur le côté du tube en PVC de la sonde permet de prélever les eaux libres précisément dans l'enceinte où sont effectuées les mesures physico-chimiques. Les analyses suivantes ont été réalisées :

- le fer Fe^{2+} et les sulfures totaux *in situ* avec un spectromètre UV-visible portable ;
- les anions et les cations majeurs au laboratoire, respectivement par chromatographie ionique et ICP-AES.

5.3 Résultats du suivi *in situ* de la minéralogie des rouilles vertes dans les sols hydromorphes

5.3.1 Les rouilles vertes caractérisées *in situ*

En l'absence de références préalables, le premier résultat significatif de ces travaux a été l'identification et la caractérisation des rouilles vertes naturelles directement sur le terrain. La figure 5.4 présente l'un des premiers spectres Mössbauer acquis en trois jours à la profondeur de 106 cm. Comme tout les spectres de rouilles vertes obtenus *in situ* à Fougères, celui-ci se décompose en une combinaison de trois doublets, partiellement superposés et nommés D1, D2 et D3. Les deux premiers correspondent à du Fe^{2+} tandis que le troisième correspond à du Fe^{3+}. Le pourcentage de chaque doublet calculé à partir de la courbe enveloppe représentant 100 % du fer, est utilisé pour calculer le ratio $x = Fe^{3+}/Fe_{tot.}$. Les paramètres hyperfins δ et ΔE_Q de ces doublets sont caractéristiques de ces rouilles vertes (Feder *et al.*, 2005). En outre, une analyse de tout les spectres acquis aux différentes profondeurs et au cours de toute notre étude montre une faible variabilité de ces paramètres hyperfins. Cela confirme la prédominance des rouilles vertes dans cet environnement et la constance des paramètres hyperfins malgré une stœchiométrie variable : $x = Fe^{3+}/Fe_{tot.}$ varie de 1/3 à 2/3 (Feder *et al.*, 2005 ; Trolard *et al.*, 2007).

5.3.2 Évolution avec la profondeur

Le ratio $x = Fe^{3+}/Fe_{tot.}$ calculé à partir des doublets des spectres, présente des valeurs remarquables avec la profondeur d'acquisition. En effet, les rouilles vertes identifiées

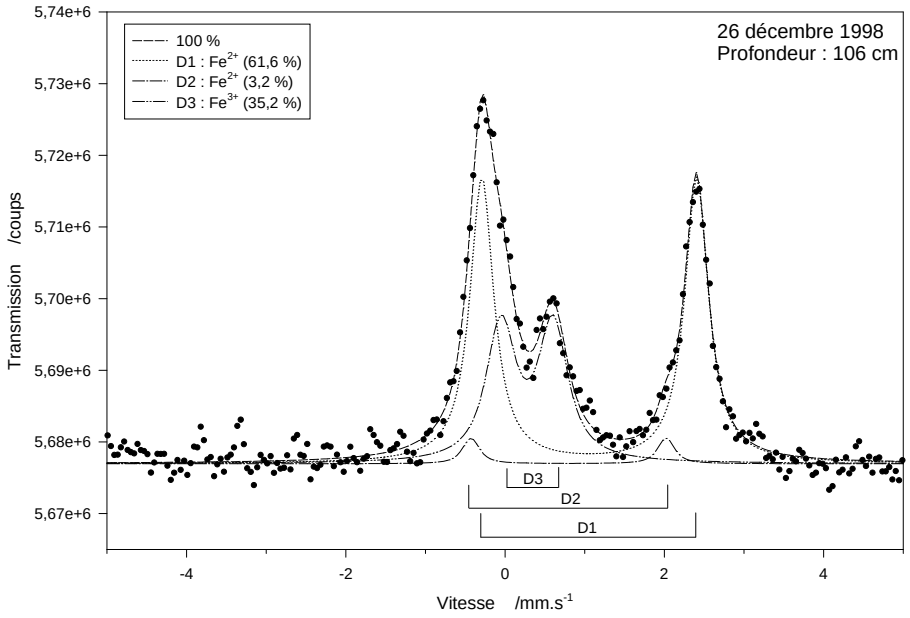

FIGURE 5.4 – *Spectre Mössbauer acquis à 106 cm de profondeur le 26 décembre 1998.*

couvrent toute la gamme possible de variation du ratio x. À la profondeur de 106 cm, les valeurs minimales et maximales du ratio x sont respectivement de 0,347 et 0,375 (moyenne de 0,361 pour les quatre spectres acquis entre décembre 1998 et avril 1999). Or, Feder *et al.* (2005) et Trolard *et al.* (2007) ont démontré que pour les rouilles vertes la valeur minimale de ce ratio x était de 1/3. Ainsi, non seulement nos calculs du ratio x sont donc conformes aux limites théoriques mais en outre, nous sommes en présence des rouilles vertes les plus réductrices à cette profondeur de 106 cm. Inversement, à la profondeur de 48 cm, les valeurs minimales et maximales du ratio x sont respectivement de 0,607 et 0,667 (moyenne de 0,638 pour les trois spectres acquis entre novembre 1998 et mai 1999). Les rouilles vertes observées correspondent donc ici au pôle le plus oxydant de la solution solide où le ratio x prend la valeur maximale de 2/3 (figure 5.5).

Ces caractéristiques sont cohérentes avec les observations faites sur le terrain. Au cours de l'hiver, la nappe est au plus haut et le sol est complètement et longuement engorgé à la profondeur de 106 cm. Les rouilles vertes sont ainsi plus proches du pôle réductique ($x = 1/3$; figure 5.5). En revanche, dans l'horizon limoneux rédoxique (15–50 cm de profondeur), le niveau de la nappe fluctue entre 30 et 50 cm de profondeur pendant le printemps créant ainsi des alternances de périodes oxydantes et réductrices. Les rouilles vertes identifiées à la profondeur de 48 cm sont ici proches de leur pôle le plus oxydé ($x = 2/3$). Entre ces deux profondeurs et ces deux pôles extrêmes, les rouilles vertes présentent des ratios x qui diminue avec la profondeur de manière monotone. À 78 cm de profondeur, le ratio x prend la valeur moyenne de 0,6 puis entre 85 et 90 cm de profondeur, la valeur 0,5.

Le changement de valence du fer dans les minéraux n'est toutefois pas l'apanage des rouilles vertes. De nombreux travaux ont montré :

- que le fer pouvait changer de degré d'oxydation dans les argiles notamment dans les nontronites (Stucki & Tessier, 1991 ; Komadel *et al.*, 1995 ; Heller-Kallai, 1997) ;
- que ces réactions pouvaient être réversibles (Stucki *et al.*, 1984 ; Fanning *et al.*, 1989 ; Badaut *et al.*, 1992 ; Drits & Manceau, 2000).

En conséquence, la densité et la répartition des charges des feuillets de ces minéraux sont modifiées. Les propriétés thermodynamiques sont donc différentes et les équilibres avec la solution du sol doivent être reconsidérés pour chaque espèce minérale.

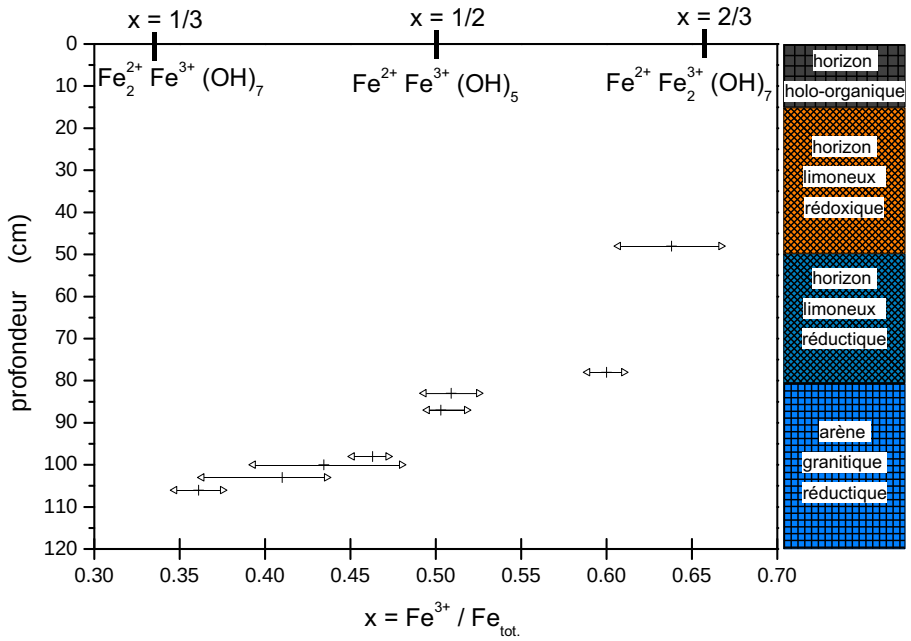

FIGURE 5.5 – *Pour différentes profondeurs, valeurs moyennes, minimales et maximales du rapport* $x = Fe^{3+}/Fe_{tot.}$ *des rouilles vertes identifiées et correspondance avec les différentes formulations d'oxy-hydroxydes mixtes de* Fe^{2+} *et de* Fe^{3+}.

5.4 Géochimie de la solution du sol et équilibres thermodynamiques

Les concentrations des éléments majeurs de la solution du sol ont été utilisées afin de calculer les activités chimiques de chaque espèce en solution. En effet, en solution aqueuse, les espèces chimiques sont associées entre elles et forment des ions complexes. Il existent plusieurs logiciels tels PhreeQc, Minteq ou Chess qui utilisent des algorithmes pour calculer par itération une distribution des espèces chimiques présentes dans la solution pour les différents ions, en tenant compte des constantes d'équilibre de chaque complexe et ce, en fonction de la température. Quel que soit le logiciel utilisé, les variables à renseigner sont la composition chimique de la solution et les conditions physico-chimique du milieu (pH, Eh, température). Les principales différences entre ces logiciels sont dans la prise en compte de l'interface entre les phases solides et aqueuses et dans la base de données utilisée. Nous avons utilisé un logiciel plus ancien, mais aussi plus simple (Equil(T)), dont l'algorithme de calcul a été développé par Helgeson (1968) parce que nous n'avions besoin que de la spéciation en solution des différentes espèces chimiques.

5.4.1 Variation du pH et du potentiel d'oxydo-réduction

Notion de $pe_{critique}$

Le pH et le potentiel d'oxydo-réduction sont, avec la température, les paramètres physico-chimiques essentiels pour décrire et comprendre les réactions chimiques en solution. Ainsi, les diagrammes de Pourbaix Eh–pH permettent une représentation des variations de ces paramètres pour une activité des espèces chimiques donnée. Toutefois, les réactions d'oxydo–réduction dans les sols sont parfois hétérogènes, c'est-à-dire qu'elles se produisent

TABLEAU 5.2 – *Équations et données thermodynamiques des réactions standard utilisées dans la figure 5.6.*

Réactions			$pe_{critique}$ à pH=4	$pe_{critique}$ à pH=7	$pe_{critique}$ à pH=9
$1/4\ O_{2\,(g)} + H^+ + e^-$	$\rightleftharpoons$	$1/2\ H_2O_{(liq.)}$	16,6	13,6	11,6
$1/8\ NO_3^- + 5/4\ H^+ + e^-$	$\rightleftharpoons$	$1/8\ NH_4^+ + 3/8\ H_2O$	9,24	5,4	2,85
$NO_3^- + 2\ H^+ + 2\ e^-$	$\rightleftharpoons$	$NO_2^- + H_2O$	7,3	4,3	2,3
$1/2\ MnO_2 + 2\ H^+ + e^-$	$\rightleftharpoons$	$1/2\ Mn^{2+} + H_2O$	9,35	3,35	–0,65
$Fe_3(OH)_8 + 8/3\ H^+ + 2/3\ e^-$	$\rightleftharpoons$	$Fe^{2+} + 8/3\ H_2O$	17,7	5,7	–2,3
$\gamma\ FeOOH + 3\ H^+ + e^-$	$\rightleftharpoons$	$Fe^{2+} + 2\ H_2O$	11,8	2,7	–3,41
$\alpha\ FeOOH + 3\ H^+ + e^-$	$\rightleftharpoons$	$Fe^{2+} + 2\ H_2O$	10,0	1,0	–5,0
$1/8\ SO_4^{2-} + H^+ + e^-$	$\rightleftharpoons$	$1/8\ S^{2-} + 1/2\ H_2O$	–2,2	–5,2	–7,2

entre une phase solide et une phase aqueuse. Aussi, Sposito (1981) propose de se placer à un pH de référence donné (pH = 7) et de calculer la valeur du potentiel d'oxydo-réduction pour laquelle le rapport des activités des espèces réduites et oxydées est supérieur à un seuil fixé conventionnellement. C'est la notion de $pe_{critique}$ où le pe est le logarithme du potentiel d'oxydo-réduction à l'image du pH.
Dans les réactions hétérogènes, les activités des phases solides sont prises égales à 1 et le $pe_{critique}$ est défini comme la valeur à partir de laquelle l'activité de l'espèce aqueuse est supérieure à 10^{-7}. Pour les réactions homogènes, c'est-à-dire lorsque les phases sont identiques, la valeur seuil du rapport des activités espèce réduite/espèce oxydée est 10^6.

Représentation dans un diagramme de Pourbaix

Le tableau 5.2 présente les réactions d'équilibre que nous avons considérées. Ces réactions d'oxydo-réduction sont les plus courantes dans les sols qui présentent des signes d'hydromorphie puisque dans les sols bien aérés les conditions restent oxydantes. Les $pe_{critique}$ sont calculés pour différents pH étant entendu que le pH = 7 est la référence pour comparer ces réactions. Les mesures réalisées *in situ* sont présentées sur la figure 5.6 avec les droites d'équilibre des différentes réactions excepté pour le couple $O_{2\,(g)}/H_2O_{(liq.)}$ situé hors du graphique. Par exemple, la droite correspondant au couple $Fe_3(OH)_8/Fe^{2+}$ représente le seuil à partir duquel l'activité du fer dissous Fe^{2+} est supérieure à 10^{-7}. C'est donc la limite à partir de laquelle les rouilles vertes commencent à se dissoudre ou finissent de précipiter. La droite de l'équilibre SO_4^{2-}/S^{2-} représente le seuil à partir duquel le rapport des activités $(S^{2-})/(SO_4^{2-})$ est supérieur à 10^6. C'est donc la limite à partir de laquelle la réduction des sulfates est quasiment totale ou à partir de laquelle les sulfates commencent à apparaître.
La figure 5.6 se décompose en trois domaines distincts délimités par des lignes en pointillé et numérotés en chiffres romains, respectivement I, II et III et qui correspondent à ceux définis par Sposito (1981) à pH = 7 :

- le premier appartient aux sols modérément réduits où le pe présente des valeurs supérieures à 2 (soit pe + pH > 9) ;
- le second domaine correspond aux sols réduits avec –2 < pe < 2, c'est-à-dire lorsque 5 < pe + pH < 9 ;
- le troisième domaine est défini par pe < –2 (*i.e.* pe + pH <5) ; le sol est considéré comme très réduit.

La position des couples de valeurs Eh–pH mesurés *in situ* sont essentiellement dans le champ III, le domaine le plus réducteur. Quelques couples de mesures sont dans le champ

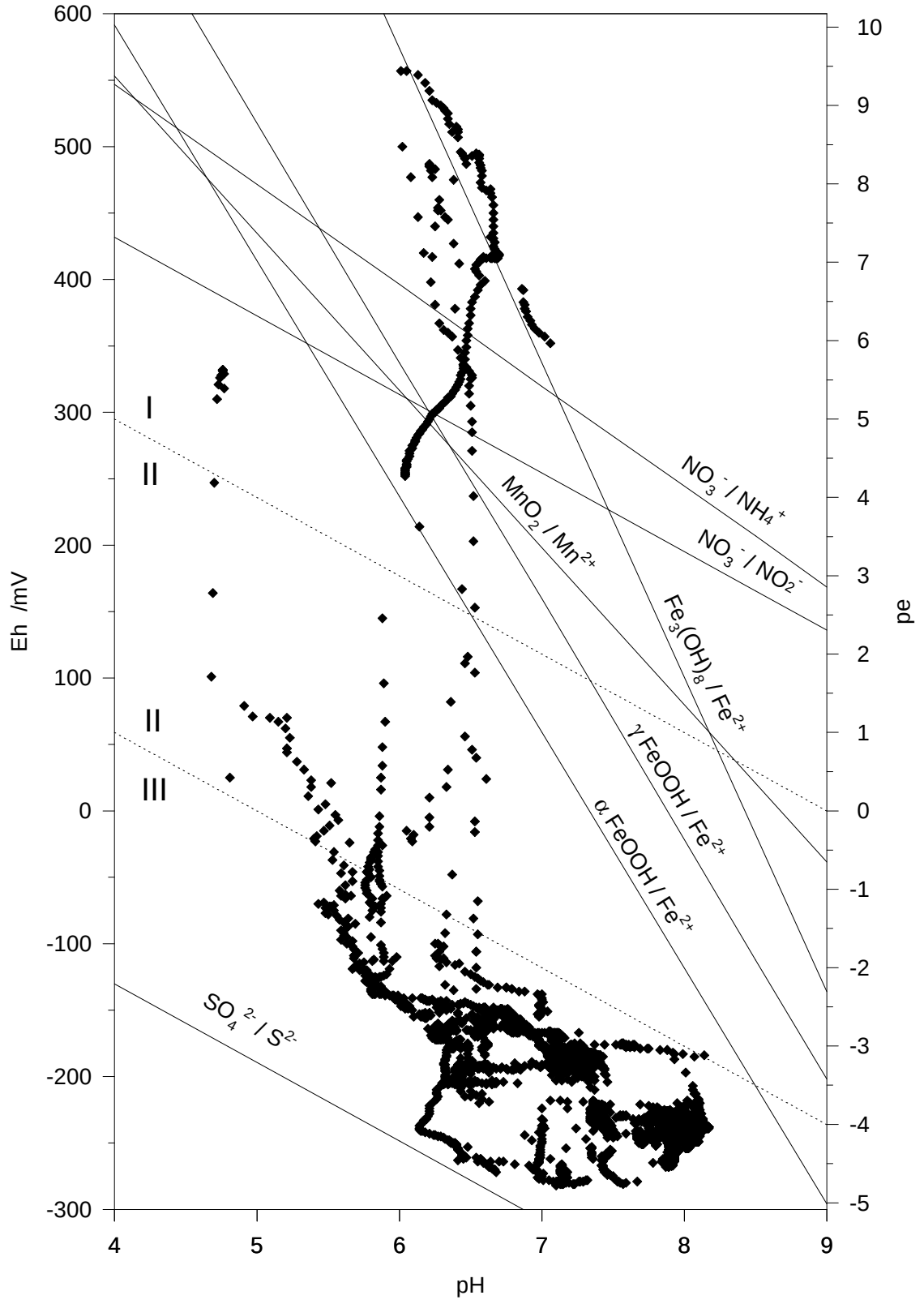

FIGURE 5.6 – *Mesures des potentiels d'oxydo-réduction et du pH des eaux de la solution du sol au cours du temps ; les droites correspondent aux réactions d'équilibre pour les valeurs de* $pe_{critique}$ *reportées dans le tableau 5.2.*

TABLEAU 5.3 – *Équations de réactions de la gœthite, de l'hydroxyde ferreux ainsi que de trois rouilles vertes, avec des rapports x = 1/3, 1/2 et 2/3.*

$Fe_2(OH)_5 + 5\ H^+ + e^-$	$\rightleftharpoons$	$2\ Fe^{2+} + 5\ H_2O$	$pFe^{2+} + 1/2\ pe + 5/2\ pH = 12{,}7$
$Fe_3(OH)_7 + 7\ H^+ + e^-$	$\rightleftharpoons$	$3\ Fe^{2+} + 7\ H_2O$	$pFe^{2+} + 1/3\ pe + 7/3\ pH = 9{,}4$
$Fe_3(OH)_8 + 8\ H^+ + 2\ e^-$	$\rightleftharpoons$	$3\ Fe^{2+} + 8\ H_2O$	$pFe^{2+} + 2/3\ pe + 8/3\ pH = 15{,}26$
γ FeOOH $+ 3\ H^+ + e^-$	$\rightleftharpoons$	$Fe^{2+} + 2\ H_2O$	$pFe^{2+} + 3\ pH + pe = 16{,}65$
α FeOOH $+ 3\ H^+ + e^-$	$\rightleftharpoons$	$Fe^{2+} + 2\ H_2O$	$pFe^{2+} + 3\ pH + pe = 14{,}97$
$Fe(OH)_2 + 2\ H^+$	$\rightleftharpoons$	$Fe^{2+} + 2\ H_2O$	$pFe^{2+} + 2\ pH = 13{,}32$

II et un groupe se situe dans le premier champ, le domaine le plus oxydant. Plusieurs séries de points montrent des évolutions continues et rapides du potentiel d'oxydo-réduction, le pH restant constant. Ces basculements rapides entre les domaines très réducteur et oxydant s'observent lorsque la nappe est au plus bas (autour de 60 cm de profondeur pendant l'été 1999). En effet, pendant cette période, le sommet de la nappe est donc plus proche de notre profondeur de mesure (70 cm de profondeur) et les conditions sont plus oxydantes du fait de la proximité avec l'oxygène de l'air.
La droite d'équilibre du couple SO_4^{2-}/S^{2-} correspond à la limite inférieure des couples de mesure Eh–pH. À l'inverse, le couple $Fe_3(OH)_8/Fe^{2+}$ dessine la limite supérieure dans le domaine oxydant. Ces deux couples d'oxydo-réduction semblent ainsi contrôler, tamponner les évolutions du pH et du potentiel d'oxydo-réduction. En revanche, les autres droites d'équilibre sont traversées rapidement et les espèces chimiques correspondantes ne semblent pas jouer un rôle sur la géochimie de la solution du sol. Dans la partie suivante, nous allons donc rechercher quelles sont les phases ferrifères qui sont à l'équilibre, au sens thermodynamique, avec la solution du sol.

5.4.2 Équilibres thermodynamiques entre la solution du sol et les phases ferrifères

Pour calculer les équilibres entre les phases minérales et la solution du sol, nous avons utilisé les réactions d'équilibre et les produits d'activités ioniques de différentes phases ferrifères, dont les rouilles vertes avec trois valeurs du ratio x, 1/3, 1/2 et 2/3 (tableau 5.3). La différence log Q – log K, où Q est le produit ionique et K, la constante d'équilibre, évalue ces états d'équilibre (figure 5.7) :

- lorsque log Q $>$ log K, la solution est sur-saturée par rapport au minéral ;
- lorsque log Q $=$ log K, la réaction est à l'équilibre ;
- lorsque log Q $<$ log K, la solution est sous-saturée.

La figure 5.7 peut être découpée selon trois saisons similaires à celles mises en évidence précédemment. De février à mi-juillet 1999, la forme réduite des rouilles vertes $Fe_3(OH)_7$ (*i.e.* $x = 1/3$) est la forme minéralogique la plus stable et ce, durant toute la période d'étude puisque la solution du sol est sur-saturée par rapport à ce minéral. De plus, la forme $Fe_2(OH)_5$, où $x = 1/2$, ainsi que la gœthite α FeOOH sont deux espèces quasiment à l'équilibre. De mi-juillet 1999 à mi-octobre 1999, le niveau piézométrique de la nappe est au plus bas. Le pH est au plus bas, les potentiels d'oxydo-réduction mesurés sont élevés, les concentrations en fer Fe^{2+} sont très faibles et les solutions sont toutes sous-saturées par rapport aux minéraux, sauf la forme réduite des rouilles vertes $Fe_3(OH)_7$. Enfin, de mi-octobre 1999 à juin 2000, en même temps que le niveau de la nappe remonte, le pH augmente, le potentiel d'oxydo-réduction diminue (autour de –250 mV contre –200 mV lors de la première saison). Les solutions du sol sont sur-saturées par rapport aux phases $Fe_3(OH)_7$ principalement, $Fe_2(OH)_5$ et α FeOOH secondairement.

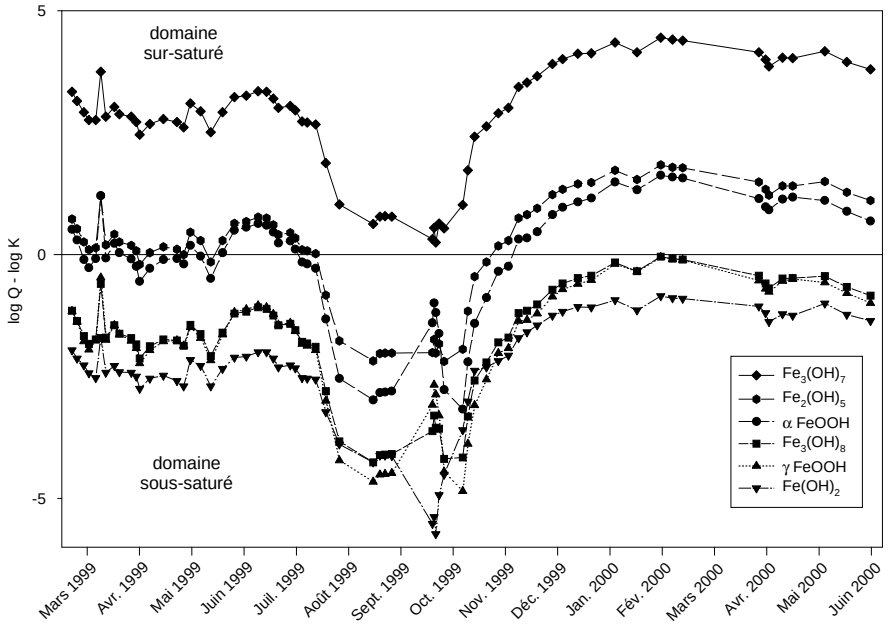

FIGURE 5.7 – *Différence entre les logarithmes des produits ioniques Q et des constantes de stabilité K de plusieurs espèces ferrifères au cours de la période d'étude.*

Ainsi, à la profondeur étudiée de 70 cm, les variations saisonnières du niveau de la nappe engendrent des modifications des conditions physico-chimiques (pH, potentiel d'oxydo-réduction, teneur en oxygène dissous) de la solution du sol. Celles-ci sont associées à des variations de la concentration en fer Fe^{2+} et modifient donc les équilibres thermodynamiques entre les phases ferrifères et la solution du sol. La forme réduite des rouilles vertes $Fe_3(OH)_7$ est toujours sur-saturée et peut précipiter.

5.5 Synthèse et conclusion

L'objectif général de ma thèse était de comprendre la dynamique des processus d'oxydo-réduction *in situ* dans un sol hydromorphe ainsi que les équilibres thermodynamiques entre les phases minérales et la solution du sol. En premier lieu, nous avons montré, par spectrométrie Mössbauer, que les rouilles vertes caractérisées *in situ* présentent des compositions chimiques variables. Leurs ratios $x = Fe^{3+}/Fe_{tot.}$ diminuent avec la profondeur passant de 2/3 à 48 cm de profondeur à 1/3 à 106 cm de profondeur. Ces résultats sont cohérents avec les observations ponctuelles du sol puisque les caractères rédoxiques sont présents dès 15 cm de profondeur et les caractères réductiques à partir de 50 cm de profondeur.
Nous avons ensuite démontré que le fonctionnement hydrologique du site gouvernait les variations de la géochimie de la solution du sol selon un rythme saisonnier. Ainsi, en automne, en hiver et au printemps, lorsque le niveau piézométrique de la nappe est au plus haut, les mesures réalisées à 70 cm de profondeur montrent une faible teneur en oxygène dissous et un potentiel d'oxydo-réduction au plus bas ; les rouilles vertes les plus réductrices $Fe_3(OH)_7$ précipitent. En revanche, durant la période estivale, lorsque le niveau de la nappe diminue, la forme $Fe_3(OH)_7$ est à l'équilibre et les formes plus oxydées telle $Fe_2(OH)_5$ ne sont plus stables (sous-saturation). Ces résultats démontrent que la composition stœchiométrique des rouilles vertes est étroitement corrélée à la géochimie de la solution du sol expliquant ainsi, en fonction des paramètres physico-chimique et de la teneur en fer Fe^{2+}, leurs variabilités tant avec la profondeur qu'au cours du temps.

Le dispositif que nous avons mis en place s'est avéré correctement adapté pour répondre à nos objectifs ; nous n'avions alors pas de recul puisque c'était sa première utilisation dans ces conditions. Toutefois, l'acquisition de la géochimie de la solution du sol à différentes profondeurs (au lieu d'une seule) aurait permis :

- une meilleure compréhension des processus d'oxydo-réduction au cours du temps ;
- une plus grande précision dans les calculs des équilibres thermodynamiques et ainsi une meilleure cohérence spatiale avec les caractéristiques des phases minérales par spectrométrie Mössbauer.

En revanche, il aurait été impossible techniquement d'acquérir plus de spectres Mössbauer puisque l'instrument doit rester positionné plusieurs jours afin d'obtenir un spectre de qualité.

Ainsi, les sols hydromorphes sont le théâtre de processus d'oxydo-réduction complexes où la dynamique saisonnière du niveau de la nappe, et donc la profondeur d'engorgement des sols, joue un rôle majeur. Lorsque le potentiel d'oxydo-réduction varie de $+550$ à -300 mV et le pH de 5 à 8, plusieurs couples sont impliqués et différentes phases minérales de la famille des rouilles vertes sont à l'équilibre ou peuvent précipiter. Ces changements géochimiques et minéralogiques rapides sont exceptionnels dans les sols si l'on excepte les réactions chimiques avec les sels. Cette instrumentation *in situ* était donc indispensable pour les suivre. Les rouilles vertes sont ainsi les principales phases minérales ferrifères dans les sols hydromorphes, elles précipitent, s'oxydent ou se dissolvent très rapidement selon les propriétés du milieu et contrôlent ainsi la dynamique du fer en solution. La connaissance de ces processus peut favoriser une meilleure prise en compte et une meilleure gestion des zones humides par une définition plus précise de leur extension et de leur zone d'influence, deux caractéristiques variables au cours des saisons et du fonctionnement hydrologique des sites.

CHAPITRE 6

LE TRANSFERT DE CONTAMINANTS DANS LES SOLS DE LA RÉUNION À DIFFÉRENTES ÉCHELLES

Ce chapitre présente une synthèse de mes recherches menées après mes travaux de thèse sur la dynamique des processus d'oxydo-réduction dans les sols hydromorphes. Si la minéralisation de la matière organique est réduite dans ces sols, elle est toutefois à l'origine de nombreux processus géochimiques qui peuvent être exacerbés selon la nature et les quantités de matières organiques mises en jeu. Les apports anthropiques de matières organiques exogènes, notamment lors du recyclage agricole des déchets, correspondent à de telles situations puisque les quantités apportées sont importantes et leurs caractéristiques très variables. De plus, dans ce contexte, les matières organiques peuvent apporter des contaminants susceptibles de migrer entre les différents compartiments des agro-écosystèmes. Aussi, j'ai poursuivi mes recherches sur l'interaction entre la solution du sol, le vecteur principal des contaminants, et les phases minéralogiques dans le contexte du recyclage agricole des matières organiques sur les sols volcaniques et tropicaux de la Réunion.
La première section de ce chapitre aura pour objectifs (i) d'établir un état des lieux du recyclage des matières organiques à la Réunion, (ii) de présenter les principales caractéristiques géologiques et pédologiques de la Réunion et (iii) de fournir les éléments de compréhension essentiels de la modélisation du transport et de l'adsorption que nous avons appliqué à l'étude de deux types de contaminants, les nitrates et les éléments traces métalliques. La deuxième section traitera des transferts de nitrates de l'échelle de la colonne de sol au territoire. La troisième section abordera la contamination des sols par les éléments traces métalliques (ETM) à travers l'expérimentation et la modélisation à l'échelle de la colonne et de la parcelle.

6.1 Contexte et problématique

6.1.1 Le recyclage des produits résiduaires organiques en agriculture et à la Réunion

Les produits résiduaires organiques (PRO) proviennent essentiellement des activités agricoles, urbaines et industrielles. Après l'essor des engrais chimiques au XX^{e} siècle, le recourt aux PRO en agriculture se renforce en même temps que leurs nombreux effets bénéfiques sont redécouverts :

- ils sont une source notable d'éléments fertilisants et peuvent totalement ou partiellement se substituer aux engrais minéraux ;
- l'apport de PRO aux sols concourt à améliorer leur fertilité tant physique (Abiven

et al., 2009) que chimique à long terme (Diacono & Montemurro, 2010) ;

- les PRO favorisent l'activité microbiologique des sols (Ros *et al.*, 2006) ;
- le recyclage des PRO en agriculture présente un faible coût par comparaison avec d'autres filières de traitement (Veronica *et al.*, 2013).

Par ailleurs, avant leur recyclage en agriculture, les PRO peuvent être mélangés entre eux (par exemple afin d'équilibrer leur composition ou d'améliorer leur structuration physique finale), transformés (par compostage, etc.) ou être utilisés pour produire de l'énergie (par exemple du méthane) sans réduire certains effets bénéfiques pour les sols cultivés. Malgré ces avantages indéniables, les PRO souffrent toujours d'une image négative véhiculée par leur nature de déchets qui leur reste attachée mais également par la présence de contaminants de différentes natures.
Comme tout système complexe multifactoriel, le choix d'usage d'un PRO se raisonne en confrontant les avantages et les risques tout en respectant les contraintes réglementaires. Pour les PRO, en regard de leurs bénéfices, les principaux risques résultent de leur teneur en contaminants de différentes natures :

- les éléments traces métalliques (ETM) possède parfois cette ambivalence d'être des oligo-éléments nécessaires aux systèmes vivants et des éléments potentiellement toxiques même à de faibles concentrations. Les éléments les plus fréquemment suivis, notamment dans le cadre législatif[1], sont le cuivre, le zinc, le nickel, le chrome, le cadmium, le plomb et le mercure ;
- les contaminants traces organiques (CTO) dont les plus étudiés (également pour des raisons réglementaires) sont les PCB (polychlorobiphényles), les HAP (hydrocarbures aromatiques polycycliques), les dioxines et les furanes. Hormis pour les PCB qui sont des molécules synthétisées industriellement, ces CTO résultent d'une combustion souvent incomplète puis sont émis dans l'atmosphère et redistribués dans les écosystèmes. Selon les molécules considérées de ces familles très nombreuses[2], les effets biologiques négatifs avérés ou suspectés sont variables : perturbateurs endocriniens, cancérigènes, mutagènes, etc. ;
- les contaminants biologiques regroupent principalement les organismes pathogènes (virus, bactéries, etc.) et l'antibiorésistance. Qu'ils soient d'origine humaine ou animale, les pathogènes proviennent des excrétions et induisent essentiellement des maladies digestives. Les antibiotiques résiduels présents dans les PRO contribuent à sélectionner et diffuser des bactéries résistantes ; le transfert de gènes résistants à d'autres bactéries amplifie ce problème.

Dans le contexte insulaire de la Réunion, le fort développement agricole et urbain des dernières décennies associé à un environnement physique contraignant (climat tropical, faible superficie, relief montagneux, espaces remarquables et protégés, etc.), génère de multiples difficultés pour le développement de la valorisation de ces PRO en agriculture. La méconnaissance des impacts de leur recyclage sur les écosystèmes a justifié de nombreux travaux de recherche au sein de l'équipe du Cirad de l'unité « recyclage et risque ». Si les sources et les puits de matières organiques apparaissent aussi diversifiées (figure 6.1) que les règles de décision des agriculteurs (Aubry *et al.*, 2006), une voire deux filières principales de valorisation monopolise les plus grands volumes pour un gisement donné.

1. Arrêté du 8 janvier 1998 fixant les prescriptions techniques applicables aux épandages de boues sur les sols agricoles pris en application du décret n° 97-1133 du 8 décembre 1997 relatif à l'épandage des boues issues du traitement des eaux usées.

2. Les PCB forment, par exemple, une famille de 209 composés aromatiques organochlorés dérivés du biphényle.

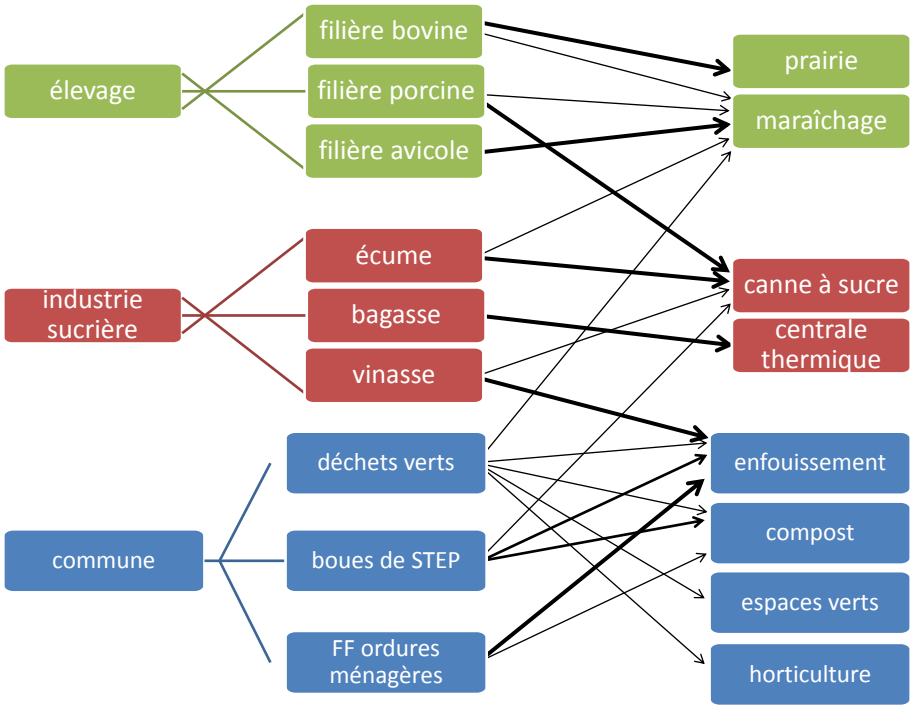

FIGURE 6.1 – *Représentation des gisements de matières organiques selon leur origine et de leurs principales filières de valorisation à la Réunion.*

6.1.2 La géologie et les informations pédologiques existantes à la Réunion

L'île de la Réunion est un stratovolcan intraplaque issu d'un point chaud et dont les laves sont essentiellement de composition basaltique. Elle est constituée des massifs du piton des Neiges et du piton de la Fournaise qui culminent respectivement à 3 069 et 2 631 mètres d'altitude. L'érosion particulièrement intense a entaillé l'île de profondes vallées et créé trois cirques volcaniques d'effondrement. Son sous-sol est hétérogène puisque les alternances de niveaux rocheux compacts et de bancs scoriacés sont entrecoupés de structures majeures (fractures, failles, sills et dykes[3]).
Dans cette zone non-saturée, la vitesse d'infiltration des eaux dépend essentiellement de la nature et de l'état des roches volcaniques. La recharge de la nappe phréatique de base provient principalement de ces flux souterrains depuis les reliefs puis des eaux d'infiltrations dans les alluvions et les cônes détritiques. Si les nappes perchées sont logiquement plus sensibles aux pollutions de surface d'origine anthropiques, depuis les années 2000, les nappes de base, éloignées donc des sources de contaminations, ont montré également des augmentations significatives de leurs concentrations en nitrates et en divers pesticides.

La couverture pédologique de l'île de la Réunion a été étudiée à diverses échelles et par différents auteurs depuis 1960 ; les travaux les plus significatifs sont :

- la carte de Riquier au 1:100 000 et sa notice (Riquier, 1960) ;
- la climatoséquence de Zebrowski (1975) ;
- les cartes de Raunet (1988 ; 1989 ; 1991b) et son ouvrage de synthèse (Raunet, 1991a).

Ces trois auteurs reconnaissent que les sols sont distribués selon une séquence altitudinale de grands types génétiques. En fait, cette séquence est aussi climatique puisque l'augmentation de l'altitude et de la pluviosité annuelle sont concomitantes avec la baisse des

3. Un dyke est un filon volcanique vertical traversant un encaissant en ayant profité d'une fracturation ; un sill est plutôt horizontal et ne recoupe pas de couche.

températures moyennes et de l'ensoleillement. Sur la zone ouest de l'île, les conditions climatiques moyennes extrêmes du littoral, 24°C et 500 mm/an, contrastent ainsi fortement avec celles des sommets, 10°C et 1700 mm/an. Riquier, Zebrowski et Raunet considèrent les termes les plus évolués de la couverture pédologique, c'est-à-dire pratiquement tous les sols pour Riquier (1960) et ceux situés vers le bas de la séquence pour les deux autres, comme des sols ferrallitiques au sens que l'on donnait à ce terme dans les années 1960 et qui sera repris dans leur définition par l'ancienne classification française (Aubert & Ségalen (1966) ; CPCS (1967)). L'analyse préalable de l'ensemble des informations pédologiques disponibles nous montre que l'amélioration de la connaissance de la couverture pédologique de l'île de la Réunion a été fortement conditionnée par les progrès de l'exploration géologique de l'île, notamment par les datations des phases du volcanisme, ainsi que par l'évolution propre à la science des sols, à ses méthodes d'analyses et à ses concepts. Les sols ont été d'abord considérés comme résultant d'un seul type de pédogenèse, la ferrallitisation (Riquier, 1960). Dans un second temps, l'andosolisation a été identifé dans la partie haute des versants du massif du piton des Neiges et pour tous les sols les plus récents sur la massif du piton de la Fournaise. Avec Raunet (1988 ; 1989), l'extension des sols ferrallitiques a été réduite à son minimum car il ne s'est pas appuyé sur les valeurs du rapport Ki[4]. Par ailleurs, il a certainement identifié une incompatibilité de plus en plus flagrante entre l'âge des roches d'une part, et la possibilité que la ferrallitisation en ait affecté une épaisseur importante au cours de la pédogénèse, d'autre part. Dans l'ouest, le haut du versant est marqué, jusqu'à 900 mètres d'altitude par l'andosolisation. La podzolisation s'y superpose sous forêt entre 1600 et 1800 mètres d'altitude. Elle est certainement facilitée par l'existence d'une couche de phytolithes issus d'une végétation non actuelle de bambous (*Nastus borbonicus*) comme l'a montré Alarcon (1995). Cependant, elle correspond bien au développement de véritables horizons spodiques sous l'effet de la migration de composés organiques comme l'indiquait déjà Zebrowski (1975). La limite basse de l'andosolisation (900 mètres d'altitude) que proposait Zebrowski (1975) est nettement plus haute que celle proposée par Raunet (1991b) : en moyenne 700 mètres d'altitude. Le reste du versant est marqué par des teneurs en matière organique toujours fortes, mais qui vont en décroissant vers le littoral. C'est la saturation du complexe absorbant qui permet de distinguer une zone moyenne, où les Umbrisols dominent, d'une zone basse, domaine des Phaeozems et d'autres sols associés et minoritaires.
Si l'organisation des sols sur le flanc ouest du piton des Neiges en fonction de l'altitude est très didactique, les autres zones de l'île sont souvent plus complexes et la superposition d'une pédogenèse tropicale sur des roches mères volcaniques d'âges variables[5] génère des sols très différents et aux propriétés atypiques et complexes.

6.1.3 La modélisation des flux d'eau et de solutés dans les sols

Le formalisme mécaniste de représentation des flux d'eau dans les milieux poreux tels que les sols est couramment utilisé et transposé dans de nombreux logiciels. Il nécessite la connaissance de peu de paramètres hydrodynamiques des sols (par exemple la conductivité hydraulique), mais surtout de la mesure précise de la pression matricielle, de la teneur en eau et des flux d'eau en entrée ou en sortie du système considéré. Armé de ces informations, les outils de modélisation mécaniste reproduisent avec précision les flux hydrodynamiques ou sont susceptibles de simuler des mesures manquantes. Aux échelles de la colonne de sol et de la parcelle, j'ai utilisé ces modèles mécanistes avec deux objectifs principaux qui étaient (i) de valider les mesures des flux d'eau dans les sols et (ii) de simuler des évènements non

4. Le rapport Ki correspond au rapport silice / alumine sur les résultats de l'analyse triacide couramment pratiquée alors.

5. En effet, les roches les plus anciennes, actuellement datées à 2,1 millions d'années, côtoient quasiment les éruptions actuelles.

mesurés (flux hydriques sur une longue période de temps, etc.). Les équations générales qui régissent les flux d'eau et par extension les flux de solutés sont rappelées ici.
La conservation de la masse d'eau dans un sol non saturé est représentée par l'équation suivante :

$$\frac{\delta\theta}{\delta t} = -\frac{\delta q}{\delta z}$$

où θ est la teneur en eau volumique ($L^3.L^{-3}$), t, le temps (T), q le flux d'eau ($L.T^{-1}$) et z, la profondeur (L) orientée positivement vers le bas. La variation au cours du temps de l'humidité égale donc la variation du flux d'eau en fonction de la profondeur.
Or, la loi de Darcy exprime le flux d'eau q ainsi :

$$q = -K(\theta)\frac{dH}{dz}$$

où K est la conductivité hydraulique ($L.T^{-1}$), fonction de θ et H, la charge hydraulique (L) définie par $H = h - z$ où h est la pression matricielle de l'eau dans le sol (L).
En couplant ces deux premières équations, les transferts d'eau dans les sols en condition non saturé peuvent ainsi être décrits et modélisés par l'équation de Richards modifiée pour prendre en compte également les prélèvements d'eau par la plante :

$$\frac{\delta\theta}{\delta h}\frac{\delta h}{\delta t} = \frac{\delta}{\delta z}\left[K(\theta)\left(\frac{\delta h(\theta)}{\delta z} - 1\right)\right] - S(z,t)$$

où S est un terme « puit » correspondant aux prélèvements d'eau par la plante (T^{-1}), fonction de la profondeur d'enracinement et du temps.
De la même façon que pour la masse d'eau, nous pouvons définir l'équation de la conservation de la masse d'un élément chimique M au cours du temps et selon la profondeur.

$$\frac{\delta M}{\delta t} = -\frac{\delta q_M}{\delta z}$$

$$\text{où } M = \theta C + \rho_d K_d C \quad \text{et } q_M = qC - \theta D\frac{\delta C}{\delta z}$$

avec C, la concentration de l'élément dans la solution du sol, ρ_d, la masse volumique du sol ($M.L^{-3}$), K_d, le coefficient de distribution de l'élément entre les phases aqueuses et solide ($L^3.M^{-1}$) et D, le coefficient de dispersion dans le sol ($L^2.T^{-1}$).
Ainsi, nous obtenons l'équation de transfert des solutés suivante :

$$\frac{\delta}{\delta t}\left(\theta C + \rho_d K_d C\right) = \frac{\delta}{\delta z}\left(\theta D\frac{\delta C}{\delta z}\right) - \frac{\delta}{\delta z}\left(qC\right) + \sum_{i=1}^{n}\varphi_i$$

où φ_i est un terme « puit » incluant les prélèvements par la plante et les autres transformations ($M.L^{-3}.T^{-1}$).
Le facteur retard R (figure 6.2) de l'élément chimique est ainsi défini :

$$R = 1 + \frac{\rho_d K_d}{\theta}$$

Dans le cas particulier où l'élément chimique considéré n'interagit pas avec la phase solide, K_d vaut 0 et le facteur retard R vaut donc 1 signifiant qu'il n'y a pas de retard.
Dans le cas général, l'équation du transfert de solutés s'écrit également :

$$\frac{\delta}{\delta t}\left(R\theta C\right) = \frac{\delta}{\delta z}\left(\theta D\frac{\delta C}{\delta z}\right) - \frac{\delta}{\delta z}\left(qC\right) + \sum_{i=1}^{n}\varphi_i$$

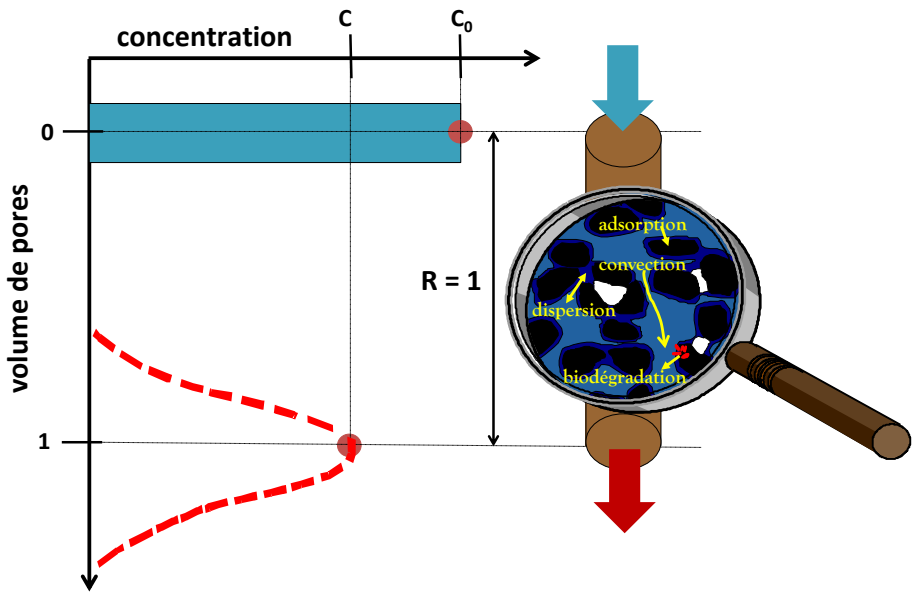

FIGURE 6.2 – *Représentation d'un pulse d'injection d'un élément à la concentration C_0 en haut d'une colonne et de sa courbe d'élution à l'exutoire à la concentration maximale C. Les aires restent constantes et il n'y a pas d'adsorption lorsque le facteur retard $R = 1$. La dispersion au sein du sol induit un élargissement de la base de la courbe d'élution.*

Ainsi, pour un élément en solution réactif avec la phase solide, dans un système sans plante et sans prendre en compte d'autres transformations, lorsque le régime hydrodynamique est permanent, R, θ, q et D sont constants et l'équation se simplifie :

$$R\frac{\delta C}{\delta t} = D\frac{\delta^2 C}{\delta z^2} - v\frac{\delta C}{\delta t}$$

où v est une vitesse apparente moyenne de pore ($\mathrm{L.T^{-1}}$).

6.1.4 Les transferts et l'adsorption des contaminants

Le cas des nitrates à la Réunion

Les nitrates correspondent à la principale forme d'azote assimilable par les végétaux. Ils proviennent de la nitrification de l'ammonium issu de la minéralisation de divers composés organiques (matière organique du sol, résidus de cultures, PRO apportés, etc.) ou d'apports directs (engrais, eaux d'irrigation, etc.). Très solubles dans l'eau, les nitrates sont habituellement peu retenus dans la plupart des sols parce que de nature anionique. Toutefois, les sols volcaniques possèdent des charges de surface positives, variables avec le pH et la force ionique de la solution du sol du fait de la présence de complexes organo-minéraux et de certains minéraux mal cristallisés tels la ferrihydrite ou l'allophane et l'imogolite spécifiques aux andosols. En raison de la présence importante d'oxydes de fer et d'aluminium, les sols tropicaux présentent également des charges de surfaces positives, permanentes pour certaines mais aussi variables avec le pH et la force ionique pour d'autres. Ainsi les sols de la Réunion offrent une capacité d'échange anionique et sont donc susceptibles d'adsorber significativement les anions.
Selon l'agence régionale de santé océan Indien, le pourcentage des captages présentant des teneurs en nitrates supérieures à 10 $\mathrm{mg.l^{-1}}$ est passé de 12 à 42 % de 1994 à 2008 ; les aquifères de la côte ouest jusqu'à Saint-Pierre sont les plus impactés. Ces pollutions sont d'origine urbaines (assainissement non collectif) et agricoles (Payet *et al.*, 2010).

Le cas des éléments traces métalliques

Bien que leurs concentrations soient très faibles, les éléments trace métallique (ETM) sont ubiquistes dans les roches. Pour les règnes animal et végétal, ils présentent parfois cette ambivalence d'être des oligo-éléments et des éléments toxiques. Dans les sols, les ETM sont principalement hérités de la roche mère ou d'origine anthropique : apportés par les engrais et les PRO, l'eau d'irrigation, la redéposition atmosphérique d'origine naturelle (volcanisme, feux de forêt) ou anthropique, etc.
Les principaux travaux menés à la Réunion par E. Doelsch ont porté sur l'identification des origines des ETM dans les sols et les PRO, leur spéciation en phase solide (Doelsch, 2010). J'ai apporté une contribution complémentaire à cette approche en étudiant leur transfert en conditions hydrodynamiques contrôlées de laboratoire ou en conditions réelles au champ. En effet, il était essentiel de comprendre les déterminants des transferts de cuivre et zinc dans les sols de la Réunion (§ 6.3, page 75). Ces deux éléments chimiques présentent en effet la particularité d'être ajouté à l'alimentation des porcs puis d'être excrétés.

6.1.5 À travers les échelles étudiées, une approche multidisciplinaire

Au laboratoire, en colonnes de sol, il est aisé de maintenir des conditions contrôlées. Les variables hydrodynamiques peuvent être précisément mesurées à différentes profondeurs : les volumes d'eau apportés et recueillis, l'humidité et les pressions matricielles au sein des colonnes. La reconstitution dans les colonnes des sols remaniés garantit une excellente homogénéité mais nécessite de vérifier que leur fonctionnement hydrodynamique reproduit bien les conditions de terrain. En outre, l'installation de préleveurs sans tension de la solution du sol permet de suivre sa composition chimique. Enfin, une température constante et l'absence de plante réduisent les perturbations au cours de l'expérimentation. Au-delà du contrôle de ces paramètres, mes objectifs de recherche étaient de comprendre les processus qui gouvernent l'impact des PRO suite à leur apport sur un sol cultivé en terme de transfert des contaminants lors de flux hydriques imposés. Inversement, à la parcelle en conditions réelles, l'hétérogénéité du sol, la présence d'une culture, les pluviométries variables, etc. sont prises en compte. Les processus sont certes plus difficiles à dissocier et à étudier mais *a contrario* leurs interactions sont observées. La culture induit des modifications importantes dans la dynamique des PRO et des contaminants associés de part ses prélèvements d'eau et de nutriments.
L'échelle du territoire est progressivement apparue cruciale pour répondre aux enjeux liés aux risques de pollutions. En effet, à la Réunion et notamment sur le territoire de la côte ouest, l'intrication de l'habitat (avec son assainissement non collectif) dans les zones agricoles associé à un contexte hydrogéologique complexe ne permettant pas de découper l'espace en petits bassins versants et limite l'identification avec certitude des sources des pollutions. Aussi, mon approche a consisté à étudier spécifiquement la vulnérabilité des sols aux transferts des contaminants vers les aquifères. En effet, les travaux menés aux échelles des colonnes de sol et de la parcelle avait préalablement montré que le sol jouait toujours un rôle prépondérant dans les transferts des contaminants et notamment des nitrates. De plus, quelles que soient les vitesses de transfert d'un contaminant, lorsqu'il est conservatif, une fois la zone racinaire dépassée, celui-ci ne pourra que continuer à progresser pour contaminer les aquifères du sous-sol.
La suite de ce chapitre de présentation des résultats suivra les objectifs scientifiques que j'ai poursuivi :

- quels sont les déterminants du transfert des nitrates dans les sols et vers les aquifères de l'échelle de la colonnes de sol à celle du territoire ?
- quelles sont les modalités de contaminations des sols par les ETM aux échelles de la colonnes de sol et de la parcelle ainsi que sur de longues durées ?

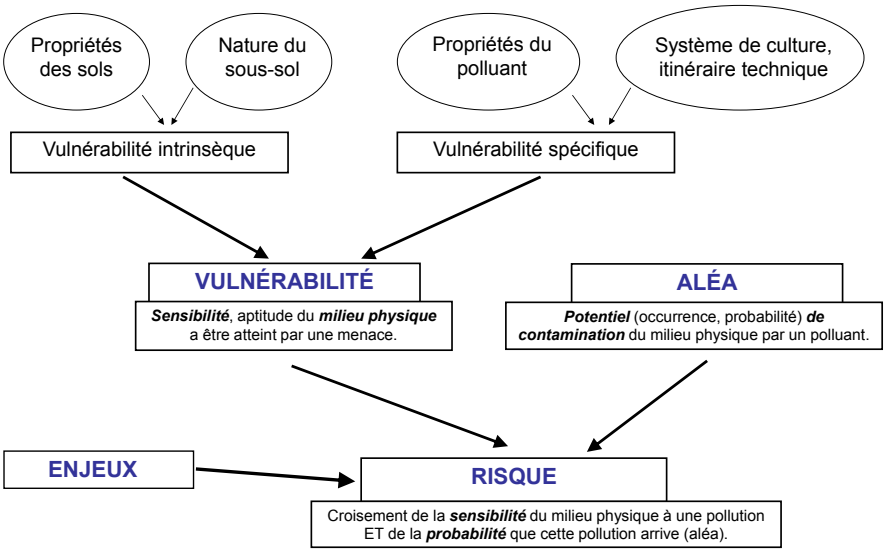

FIGURE 6.3 – *Représentation schématique des concepts de vulnérabilité, d'aléa et de risque de transfert d'un polluant vers les aquifères.*

6.2 Les transferts de nitrates de l'échelle des colonnes de sol au territoire

La problématique de la pollution par les nitrates est complexe notamment du fait des différentes échelles auxquelles les études doivent être menées. En effet, ce sont en premier lieu les processus microbiologiques dans le sol qui interviennent dans le cycle de transformation de l'azote et donc de la production, voire de la disparition, des nitrates. À l'échelle de la parcelle, les processus prépondérants sont les prélèvements par les cultures, les pertes par volatilisation ou par lixiviation. Enfin, à l'échelle territoriale ou du bassin versant, au delà des aspects de gestion des intrants, les transferts dans le sous-sol aboutissent à l'identification des pollutions en nitrates dans les cours d'eau ou les aquifères.
Les résultats présentés dans cette section ont fait l'objet de cinq publications dans des revues à comité de lecture et à facteur d'impact (Feder & Findeling (2007), Payet *et al.* (2009), Alary *et al.* (2013), Feder (2013), Feder *et al.* (2015)), neuf communications orales et cinq communications poster dans des congrès internationaux.

6.2.1 Compétition entre les nitrates et les chlorures pour l'adsorption et la lixiviation dans deux types de sols de la Réunion

Expérimentation en colonnes de sol remanié avec un nitisol

Le nitisol a été prélevé sur la station du Cirad de La Mare. Dans trois larges colonnes de 37,5 cm de diamètre, nous avons reconstitué les deux horizons de sol (0–45 et 45–85 cm) en respectant les densités apparentes mesurées *in situ*. Deux apports de lisier de porc ont été réalisés sur les colonnes C1 et C2, la troisième colonne C3 servant de témoin ; les apports d'eau ont été réalisés régulièrement afin de reproduire le régime hydrique annuel de cette zone. À 17, 30, 55 et 80 cm de profondeur, chaque colonne a été équipé de tensiomètres pour mesurer le potentiel matriciel de l'eau dans le sol et de sondes TDR[6] pour mesurer l'humidité volumétrique. Aux mêmes profondeurs, la solution du sol est échantillonnée par des préleveurs sans tension. À l'exutoire, le flux d'eau est également mesuré et prélevé.

6. Time Domain Reflectometry : réflectomètrie dans le domaine temporel.

Les mesures ont été enregistrées toutes les 10 secondes. Les mesures des flux entrants et sortants sont confrontées aux calculs des flux d'eau aux différentes profondeurs au sein de la colonne réalisés avec l'équation de Richards et les mesures d'humidité et de potentiel hydrique. Compte-tenu des propriétés très proches des ions nitrates et chlorures et de leurs présences dans le lisier apporté, nous avons systématiquement suivi leurs concentrations en solution aux différentes profondeurs.
Les trois colonnes présentent une dynamique de l'eau similaire attestée par des écarts sur les mesures d'humidité volumique inférieurs à 0,03 $m^3.m^{-3}$. Toutefois, avec la profondeur, les facteurs retard augmentent pour les chlorures et diminuent pour les nitrates (figure 6.4). À 17 cm de profondeur, le facteur retard des chlorures est proche de 1 volume de pores (VP) (en moyenne pour les deux colonnes et les deux apports) indiquant l'absence d'adsorption entre 0 et 17 cm. Avec la profondeur, l'adsorption des chlorures augmente linéairement puisque le facteur retard atteint la valeur de 2 VP à 85 cm de profondeur. En revanche, pour les nitrates, non seulement il n'existe pas de relation linéaire avec la profondeur mais les facteurs retard sont différents pour les deux apports de lisier (figure 6.5). En effet, à 17 cm de profondeur, le facteur retard est de 4,9 VP pour le premier apport de lisier et de 3,5 VP pour le second apport de lisier. À partir de 30 cm de profondeur, le facteur retard diminue linéairement jusqu'à atteindre des valeurs proches de celui des chlorures. Cette forte différence entre les deux anions s'explique par l'absence nativement de nitrates dans les lisiers apportés, contrairement aux chlorures. En effet, les nitrates sont produits par la nitrification du lisier selon une cinétique du premier ordre :

$$NH_4^+ + 2\,O_2 \rightleftharpoons NO_3^- + 2\,H^+ + H_2O$$

Dans l'horizon de surface, le facteur retard des nitrates n'est donc qu'apparent puisque, contrairement aux chlorures, il intègre deux composantes : l'adsorption sur le sol et la nitrification du lisier. Les mesures du pH et de la concentration en ammonium dans la solution du sol (figure 6.6) montrent que la nitrification est rapide et complète dès 17 cm de profondeur. Une fois ce processus achevé, les nitrates sont lixiviés en profondeur. Toutefois, jusqu'à l'exutoire de la colonne, le calcul du facteur retard des nitrates intègre ce décalage initial.
À la profondeur de 85 cm, les facteurs retard des nitrates et des chlorures se rejoignent (figure 6.5). Or, bien que les nitrates aient été produits par nitrification, leur retard vis-à-vis des chlorures s'est progressivement amoindri avec la profondeur. En effet, les chlorures précédent les nitrates et présentent une affinité pour l'adsorption légèrement supérieurs à celle des nitrates (Katou *et al.*, 1996) saturant ainsi préférentiellement les sites d'échange disponibles. Le transfert des nitrates est donc indirectement favorisé du fait principalement de cet asynchonisme.
À la profondeur de 17 cm, les facteurs retards pour les nitrates sont significativement différents entre le premier et le second apport (figure 6.5). Les courbes d'élution montrent une dispersion plus faible indiquant une nitrification plus rapide ou plus efficace. En effet, les apports répétés de matières organiques améliorent le fonctionnement microbiologique des sols (Diacono & Montemurro, 2010) et notamment les processus de nitrification (Müller *et al.*, 2003).

Expérimentation en colonnes de sol remanié avec un cambisol andique

Une expérimentation très similaire a été menée avec un cambisol andique prélevé dans les hauts de l'ouest de la Réunion à 800 m d'altitude au coeur de la toposéquence caractérisé par Feder *et al.* (2006). Dans trois colonnes de 37,5 cm de diamètre, nous avons reconstitué deux horizons de sol (0–40 et 40–100 cm). Un lisier de porc a été apporté sur deux d'entre elles, la troisième servant de témoin, et des apports d'eau ont été réalisé régulièrement afin

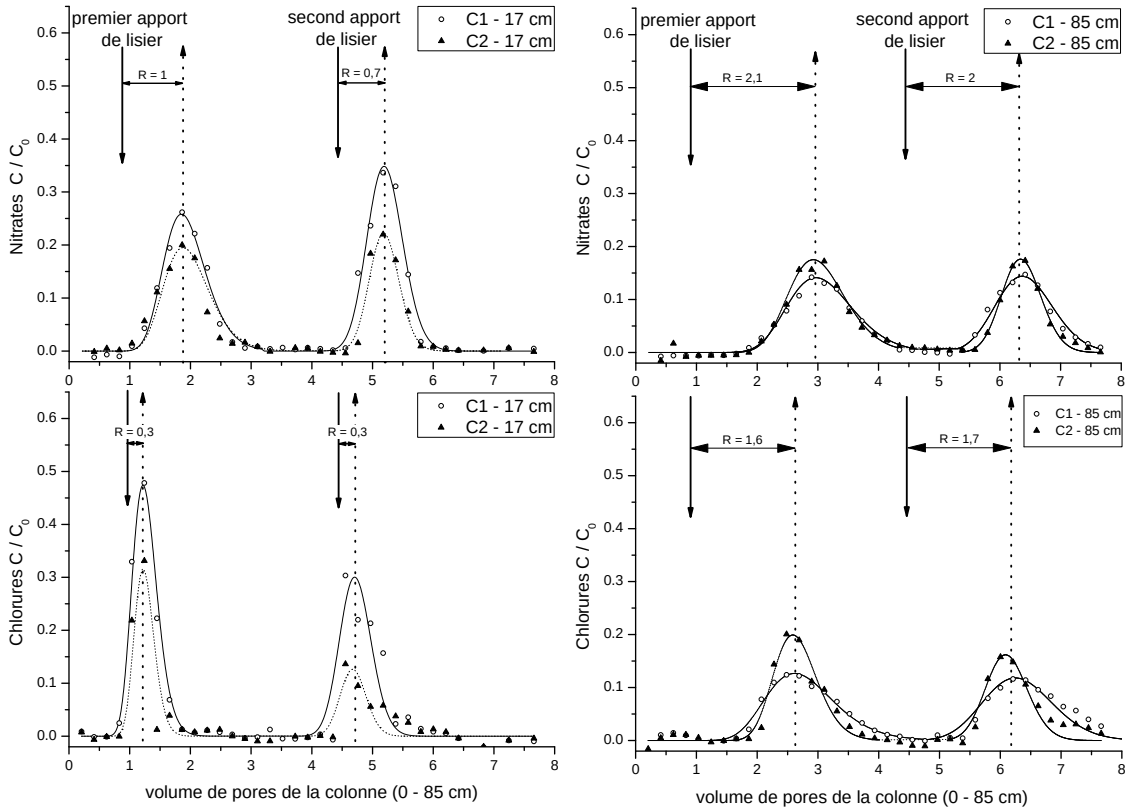

FIGURE 6.4 – *Courbes d'élution des nitrates (en haut) et des chlorures (en bas) à 17 cm de profondeur (à gauche) et à l'exutoire (à droite) des colonnes C1 et C2 après les deux apports de lisier. Les flèches en pointillés passent par les valeurs moyennes des pics d'élution de C1 et de C2. Les facteurs retard R correspondent aux écarts entre les flèches pleines et en pointillées, exprimés en volume de pores (de toute la colonne).*

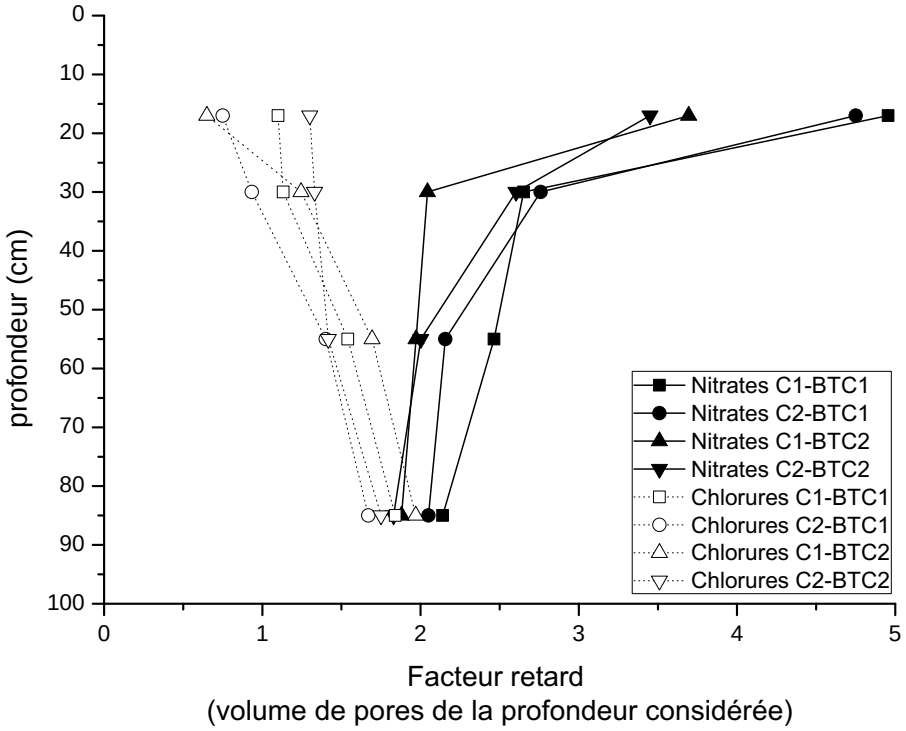

FIGURE 6.5 – *Facteurs retard des nitrates et des chlorures en fonction de la profondeur pour le premier (BTC1) et le second (BTC2) apport de lisier, pour les colonnes C1 et C2.*

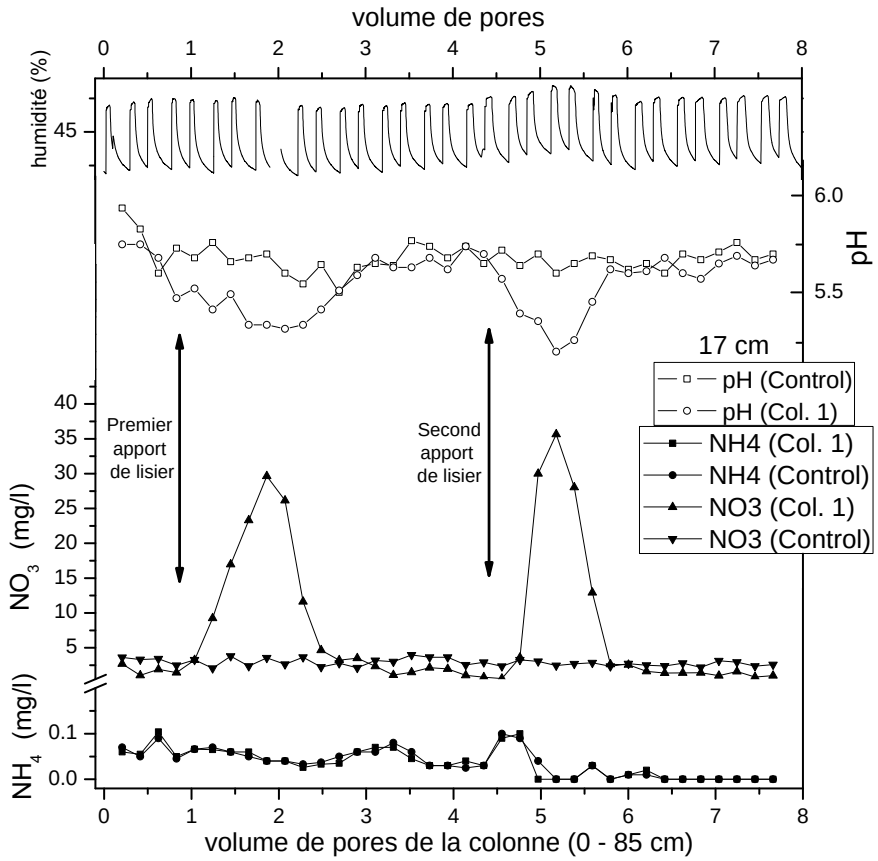

FIGURE 6.6 – *À 17 cm de profondeur, évolution du pH, de l'humidité du sol et des concentrations en nitrates et ammonium.*

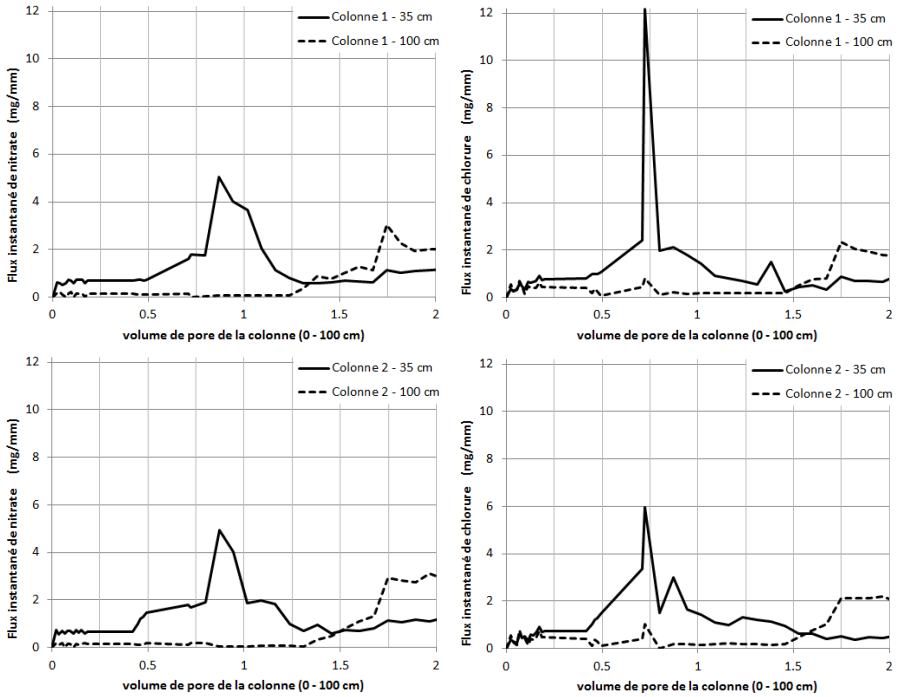

FIGURE 6.7 – *Flux instantanés des nitrates (à gauche) et des chlorures (à droite) à 35 cm de profondeur (traits pleins) et à l'exutoire (traits en pointillés) des colonnes C1 (en haut) et C2 (en bas) après un apport de lisier ; exprimés en volume de pores (de toute la colonne).*

de reproduire le régime hydrique annuel de cette zone. À 15, 35 et 95 cm de profondeur, chaque colonne a été équipé de tensiomètres et de sondes TDR ; le flux d'eau est également mesuré à l'exutoire. La solution du sol est prélevée à 7,5, 15 et 35 cm de profondeur par des préleveurs sans tension ainsi qu'à l'exutoire.

Les trois colonnes présentent une dynamique de l'eau similaire et l'erreur globale estimée sur le bilan de l'eau est inférieure à 7 %. À 35 cm de profondeur, les flux instantanés de chlorures précédent ceux des nitrates alors que ces flux sont synchrones à 100 cm de profondeur (figure 6.7). Les facteurs retard pour les nitrates et les chlorures sont respectivement de 0,85 et 0,7 volume de pores à 35 cm de profondeur et de 1,75 VP à 100 cm de profondeur. Pour les chlorures les facteurs retards sont semblables à ceux de l'expérimentation avec le nitisol puisque les valeurs étaient deux fois moindre mais à une profondeur deux fois moindre aussi. En revanche, pour les nitrates, les facteurs retards à 35 cm avec le cambisol andique (Feder & Findeling, 2007) sont similaires à ceux obtenus à 17 cm de profondeur avec le nitisol. Cela indique que la nitrification est plus rapide et plus intense pour le cambisol andique et que l'adsorption des nitrates est plus forte à cette profondeur pour le nitisol. En effet, l'acidification de la solution du sol liée à la nitrification est significativement plus marquée dans le cambisol andique (Feder & Findeling, 2007) que dans le nitisol puisque les différences de pH avec les colonnes témoins sont respectivement pour ces deux sols de 1,2 et 0,5 unité pH.

Ainsi, dans les deux expérimentations que nous avons menées, la nitrification du lisier induit une acidification et un retard significatif aux faibles profondeurs des flux de nitrates par rapport aux flux de chlorures. En revanche, aux exutoires des colonnes, la nitrification est complète et les facteurs retards sont semblables pour les nitrates et les chlorures et pour les deux types de sols.

Conclusions sur les expérimentations à l'échelle des colonnes de sol

La problématique de la pollution des cours d'eau et des aquifères par les nitrates est apparue au sein de régions comme la Bretagne, la Hollande, etc. pratiquant une agriculture intensive et présentant de forts excédents structurels en azote (Rivett *et al.*, 2008). Situées le plus souvent dans les pays développés, ces régions ne présentent habituellement pas de sols tropicaux ou volcaniques susceptibles d'interférer avec les transferts de nitrates (Barrow, 1986). Très peu d'étude ont donc été conduites sur ces types de sols soumis à des apports de PRO ; la plupart d'entre elles se focalisant sur les transferts et l'adsorption des nitrates, mais également des chlorures, apportés sous forme de sels (Katou *et al.*, 1996 ; Vogeler *et al.*, 1998 ; Duwig *et al.*, 1999 ; Qafoku *et al.*, 2000 ; Clay *et al.*, 2004 ; Katou, 2004). Les nitrates et les chlorures sont les deux principaux anions monovalents fréquemment apportés ou mesurés dans les sols ; aussi, ils sont souvent étudiés conjointement. Ils présentent des constantes d'adsorption semblables et entrent ainsi en compétition pour l'adsorption sur les sols. Ces études, toutes menées à l'échelle de la colonne de sol, démontrent que cette première étape ou « échelle d'étude », est la plus simple à mettre en œuvre pour obtenir des résultats préliminaires en l'absence d'autres références ou études (Mochoge, 1984).
En effet, dans les conditions contrôlées du laboratoire, la précision des mesures et leur bonne répétabilité ont permis de suivre la minéralisation du lisier et notamment sa nitrification en fonction de la profondeur dans deux types de sol représentatifs de la Réunion. Bien que l'observation de la nitrification et son suivi au cours du transfert des solutés ne soit pas en soi novateur (Ardakani *et al.*, 1974 ; Sierra, 2002), la cinétique de minéralisation du PRO apporté est très dépendante des caractéristiques du PRO et du sol (Paul & Clark, 1989 ; Rivett *et al.*, 2008). Mon premier apport fondamental est donc une mesure de la capacité des ces sols à retenir les nitrates lorsqu'ils sont nitrifiés à partir d'un PRO et lorsqu'ils entrent en compétition avec les chlorures de façon asynchrone ; cette mesure se traduit par le facteur retard. L'originalité de mes travaux réside également dans le fait que, dans les études précédemment menées, les sels sont apportés en même temps. Ainsi, en l'absence de mesures des flux d'eau et d'analyses physico-chimique des solutés aux différentes profondeurs, nous aurions simplement observé que les facteurs retards étaient semblables à l'exutoire des colonnes pour les deux anions étudiés. En réalité, dans les couches de surface, la lixiviation et l'adsorption des anions sont asynchrones et dépendent de la cinétique de minéralisation du lisier, des caractéristiques minéralogiques et microbiologiques du sol ; les facteurs retards sont donc très différents pour ces deux anions contrairement à d'autres résultats (Katou *et al.*, 1996 ; Clay *et al.*, 2004). L'identification et l'analyse de processus jouant un rôle majeur dans nos expérimentations (nitrification, adsorption asynchrone) expliquent les différences majeures avec d'autres études et éclairent sur les conséquences agronomiques.
La première conséquence est que les nitrates ne présentent pas une dynamique uniforme même si les propriétés du sol sont constantes avec la profondeur ; la modélisation des flux de nitrates s'en trouve complexifiée. La seconde conséquence est que la disponibilité des nitrates pour les cultures au cours du temps et selon la profondeur n'est pas constante également. En effet, les nitrates ne sont pas produits immédiatement puis, ils sont lixiviés plus rapidement qu'ils ne l'auraient été s'ils avaient été apportés ou produits en même temps que les chlorures du fait de la compétition entre ces deux espèces pour l'adsorption. Ces éléments justifient une approche plus intégrative, à l'échelle de la parcelle cultivée.

6.2.2 Suivi des flux de nitrates dans un cambisol andique

À l'échelle de la parcelle, nous avons suivi les transferts de nitrates dans le cambisol andique précédemment étudié en colonnes de sol. Une parcelle a été amendée annuellement par du lisier de porc tandis qu'une parcelle servait de témoin sans apport. La superficie de la parcelle demeurant faible, nous avons pu maitriser les quantités de lisiers apportés ;

les épandages étaient réalisés manuellement à l'aide d'une lance à incendie directement connectée à la tonne à lisier. Les pertes gazeuses par volatilisation ont ainsi été réduites. En outre, la possibilité de choisir précisément la période, voire le jour d'épandage, nous ont permis de les réaliser dans des conditions optimales (absence de vent...). Pour palier à l'absence de répétition dans ce dispositif, nous avons réduit la variabilité inhérente du sol en réalisant systématiquement plusieurs prélèvements pour la parcelle lisier et la parcelle témoin ; cette variabilité s'est toujours avérée faible.
Les flux d'eau et de solutés ont été suivis avec la même méthodologie qu'en colonnes de sol par des mesures de la pression de l'eau dans le sol et de l'humidité volumétrique enregistrées en continu à différentes profondeurs. Les stocks d'azote minéral du sol[7] ont été suivis régulièrement ainsi que les exportations par les cultures.
De 2003 à 2005, la première campagne de suivi s'est déroulée dans le cadre de la thèse de N. Payet (2005). Nous avons suivi une rotation maïs/avoine pendant deux saisons avec un épandage de lisier en octobre ou en novembre au début de la saison chaude. De 2007 à 2009, nous avons mené une seconde campagne de suivi. Nous avons également suivi deux saisons mais sur une prairie de *bracharia* recevant également une fois par an aux mêmes périodes un épandage de lisier.

Première campagne de suivi

La dynamique du stock de nitrates dans les différentes couches de sol au cours de la première campagne de suivi (2003–2005) est rythmée par plusieurs évènements. Après l'apport de lisier en octobre 2003, le stock de nitrate augmente régulièrement et significativement dans la couche 0 – 30 cm jusqu'en janvier 2004 puis par transfert dans la couche 30 – 60 cm (figure 6.8). Cette augmentation est régulière puisque l'azote organique du lisier apporté en surface doit se minéraliser et l'ammonium se nitrifier préalablement. Les fortes pluies de janvier 2004 couplées aux prélèvements par la culture de maïs réduisent drastiquement le stock de nitrates notamment dans la couche de surface. Ensuite, d'avril à octobre 2004, les pluies sont quasiment nulles et le stock de nitrate dans les différentes couches de sol analysées se reconstitue par la minéralisation des résidus de la culture de maïs et de la matière organique du sol.
Le deuxième épandage de lisier en novembre 2004 engendre également une augmentation régulière et significative du stock de nitrate dans la couche de surface puis progressivement des couches sous-jacentes. De janvier 2005 à mars 2005, trois épisodes pluviométriques intenses d'environ dix jours chacun se succèdent et induisent un transfert significatif des nitrates vers les couches plus profondes puis hors du profil de sol ainsi qu'une diminution globale du stock de nitrates.
La lixiviation des nitrates en dessous de la profondeur racinaire (150 cm) et les prélèvements d'azote par les cultures représentent chacun environ 150 kg_N/ha pour la seconde saison de culture (figure 6.9). Si les exportations d'azote par la culture de maïs sont cohérentes avec la fertilisation apportée et les rendements obtenus, les pertes par lixiviation, en revanche, apparaissent très importantes. En effet, en moins de deux mois, de début février 2005 à fin mars 2005, le cumul des pluies atteint 570 mm. En l'absence de ruissellement, ces pluies ont lixivié progressivement les nitrates. Par ailleurs, après ces évènements, le stock d'azote dans la couche 0–60 cm est très faible (inférieure à 20 kg_N/ha) tandis que le stock total dans le profil de sol dépasse 150 kg_N/ha (figure 6.8).
Ces mesures ont été utilisées dans le cadre de la thèse de N. Payet (2005) afin de caler et de valider le modèle WAVE dans nos conditions spécifiques (Payet *et al.*, 2009). Outre les paramètres agronomiques demandés par le modèle, le coefficient de dispersion D et le

7. Compte-tenu des concentrations toujours très faibles en azote ammoniacal, les teneurs en nitrates sont similaires aux teneurs totales en azote minéral.

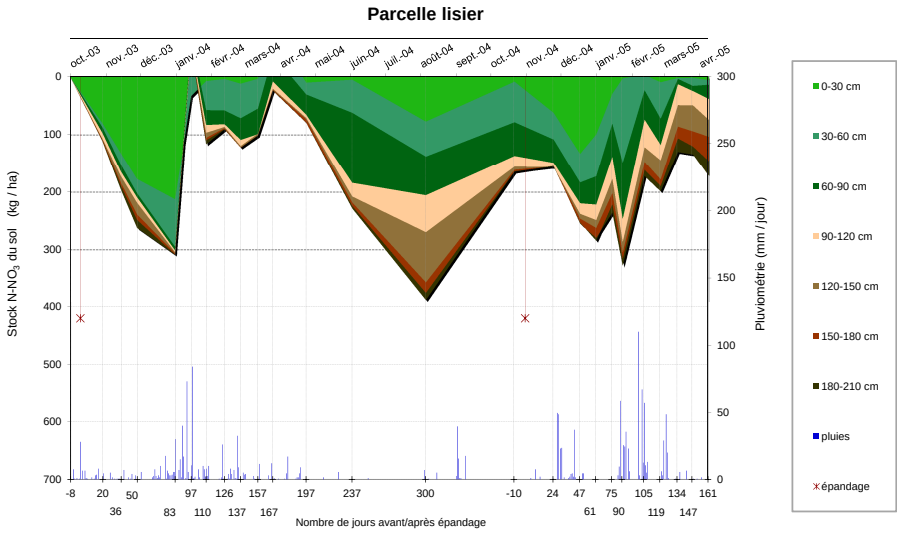

FIGURE 6.8 – *Évolution des stocks de nitrates dans les différentes couches de sol au cours de la première campagne de suivi (2003–2005).*

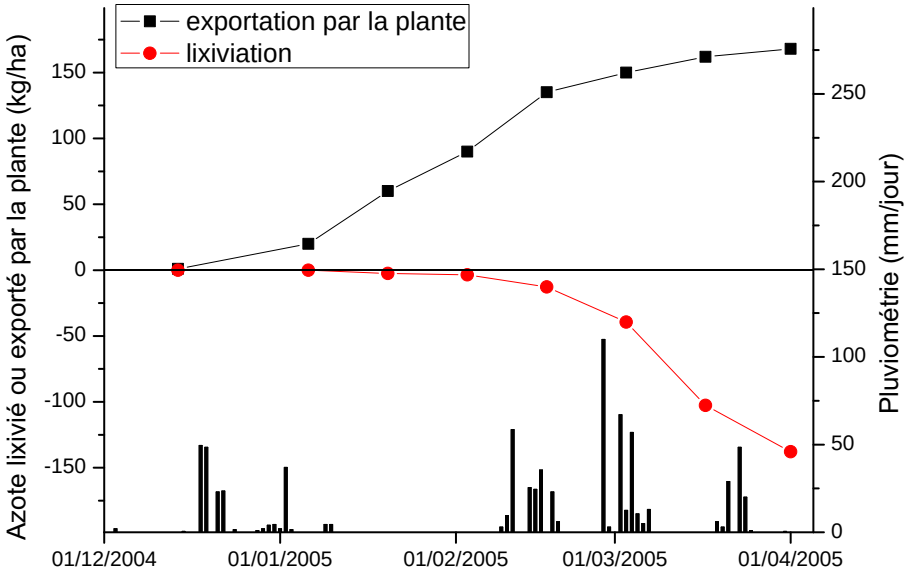

FIGURE 6.9 – *Quantités d'azote lixivié sous forme de nitrates en deçà de la profondeur racinaire et prélevé par la plante au cours de la seconde saison sur la parcelle lisier.*

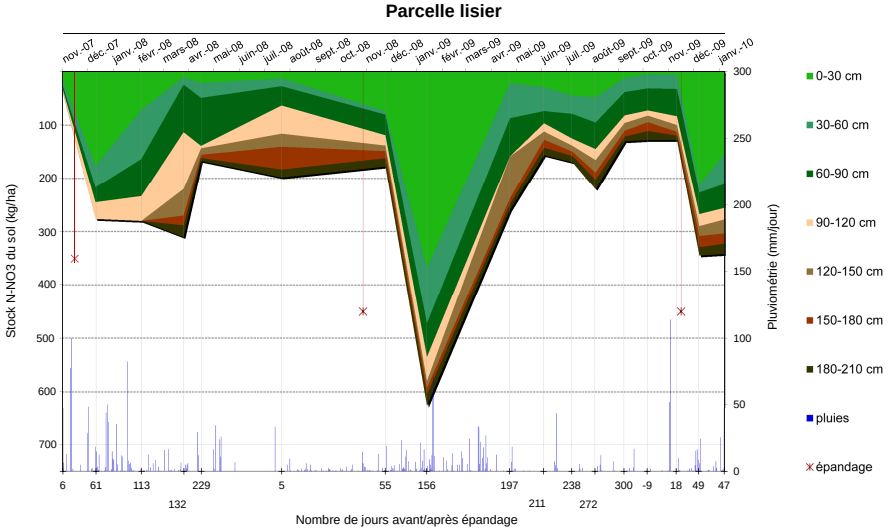

FIGURE 6.10 – *Évolution des stocks de nitrates dans les différentes couches de sol au cours de la seconde campagne de suivi (2007–2009).*

coefficient de distribution K_d du nitrate (cf. § 6.1.3, page 57) ont été calé sur la première période de suivi. Ainsi, les flux d'eau et de nitrates, l'évolution des stock d'azote dans le sol et les prélèvements par la plante ont été correctement reproduits par ce modèle. Duwig *et al.* (2003) avait déjà démontré la robustesse de ce modèle dans une autre situation tropicale (sol ferrallitique, îles Loyautés, Nouvelle-Calédonie).

Seconde campagne de suivi

L'apport de lisier en novembre 2007 débute la seconde campagne de suivi (figure 6.10). Jusqu'en février 2008, les fortes pluies redistribuent les nitrates sur le profil de sol jusqu'à 120 cm de profondeur. Contrairement à la première campagne de suivi, le stock d'azote du sol augmente immédiatement puis il évolue très peu en deçà de 60 cm de profondeur. En effet, en l'absence de pluies significatives à partir de février 2008 et compte tenu de l'enracinement moins profond de la *bracharia* (environ 40 cm), les nitrates ne sont ni lixiviés ni prélevés par la plante à ces profondeurs.
En novembre 2008 et 2009, deux autres apports de lisiers renouvellent rapidement le stock d'azote du stock dans les couches de surface. Dans la couche 0–30 cm, l'azote est intensément prélevé par la culture pendant la saison chaude et humide mais également redistribué vers les couches sous-jacentes. L'absence d'épisode cyclonique ou de pluies importantes expliquent cette dynamique.

Conclusions sur les expérimentations à l'échelle de la parcelle

J'ai précédemment démontré et mesuré la capacité de deux types de sols de la Réunion a retenir les nitrates à l'échelle de la colonne de sol (§ 6.2.1, page 65). Les expérimentations à l'échelle de la parcelle présentées ici ont permis principalement de quantifier les prélèvements d'azote apporté par les lisiers selon les caractéristiques des cultures. En effet, la *bracharia* couvre intégralement le sol et possède un système racinaire permanent et plus efficient dans les couches de surface. Inversement, les cultures de maïs et d'avoine couvrent peu le sol mais présentent un système racinaire qui explore également les horizons profonds ; le système racinaire du maïs a été observé sur la parcelle jusqu'à 1,4 mètre de profondeur tandis que celui de la *bracharia* ne dépasse pas 60 cm. L'efficience des prélè-

vements d'azote par la plante est directement corrélée à la profondeur et à la densité de son système rhizosphérique. Les références agronomiques et pédologiques disponibles sur ces sols, notamment pour renseigner les modèles, étant peu nombreuses voire inexistantes, nos résultats ont contribués à combler ces lacunes.
Par ailleurs, mes expérimentations ont également permis de quantifier en conditions réelles la rétention des nitrates dans le cambisol andique et d'obtenir les paramètres nécessaires à la modélisation de ces flux. Ainsi, j'ai mesuré la lixiviation des nitrates suite aux épandages de lisier et aux premières pluies. Dans ces sols, les différentes cultures ont plus longtemps accès aux nitrates, notamment dans les horizons de surface, avant que ceux-ci soient lixiviés. En outre, nos résultats ont montré qu'un modèle comme WAVE peut être calé et validé sur un sol présentant des propriétés andiques (Payet *et al.*, 2009). Bien que la modélisation des flux d'azote n'ait pas été menée lors de la seconde campagne de suivi, les mesures réalisées ont confirmé cette plus longue disponibilité des nitrates pour les cultures. Eneji *et al.* (2002) et Maeda *et al.* (2003) ont également démontré cet effet pour des andosols du Japon, dont les caractéristiques pédologiques sont assez proches du cambisol andique de la station des Colimaçons. Enfin, le lisier de porc apporté s'est minéralisé plus rapidement lors de la seconde campagne de suivi. Cet effet, également observé précédemment en colonne de sol, s'explique principalement par une meilleure activité microbiologique du sol après plusieurs épandages (Diacono & Montemurro, 2010).
En résumé, les sols volcaniques et tropicaux de la Réunion présentent une capacité d'échange anionique (CEA) qui ralentie la lixiviation des nitrates et des chlorures. Mais lorsque les nitrates sont apportés après les chlorures, cette capacité d'adsorption est moindre pour les nitrates et ceux-ci sont alors lixiviés plus rapidement que les chlorures ; cet effet se compensant à partir d'une certaine profondeur (environ 1 mètre dans nos expérimentations). Bien que les conséquences agronomiques et environnementales soient indéniables, il apparait difficile de les prendre en considération pour faire des recommandations tant les situations agro-pédologiques et climatiques sont contrastées. En effet, si les seuls aspects agro-pédologiques peuvent faire l'objet de recommandations[8], la prise en compte de la pluviométrie nécessiterais de renseigner un modèle afin de simuler les transferts de solutés. Bien que cela eût été ambitieux et novateur, la diversité des sols et des pratiques agricoles à la Réunion, m'a plutôt orienté dans une autre direction à savoir la prise en compte des caractéristiques des sols pour évaluer les transferts de nitrate à l'échelle régionale.

6.2.3 La vulnérabilité des aquifères de l'ouest de la Réunion aux pollutions par les nitrates

Aux échelles de la colonne de sol et de la parcelle, mes travaux ont montré le rôle clé joué par les sols dans la rétention et les transferts des nitrates. Or, bien que la superficie de la Réunion soit modeste (2 512 km^2), les sols présentent une très forte diversité et des propriétés physiques et géochimiques particulières, spécifiques aux sols tropicaux et aux sols volcaniques. Le sous-sol quant à lui est très hétérogène puisqu'à la superposition de matériaux aux caractéristiques différentes s'ajoute des structures géologiques telles des dykes ou des fissures et des fractures. À l'échelle du territoire, le contexte morphologique ne dessine pas des bassins versants qu'il serait possible d'étudier individuellement. En outre, des études stationnelles, telle que celle menée sur la station des Colimaçons, ne peuvent être démultipliées afin d'appréhender les impacts des apports de PRO sur la pollution des aquifères par les nitrates d'origine anthropiques. Aussi, j'ai cherché une méthode pour évaluer ces impacts en tenant particulièrement compte de la nature des sols de l'ouest de la Réunion.

8. Pour un type de sol donné, en connaissant la CEA ou l'intensité potentielle de la nitrification, un conseil agronomique pourrait être donné pour orienter la gestion de la fertilisation organique.

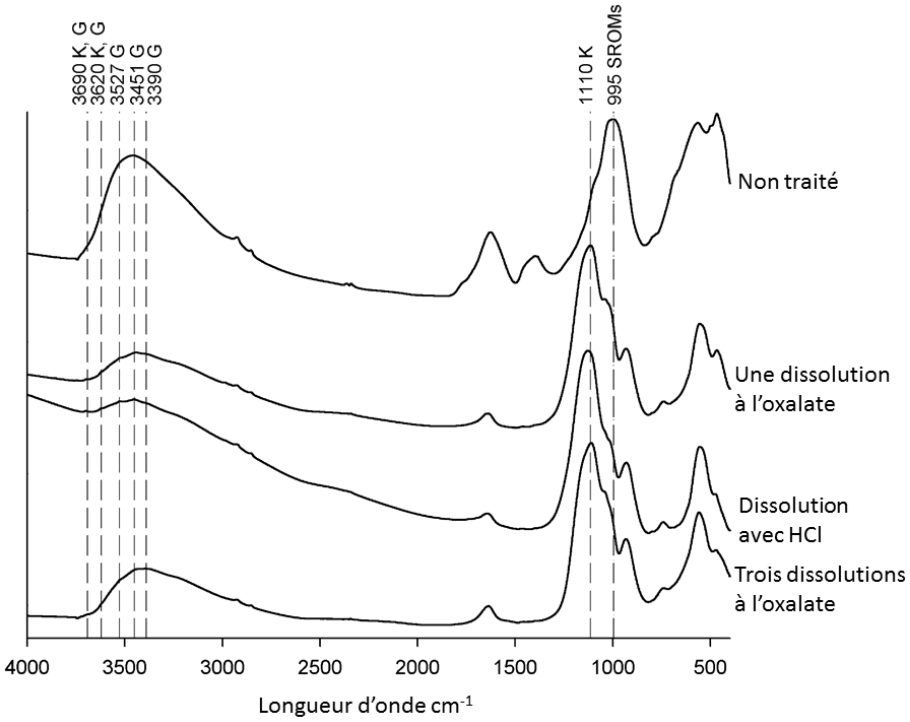

FIGURE 6.11 – *Spectre infrarouge à transformée de Fourier sur le sol non traité et après un ou trois traitements à l'oxalate et avec HCl; G = gibbsite, K = kaolinite, SROMs = minéraux cristallisés à courte distance (e.g. allophane et imogolite).*

À partir des données acquises aux échelles de la colonne de sol et de la parcelle, j'ai identifié les propriétés jouant un rôle prépondérant dans les transferts des nitrates spécifiquement pour les sols de la Réunion. Ensuite, j'ai cherché à les agréger puis à les représenter spatialement à l'échelle du territoire. Ces propriétés de nature physique (conductivité hydraulique, granulométrie, épaisseur du sol) s'associent aux propriétés chimiques (capacité d'échange anionique, etc.) pour caractériser la capacité intrinsèque des sols à retenir ou transmettre les flux de nitrates vers le sous-sol et donc vers les nappes phréatiques.
Néanmoins, pour construire cette cartographie de la vulnérabilité des aquifères au transfert des nitrates, j'ai très vite été confronté au manque de données pédologiques et à l'ancienneté de la carte de Raunet (1991a). Dans le cadre du projet « évaluation des risques de transfert des polluants à travers les sols », j'ai été amené à réaliser une cartographie de la vulnérabilité des nappes au transfert des nitrates. La première étape a consisté à développer une méthode de mesure de la granulométrie adaptée aux sols présentant des propriétés andiques (Alary *et al.*, 2013). Pour la deuxième étape, en plus de ces analyses granulométriques, j'ai acquis de nouvelles informations pédologiques afin d'actualiser la carte pédologique existante (Feder & Bourgeon, 2009 ; Feder, 2013). Enfin, la réalisation d'une carte de vulnérabilité au transfert des nitrates a constitué la troisième étape (Feder *et al.*, 2008).

Développement d'une méthode de détermination de la granulométrie pour les sols andiques

L'étude de la pédogenèse sur le flanc ouest du piton des Neiges est complexe du fait du fort gradient climatique altitudinal, de l'âge variable des roches mères et de l'impossibilité de réaliser des analyses granulométriques classiques sur les sols présentant des propriétés andiques. Or, ce dernier paramètre est indispensable pour l'identification d'horizons

argiques, pour évaluer l'intensité de la pédogenèse et caractériser les minéraux argileux. Aussi, nous avons développé une méthode de détermination de la granulométrie dans les sols andiques.
Dans les sols tropicaux riches en oxydes de fer et d'aluminium, un traitement à l'acide chlorhydrique à 2 $mol.l^{-1}$ est fréquemment utilisé pour dissoudre les ciments ferrugineux qui perturbent la mesure de la taille des particules. Toutefois, ce traitement peut également dissoudre d'autres minéraux. Or, ce traitement est souvent nécessaire dans les sols de la Réunion dès lors qu'ils présentent de telles caractéristiques. Dans les sols aux propriétés andiques, ce sont les phases cristallisées à courte distance (e.g. allophane et imogolite) qui perturbent habituellement la mesure granulométrique. Aussi, nous avons comparé l'effet d'un traitement HCl avec un traitement consistant à réaliser une à trois dissolutions avec de l'oxalate d'ammonium à pH 3.
Le traitement à l'oxalate dissout correctement les minéraux cristallisés à courte distance (figure 6.11) puisque le pic caractéristique à la longueur d'onde de 995 cm^{-1} disparait. Toutefois, contrairement au traitement à l'HCl, les autres minéraux tels que la gibbsite et la kaolinite ne sont pas dissous. De la même façon, par diffraction aux rayons X (Alary *et al.*, 2013), la smectite est préservée par le traitement à l'oxalate mais dissoute par le traitement à l'acide.
Au-delà de cette possibilité désormais offerte de réaliser des analyses granulométriques pour comprendre plus finement la pédogenèse des sols aux propriétés andiques, l'application de cette méthode sur les sols andiques du flanc ouest du piton des Neiges a permis d'identifier deux phases minérales (smectite et kaolinite) qui n'avaient pas été observées auparavant sur ces sols (Alary *et al.*, 2013). En outre, l'enrichissement en argiles de certains horizons a pu être mis en évidence afin de distinguer entre eux certains sols aux propriétés andiques.

Actualisation de la carte pédologique de l'ouest de l'île de la Réunion

Au cours de la deuxième étape, j'ai acquis de nombreuses et nouvelles données pour actualiser la carte pédologique de l'ouest de la Réunion en utilisant comme système de classification des sols la WRB (IUSS working group WRB, 2007). En effet, l'évolution des concepts en science du sol et corrélativement des systèmes de classification des sols, ne permettent pas systématiquement d'actualiser, sans erreurs ou imprécisions, d'anciennes cartes pédologiques. Les paramètres pédologiques, les caractérisations analytiques deviennent avec le temps imprécis, incomplets, parfois inexploitables.
Aussi, j'ai mené une campagne de caractérisation et de prélèvement des sols en deux étapes : dans un premier temps, sur un secteur de référence autour d'une toposéquence (Feder *et al.*, 2006) puis sur l'intégralité de la zone d'étude. Les observations et les analyses de 70 fosses de référence et de 175 sondages à la tarière m'ont permis d'identifier trente types de sols correspondant à des groupes de références de la WRB (IUSS working group WRB, 2007) et à leurs subdivisions par des qualificatifs, préfixes et suffixes (figure 6.12). La confrontation de cette nouvelle cartographie avec celles précédemment acquises par Riquier (1960) et Raunet (1991a) principalement, a montré les difficultés d'actualisation de cette carte pédologique notamment du fait du changement dans le système de classification des sols utilisé (Feder, 2013). Toutefois, cette comparaison fait également ressortir des constantes. Si nous admettons que les sols ferrallitiques beiges de Riquier (1960) sont en fait des andosols non identifiés comme tels pour des raisons historiques, la succession podzols – andosols – autres sols est reconnue de tous. Autre constante, aucun de ces auteurs n'a identifié de sols brun-rouille à halloysite comme signalé dans de nombreuses autres études de sols tropicaux développés sur matériau volcanique (Colmet-Daage *et al.*, 1973 ; Albrecht *et al.*, 1992) ou simplement des sols bruns dont la fraction argileuse serait dominée par l'halloysite comme en Équateur (Winckell *et al.*, 1991).

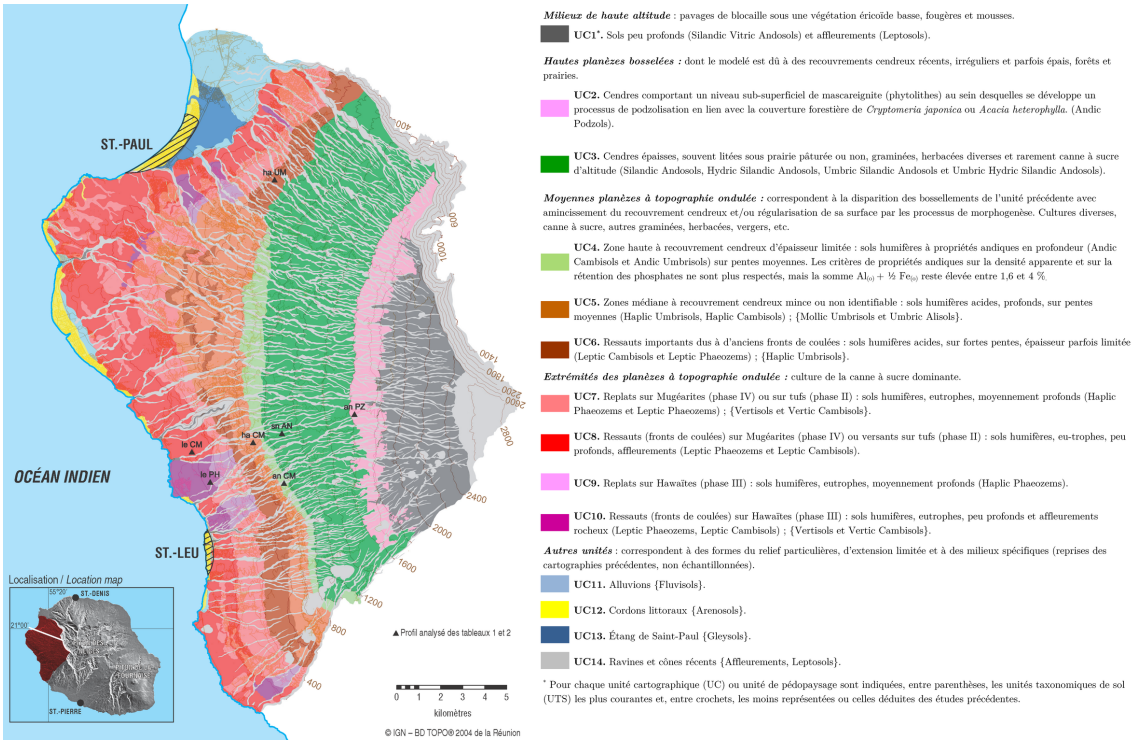

FIGURE 6.12 – *Nouvelle cartographie des sols de l'ouest de la Réunion.*

Cartographie de la vulnérabilité des aquifères au transfert de nitrates

Pour élaborer la cartographie de la vulnérabilité des aquifères, je me suis inspiré en premier lieu des modèles hydrogéologiques tels que DRASTIC (Aller *et al.*, 1987 ; Shirazi *et al.*, 2012). Cet outil utilise différentes variables (type de sol, profondeur de l'aquifère, pente, conductivité hydraulique de l'aquifère, recharge, etc.) ; chacune de ces variables est normalisée entre 1 et 10 et possède un poids, en fonction de leur importance, dans le calcul final d'un indice de vulnérabilité[9]. Ainsi pour la variable « sol », un sol argileux ou très peu filtrant aura un indice de 1 tandis qu'un sol sableux (ou l'absence de sol) possédera un indice de 10. Cet indice sera, pour la variable « sol », ensuite pondéré par un facteur 2 ; les autres variables ayant un facteur de pondération compris entre 1 et 5. Bien que cet outil soit assez simple à mettre en oeuvre, les principales critiques à son encontre dans notre situation, sont les suivantes :

- il nécessite des données hydrogéologiques dont nous ne disposons pas toujours ;
- il n'est pas adapté au contexte volcanique ;
- il minimise le rôle du sol ;
- l'échelle de représentation n'est pas adapté puisque en surface nous avons une diversité de type de sol alors que l'aquifère sous-jacent est unique et homogène.

En outre, l'intérêt d'un tel modèle à indexation et pondération réside dans la comparaison de situations complexes et contrastées puisque l'information finale est un indice relatif. Or, le sol est la seule variable pour laquelle nous avons une bonne connaissance et qui présente des différences à l'échelle de notre zone d'étude. Aussi, j'ai choisi d'élaborer un modèle à l'image de DRASTIC mais dont les variables seraient uniquement pédologiques. L'hypothèse que j'ai faite est que le sous-sol de notre zone d'étude était soit homogène (nature et propriétés de la roche mère, etc.) soit connu trop imprécisément.
Toutefois, la difficulté rencontrée dans les modèles à indexation est la hiérarchisation et

9. Plus l'indice est élevé, plus la vulnérabilité est forte.

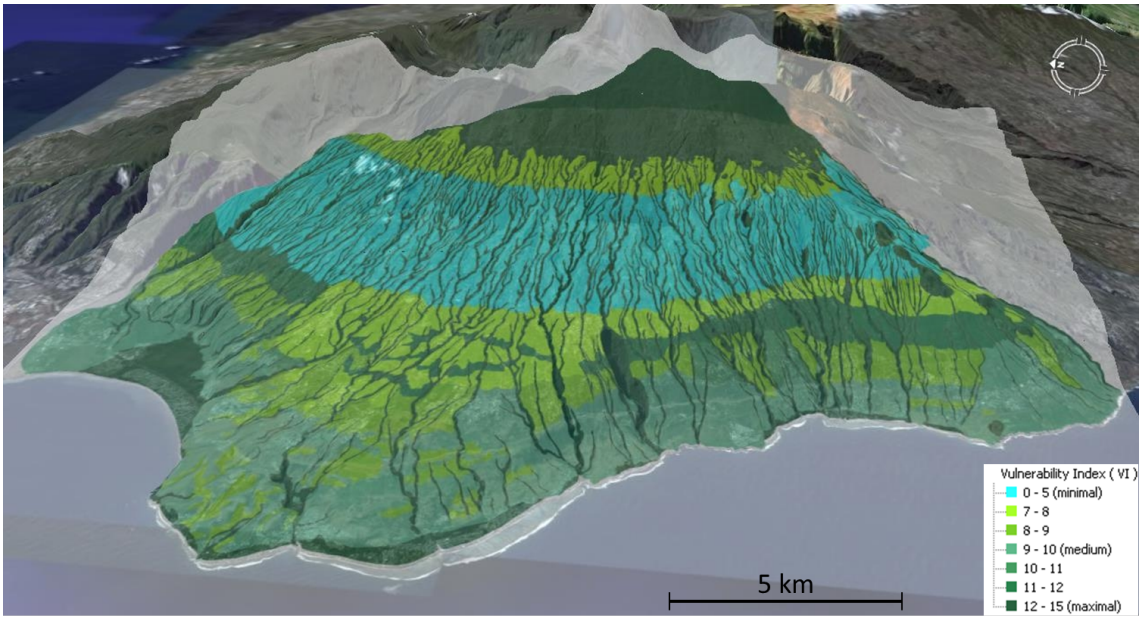

FIGURE 6.13 – *Représentation de l'indice de vulnérabilité de la zone d'étude comprise entre la rivière des Galets au nord et la ravine des Avirons au sud.*

surtout la pondération des différents critères. Ici, ce sont les variables pédologiques que nous avons identifiées comme jouant un rôle majeur dans le transfert des nitrates a travers les sols. Certains modèles permettent de lever le problème de la pondération, ne nécessitant simplement que la résolution de la hiérarchisation des critères à prendre en compte. C'est le cas de la méthode Siris (système d'intégration des risques par interaction des scores) proposée par Vaillant *et al.* (1995). C'est une méthode hiérarchique qui ne nécessite pas la définition de la gravité des facteurs (semblable à la pondération dans les autres méthodes) mais seulement leur classement hiérarchique relatif les uns par rapport aux autres. Elle met en fait en œuvre des règles (auto-pénalisation, etc.) peu explicites. La méthode Siris est un outil d'aide à la décision pour le classement de situation à risque les unes par rapport aux autres (Guerbet & Jouany, 2002). Les propriétés des contaminants composent essentiellement la vulnérabilité spécifique tandis que les propriétés des sols forment la vulnérabilité intrinsèque (figure 6.3, page 60). Ainsi, l'application à d'autres contaminants ne nécessiterait pas d'acquérir de nouvelles informations fondamentales sur les sols du territoire considéré. En effet, cette méthode est également appliquée afin de représenter la potentialité des substances phytosanitaires à se retrouver dans les eaux de surface ou les eaux souterraines (voir par exemple www.ineris.fr/siris-pesticides).

La carte de la vulnérabilité des aquifères au transfert des nitrates (figure 6.13) utilise une échelle relative de 1 à 15 correspondant respectivement aux vulnérabilités les plus faibles et les plus fortes. Ainsi, nous observons immédiatement que les zones où le sol est très peu épais voire absent (fond de ravine, forte pente, zone d'altitude, etc.) présentent les vulnérabilités maximales (classe entre 12 et 15). En effet, la rétention des nitrates est, par comparaison avec les autres situations où un sol est présent, nulle ou très faible. À l'inverse, les sols les plus épais, avec une faible conductivité hydraulique et une forte capacité d'échange anionique (typiquement les andosols), montrent un indice de vulnérabilité au transfert des nitrates très faible (classe entre 0 et 5).

Cette vulnérabilité ne préjuge en rien d'un éventuel aléa. En effet, l'aléa, selon la représentation schématique de la figure 6.3, correspondrait à un apport de PRO ou de tout autre fertilisant contenant des nitrates. Or, c'est bien le croisement de cet aléa et de la vulnérabilité qui induit un risque de pollution. Dans le fond des ravines, bien que la vulnérabilité

soit très forte, l'aléa serait certainement très faible ; au final, ce n'est donc potentiellement pas une zone à risque. Enfin, cette vulnérabilité est essentiellement invariable au cours du temps puisque construite à partir de paramètres pédologiques, contrairement à l'aléa qui est ponctuel dans le temps et indéterminé a priori. Cette carte de la vulnérabilité est donc un premier élément qu'il est nécessaire de croiser avec une cartographie de l'aléa qui pourrait par exemple représenter spatialement, la fertilisation en azote des cultures. L'objectif principal de cette cartographie est de pouvoir orienter des actions, notamment des pouvoirs publics, vers les zones présentant les vulnérabilités les plus fortes, a fortiori si l'aléa est également fort.

Conclusions des travaux sur les nitrates à l'échelle du territoire

Contrairement aux échelles de la colonne de sol et de la parcelle pour lesquelles les outils et la nature des mesures étaient similaires et les concepts proches, mes travaux à l'échelle du territoire marquent une rupture franche. En effet, si les objets « colonne de sol » et « parcelle » sont fondamentalement identiques (seule la taille considérée change), le territoire ne peut plus aussi simplement être considéré comme une grande ou comme une mosaïque de parcelles, du fait notamment de l'émergence d'autres processus (redistribution complexe de matière par ruissellement, hétérogénéité du territoire, etc.). En outre, les flux de contaminants sont observés ou considérés soit à la base de la colonne ou du profil de sol aux échelles de la colonne de sol et de la parcelle, soit dans l'aquifère sous jacent à l'échelle du territoire ; c'est un autre élément distinctif majeur puisque dans la première situation nous mesurons un flux ponctuel ou continu tandis que dans la seconde situation, nous mesurons une concentration à un moment donné.
À cette échelle d'étude, mes travaux sur la granulométrie dans les sols andiques ont constitué une réelle nouveauté (Alary *et al.*, 2013). En effet, Nanzyo *et al.* (1993) et plus récemment Buurman *et al.* (1997) ont détaillé les problèmes rencontrés dans l'analyse granulométriques des andosols (dispersion incomplète, influence du pH) et les difficultés d'interprétation de leur pédogénèse (lessivage des argiles, etc.). La procédure développée contourne désormais ces difficultés (Feder, 2013) alors que les classifications pédologiques avait abandonnée cette détermination comme critère caractéristique (Soil Survey Staff, 2014).
Au delà de nos besoins pour étudier la vulnérabilité des sols aux transferts de nitrates, l'actualisation de la carte pédologique de l'ouest de la Réunion a défini un cadre méthodologique et conceptuel qui permet d'envisager une transposition sur toute l'île de la Réunion. J'ai détaillé ces problèmes rencontrés (Feder & Bourgeon, 2009) parce que de nombreuses autres cartes pédologiques ont également été réalisées avec la CPCS (1967), notamment en Afrique pour des raisons historiques évidentes. Ainsi, par extension, les travaux d'actualisation de ces cartes (i) éviteront les transpositions trop rapides entre deux systèmes de classification (nous avons démontré l'infaisabilité systématique), (ii) cibleront efficacement les nouvelles mesures et observations à réaliser. Plus largement, ce travail fournit également des éléments de réflexion sur (i) la prise en compte de l'évolution des concepts en science du sol et leurs transpositions dans les classifications, (ii) les différences entre les grandes classifications internationales et (iii) le choix de l'une d'entre elles pour actualiser une ancienne carte pédologique.
Enfin, bien que mon travail sur la vulnérabilité aux transferts de nitrates soit à l'origine spécifiquement développé pour le contexte de l'ouest de la Réunion, l'approche conceptuelle est générique et réutilisable aussi bien pour le transfert d'autres contaminants sur le même territoire que dans d'autres situations pédologiques. En effet, l'évaluation de la vulnérabilité des aquifères fait l'objet de nombreux travaux notamment grâce à l'essor des systèmes d'information géographique aussi bien pour les nitrates (Shirazi *et al.*, 2012) que pour d'autres contaminants (Brown *et al.*, 2003).

6.3 Contamination des sols par les éléments traces métalliques : expérimentation et modélisation à l'échelle de la colonne et de la parcelle

La problématique de la contamination des sols et des végétaux par les ETM est assez récente à la Réunion pour plusieurs raisons. Le secteur industriel lié à la production ou la transformation de matières premières (mines, métallurgie, chimie...) et générateur de rejets métalliques est très peu présent. De plus, dans les années 2000, le recyclage des déchets non agricoles à la Réunion est embryonnaire et l'enfouissement demeure la voie d'élimination principale. Ainsi, les principaux déchets recyclés en agriculture (lisiers, fumiers, écumes, etc.) ne sont pas contraints à un suivi réglementaire des ETM. Par ailleurs, à la même période, la mise aux normes et le développement des stations d'épuration des eaux usées a induit une augmentation de la production de boues de STEP pour lesquelles la valorisation en agriculture est la voie privilégiée en France. Or, ces épandages ont longtemps été impossible à la Réunion à cause du fond pédogéochimique naturel en ETM trop riche[10] ; les travaux de Collin & Doelsch (2008) ont apporté les éléments scientifiques permettant de lever cette interdiction. Le recyclage des PRO d'origine agricole et urbaine et contenant des ETM s'est donc accentué et compte tenu des contraintes réglementaires le besoin de références sur les différents types de sol de la Réunion a émergé. De même que pour les nitrates, j'ai abordé cette problématique selon plusieurs échelles pour deux types de sol contrastés de la Réunion, mais compte-tenu des propriétés des ETM, en mettant en place des expérimentations différentes ou des modèles spécifiques.
Au sein du troisième thème du projet scientifique de l'unité « recyclage et risque » (interactions entre PRO, eau, sols et plantes), mes collègues E. Doelsch et M. Bravin s'intéressent respectivement à la spéciation des ETM en phase solide et à leurs phytodisponibilités tandis que j'apporte une complémentarité en focalisant mon approche sur le transfert de ces éléments dans les sols. En effet, la mobilité des ETM présente de significatives différences en premier lieu selon les caractéristiques du sol et principalement ses capacités d'adsorption liées à sa minéralogie (argiles, oxydes de fer et d'aluminium), sa teneur en matière organique (McBride, 1989 ; Bradl, 2004 ; Carrillo-Gonzalez *et al.*, 2006). Dans un second temps, les quantités et les propriétés du PRO apportés jouent un rôle majeur de part l'apport de composés organiques facilement solubles et pouvant complexer les ETM (Saar & Weber, 1982 ; Kramer & Duinker, 2013) mais également du fait des modifications (pH, potentiel d'oxydo-réduction, force ionique...) induites sur le milieu (Diacono & Montemurro, 2010). Enfin, le contexte climatique (pluviométrie, température) ne joue pas un rôle moins important notamment lorsque les flux d'eau dans les sols sont importants que cela peut l'être à la Réunion du fait des fortes pluviométries. Dans ce cadre, mes objectifs ont été :

- de quantifier les transferts d'ETM après des apports de différents PRO dans deux grands types de sol de la Réunion ;
- de modéliser leur accumulation à long terme.

Ma contribution aux études sur les ETM présentées dans cette section ont fait l'objet de quatre publications dans des revues à comité de lecture (Doelsch *et al.* (2011) ; Lahbib-Burchard *et al.* (2012) ; Legros *et al.* (2013) ; Wassenaar *et al.* (2014)), trois communications orales et deux communications posters dans des congrès internationaux.

10. Les fortes teneurs en ETM des sols réunionnais sont dues aux roches mères d'origine volcanique sur lesquelles les sols se développent (Doelsch *et al.*, 2006).

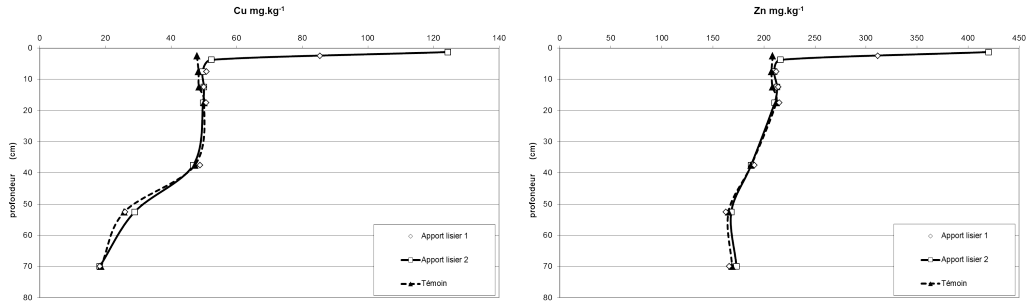

FIGURE 6.14 – *Nitisol de La Mare : concentrations en cuivre et en zinc en fonction de la profondeur dans le sol témoin n'ayant reçu que les apports d'eau et dans le sol des colonnes 1 et 2 (valeurs moyennes) ayant reçu deux apports de lisier.*

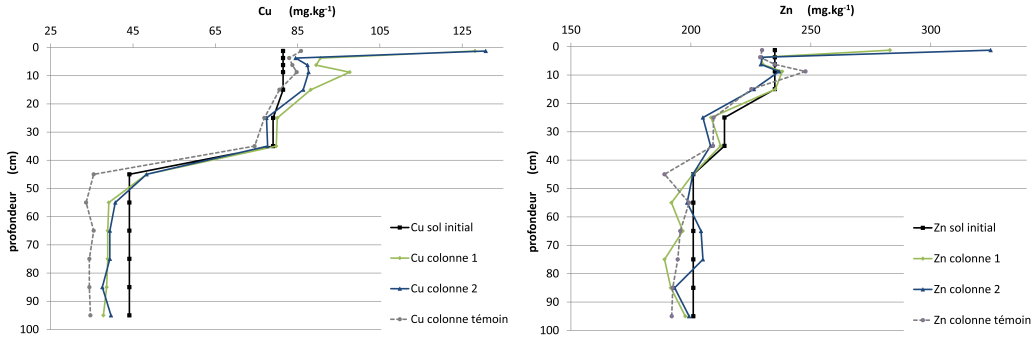

FIGURE 6.15 – *Cambisol andique des Colimaçons : concentrations en cuivre et en zinc en fonction de la profondeur dans le sol initial, dans le sol de la colonne témoin n'ayant reçu que les apports d'eau et dans le sol des colonnes 1 et 2 ayant reçu un apport de lisier.*

6.3.1 Suivi des flux d'éléments traces métalliques à l'échelle de la colonne de sol

Afin de suivre les transferts d'ETM à l'échelle de la colonne de sol, j'ai utilisé les mêmes dispositifs expérimentaux que ceux présentés dans les sections 6.2.1 (page 60) et 6.2.1 (page 61). Le cambisol andique et le nitisol, prélevés respectivement sur les stations du Cirad de La Mare et des Colimaçons, ont donc reçu respectivement un et deux apports de lisier de porc suivis d'apports d'eau reproduisant une à deux années pluviométriques. Les teneurs en ETM dans les sols ont été mesuré :

- avant l'expérimentation pour chaque couche prélevée *in situ* puis reconstituée dans les colonnes ;
- après l'expérimentation dans chacune des trois colonnes tous les 2,5 cm entre 0 et 10 cm de profondeur puis tous les 10 cm jusqu'à la base de la colonne.

Pour les deux types de sol, dans l'horizon de surface, les teneurs initiales en cuivre et en zinc ne présentent pas de différences significatives avec le sol de la colonne témoin (figures 6.14 et 6.15).

Le comportement du cuivre dans le nitisol et du zinc dans les deux types sols est similaire : les bilans massiques ont montré que la quasi-totalité de ces éléments apportés par le lisier de porc, s'était accumulée dans la couche la plus superficielle 0 – 2,5 cm. Les préleveurs de la solution du sol placés à 17 cm de profondeur n'ont d'ailleurs jamais révélé de concentrations en zinc plus élevées pour les colonnes ayant reçu du lisier par comparaison avec la colonne témoin du cambisol andique ni même pour le cuivre dans le nitisol. Les analyses de ces deux compartiments (sol et lixiviat) ont donc confirmé l'absence de transfert de cuivre à travers le nitisol et de zinc à travers les deux types de sol dans ces conditions

hydrodynamiques. En revanche, les concentrations en cuivre dans le cambisol andique ont été plus élevées pour les deux colonnes lisier par rapport à la colonne témoin pour toutes les couches jusqu'à 15 cm de profondeur. En deçà, dans la couche 20 – 40 cm, les teneurs en cuivre des colonnes lisier et témoin redeviennent similaires aux teneurs dans le sol initial. Ces résultats sont cohérents avec les caractéristiques granulométriques et minéralogiques de ces sols. Pour le nitisol, la quantité d'argile est particulièrement importante (75 % d'argile dans l'horizon de surface) et les principales phases minérales observées par diffraction aux rayon X (halloysite, goethite, magnétite, hématite, ilménite, gibbsite) sont de nature à adsorber les ETM. En outre, la teneur en matière organique est assez élevée (3,1 %). Malgré le pH acide du sol et l'acidification de la solution du sol corrélative à la nitrification du lisier (cf. paragraphe 6.2.1, page 60), cette adsorption du cuivre et du zinc dès la couche de surface est donc cohérente avec d'autres résultats acquis sur des sols tropicaux lors d'expérimentations d'apport de PRO en colonnes (Richards *et al.*, 2000 ; Cornu *et al.*, 2001). Pour le cambisol andique, les caractéristiques minéralogiques (halloysite, gibbsite, maghémite, hématite, ilménite) déduites des spectres de diffraction aux rayons X et les fortes teneurs en complexes organo-minéraux déduites des extractions à l'oxalate d'ammonium et au pyrophosphate de sodium expliquent cette forte adsorption dès les couches de surface ; ces résultats sont similaires à ceux observés pour les sols tempérés (Novak *et al.*, 2004 ; Lipoth & Schoenau, 2007) et des andosols (Fujikawa & Fukui, 2001 ; Soubrand-Colin *et al.*, 2007). Toutefois, ces suivis en colonne de sol ne prennent pas en compte les prélèvements d'ETM par les cultures ni les processus rhizosphériques. Les conditions de terrain, notamment la préservation de la structure du sol, peuvent également modifier les transferts. Aussi, nous avons choisi de travailler également à l'échelle de la parcelle.

6.3.2 À l'échelle de la parcelle, suivi des flux d'éléments traces métalliques dans un cambisol andique

Contexte et méthodologie

Dans cadre de la thèse de S. Legros (2008), nous avons complété le dispositif de suivi des flux d'eau et de soluté *in situ* mis en place initialement dans le cadre de la thèse de N. Payet (2005) mais pour suivre les transferts d'ETM et particulièrement du cuivre et du zinc dont on sait que les teneurs dans les lisiers de porc sont importantes. Les flux d'eau sont calculés à partir de la loi de Richards à l'aide des mesures tensiomètrique et de l'humidité volumétrique selon la même méthodologie qu'en colonne de sol. Le logiciel Hydrus 1D a ainsi été utilisé pour modéliser ces flux d'eau et calculer les différentes composantes du bilan hydrique. Les flux de solutés sont récupérés à l'aide de plaques lysimétriques équipées de mèches en fibre de verre. La solution du sol a également été récupérée par centrifugation de 50 g de sol frais. Deux épandages de lisiers ont été réalisés (novembre 2006 et juillet 2007) à la suite desquels les teneurs en ETM des lixiviats, de la solution du sol, des PRO et des végétaux ont été mesurées.

Le cuivre et le zinc dans le lisier et les compartiments eau-sol-plante

La qualité de la paramétrisation du modèle Hydrus 1D a été estimée par le coefficient de Willmott (Willmott, 1981) et s'est avérée satisfaisante. Dès lors, nous avons établi le bilan hydrique de chacune les deux périodes de suivi (figure 6.16). La première période se caractérise par un évènement pluviométrique court et intense (jour 115) qui est à l'origine de la quasi-totalité du flux d'eau cumulé drainé à 60 cm de profondeur. À l'inverse, au cours de la seconde période, le drainage est la conséquence de six à huit évènements pluviométriques bien distincts. Nous avons ensuite couplé ces flux d'eau avec les concentrations en cuivre et en zinc mesurées à 60 cm de profondeur. Les flux ainsi calculés sont très peu

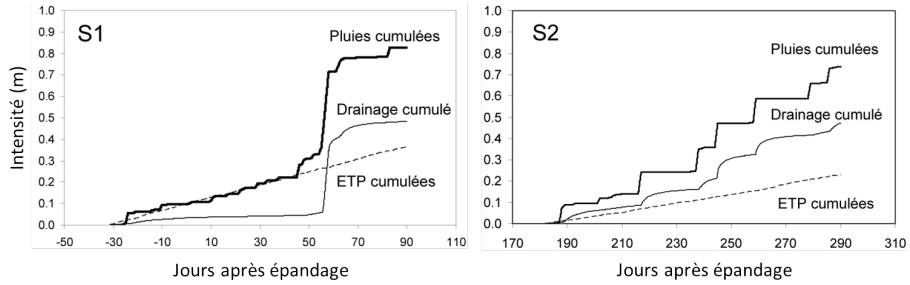

FIGURE 6.16 – *Cumul des pluies, du flux d'eau drainé et de l'évapotranspiration potentielle au cours de la première (à gauche) et de la seconde campagne de suivi (à droite) ; d'après Legros* et al. *(2013).*

différents entre la parcelle amendée par du lisier et la parcelle témoin.

Les concentrations en cuivre dans les végétaux ont montré des valeurs significativement plus élevées dans la parcelle lisier que dans la parcelle témoin (tableau 6.1) ; la différence reste toutefois faible. En revanche, les concentrations en zinc dans les végétaux sont similaires entre les deux modalités. Ainsi, les exportations de cuivre et de zinc par les végétaux, quelles soient les modalités, demeurent très faibles.

À la fin de l'expérimentation, nous avons mesuré les stocks de cuivre et de zinc dans le sol de la parcelle lisier et à partir du fond pédogéochimique de la même parcelle (tableau 6.1). Pour le cuivre, entre 0 et 60 cm de profondeur, seule la couche 0 – 20 cm présente une différente significative entre ces deux mesures. En revanche, pour le zinc, c'est l'inverse puisque seule la couche 0 – 20 ne présente pas de différence significative : les couches 20 – 40 et 40 – 60 cm présentent des concentrations toujours supérieures pour la parcelle ayant reçue du lisier.

TABLEAU 6.1 – *Concentrations en cuivre et en zinc dans les lisiers apportés, les plantes des deux parcelles et dans les couches de sol de surface de la parcelle lisier par comparaison avec son fond pédogéochimique ; d'après Legros* et al. *(2013).*

	parcelle	Cu ($mg.kg^{-1}$)	Zn ($mg.kg^{-1}$)
lisier (nov. 2006)		402,5	720,5
lisier (juillet 2007)		423	415
plante	parcelle témoin	7 ±1,7 † [a]	39 ±9,1 †
	parcelle lisier	10 ±1,4 ‡	47 ±13,9†
sol 0–20 cm	parcelle lisier	75 ±5 †	235 ±12 †
	fond pédogéochimique [b]	71 ±3,7 ‡	237 ±6,9 †
sol 20–40 cm	parcelle lisier	79 ±7 †	238 ±15 †
	fond pédogéochimique	75 ±16,9 †	226 ±15.4 ‡
sol 40–60 cm	parcelle lisier	76 ±10 †	241 ±14 †
	fond pédogéochimique	82 ±35,4 †	224 ±15,7 ‡

[a] Déviation standard ; les valeurs suivies de signes différents dans une même colonne, à une profondeur donnée, sont significativement différentes au seuil de 5 % par le test de Student.

[b] Calculé pour la parcelle lisier à partir de la méthode typologique (Baize, 1997).

6.3.3 Conclusions des expérimentations aux échelles de la colonne de sol et de la parcelle

Les concentrations en cuivre et en zinc mesurées dans le lisier sont élevées du fait de l'ajout de ces éléments dans l'alimentation des animaux mais elles sont cohérentes avec d'autres valeurs relevées dans la littérature (Nicholson *et al.*, 1999 ; Sánchez & González, 2005). À l'échelle de la parcelle, les prélèvements par les végétaux de type herbacé sont ici extrêmement faibles comme cela a été observé par ailleurs pour d'autres plantes (Mantovi *et al.*, 2003 ; Lipoth & Schoenau, 2007) ; ils correspondent ici à 0,005 $kg.ha^{-1}$.
En colonne de sol comme à la parcelle, les concentrations en cuivre et en zinc dans la solution du sol ne présentent pas de différence entre les traitements (lisier versus témoin). Ce résultat est cohérent avec d'autres observations (L'Herroux *et al.*, 1997 ; Egiarte *et al.*, 2006 ; Chahal & Toor, 2011) pour d'autres types de sols présentant a priori une granulométrie et une minéralogie moins propice à l'adsorption des ETM. De plus, dans les couches 20 – 60 cm, l'absence de cuivre pour les deux sols et de zinc pour le nitisol confirme cette accumulation. Lorsque des bilans massiques ont pu être réalisés, ils montrent également que tout le cuivre et le zinc se sont accumulés dans la couche de surface 0 – 20 cm. En effet, les fortes teneurs naturelles en cuivre et en zinc de ces deux sols résultent de la nature volcanique de la roche mère (Doelsch *et al.*, 2006) et sont dans des fractions peu mobiles (Doelsch *et al.*, 2010). De plus, la spéciation du cuivre dans le lisier est essentiellement sous la forme de Cu_2S très peu soluble dans les sols même lorsque le pH est supérieur à 4,5 (Legros *et al.*, 2010).
Tout ces éléments sont concordants dans nos expérimentations aux échelles de la colonne de sol et de la parcelle excepté pour le zinc qui pourrait s'être accumulé dans les couches 20 – 60 cm du cambisol andique (échelle de la parcelle). Ce serait un résultat original puisque dans les sols tempérés (Novak *et al.*, 2004 ; Lipoth & Schoenau, 2007) comme dans les sols tropicaux (Formentini *et al.*, 2015) le zinc est habituellement accumulé dans la couche superficielle. Néanmoins, la forte variabilité spatiale mesurée pour cet élément réduit la robustesse de cette observation qui n'a pas été faite lors des expérimentations à l'échelle de la colonne de sol alors que les prélèvements en fonction de la profondeur sont plus nombreux et la variabilité spatiale moindre.
Ainsi, contrairement aux nitrates qui sont rapidement lixiviés ou prélevés par les plantes, le suivi de la contamination par les ETM et l'évaluation des impacts environnementaux doit se faire à une échelle de temps plus longue et avec des outils différents. J'ai donc poursuivi mes travaux avec pour objectif de quantifier l'accumulation des ETM dans ces sols sur le long terme.

6.3.4 Élaboration d'un modèle de prévision de l'accumulation à long terme des éléments traces métalliques dans les sols

Dans le cadre du projet GIROVAR[11], j'ai utilisé les données précédemment acquises sur les sols de l'ouest de la Réunion (section 6.2.3, page 71) pour caractériser leur aptitude aux épandages de PRO. La question de la durabilité de cette pratique s'est posée puisque, alors que les nitrates sont prélevés par les plantes ou lixiviés, les ETM sont essentiellement stockés dans les premiers centimètres des sols de la Réunion étudiés puisque peu prélevés par les cultures et très peu mobiles. Or, le recyclage des PRO en agriculture, principale source de ces contaminations en ETM, reste à ce jour la voie de valorisation la plus intéressante et la plus faisable en France et à la Réunion notamment du fait des nombreux effets positifs. Les travaux actuels montrent que l'impact environnemental des ETM est faible à court terme

11. GIROVAR est l'acronyme du projet « gestion intégrée des résidus organiques par la valorisation agronomique à la Réunion » coordonné par T. Wassenaar (Cirad) et financé dans le cadre de l'appel d'offre CAS-DAR 2010.

mais les prévisions sur le long terme sont encore débattues. Celles-ci s'appuient notamment sur des modèles empiriques simples faisant des bilans « entrées / sorties » (Franco *et al.*, 2006). En outre, ces modèles ne sont que très peu validés par des suivis sur le terrain avec suffisamment de recul et particulièrement pour les environnements tropicaux.
C'est dans ce contexte que nous avons élaboré un modèle de prédiction de l'accumulation des ETM dans les sols de l'ouest de la Réunion (Lahbib-Burchard *et al.*, 2012 ; Oustrière *et al.*, 2013) en nous appuyant sur les données pédologiques les plus récentes (section 6.2.3, page 71) ; ses principales caractéristiques sont les suivantes :

- les flux d'ETM en entrée sont les PRO (E_{PRO}), les engrais minéraux (E_{MIN}) et les produits phytosanitaires (E_{PHY}) ;
- les flux d'ETM en sortie sont les exportations par les végétaux (S_{PL}) et la lixiviation (S_L) en dessous de l'horizon de surface travaillé du sol.

Ainsi, la concentration en un ETM (C_{ETM} en mg.kg^{-1}) dans l'horizon de surface travaillé à un temps t (en année ou en nombre de cycles de culture) est :

$$C_{ETM(t)} = C_{ETM(t-1)} + \frac{E_{PRO} + E_{MIN} + E_{PHY} - S_{PL} - S_L}{10\,\rho\,P}$$

où ρ est la masse volumique apparente de l'horizon de sol (kg.m^{-3}) et P est la profondeur de l'horizon de surface travaillé du sol (m).
Pour la validation du modèle, nous avons utilisé un essai de terrain mené sur la station du Cirad des Colimaçons avec les caractéristiques suivantes :

- cinq espèces maraîchères différentes (chou, laitue, carotte, tomate, haricot) ont été conduites ;
- en sept ans, quatorze cycles de culture successifs ont été menés ;
- à chaque cycle de culture, trois modalités de fertilisation ont été menées : engrais minéral, compost de lisier de porcs et compost de fumier de volaille ;
- chaque modalité a été répétée trois fois ; ainsi, le dispositif est composé de $5 \times 3 \times 3 = 45$ parcelles.

La validation du modèle s'est révélée satisfaisante puisque les apports de compost de lisier de porc pendant quatorze cycles successifs de cultures ont engendré une augmentation de 48 mg.kg^{-1} de zinc correctement reproduite (figure 6.17). De même, les apports d'engrais minéraux (ne contenant pas de zinc) ont été correctement simulés puisque les concentrations en zinc sont restées stables autour de 245 mg.kg^{-1} dans le sol. Pour le cuivre, après les apports de compost de lisier de porc, le modèle a légèrement surestimé les concentrations (22 mg.kg^{-1}) alors que les mesures n'ont montré qu'une augmentation de 16 mg.kg^{-1}. En revanche, pour les apports d'engrais minéraux, le modèle a correctement reproduit la stagnation de la concentration du cuivre dans l'horizon de surface du sol.
Les simulations sur le long terme sont le principal intérêt de ce modèle. Aussi, nous avons simulé l'accumulation des ETM dans un type de sols de l'ouest de la Réunion (un cambisol andique des moyennes planèzes ondulées, cf. figure 6.12) après 100 années d'apports de trois types de PRO. Ceux-ci correspondent à des mélanges des différentes sources de matières organiques présentes sur ce territoire :

- PRO-1 : broyats de déchets verts, fumier de volailles et lisier de porc ;
- PRO-2 : broyats de déchets verts, fientes de volailles et vinasses de distillerie ;
- PRO-3 : broyats de déchets verts, boues de STEP et vinasses de distillerie.

Les trois PRO ont montré une accumulation systématique dans les horizons de surface des sols : 0,15 à 0,25 mg.kg^{-1} pour le cadmium, 40 à 60 mg.kg^{-1} pour le cuivre, 30 à 65 mg.kg^{-1} pour le nickel et 120 à 250 mg.kg^{-1} pour le zinc. Le PRO-1 est celui qui accumule le plus de cuivre, de zinc et de nickel (figure 6.18) en raison de sa teneur une fois et demi

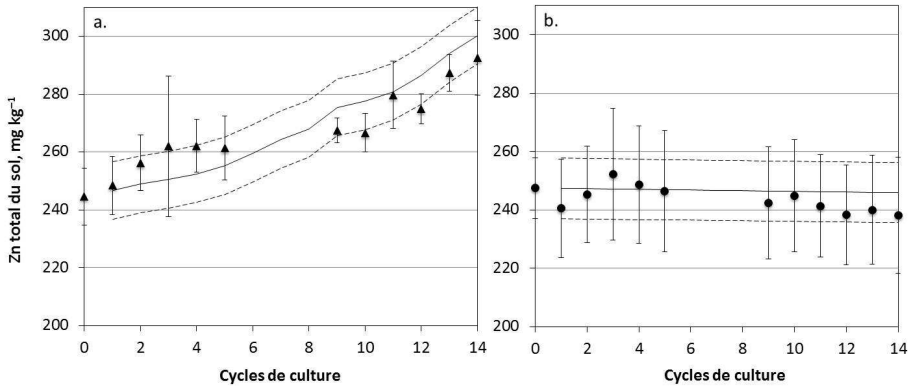

FIGURE 6.17 – *Concentrations en zinc mesurées (triangles et ronds) et modélisées (courbes en trait plein) dans l'horizon de surface de l'essai de terrain après apport de compost de lisier de porc à gauche (a) et d'engrais minéral à droite (b) pendant quatorze cycles de culture ; les écart-types sont représentés par les barres d'erreur pour les mesures des concentrations et par les lignes en pointillée pour les valeurs modélisées.*

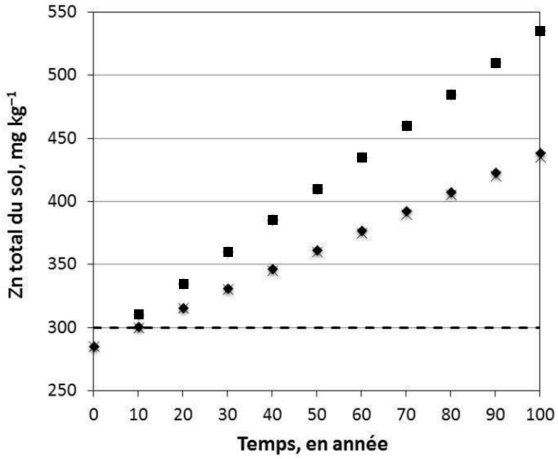

FIGURE 6.18 – *Simulation de l'accumulation de zinc dans les sols des moyennes planèzes ondulées après apport des* PRO-1 *(carré),* PRO-2 *(croix) ou* PRO-3 *(losanges).*

supérieure à celle des PRO-2 et PRO-3 en ces éléments. Après six années d'épandage du PRO-1 sur ce sol, le seuil fixé par l'arrêté boues de 1998 serait dépassé pour le zinc. En revanche, sur les sols des hautes planèzes (figure 6.12) initialement moins riches en zinc, ce seuil ne serait dépassé qu'après vingt-six années. Pour le cuivre, ce seuil serait franchi après 91 années mais uniquement sur les sols des moyennes planèzes.

La simplicité de ce modèle permet de réaliser de nombreuses simulations avec des jeux de données sur les sols, les PRO et les cultures assez légers. Toutefois, il n'a été validé que pour une seule situation agro-pédologique (maraîchage sur cambisol andique). En outre, du fait qu'il soit empirique, ce modèle ne préjuge pas d'une éventuelle modification de la spéciation des ETM qui pourrait modifier la répartition des flux vers les cultures ou par lixiviation. De même, sur le long terme, l'évolution des propriétés physiques (conductivité hydraulique, porosité, etc.) ou chimiques (pH, teneurs en matières organiques, etc.) des sols est susceptible d'engendrer de substantielles modifications du comportement des ETM (Houot *et al.*, 2009).

6.3.5 Conclusions sur le suivi et la modélisation des transferts d'éléments traces métalliques aux échelles de la colonne de sol et de la parcelle

La problématique de la contamination des sols et des végétaux par les ETM a débuté à la Réunion dans les années 2000. Les premiers éléments d'inventaire et d'identification des origines de ces ETM dans les sols (Doelsch *et al.*, 2006) ne permettaient pas d'établir des bilans complets lors du recyclage des PRO. Ma contribution principale a donc été de montrer que les ETM apportés par les PRO n'étaient pas mobiles dans deux des principaux types de sol de la Réunion et ce, dans le contexte d'un fond pédogéochimique naturel élevé. À l'échelle de la colonne de sol, l'absence d'une culture et la modification de la structure du sol modifient les conditions de transfert et de prélèvement des ETM tandis qu'à l'échelle de la parcelle, la précision des mesures des ETM et la variabilité spatiale des sols réduit la robustesse de certaines interprétations. Ces difficultés ont justifié le choix de plusieurs échelles d'expérimentation pour atteindre des objectifs spécifiques différents.
Quelle que soit l'échelle de travail, dans les deux types de sols choisis, les ETM étudiés ne montrent pas une grande mobilité ; ici le cuivre et le zinc sont principalement détaillés. Bien qu'attendus au regard des autres études essentiellement en contexte tempéré (Houot *et al.*, 2014), ces résultats apportent néanmoins pour les sols de la Réunion de nouvelles connaissances scientifiques.
En premier lieu, la répartition précise selon la profondeur (par tranche de 2,5 cm) du cuivre et du zinc après un ou plusieurs apports de lisier par comparaison avec un témoin, nous indique que tous les ETM apportés par les lisiers sont stockés entre 0 et 5 cm de profondeur. Seul le cuivre dans le cambisol andique s'accumule un peu plus profondément jusqu'à 15 cm de profondeur.
Deuxièmement, les flux de cuivre et de zinc en solution dans le sol ne sont pas plus importants après apports de lisier, par comparaison avec un témoin, à la profondeur de 15 cm (en colonne) ou de 60 cm (*in situ*). Dans la littérature, les résultats expérimentaux sur les flux d'ETM divergent sensiblement selon la forme sous laquelle les ETM sont apportés (Chang *et al.*, 1984), la nature et les propriétés du sol (McBride, 1989 ; Bradl, 2004), l'intensité des flux d'eau (Vogeler, 2001 ; Egiarte *et al.*, 2006 ; Chahal & Toor, 2011) démontrant ainsi la nécessité d'acquérir des informations représentatives des conditions réelles spécifiques. Pour des expérimentations de court terme, si nous envisageons d'étudier la spéciation de ces métaux en solution dans le sol, nous devons prélever celle-ci dans la couche de surface, plutôt autour de 10 cm. En revanche, dans l'hypothèse d'un suivi à plus long terme, il est possible que les flux de cuivre et de zinc soient observables après des apports de lisier à des profondeurs supérieures ou égales à 20 cm.
Troisièmement, les quantités de cuivre et de zinc prélevées par une plante herbacée fréquente à la Réunion sont très faibles. Ces valeurs confirment d'autres résultats (Mantovi *et al.*, 2003) mais sont plus adaptées au contexte agro-pédologique tropical et volcanique. En terme de bilan d'exportation, ce compartiment « plante » sera certainement toujours négligeable à court terme (Chaney, 2012).
Quatrièmement, la modélisation empirique que nous avons calée et utilisée spécifiquement dans notre contexte confirme, pour plusieurs types de sols de la Réunion, l'atteinte des seuils réglementaires pour plusieurs ETM à court terme pour le zinc et à long terme pour le cuivre et soulève le problème également sous l'angle de la phytotoxité (McBride, 1995).

L'acquisition de données de référence et le suivi sur le long terme des contaminants est une étape indispensable pour renseigner et utiliser des modèles permettant d'évaluer leur devenir et de prédire les éventuels risques associés. Je développe certaines perspectives de recherche dans cette direction.

TROISIÈME PARTIE : PERSPECTIVES DE RECHERCHE

CHAPITRE 7

À LA RÉUNION ET AU SÉNÉGAL

Mon projet scientifique personnel est à ce jour indissociable de celui de l'unité de recherche « recyclage et risque » à laquelle je suis rattaché et plus particulièrement à l'axe « interactions entre PRO, eau, sols et plantes ». Après mes travaux de recherches menés à la Réunion, j'ai été affecté au Sénégal en 2011 au sein du laboratoire mixte international (LMI) IE SOL dont la coordination est assurée conjointement par l'IRD et l'ISRA ; l'unité de recherche « recyclage et risque » est l'une des équipes constituantes de ce LMI. Aussi, dans la continuité de mes travaux précédemment présentés, mon projet de recherche est construit en m'appuyant sur deux terrains d'étude en milieu tropical mais présentant des contextes agro-pédologiques et climatiques très différents.
Le premier site d'expérimentation est celui de l'île de la Réunion ; il est localisé sur la station du Cirad à La Mare et fait partie du dispositif SOERE PRO. Ce terrain est celui des travaux que j'ai présenté sur les nitisols à l'échelle de la colonne de sol essentiellement. Le second site est localisé au Sénégal sur la station de l'ISRA à Sangalkam. En effet, dans le cadre du projet ISARD[1], notre unité a commencé à travailler dans un contexte foncièrement différent de celui de la Réunion : l'intensification du maraîchage en milieu périurbain par l'usage de PRO. Depuis mon affectation au Sénégal, je m'approprie et développe ce thème. Sur chacun de ces deux terrains, mes perspectives de recherche se focalisent sur les impacts des apports répétés de PRO. Sur le site de la Réunion, du fait de la présence de certains contaminants et de la nature des PRO apportés sur la canne à sucre, mes perspectives se focaliseront plus particulièrement sur la compréhension des déterminants du transfert des contaminants entre les compartiments eau, sol et plante. En revanche, au Sénégal, les cultures maraîchères, contrairement à la canne à sucre, sont directement consommées. Il semble donc plus pertinent de s'intéresser alors aux points suivants :

- la qualité nutritionnelle et l'absence de différents contaminants (ETM, CTO) dans les cultures maraîchères ;
- la sécurisation de cette production par l'étude de la durabilité des pratiques d'intensification par les PRO : quelles sont les pratiques optimales et durables ?
- l'acquisition de données de référence sur les grands cycles biogéochimiques de la matière organique et des éléments majeurs afin de renseigner et d'utiliser des modèles de simulation.

1. ISARD est l'acronyme du projet « intensification écologique des systèmes de production agricoles par le recyclage des déchets » financé par l'ANR (2009–2012).

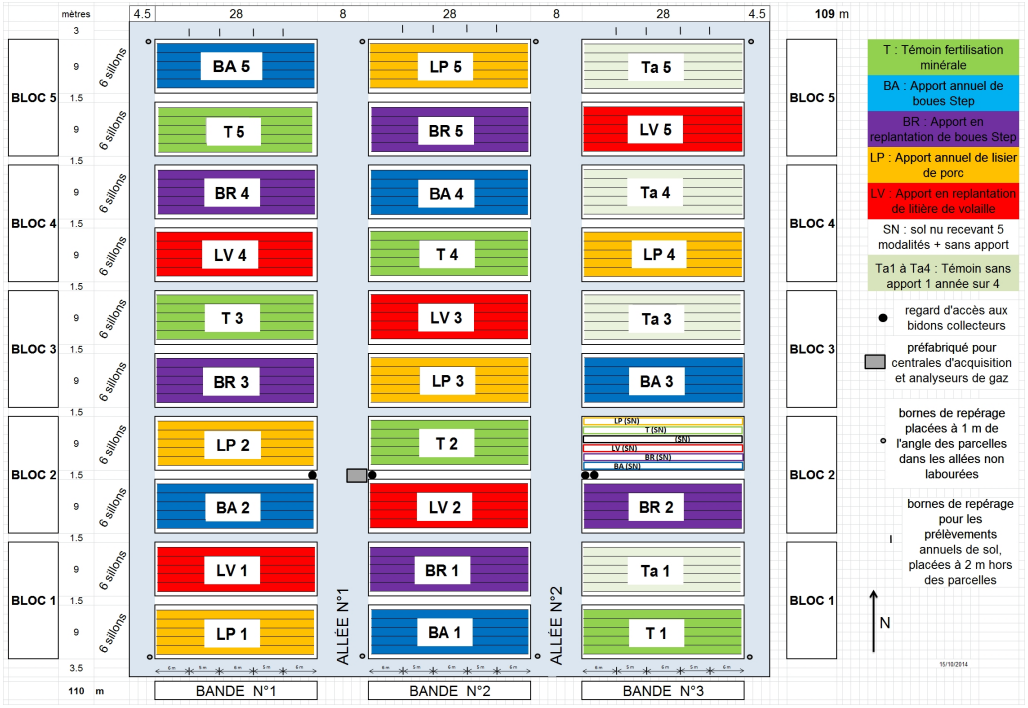

FIGURE 7.1 – *Schéma du dispositif expérimental du site du* SOERE PRO *à la Réunion.*

7.1 Le site du Soere Pro à la Réunion

Les SOERE (systèmes d'observation et d'expérimentation au long terme pour la recherche en environnement) sont des réseaux d'observatoire de l'environnement pour lesquels AllEnvi[2] est en charge de leur évaluation, leur structuration, leur labellisation et leur suivi. Le SOERE PRO s'intéresse donc aux impacts environnementaux des produits résiduaires organiques. Il a été labellisé en 2010 et il regroupe, depuis 2013, quatre sites lourdement instrumentés : trois sites en France métropolitaine (Feucherolles, Colmar et Rennes) et le site de la Réunion. Il est coordonné par S. Houot de l'UMR ECOSYS.

7.1.1 Description du dispositif

Le site du SOERE PRO à la Réunion a été mis en place en 2013 au sein de la station de La Mare (nitisol). La station expérimentale est plantée en canne à sucre, culture semi-pérenne représentant près de 60 % de la surface agricole utile de la Réunion. Dans notre essai, la canne à sucre est replantée tous les quatre ans. La température annuelle moyenne est proche de 25°C et les précipitations annuelles sont d'environ 2000 mm. Différents PRO d'origine urbaine et agricole sont apportés selon les modalités suivantes :

- BA : apport annuel de boues de STEP ;
- BR : apport en replantation de boues de STEP ;
- LP : apport annuel de lisier de porc ;
- LV : apport en replantation de litière de volaille ;
- T : témoin fertilisation minérale ;
- SN : sol nu recevant les cinq modalités et une modalité sans apport.

2. AllEnvi est une alliance nationale de recherche pour l'environnement dont l'objectif est de contribuer à faire de la France l'un des acteurs de référence des sciences et technologies de l'environnement et de l'alimentation au sein de l'espace européen de la recherche.

Toutes les modalités avec PRO sont complétées afin d'équilibrer les apports des éléments majeurs (N, P, K, Ca et Mg). Sur près d'un hectare, l'essai est constitué de cinq blocs identiques (figure 7.1). Sur le bloc 2, toutes les modalités sont équipées de tensiomètres et de sondes TDR pour mesurer les flux d'eau en continu sur tout le profil de sol. Les températures et la conductivité électrique sont également mesurées sur tout le profil de sol. Les solutés sont prélevés à l'aide de plaques lysimétriques installées à un mètre de profondeur. Sur les parcelles BA, LP, LV et T, les gaz CO_2 et N_2O sont mesurés quatre fois par jour dans des enceintes climatiques dont l'ouverture et la fermeture sont automatisées. L'enregistrement automatisé des données hydrodynamiques et les instruments d'analyse des gaz sont centralisés dans un local technique au sein de la parcelle.

7.1.2 Perspectives de recherche

Mes perspectives de recherche dans le contexte de l'île de la Réunion concernent, en premier lieu, l'évolution de deux types de contaminants (les ETM et les composés traces organiques (CTO)) et les grands cycles biogéochimiques, dans un second temps.
Dans mes travaux précédemment présentés, j'ai établi à l'aide des bilans de masse des ETM que sur ce nitisol ces éléments, qu'ils soient apportés par les PRO ou déjà présents dans le sol, étaient essentiellement immobiles et qu'ils s'accumulaient dans les premiers centimètres en surface du sol. Toutefois, la spéciation des ETM peut être différente pour chaque ETM et pour chaque PRO : le cuivre dans les lisiers de porc est essentiellement sous la forme Cu_2S (Legros *et al.*, 2010) alors que pour d'autres PRO le cuivre est surtout lié aux fractions organiques et le zinc essentiellement adsorbé sur les oxydes de fer (Tella *et al.*, 2016). Cette diversité de la spéciation des ETM dans les PRO se répercute naturellement lorsque ceux-ci sont apportés aux sols. Or, suite à l'apport de PRO à long terme, l'évolution de cette spéciation dans les sols reste méconnue (Franco *et al.*, 2006) et répond certainement à de nombreux paramètres. Formentini *et al.* (2015) ont montré dans un latosol du Brésil, aux propriétés assez proche du nitisol, que le cuivre et le zinc migraient jusqu'à 15 cm de profondeur après onze années d'apports de 200 $m^3 .ha^{-1} .an^{-1}$ de lisiers de porc alors que ces éléments restaient dans les 5 premiers centimètres du sol pour des apports deux à quatre fois plus faibles. En outre, à l'aide d'extractions sélectives, ces mêmes auteurs ont montré que le cuivre était essentiellement lié à la fraction organique alors que le zinc était distribué entre les fractions organique et adsorbable.
Dans un premier temps, il m'apparait important d'affiner nos connaissances sur la spéciation de certains ETM dans les PRO apportés. La répartition des ETM dans les différentes fractions des extractions sélectives, par exemple, aussi bien dans les PRO que dans les sols déjà amendés, devraient nous renseigner sur certaines de leurs propriétés à long terme que nous pourrons confronter régulièrement aux suivis que nous réalisons. Ces techniques « chimiques » montrent rapidement leurs limites et nécessiteront d'être complétées. La séparation et l'individualisation des phases porteuses des ETM par des méthodes physiques (séparation granulométrique ou densitométrique par exemple), pourrait nous permettre d'affiner ces connaissances.
Dans le cadre du projet Digestate[3], des travaux sont également envisagés pour étudier l'évolution de la spéciation des ETM au cours des processus de transformation des PRO (compostage, digestion anaérobie, etc.). En effet, en amont de l'épandage des PRO, la diversité de la spéciation des ETM résulte principalement d'une diversité des modes de production de ces PRO et de leurs évolutions, essentiellement liés aux conditions physico-chimiques. Il est intéressant de déterminer dans quelles conditions physico-chimiques les ETM acquièrent leurs spéciations et dans quelles conditions hydrodynamiques ils deviennent

3. Digestate est l'acronyme du projet « Diagnosis of Waste Treatments for Contaminant Fates in the Environment » financé par l'ANR (2016-2019).

mobiles et migrent dans le sol. Ici, une difficulté réside dans le suivi de cette spéciation à différents stades de transformation du PRO. Un enjeu d'importance sera *in fine* de comprendre comment la spéciation des ETM influence leur mobilité sur le long terme.

Dans un second temps, je m'intéresserais aux divers et nombreux composés traces organiques (CTO). Plusieurs d'entre eux font l'objet de réglementations et sont donc étudié depuis plus longtemps : les hydrocarbures aromatiques polycycliques (HAP), les polychlorobiphényles (PCB), les dioxines et les furanes. Les HAP, constitués d'au moins deux cycles aromatiques fusionnés, sont issus des produits pétroliers et résultent notamment d'une combustion incomplète. Les PCB sont des composés aromatiques organochlorés qui ont été produits entre 1930 et le début des années 1980 pour leurs qualités d'isolants électriques, leur stabilité thermique, leur excellente lubrification et leur résistance au feu. Toutefois, il existe des centaines d'autres composés qui ne sont pas réglementés mais qui font l'objet de nombreuses études scientifiques. L'intérêt croissant pour les CTO résultent des risques graves pour la santé humaine, avérés ou suspectés, parfois même à de très faibles concentrations.
Mon objectif principal sera de suivre l'évolution au cours du temps et les transferts entre les compartiments de l'écosystème de quelques CTO identifiés dans les différents PRO apportés. En effet, les études permettant d'établir des bilans des CTO restent disparates et sont confrontées à de nombreuses difficultés. La plupart des CTO sont ubiquistes dans les sols et dans les PRO et il peut être difficile d'identifier leurs origines. Par ailleurs, les méthodes d'analyses sont encore souvent en développement du fait des faibles concentrations des CTO, des méthodes d'extraction encore perfectibles et des effets matriciels. Ces difficultés analytiques et méthodologiques pourront être partiellement compensées par un suivi sur le long terme et une répétition dans le temps des analyses de CTO dans des parcelles où les concentrations de base sont connues.

Ma dernière perspective de recherche sur ce site concerne l'acquisition de données de références sur les grands cycles biogéochimiques de la matière organique et des éléments majeurs associés aux différents apports de PRO (azote, phosphore, potassium). En effet, notre dispositif expérimental permet de suivre l'évolution des stocks dans le sol à différentes profondeurs, les exportations par les cultures et les pertes par lixiviation. Par ailleurs, la mise en place des enceintes de mesure des gaz CO_2 et N_2O ainsi que les mesures ponctuelles de NH_3, nous permettra d'évaluer finement les pertes gazeuses au cours de l'année. L'utilisation du marquage isotopique de l'azote par enrichissement des paillis, des apports d'engrais minéraux, etc. sera un outil complémentaire qui nous permettra de déterminer les contributions respectives des différents compartiments dans son cycle complexe. Ces données nous permettraient de renseigner des modèles mécanistes, à l'image du modèle WAVE déjà utilisé, afin de simuler les impacts de l'épandage de PRO sur le long terme ou avec des doses d'apport différentes.

7.2 Perspectives de recherche au Sénégal

7.2.1 Contexte de l'agriculture maraîchère dans la zone périurbaine de Dakar

L'agriculture urbaine est indispensable pour répondre aux besoins alimentaires de la population et elle favorise la proximité d'un marché de consommation en ville. Elle contribue essentiellement à l'approvisionnement de denrées alimentaires, à la création d'emplois et de revenus et à la gestion des déchets organiques. Ce système de production dépend essentiellement de la disponibilité des terres, de l'eau et des intrants organiques et miné-

raux. De ce fait, l'urbanisation accélérée et l'accroissement de la population dans certaines régions en Afrique de l'ouest intensifient considérablement les défis d'une sécurité alimentaire. Ces deux facteurs sont aussi associés à la présence importante de différentes sources de matières organiques. Ainsi, pour maintenir une production élevée, dans un contexte d'enchérissement des engrais minéraux, les agriculteurs ont recours fréquemment aux matières organiques d'origine agricole (lisiers, fumiers, fientes, composts, etc.), urbaine (boues de station d'épuration, déchets ménagers, etc.) et agro-industrielle (déchets d'abattoirs, tourteaux, vinasses, etc.), mais sans pouvoir les maîtriser (Cofie *et al.*, 2006 ; N'Dienor, 2006 ; Doelsch *et al.*, 2011).

Au Sénégal, les pratiques agricoles autour des villes, particulièrement dans la zone des Niayes couvrent plus de 80 % de la production horticole nationale avec une large diversité de cultures maraîchères à haute valeur ajoutée (Fall *et al.*, 2001). La diversité et l'intensification des cultures dans la zone des Niayes s'expliquent par l'existence de caractéristiques pédologiques favorables, assez variées et d'un climat propice. S'y ajoute la présence de grandes villes (Dakar, Louga, Thiès et Saint-Louis) qui offrent des marchés de proximité avec un pouvoir d'achat conséquent. Ainsi, la contribution de la région de Dakar est considérable puisqu'elle abrite 23,2 % de la population nationale. La présence de ce grand centre de consommation a été un facteur déterminant pour le développement du maraîchage dans les Niayes puisque la région de Dakar couvrirait plus de 60 % de la consommation de la ville de Dakar en légumes (Gaye & Niang, 2010).

Deux grands bassins de productions maraîchères sont présents dans cette zone des Niayes, à proximité de Dakar. Sur le bassin de Pikine, les principales cultures maraîchères sont respectivement : la laitue, la tomate (Lycopersicon esculentum), l'aubergine et le poivron (Capsicum annuum L.). Sur le bassin de Rufisque, les principales spéculations sont : le chou pomme (Brassica oleracea), la carotte (Daucus carota var.), le poivron, la laitue, l'oignon (Allium cepa) et la tomate. Dans cette zone, la production est essentiellement assurée par de petites exploitations, souvent familiales (Badiane *et al.*, 2000 ; Fall *et al.*, 2001), soumises fréquemment à des pressions budgétaires. Ces systèmes de production utilisent généralement des PRO pour maintenir la production, seuls ou associés à des engrais minéraux. Toutefois, le manque de références agronomiques actualisées fait qu'actuellement la maîtrise de la fertilisation organique des sols cultivés dans les Niayes reste une problématique (Hodomihou *et al.*, 2016). En effet, les agriculteurs des Niayes se basent jusqu'à présent sur des connaissances traditionnelles pour fertiliser leurs cultures (Fall *et al.*, 2001). Les modalités d'apports mal maitrisées de PRO et répétées à chaque cycle de culture peuvent ainsi induire des conséquences environnementales négatives. Par exemple :

- lorsque l'azote est apporté en trop grandes quantités par rapport aux besoins des cultures, les nappes phréatiques des Niayes peuvent être contaminées (Sall & Vanclooster, 2009). De même, un mauvais usage des pesticides engendre une contamination significative des nappes phréatiques des Niayes (Ngom *et al.*, 2012) ;
- lorsque les PRO sont apportés en trop grandes quantités, Hodomihou *et al.* (2015) ont observé une accumulation des ETM dans les horizons superficiels des deux grands types de sols de la zone des Niayes ;
- les ETM, apportés de manière répétée par certains PRO, peuvent avoir aussi une influence sur les organismes du sol, conduisant à des modifications de la biodiversité (Kelly *et al.*, 2003 ; Hinojosa *et al.*, 2010). Mais les PRO, par leur apport massif en matière organique, peuvent également stimuler les populations et la diversité microbienne en fonction de leur composition biochimique. Les communautés microbiennes du sol sont alors utilisées telles un bioindicateur sensible de l'impact des pratiques.

Ces impacts négatifs sur les sols et les nappes phréatiques, voire les cultures, des Niayes pourraient ensuite induire une réduction de la productivité des sols à moyen terme et engendrer l'apparition de symptômes sur les cultures à court terme. En vue de la préser-

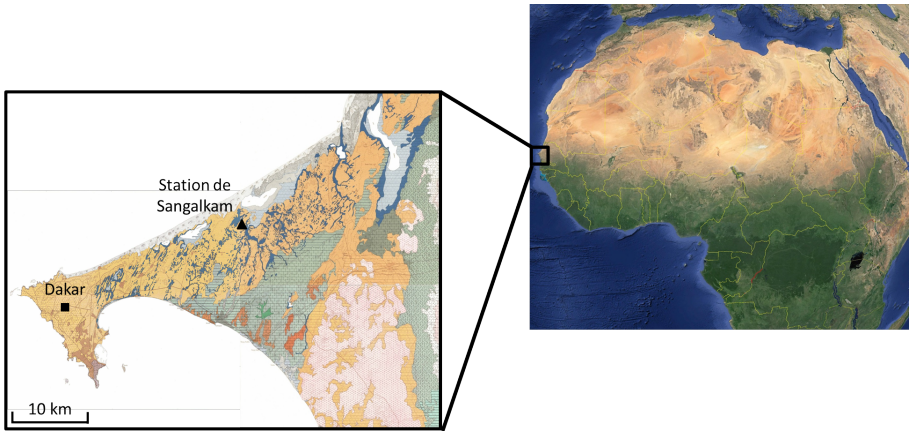

FIGURE 7.2 – *Localisation du Sénégal en Afrique de l'ouest (figure de droite) et de la station de Sangalkam dans la région de Dakar (figure de gauche).*

vation durable des agrosystèmes, la préoccupation majeure dans cette région devrait être la compréhension des trajectoires d'évolution des sols amendés par de fortes quantités de matières organiques et les impacts environnementaux associés. Aussi, dans le cadre de mes projets de recherche, ma démarche sera :

- de mettre en place et de suivre un site expérimental sur la station de l'ISRA de Sangalkam (figure 7.2) afin de connaitre précisément les impacts à long terme de l'épandage des PRO sur des cultures maraîchères ;
- de développer des expérimentations connexes sur les mêmes types de sol pour répondre à des questions plus spécifiques.

7.2.2 Description de l'expérimentation pour le suivi à long terme de l'impact des produits résiduaires organiques

Le climat de la région de Dakar est de type sahélo-soudanien mais fortement influencé par l'alizé boréal maritime issu de l'anticyclone des Açores. La pluviométrie moyenne est comprise entre 450 et 500 mm/an et elle est concentrée au cours de la saison des pluies allant de juillet à septembre. Elle présente toutefois une forte variabilité interannuelle. La température moyenne annuelle est de 24,4°C, oscillant de 20,4°C en février à 28,2°C en septembre. L'évaporation journalière moyenne présente peu de variation à l'échelle annuelle puisqu'elle est comprise entre 4,6 et 5,8 mm.
Le dispositif expérimental consistera à comparer une fertilisation minérale témoin aux trois PRO suivant :

- une boue de station d'épuration (B);
- une litière de volaille (LV) ;
- un digestat de méthanisation (DM).

La fertilisation minérale témoin correspondra pour chaque spéculation aux recommandations locales. Les doses de PRO seront ajustées à 100 % et 200 % de cette fertilisation témoin.
Les cultures maraîchères seront conduite à l'identique pour toutes les parcelles et donc pour toutes les modalités d'apports de PRO. Ainsi, plusieurs cultures successives au cours de l'année seront conduites sur la base de celles observées dans les deux principaux bassins maraîchers de la zone des Niayes. Les cultures ont été choisies en fonction du calendrier cultural de la zone, de leur précocité et de leur physionomie. À partir des enquêtes déjà réalisées et des observations, la rotation sera, dans l'ordre, à partir de la sortie de l'hivernage (octobre ou novembre) : tomate, laitue et carotte.

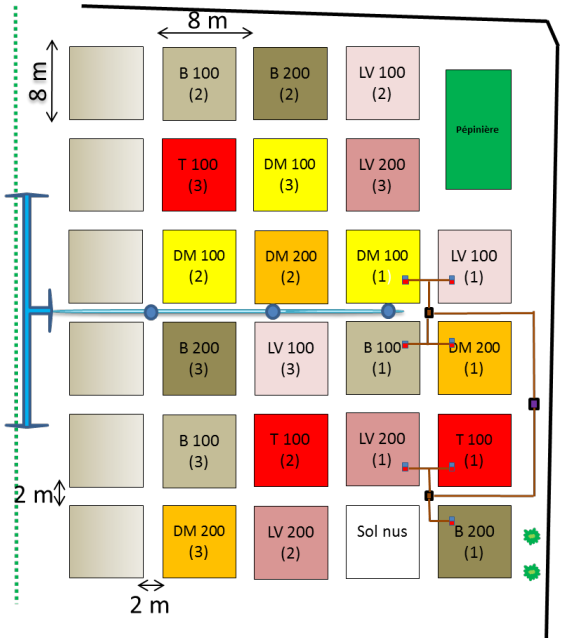

FIGURE 7.3 – *Schéma du dispositif expérimental sur la station de Sangalkam.*

Nous avons subdivisé notre expérimentation en parcelle carrées de 8 mètres de côté séparées par des allées de 2 mètres de largeur (figure 7.3). Chaque parcelle est constituée de six planches de 1 mètre de large et 8 mètres de long (soit 8 m^2) espacées de 0,4 mètre. Le dispositif a été randomisé avec trois répétitions par traitement. Ainsi, pour chaque traitement les parcelles ont été numérotées de 1 à 3.
Sur l'une des répétitions de chaque modalité, des tensiomètres et des sondes TDR mesurerons les flux d'eau en continu aux profondeurs de 20, 40 et 60 cm. Les températures et la conductivité électrique sont également mesurées sur tout le profil de sol. Les solutés sont prélevés à l'aide de plaques lysimétriques installées en deçà de la profondeur racinaire des différentes spéculations (40 centimètre de profondeur).

7.2.3 Perspectives de recherche

Sur l'essai de longue durée

Mon premier objectif majeur sera de déterminer et de modéliser la dynamique de la matière organique et le fonctionnement des cycles biogéochimiques des éléments majeurs apportés par les PRO (azote, phosphore, potassium...). En effet, le dispositif permettra d'acquérir toutes les composantes de ces flux dans les PRO, dans les sols, dans les plantes et les lixiviats ; seules les émissions gazeuses ne seront pas mesurées *in situ*. Pour combler ce dernier manque, celles-ci seront mesurées au laboratoire en conditions contrôlées au sein du LMI IE SOL. En effet, les apports répétés de PRO modifient positivement les caractéristiques structurales du sol (Abiven *et al.*, 2009), améliorent le fonctionnement microbiologique du sol (Ros *et al.*, 2006) et la fertilité chimique du sol (Diacono & Montemurro, 2010). Toutefois, les données de référence et les travaux dans les contextes semblables au nôtre, ne sont pas assez nombreuses pour paramétrer et valider des modèles de simulation de ces grands cycles biogéochimiques et de l'évolution des caractéristiques physiques et physico-chimiques des sols.

Le second objectif consistera à suivre l'évolution et les transferts des contaminants (ETM et CTO) apportés par les PRO. Si les travaux de Tella *et al.* (2013) ont montré que

certains PRO au Sénégal contenaient de fortes teneurs en ETM, il n'existe pas de données actuellement sur les teneurs en CTO dans les PRO au Sénégal. Dans le cadre du projet « mise en œuvre du volet recherche scientifique du programme national de biogaz domestique au Sénégal », nous avons d'ores-et-déjà prévu d'analyser ces contaminants sur des digestats de méthanisation. Il sera judicieux d'étendre ces analyses à d'autres PRO afin d'établir un inventaire de la présence de ces contaminants. Par ailleurs, nous suivrons l'évolution et le devenir des CTO présents dans les PRO apportés sur l'expérimentation.

Le troisième objectif sera de déterminer si les PRO ont un impact sur la qualité nutritionnelle des cultures maraîchères et sur la résistance de ces cultures aux bio-agresseurs et aux ravageurs. En effet, dans le cadre du projet IntenseMaraichage (2016-2018), financé par le métaprogramme Glofoods, nous prévoyons de réaliser des analyses des micro-nutriments sur les cultures maraîchères, afin d'identifier d'éventuels déséquilibres en lien avec la fourniture minérale du sol, ainsi que des analyses de la fermeté des parties comestibles. De plus, les maladies et les attaques sur les cultures seront caractérisées régulièrement par deux variables : l'incidence (représentant le pourcentage de plantes atteintes dans une parcelle) et la sévérité (caractérisant la gravité des attaques, calculée à partir des notes de gravité ou des indices).

Dans la région des Niayes

Bien que les pratiques agricoles soient variées dans la région des Niayes de Dakar, les apports de PRO sur les cultures maraîchères sont systématiques au début de chaque nouveau cycle de culture. Ainsi, trois à cinq apports annuels peuvent être réalisés et ce, dans des proportions peu maitrisées. Le récent diagnostique réalisé par Hodomihou *et al.* (2016) a montré qu'après plusieurs décennies, les contaminations de ces sols maraîchers en ETM étaient significatives. Or, la sécurisation des productions maraîchères passe indéniablement par une intensification *durable* de la productivité des sols.
Dans le cadre du projet IntenseMaraichage, mes perspectives de recherche seront de déterminer *les critères et le niveau d'intensification durable optimal* préservant la qualité des sols et n'impactant pas négativement les autres compartiments de l'écosystème dont les cultures. Pour cela, j'envisage de tester plusieurs itinéraires techniques avec des doses de PRO variables, voire des mélanges de PRO, et de suivre les compartiments potentiellement impactés à l'échelle fine des processus biogéochimiques.

7.3 Conclusion générale

Après avoir mis en oeuvre des approches multi-échelles pour étudier les transferts de contaminants majeurs et traces, mes perspectives scientifiques se recentrent principalement vers l'expérimentation à l'échelle de la parcelle. Toutefois, bien que les thématiques de mes perspectives scientifiques soient sensiblement les mêmes sur les deux sites tropicaux que j'envisage de suivre, les finalités sont différentes.
En effet, sur le site de la Réunion, l'enjeu majeur est de comprendre le devenir des contaminants traces, particulièrement les CTO pour lesquels certaines connaissances sont balbutiantes alors que certains effets toxiques sont reconnus. Les enjeux, en terme de toxicité, sont donc prégnants notamment concernant les risques de transfert vers l'homme. En revanche, sur le site du Sénégal, les préoccupations sociétales, qui orientent mes perspectives de recherche, sont plus directes et liées à la qualité sanitaire des productions maraîchères. Dans tous les cas, l'objectif recherché, sur le long terme, est la préservation durable des écosystèmes non-renouvelables à l'échelle humaine, principalement le sol et les ressources en eau.

RÉFÉRENCES BIBLIOGRAPHIQUES

Abiven, S., Menasseri, S., & Chenu, Cl. 2009. The effects of organic inputs over time on soil aggregate stability – A literature analysis. *Soil Biology and Biochemistry*, **41**(1), 1–12.

Alarcon, Cl. 1995. *Cycle biogéochimique du silicium en environnement tropical : application à l'étude des sols à mascareignite de l'île de la Réunion.* Thèse de l'université d'Aix-Marseille III.

Alary, K., Babre, D., Caner, L., Feder, F., Szwarc, M., Naudan, M., & Bourgeon, G. 2013. Pretreatment of Soil Samples Rich in Short-Range-Order Minerals Before Particle-Size Analysis by the Pipette Method. *Pedosphere*, **23**(1), 20–28.

Albrecht, A., Brossard, M., Chotte, J.-L., & Feller, Ch. 1992. Les stocks organiques des principaux sols cultivés de la Martinique (Petites Antilles). *Cahiers ORSTOM, série Pédologie*, **27**(1), 23–36.

Aller, L., Bennett, T., Lehr, J.H., Hackett, G., Petty, R.J., & Thornhill, J. 1987. *DRASTIC : a standarized system for evaluating ground water pollution potential using hydrogeologic settings.* U.S. Environmental Protection Agency.

Ardakani, M. S., Rehbock, J. T., & McLaren, A. D. 1974. Oxidation of ammonium to nitrate in a soil column. *Soil Science Society of America Journal*, **38**(1), 96–99.

Aubert, G., & Ségalen, P. 1966. Projet de classification des sols ferrallitiques. *Cahiers ORSTOM, série Pédologie*, **4**(4), 97–112.

Aubry, Ch., Paillat, J.-M., & Guerrin, F. 2006. A conceptual representation of animal waste management at the farm scale: The case of the Reunion Island. *Agricultural Systems*, **88**(2-3), 294–315.

Badaut, D., Decarreau, A., & Besson, G. 1992. Ferripyrophyllite and related Fe^{3+}-rich 2:1 clays in recent deposits of Atlantis II Deep, Red Sea. *Clay minerals*, **27**(2), 227–244.

Badiane, A. N., Diagne, M., Fall, A., Faye, A., Kébé, M., Kholjma, M., & Sène, M. 2000. *Gestion et transformation de la matière organique : synthèse des travaux de recherche menés au Sénégal depuis 1945.* Institut sénégalais de la recherche agricole (Isra).

Baize, D. 1997. *Teneurs totales en éléments traces métalliques dans les sols (France).* Inra (éd.), Paris.

Barrow, N.J. 1986. Reaction of Anions and Cations with Variable-Charge Soils. *Advances in Agronomy*, **38**, 183–230.

Bourrié, G., Berthelin, J., Génin, J.-M. R., Trolard, F., Klingelhöfer, G., Abdelmoula, M., Appenzeller, B., Benali, O., Bernhardt, B., Block, J.-C., Ehrhardt, J.-J., Feder, F., Géhin, A., Gury, M., Herbillon, A. J., Jeanroy, E., Jorand, F., Ona-Nguema, G., Refait, Ph., & Stemmler, S. 2000. Rôle des processus biogéochimiques sur les transformations

minéralogiques des oxydes de fer dans les sols hydromorphes. *Les composés lamellaires. Réunion de la société française de minéralogie et de cristallographie et du groupe français des argiles, Porquerolles, France, 2000/10/09-11.*

Bourrié, G., Trolard, F, Refait, Ph., & Feder, F. 2002. A solid solution model for FeII–FeIII–Mg green rust (fougerite): structural and geochemical constraints. *17th World Congress of Soil Science, Bangkok, Thailand, 2002/08/14-21.*

Bourrié, G., Trolard, F., Refait, Ph., & Feder, F. 2004. A solid-solution model for Fe(II)-Fe(III)-Mg green rust and Fougerite and estimation of their Gibbs free energies of formation. *Clays and Clay Minerals*, **52**(3), 382–394.

Bourrié, G., Trolard, F., & Feder, F. 2007. Critère d'identification de la fougérite dans les sols hydromorphes et nature de l'anion compensateur. *9es journées nationales d'études des sols, Angers, France, 2007/04/03-05.*

Bradl, H. B. 2004. Adsorption of heavy metal ions on soils and soils constituents. *Journal of Colloid and Interface Science*, **277**(1), 1–18.

Brown, C., Hart, A., Lewis, K., & Dubus, I. 2003. p-EMA (I): simulating the environmental fate of pesticides for a farm-level risk assessment system. *Agronomie*, **23**(1), 67–74.

Buurman, P., de Boer, K., & Pape, Th. 1997. Laser diffraction grain-size characteristics of Andisols in perhumid Costa Rica: the aggregate size of allophane. *Geoderma*, **78**, 71–91.

Carrillo-Gonzalez, R., Simunek, J., Sauvé, S., & Adriano, D. 2006. Mechanisms and Pathways of Trace Element Mobility in Soils. *Pages 111–178 of: Advances in Agronomy*, vol. 91. Elsevier.

Chahal, M. K., & Toor, G. S. 2011. Trace metal leaching in a spodosol irrigated with tomato packinghouse wastewater: Trace metal leaching in a spodosol. *Soil Use and Management*, **27**(4), 480–490.

Chaney, R. L. 2012. Food safety issues for mineral and organic fertilizers. *Advances in Agronomy*, **117**(51), e116.

Chang, A. C., Warneke, J. E., Page, A. L., & Lund, L. J. 1984. Accumulation of Heavy Metals in Sewage Sludge-Treated Soils. *Journal of Environmental Quality*, **13**(1), 87–91.

Clay, D. E., Zheng, Z., Liu, Z., Clay, S. A., & Trooien, T. P. 2004. Bromide and Nitrate Movement through Undisturbed Soil Columns. *Journal of Environment Quality*, **33**(1), 338.

Cofie, O., Bradford, A. A., & Dreschel, P. 2006. Recycling of urban organic waste for urban agriculture. *Pages 209–242 of: Cities farming for the future - Urban agriculture for sustainable cities.* René van Veenhuizen (ed.), RUAF Foundation, IDRC and IIRR.

Collin, B., & Doelsch, E. 2008. *Evaluation de la mobilité et de la phytodisponibilité des éléments traces métalliques des sols.* Cirad.

Colmet-Daage, F., Gautheyrou, J., Gautheyrou, M., & de Kimpe, C. 1973. Étude des sols à allophane dérivés de matériaux volcaniques des Antilles et d'Amérique latine à l'aide de techniques de dissolution différentielle. *Cahiers ORSTOM, série Pédologie*, **11**(2), 97–120.

Cornell, R.M., & Schwertmann, U. 1996. *The Iron Oxides: Structure, Properties, Reactions, Occurences and Uses.* Second Edition. VCH, Weinheim, Basel, New York.

Cornu, S., Neal, C., Ambrosi, J.-P., Whitehead, P., Neal, M., Sigolo, J., & Vachier, P. 2001. The environmental impact of heavy metals from sewage sludge in ferralsols (Sao Paulo, Brazil). *Science of the total environment*, **271**(1), 27–48.

CPCS. 1967. *Classification des sols.* Commission de pédologie et cartographie des sols. École nationale supérieure agronomique, Grignon, France.

Diacono, M., & Montemurro, F. 2010. Long-term effects of organic amendments on soil fertility. A review. *Agronomy for Sustainable Development*, **30**(2), 401–422.

Doelsch, E. 2010. *Étude du comportement des éléments majeurs et traces à l'interface eau-sol-plante : une approche multi-technique et multi-échelle.* Mémoire pour l'obtention de l'habilitation à diriger des recherches. Université de Aix-Marseille III.

Doelsch, E., Van de Kerchove, V., & Saint Macary, H. 2006. Heavy metal content in soils of Réunion (Indian Ocean). *Geoderma*, **134**(1-2), 119–134.

Doelsch, E., Masion, A., Moussard, G. D., Chevassus-Rosset, Cl., & Wojciechowicz, O. 2010. Impact of pig slurry and green waste compost application on heavy metal exchangeable fractions in tropical soils. *Geoderma*, **155**(3-4), 390–400.

Doelsch, E., Basile-Doelsch, I., Bottero, J. Y., Cazevieille, P., Chevassus-Rosset, C., Feder, F., Garnier, J. M., Gaudet, J. P., Legros, S., Levard, C., Masion, A., Moussard, G. D., Rose, J., & Saint Macary, H. 2011. Recyclage agricole des déchets organiques dans les sols tropicaux (île de la Réunion) : quel impact sur les transferts d'éléments traces métalliques? *Étude et Gestion des Sols*, **18**(3), 175–186.

Drits, V.A., & Manceau, A. 2000. A model for the mechanism of Fe^{3+} to Fe^{2+} reduction in dioctahedral smectites. *Clays and Clay Minerals*, **48**(2), 185–195.

Duwig, C., Becquer, Th., Clothier, B. E., & Vauclin, M. 1999. A simple dynamic method to estimate anion retention in an unsaturated soil. *Comptes Rendus de l'Académie des Sciences - Series IIA - Earth and Planetary Science*, **328**(11), 759–764.

Duwig, C., Normand, B., Vauclin, M., Vachaud, G., Green, S.R., & Becquer, Th. 2003. Evaluation of the WAVE model for predicting nitrate leaching for two contrasted soil and climate conditions. *Vadose Zone Journal*, **2**(1), 76–89.

Egiarte, G., Camps Arbestain, M., Ruíz-Romera, E., & Pinto, M. 2006. Study of the chemistry of an acid soil column and of the corresponding leachates after the addition of an anaerobic municipal sludge. *Chemosphere*, **65**(11), 2456–2467.

Eneji, A.E., Honna, T., Yamamoto, S., Saito, T., & Masuda, T. 2002. Nitrogen transformation in four japanese soils following manure + urea amendment. *Communications in Soil Science and Plant Analysis*, **33**(1&2), 53–66.

Fall, A. S., Fall, S. T., Cissé, I., Badiane, A. N., Diao, M. B., & Fall, C. A. 2001. *Cités horticoles en sursis? L'agriculture urbaine dans les grandes Niayes au Sénégal.* Centre de recherches pour le développement international (CRDI).

Fanning, D.S., Rabenhorst, M.C., May, L, & Wagner, D.P. 1989. Oxidation state of iron in glauconite from oxidized and reduced zones of soil-geologic columns. *Clays and Clay Minerals*, **37**(1), 59–64.

Feder, F. 2013. Soil map update: Procedure and problems encountered for the island of Réunion. *Catena*, **110**, 215–224.

Feder, F., & Bourgeon, G. 2009. Mise à jour de la carte des sols de l'île de la Réunion. Démarche suivie et problèmes rencontrés. *Étude et Gestion des Sols*, **16**(2), 85–99.

Feder, F., & Findeling, A. 2007. Retention and leaching of nitrate and chloride in an andic soil after pig manure amendment. *European Journal of Soil Science*, **58**(2), 393–404.

Feder, F., Bourrié, G., & Trolard, F. 1998. *In situ* continuous monitoring of soil solution chemistry. *Mineralogical magazine*, **A, 62**, 441–442.

Feder, F., Bourrié, G., & Trolard, F. 1999a. Mesures en continu et *in situ* des paramètres de la solution du sol. *Réunion de la direction scientifique « Environnement Forêt et Agriculture », Évian, France, 1999/02.*

Feder, F., Trolard, F., Bourrié, G., Klingelhöfer, G., & Génin, J.-M. R. 1999b. Utilisation *in situ* de la spectrométrie Mössbauer pour la caractérisation des oxydes de fer dans les sols hydromorphes. *Journées « jeunes chercheurs », association française pour l'étude du sol (AFES), Paris, France, 1999/11/18.*

Feder, F., Klingelhofer, G., Trolard, F., Bernhardt, B., Bourrié, G., & Génin, J.-M. R. 2000. Suivi *in situ* par spectrométrie Mössbauer de la dynamique des oxydes de fer dans un sol hydromorphe. *6es journées nationales d'étude des sols, Nancy, France, 2000/04/25-28.*

Feder, F., Klingelhofer, G., Trolard, F., & Bourrie, G. 2002. In situ Mossbauer spectroscopy and soil solution monitoring to follow spatial and temporal iron dynamics. *17th World Congress of Soil Science, Bangkok, Thailand, 2002/08/14-21.*

Feder, F., Trolard, F., Klingelhöfer, G., & Bourrié, G. 2005. *In situ* Mössbauer spectroscopy: Evidence for green rust (fougerite) in a gleysol and its mineralogical transformations with time and depth. *Geochimica et Cosmochimica Acta*, **69**(18), 4463–4483.

Feder, F., Olivier, R., Alary, K., & Bourgeon, G. 2006. Characterization of a soil catena on the western slope of the Piton des Neiges volcano (la Réunion). *In: 18th world Congress of Soil Science, 2006/07/9-15, Philadelphia, Pennsylvania, USA.*

Feder, F., Robin, J.-G., & Bourgeon, G. 2008. Cartographie de la vulnérabilité des aquifères de l'ouest de l'île de la Réunion au transfert de polluants = Cartography of groundwater vulnerability to polluants transfer in Western part of La Reunion Island. *In: IWRA, 13^{e} congrès mondial de l'eau, Montpellier, 1-4 septembre 2008.*

Feder, F., Bochu, V., Findeling, A., & Doelsch, E. 2015. Repeated pig manure applications modify nitrate and chloride competition and fluxes in a Nitisol. *Science of The Total Environment*, **511**, 238–248.

Formentini, T., Mallmann, F., Pinheiro, A., Fernandes, C., Bender, M., da Veiga, M., dos Santos, D., & Doelsch, E. 2015. Copper and zinc accumulation and fractionation in a clayey Hapludox soil subject to long-term pig slurry application. *Science of The Total Environment*, **536**(Dec.), 831–839.

Franco, A., Schuhmacher, M., Roca, E., & Luis Domingo, J. 2006. Application of cattle manure as fertilizer in pastureland: Estimating the incremental risk due to metal accumulation employing a multicompartment model. *Environment International*, **32**(6), 724–732.

Fujikawa, Y., & Fukui, M. 2001. Vertical Distribution of Trace Metals in Natural Soil Horizons from Japan Part 2: Effects of Organic Components in Soil. *Water, Air, and Soil Pollution*, **131**(1-4), 305–328.

Gaye, M., & Niang, S. 2010. *Manuel des bonnes pratiques de l'utilisation saine des eaux usées dans l'agriculture urbaine.* ENDA RUP, Dakar.

Guerbet, M., & Jouany, J. M. 2002. Value of the SIRIS method for the classification of a series of 90 chemicals according to risk for the aquatic environment. *Environmental Impact Assessment Review*, **22**(4), 377–391.

Helgeson, H. C. 1968. Evaluation of irreversible reactions in geochemical processes involving minerals and aqueous solutions – I. Thermodynamic relations. *Geochimica et Cosmochimica Acta*, **32**, 853–877.

Heller-Kallai, L. 1997. Reduction and reoxidation of nontronite: the data reassessed. *Clays and clay minerals*, **45**(3), 476–479.

Hinojosa, B. M., García-Ruiz, R., & Carreira, J. A. 2010. Utilizing microbial community structure and function to evaluate the health of heavy metal polluted soils. *Pages 185–224 of: Soil Biology - Soil Heavy Metals.* Springer.

Hodomihou, N. R., Feder, F., Doelsch, E., Agbossou, E. K., Amadji, G. L., Ndour-Badiane, Y., Cazevieille, P., Chevassus-Rosset, C., & Masse, D. 2015. Caractérisation des risques de contamination des agrosystèmes périurbains de Dakar par les éléments traces métalliques. *Agronomie Africaine*, **27**(1), 69–82.

Hodomihou, N. R., Feder, F., Masse, D., Agbossou, E. K., Amadji, G. L., Ndour-Badiane, Y., & Doelsch, E. 2016. Diagnostic de contamination des agrosystèmes périurbains

de Dakar par les éléments traces métalliques. *Biotechnologie, Agronomie, Société et Environnement*, **20**(3).

Houot, S., Cambier, Ph., Benoit, P., Bodineau, G., Deschamps, M., Jaulin, A., Lhoutellier, C., & Barriuso, E. 2009. Effet d'apports de composts sur la disponibilité de micropolluants métalliques et organiques dans un sol cultivé. *Étude et gestion des sols*, **16**(3/4), 255–274.

Houot, S., Pons, M.-N., Pradel, M., Aubry, Ch., Augusto, L., Barbier, R., Benoit, P., Brugère, H., Casellas, M., Chatelet, A., Dabert, P., Doussan, I., Etrillard, Cl., Fuchs, J., Genermont, S., Giamberini, L., Helias, A., Jardé, E., Lupton, S., Marron, N., Menasseri, S., Mollier, A., Morel, Ch., Mougin, Ch., Parnaudeau, V., Pourcher, A.-M., Rychen, G., Smolders, E., Topp, E., Vieublé, L., Viguie, C., Caillaud, M. A., Girard, F., Savini, I., De Marechal, S., & Le Perchec, S. 2014. *Valorisation des matières fertilisantes d'origine résiduaire sur les sols à usage agricole ou forestier. Impacts agronomiques, environnementaux, socio-économiques.* Synthèse de l'expertise scientifique collective, INRA, CNRS, IRSTEA.

IUSS Working Group, WRB. 2007. *World Reference Base for Soil Resources 2006, first update 2007.* World Soil Resources Reports No. 103. Rome: FAO.

Katou, H. 2004. Determining competitive nitrate and chloride adsorption in an andisol by the unsaturated transient flow method. *Soil Science and Plant Nutrition*, **50**(1), 119–127.

Katou, H, Clothier, B. E., & Green, S.R. 1996. Anion Transport Involving Competitive Adsorption during Transient Water Flow in an Andisol. *Soil Science Society of America Journal*, **60**(5), 1368.

Kelly, J. J., Haggblom, M. M., & Tate, R. L. 2003. Effects of heavy metal contamination and remediation on soil microbial communities in the vicinity of a zinc smelter as indicated by analysis of microbial community phospholipid fatty acid profiles. *Biology and Fertility of Soils*, **38**(2), 65–71.

Klingelhöfer, G., Trolard, F., Bernhardt, B., Bourrié, G., Feder, F., & Génin, J.-M. R. 1999a. The monitoring of iron mineralogy and oxidation states by Mössbauer spectroscopy in the field; the green rust mineral in hydromorphic soils. *International conference on applications of Mössbauer effect, Garmisch-Partenkirchen, Germany, 1999/08/30-09/03.*

Klingelhöfer, G., Trolard, F., Bourrié, G., Feder, F., & Génin, J.-M. R. 1999b. The monitoring of iron mineralogy and oxidation states by Mössbauer spectroscopy in the field; the Green Rust mineral in hydromorphic soils. *American Geophysical Union, Fall Meeting, San Francisco, USA, 1999/12/13-17.*

Komadel, P., Madejova, J., & Stucki, J. W. 1995. Reduction and reoxidation of nontronite: Questions of reversibility. *Clays and Clay Minerals*, **43**(1), 105–110.

Kramer, C. J., & Duinker, J. C. (Eds). 2013. *Complexation of trace metals in natural waters.* Proceedings of the International Symposium, May 2–6 1983, Texel, The Netherlands (Vol. 1). Springer Science & Business Media.

Lahbib-Burchard, T., Wassenaar, T., Doelsch, E., Feder, F., & Bravin, M. 2012. Prédiction de l'accumulation à long-terme des éléments traces métalliques dans les sols en contexte de recyclage agricole de produits résiduaires organiques en milieu tropical : validation d'un modèle par mesures in situ. *50 ans de l'Orgeval et 37es journées du GFHN.*

Legros, S., Chaurand, P., Rose, J., Masion, A., Briois, V., Ferrasse, J.-H., Saint Macary, H., Bottero, J.-Y., & Doelsch, E. 2010. Investigation of copper speciation in pig slurry by a multitechnique approach. *Environmental science & technology*, **44**(18), 6926–6932.

Legros, S., Doelsch, E., Feder, F., Moussard, G., Sansoulet, J., Gaudet, J. P., Rigaud, S., Basile-Doelsch, I., Saint Macary, H., & Bottero, J. Y. 2013. Fate and behaviour of Cu

and Zn from pig slurry spreading in a tropical water–soil–plant system. *Agriculture, Ecosystems & Environment*, **164**, 70–79.

L'Herroux, L., Le Roux, S., Appriou, P., & Martinez, J. 1997. Behaviour of metals following intensive pig slurry applications to a natural field treatment process in Brittany (France). *Environmental Pollution*, **97**(1), 119–130.

Lipoth, S. L., & Schoenau, J. J. 2007. Copper, zinc, and cadmium accumulation in two prairie soils and crops as influenced by repeated applications of manure. *Journal of Plant Nutrition and Soil Science*, **170**(3), 378–386.

Maeda, M., Zhao, B., Ozaki, Y., & Yoneyama, T. 2003. Nitrate leaching in an Andisol treated with different types of fertilizers. *Environmental Pollution*, **121**(3), 477–487.

Mantovi, P., Bonazzi, G., Maestri, E., & Marmiroli, N. 2003. Accumulation of copper and zinc from liquid manure in agricultural soils and crop plants. *Plant and soil*, **250**(2), 249–257.

McBride, M. B. 1989. Reactions Controlling Heavy Metal Solubility in Soils. *Advances in Soil Science*, **10**, 1–56.

McBride, M. B. 1995. Toxic Metal Accumulation from Agricultural Use of Sludge: Are USEPA Regulations Protective? *Journal of environmental quality*, **24**, 5–18.

Müller, C., Stevens, R.J., & Laughlin, R.J. 2003. Evidence of carbon stimulated N transformations in grassland soil after slurry application. *Soil Biology & Biochemistry*, **35**, 285–293.

Mochoge, B.O. 1984. Simulation of nitrate movement in undisturbed soil columns. *Agriculture, Ecosystems & Environment*, **11**, 105–115.

Nanzyo, M., Shoji, S., & Dahlgren, R.A. 1993. Physical characteristics of volcanic ash soils. *Pages 189–207 of: Volcanic Ash Soils—Genesis, Properties and Utilization. S. Shoji, M. Nanzyo and R.A. Dahlgren Eds.* Developments in Soil Science, no. 21. Elsevier, Amsterdam.

N'Dienor, M. 2006. *Fertilité et gestion de la fertilisation dans les systèmes maraîchers périurbains des pays en développement: intérêts et limites de la valorisation agricole des déchets urbains dans ces systèmes, cas de l'agglomération d'Antananarivo (Madagascar).* Thèse de doctorat de l'université d'Antananarivo, école supérieure des sciences agronomiques (ESSA), INA Paris-Grignon.

Ngom, S., Seydou, T., Thiam, M. B., & Anastasie, M. 2012. Contamination des produits agricoles et de la nappe phréatique par les pesticides dans la zone des Niayes au Sénégal. *Synthèse: Revue des Sciences et de la Technologie*, **25**(1), 119–130.

Nicholson, F. A., Chambers, B. J., Williams, J. R., & Unwin, R. J. 1999. Heavy metal contents of livestock feeds and animal manures in England and Wales. *Bioresource Technology*, **70**(1), 23–31.

Novak, J. M., Watts, D. W., & Stone, K. C. 2004. Copper and zinc accumulation, profile distribution, and crop removal in coastal plain soils receiving long-term, intensive applications of swine manure. *Transactions of the ASAE*, **47**(5), 1513–1522.

Oustrière, N., Lahbib-Burchard, T., Doelsch, E, Feder, F., Wassenaar, T., & Bravin, M. 2013. Predictive modelling of the long-term accumulation of trace metals in tropical soils amended with organic wastes - field trial validation. *In: 15e conférence internationale Ramiran : recyclage des résidus organiques pour l'agriculture : de la gestion des déchets aux services écosystémiques. Versailles, France, 2013/06/03-05.*

Paul, E.A., & Clark, F.E. 1989. Reduction and transport of nitrate. *Pages 81–85 of: Soil microbiology and biochemistry*, vol. 9.

Payet, N. 2005. *Impact des apports de lisier sur un sol cultivé de la Réunion : étude expérimentale et modélisation des flux d'eau et de nitrate dans la zone non saturée.* Thèse de l'université de la Réunion.

Payet, N., Findeling, A., Chopart, J.-L., Feder, F., Nicolini, E., Saint Macary, H., & Vauclin, M. 2009. Modelling the fate of nitrogen following pig slurry application on a tropical cropped acid soil on the island of Réunion (France). *Agriculture, Ecosystems & Environment*, **134**(3–4), 218–233.

Payet, N., Nicolini, E., Rogers, K., Saint Macary, H., & Vauclin, M. 2010. Evidence of soil pollution by nitrates derived from pig effluent using ^{18}O and ^{15}N isotope analyses. *Agronomy for Sustainable Development*, **30**(4), 743–751.

Qafoku, N. P., Sumner, M. E, & Radcliffe, D. E. 2000. Anion transport in column of variable charge subsoils: Nitrate and chloride. *Journal of Environmental Quality*, **29**(2), 484–493.

Raunet, M. 1988. *Carte morpho-pédologique au 1:50 000 en quatre feuilles.* Département de la Réunion. Cirad-Irat et région Réunion.

Raunet, M. 1989. *Littoral ouest – Rivière des Galets à ravine du Cap. Carte morpho-pédologique. Aptitudes à l'irrigation au 1:10 000 en cinq feuilles.* Cirad-Irat et conseil général de la Réunion.

Raunet, M. 1991a. *Le milieu physique et les sols de l'île de la Réunion.* Cirad Réunion.

Raunet, M. 1991b. *Périmètres du bras de Cilaos et du bras de la Plaine. Carte morpho-pédologique. Aptitudes à l'irrigation au 1:10 000 en six feuilles.* Cirad-Irat et conseil général de la Réunion.

Richards, B. K., Steenhuis, T. S., Peverly, J. H., & McBride, M. B. 2000. Effect of sludge-processing mode, soil texture and soil pH on metal mobility in undisturbed soil columns under accelerated loading. *Environmental pollution*, **109**(2), 327–346.

Riquier, J. 1960. *Notice de la carte pédologique de reconnaissance. Ile de la Réunion.* I.S.R.M. Tananarive – Tsimbazaza. + carte à 1/100 000 en couleur.

Rivett, M. O., Buss, S. R., Morgan, Ph., Smith, J. W. N., & Bemment, Ch. D. 2008. Nitrate attenuation in groundwater: A review of biogeochemical controlling processes. *Water Research*, **42**(16), 4215–4232.

Ros, M., Klammer, S., Knapp, B., Aichberger, K., & Insam, H. 2006. Long-term effects of compost amendment of soil on functional and structural diversity and microbial activity. *Soil Use and Management*, **22**(2), 209–218.

Saar, R. A., & Weber, J. H. 1982. Fulvic acid: modifier of metal-ion chemistry. *Environmental science & technology*, **16**(9), 510A–517A.

Sall, M., & Vanclooster, M. 2009. Assessing the well water pollution problem by nitrates in the small scale farming systems of the Niayes region, Senegal. *Agricultural Water Management*, **96**(9), 1360–1368.

Shirazi, S.M., Imran, H.M., & Akib, S. 2012. GIS-based DRASTIC method for groundwater vulnerability assessment: a review. *Journal of Risk Research*, **15**(8), 991–1011.

Sierra, J. 2002. Nitrogen mineralization and nitrification in a tropical soil: effects of fluctuating temperature conditions. *Soil Biology and Biochemistry*, **34**(9), 1219–1226.

Sánchez, M., & González, J.L. 2005. The fertilizer value of pig slurry. I. Values depending on the type of operation. *Bioresource Technology*, **96**(10), 1117–1123.

Soubrand-Colin, M., Neel, C., Bril, H., Grosbois, C., & Caner, L. 2007. Geochemical behaviour of Ni, Cr, Cu, Zn and Pb in an Andosol–Cambisol climosequence on basaltic rocks in the French Massif Central. *Geoderma*, **137**(3-4), 340–351.

Sposito, G. 1981. *The thermodynamics of soil solutions.* Oxford University Press.

Staff, Soil Survey. 2014. *Keys to Soil Taxonomy, 12th ed.* USDA-Natural Resources Conservation Service, Washington, DC.

Stucki, J. W., & Tessier, D. 1991. Effects of iron oxidation state on the texture and structural order of Na-nontronite gels. *Clays and Clay Minerals*, **39**(2), 137–143.

Stucki, J. W., Golden, D. C., & Roth, Ch. B. 1984. Effects of reduction and reoxidation of structural iron on the surface charge and dissolution of dioctahedral smectites. *Clays and Clay Minerals*, **32**(5), 350–356.

Tella, M., Doelsch, E., Letourmy, P., Chataing, S., Cuoq, F., Bravin, M.N., & Saint Macary, H. 2013. Investigation of potentially toxic heavy metals in different organic wastes used to fertilize market garden crops. *Waste Management*, **33**(1), 184–192.

Tella, M., Bravin, M., Thuriès, L., Cazevieille, P., Chevassus-Rosset, Cl., Collin, B., Chaurand, P., Legros, S., & Doelsch, E. 2016. Increased zinc and copper availability in organic waste amended soil potentially involving distinct release mechanisms. *Environmental Pollution*, **212**(May), 299–306.

Trolard, F., Génin, J.-M. R., Abdelmoula, M., Bourrié, G., Humbert, B., & Herbillon, A. J. 1997. Identification of a green rust mineral in a reductomorphic soil by Mossbauer and Raman spectroscopies. *Geochimica et Cosmochimica Acta*, **61**(5), 1107–1111.

Trolard, F., Bourrié, G., Abdelmoula, M., Refait, Ph., & Feder, F. 2007. Fougerite, a New Mineral of the Pyroaurite-Iowaite Group: Description and Crystal Structure. *Clays and Clay Minerals*, **55**(3), 323–334.

Vaillant, M., Jouany, J.M., & Devillers, J. 1995. A multicriteria estimation of the environmental risk of chemicals with the SIRIS method. *Toxicology modeling*, **1**(1), 57–72.

Veronica, Ch., Francisco, S.S., Francisco, M.J., & Maria, A. H. 2013. Comparative analysis of cost on slurry application in Chile and Argentina dairy farms. *In: 15^{e} conférence internationale Ramiran : recyclage des résidus organiques pour l'agriculture : de la gestion des déchets aux services écosystémiques. Versailles, France, 2013/06/03-05.*

Vogeler, I. 2001. Copper and calcium transport through an unsaturated soil column. *Journal of environmental quality*, **30**(3), 927–933.

Vogeler, I., Scotter, D. R., Clothier, B. E., & Tillman, R. W. 1998. Anion transport through intact soil columns during intermittent unsaturated flow. *Soil and Tillage Research*, **45**(1–2), 147–160.

Wassenaar, T., Doelsch, E., Feder, F., Guerrin, F., Paillat, J. M., Thuriès, L., & Saint Macary, H. 2014. Returning Organic Residues to Agricultural Land (RORAL) – Fuelling the Follow -the- Technology approach. *Agricultural Systems*, **124**, 60–69.

Willmott, C. J. 1981. On the validation of models. *Physical geography*, **2**(2), 184–194.

Winckell, A., Zebrowski, Cl., & Delaune, M. 1991. Évolution du modèle quaternaire et des formations superficielles dans les Andes de l'Équateur : 2. Quelques aspects de l'histoire paléogéographique quaternaire. *Géodynamique*, **6**(2), 119–139.

Zebrowski, Cl. 1975. Etude d'une climatoséquence dans l'île de la Réunion. *Cahiers ORSTOM, série Pédologie*, **13**(314), 255–278.

TABLE DES MATIÈRES

TABLE DES FIGURES

LISTE DES TABLEAUX

ANNEXES

Sélection d'articles relatifs aux processus d'oxydo-réduction dans les sols hydromorphes :

- Feder, F., Trolard, F., Klingelhöfer, G. and Bourrié, G. 2005. *In situ* Mössbauer spectroscopy: Evidence for green rust (fougerite) in a gleysol and its mineralogical transformations with time and depth. *Geochimica et Cosmochimica Acta*, 69(18), 4463-4483. http://dx.doi.org/10.1016/j.gca.2005.03.042
- Bourrié, G., Trolard, F., Refait, Ph. and Feder, F. 2004. A solid solution model for Fe(II)-Fe(III)-Mg green rust "Fougerite": structural and geochemical constraints. *Clays and Clay Minerals*, 52(3), 382-394. http://dx.doi.org/10.1346/CCMN.2004.0520313

Sélection d'articles relatifs aux transferts de nitrates à l'échelle de la colonne de sol :

- Feder, F., Bochu, V., Findeling, A. and Doelsch, E. 2015. Repeated pig manure applications modify nitrate and chloride competition and fluxes in a Nitisol. *Science of the Total Environment*, 511, 238–248. http://dx.doi.org/10.1016/j.scitotenv.2014.12.059
- Feder, F. and Findeling, A. 2007. Retention and leaching of nitrate and chloride in an andic soil after pig manure amendment. *European Journal of Soil Science*, 58(2), 393-404. http://dx.doi.org/10.1111/j.1365-2389.2006.00885.x

Sélection d'un article relatif aux transferts de nitrates de l'échelle de la parcelle :

- Payet, N., Findeling, A., Chopart, J.-L., Feder, F., Nicolini, E., Saint Macary, H. and Vauclin, M. 2009. Modelling the fate of nitrogen following pig slurry application on a tropical cropped acid soil on the island of Réunion (France). *Agriculture, Ecosystems & Environment*, 134(3-4), 218-233. http://dx.doi.org/10.1016/j.agee.2009.07.004

Sélection d'articles relatifs aux transferts des nitrates à l'échelle du territoire :

- Alary, K., Babre, D., Caner, L., Feder, F., Szwarc, M., Naudan, M. and Bourgeon, G. 2013. Pretreatment of Soil Samples Rich in Short-Range-Order Minerals Before Particle-Size Analysis by the Pipette Method. *Pedosphere*, 23(1), 20-28. http://dx.doi.org/10.1016/S1002-0160(12)60076-9
- Feder, F. 2013. Soil map update: Procedure and problems encountered for the island of Réunion. *Catena*, 110, 215-224. http://dx.doi.org/10.1016/j.catena.2013.06.019

Sélection d'un article relatif aux transferts des ETM à l'échelle de la parcelle :

- Legros, S., Doelsch, E., Feder, F., Moussard, G. D., Sansoulet, J., Gaudet, J.-P., Rigaud, S., Basile-Doelsch, I., Saint Macary, H. and Bottero, J. Y. 2013. Fate and behaviour of Cu and Zn from pig slurry spreading in a tropical water-soil-plant system. *Agriculture, Ecosystems & Environment*, 164, 70-79. http://dx.doi.org/10.1016/j.agee.2012.09.008

Geochimica et Cosmochimica Acta, Vol. 69, No. 18, pp. 4463–4483, 2005

0016-7037/05 $30.00 + .00

doi:10.1016/j.gca.2005.03.042

In situ Mössbauer spectroscopy: Evidence for green rust (fougerite) in a gleysol and its mineralogical transformations with time and depth

FRÉDÉRIC FEDER,[1,2,*] FABIENNE TROLARD,[2] GÖSTAR KLINGELHÖFER,[3] and GUILHEM BOURRIÉ[2]

[1]Centre de Coopération Internationale en Recherche Agronomique pour le Développement, Internal Research Unit "Environmental Risks of Recycling," station de La Bretagne, BP 20, F-97408 Saint-Denis Messagerie Cedex 9, Île de La Réunion, France
[2]Institut National de la Recherche Agronique, Unité de Recherche de Géochimie des Sols et des Eaux, Europôle de l'Arbois, BP 80, F-13545 Aix-en-Provence CEDEX 04, France
[3]Institut für Anorganische und Analytische Chemie, Johannes Gutenberg-Universität Mainz, Staudinger Weg 9, D-55099 Mainz, Germany

(*Received August 4, 2004; accepted in revised form March 16, 2005*)

Abstract—A miniaturized Mössbauer spectrometer, adapted to the Earth's conditions from the instrument developed for Mars space missions, has been used for the first time to study in situ variations with depth and transformations with time of iron minerals in a gleysol. The instrument is set into a PVC tube and can be moved up and down precisely (±1 mm) at the desired depth. Mössbauer spectra were obtained from 15 to 106 cm depth and repeated exactly at the same point at different times to follow mineralogical transformations with time. X-ray diffraction (XRD) and selective extraction techniques were performed on soil samples. The piezometric level of the water table was measured and the composition of the soil solution was monitored in situ and continuously, with a multiparametric and automatic probe. All the Mössbauer spectra obtained are characteristic of Fe(II)-Fe(III) green rust–fougerite, a natural mineral of the meixnerite group, that is, whose structural formula is: $[Fe^{II}_{1-x}\,Mg_y\,Fe^{III}_x\,(OH)_{2+2y}]^{x+}[xA, mH_2O]^{x-}$, where x is the ratio $Fe^{3+}/Fe_{tot.}$ and A the intercalated anion. The name of fougerite has been formally approved by the Commission on New Minerals and Mineral Names of IMA (number 2003-057), on January 29, 2004. No other iron phases have been found by this way or by XRD. About 90% of total iron is extractible by dithionite-citrate-bicarbonate, and 60% by citratebicarbonate. In the horizons showing oximorphic properties that are in the upper part of the studied soil profile, x ratio in fougerite, deduced from Mössbauer spectra, is approximately 2/3. In the deepest horizons that show reductomorphic properties, x ratio is only 1/3. Fast mineralogical transformations were observed at well-defined points in soil, as evidenced by x ratio variations observed when Mössbauer spectra were acquired at different times at the same depth. Variations of the level of the water table and of pe and pH of the soil solution were simultaneously observed and could explain these mineralogical transformations. A ternary solid solution model previously proposed for OH-fougerite has been extended to chloride, sulphate, and carbonate green rusts to estimate the Gibbs free energies of formation of fougerite, providing for possible anions other than OH^- in the interlayer and for Mg substitution. Soil solutions appear as largely oversaturated with respect to OH-fougerite, either oversaturated or undersaturated to "carbonate-fougerite" and "sulphate-fougerite", and largely undersaturated with respect to "chloro-fougerite". Fougerite forms most likely from oversaturated solutions by coprecipitation of Fe^{3+} with Fe^{2+} and Mg^{2+}. Oxidation and reduction are driven by pH and pe variations, with both long timescale variations and short duration events. Exactly as synthetic green rusts are very reactive compounds in the laboratory, fougerite is thus a very reactive mineral and readily forms, dissolves, or evolves in soils. *Copyright © 2005 Elsevier Ltd*

1. INTRODUCTION

Iron in soil is one of the five most important chemical elements in abundance. It plays a major role in biogeochemical cycles as electron donor and acceptor in oxido-reduction reactions; they are tthe main source of energy for life. By decreasing order of abundance, iron minerals found in soils are iron oxides, clay minerals, and less commonly, iron sulfides and carbonates (Stucki, 1988). Soil genesis and soil properties are influenced by iron in minerals (Schwertmann, 1988) and in soil solution (Ponnamperuma, 1972).

Indeed, iron oxides can be precipitated by various organisms (Fischer, 1988; Fredrickson et al., 1998): Fe^{3+} in clay minerals can be reduced to Fe^{2+} by bacteria (Stucki et al., 1987; Kostka et al., 1996) and iron in solution can be complexed by organic ligands (Stevenson, 1994; Stumm and Morgan, 1996; Zsolnay, 1996).

Iron minerals occur mainly as fine particles that develop a large surface area and closely associate to other colloidal particles (De Boodt et al., 1991; Jolivet, 1994). Due to the low solubility of Fe^{3+} minerals, iron in soil is essentially mobile in solution as Fe^{2+}. Iron distribution in soil landscape is the consequence of oxido-reduction processes (Van Breemen, 1988; Stumm and Sulzberger, 1992) that influence soil colour. Generally, white (albic) horizons are characteristic of the absence of iron oxides. In well drained soils, hematite gives a red colour, goethite a yellow colour, and ferrihydrite a brown colour (Cornell and Schwertmann, 2003). But in hydromorphic soils, while lepidocrocite gives an orange colour, green and blue colours have been ascribed to mixed Fe^{2+} and Fe^{3+} hydroxides known as green rusts (GRs; FAO, 1998; Taylor, 1980). Similar in structure to pyroaurite, they consist of positively charged brucitelike layers, alternating with interlayer anions and water molecules (Allmann, 1968).

Many physical and chemical techniques have been used to

* Author to whom correspondence should be addressed (frederic.feder@cirad.fr).

study iron oxides, such as X-ray diffraction (XRD), electron microscopy, Mössbauer (Murad, 1988; Murad and Cashion, 2004), Raman or, extended X-ray absorption fine structure (EXAFS), spectroscopy, thermal analysis, and selective extraction (Mehra and Jackson, 1960; Borggaard, 1988). Mössbauer spectroscopy has emerged as a key tool to study precipitations, transformations, substitutions, reactivities, etc. of iron minerals (Schwertmann and Cornell, 1991), with a detection limit of about one percent (absolute; Murad, 1988), and to define the conditions of synthesis of green rusts (Drissi et al., 1995; Hansen and Koch, 1995).

It has been shown that several iron phases, especially green rusts and ferrous clay minerals, are very reactive because iron can be oxidized or reduced in their structures. However, their lability makes the study difficult, and special care must be taken, both in the field and in the laboratory, for the conservation of these minerals (Badaut et al., 1985; Trolard et al., 1996). Green rusts thus readily oxidize when in contact with air and have been shown to be precursors of goethite and lepidocrocite (Refait and Génin, 1993; Schwertmann and Fechter 1994).

The first studies realised at Fougères (Brittany, France) in a gleysol under forest have shown, by Raman and Mössbauer spectroscopies and kinetic selective extraction, that the major iron mineral is a green rust (Trolard et al., 1996; Trolard et al., 1997) now known as fougerite, named for the city of Fougères. The name of fougerite has been formally approved by the Commission on New Minerals and Mineral Names of IMA (number 2003-057), on January 29, 2004.

As synthetic green rust, fougerite contains both Fe(II) and Fe(III), and the Mössbauer spectra show two or three doublets, each doublet being characterized by two hyperfine parameters. Well-crystallized, Al-free goethite and hematite show sextets, but soil goethite and hematite are frequently small-sized and Al-substituted, and the room temperature (RT) spectra consist of a doublet (Cornell and Schwertmann, 2003); lepidocrocite is paramagnetic at RT and its spectrum shows a doublet. The distinction between fougerite, lepidocrocite, and paramagnetic goethite or hematite in soils requires the consideration of the different values of the hyperfine parameters at field temperature, and the spectra obtained at low temperatures in the laboratory.

A recent EXAFS study at the Fe-*K* absorption edge (Refait et al., 2001) has confirmed that fougerite is very similar to synthetic layered double hydroxysalt green rusts unambiguously identified by XRD and Mössbauer spectroscopy and led to the cell parameters and the space group of the mineral. However, a partial substitution of Fe^{2+} by Mg^{2+} was found, leading to the following general formula for fougerite: $[Fe^{II}_{1-x}\ Mg_y\ Fe^{III}_x(OH)_{2+2y}]^{x+}\ [xA,\ mH_2O]^{x-}$.

Though Mössbauer spectroscopy is not an absolute method, the *relative* proportions of Fe(II) and Fe(III) can be quantitatively determined, and the mole ratio x can be directly derived from the spectra, independently of the magnesium content.

In the same site, variations of x were observed with depth (Abdelmoula et al., 1998): 0.44 at 20 cm, 0.40 at 40 cm, 0.36 at 60 cm, in addition, some lepidocrocite was observed at the lowest depth. Fougerite has been proposed to control iron in soil solutions (Bourrié et al., 1999). As green rusts are very reactive, x could seasonally vary due to fluctuations in the water table. Such variations cannot be demonstrated by destructive techniques, and must be measured in situ.

In order to monitor in situ transformations of iron minerals in soils, a miniaturized Mössbauer spectrometer (MIMOS), designed for Mars missions with NASA and European Space Agency supports (Klingelhöfer et al., 1996), was adapted to Earth conditions (Klingelhöfer et al., 1999) and installed in the field. The miniaturized Mössbauer spectrometer works in backscattering geometry so that no soil preparation is necessary and no matrix effect perturbs the measurement as opposed to classical transmission Mössbauer spectroscopy. It can be deployed at different depths in a PVC tube, and used to characterize iron minerals in situ and follow their transformations in soils. The aim of the present paper is thus to present the first results obtained on iron dynamics and the first evidence for in situ variations of the molar x ratio, $Fe^{3+}/Fe_{tot.}$ in soils with time and space, under natural conditions.

2. MÖSSBAUER PARAMETERS OF FOUGERITE AND FERRIC OXIDES

From the Mössbauer spectra, information about iron valence (Fe^{2+} or Fe^{3+}) and crystallographic environment (tetrahedal or octahedral coordinations) can be gained with the different hyperfine parameters that are a fingerprint of iron minerals (Cornell and Schwertmann, 2003; Murad and Cashion, 2004). In the following, we are only concerned with doublets, which are characterized by their isomer shift δ and their quadrupole splitting ΔE_Q.

The isomer shift δ is measured with respect to a α-Fe foil reference and is determined by the electron density at the nucleus. Thus, δ reflects specifically the oxidation states: Fe^{2+} or Fe^{3+}. The quadrupole splitting ΔE_Q originates from nonuniform charge density and electric field gradient interactions with the iron nucleus. ΔE_Q is influenced by crystallinity, specifically by site distortion (Cornell and Schwertmann, 2003).

Synthetic purely Fe(II)-Fe(III) green rusts show two main doublets at 78 K by classical transmission Mössbauer spectroscopy: D1 (δ = 1.27 mm s^{-1} and ΔE_Q = 2.87–2.92 mm s^{-1}), and D3 (δ = 0.47–0.48 mm s^{-1} and ΔE_Q = 0.38–0.43 mm s^{-1}). D1 is ascribed to Fe^{2+} and D3 to Fe^{3+}. A slightly better fit is sometimes obtained by considering a second ferrous doublet D2 (δ = 1.27–1.28 mm s^{-1} and ΔE_Q = 2.55–2.69 mm s^{-1}). This occurs when the structure is GR1, that is, when interlayered anions are spherical or planar (carbonate, chloride, oxalate) and the space group is $R\bar{3}m$ (Drissi et al., 1994; Refait et al., 1998a; Refait et al., 1998b). Conversely, in GR2, when interlayered anions are tetrahedral and the space group is $P\bar{3}m1$ (Simon et al., 2003), the consideration of ferrous doublet D2 is not necessary. Refait et al. (1998b) assign the D1 doublet to Fe(II) in the octahedral sites of the brucitelike sheets of GRs, as its hyperfine parameters are close to those of $Fe(OH)_2$, and the D2 doublet to Fe(II) atoms situated close to the anions.

The first spectrum of fougerite was originally obtained in Fougères by classical transmission Mössbauer spectroscopy, at 77 to 78 K, the sample being taken at 20 cm depth (Trolard et al., 1996; Trolard et al., 1997). The total concentration of Fe in the sample is only about 4% Fe_2O_3. The spectrum could be fitted with only two doublets: D1 (δ = 1.25 mm s^{-1}, ΔE_Q = 2.87 mm s^{-1}), D3 (δ = 0.45 mm s^{-1}, ΔE_Q = 0.54 mm s^{-1}).

Three other samples were later taken in the same site at different depths (20, 40, 60 cm). No sextet was observed in any case. The spectra could be fitted with only two doublets D1 (δ = 1.25 mm s^{-1} and ΔE_Q = 2.81; 2.81, and 2.88 mm s^{-1}) and D3 (δ = 0.43; 0.44, and 0.45 mm s^{-1} and ΔE_Q = 0.72; 0.61, and 0.58 mm s^{-1}), by order of increasing depths (Abdelmoula et al., 1998). Siderite $FeCO_3$ and vivianite $Fe_3(PO_4)_2.8H_2O$ are not present as they give rise to a magnetically split sextet or a ferrous doublet with a large ΔE_Q = 3.12 mm s^{-1} at 78 K, respectively (Génin et al., 1998). A distinct ferric doublet D′3 (δ = 0.53 mm s^{-1} and ΔE_Q = 0.55 mm s^{-1}) observed in the deeper level (60 cm) was ascribed to lepidocrocite. This latter sample was yellowish, whereas the other three samples showed the typical greenish blue colour of gleys. The positions of D1 and D3 doublets were thus very close to the values obtained for synthetic green rusts, and conform with the observation by Murad and Taylor (1986) that Fe^{2+} in synthetic green rusts has a very constant, oxidation-insensitive ΔE_Q = 2.8 mm s^{-1}. These observations, in addition to Raman spectra, demonstrated the existence of GR as a natural mineral, fougerite.

More recently (Refait et al., 2001), another sample was taken in the same profile at 90 cm depth. Transmission Mössbauer spectroscopy was performed at 78 K, along with X-ray absorption spectroscopy. By comparison with synthetic Mg-Fe(II)-Fe(III) pyroaurites, four doublets were fitted: D1 (δ = 1.27 mm s^{-1}, ΔE_Q = 2.86 mm s^{-1}), D2 (δ = 1.27 mm s^{-1}, ΔE_Q = 2.48 mm s^{-1}), D3 (δ = 0.46 mm s^{-1}, ΔE_Q = 0.48 mm s^{-1}) and D4 (δ = 0.46 mm s^{-1}, ΔE_Q = 0.97 mm s^{-1}). It can be seen that D1, D2, and D3 are identical within experimental error to the values quoted above at the same temperature. Doublet D4 was added for a slightly better refinement. The experimental error was estimated at $\pm$0.2 mm s^{-1} by analyzing three samples of the same product.

The presence of a ferrous doublet clearly separates GRs and fougerite from paramagnetic Fe(III) oxides. The parameters of the ferric doublet for paramagnetic Fe(III) oxides at RT for goethite (δ = 0.37 mm s^{-1}, ΔE_Q = 0.48 mm s^{-1}), hematite (δ = 0.37 mm s^{-1}, ΔE_Q = 0.46 mm s^{-1}) and lepidocrocite (δ = 0.37 mm s^{-1} and ΔE_Q = 0.53 mm s^{-1}), from Cornell and Schwertmann (2003) are recalled here for comparison with the values obtained at field temperature. The distinction between fougerite and Fe-bearing clay minerals is more difficult and discussed below.

Though Mössbauer spectroscopy is not truly an absolute method, the ratios between Fe(II) and Fe(III) can be derived from the relative areas of the peaks obtained by deconvolution of the spectra. The x mole ratio of Fe(III) in the mineral can thus be obtained directly as $x = RA(D3)$ or $x = RA(D3) + RA(D4)$, while total Fe in the sample is readily obtained by chemical analysis. The goodness of fit, as estimated from the difference between the experimental spectrum and the theoretical one in the last spectrum of fougerite was within 0.2% (absolute), that is, the relative area of Fe(III) (D3 + D4) was 34 $\pm$ 0.2% of total Fe (Refait et al., 2001). With the notation in mole ratio, this gives x = 0.34 $\pm$ 0.002.

3. MATERIALS AND METHODS

3.1. Sampling Site

The sampling site is located in the domanial forest (15 km^2) of Fougères in Brittany, France (48°25′N, 1°10′W). Climatic conditions are oceanic (Fig. 1). Oak and especially beech are dominant with holly, fern, nettle, and bramble. The altitude is 180 m above sea level at the bottom of a hill cut by many thalwegs into small watersheds, about 800 m long. The site is located near a spring area upslope about 200 m from the top of the hill. The soils are developed on saprolite (several meters deep) derived from a cordieritic granodiorite. This saprolite is covered by two silty layers, a lower one is a saprolite covered by Weichselian loess (Van Vliet-Lanoë et al., 1995) as evidenced by the discontinuities of the grain size distribution near 30 and 70 cm (Table 1). The clay fraction has a maximum near 70 cm at the top of granitic saprolite.

The profile chosen is situated in a soil catena of cambisols upslope and gleysols downslope (FAO, 1998). Soil physicochemical data are given in Table 1. The soil where the instruments were placed is a gleysol and the different horizons observed are (Fig. 2) (1) 0 to 15 cm: black organo-mineral horizon without oxido-reduction phenomens and with a diffuse transition; (2) 15 to 50 cm: silty with oximorphic properties, that is, grey colours in cores with some bleaching along roots and numerous oxido-reduction mottles (specifically 5 Y 6/4 and 2.5 Y 5/6, moist according to Munsell's chart). The water table is most frequently in this horizon (Fig. 3); (3) 50 to 80 cm: silty with reductomorphic properties, that is, homogeneous blue (5 BG 6/1), almost permanently waterlogged (10 months/year), without roots. No oxido-reduction mottles. Texture changes progressively from 60 cm to 80 cm; (4) 80 to 120 cm: granitic saprolite with reductomorphic properties, that is, permanently waterlogged.

3.2. Soil Analyses

Fresh soil samples were kept under anoxic conditions in a sealed container in the dark to avoid both oxidation and photoreduction. All measurements were performed immediately after sampling. X-ray diffraction patterns were obtained with a Siemens D 500 diffractometer (40 kV, 20 mA) using Co-Kα1 radiation and a graphite monochromator. The clay fraction (<2 μm) was analysed after Mg, K, and ethylene glycol saturations and heating to 623, 723, and 823 K (Robert, 1975).

These treatments were performed in the glove box under anoxic conditions, to prevent any modification of clay behaviour by interaction with Fe(III) oxides. Samples were extracted by citrate-bicarbonate (CB; Trolard et al., 1993; Troland et al., 1995) and dithionite- citrate-bicarbonate (DCB; Mehra and Jackson, 1960) to quantify iron oxides. Structural iron in phyllosilicate minerals is not extractible by these reagents (Mitchell et al., 1971). DCB extracts all non-silicated Fe oxides, as it combines reduction by dithionite and complexation by citrate at pH buffered by bicarbonate. Natural and synthetic green rusts are dissolved by CB within a few hours, while the other iron oxides are not dissolved (Trolard et al., 1996).

The CB reagent is obtained by dissolving 9.82 g $NaHCO_3$ and 78.43 g $Na_3C_6H_5O_7$,2 H_2O in 1 L H_2O. Extractions were performed at room temperature in a glove box under nitrogen atmosphere, according to the following procedure: 0.5 g of soil sample from a sealed container is mixed with 50 mL of reagent. For the DCB extraction, add 1 g of $Na_2S_2O_4$ to 0.5 g of soil sample and 50 mL of CB reagent. To ensure that the dissolution is quasi-complete, the whole kinetic curve was acquired by sampling after 1, 6, 48, 168, 336, and 504 h (Trolard et al., 1995). The samples were shaken three times a day. Analyses of Fe, Mg, Si, and Al were performed by inductively coupled plasma-atomic emission spectrometry (ICP-AES), relative precision ranged from 2 to 5%.

3.3. In Situ Measurements and Instrumentations

3.3.1. In situ Mössbauer spectrometry

As any Mössbauer spectrometer dedicated to Fe, the instrument consists of a source of 14.4 keV γ ray source, a drive generating by Doppler-effect a variation of the incident wavelength, and detectors. Thus, Mössbauer spectra are presented with the velocity of the source in mm s^{-1} in abscissa and the number of γ rays re-emitted by the sample in ordinate, but it operates in backscattering geometry and not in transmission. Klingelhöfer et al. (1996, 1998) have demonstrated experimentally that standard transmission and the backscattering data obtained with MIMOS give the same results within experimental error.

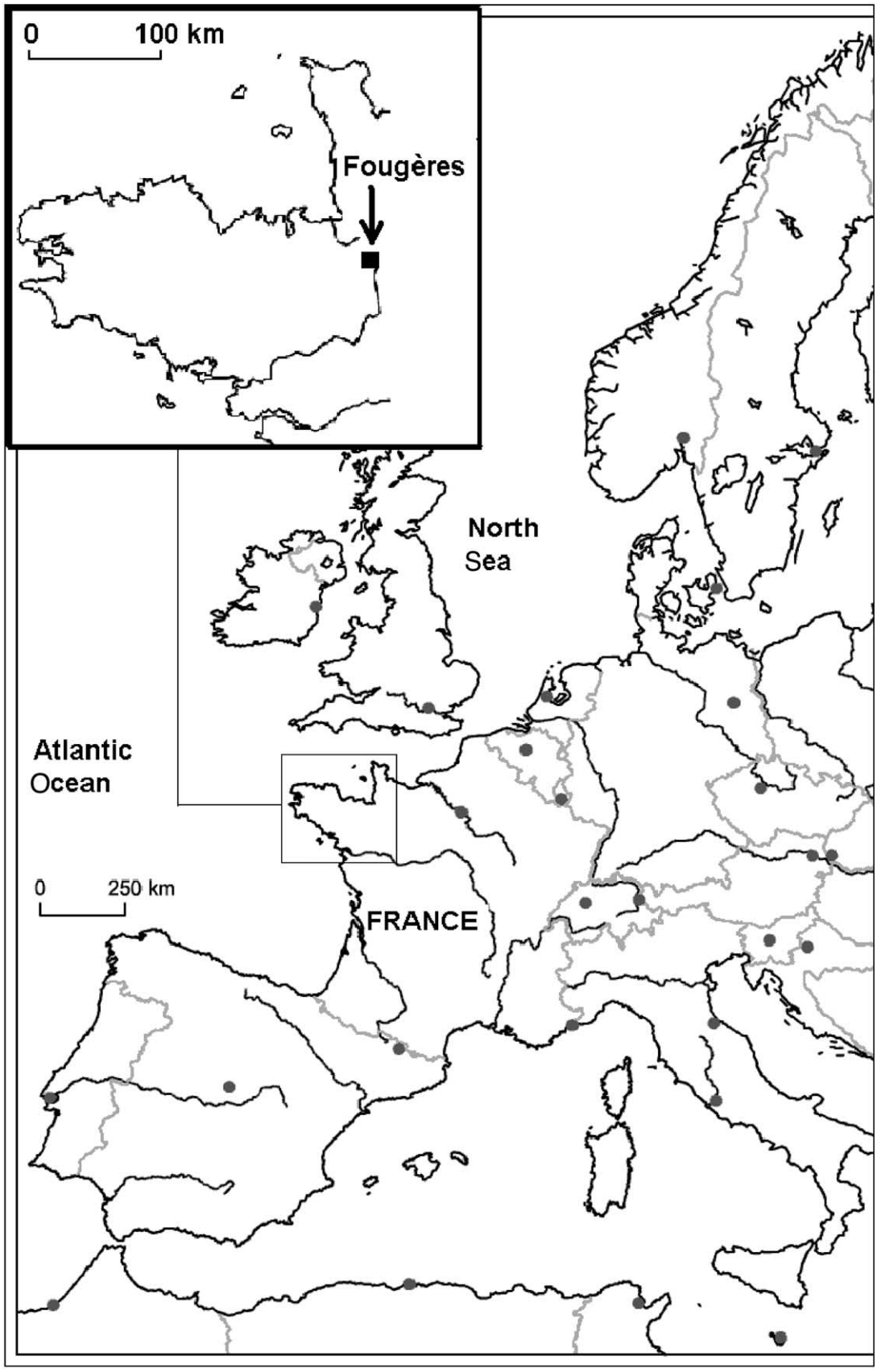

Fig. 1. Localization of sampling site.

Table 1. Chemical analyses of some major elements obtained by ICP-AES (precision ranged from 2% to 5%) in mmol kg^{-1} of the bulk soil sample, pH, and grain size distribution for the different depths.

Depth/cm	Si mmol kg^{-1}	Al mmol kg^{-1}	Fe mmol kg^{-1}	C mmol kg^{-1}	pH_{water}	pH_{KCl}	CF g kg^{-1}	ES g kg^{-1}	CS g kg^{-1}	S g kg^{-1}
0–20	13897	824	209	6227	4.46	3.69	76	364.7	450.9	108.4
20–30	13697	838	174	4420	4.08	3.54	96.5	305.9	452.8	144.7
30–40	13747	819	253	1373	4.55	3.75	109.6	262	536.5	91.9
40–60	13464	894	302	582	4.85	3.82	157.3	240.6	525	77.1
60–70	13381	1027	346	457	4.85	3.75	167.8	206.3	453	172.9
70–80	12033	1456	468	316	4.21	3.42	119.5	185.3	278.9	416.3
80–90	10585	1648	604	566	5.18	4.03	118.8	197.4	150.1	533.7
90–100	11268	1726	642	358	4.85	3.72	98.6	182.8	131.4	587.3
Granodiorite	11155	2983	684							

CF = clay fraction (<2 μm); FS = fine silt (2–20 μm); CS = coarse silt (20–50 μm); and S = sand (50–2000 μm).

The instrument was designed for Mars missions, which require a high-detection efficiency. Backscattering geometry is not influenced by the thickness of the sample. The main disadvantage is the secondary radiation caused by primary 122 keV radiation, for which an effective shielding of the detectors has been designed. Si-PIN diodes are used as detectors, with efficiencies nearly 100% and 65% for 6.4 and 14.4 keV radiations, respectively.

The spectra are fitted to Lorentzian curves. A set of free parameters are then adjusted in such a way that a goodness-of-fit criterion, the minimal χ^2, is optimized. The free parameters are those which are only mutually bounded via the χ^2 minimization procedure. These parameters are the isomer shift δ, the quadrupole splitting ΔE_Q, the half-widths at half maximum, and the height of the peaks, constrained to be equal for both lines of the doublet. Quality of spectra depends essentially on iron concentration in the samples and the time of acquisition. The relative abundance of components is obtained by integration of the corresponding areas.

The reproducibility of the curve fitting was checked by repeating the data treatment 10 times. The standard deviation obtained on the sum of relative areas of ferric doublets was obtained as 0.01 mole ratio (1% absolute). This is five times larger than the value obtained at 78 K and discussed above (0.2% absolute), and as can be expected, the signal/noise ratio is better at lower temperature. Of course, this paper does not intend to suggest that in situ Mössbauer spectroscopy could substitute

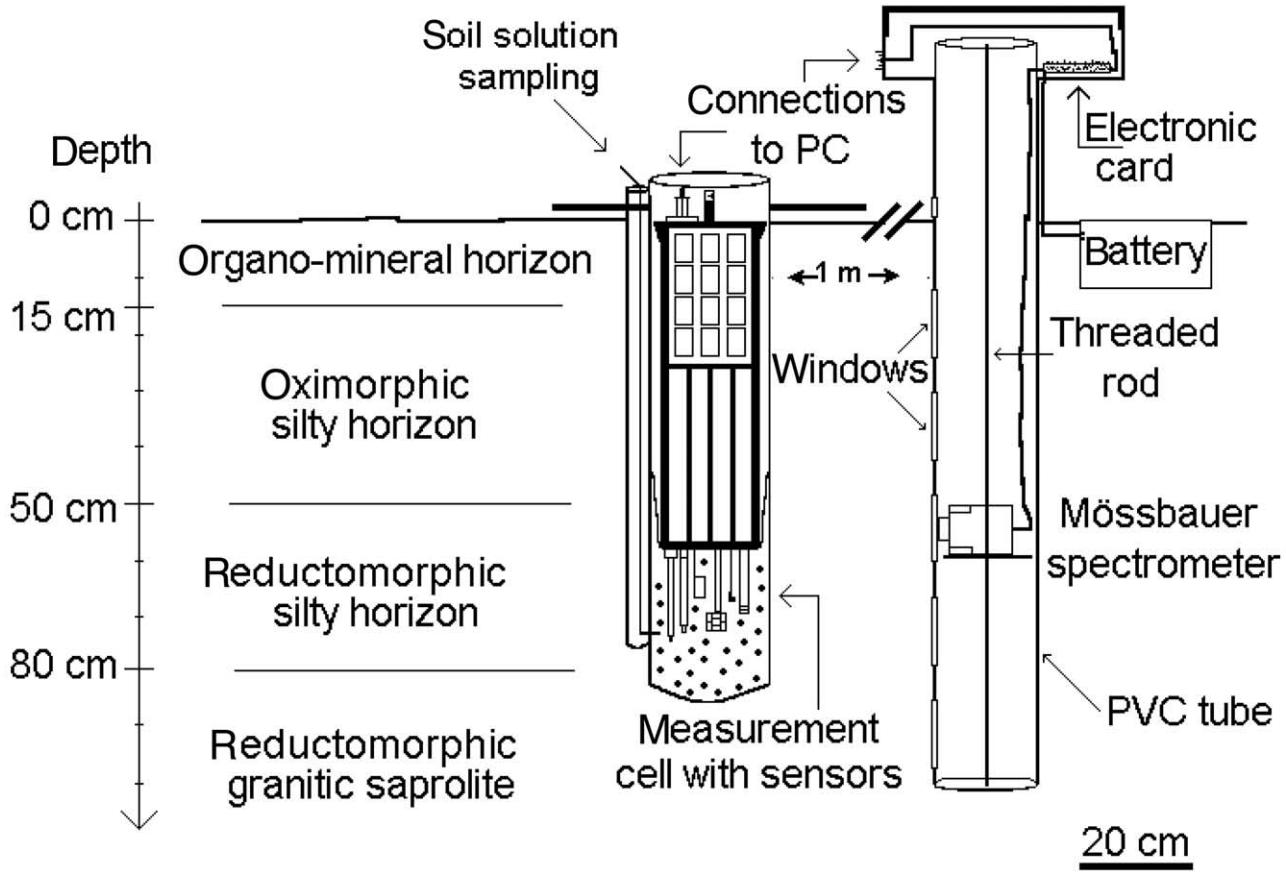

Fig. 2. Soil profile and devices for in situ monitoring: Mössbauer spectrometer and multiparametric probe.

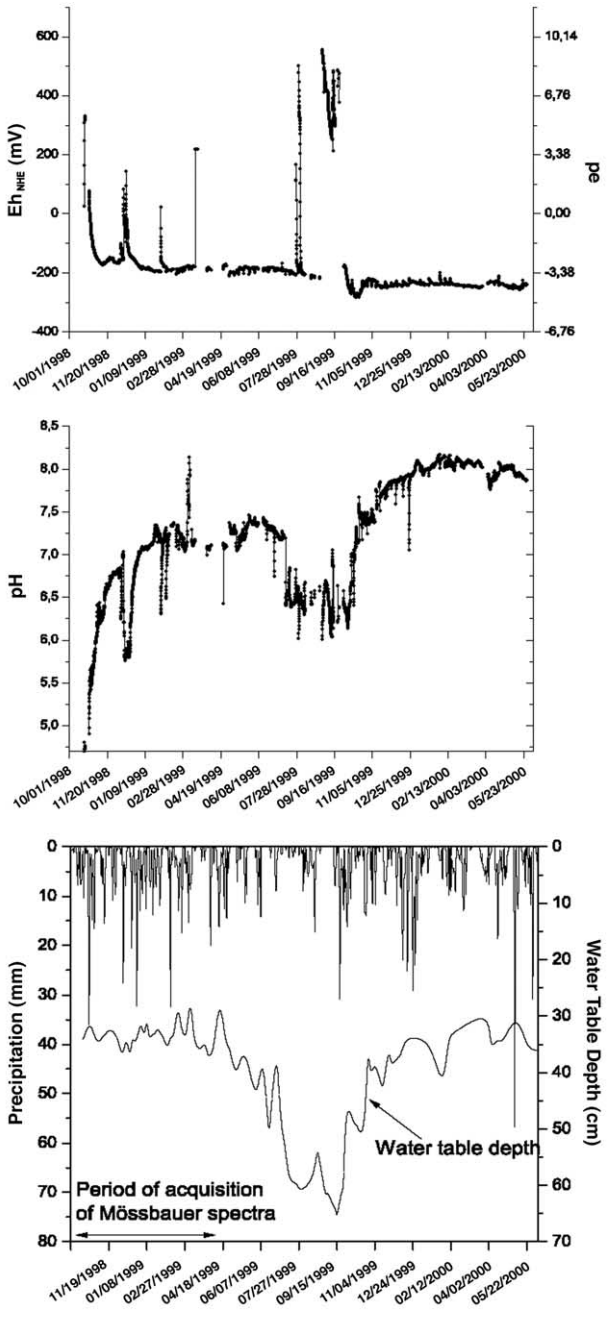

Fig. 3. Piezometric watertable level, daily precipitation and pH and pe automatically measured in the site at 70 cm depth.

classical Mössbauer spectroscopy (transmission or backscattering) in the laboratory. Once a site is characterized by classical transmission Mössbauer spectroscopy, and spectra are obtained at low temperatures to identify unambiguously the minerals present; in situ Mössbauer spectroscopy, as a nondestructive technique, can be fruitfully used to monitor Fe transformations directly in the field.

Total mass of the MIMOS is less than 400 g, and the power consumption of approximately 2 W is supplied by a battery, which provides power for ~10 days. The spectrometer is fixed on an 18 cm diameter platform inside a PVC tube (Fig. 2). It is mobile with depth with the help of a threaded rod (1.75 mm per turn). The depth accuracy is about 1.0 mm. The tube is watertight and five large windows are drilled vertically. The instrument is placed in front of a window to acquire a spectrum. The investigation depth of the incident γ ray radiations is approximately 0.5 mm, and the circular field of view is 2 cm diameter. A good physical contact between the soil and the windows was observed and velocity noise was not noticeable. Temperature was measured, and annual variations observed range from 279 to 288 K (283 $\pm$ 5 K). A series of twenty reference positions was defined from the surface to 106 cm depth: 106 cm, 103 cm, 100 cm, 98 cm, 87 cm, 83 cm, 78 cm, 48 cm, etc. During six months, the spectrometer was moved between all these positions; two or three days are sufficient to acquire a good quality spectrum; 46 spectra were acquired in the field.

3.3.2. *In situ measurements of pH and pe*

A multiparametric probe designed for oceanic measurements in seawater by Meerestechnik Electronik was adapted to monitor in situ changes of physical and chemical parameters in soil solution (Feder et al., 1998). No battery changes or sensor maintenance were required for several weeks. The probe was put into another PVC tube ~80 cm length and 12 cm diameter (Fig. 2), 1 m away from the Mössbauer spectrometer. The lower portion and three large windows in the front remained open to ease the entry and the circulation of soil water in the cell of the pipe where the measurements were performed, first at 40 cm in the groundwater level fluctuation zone in spring 1998, and then at 70 cm depth in the permanently waterlogged horizons, from autumn 1998 to spring 2000. To avoid the penetration of particles, the cell was wrapped in a synthetic and inert cloth. Precaution was taken to avoid preferential outflow along the tube and to isolate thoroughly the measurement cell from the atmosphere. The instrument was completed with external tubings to precisely sample the soil solution in the cell, free from contact with atmospheric oxygen; pH, oxido-reduction potential, dissolved oxygen, electric conductivity, and temperature are measured hourly and directly, and continuously stored in the internal memory of the probe.

The oxido-reduction potential is measured with a platinum electrode against a standard Ag/AgCl electrode and is converted to the normal hydrogen scale (NHE) with temperature correction. The oxido-reduction potential measured in the soil solution by the probe is converted into pe, according to: $\mathrm{pe} = \dfrac{\mathrm{F}E_{\mathrm{NHE}}}{(\ln 10)\,\mathrm{R}T}$, where T is the absolute temperature, $\mathrm{F} = 96485.309\ \mathrm{C\ mol^{-1}}$ and $\mathrm{R} = 8.31451\ \mathrm{J\ mol^{-1}\ K^{-1}}$.

3.3.3. *Soil solution analyses and equilibrium calculations*

After filtration at 0.45 μm, dissolved iron of soil solution samples is analyzed immediately in situ by colorimetry at 660 nm after di-2-pyridyl ketone benzoylhydrazone (DPKBH) complexation (Suarez Iha et al., 1994; Bourrié et al., 1999) with a portable spectrometer Hach DR/2010.

DPKBH is specific of aqueous total Fe(II), does not complex Fe(III), and is not influenced by the presence of "colloidal" particles. Major cations in soil solution are analyzed by ICP- AES, anions by ion chromatography (DIONEX Isocratic) and alkalinity by acidimetry with Gran-method for detection of the endpoint. As previously (Bourrié et al., 1999), the activity of Fe^{2+} is derived from total Fe(II), providing for the different ion pairs formed by Fe(II) with Cl^-, OH^-, and SO_4^{2-}, and the activity of Fe^{3+} is derived from the activity of Fe^{2+} and pe. This method prevents the overestimation of the activity of Fe^{2+}, as total Fe measured by physical techniques always includes colloidal particles that are neither quantitatively separated by ultrafiltration nor by dialysis. Activity coefficients are computed with the Debye-Hückel extended equation with provision for ion-pair formation using EQUIL(T) code (Bourrié et al., 1999), from which activities of free elements are derived. All equilibrium reactions are written with pe, pH, and the activity of Fe^{2+} as master variables.

In addition, the water table level is followed with a piezometer. It was observed that the water table level stays generally at ~40 cm depth during winter and moves down to 80 cm during the driest summers (Fig. 3).

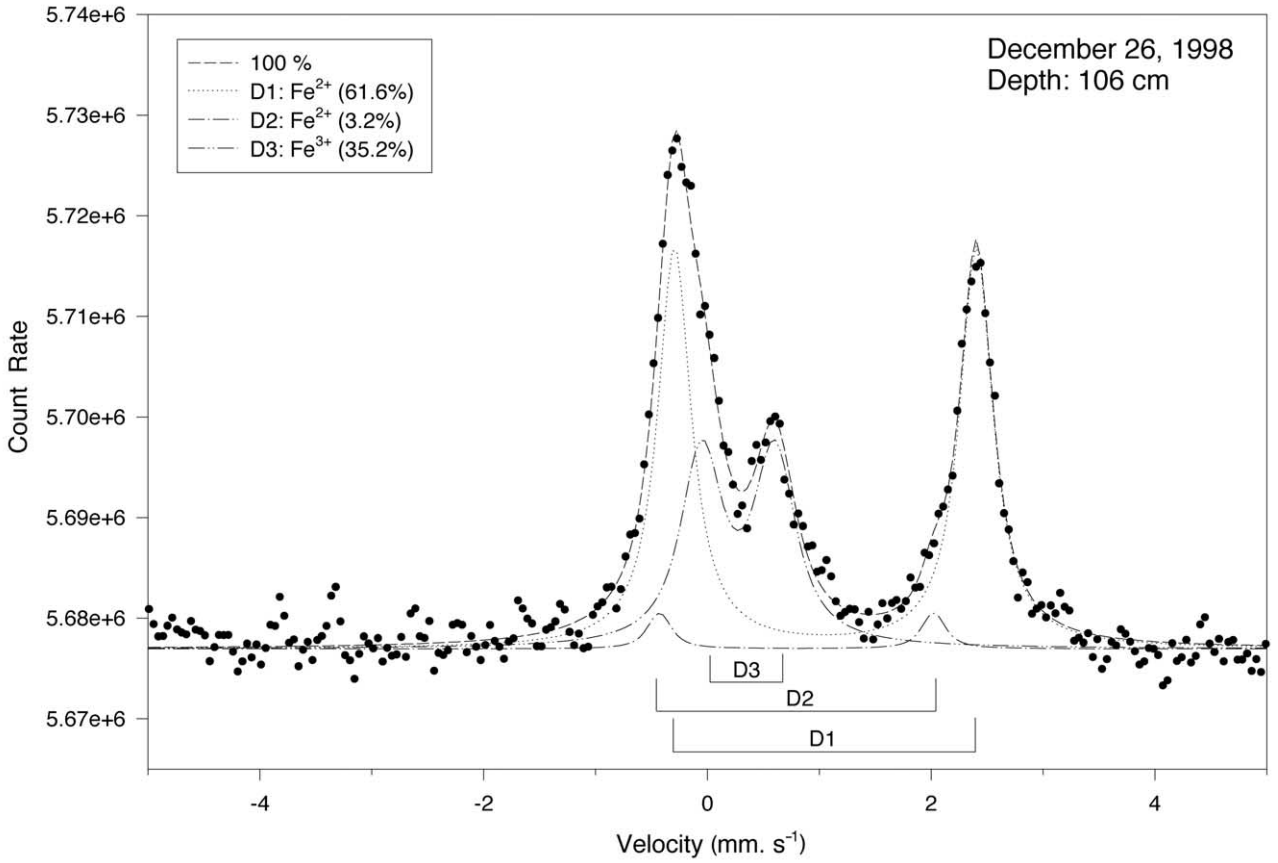

Fig. 4. Backscattered Mössbauer spectrum measured in situ at 106 cm depth in the soil. The field temperature is ~283 K, and the hyperfine interaction parameters are reported in Table 2.

4. RESULTS AND DISCUSSION

4.1. XRD and Selective Dissolutions

Concentration of total iron in soil increases with depth, from 20 to 100 cm (Table 1), from 174 to 642 mmol kg^{-1}, respectively, (i.e., 1–3.6%), but no iron minerals have been determined by X-ray diffraction, either on silty or on clay fraction. Primary minerals recognized are: quartz, micaceous illites, plagioclase feldspars, and K-feldspars. Secondary minerals are: kaolinite, vermiculite, and interstratified minerals. At ambient temperature and 623, 723, and 823 K, magnesium, potassium, or ethylene glycol saturation did not reveal any swelling characteristic of smectite. We can thus conclude that smectite is absent. But in the saprolite, at 110 cm, a mineral behaving as a hydroxy-aluminous vermiculite (VH-Al) is identified: after K-saturation, it shows a peak at 14.2 Å, which after heating to 823 K, shifts only to 12.3 Å. Instead, in the topsoil at 20 cm, a true-vermiculite peak is observed that shifts to 10 Å.

Iron phases extracted by dithionite-citrate-bicarbonate (DCB) in oximorphic silty (15–50 cm) and in reductomorphic silty (50–80 cm) horizons (Fig. 2) amount to 86 to 95% of total iron, respectively, while iron phases extracted by citrate-bicarbonate (CB) amount to 60 to 70% of total iron. The maximum content of silicated iron is thus 10% of total iron (4%), that is, 0.4%. As an average, *in bulk samples,* iron oxides amount to 90% of total iron, and 2/3 of those iron oxides consist of labile iron oxide such as fougerite (Trolard et al., 1996).

4.2. Fougerite Identification

All spectra show the presence of Fe^{2+} in the structure, and except for two, needed to be fitted with three doublets (e.g., Fig. 4, 5, and Table 2). The D1 doublets observed here (δ = 1.03–1.07 mm s^{-1}, ΔE_Q = 2.60–2.74 mm s^{-1}), and the D2 doublets observed here (δ = 0.6–1.0 mm s^{-1}, ΔE_Q = 2.2–2.7 mm s^{-1}) can be compared with the data obtained by Refait et al. (1998a) on GR1(Cl): Da (δ = 1.22 mm s^{-1}, ΔE_Q = 2.34 mm s^{-1}), Db (δ = 1.11 mm s^{-1}, ΔE_Q = 2.02 mm s^{-1}).

The D3 doublets observed here (δ = 0.21–0.32 mm s^{-1}, ΔE_Q = 0.65–0.80 mm s^{-1}) are clearly different from the values, at RT, of all purely ferric oxides, goethite, lepidocrocite, and hematite, at RT: (δ = 0.37 mm s^{-1}, ΔE_Q = 0.48–0.53 mm s^{-1}). The D3 doublets observed here are closer to the two ferric doublets observed at RT by Refait et al. (1994) in synthetic Ni(II)-Fe(III) GR1 compounds, where only ferric doublets were present and which were isomorphic to GR1: Dc (δ = 0.336 mm s^{-1}, ΔE_Q = 0.445 mm s^{-1}) and Dd (δ = 0.352 mm s^{-1}, ΔE_Q = 0.861 mm s^{-1}). The values of ΔE_Q observed here are in between the values for Dc and Dd. The D3 doublet observed at RT for synthetic GR1(Cl) (Refait et al., 1998a) is: D3 (δ = 0.35 mm s^{-1}, ΔE_Q = 0.58 mm s^{-1}).

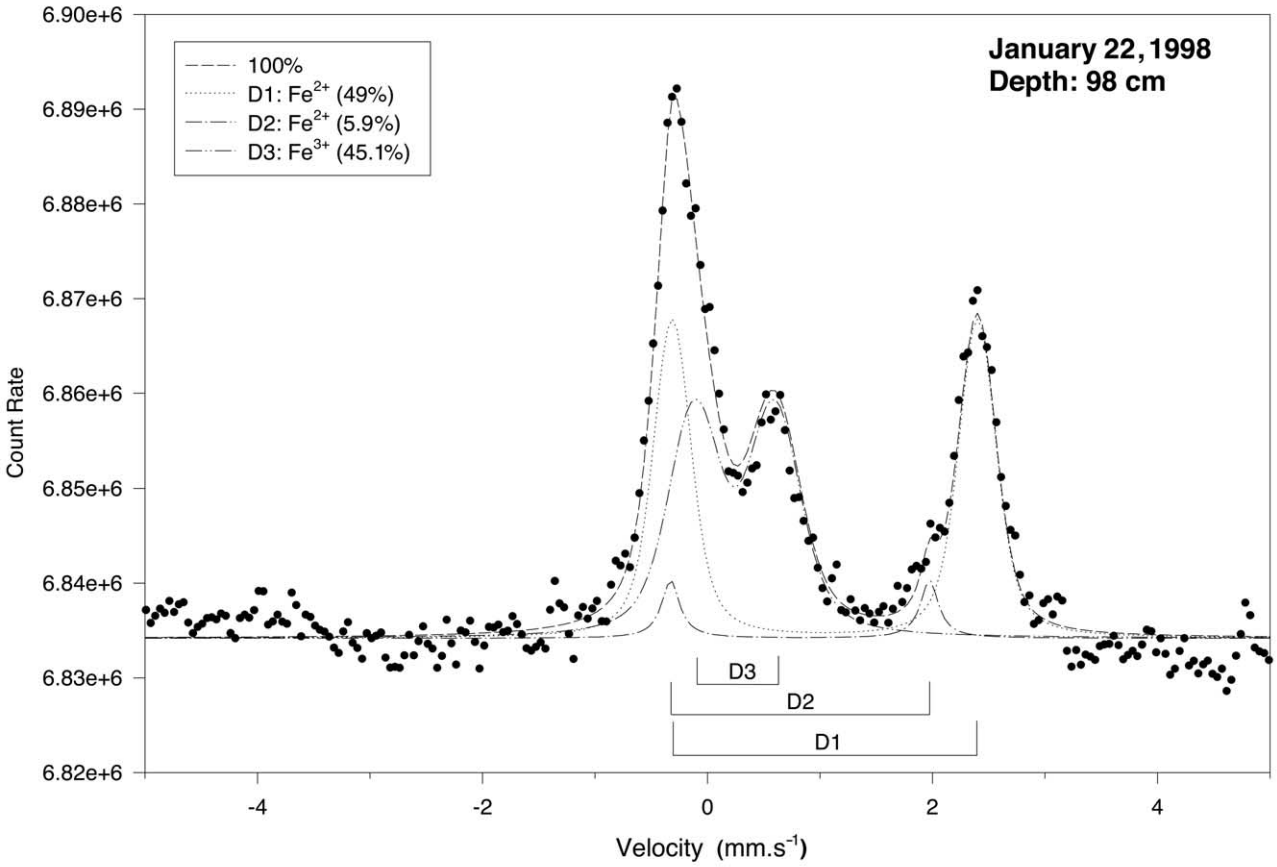

Fig. 5. Backscattered Mössbauer spectrum measured in situ at 98 cm depth in the soil. The field temperature is ~283 K, and the hyperfine interaction parameters are reported in Table 2.

Most of the spectra were acquired during late autumn, winter, and early spring, and ferric oxides were not present, which is identical to what was observed by Abdelmoula et al. (1998) by classical transmission Mössbauer spectroscopy at 78K, but different from what was observed at 60 cm, where lepidocrocite was present in addition to fougerite, in the respective proportions 30% lepidocrocite to 70% fougerite (with x = 0.36). We can thus conclude that the contribution of Fe(III) oxides during these periods is small and that Fe(III) is mainly present in the structure of the fougerite mineral. There exist clearly both striking similarities and nonnegligible differences in the values of the hyperfine parameters for ferrous doublets, especially for D2, as the smaller the relative area, the larger the uncertainty. This suggests that the fougerite structure is not exactly the same as that of the synthetic purely Fe(II)-Fe(III) GR1(Cl), probably due to the presence of Mg, which modifies site distortion.

The distinction between fougerite and a mixed Fe(II)-Fe(III) clay mineral is more difficult, as the octahedral layer of clay minerals is close to the brucitic layer of green rusts, from which it differs by the bonding to tetrahedral layers. However, by plotting δ vs. ΔE_Q, for D1 and D3, fougerite and iron silicates (data from the literature) do not show both the same hyperfine parameters (Fig. 6). This difference can be ascribed to the difference of the b parameters between fougerite and the octahedral layer of a 2/1 clay mineral, due to the distortion of tetrahedral layer necessary to accommodate the differences of the cell parameters of tetrahedral and octahedral layers, and to the difference of chemical composition: in the octahedral layers of clay minerals, Fe, if present, is largely minor with respect to Al in this milieu. Moreover, no tetrahedral Fe was observed in Mössbauer spectra. The spectra could be fitted with the three doublets of green rusts, while the presence of other doublets would have significantly enlarged the peaks. As in our samples, silicated Fe amounts to less than 10% total Fe, and clay minerals present are mainly aluminous minerals such as hydroxy-aluminous vermiculite and kaolinite. It can thus be concluded that the contribution of silicated Fe, if any, can be neglected.

All the spectra are not exactly of the same quality, but the precision obtained on the x ratio can be estimated as ± 0.01. The quality is thus similar in situ to that of spectra acquired in the laboratory by classical transmission Mössbauer spectroscopy on the same sample (Génin et al., 1998).

4.3. In situ Mineralogical Transformations of Fougerite

At 12 depths, especially near the surface, the spectra did not allow interpretation because the total concentration of iron on the analyzed point was too small (less than 1%). This soil profile (described previously) showed a heterogeneous distri-

Table 2. Hyperfine interaction parameters of in situ Mössbauer spectra obtained at 283 K at different depths. D1, D2 and D3 are the three doublets (cf. Figs. 4 and 5); δ is the isomer shift (in mm s^{-1}) with respect to a α-Fe foil reference; ΔE_Q is the quadrupole splitting (in mm s^{-1}); RA is the relative area of the components (in %); $x = Fe^{3+}/Fe_{tot.}$ is equal to the relative area of D3 doublets (see Fig. 7); the estimation error on x is ± 0.01.

	D1			D2			D3		
Depth cm	δ	ΔE_Q	RA	δ	ΔE_Q	RA	δ	ΔE_Q	RA
100	1.054	2.705	38.6	0.770	2.700	16.3	0.230	0.773	45.1
100	1.061	2.695	44.0	0.777	2.412	13.1	0.276	0.665	42.9
87	1.042	2.650	45.1	0.826	2.470	3.2	0.257	0.682	51.8
48	1.046	2.633	33.3	–	–	0.0	0.220	0.763	66.7
100	1.045	2.677	45.1	0.750	2.400	12.5	0.284	0.686	42.5
100	1.033	2.767	43.3	0.934	2.250	12.7	0.248	0.728	44.1
87	1.000	2.600	20.7	0.860	2.220	29.8	0.240	0.650	49.5
78	1.080	2.650	31.5	0.750	2.470	9.7	0.300	0.749	58.9
83	1.069	2.700	27.2	0.600	2.700	23.6	0.300	0.700	49.3
98	1.055	2.741	44.6	0.908	2.430	9.8	0.286	0.648	45.6
106	1.055	2.696	61.6	0.799	2.462	3.2	0.275	0.656	35.3
103	1.058	2.702	55.9	0.791	2.412	5.3	0.251	0.720	38.8
98	1.048	2.711	47.6	0.838	2.392	5.3	0.239	0.679	47.1
48	1.080	2.660	27.9	0.799	2.297	8.1	0.240	0.700	64.0
78	1.073	2.684	39.0	–	–	0.0	0.270	0.750	61.0
83	1.034	2.717	40.1	0.628	2.475	7.4	0.319	0.689	52.5
87	1.047	2.707	28.2	0.776	2.397	22.2	0.273	0.619	49.6
98	1.044	2.712	48.2	0.823	2.300	5.2	0.241	0.713	46.7
100	1.050	2.706	51.4	0.861	2.296	4.4	0.264	0.697	44.2
103	1.054	2.687	60.4	0.701	2.196	3.3	0.252	0.732	36.3
106	1.057	2.705	56.5	0.733	2.314	6.0	0.277	0.604	37.5
103	1.052	2.714	52.9	0.851	2.363	4.3	0.269	0.803	42.7
100	1.066	2.718	48.0	0.892	2.668	8.0	0.215	0.651	44.0
98	1.055	2.728	50.3	0.844	2.362	4.6	0.245	0.723	45.1
106	1.059	2.722	53.9	0.892	2.548	9.1	0.268	0.664	37.0
103	1.041	2.716	53.6	0.789	2.191	5.4	0.250	0.723	41.0
100	1.048	2.707	56.2	0.811	2.300	4.5	0.256	0.731	39.3
98	1.051	2.724	47.5	0.863	2.399	5.3	0.254	0.679	47.2
100	1.056	2.699	48.1	0.768	2.205	4.0	0.281	0.721	48.0
103	1.051	2.695	47.7	0.779	2.384	8.9	0.253	0.716	43.5
106	1.070	2.672	60.8	0.768	2.588	4.5	0.212	0.677	34.7
103	1.080	2.716	47.7	0.803	2.631	8.8	0.213	0.692	43.6
100	1.059	2.723	40.4	0.85	2.616	18.7	0.282	0.667	41.0
48	1.030	2.730	29.5	1.001	2.470	9.8	0.251	0.700	60.7

bution of the total iron between 0 and 50 cm depth, characteristic of the gleysol (oxido-reduction mottles, discolorations along roots). The 12 depths at which the absence of any doublets on the spectra demonstrate absence of iron phases were evenly distributed beetween 0 and 50 cm depth. The spatial resolution of the Mössbauer instrument is thus small enough to probe soil heterogeneity.

At 8 depths, spectra showed clear evidence of the presence of fougerite; 34 spectra were acquired at these 8 depths, that is, several spectra at the same point. The variation between 48 and 106 cm depth of the x ratio is large, from 0.34 to 0.64 (Table 2), and much larger than the estimation error on x (± 0.01, about half the size of the symbol in Fig. 7). The general tendency observed is consistent with field observations: x is minimum in the deeper reductomorphic horizons, and maximum in the upper oximorphic horizons (Table 2). This is consistent too with the previous observations (Abdelmoula et al., 1998) made with destructive sampling and classical transmission Mössbauer spectroscopy at 78 K. For example, at 106 cm depth, x is equal to 0.36, close to $x = 1/3$ for which the corresponding abridged chemical formula for green rust (omitting Mg, not detected by Mössbauer spectroscopy) is: $Fe^{II}_2\,Fe^{III}(OH)_7$. At 48 cm depth, x ratio is 0.62, close to $x = 2/3$, for which the abridged chemical formula for green rust is: $Fe^{II}\,Fe^{III}_2(OH)_8$ (cf. for the incorporation of Mg in the mineral).

The variation of x ratio observed is large and monotonous between these limits. At 2 depths (78 and 98 cm), variations of the x ratio are not larger than twice the estimation error (± 0.01). In these horizons, x ratio can be considered as constant during the experimental period. In contrast, sharp variations in x ratio are observed with time at 48, 83, 87, 100, 103, and 106 cm in soil (Fig. 7): for example at 100 cm depth, x ratio is initially equal to 0.39 and then increases to 0.48 one week later, suggesting that the $Fe^{3+}/Fe_{tot.}$ ratio of the mineral can change quickly, that is, in a few days, in soil.

A special phenomenon is observed at 78 cm depth: the first recorded spectrum does not show any iron minerals (see arrow on Fig. 7), but one month later a significant signal appears, suggesting that fougerite has precipitated meanwhile. The soil may contain aqueous Fe^{2+}, but aqueous Fe does not contribute to the Mössbauer signal. We will discuss this point later.

4.4. Soil Solution Composition

The range of soil solution variation of pe and pH is plotted in Figure 3. The data of the first month show the perturbation

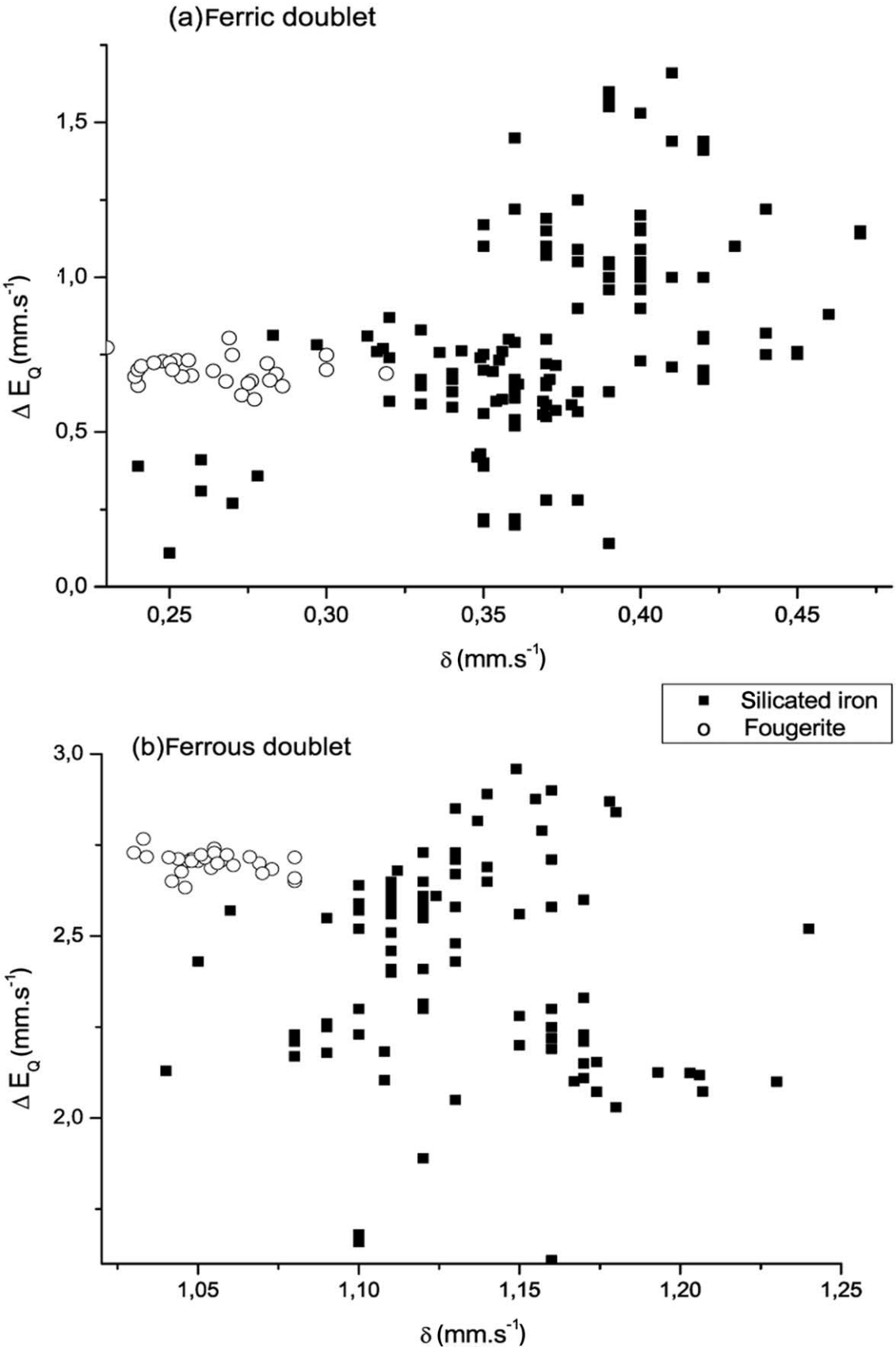

Fig. 6. Hyperfine interaction parameters at 283 K of (a) ferric doublet and (b) ferrous doublet. Closed squares refer to data for iron silicates taken from the literature; open circles refer to data from Fougères (this study).

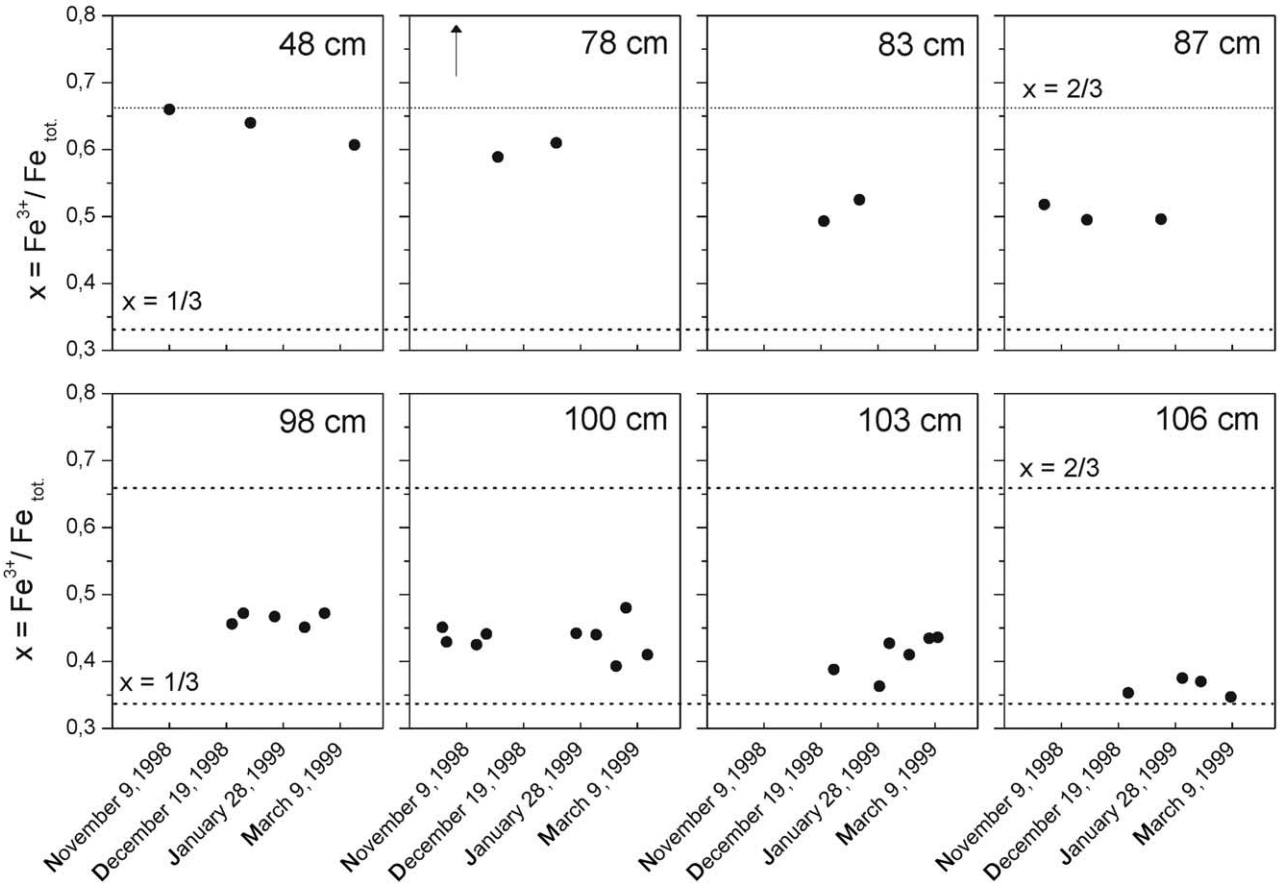

Fig. 7. Variations of $x = Fe^{3+}/Fe_{tot.}$ with time at different depths. The short dashed and dotted lines correspond to x ratios equal to 1/3 and to 2/3 with corresponding abridged chemical formula. The arrow in the 78 cm diagram indicates the absence of green rusts Mössbauer spectrum at this time (see text). The estimation error on x is ± 0.01, about half the size of the symbol.

due to the installation of the probe, with air entry; then pH stabilized to about 6.2 and pe to about −3. Then, in winter 1998–1999, short duration events superimposed to large seasonal variations. Considering the latter first pH fluctuated between 6 and 8.2, pe between −4.7 and −3.5, and pe + pH between 2 and 6.2. Most frequent values were close to pe + pH = 2.5 to 4.5. During intense storm events and especially after long dry periods, sharp changes were observed in a few hours: ΔpH = 1, ΔEh = 0.1 V, that is, Δpe = 2 (Feder et al., 1998). Dissolved oxygen was generally not detectable except during these short duration events in which as large values as Eh = 0.2 V (pe = 3.4) are recorded.

In summer 1999, the level of the water table lowered to deeper than 70 cm, until no sample could be obtained; pH decreased to an average value of 6.5, with sharp variations ΔpH = 0.5; Eh increased to the completely oxidized value (Eh = 0.55 V, pe = 9.3).

From autumn 1999 to spring 2000, the level of the water table increased, pH increased to as large as pH = 8.2, and Eh decreased to about −0.25 V (pe = −4.2). Short duration events were much less frequent than in the previous year. It must be added that after the big storm in December 1999, all the trees fell, so that there was no biological uptake in spring 2000 by trees. According to FAO (1998), gleyic properties appear when rH < 19, where rH is defined by rH = 2 (pe + pH), or equivalently pe + pH < 9.5. Our results show that pe + pH ranges from 2 to 6.2. The system remains in moderately reducing conditions, though significant and fast variations are observed with time. This is in agreement with the gleyic properties observed.

4.5. Check of Fougerite/Soil Solution Equilibria

All the x ratios observed in the field range between 1/3 and 2/3. No values have been found out of these limits. This is consistent with the earlier field results and the previous-structural formulae proposed (Bourrié et al., 1999). As all synthetic green rusts were binary Fe(II)-Fe(III) compounds, fougerite was considered as a binary solid solution (Génin et al., 2001).

The exact nature of the interlayer compensating anion cannot be determined by Mössbauer spectroscopy, and the mineral cannot be separated from the surrounding minerals as it is labite. Synthetic green rusts can accommodate a variety of anions such as carbonate, chloride, oxalate, selenate, sulphite, sulphate, etc. As in Fougères, the milieu is acidic and solutions were largely undersaturated with respect to carbonate, chloride, and sulphate green rusts; it was

simply assumed that the compensating anion is OH^- (Trolard et al., 1997; Génin et al., 1998). The discussion of equilibria between soil solutions and the mineral in different sites led us to propose tentative values for the Gibbs free energies of formation of GR1(OH) for $x = 1/3$ (*i.e.,* $Fe_3(OH)_7$), $x = 1/2$ (*i.e.,* "$Fe_2(OH)_5$") and $x = 2/3$ (*i.e.,* "$Fe_3(OH)_8$") (Bourrié et al., 1999). Quotes indicate that the mineral cannot exist as such.

However, X-ray absorption spectroscopy showed that magnesium is present in the solid in addition to Fe (Refait et al., 2001), so that the possible influence of magnesium concentration on equilibria, along with the presence of other anions, must be assessed.

4.5.1. Ternary solid solution model for OH^- fougerite

Assuming first that OH^- is the interlayer compensating anion, fougerite is thus a ternary solid solution in the system $Fe(OH)_2$-$Fe(OH)_3$-$Mg(OH)_2$. The general structural formula for the mineral must then be modified as: $[Fe^{II}_{(1-x)}\,Fe^{III}_{x}\,Mg^{II}_{y}\,(OH)_{2+2y}]^{+x}\,[x\,OH{\cdot}mH_2O]^{-x}$, with $m \leq 1 - x + y$, or as a function of the mole fractions of the three components $Fe(OH)_2$, $Fe(OH)_3$, and $Mg(OH)_2$, such that:

$$X_1 = \frac{1-x}{1+y}, \quad X_2 = \frac{x}{1+y}, \quad X_3 = \frac{y}{1+y} \tag{1}$$

A model of regular nonideal solid solution was developed, assuming the substitution of Fe^{2+} by Mg^{2+} is ideal, and examining the structural and geochemical constraints that limit the extension of the solid solution (Bourrié et al., 2004).

The basic equations of the model are:

$$\mu_1 = \mu_1^0 + RT \ln X_1 - A_{12}X_2^2, \tag{2}$$

$$\mu_2 = \mu_2^0 + RT \ln X_2 - A_{12}(1 - X_2)^2, \tag{3}$$

$$\mu_3 = \mu_3^0 + RT \ln X_3 - A_{12}X_2^2, \tag{4}$$

$$\mu = X_1\mu_1 + X_2\mu_2 + X_3\mu_3 \tag{5}$$

$$= X_1\mu_1^0 + X_2\mu_2^0 + X_3\mu_3^0 + RT[X_1 \ln X_1 + X_2 \ln X_2 + X_3 \ln X_3] + A_{12}X_2(1 - X_2). \tag{6}$$

When no Mg is present in the mineral, $X_3 = 0$, and Eqn. 6 simplifies to:

$$\mu = X_1\mu_1^0 + X_1\mu_2^0 + RT[X_1 \ln X_1 + X_2 \ln X_2] + A_{12}X_2(1 - X_2), \tag{7}$$

or equivalently, from Eqn. 1 with $y = 0$:

$$\mu = (1 - x)\mu_1^0 + x\mu_2^0 + RT[(1 - x) \ln (1 - x) + x \ln x] + A_{12}x(1 - x). \tag{8}$$

The Gibbs free energy of formation of $Fe(OH)_2$ is $\mu_1^0 = -489.8$ kJ mol^{-1} (Bourrié et al., 1999). There are two unknowns in the right member of Eqn. 8: μ_2^0 for $Fe(OH)_3$, which is a virtual endmember, and the parameter of nonideality of the solid solution, A_{12}.

A close examination of the structural and geochemical constraints in this system led to the following conclusions (Bourrié et al., 2004):

1. Each Fe^{3+} ion must be surrounded by six divalent cations, either Fe^{2+} or Mg^{2+}, so that the mole fraction of ferric hydroxide in the solid solution, X_2 obeys to: $X_2 \leq 1/3$;
2. As $Fe(OH)_2$ and $Mg(OH)_2$ are very soluble, the mole fraction X_2 must not be too small; experimentally, green rusts form from $X_2 \geq 1/4$; the domain of existence of fougerite is thus limited to the narrow range: $1/4 \leq X_2 \leq 1/3$ or $X_2 = 7/24 \pm 1/24$.

As the range of variation of x is restricted to the narrow range $[7/24 \pm 1/24]$, it was assumed that μ is minimum in this range, so that its derivative is zero.

By taking the derivative with respect to x, one obtains (Prigogine and Defay (1946)):

$$\frac{\partial \mu}{\partial x} = \mu_2 - \mu_1 \tag{9}$$

which leads to:

$$\mu_1 = \mu_2 \tag{10}$$

Now, from the definition of μ, one has:

$$\mu = (1 - x)\mu_1 + x\mu_2, \tag{11}$$

so eventually, at the minimum, one has:

$$\mu = \mu_1 = \mu_2, \tag{12}$$

whose physical meaning is that the chemical potential of the solid solution is minimum when the contributions of the endmembers are identical.

Bourrié et al. (2004) have shown that the experimental Gibbs free energies of formation of synthetic green rusts, without Mg, and $Fe(OH)_2$ are linearly related to the electronegativities of the anions by the empirical law:

$$\mu = -76.887\chi - 491.5206, \quad r^2 = 0.9985, \quad N = 4, \tag{13}$$

where χ is the electronegativity of the *unhydrated* anion, calculated from the model of partial charges developed by Jolivet (1994), such that:

$$\chi = \frac{\Sigma_i \sqrt{\chi_i^*} + 1.36Z}{\Sigma_i \frac{1}{\sqrt{\chi_i^*}}} \tag{14}$$

where χ_i^* are the electronegativities of the elements taken on the Allred and Rochow scale and Z is the electric charge of the molecule or ion. The electronegativities of the anions are: $X_i = 0.54$ for Cl^-, 1.60 for OH^-, 1.86 for SO_4^{2-}, and 2.0 for CO_3^{2-}.

From Eqn. 13, with $\chi = 1.60$ for OH^-, one obtains: $\mu = \mu_1 = \mu_2 = -614.5$ kJ mol^{-1} for fougerite normalized to 1 atom Fe per mole formula, and with OH^- as interlayered anion. By successively substituting these values in the basic equations for each endmember, Eqns. 2 and 3, with $\mu_1{}^0 = -489.8$ kJ mol^{-1}, $X_1 = 1 - x = 1 - 7/24 = 17/24$ and $X_2 = x = 7/24$, one obtains the two unknown parameters: $\mu_2{}^0 = +119.18$ kJ mol^{-1}

Table 3. Basic equation and parameters of the regular ternary solid solution models for Fe(II)-Fe(III)-Mg(II) green rust, fougerite, at 298.15 K, 1 bar.

Equation			
$\mu = X_1\mu_1^0 + X_2\mu_2^0 + X_3\mu_3^0 + RT[X_1 \ln X_1 + X_2 \ln X_2 + X_3 \ln X_3] + A_{12}X_2(1 - X_2)$ Eq. 6			
Thermodynamic parameters			
Name of pole	Mole formula	μ kJ mol^{-1}	A_{12} kJ mol^{-1}
Pole 1: ferrous hydroxide	$Fe(OH)_2$	−489.8	-
Pole 2: Cl-fougerite	$[Fe(OH)_2]^+[Cl]^-$	−280.00	−498.24
Pole 2: OH-fougerite	$[Fe(OH)_2]^+[OH]^-$ (virtual)	+119.18	−1456.28
Pole 2: SO_4-fougerite	$[Fe(OH)_2]^+[1/2SO_4]^-$ (virtual)	+217.10	−1691.27
Pole 2: CO_3-fougerite	$[Fe(OH)_2]^+[2/3HCO_3 \cdot 1/6CO_3]^-$ (virtual)	+394.09	−2116.06
Pole 3: Brucite	$Mg(OH)_2$	−832.16	
μ at minimum (x = 7/24) and at the limits, for fougerite without Mg			
Anion	$\mu(x = 7/24)$ kJ mol^{-1}	$\mu(x = 1/4$ *or* $1/3)$ kJ mol^{-1}	$\Delta\mu$ %
Cl^-	−533.04	−532.16	0.16
OH^-	−614.54	−612.00	0.41
SO_4^{2-}	−634.53	−631.58	0.46
CO_3^{2-}/HCO_3^-	−670.67	−666.98	0.55

for $Fe(OH)_3$ (virtual), and $A_{12} = -1456.28$ kJ mol^{-1} (nonideality parameter), at 298.15 K, 1 bar.

The ternary solid solution model for fougerite is now completed with the value for the pure $Mg(OH)_2$ endmember, for which we take the value for brucite. The value from Bratsch (1989) is $\mu_3^0 = -833.67$ kJ mol^{-1}, from $E^0 = -2.690$ V for the redox couple $Mg(OH)_{2,c}/Mg_c,OH^-$. However, the value proposed by Harvie et al. (1984) is different (log $K_{sp} = 17.1$ for the solubility of $Mg(OH)_{2,cr.}$). This latter value was recently confirmed by Altmeier et al. (2003), who retain 17.1 ± 0.2. This leads to $\mu_3^0 = -832.16$ kJ mol^{-1}, consistent with $\Delta_f G^0(Mg^{2+}, aq.) = -454.8$ kJ mol^{-1} and $\Delta_f G^0(H_2O, 1.) = -237.18$ kJ mol^{-1}. The parameters of the model are given in Table 3 at 298.15 K, 1 bar.

4.5.2. *Ternary solid solution model for Cl^-, CO_3^{2-}, and SO_4^{2-} green rusts*

The same method can be used to obtain the thermodynamic parameters when the compensating anion is not OH^-. The (virtual) ferric endmembers are now $[Fe(OH)_2]^+[A]^-$, where A = Cl^-, 1/2 SO_4^{2-}, 1/2 CO_3^{2-}, or HCO_3^-.

With $\chi = 0.54$ for Cl^-, and $x = 7/24$ for GR1(Cl), Eqn. 13 gives $\mu_{calc.} = -2132$ kJ mol^{-1} against $\mu_{exp.} = -2145 \pm 7$ kJ mol^{-1}. The value normalized to 1 atom Fe per mole formula is then: $\mu = \mu_1 = \mu_2 = -533$ kJ mol^{-1} for GR1(Cl) $[Fe^{II}_{3/4}\, Fe^{III}_{1/4}(OH)_2]^{+1/4}[1/4\, Cl]^{-1/4}$. By substituting the value of μ as above in Eqns. 2 and 3, one obtains: $A_{12} = -498.24$ kJ mol^{-1} and $\mu_2^0 = -280.00$ kJ mol^{-1}. With $\chi = 1.66$ for SO_4^{2-}, the values obtained are $A_{12} = -1691.27$ kJ mol^{-1} and $\mu_2^0 = 217.10$ kJ mol^{-1}.

The value used here for GR1(CO_3) is indeed relative to a mixture of CO_3^{2-} and HCO_3^- in the interlayer (Bourrié et al., 2004), so that the average value is $\chi = 2.33$. As the proportion of carbonate and hydrogen-carbonate in the interlayer may vary as a function of pH in the milieu, this introduces an uncertainty. The values obtained are $A_{12} = -2116.06$ kJ mol^{-1} and $\mu_2^0 = 394.09$ kJ mol^{-1} (Table 3).

The values of A_{12} are all negative, which ensures that green rusts will not demix at any temperature, as the second derivative of μ with respect to x is given by:

$$\frac{\partial^2\mu}{\partial x^2} = -2A_{12} + \frac{RT}{x(1-x)}. \quad (15)$$

This derivative is then always positive.

However, whereas μ_2^0 is positive for pure endmembers with OH^-, SO_4^{2-} and CO_3^{2-}, which means that these endmembers are virtual, it is negative for Cl^-, which means that this endmember could a priori exist. Solving the equation ${\mu_2}^0 = 0$ for χ gives $\chi = 1.2835$. For anions such that $\chi \leq 1.2835$, the pure endmember might exist. However, in the case of GR1 (Cl) it was observed that the compound decomposes into "hydrated magnetite" when $x \geq 1/3$ (Refait and Génin, 1993).

From Eqn. 8, μ can be computed for $x = 1/4$, and $x = 1/3$. The values are identical as the equation is symmetrical around $x = 7/24$ and are reported in Table 3. The ranges of variation of μ are very narrow and within 1 to 4 kJ mol^{-1}, that is, within 0.2 to 0.55%.

As previously, the ternary model is completed with the value for $Mg(OH)_2$, and full Eqn. 6 can be used to compute the Gibbs free energies of formation of any Fe(II)-Fe(III)-Mg(II)-A^- green rust. No attempt is made here to mix anions in the interlayer.

4.5.3. *Check of equilibria*

By definition, the mole ratio x is related to the mole fractions of endmembers in the solid by:

$$x = \frac{X_2}{X_1 + X_2}. \quad (16)$$

From the value of x and with either $X_2 = 1/4$ or $X_2 = 1/3$, X_1 is obtained, and $X_3 = 1 - (X_1 + X_2)$, so that the composition of fougerite is obtained from in situ Mössbauer measurements and our solid solution model.

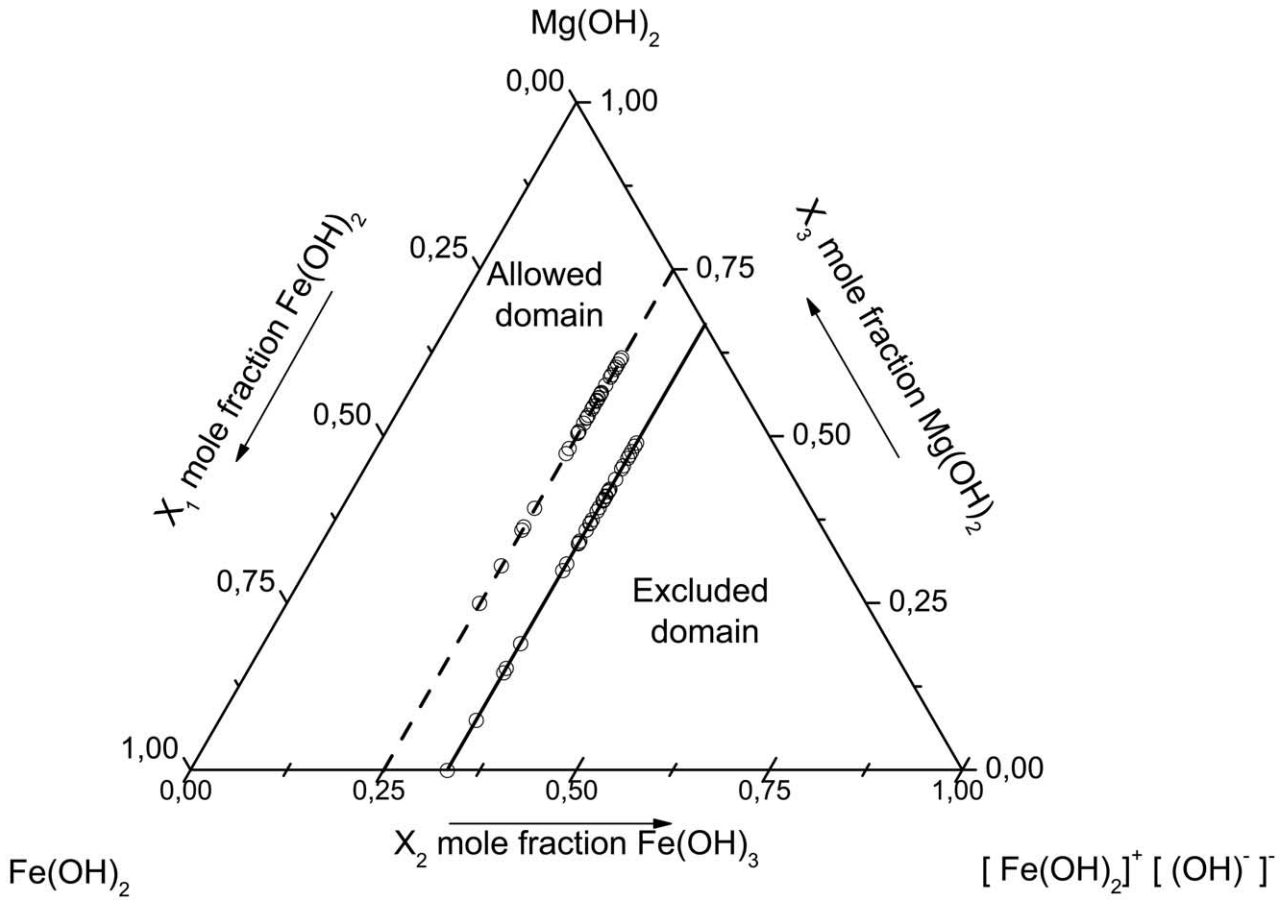

Fig. 8. Diagram for the ternary system $Fe(OH)_2$ - $Fe(OH)_3$ - $Mg(OH)_2$. The solid line is the limit between the excluded and the allowed domains constrained by the green rust structure. The dashed line is the limit of the incipient precipitation of green rust. For each Mössbauer spectrum acquired in the field, we drew a circle on both solid and dashed lines.

The values obtained are plotted in the ternary diagram (Fig. 8) for the two limits of X_2. Values of x larger than 1/3 are not possible in a purely ferric minerals and correspond to fougerite richer in Mg.

At the depth where soil solutions were sampled, x is quasi-constant around 0.6. This implies that magnesium is present in the mineral. From this value of x, and in the range of variation admitted for X_2, two limits of the composition of the layer are obtained:

Table 4. Equilibrium reactions for fougerite F1 with different interlayer anions.

Mole formula of fougerite F1 $[1/6\ Fe^{II}(OH)_2 \cdot 1/4\ Fe^{III}(OH)_2 \cdot 7/12\ Mg(OH)_2]^{1/4+}\ [1/4\ A]^{1/4-}$	$X_2 = 1/4$
Reaction with $A^- = Cl^-$	$\mu = -732.86$ kJ mol^{-1}
$F1 + 1/4\ e^- + 2H^+ \rightleftarrows 5/12\ Fe^{2+} + 7/12\ Mg^{2+} + 1/4\ Cl^- + 2H_2O$	$\Delta_R G^0 = -28.10$ kJ mol^{-1}
Equilibrium equation	
$5/12\log(Fe^{2+}) + 7/12\log(Mg^{2+}) + 1/4\log(Cl^-) + 2\log a_w + 1/4pe + 2pH$	$\log K = 13.68$
Reaction with $A^- = OH^-$	$\mu = -812.70$ kJ mol^{-1}
$F1 + 1/4\ e^- + 9/4H^+ \rightleftarrows 5/12\ Fe^{2+} + 7/12\ Mg^{2+} + 9/4H_2O$	$\Delta_R G^0 = -24.74$ kJ mol^{-1}
Equilibrium equation	
$5/12\log(Fe^{2+}) + 7/12\log(Mg^{2+}) + 9/4\log a_w + 1/4pe + 9/4pH$	$\log K = 4.33$
Reaction with $A^- = 1/2SO_4^{2-}$	$\mu = -832.28$ kJ mol^{-1}
$F1 + 1/4\ e^- + 2H^+ \rightleftarrows 5/12\ Fe^{2+} + 7/12\ Mg^{2+} + 1/8\ SO_4^{2-} + 2H_2O$	$\Delta_R G^0 = -38.91$ kJ mol^{-1}
Equilibrium equation	
$5/12\log(Fe^{2+}) + 7/12\log(Mg^{2+}) + 1/8\log(SO_4^{2-}) + 2\log a_w + 1/4pe + 2pH$	$\log K = 6.82$
Reaction with $A^- = 2/3HCO_3^- \cdot 1/6CO_3^{2-}$	$\mu = -867.68$ kJ mol^{-1}
$F1 + 1/4\ e^- + 49/24H^+ \rightleftarrows 5/12\ Fe^{2+} + 7/12\ Mg^{2+} + 5/24\ HCO_3^- + 2H_2O$	$\Delta_R G^0 = -32.71$ kJ mol^{-1}
Equilibrium equation	
$5/12\log(Fe^{2+}) + 7/12\log(Mg^{2+}) + 5/24\log(HCO_3^-) + 2\log a_w + 1/4pe + 49/24pH$	$\log K = 5.73$

Table 5. Equilibrium reactions for fougerite F2 with different interlayer anions.

Mole formula of fougerite F2 $[2/9Fe^{II}(OH)_2 \cdot 1/3\ Fe^{III}(OH)_2 \cdot 4/9\ Mg(OH)_2]^{1/3+}[1/3A^-]^{1/3-}$	$X_2 = 1/3$
Reaction with $A^- = Cl^-$	$\mu = -685.38$ kJ mol^{-1}
F2 + 1/3 e^- + 2H^+ ⇄ 5/9 Fe^{2+} + 4/9 Mg^{2+} + 1/3 Cl^- + 2H_2O	$\Delta_R G^0 = -85.77$ kJ mol^{-1}
Equilibrium equation	
5/9log(Fe^{2+}) + 4/9log(Mg^{2+}) + 1/3log(Cl^-) + 2log a_w + 1/3pe + 2pH	log K = 15.06
Reaction with $A^- = OH^-$	$\mu = -765.22$ kJ mol^{-1}
F2 + 1/3 e^- + 7/3H^+ ⇄ 5/9 Fe^{2+} + 4/9 Mg^{2+} + 7/3H_2O	$\Delta_R G^0 = -41.44$ kJ mol^{-1}
Equilibrium equation	
5/9 log(Fe^{2+}) + 4/9log(Mg^{2+}) + 7/3log a_w + 1/3pe + 7/3pH	log K = 7.26
Reaction with $A^- = 1/2SO_4^{2-}$	$\mu = -784.80$ kJ mol^{-1}
F2 + 1/3 e^- + 2H^+ ⇄ 5/9 Fe^{2+} + 4/9 Mg^{2+} + 1/6 SO_4^{2-} + 2H_2O	$\Delta_R G^0 = -66.86$ kJ mol^{-1}
Equilibrium equation	
5/9 log(Fe^{2+}) + 4/9log(Mg^{2+}) + 1/6log(SO_4^{2-}) + 2loga_w + 1/3pe + 2pH	log K = 11.71
Reaction with $A^- = 2/3HCO_3^- \cdot 1/6CO_3^{2-}$	$\mu = -820.20$ kJ mol^{-1}
F2 + 1/3 e^- + 37/18H^+ ⇄ 5/9 Fe^{2+} + 4/9 Mg^{2+} + 5/18 HCO_3^- + 2H_2O	$\Delta_R G^0 = -70.39$ kJ mol^{-1}
Equilibrium equation	
5/9 log(Fe^{2+}) + 4/9 log(Mg^{2+}) + 5/18 log(HCO_3^-) + 2 log a_w + 1/3pe + 37/18pH	log K = 12.33

1. $x = 0.6$ and $X_2 = 1/4$ give $X_1 = 1/6$ and $X_3 = 7/12$, that is, the formula: $\left[\frac{1}{6}Fe^{II}(OH)_2 \cdot \frac{1}{4}Fe^{III}(OH)_2 \cdot \frac{7}{12}Mg(OH)_2\right]^{+\frac{1}{4}}\left[\frac{1}{4}A\right]^{-\frac{1}{4}}$, hereafter designated as F1;
2. $x = 0.6$ and $X_2 = 1/3$ give $X_1 = 2/9$ and $X_3 = 4/9$, that is, the formula: $\left[\frac{2}{9}Fe^{II}(OH)_2 \cdot \frac{1}{3}Fe^{III}(OH)_2 \cdot \frac{4}{9}Mg(OH)_2\right]^{+\frac{1}{3}}\left[\frac{1}{3}A\right]^{-\frac{1}{3}}$, hereafter designated as F2.

From the solid solution model generalized to different anions, the chemical potentials of F1 and F2 are computed, hence the $\Delta_r G^0$ and the log K for the equilibrium reactions (cf. Tables 4 and 5). As the extent of variation of μ for a given interlayer anion is very narrow (less than 0.6%), equilibria are written in the classical way for constant composition minerals, as previously (Bourrié et al., 2004). It is here extended to other anions than OH^-.

The set of soil solutions sampled in Fougères during 16 months is used to check the equilibria (Table 6; Fig. 9). The soil solution is always undersaturated when chloride is the interlayer anion, and always oversaturated when the anion is OH^-. With the carbonate or the sulfate anion, depending on X_2 value and date, the solutions are either undersaturated or oversaturated. For all species, the lowest values of log IAP − log K occur between 7/15/1999 and 10/15/1999.

If one compares those results with the preceding results obtained in the same milieu, not considering magnesium incorporation in the mineral, it appears that the presence of magnesium stabilizes fougerite. This is logical, as Mg dilutes Fe atoms and cannot undergo oxidation. The solid solution model shows that this effect increases when the electronegativity of the interlayer anion increases. In addition to being more stable from a thermodynamic point of view, Mg-fougerite should be less labile from a kinetic point of view, due to the smaller number of neighbouring Fe atoms, likely to oxidize and destabilize the lattice by an oxolation process.

4.6. Interactions Between Fougerite and Soil Solution

The preceding results can now be used to draw the consequences of the observed variations of x or of its constancy on the chemical composition of soil solution. Variations of x can occur (1) at a constant number of moles of fougerite, that is, by reducing or oxidizing Fe in the mineral. In this case, the total number of moles of Fe and Mg in the solid does not change, hence, there is no exchange of Fe or Mg with the soil solution, and the elementary reaction can be simply written as the oxidation of a unit-cell of $Fe(OH)_2$: $Fe(OH)_2 \cdot H_2O$ ⇄ $Fe(OH)_3 + H^+ + e^-$, which would lead at equilibrium to: pe + pH = constant; and (2) with precipitation or dissolution of fougerite, at equilibrium or not, thus with exchange of Fe and Mg between the solid phase and the soil solution. Conversely, x constancy does not imply there is no precipitation or dissolution of fougerite, but simply that fougerite precipitates or dissolves as if it were a mineral of fixed composition. In this case, pe + pH is not constant (see equations in Tables 4 and 5).

This can be discussed considering the (pe, pH) diagram (Fig. 10). It appears that the first hypothesis can be ruled out, as pe + pH is not constant, (slope −1 corresponds to dotted lines), that is, there is no complete buffering of pH by pe variations. Instead, the system shifts rapidly from a state of strong reducing conditions (domain III, according to Sposito (1981); Fig. 10) to oxidizing conditions (domain I) during short duration events, then back to domain III. In this domain, SO_4^{2-} is the stable species, though in extreme cases, sulfides were measured. The solid line corresponds, according to Sposito (1981), to the critical pe value under which the activity of $Fe^{2+}_{aq.}$ begins to be significantly different from zero (by convention 10^{-7}). Hence, points situated above the line $Fe_3(OH)_7/Fe^{2+}$ represent solutions for which the variety of fougerite without magnesium is stable. The majority of points lie in the field of stability of $Fe_3(OH)_7$ and some in the field of stability of goethite or lepidocrocite.

Variations of x ratio with time and depth can be driven by the fluctuations of the groundwater level and by the variations of the groundwater chemistry as influenced by rain events. We

Table 6. Temperature, pH, pe, and log activities of free ions in soil solutions from Fougères.

Date	t °C	pH	pe	log (Fe^{2+})	log (Mg^{2+})	log (SO_4^{2-})	log (Cl^-)	log (HCO_3^-)
February 19, 1999	280.15	7.30	−3.171	−3.2192	−3.6820	−5.5277	−2.8378	−7.0999
February 22, 1999	280.75	7.24	−3.162	−3.2669	−3.7055	−5.5877	−3.0034	−7.0258
February 26, 1999	280.75	7.12	−3.298	−3.1798	−3.7981	−5.6337	−2.8791	−7.6193
March 1, 1999	280.75	7.11	−3.297	−3.3108	−3.8118	−5.4779	−3.0405	−7.0451
March 5, 1999	281.15	7.15	−3.049	−3.4950	−3.8474	−5.4371	−2.9296	−7.1276
March 8, 1999	280.65	7.52	−2.975	−3.4050	−3.9167	−5.4466	−3.0480	−7.1543
March 11, 1999	280.75	7.16	−3.162	−3.4033	−3.8488	−5.4008	−3.0308	−7.6677
March 16, 1999	281.45	7.19	−3.037	−3.3255	−3.8661	−5.5452	−2.9134	−7.3488
March 19, 1999	281.55	7.15	−3.054	−3.3688	−3.8448	−5.5225	−3.0575	−6.6982
March 26, 1999	281.65	7.12	−3.140	−3.3212	−3.8141	−5.4839	−2.9894	–
March 29, 1999	281.85	7.10	−3.193	−3.3636	−3.8877	−5.4423	−3.0376	−6.9003
March 31, 1999	281.85	7.08	−3.227	−3.5740	−3.9257	−5.2808	−3.0280	−7.5714
April 6, 1999	282.75	7.11	−3.205	−3.4210	−3.8750	−5.4234	−3.0500	−7.3829
April 14, 1999	282.65	7.10	−3.069	−3.3455	−3.8794	−5.5113	−3.0415	−7.5040
April 22, 1999	282.25	7.07	−2.911	−3.3949	−3.8852	−5.3691	−2.9550	−7.4500
April 26, 1999	282.45	7.11	−2.948	−3.5895	−3.9202	−5.2860	−3.0283	−7.4200
April 30, 1999	283.05	7.31	−3.311	−3.4456	−3.9432	−5.3962	−3.0354	−7.3498
May 6, 1999	284.05	7.24	−3.339	−3.4326	−4.2152	−5.3409	−2.9963	–
May 12, 1999	284.35	7.08	−3.225	−3.5259	−3.9408	−5.3429	−3.0788	−7.4536
May 19, 1999	284.15	7.24	−3.206	−3.4911	−3.9631	−5.3903	−3.0882	−7.1667
May 26, 1999	284.45	7.37	−3.108	−3.5162	−3.9127	−5.3526	−3.0052	–
June 2, 1999	285.55	7.37	−3.072	−3.5067	−3.9095	−5.4288	−2.974	−7.0954
June 9, 1999	285.35	7.40	−3.103	−3.4819	−4.0459	−5.3721	−2.9849	−6.6539
June 14, 1999	285.25	7.41	−3.152	−3.5040	−4.1734	−5.4057	−3.0059	−6.7293
June 18, 1999	285.65	7.36	−3.124	−3.5290	−3.8986	−5.4292	−3.0034	−6.6525
June 21, 1999	285.85	7.28	−3.076	−3.5506	−3.9309	−5.3836	−3.0878	−6.4321
June 28, 1999	286.05	7.31	−3.112	−3.5700	−3.9202	−5.4200	−3.0639	−6.7291
July 1, 1999	286.15	7.24	−3.147	−3.4891	−3.9258	−5.4235	−3.0778	−6.5986
July 5, 1999	286.65	7.19	−3.153	−3.5945	−3.9605	−5.4248	−3.0869	−6.8323
July 8, 1999	286.75	7.18	−3.188	−3.576	−3.9579	−5.4439	−3.0961	−6.9605
July 13, 1999	287.25	7.19	−3.262	−3.6222	−3.9249	−5.4844	−3.1008	−6.6544
July 19, 1999	287.35	6.85	−3.280	−3.6148	−3.9439	−5.5041	−3.0539	−6.7084
July 27, 1999	287.75	6.49	−3.489	−3.5465	−3.9449	−5.6702	−3.0518	−6.6491
August 16, 1999	287.75	6.42	−3.489	−3.7836	−4.0035	−5.4525	−3.0753	−6.7750
August 20, 1999	287.45	6.40	−3.468	−3.5966	−4.0463	−5.4010	−3.0485	−6.7935
August 23, 1999	287.65	6.42	−3.471	−3.6374	−4.0463	−5.3436	−3.0808	−7.0247
August 27, 1999	288.05	6.45	−3.475	−3.7095	−4.0562	−5.6275	−3.0924	−6.9099
September 20, 1999	287.35	6.28	−0.508	−4.7590	−4.2918	−5.7412	−3.2604	−7.0741
September 21, 1999	287.35	6.30	−0.255	−4.6622	−4.2920	−5.7417	−3.2722	−6.7113
September 22, 1999	287.25	6.40	−0.203	−5.2148	−4.2621	−5.7407	−3.2748	−6.6123
September 24, 1999	287.25	6.40	−1.437	−4.4113	−4.2361	−5.6022	−3.1719	−6.7129
September 27, 1999	287.35	6.37	−2.976	−3.9306	−4.2303	−5.5354	−3.2688	−7.3376
October 8, 1999	286.05	6.68	−4.600	−3.6381	−4.0630	−5.2515	−3.1908	−6.5760
October 11, 1999	286.05	6.96	−4.498	−3.6099	−4.0562	−5.0545	−3.2018	−6.6188
October 15, 1999	285.95	7.32	−4.700	−3.6958	−4.0325	−5.0884	−3.1921	−6.6339
October 22, 1999	285.35	7.35	−4.269	−3.6936	−4.0210	−5.1681	−3.1900	−6.5649
October 29, 1999	285.35	7.36	−3.864	−3.5836	−4.0095	−5.1282	−3.1761	−6.4220
November 4, 1999	285.35	7.40	−3.915	−3.5536	−4.0016	−5.1934	−3.1375	−6.5210
November 10, 1999	284.55	7.60	−3.921	−3.5867	−3.9871	−5.2073	−3.1187	−6.3368
November 15, 1999	283.85	7.68	−4.098	−3.6275	−3.9739	−5.1370	−3.1088	−6.3312
November 21, 1999	282.85	7.74	−4.170	−3.6114	−3.9589	−5.3432	−3.1040	−6.4132
November 30, 1999	282.65	7.85	−4.133	−3.6294	−3.9305	−5.3540	−3.0773	−6.4160
December 6, 1999	282.65	7.87	−4.083	−3.5890	−3.9465	−5.2840	−3.0664	−6.5791
December 15, 1999	282.15	7.90	−4.093	−3.5524	−3.9384	−5.1327	−3.0593	−6.4334
December 23, 1999	281.25	7.94	−4.047	−3.6430	−3.9465	−5.2110	−3.0682	−6.5725
January 7, 2000	281.35	8.07	−3.999	−3.7465	−3.9647	−4.9614	−3.1280	−6.5083
January 19, 2000	279.75	8.01	−3.893	−3.8189	−4.0815	−5.3508	−3.1664	−6.4385
February 2, 2000	279.45	8.17	−4.042	−3.8464	−4.0153	−5.2541	−3.1595	−6.4016
February 9, 2000	280.15	8.14	−4.017	−3.8270	−4.0813	−5.1909	−3.1812	−6.3609
February 15, 2000	280.35	8.16	−4.036	−3.8840	−4.1167	−5.1671	−3.1961	−6.4925
March 31, 2000	281.65	8.02	−4.154	−3.7619	−4.0837	−5.6413	−3.2256	−6.4042
April 4, 2000	281.55	7.90	−4.069	−3.6635	−4.0947	−5.3645	−3.2171	−6.4128
April 6, 2000	281.45	7.87	−3.915	−3.7811	−4.0651	−5.0595	−3.2465	−6.4380
April 14, 2000	281.45	7.91	−3.898	−3.7022	−4.1409	−5.1375	−3.2378	−6.4503
April 20, 2000	281.75	7.95	−3.868	−3.8145	−4.1375	−5.1887	−3.2456	−6.3915
May 9, 2000	284.95	8.03	−4.264	−3.7276	−4.0840	−5.4451	−3.2386	−6.5704
May 22, 2000	286.05	7.92	−4.144	−3.7362	−4.1214	−5.3934	−3.2533	−6.4522
June 5, 2000	286.45	7.90	−4.199	−3.8221	−4.1383	−5.4449	−3.2375	−6.5481

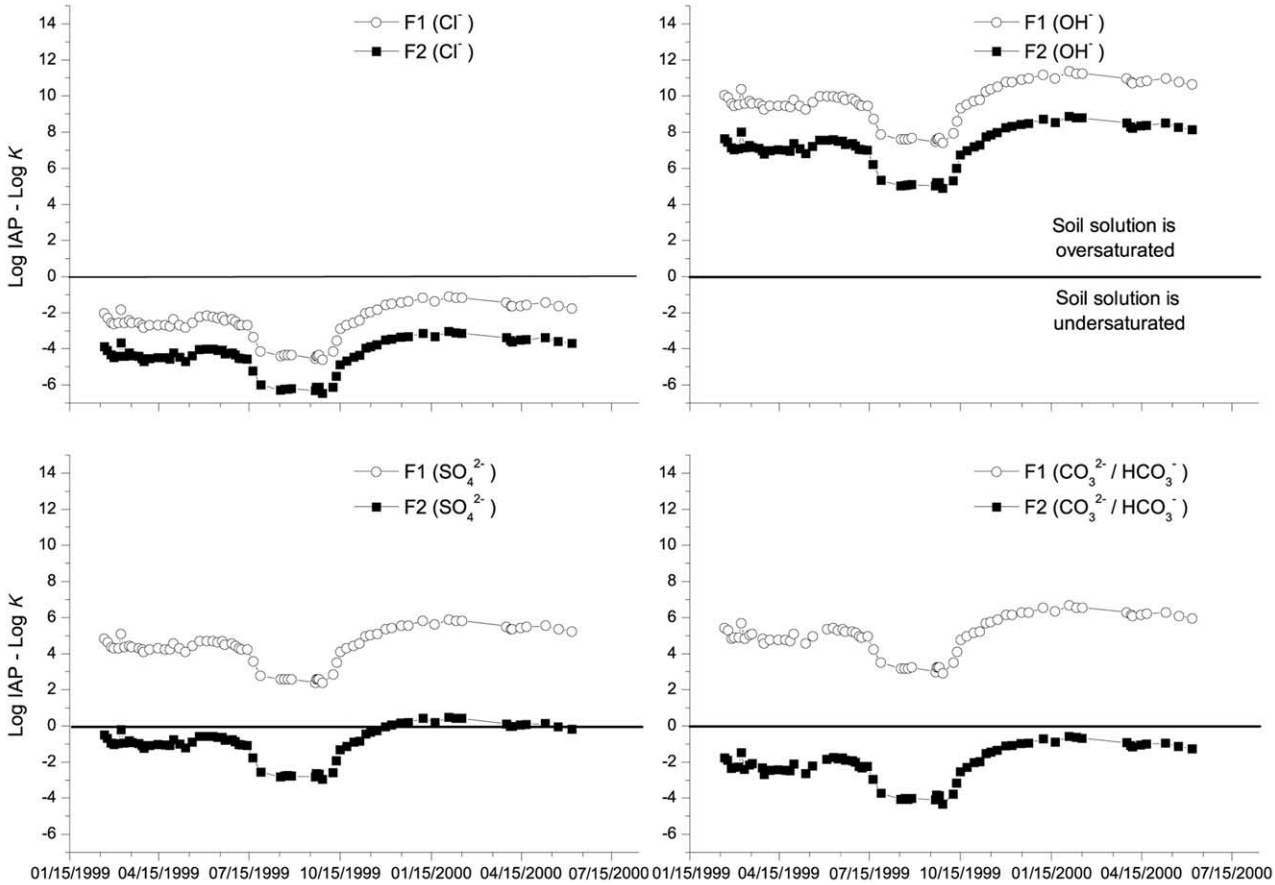

Fig. 9. Variations with time of log IAP − log K for green rusts with different anions (Cl^-; OH^-, SO_4^{2-} or HCO_3^-/CO_3^{2-} and for the limits of variation admitted for X_2: 1/4 (F1) to 1/3 (F2). The solid line (log IAP = log K) corresponds to the equilibrium between mineral and soil solution. The oversaturation of the soil solution is observed when log IAP − log $K > 0$; the undersaturation corresponds to log IAP − log $K < 0$.

will first address large timescale variations, then short duration events.

4.6.1. Large timescale variations

During the seasons that Mössbauer spectra were acquired, the water table fluctuated from 25 to 40 cm depth. Thus, all points observed by Mössbauer spectroscopy are situated in the permanently waterlogged horizons. The seasonal decrease of the water table (Fig. 3) from steadily high values (October 1998 to April 1999) to low values (april to august 1999) does not immediately result in an increase of pe at the depth where the probe is situated (70 cm). Indeed, pe remains constant at about −2.9 (Eh ≃ −165 mV), but pH increases generally from 6.2 to 7.3. An increase of pH at constant pe drives reactions towards oxidation, as slopes in (pe, pH) diagrams are negative. The Mössbauer data do not show a definite tendency with time at given depth. As soil solution is transferred, its chemical composition cannot be directly compared with the x ratio at the same depth. Instead, the clear general tendency of x to decrease with depth, as the milieu becomes more reducive, suggests that x is a better proxy of average oxidizing conditions than pe, which is subject to fast variations.

As an average, goethite and lepidocrocite are frequently destabilized, while fougerite is generally stable even in its purely ferroso-ferric form, the endmember $Fe_3(OH)_7$. The presence of magnesium makes fougerite always stable when goethite and lepidocrocite are not stable.

4.6.2. Short duration events

Sharp pe increase to +9.5 is observed following summer storms at quasi-constant pH. This can be ascribed to oxygen input by rainwater saturated with atmospheric O_2 just preceding air entry in the system (iron concentration falls to zero, and later no sample could be obtained). In these conditions, goethite and lepidocrocite are stable. In Fougères, goethite was not observed, but lepidocrocite was observed previously by transmission Mössbauer spectroscopy at 60 cm depth (Abdelmoula et al., 1998).

As soon as, in autumn, the water table rises, pe decreases to lower values, as low as −4.7 (Eh ≃ −263 mV), probably due to supply of fresh dissolved organic matter. Except in summer during storms of short duration and when air enters soil at the driest period, pe remains quasi-constant and low. This, however, does not imply that there are no oxido-reduction varia-

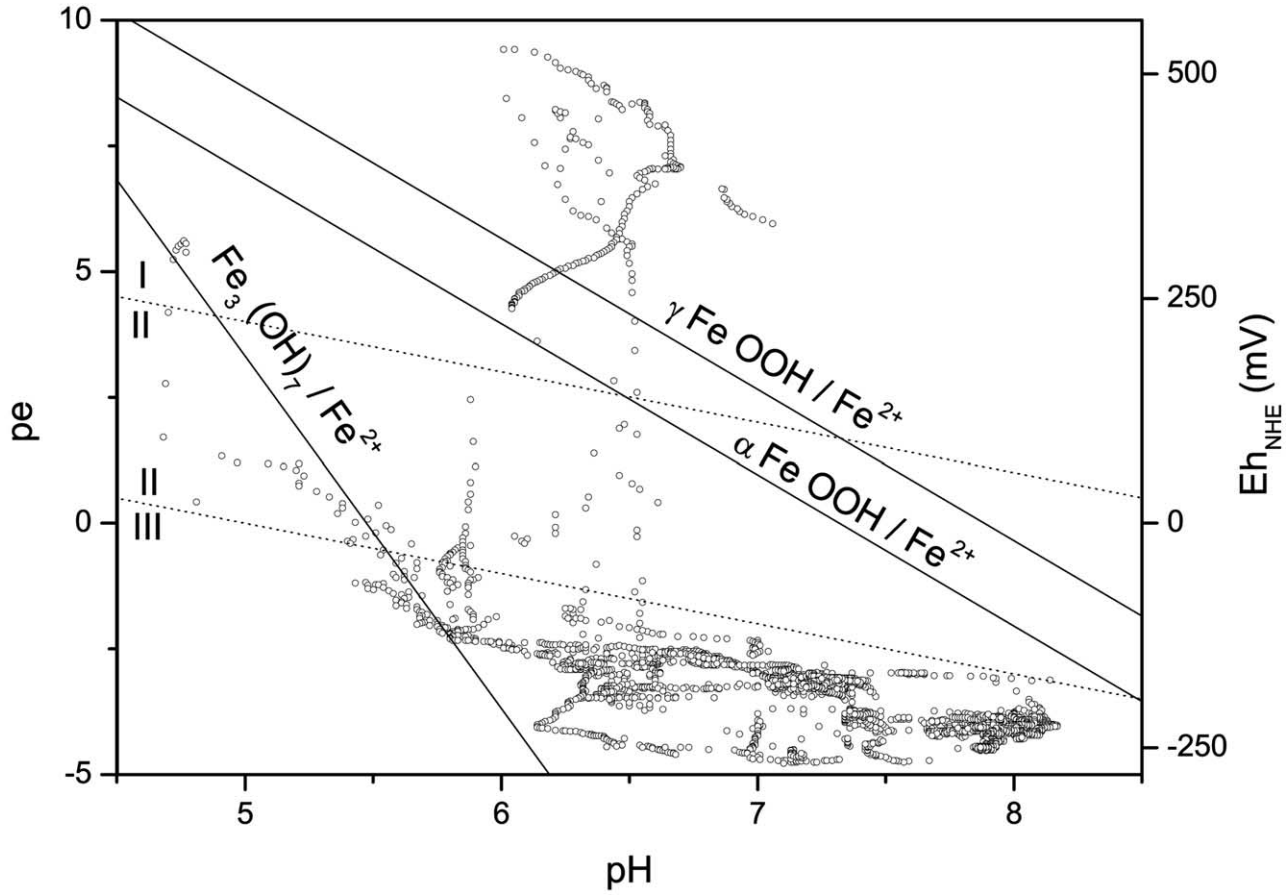

Fig. 10. pe and pH variations of soil solutions at 70 cm depth.

tions, but geochemical processes are then driven by sharp pH variations at quasi-constant pe ($-4 < pe < -3$). Such sharp pH variations, which are all significant, can be ascribed to acid inputs transferred by rainwater percolating through the litter and organic horizons, and to nitrification. Such sharp acid events are recorded at 40 cm depth during several months (Fig. 11). During those events, pH decreases sharply at quasi-constant pe, thus pe + pH (or equivalently rH) decreases, which favours reduction of green rusts and decrease of the *x* ratio. The rH values (between 6 and 12) correspond to a gleysol (according to the WRB limits, *i.e.,* $rH < 19$). One can thus oppose (i) pe variations at quasi-constant pH during summer storms at the driest period, and (ii) long periods where soil is saturated with water and reducing conditions prevail, oxido-reduction processes being driven by sharp pH variations.

We will now discuss the possibility of green rusts to form quickly, as evidenced at 78 cm depth (Fig. 7). From the investigation depth (0.05 cm) and the field of view of the instrument (2 cm diameter), the volume probed is obtained at $\sim$0.2 cm^3, while the molar volume of green rust (for 1 iron in the cell) is $\sim$20 nm^3. The complete filling of the volume probed by newly formed green rust would imply precipitation of 10^9 unit cells, that is, 20 micromoles of iron. The iron concentration in solution being ca. $4 \cdot 10^{-4}$ M in reducing conditions, the contribution of only 5 mL of soil solution is required to entirely fill this volume with green rust. However, the sensitivity of the Mössbauer spectrometer is such that green rusts can be detected from abundance of 5% in the volume probed, so that the preceding figure can be divided by 20, which shows that the precipitate can form from dissolved iron contained in 0.25 mL soil solution. As green rusts are known to form very quickly in the laboratory, we can conclude that we have evidence for the direct formation of fougerite in the field. Then, the mechanism would simply be to precipitate locally all the iron contained in soil solution as dissolved oxygen enters the system, for example, when the water table gets deeper.

5. CONCLUSIONS

We used a portable Mössbauer spectrometer for the first time in situ to study iron oxide mineralogy in a hydromorphic soil. During alternating aerobic and anaerobic conditions, the soil colour changes from ochre to blue in horizons deeper than 70 cm. Fougerite is the only iron mineral identified, except in summer when lepidocrocite is present in addition to fougerite, whereas goethite was not observed. Silicated iron is negligible.

Variations of $Fe^{3+}/Fe_{tot.}$ are observed with depth: (i) more ferric fougerite ($Fe^{II}\ Fe_2^{III}\ (OH)_8$) is present in the upper oximorphic horizons; (ii) more ferrous fougerite ($Fe_2^{II}\ Fe^{III}\ (OH)_7$) is present in the lower reductomorphic horizons. These variations are consistent with soil morphology. Rapid temporal variations of $Fe^{3+}/Fe_{tot.}$ are correlated with fluctuations of the

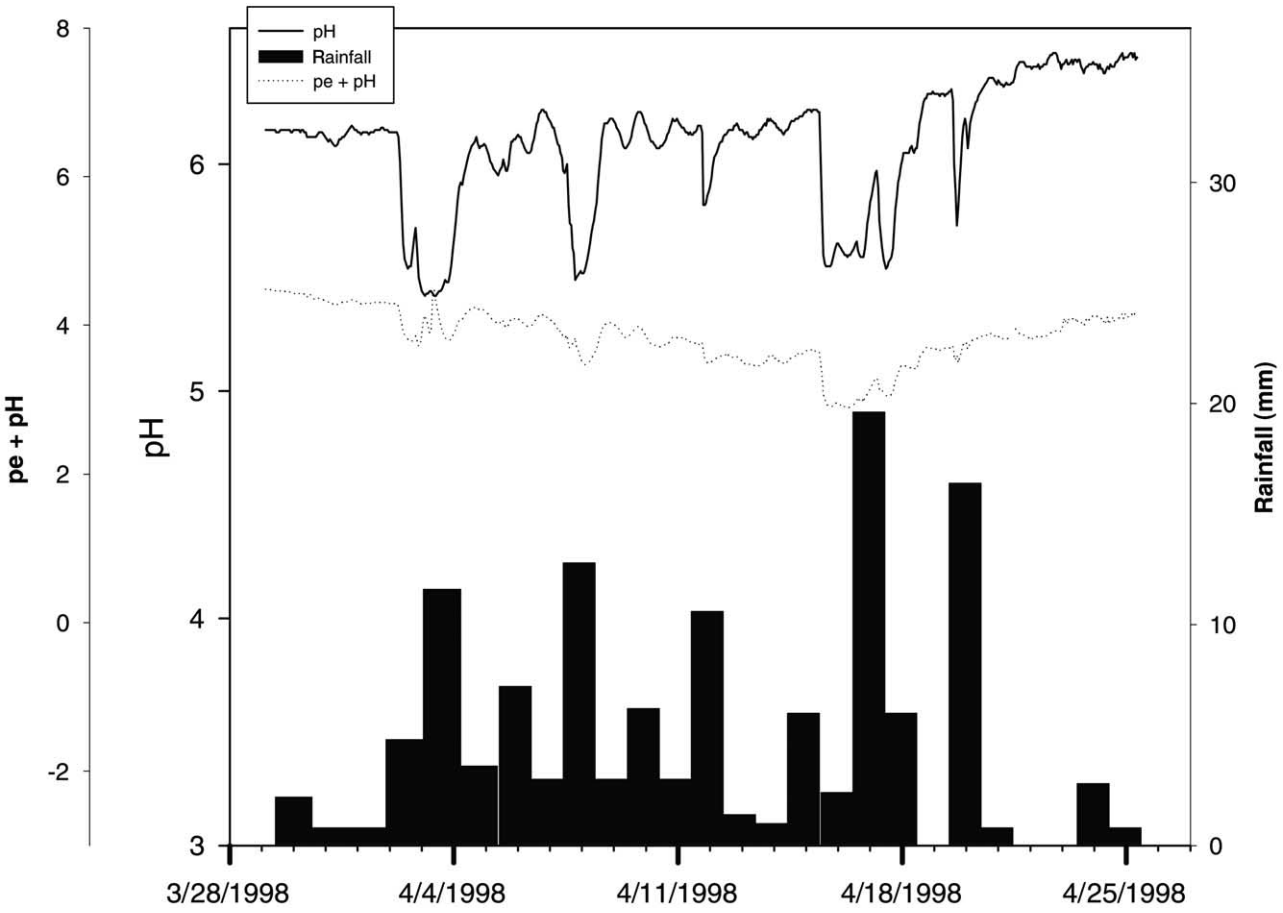

Fig. 11. Rainfall, pH, and pe, and pH variations at shallow depth (40 cm).

water table, causing alternating aerobic and anaerobic conditions.

This demonstrates that fast and reversible mineralogical transformations of iron oxides exist in these soils. Fast geochemical phenomena in soils are thus not restricted to ion exchange or precipitation and dissolution of soluble salts, as classically considered. In situ Mössbauer spectroscopy appears as an essential tool to monitor mineralogical transformations of iron oxides. It allows both the identification of solid phases and the quantitative measurement of Fe^{2+} and Fe^{3+}, is a nondestructive technique, and is a means to follow the influence of anaerobic and aerobic alternations, in which iron plays the role of electron donor or acceptor. Fougerite is an essential actor in this interplay of biogeochemical cycles.

An automatic probe was used to monitor pH and pe in soil solution at 1 h interval. Seasonal dynamics could thus be registered. Both sharp variations of pe at quasi-constant pH and sharp variations of pH at quasi-constant pe were observed.

To check soil-solutions equilibria, a solid solution model for fougerite is proposed, allowing the Mg-Fe(II)-Fe(III) hydroxide to accommodate different anions in the interlayer. As an average, log IAP variations closely parallel pH variations. The soil solutions are largely oversaturated with respect to OH-fougerite, either undersaturated or oversaturated with respect to CO_3^{2-}/HCO_3^- or SO_4^{2-} green rusts, and always undersaturated with respect to Cl^- green rust. The soil solution shifts quickly from a reduced state in the field of stability of fougerite to an oxidized state in the field of stability of lepidocrocite. The field of stability of goethite is quickly crossed.

This strongly suggests that fougerite forms from oversaturated soil solutions, when dissolved oxygen enters the system and Fe^{3+} coprecipitates with Fe^{2+} and Mg^{2+}.

We can thus propose that the following mineralogical transformations occur seasonally:

1. In the driest periods of summer, fougerite is completely oxidized to Fe(III) oxides (lepidocrocite).
2. In autumn, due to the supply of fresh organic matter and water saturation, the milieu turns anoxic, and lepidocrocite is reduced and dissolves, releasing Fe^{2+} into solution.
3. When dissolved oxygen is replenished by air-saturated rainfall, Fe^{2+} oxidizes to Fe^{3+} that coprecipitates with Fe^{2+} and Mg^{2+} to form fougerite, with a variable x ratio, following alternatively anoxic and oxic periods.
4. Eventually, during the next summer when the water table falls and air enters the soil profile, fougerite transforms back by complete oxidation into lepidocrocite, releasing Mg^{2+} in solution.

Acknowledgments—This work was supported by the Ministère de la Recherche (pre-doctoral grant F.F.), the Institut National de la Recherche Agronomique (post-doctoral grant G.K.), the Région Bretagne (programme PRIR), the German Space Agency (DLR) and the Pro-

gramme National Sol et Erosion (CNRS/INRA/INSU/IRD). The authors are particularly grateful to Dr P. Stengel, Dr P. Chassin, Prof. A. Mariotti, Dr P. Thivend and B.Bernhardt for their help. Thanks are expressed to the three anonymous referees for their comments and help to improve the manuscript.

Associate editor: D. L. Sparks

REFERENCES

Abdelmoula M., Trolard F., Bourrié G., and Génin J.-M. R. (1998) Evidence for the Fe(II)-Fe(III) green rust "fougerite" mineral occurrence in a hydromorphic soil and its transformation with depth. *Hyperfine Interactions* **112,** 235–238.

Allmann R. (1968) The crystal structure of pyroaurite. *Acta Crystallographica* **B24**, 972–977.

Altmeier M., Metz V., Neck V., Müller R., and Fanghänel T. (2003) Solid-liquid equilibria of $Mg(OH)_{2(cr)}$ and $Mg(OH)_3\ Cl \cdot 4H_2O_{(cr)}$ in the system Mg - Na - H - OH - Cl - H_2O at 25°C. *Geochim. Cosmochim. Acta* **67,** 3595–3601.

Badaut D., Besson G., Decarreau A., and Rautureau R. (1985) Occurrence of a ferrous, trioctahedral smectite in recent sediments of Atlantis II deep, Red Sea. *Clay Minerals*, **20,** 389–404.

Borggaard O. K. (1988) Phase identification by selective dissolution techniques. In *Iron in Soil and Clay Minerals,* NATO series, (ed J. W. Stucki et al.) p. 83–98 Dordrecht Reidel Publishing Company.

Bourrié G., Trolard F., Génin J.-M. R., Jaffrezic A., Maître V., and Abdelmoula M. (1999) Iron control by equilibria between hydroxygreen rusts and solutions in hydromorphic soils. *Geochim. Cosmochim. Acta* **63,** 3417–3427.

Bourrié G., Trolard F., Refait P., and Feder F. (2004) A solid solution model for Fe(II)-Fe(III)-Mg(II) green rusts and fougerite and estimation of their Gibbs free energies of formation. *Clays and Clay Minerals* **52,** 383–395.

Bratsch, S. G. (1989). Standard electrode potentials and temperature coefficients in water at 298. 15 K. *J. Physical and Chemical Reference Data* **18,** 1–21.

Cornell R. M. and Schwertmann U. (2003) *The Iron Oxides: Structure, Properties, Reactions Occurrences and Uses*. VCH.

DeBoodt M. F., Hayes M. H. B., and Herbillon A. J. ed. (1991) *Soil Colloids and Their Associations in Aggregates,* NATO series. Plenum Press.

Drissi H., Refait Ph., and Génin, J.-M. R. (1994) The oxidation of $Fe(OH)_2$ in the presence of carbonate ions: structure of carbonate green rust one. *Hyperfine Interactions* **90,** 395–400.

Drissi S. H., Refait Ph., Abdelmoula M., and Génin J.-M. R. (1995) Preparation and thermo-dynamic properties of Fe(II)-Fe(III) hydroxide-carbonate (green rust one): Pourbaix diagram of iron in carbonate-containing aqueous media. *Corrosion Science* **37,** 2025–2041.

FAO (1998) *World Reference Base for Soil Resources, Vol. 84*. FAO, ISRIC, and AISS, Rome.

Feder F., Bourrié G., and Trolard F. (1998) *In situ* continuous monitoring of soil solution chemistry. *Mineralogical Magazine* **62A,** part 1; 441–442.

Fischer W. (1988) Microbiological reactions of iron in soil. In *Iron in Soil and Clay Minerals,* NATO series (ed. J. W. Stucki et al.), pp. 715–748. Dordrecht Reidel Publishing Company.

Fredrickson J. K., Zachara J. M., Kennedy D. W., Dong H., Onstott T. C., Hinman N. W., and Li S.-M. (1998) Biogenic iron mineralization accompanying the dissimilatory reduction of hydrous ferric oxide by a groundwater bacterium. *Geochim. Cosmochim. Acta* **62,** 3232–3257.

Génin J.-M. R., Bourrié G., Trolard F., Abdelmoula M., Jaffrezic A., Refait Ph., Maître V., Humbert B., and Herbillon A. J. (1998) Thermodynamic equilibria in aqueous suspensions of synthetic and natural Fe(II)-Fe(III) green rusts: occurrences of the mineral in hydromorphic soils. *Environmental Science and Technology* **32,** 1058–1068.

Génin J.-M. R., Refait Ph., Bourrié G., Abdelmoula M., and Trolard F. (2001) Structure and stability of the Fe(II)-Fe(III) green rust "fougerite" mineral and its potential for reducing pollutants in soil solutions. *Applied Geochemistry* **16,** 559–570.

Hansen H. C. B. and Koch C. B. (1995) Synthesis and characterization of pyroaurite. *Applied Clay Science* **10,** 5–19.

Harvie C. E., MoÏller N., and Weare J. H. (1984) The prediction of mineral solubilities in natural waters: the Na - K - Mg - Ca - H - Cl - SO_4 - OH - HCO_3 - CO_3 - CO_2 - H_2O system to high ionic strengths at 25 °C. *Geochim. Cosmochim. Acta* **48,** 723–751.

Jolivet J. P. (1994) *De la Solution à l'Oxyde-Condensation des Cations en Solution Aqueuse- Chimie de Surface des Oxydes*. InterEditions/ CNRS Editions.

Klingelhöfer G., Fegley B. Jr., Morris R. V., Kankeleit E., Held P., and Evlanov E. P. O. (1996) Mineralogical analysis of martian soil and rock by a miniaturized backscattering Mössbauer spectrometer. *Planetary Space Science* **44,** 1277–1288.

Klingelhöfer G., Held P., Bernhardt B., Foh J., Teucher R., and Kankeleit E. (1998) In situ phase analysis by a versatile miniaturized Mössbauer spectrometer. *Hyperfine Interactions* **111,** 331–334.

Klingelhöfer G., Trolard F., Bourrié G., Feder F., and Génin J.-M. R. (1999) The monitoring of iron mineralogy and oxidation states by Mössbauer spectroscopy in the field; the Green Rust mineral in hydromorphic soils. In *American Geophysical Union,* Fall Meeting, San Francisco, 13–17 December 1999; H129-01.

Kostka J. E., Stucki J. W., Nealson K. H., and Wu J. (1996) Reduction of structural Fe(III) in smectite by a pure culture of *Shewanella putrefaciens* strain MR-1. *Clays and Clay Minerals* **44,** 522–529.

Mehra O. P. and Jackson M. L. (1960) Iron oxides removal from soils and clays by a dithionite-citrate system buffered with sodium bicarbonate. *Clays and Clay Minerals* **7,** 317–327.

Mitchell B. D., Smith B. F. L., and De Endredy A. S. (1971) The effect of buffered sodium dithionite solution and ultrasonic agitation on soil clays. *Israël Journal of Chemistry* **9,** 45–52.

Murad E. (1988) Properties and behavior of iron oxides as determined by Mössbauer spectroscopy. In *Iron in Soil and Clay Minerals.* NATO series. J. W. Stucki et al. p. 309–350, Dordrecht Reidel Publishing Company.

Murad E. and Cashion J. (2004) *Mössbauer-Spectroscopy of Environmental Materials and Their Industrial Utilization*. Kluwer Academic Publishers.

Murad E. and Taylor R. M. (1986) The oxidation of hydroxycarbonate green rusts. In *Industrial Applications of the Mössbauer Effect*, (ed. G. J. Long and J. G. Stevens) pp. 585–593, Plenum.

Ponnamperuma F. N. (1972) The chemistry of submerged soils. *Advances in Agronomy* **24,** 173–189.

Prigogine I. and Defay R. (1946) *Thermodynamique Chimique Conformément aux Méthodes de Gibbs et De Donder,* Tome I and Tome II, Dunod, Paris.

Refait P. and Génin J. (1993) The oxidation of Fe(II) hydroxide in chloride-containing aqueous media and Pourbaix diagrams of green rust one. *Corrosion Science* **34,** 797–819.

Refait P., Drissi H., Marie Y., and Génin J.-M. R. (1994) The substitution of Fe^{2+} ions by Ni^{2+} ions in green rust one compounds. *Hyperfine Interactions* **90,** 389–394.

Refait P., Abdelmoula M., and Génin J.-M. R. (1998a) Mechanisms of formation and structure of green rust one in aqueous corrosion of iron in the presence of chloride ions. *Corrosion Science* **40** 1547–1560.

Refait P., Charton A., and Génin J.-M. R. (1998b) Identification, composition, thermodynamic and structural properties of a pyroaurite-like iron(II)-iron(III) hydroxy-oxalate greenrust. *European J. of Solid State and Inorganic Chemistry* **35,** 655–666.

Refait P., Abdelmoula M., Trolard F., Génin J.-M. R., Ehrhardt J. J., and Bourrié G. (2001) Mössbauer and EXAFS study of the green rust mineral; the partial substitution of Fe(II) by Mg(II). *American Mineralogist* **86,** 731–739.

Robert M. (1975) Principes de détermination qualitative des minéraux argileux à l'aide des rayons X. Problèmes particuliers posés par les minéraux argileux les plus fréquents danslessols des régions tempérées. *Annales Agronomiques* **26,** 363–399.

Schwertmann U. (1988) Occurrence and formation of iron oxides in various pedoenvironments. In *Iron in Soil and Clay Minerals,* NATO series (ed. J. W. Stucki et al.), pp. 267–308. Dordrecht Reidel Publishing Company.

Schwertmann U. and Cornell R. M. (1991) *Iron Oxides in the Laboratory, Preparation and Characterization*. VCH.

Schwertmann U. and Fechter H. (1994) The formation of green rust and its transformation to lepidocrocite. *Clay Minerals* **29,** 87–92.

Simon L., François M., Refait P., Renaudin G., Lelaurain M., and Génin J.-M. R. (2003) Structure of the Fe(II-III) layered double hydroxy-sulphate green rust two from Rietveld analysis. *Solid State Sciences* **5,** 327–334.

Sposito G. (1981) *The Thermodynamics of Soil Solutions*. Oxford University Press.

Stevenson F. (1994) *Humus Chemistry-Genesis, Composition, Reactions*, 2nd ed. John Wiley.

Stucki J. W. (1988). Structural iron in smectites. In *Iron in Soil and Clay Minerals,* NATO series (ed. J. W. Stucki et al.), pp. 625–675. Dordrecht Reidel Publishing Company.

Stucki J. W., Komadel P., and Wilkinson H. T. (1987) Microbial reduction of structural Fe^{3+} in smectites. *Soil Science Society of America J.* **51,** 1663–1665.

Stumm W. and Morgan J. (1996) *Aquatic Chemistry-Chemical Equilibria and Rates in Natural Waters*, 3rd ed., John Wiley.

Stumm W. and Sulzberger B. (1992) The cycling of iron in natural environments: considerations based on laboratory studies of heterogeneous redox processes. *Geochim. Cosmochim. Acta* **56,** 3233–3257.

SuarezIha M. E. V., Pehkonen S. O., and Hoffmann M. R. (1994) Stability, stoichiometry, and structure of Fe (II) and Fe (III) complexes with di-2-pyridyl ketone benzoylhydrazone: environmental applications. *Environmental Science and Technology* **28,** 2080–2086.

Taylor R. M. (1980) Formation and properties of Fe(II)-Fe(III) hydroxy-carbonate and its possible significance in soil formation. *Clay Minerals* **15,** 369–372.

Trolard F., Soulier A., and Curmi P. (1993) Les formes solides du fer en milieu hydromorphe acide: une approche compartimentale par dissolution sélective. *Comptes rendus de l'Académie des Sciences* **316-II**, 1463–1468.

Trolard F., Bourrié G., Jeanroy E., Herbillon A. J., and Martin H. (1995) Trace metals in natural iron oxides from laterites: a study using selective kinetic extraction. *Geochim. Cosmochim. Acta* **59,** 1285–1297.

Trolard F., Abdelmoula M., Bourrié G., Humbert B., and Génin J.-M. R. (1996) Mise enévidence d'un constituant de type "rouilles vertes" dans les sols hydromorphes. Proposition de l'existence d'un nouveau minéral: la "fougérite". *Comptes rendus de l'Académie des Sciences* **323,** 1015–1022.

Trolard F., Genin J.-M. R., Abdelmoula M., Bourrié G., Humbert B., and Herbillon A. J. (1997) Identification of a green rust mineral in a reductomorphie soil by Mössbauer and Raman spectroscopie. *Geochim. Cosmochim. Acta* **61,** 1107–1111.

Van Breeman N. (1988) Effects of seasonal redox processes involving iron on the chemistry of periodically reduced soils. In *Iron in Soil and Clay Minerals,* NATO series (ed. J. W. Stucki et al.), pp. 797–809. Dordrecht Reidel Publishing Company.

VanVliet-Lanoë B., Pellerin J., and Helluin M. (1995) Morphogenèse-pédogenèse: Les héritages du dernier cycle glaciaire en forêt de Fougères (Ille et Vilaine, France). *Zeitschrift für Geomorphologie N.F.* **39,** 489–510.

Zsolnay A. (1996) Dissolved humus in soil waters. In *Humic Substances in Terrestrial Ecosystems* (ed. A. Piccolo), pp. 171–223. Elsevier, Amsterdam.

Clays and Clay Minerals, Vol. 52, No. 3, 382–394, 2004.

A SOLID-SOLUTION MODEL FOR Fe(II)-Fe(III)-Mg(II) GREEN RUSTS AND FOUGERITE AND ESTIMATION OF THEIR GIBBS FREE ENERGIES OF FORMATION

GUILHEM BOURRIÉ[1,*], FABIENNE TROLARD[1], PHILIPPE REFAIT[2] AND FRÉDÉRIC FEDER[1,3]

[1] INRA, Unité de Recherche de Géochimie des Sols et des Eaux, URGSE, Europôle de l'Arbois, BP 80, F13545 Aix-en-Provence cedex 04, France

[2] LEMMA, Université de La Rochelle, Bâtiment Marie Curie, 25 rue Enrico Fermi, F17000 La Rochelle, France

[3] CIRAD, Equipe "REGARD", Station de La Bretagne, BP 20 F97408 Saint-Denis Messag, cedex 9, La Réunion, France

Abstract—Fe(II)-Fe(III) green rust identified in soil as a natural mineral is responsible for the blue-green color of gley horizons, and exerts the main control on Fe dynamics. A previous EXAFS study of the structure of the mineral confirmed that the mineral belongs to the group of green rusts (GR), but showed that there is a partial substitution of Fe(II) by Mg(II), which leads to the general formula of the mineral: $[Fe^{2+}_{1-x}Fe^{3+}_{x}Mg_{y}(OH)_{2+2y}]^{x+}[xOH^{-}\cdot mH_2O]^{x-}$. The regular binary solid-solution model proposed previously must be extended to ternary, with provision for incorporation of Mg in the mineral. Assuming ideal substitution between Mg(II) and Fe(II), the chemical potential of any Fe(II)-Fe(III)-Mg(II) hydroxy-hydroxide is obtained as: $\mu = X_1\mu^{\circ}_1 + X_2\mu^{\circ}_2 + X_3\mu^{\circ}_3 + RT[X_1\ln X_1 + X_2\ln X_2 + X_3\ln X_3] + A_{12}X_2(1 - X_2)$.
All experimental data show that the mole ratio $X_2 = Fe(III)/[Fe_{total} + Mg]$ is constrained (1) structurally and (2) geochemically. Structurally, Fe(III) ions cannot neighbor each other, which leads to the inequality $X_2 \leqslant \frac{1}{3}$. Geochemically, Fe(III) cannot be too remote from each other for GR to form as $Fe(OH)_2$ and $Mg(OH)_2$ are very soluble, so $X_2 \geqslant \frac{1}{4}$. A linear relationship is obtained between the Gibbs free energy of formation of GR, normalized to one Fe atom, and the electronegativity χ of the interlayer anion, as: $\mu^{\circ}/n = -76.887\chi - 491.5206$ ($r^2 = 0.9985$, $N = 4$), from which the chemical potential of the mineral fougerite μ is obtained in the limiting case $X_3 = 0$, and knowing $\mu^{\circ}_1 = -489.8$ kJmol^{-1} for $Fe(OH)_2$, and $\mu^{\circ}_3 = -832.16$ kJmol^{-1} for $Mg(OH)_2$, the two unknown thermodynamic parameters of the solid-solution model are determined as:
$\mu^{\circ}_2 = +119.18$ kJmol^{-1} for $Fe(OH)_3$ (virtual), and $A_{12} = -1456.28$ kJmol^{-1} (non-ideality parameter).
From Mössbauer *in situ* measurements and our model, the chemical composition of the GR mineral is constrained into a narrow range and the soil solutions-mineral equilibria computed. Soil solutions appear to be largely overstaurated with respect to the two forms observed.

Key Words—Fe, Fougerite, Gley, Green Rust, Hydroxide, Mg, Model, Oxide, Soil, Thermodynamics.

INTRODUCTION

A green-blue color in soils has been used as a diagnostic criterion in the definition of gley and soil classification since the beginning of soil science, and ascribed immediately to the presence of Fe(II) oxide, called "protoxide", by Vysostskii (1905, [1999]). The green-blue color of soils and sediments was ascribed to the presence of "the theoretical compound hydro-magnetite $Fe_3(OH)_8$" by Ponnamperuma *et al.* (1967) and more generally to double hydroxy-carbonate-GR by Taylor (1981). The discovery of these compounds in natural environments, specifically acid to neutral gley soils (Trolard *et al.*, 1996, 1997), has confirmed the hypothesis formulated by Vysotskii (1905) and demonstrated for the first time the existence of GR as a mineral. The mineral name "fougerite" has been approved by the Commission on New Minerals and Mineral Names of the International Mineralogical Association.

An extended X-ray absorption fine structure (EXAFS) study was recently undertaken on fougerite and synthetic GR and pyroaurites, which (1) confirmed that the mineral belongs to the GR group, but (2) led to the conclusion that it contains Mg(II) (which cannot be seen by Mössbauer spectroscopy) as well as Fe(II) and Fe(III) (Refait *et al.*, 2001). This was not taken into account in checking the soil-solution equilibria (Bourrié *et al.*, 1999) and in the solid-solution model proposed earlier (Génin *et al.*, 2001).

The aims of this paper are thus: (1) to derive a generalized ternary solid-solution model for Fe(II)-Fe(III)-Mg(II) GR and fougerite; (2) to discuss the structural and geochemical constraints that must satisfy this model; (3) to estimate the parameters of this model on the basis of experimental data available on GR and of a relation obtained between the Gibbs free energy of formation of GR and the electronegativity of the unhydrated interlayer anion; and (4) to apply the model to check soil solution–solid solution equilibria on the basis of field data.

* E-mail address of corresponding author:
bourrie@aix.inra.fr
DOI: 10.1346/CCMN.2004.0520313

STRUCTURE OF GREEN RUSTS AND STRUCTURAL CONSTRAINTS FOR A SOLID-SOLUTION MODEL

Structure of green rusts and of fougerite

Green rusts consist of brucite-like sheets of $Fe(OH)_2$ in which part of the Fe(II) is oxidized to Fe(III), the excess charge being compensated by interlayered anions; the interlayers are hydrated. Two types of structure – rhombohedral GR1 and trigonal GR2 – exist, depending on the nature of interlayered anions. With small spherical or planar anions such as chloride and carbonate, GR1 compounds are obtained, while with large tetrahedral anions, such as sulfate and selenate, GR2 compounds form (Génin *et al.*, 1998a; Simon *et al.*, 2003) (Figure 1).

The exact nature of the compensating anion in fougerite cannot be determined directly as its abundance is small (total Fe_2O_3 content in soil is only ~4%), the mineral is labile and cannot be separated from the other minerals and Mössbauer spectroscopy is only sensitive to Fe. From the composition of soil solutions analyzed in the localities where GR were identified, it was concluded that the most likely anion is simply OH^-. The structure was thus assumed to be analogous to GR1(Cl), since OH^- is spherical as is Cl^-. Accordingly, the symmetry group was predicted to be the same as that of GR1(Cl), $R\bar{3}m$, with unit-cell parameters $a \approx 0.32$ nm and $c \approx 2.25$ nm, *i.e.* the same value for a, but a smaller value for c, due to the smaller size of OH^- (Génin *et al.*, 2001). In GR1(OH), the interlayer space can at most be completely filled with water molecules and OH^- ions that are of the same size, in a compact arrangement which leads to the complete general formula $[Fe^{2+}_{1-x}Fe^{3+}_x(OH)_2]^{x+}[xOH^-\cdot mH_2O]^{x-}$, or globally $Fe(OH)_{2+x}$, with x ranging from ⅓ to ⅔, and $m \leqslant 1-x$. The Mössbauer and X-ray absorption spectroscopy (XAS) studies of fougerite have confirmed that it belongs to the GR1 group, but have shown that Mg substitutes for Fe in the mineral and that the local ratio of Mg/Fe is ~2±1. Its general structural formula must then be modified as: $[Fe^{2+}_{1-x}Fe^{3+}_xMg_y(OH)_{2+2y}]^{x+}[xOH^-\cdot mH_2O]^{x-}$, with $m \leqslant 1 - x + y$. As x is the parameter measurable by Mössbauer spectroscopy, the preceding notation will be used to discuss the corpus of available experimental data. However, the solid-solution model is more conveniently, and symmetrically, written on the basis of mole fractions of the three components $Fe(OH)_2$, $Fe(OH)_3$ and $Mg(OH)_2$ respectively:

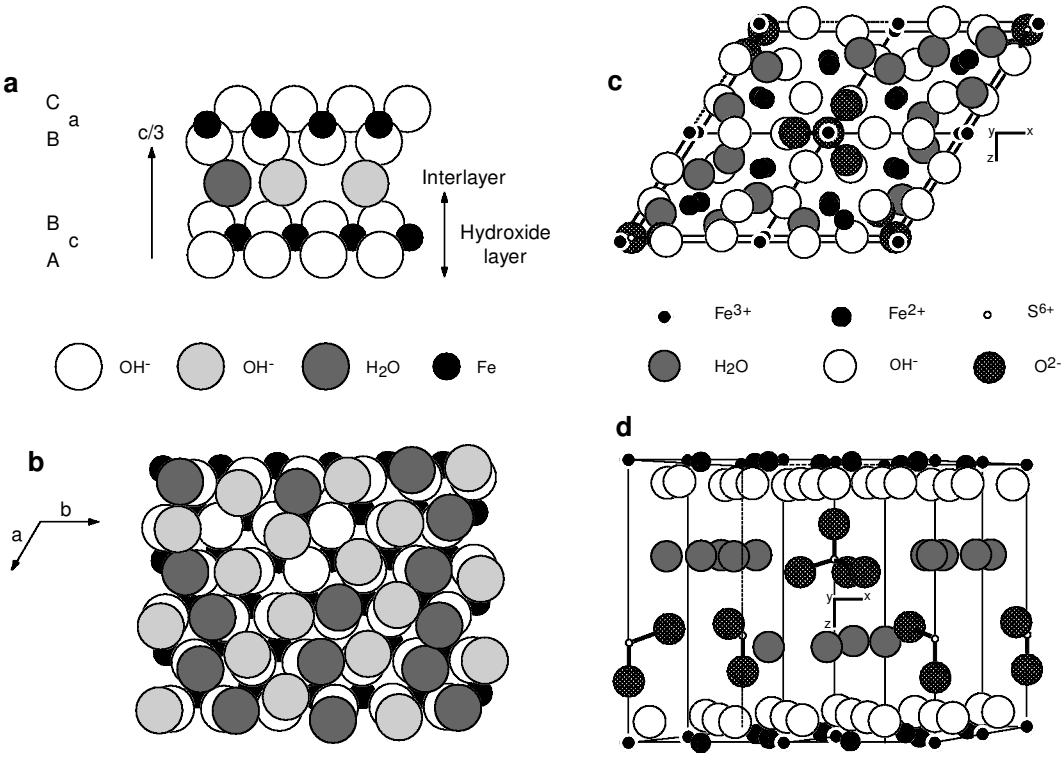

Figure 1. Structures of GR1 and GR2. (a) Stacking sequence for the crystal structure of the GR1(OH) mineral, fougerite, in the limiting case $Fe_3(OH)_7$; (b) position of water molecules and OH^- ions in an interlayer viewed along [001]; only one interlayer, one OH^- and one Fe layer below are represented, from Génin *et al.* (2001); (c) projection of an ordered representation of the (2a, 2a, c) lattice of GR2(SO_4^{2-}) structure on the (001) plane; (d) stacking sequence for the crystal structure of GR2(SO_4^{2-}), from Simon *et al.* (2003).

$$X_1 = \frac{1-x}{1+y} \quad X_2 = \frac{x}{1+y} \quad X_3 = \frac{y}{1+y} \qquad (1)$$

The formula of fougerite can be written in a simplified way as: $(Fe^{2+},Mg)_{X_1+X_3}Fe^{3+}_{X_2}(OH)_{2X_1+2X_3+3X_2}$

Structural constraints for the solid-solution model

From structural considerations, the smallest possible value for x is zero, which would correspond to a solid-solution between $Fe(OH)_2$ and $Mg(OH)_2$. The effective ionic radii of Fe^{2+} and Mg^{2+} are very close to each other, 0.078 nm and 0.072 nm, respectively (Shannon, 1976), so that extensive substitution is possible. Indeed, most natural Fe(II) oxides, hydroxides and silicates admit continuous series between pure Fe(II) and Mg(II) end-members.

The upper limit for GR1(OH) was proposed as $x = ⅔$ (Génin *et al.*, 2001). According to Vucelic *et al.* (1997), there exists a local ordering so that Fe^{3+} cations are never neighbors to each other. As each cation is surrounded by six cations, this means that this rule can be generalized now as: every Fe^{3+} must be surrounded by six bivalent cations, either Fe^{2+} or Mg^{2+}. The basic question is thus: what is the exact structural cause of this limitation?

For GR1(OH), the excess positive charge is compensated in the interlayer by deprotonation of the water molecule, the elementary reaction of oxidation being written in Figure 2. Further oxidation leading to two neighboring Fe(III) would then result in two neighboring OH^- in the interlayer (Figure 2). This is *a priori* structurally possible, but rather than deprotonating the remote interlayer water molecule, the repulsive field exerted by the two Fe(III) atoms would result in the deprotonation of the OH of the layer itself by an 'oxolation' process (Jolivet, 1994) and to Fe(III)–O–Fe(III) bonds. The GR structure is then no longer stable and it transforms into magnetite with spinel inverse structure, or into an oxyhydroxide such as lepidocrocite (Olowe and Génin, 1991). Substitution of Fe(II) by Mg(II) in the structure stabilizes the green rust structure and the x mole ratio is allowed to increase to a limit given by the inequality:

$$\frac{Fe(II)+Mg(II)}{Fe(III)} \geq 2 \Longleftrightarrow \frac{1-y+y}{x} \geq 2 \Longleftrightarrow x \leq \frac{1+y}{3} \qquad (2)$$

which with equation 1 gives:

$$X_2 \leqslant ⅓ \qquad (3)$$

The limiting case of pure Fe-GR. For $y = 0$, equation 2 simplifies to $x \leqslant ⅓$, which corresponds to the global formula $Fe_3(OH)_7$. This implies that the values obtained earlier for $x = ½$ '$Fe_2(OH)_5$' and $x = ⅔$ '$Fe_3(OH)_8$' must be ascribed in fact to Fe(II)–Fe(III)–Mg(II) GR. It is worth noting that the GR synthesized heretofore without Mg have x values of <⅓ (Table 1), except in one case, GR1(Cl), with a slightly larger value ($x = 0.36$), which either is not significantly different from $x = ⅓$ or would indicate that with some anions it is possible to accommodate a small increase of Fe(III). Moreover, in the case of selenate-GR2, the precipitate starts with $x = ⅓{,}25$, then x increases to a maximum value $x = ⅓$, over which it oxidizes into Fe(III) oxyhydroxides FeOOH.

It can thus be concluded that the inequality $x \leqslant ⅓$ is satisfied when $y = 0$, from all the experimental results obtained so far. Any further oxidation leads to the formation of Fe oxyhydroxides, lepidocrocite, goethite, or akaganeite, or to the formation of magnetite-maghemite minerals. Similar conclusions apply also to compounds based on trivalent cations other than Fe. It is for example the case for synthetic meixnerite, $[Mg^{2+}_{1-x}Al^{3+}_x(OH)_2]^{x+}[x\ OH^-\cdot(0.81-x)H_2O]^{x-}$, for which $0.23 \leqslant x \leqslant 0.33$ (Mascolo and Marino, 1980).

The general case of the ternary solid-solution. The Fe(III) mole fraction must be <⅓, which separates the excluded domain from the domain where it is structurally possible for GR to form. The inequality 2 can be drawn graphically in a triangular diagram in the system $Fe^{2+}(OH)_2$–$Fe^{3+}(OH)_3$–$Mg(OH)_2$ (solid line, Figure 3).

For $y \geqslant 0$, *i.e.* when other divalent metals substitute for Fe(II), further oxidation is possible as soon as the inequality (3) is fulfilled. Such a compound was synthesized, with $x = ½$ and $y = ½$, by co-precipitation

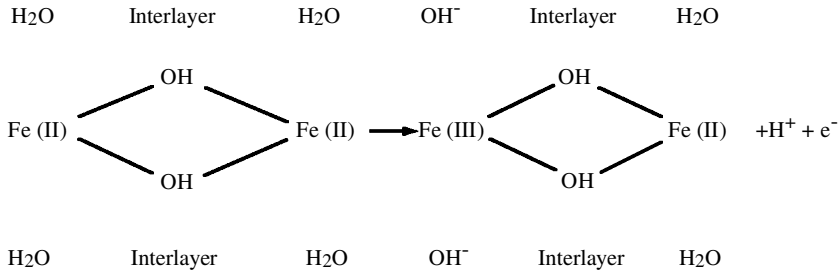

Figure 2. Modification of the composition of octahedra and interlayer in GR during the oxidation of Fe(II) to Fe(III).

Table 1. Structural formulae and Gibbs free energies of formation at 298.15 K and 1 bar of synthetic GR.

Structural formula	Group	x*	μ° exp. (kJ mol^{-1})	μ° calc.[c] (kJ mol^{-1})
$[Fe^{2+}_3Fe^{3+}(OH)_8]^+[Cl^-\cdot 2H_2O]^-$	GR1	¼[1]	−2145±7[a]	−2132
$[Fe^{2+}_6Fe^{3+}_2(OH)_{16}]^{2+}[SO^{2-}_3\cdot 4H_2O]^{2-}$	GR1	¼[2]	–	−5162
$[Fe^{2+}_6Fe^{3+}_2(OH)_{16}]^{2+}[C_2O^{2-}_4\cdot 4H_2O]^{2-}$	GR1	¼[3]	−5383±3[b]	−5365
$[Fe^{2+}_{5.5}Fe^{3+}_2(OH)_{15}]^{2+}[SeO^{2-}_4\cdot 8H_2O]^{2-}$	GR2	⅓.25[4]	–	−5007
$[Fe^{2+}_4Fe^{3+}_2(OH)_{12}]^{2+}[SeO^{2-}_4\cdot 8H_2O]^{2-}$	GR2	⅓[4]	–	−4006
$[Fe^{2+}_4Fe^{3+}_2(OH)_{12}]^{2+}[SO^{2-}_4\cdot 8H_2O]^{2-}$	GR2	⅓[5]	−3790±10	−3807
$[Fe^{2+}_4Fe^{3+}_2(OH)_{12}]^{2+}[CO^{2-}_3\cdot nH_2O]^{2-}$	GR1	⅓[6,7]	−3590±5[a]	−3872

* x = Fe(III)/Fe$_{total}$ mole ratio
[1] Refait *et al.* (1998a); [2] Simon *et al.* (1998); [3] Refait *et al.* (1998b); [4] Refait *et al.* (2000); [5] Refait *et al.* (1999); [6] Hansen (1989); [7] Drissi *et al.* (1995)
[a] Bourrié *et al.* (1999); [b] ref. 3; [c] data from this paper

of Mg^{2+}, Fe^{2+} and Fe^{3+} salts, at stoichiometry: $[Fe^{2+}_2Fe^{3+}_2Mg^{2+}_2(OH)_{12}]^{2+}[CO^{2-}_3\cdot nH_2O]^{2-}$ (Refait *et al.*, 2001).

For y = ½, the limit is $x \leqslant$ ½, which corresponds to the former formula '$Fe_2(OH)_5$' and for y = 1, the limit is $x \leqslant$ ⅔, which corresponds to the former formula '$Fe_3(OH)_8$'. These compounds, whose Fe(III)/Fe$_{total}$ ratios were observed in hydromorphic soils, can thus only be stable if they incorporate divalent cations other than Fe(II), for which Mg(II), due to its abundance in the environment is the more likely candidate. The proposed complete formulae for the mineral at remarkable points are given in Table 2 (points A, B, C, D, Figure 3), under the constraint that the total number of water molecules and OH^- ions is at most equal to the total number of cations in the mole formula, with one monolayer of water in GR1-type compounds.

Larger Mg substitutions are possible, as this consists simply of diluting Fe atoms, and for $y \geqslant 2$, the complete oxidation of Fe is possible, which leads to a compound isomorphous with pyroaurite, with OH^- as a compensating anion instead of carbonate.

Among excluded forms are thus not only $Fe(OH)_3$, but all mixed Fe hydroxides $Fe^{2+}_{1-x}Fe^{3+}_x(OH)_{2+x}$, with $x \geqslant$ ⅓, including the previously considered compounds $Fe_2(OH)_5$ and $Fe_3(OH)_8$ ("ferrosic hydroxide" of Arden, 1950). If they exist, the structure of these components instead of a GR structure, would be more consistent with the formula $Fe(OH)_2\cdot$ 2FeOOH for "hydrated magnetite" used by Olowe and Génin (1991) and Refait and Génin (1993), which implies an oxolation of Fe(III)–Fe(III) bridges, but the structures of these hypothetical compounds are not established.

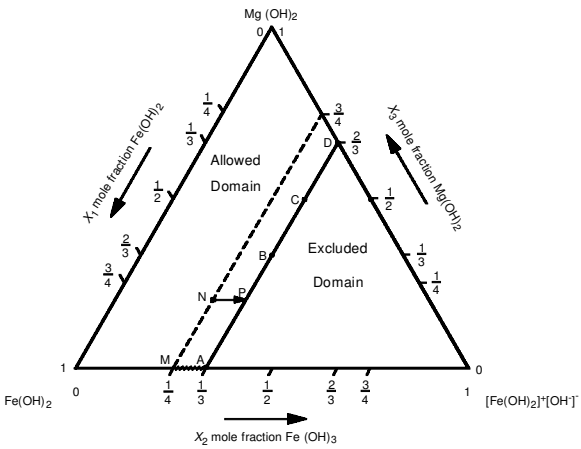

Figure 3. Diagram for the ternary system $Mg(OH)_2$-$Fe(OH)_2$-$Fe(OH)_3$. Solid line: limit between the excluded domain and the domain allowed for GR structure to be stable; dashed line: limit of the incipient precipitation of GR; M-A (hatched): interval of composition of synthetic GR. (A) $Fe_3(OH)_7$; (B) previously '$Fe_2(OH)_5$' ≡ $[MgFe^{2+}Fe^{3+}(OH)_6]^+[OH^-\cdot mH_2O]^-$; (C) previously '$Fe_3(OH)_8$' ≡ $[Mg_3Fe^{2+}Fe^{3+}_2(OH)_{12}]^{2+}[2OH^-\cdot mH_2O]^{2-}$; (D) limit with complete oxidation of Fe, $[Mg_2Fe^{3+}(OH)_6]^+[OH^-\cdot mH_2O]^-$; (N-P) path of oxidation of fougerite (see text).

GEOCHEMICAL CONSTRAINTS

The solid-solution model proposed by Génin *et al.* (2001) must be revised given the presence of Mg in the mineral. This adds a degree of freedom to the system. The solid-solution is now ternary, and the end-members are the hypothetical minerals with a GR1 structure of the same composition as $Fe(OH)_2$ and $Mg(OH)_2$, but not

Table 2. Proposed structural formulae for the GR1(OH) mineral fougerite at remarkable points, and for the isomorphous OH analogue of pyroaurite.

Structural formula (for $y = y_{min.}$)	x	$y_{min.}$	Ref. Fig. 3
$[Fe^{2+}_2Fe^{3+}(OH)_6]^+[OH^-\cdot mH_2O]^-$	⅓	0	A
$[Mg^{2+}Fe^{2+}Fe^{3+}(OH)_6]^+[OH^-\cdot mH_2O]^-$	½	½	B
$[Mg^{2+}_3Fe^{2+}Fe^{3+}_2(OH)_{12}]^{2+}[2OH^-\cdot mH_2O]^{2-}$	⅔	1	C
$[Mg^{2+}_2Fe^{3+}(OH)_6]^+[OH^-\cdot mH_2O]^-$	1	2	D

x = Fe(III)/Fe$_{total}$ mole ratio; y = Mg/Fe$_{total}$ mole ratio; $m \leqslant 1 - x + y$

necessarily with the same thermodynamic properties as their isomers of different structure.

Aqueous solution – ternary solid-solution equilibria

The equilibrium between a soil solution and a ternary solid-solution must be checked by writing a separate equilibrium equation for each pole:

$$Fe(OH)_2 + 2H^+ \rightleftharpoons Fe^{2+} + 2H_2O \quad (4)$$
$$[Fe(OH)_2]^+[OH^-]^- + 3H^+ + e^- \rightleftharpoons Fe^{2+} + 3H_2O \quad (5)$$
$$Mg(OH)_2 + 2H^+ \rightleftharpoons Mg^{2+} + 2H_2O \quad (6)$$

In the following, indices 1, 2 and 3 will refer to Fe(II), Fe(III) and Mg(II) pure end-members, respectively. Ionic activity products (IAP) for each pole are defined by:

$$\log IAP_1 = \log (Fe^{2+}) + 2 \log a_w + 2\ pH \quad (7)$$
$$\log IAP_2 = \log (Fe^{2+}) + 3 \log a_w + 3\ pH + pe \quad (8)$$
$$\log IAP_3 = \log (Mg^{2+}) + 2 \log a_w + 2\ pH \quad (9)$$

where quantities in parentheses are the activities of chemical species considered, a_w is the activity of water, pe is related to the redox potential measured with respect to the normal hydrogen electrode E_h, by $pe = (FE_h)/(\ln 10)\ RT$, T is the absolute temperature, $F = 96485.309$ C mol^{-1} and $R = 8.31451$ Jmol^{-1}K^{-1}.

At equilibrium, one has:

$$\log IAP_1 = \log K_1 + \log a_1 \quad (10)$$
$$\log IAP_2 = \log K_2 + \log a_2 \quad (11)$$
$$\log IAP_3 = \log K_3 + \log a_3 \quad (12)$$

where a_i is the activity of pole i in the solid-solution, which is different from unity, as the mineral is not a pure mineral in standard state. The activity coefficient λ_i of pole i in the solid-solution is defined by:

$$\lambda_i = a_i/X_i \quad (13)$$

where X_i is the mole fraction of pole i in the solid-solution, and the chemical potential of each pole in the solid solution is given by:

$$\mu_i = \mu_i^o + RT \ln X_i + RT \ln \lambda_i \quad (14)$$

The λ_i values are functions of P,T and the mole fractions of the solid X_i. The function defines the type of solid-solution.

For an ideal solid-solution, $\lambda_i = 1$. However, the end-members $Fe(OH)_2$ and $Mg(OH)_2$ have a brucite-like structure, with no intercalation of a monomolecular layer of water, but as soon as some Fe(II) is oxidized, the layers separate, hydrate and compensating anions enter the interlayer, which explains why the solid-solution is largely non-ideal (Génin *et al.*, 2001). As before, a regular solid-solution model will be used here.

Regular ternary solid-solution model for GR and fougerite

For a regular ternary solid-solution, the equations are (Prigogine and Defay, 1946, t. II p. 80):

$$RT \ln \lambda_1 = A_{12}X_2^2 + A_{13}X_3^2 + X_2X_3(A_{12} - A_{23} + A_{13}) \quad (15)$$

$$RT \ln \lambda_2 = A_{23}X_3^2 + A_{12}X_1^2 + X_1X_3(A_{12} + A_{23} - A_{13}) \quad (16)$$

$$RT \ln \lambda_3 = A_{13}X_1^2 + A_{23}X_2^2 + X_1X_2(-A_{12} + A_{23} + A_{13}) \quad (17)$$

where A_{ij} are the interaction parameters of the three binary solid-solutions. This implies that three parameters must be experimentally measured and fitted to a model of ternary regular solid-solution. For GR, we can make the assumption that the Fe(II)-Mg(II) substitution is ideal.

This implies that $\lambda_1 = \lambda_3$ for all X_2 and that if $X_2 = 0$, one obtains the ideal solid-solution Mg(II)-Fe(II), so that: $RT \ln \lambda_1 = A_{13}X_3^2 = 0$, hence $A_{13} = 0$. The same assumption implies that the effects of pole 1 and pole 3 on the activity coefficient of pole 2 are the same, *i.e.* $A_{12} = A_{23}$. One eventually obtains:

$$RT \ln \lambda_1 = A_{12}X_2^2 \quad (18)$$
$$RT \ln \lambda_2 = A_{12}(X_1 + X_3)^2 \quad (19)$$
$$RT \ln \lambda_3 = A_{12}X_2^2 \quad (20)$$

There remains only one adjustable parameter, $A_{12} = A_{23}$ and poles 1 and 3 play the same role, and this can be written equivalently as:

$$RT \ln \lambda_1 = A_{12}X_2^2 \quad (21)$$
$$RT \ln \lambda_2 = A_{12}(1 - X_2)^2 \quad (22)$$
$$RT \ln \lambda_3 = A_{12}X_2^2 \quad (23)$$

The chemical potentials of the three components and of the solid-solution are obtained as:

$$\mu_1 = \mu_1^o + RT \ln X_1 + A_{12}X_2^2 \quad (24)$$

$$\mu_2 = \mu_2^o + RT \ln X_2 + A_{12}(1 - X_2)^2 \quad (25)$$

$$\mu_3 = \mu_3^o + RT \ln X_3 + A_{12}X_2^2 \quad (26)$$

$$\mu = X_1\ \mu_1 + X_2\ \mu_2 + X_3\ \mu_3 \quad (27)$$

The ideal and excess Gibbs free energy of mixing are given respectively by:

$$\Delta G_{ideal}/RT = X_1 \ln X_1 + X_2 \ln X_2 + X_3 \ln X_3 \quad (28)$$
$$\Delta G_{excess}/RT = X_1 \ln \lambda_1 + X_2 \ln \lambda_2 + X_3 \ln \lambda_3 \quad (29)$$

and by substituting equations 21–23 in equations 29 and 27, one obtains:

$$\Delta G_{excess} = A_{12}\ X_2\ (1\ -\ X_2) \quad (30)$$

$$\mu = X_1\ \mu_1^o + X_2\ \mu_2^o + X_3\ \mu_3^o + RT\ [X_1 \ln X_1 + X_2 \ln X_2 + X_3 \ln X_3] + A_{12}\ X_2\ (1\ -\ X_2) \quad (31)$$

By letting $X_3 = 0$, one obtains the expression used to fit the regular solid-solution model previously (Génin *et al.*, 2001). The parameter A_{12} is identical to the parameter A_0 obtained previously, though the value proposed previously must be revised as Mg was not considered in the computation of IAP values.

Difficulty in solving the system on the basis of aqueous solution-solid solution equilibria

In principle, the system can be solved by successive iterations for each aqueous solution to check equilibrium, if K_i are known, starting with $\lambda_i = 1$ and a tentative value of A_{12}.

The condition of equilibrium can thus be checked by computing first for each pole:

$$\log X_i = \log \mathrm{IAP}_i - \log K_i - \log \lambda_i \quad (32)$$

and secondly by summing the X_i. The condition obtained is then:

$$\sum_i X_i < 1, \text{ the soil solution is undersaturated} \quad (33)$$
$$\sum_i X_i = 1, \text{ the soil solution is at equilibrium} \quad (34)$$
$$\sum_i X_i > 1, \text{ the soil solution is oversaturated} \quad (35)$$

This generalizes the classic condition IAP < K, IAP = K, IAP > K for a pure solid (Bourrié, 1983).

The values of log IAP_i can be obtained from the composition of soil solution and the computation of activities and such a set of data is available (Bourrié *et al.*, 1999). One must, however, know the values of K_i for pure end-members, which here it is not possible to measure directly as the purely ferric pole is virtual. Indeed, as the solubilities of $Mg(OH)_2$ and $Fe(OH)_2$ are very large, solutions are largely undersaturated with respect to these end-members, resulting in numerical instabilities. As explained before, the solid-solution is largely non-ideal, so that the values $\lambda_i = 1$ are not a good starting point for iterations. Moreover, the mineral is labile and cannot be separated, so that the mole fractions X_i are not measurable. Only the x mole ratio is measurable by Mössbauer spectroscopy.

Estimating both μ_2°, A_{12} and the X_i from a set of field data would imply the questionable assumption of equilibria at low temperature and give a circular character to the demonstration. Instead, hereafter, we will constrain the range of variation of the mole fraction X_2 better, then derive the chemical potential of the mineral, and eventually check equilibria independently with aqueous solutions.

Geochemical constraints on the solid-solution model

Lower limit of the mole fraction of Fe(III) in GR. On the basis of structural considerations, we have seen that the mole fraction of Fe(III) must be such that $X_2 \leqslant \frac{1}{3}$, as two Fe(III) must not be direct neighbors. Conversely, if X_2 is too small, the distance Fe(III)–Fe(III) is too large and the mineral will not form as the solubilities of $Fe(OH)_2$ and $Mg(OH)_2$ are very large. Experimentally, starting from $Fe(OH)_2$, and letting it oxidize gently in contact with air, synthetic GR form in coexistence with $Fe(OH)_2$ from $x = \frac{1}{4}$.

With Ni(II), the compound obtained with the initial ratio Fe(II)/Ni(II) = ⅓, *i.e.* $X_3 = \frac{3}{4}$, by assimilating Ni(II) to Mg(II) in Figure 3, is a GR1 isomorphous to GR1(Cl), with $x = 1$, and $X_2 = \frac{1}{4}$ (Refait and Génin, 1993). The unique product obtained corresponds to $X_2 = \frac{1}{4}$ (the point of intersection of the dashed line with the edge $Mg(OH)_2$-$Fe(OH)_3$ in the diagram). For larger initial ratios Fe(II)/Ni(II), ½ and 1, the initial products obtained bear $X_2 = \frac{1}{4}$ too.

In pyroaurite, $Mg_6^{2+}Fe_2^{3+}(OH)_{16}CO_3{\cdot}4H_2O$, $X_2 = \frac{1}{4}$; in GR1(CO_3), $Fe_x^{2+}Fe_2^{3+}(OH)_{2x+4}CO_3{\cdot}nH_2O$, x ranges from four to six, ($X_2 = \frac{1}{4}$ to ⅓) according to Murad and Taylor (1984), while $x = 4$ following Drissi *et al.* (1994) ($X_2 = \frac{1}{3}$). Similarly, when Al(III) substitutes for Fe(III), the product obtained by Taylor and MacKenzie (1980) is $Fe_6^{2+}[Al^{3+},Fe^{3+}]_2(OH)_{15.9}Cl_{1.85}$, with the mole ratio of trivalent ions $X_2 = \frac{1}{4}$, while in desautelsite, synthesized by Hansen and Taylor (1991), $Mg_{8-x}^{2+}Mn_x^{3+}(OH)_{16}(CO_3^{2-})_{x/2}$, $2 < x < 2.67$, *i.e.* $\frac{1}{4} < X_2 < \frac{1}{3}$. As mentioned above, in synthetic meixnerite, Mg(II)-Al(III) compound, the mole ratio of trivalent ion obeys $0.23 \leqslant X_2 \leqslant 0.33$. It can thus be concluded that the formation of GR or more generally of pyroaurite-type compounds begins at the mole ratio: $X_2 \equiv M(\mathrm{III})/[M(\mathrm{III}) + M(\mathrm{II})] = \frac{1}{4}$.

The value $X_2 = \frac{1}{4}$ corresponds structurally for GR1(OH), to the minimum distance Fe(III)–Fe(III), $d = a\sqrt{3}$, where a is the parameter of the hexagonal structure (Refait *et al.*, 2001). We will thus consider that the lower limit for the mole ratio X_2 is geochemically constrained to ¼, and that the upper limit is structurally constrained to ⅓. The domain of composition of either synthetic or natural GR is thus limited by $X_2 = \frac{1}{4}$ (dashed line in Figure 3) and $X_2 = \frac{1}{3}$ (solid line in Figure 3).

Minimization of the chemical potential of GR and a relationship between A_{12} and the chemical potentials of pure end-members. We can now assume that the chemical potential of GR is minimal in the range $X_2 = [\frac{1}{4}, \frac{1}{3}]$, which is rather narrow. This is true even for a pure Fe(II)-Fe(III) system. When expressed as a function of mole fractions, one has:

$$\mu \equiv G/n = X_1\,\mu_1 + X_2\,\mu_2 \quad (36)$$

and by taking the derivative with respect to X_2, one obtains (Prigogine and Defay, 1946, t. II, p. 12):

$$\frac{\partial \mu}{\partial X_2} = \mu_2 - \mu_1 \quad (37)$$

The derivative is zero for $X_2 = X_{2,\,\mathrm{min.}}$, which can be combined with equations 14, 21 and 22 and solved for A_{12}, and eventually gives:

$$A_{12} = \frac{[\mu_1^\circ - \mu_2^\circ - RT \ln(\frac{X_{2,\mathrm{min}}}{1-X_{2,\mathrm{min}}})]}{(1 - 2X_{2,\mathrm{min}})} \quad (38)$$

$$\Updownarrow$$

$$\frac{A_{12}}{RT} = \frac{[\frac{\mu_1^\circ - \mu_2^\circ}{RT} - \ln(\frac{X_{2,\mathrm{min}}}{1-X_{2,\mathrm{min}}})]}{(1 - 2X_{2,\mathrm{min}})} \quad (39)$$

By taking as an average $X_{2,min}$ = 7/24±1/24, a linear relation is obtained between A_{12} and the Gibbs free energies of formation of the ferrous and ferric end-members. As a first approximation, $(\mu_1^o - \mu_2^o)/RT$ can be considered as constant, so that from equation 39, A_{12} can be computed at any temperature. There now remains one unknown parameter instead of two.

Constraints on the chemical potentials of pure end-members. The pure end-members are $Fe(OH)_2$ for which μ_1^o = −489.8 kJmol^{-1} at 298.15 K, 1 bar, from Bourrié *et al.* (1999) and $Fe(OH)_3 \equiv [Fe^{3+}(OH)_2]^+[OH^-]^-$. However, as this end-member is virtual, μ_2^o is not measurable. This value must, however, be more positive than the values for lepidocrocite and goethite with one water molecule added, and hematite, with two water molecules added, which are the stable or metastable phases. Taking −470.7 kJmol^{-1} for lepidocrocite (Hashimoto and Misawa, 1973), −480.3 kJmol^{-1} for goethite (Détournay *et al.*,1975), −755.45 kJmol^{-1} for hematite (Bratsch, 1989) and −237.18 kJmol^{-1} for liquid water (Wagman *et al.*, 1982), one obtains a minimum value μ_2^o > −708 kJmol^{-1}. The value previously proposed was μ_2^o = −641 kJmol^{-1} (Génin *et al.*, 2001), but Mg was not considered in the mineral. Instead, for GR to form, A_{12} must be negative, which implies μ_2^o > −490 kJmol^{-1}, by letting $X_2 = X_{2,min}$ = 7/24 in equation 39. The value of μ_2^o is thus not constrained enough to give a reliable value of A_{12} from equation 31. The previously published value μ_2^o = −641 kJmol^{-1} (Génin *et al.*, 2001) leads to $X_{2,min}$ = 2/3, which is inconsistent with the structural constraints, and must be discarded.

The only way to solve the system is then to obtain a value for μ for the mineral in the range of variation of X_2 where GR exist, but as the natural mineral fougerite is labile and cannot be separated, and to date has not been synthesized, this value must be estimated from the values measured on synthetic GR.

ESTIMATION OF THE GIBBS FREE ENERGY OF FORMATION OF GR1-OH

General relation between the Gibbs free energies of formation of synthetic GR and the electronegativities of anions taken on the Allred-Rochow scale

The experimental values of the Gibbs free energies of formation of synthetic GR are reported in Table 1 at 298.15 K, 1 bar. As these compounds are essentially isostructural, we can look for a relationship between this thermodynamic property and a suitable parameter. The changes are essentially the nature of the interlayered anion, the number of moles of water, which depends on the type of GR, and to a lesser degree the mole ratio X_2. Those factors are closely correlated, and the nature of the anion is the main factor. As the interactions between the layer and the anion are of electrostatic nature, we chose the electronegativity of the anion as a parameter. More specifically, we used the Allred and Rochow electronegativity scale, as it is based on the energetics of interaction between a molecule or an ion and the electron and is a function of the global charge Z of the molecule or ion. We follow the model of partial charges developed by Jolivet (1994). Given the electronegativities χ^*_i of the elements, the electronegativity of a molecule is obtained as:

$$\chi = \frac{\sum_i \sqrt{\chi_i^*} + 1.36Z}{\sum_i \frac{1}{\sqrt{\chi_i^*}}} \qquad (40)$$

With χ_i^* = 2.50 for C and Se, 3.50 for O, 2.83 for Cl, 2.48 for S (Jolivet, 1994) the values obtained for the anions are χ = 0.54 for Cl^-, 1.86 for SO_4^{2-}, 2.0 for CO_3^{2-} and SO_3^{2-}, 2.29 for SeO_4^{2-} and 2.33 for oxalate $C_2O_4^{2-}$. The Gibbs free energies of formation of synthetic GR, normalized to 1 Fe atom, are plotted *vs.* the Allred-Rochow electronegativities of the interlayer anions in Figure 4. The value of the Gibbs free energy of formation of $Fe(OH)_2$ is plotted at χ = 0, as the interlayer is empty.

All points except GR1(CO_3) and including $Fe(OH)_2$ and GR2(SO_4) are perfectly aligned, along a straight line following the empirical law:

$$\frac{\mu^o}{n} = -76.887\chi - 491.5206,\ r^2 = 0.9985,\ N = 4 \qquad (41)$$

where n is the number of Fe atoms per mole formula, and μ^o is in kJ mol^{-1}. The differences between calculated

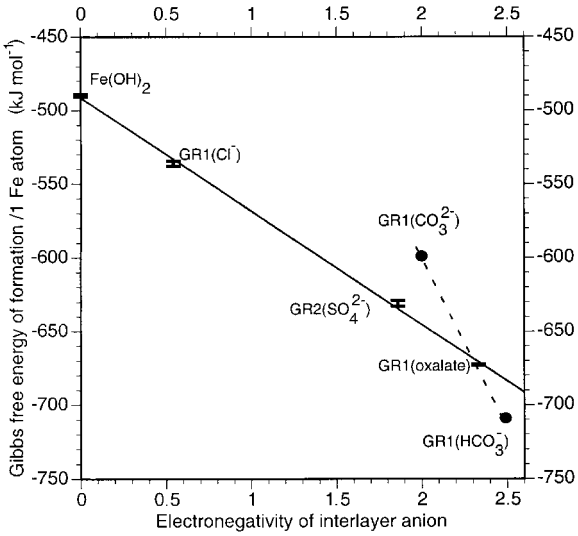

Figure 4. Relation between Gibbs free energy of formation of synthetic GR (see Table 1), normalized to one Fe atom/mole formula and the Allred and Rochow electronegativity of the interlayer anion, computed following the model of partial charges (Jolivet, 1994) (see text, equation 40). Solid line: linear regression through all points (error bars) except GR1(CO_3) (see equation 41); black circles: Gibbs free energy of formation of GR1(CO_3) (Table 1) at χ = 2 and recalculated from experimental data (Table 3) as GR1(HCO_3) (reaction 42), at χ = 2.49; the dashed line connects those two extreme values for carbonate GR.

and experimental values are within 0.6% (Table 1) except for GR1(CO_3), which will be discussed just below. It is remarkable that: (1) the value for $Fe(OH)_2$ plotted at $\chi = 0$ is aligned with GR; (2) that GR2(SO_4) is aligned with GR1s.

This confirms that the main factor is the nature of the anion. The stacking differences between the two types of GR and the number of molecules of water are not reflected in the dispersion. Considering the number of molecules of water and computing the electronegativities of $Cl^-\cdot 2H_2O$, *etc.* resulted in a large scattering of points in the diagram. The normalized Gibbs free energies of formation of GR are thus entirely explained by the electronegativity of the non-hydrated anion.

Gibbs free energy of formation of GR1(CO_3)

For GR1(CO_3), the discrepancy is 8% and is largely out of range of the experimental uncertainty, *i.e.* ±11 kJ mol^{-1}. The experimental value is derived from measurements of E_h and pH at equilibrium between $Fe(OH)_2$ and the synthetic GR from Drissi *et al.* (1994) (Table 3).

The equilibrium was considered between GR1(CO_3) and $Fe(OH)_2$. If however, HCO_3^- was the interlayer anion, the formula of the GR would be $[Fe_4^{2+}Fe_2^{3+}(OH)_{12}]^{2+}[2HCO_3^-]^{2-}$, and the equilibrium with $Fe(OH)_2$ would be:

$$6Fe(OH)_2 + 2HCO_3^- \rightleftharpoons [Fe_4^{2+}Fe_2^{3+}(OH)_{12}]^{2+}[2HCO_3^-]^{2-} + 2e^- \quad (42)$$

from which the data from Table 3 can be used to give $\mu^o = -4248.23 \pm 3$ kJ mol^{-1}. This value, when normalized to one Fe atom and plotted at $\chi(HCO_3^-) = 2.49$ is below the general regression line. Carbonate GR could thus indeed be a mixed CO_3^{2-}-HCO_3^- GR. The intersection between the solid line and dashed line in Figure 4 leads to an average value $\chi = 2.32 = \frac{2}{3}\chi(HCO_3^-) + \frac{1}{3}\chi(CO_3^{2-})$. The formula for GR1($CO_3$) could thus be:

$$\tfrac{2}{3}\{[Fe_4^{2+}Fe_2^{3+}(OH)_{12}]^{2+}[2HCO_3^-]^{2-}\}\cdot \tfrac{1}{3}\{[Fe_4^{2+}Fe_2^{3+}(OH)_{12}]^{2+}[CO_3^{2-}]^{2-}\},$$

or equivalently:

$$[Fe_4^{2+}Fe_2^{3+}(OH)_{12}]^{2+}[\tfrac{4}{3}HCO_3^-\cdot\tfrac{1}{3}CO_3^{2-}]^{2-}.$$

The activity ratio $[HCO_3^-]/[CO_3^{2-}] = 4$ in the interlayer, corresponds to pH = 9.73, which is 0.5 to 1.1 lower than the pH in the external solution, which can be ascribed to the classical surface acidity of the positively charged interlayer. There is no steric hindrance, as there are six Fe atoms, so there is space for six H_2O molecules, *i.e.* six O. In the formula proposed, there are five O, so there is the possibility of having at most one water molecule in addition in the cell. From the value $\chi = 2.32$, and equation 41, we obtain $\mu^o = -4018$ kJ mol^{-1} for GR1($\frac{4}{3}HCO_3^-\cdot\frac{1}{3}CO_3^{2-}$) at 298.15 K, 1 bar. However, the mole ratio Fe(III)/C would then be $2/(\frac{5}{3}) = 1.2$ instead of 2 as generally admitted. Thus, either the stoichiometry or the chemical potential of the hydroxy-carbonate GR must be reevaluated.

It must be noted that the intersection of the carbonate data with the regression line in Figure 4 occurs at the same point where the oxalate data point occurs. As the oxalate and carbonate functional groups are rather similar, this strengthens the main importance of the nature of the interlayer anion.

From equation 41, with $\chi(SO_3^{2-}) = 2$ and $\chi(SeO_4^{2-}) = 2.29$, we obtain the Gibbs free energies of formation of the other synthetic GR: GR1(SO_3^{2-}), GR2(SeO_4^{2-}) which are reported in Table 1, for which no published data are available.

Estimation of the Gibbs free energy of formation of the purely ferroso-ferric GR1(OH)

From equation 41, with $\chi(OH^-) = 1.60$, we eventually obtain $\mu = -614.5$ kJ mol^{-1} for GR1(OH), with one Fe atom per mole formula. This value, near the minimum at the limit $X_3 = 0$ (no Mg in fougerite) is in the range of values proposed previously for $Fe_3(OH)_7$, *i.e.* −1799.7 kJ mol^{-1} or −600 kJ mol^{-1}/1 Fe atom, and for '$Fe_2(OH)_5$', *i.e.* −1244.1 kJ mol^{-1} or −622 kJ mol^{-1}/1 Fe atom, but it must be preferred, as it is based on carefully controlled experiments on synthetic GR, thermodynamics of solid-solutions and the model of partial charges.

Table 3. Experimental data used to reevaluate the Gibbs free energy of formation of GR1(CO_3), from Drissi *et al.* (1994).

R = OH/Fe	Eh (V)[a]	pH[a]	$a(CO_3^{2-})$[a]	log $a(HCO_3^-)$[b]	log K[c]	$\Delta_R G^o$[d]	μ^{oe}
0.545	−0.598	10.82	0.027	−2.059	24.34	−138.896	−4251.24
0.600	−0.597	10.20	0.015	−1.694	23.57	−134.539	−4246.88
0.615	−0.596	10.19	0.015	−1.684	23.52	−134.232	−4246.57
Average	−0.597	10.40	0.019	−1.812	23.807	−135.89	−4248.23
σ	0.001	0.36	0.007	0.214	0.457	2.61	2.61

[a] Drissi *et al.* (1994)
[b] computed as $\log a(HCO_3^-) = \log a(CO_3^{2-}) - pH + 10.33$
[c] $\log K = -2[FE_h/(\ln 10)RT - 2\log a(HCO_3^-)]$
[d] $\Delta_R G^o = -(\ln 10)RT \log K$
[e] computed from $\mu^o = \Delta_R G^o + 2\mu^o(HCO_3^-) + 6\mu^o(Fe(OH)_2)$, with $\mu^o(HCO_3^-) = -586.77$ kJ mol^{-1} from Wagman *et al.* (1982) and $\mu^o(Fe(OH)_{2(c)}) = -489.8$ kJ mol^{-1} from Bourrié *et al.* (1999).

THE COMPLETE TERNARY SOLID-SOLUTION MODEL FOR Fe(II)-Fe(III)-Mg(II) GR

From the value of μ, we can solve entirely the binary regular solid-solution model. From equation 37, we have at the minimum, $\mu_1 = \mu_2$ and from equation 36, with $X_1 + X_2 = 1$, we obtain:

$$\mu = \mu_1 = \mu_2 = -614.5 \text{ kJ mol}^{-1} \quad (43)$$

whose physical meaning is that μ is minimal when the chemical potentials of the components of the binary solid-solution are identical.

With $X_1 = 17/24$, $X_2 = 7/24$ and $\mu_1^\circ = -489.8$ kJ mol^{-1}, by inserting the value of μ_1 in equation 24, we obtain $A_{12} = -1456.28$ kJmol^{-1}, and by inserting the value of μ_2 in equation 25, we obtain $\mu_2^\circ = +119.18$ kJ mol^{-1}.

As expected, A_{12} is negative, which implies that GR will not demix at any temperature (Prigogine and Defay, 1946). The positive value for μ_2° implies that a GR structure for $Fe(OH)_3$ is absolutely impossible. Electrostatic repulsions would be so large that this compound would be unstable with respect to the elements in their standard state, metallic Fe, $O_{2,gas}$ and $H_{2,gas}$! Indeed, this simply means that an octahedral packing of OH cannot accommodate neighboring Fe(III) and that deprotonation of OH leads by an oxolation process to other iron oxides.

The A_{12} value obtained is larger than the corresponding value for FeO-MgO, *i.e.* +15.945 kJ mol^{-1} (Davies and Navrotsky, 1983), and of opposite sign. However, this latter value is relative to the halite-like structure of oxides and valid at high temperatures (1373–1573 K). Moreover, it refers to a substitution of same-charge cations, Fe(II)-Mg(II). Our value, largely negative, refers to the simultaneous substitution $Fe(II)\cdot H_2O$-$Fe(III)\cdot OH$ (see Figure 1) and implies much more important changes in the electronic structure of the solid, so that the values cannot be directly compared. The large negative value of A_{12} we obtained compensates the positive value of μ_2° and makes the fougerite stable.

Our solid-solution model for GR is now complete with the value for the pure $Mg(OH)_2$ end-member, for which we take the value of brucite, $\mu_3^\circ = -832.16$ kJ mol^{-1}, from Altmeier *et al.* (2003). The basic equation of the model and the parameters are summarized in Table 4.

CHECK OF SOIL SOLUTION-FOUGERITE EQUILIBRIUM

Soil solution was studied in the site where fougerite was discovered (Trolard *et al.*, 1996, 1997), in a gley soil developed on granite at Fougères (Brittany, France) and simultaneously three types of data were measured (Feder, 2001): (1) Mössbauer spectra were acquired in the field at different depths and times; (2) E_h and pH were monitored in the groundwater at 70 cm depth every hour, in a gley horizon; (3) the soil solution was sampled every week or twice a month for complete analysis.

Mössbauer spectra show clear evidence of the presence of fougerite, and the mole ratio $x = Fe(III)/Fe_{total}$ in the mineral decreases monotonically with depth, from 0.64 to 0.34, as the milieu becomes more and more reducing. At a given depth, when repeated measurements are made at different times, significant variations of x are observed, though the amplitude is smaller than the entire variation in the profile. No values were observed outside the range $x = [⅓, ⅔]$.

At the depth where the composition of soil solution was monitored, x ranges from 0.59 to 0.61.

By definition, $x = X_2/(X_1 + X_2)$; hence with $x = 0.6$, $X_1 = 2X_2/3$. According to our model, $¼ \leqslant X_2 \leqslant ⅓$. With $X_2 = ¼$, we obtain: $X_1 = ⅙$, and $X_3 = 7/12$. With $X_2 = ⅓$, we obtain: $X_1 = ⅔$, and $X_3 = ⅑$.

By combining the data from Mössbauer spectroscopy in the field and the structural and geochemical constraints for fougerite composition, we can thus solve the system and obtain the three mole fractions of the components. The range of composition of fougerite at that depth is thus between:

$[Mg^{2+}_{7/12}Fe^{2+}_{1/6}Fe^{3+}_{¼}(OH)_2]^{+¼}[¼OH^-]^{-¼}$,
designated as 'fougerite1' (F1)

and

$[Mg^{2+}_{⅔}Fe^{2+}_{⅔}Fe^{3+}_{⅓}(OH)_2]^{+⅓}[⅓OH^-]^{-⅓}$,
designated as 'fougerite 2' (F2).

Table 4. Basic equation and parameters of the regular ternary solid-solution model for hydroxy-Fe(II)-Fe(III)-Mg(II) GR, fougerite, at 298.15 K and 1 bar.

Equation	
$\mu = X_1\mu_1^\circ + X_2\mu_2^\circ + X_3\mu_3^\circ + RT\,[X_1 \ln X_1 + X_2 \ln X_2 + X_3 \ln X_3] + A_{12}X_2\,(1 - X_2)$, (equation 31)	
Thermodynamic parameters	
$Fe(OH)_2$	$\mu^\circ = -489.8$ kJ mol^{-1}
$Fe(OH)_3$ (virtual)	$\mu^\circ = +119.18$ kJ mol^{-1}
$Mg(OH)_2$	$\mu^\circ = -832.16$ kJ mol^{-1}
Non-ideality parameter	$A_{12} = -1456.28$ kJ mol^{-1}

Table 5. Geochemical characteristics of soil solutions from Fougères (Feder, 2001) (N = 68).

Date	T (K)	pH	pe	log (Fe^{2+})	log (Mg^{2+})	log IAP_{F1}	log IAP_{F2}
February 19 1999	280.15	7.3	−3.171	−3.2192	−3.682	29.14	22.59
February 22 1999	280.75	7.24	−3.162	−3.2669	−3.7055	28.74	22.28
February 26 1999	280.75	7.12	−3.298	−3.1798	−3.7981	27.97	21.71
March 1 1999	280.75	7.11	−3.297	−3.3108	−3.8118	27.77	21.52
March 5 1999	281.15	7.15	−3.049	−3.495	−3.8474	27.9	21.63
March 8 1999	280.65	7.52	−2.975	−3.405	−3.9167	29.93	23.26
March 11 1999	280.75	7.16	−3.162	−3.4033	−3.8488	27.98	21.69
March 16 1999	281.45	7.19	−3.037	−3.3255	−3.8661	28.27	21.96
March 19 1999	281.55	7.15	−3.054	−3.3688	−3.8448	28.03	21.75
March 26 1999	281.65	7.12	−3.14	−3.3212	−3.8141	27.9	21.65
March 29 1999	281.85	7.1	−3.193	−3.3636	−3.8877	27.62	21.43
March 31 1999	281.85	7.08	−3.227	−3.574	−3.9257	27.23	21.09
April 6 1999	282.75	7.11	−3.205	−3.421	−3.875	27.63	21.42
April 14 1999	282.65	7.1	−3.069	−3.3455	−3.8794	27.72	21.53
April 22 1999	282.25	7.07	−2.911	−3.3949	−3.8852	27.6	21.44
April 26 1999	282.45	7.11	−2.948	−3.5895	−3.9202	27.55	21.37
April 30 1999	283.05	7.31	−3.311	−3.4456	−3.9432	28.52	22.12
May 6 1999	284.05	7.24	−3.339	−3.4326	−4.2152	27.76	21.6
May 12 1999	284.35	7.08	−3.225	−3.5259	−3.9408	27.25	21.12
May 19 1999	284.15	7.24	−3.206	−3.4911	−3.9631	28.13	21.82
May 26 1999	284.45	7.37	−3.108	−3.5162	−3.9127	28.94	22.44
June 2 1999	285.55	7.37	−3.072	−3.5067	−3.9095	28.97	22.48
June 9 1999	285.35	7.4	−3.103	−3.4819	−4.0459	28.95	22.5
June 14 1999	285.25	7.41	−3.152	−3.504	−4.1734	28.78	22.39
June 18 1999	285.65	7.36	−3.124	−3.529	−3.8986	28.88	22.39
June 21 1999	285.85	7.28	−3.076	−3.5506	−3.9309	28.41	22.04
June 28 1999	286.05	7.31	−3.112	−3.57	−3.9202	28.55	22.13
July 1 1999	286.15	7.24	−3.147	−3.4891	−3.9258	28.22	21.89
July 5 1999	286.65	7.19	−3.153	−3.5945	−3.9605	27.8	21.54
July 8 1999	286.75	7.18	−3.188	−3.576	−3.9579	27.74	21.5
July 13 1999	287.25	7.19	−3.262	−3.6222	−3.9249	27.75	21.48
July 19 1999	287.35	6.85	−3.28	−3.6148	−3.9439	25.89	20.03
July 27 1999	287.75	6.49	−3.489	−3.5465	−3.9449	23.88	18.46
August 16 1999	287.75	6.42	−3.489	−3.7836	−4.0035	23.19	17.88
August 20 1999	287.45	6.4	−3.468	−3.5966	−4.0463	23.22	17.97
August 23 1999	287.65	6.42	−3.471	−3.6374	−4.0463	23.28	18.01
August 27 1999	288.05	6.45	−3.475	−3.7095	−4.0562	23.36	18.05
September 20 1999	287.35	6.28	−0.508	−4.759	−4.2918	22.84	17.88
September 21 1999	287.35	6.3	−0.255	−4.6622	−4.292	23.2	18.21
September 22 1999	287.25	6.4	−0.203	−5.2148	−4.2621	23.26	18.13
September 24 1999	287.25	6.4	−1.437	−4.4113	−4.2361	23.36	18.22
September 27 1999	287.35	6.37	−2.976	−3.9306	−4.2303	22.76	17.65
October 8 1999	286.05	6.68	−4.6	−3.6381	−4.063	23.99	18.41
October 11 1999	286.05	6.96	−4.498	−3.6099	−4.0562	25.6	19.68
October 15 1999	285.95	7.32	−4.7	−3.6958	−4.0325	27.37	21
October 22 1999	285.35	7.35	−4.269	−3.6936	−4.021	27.81	21.4
October 29 1999	285.35	7.36	−3.864	−3.5836	−4.0095	28.23	21.8
November 4 1999	285.35	7.4	−3.915	−3.5536	−4.0016	28.46	21.98
November 10 1999	284.55	7.6	−3.921	−3.5867	−3.9871	29.52	22.79
November 15 1999	283.85	7.68	−4.098	−3.6275	−3.9739	29.82	22.99
November 21 1999	282.85	7.74	−4.17	−3.6114	−3.9589	30.14	23.23
November 30 1999	282.65	7.85	−4.133	−3.6294	−3.9305	30.78	23.72
December 6 1999	282.65	7.87	−4.083	−3.589	−3.9465	30.93	23.86
December 15 1999	282.15	7.9	−4.093	−3.5524	−3.9384	31.14	24.02
December 23 1999	281.25	7.94	−4.047	−3.643	−3.9465	31.28	24.12
January 7 2000	281.35	8.07	−3.999	−3.7465	−3.9647	31.88	24.58
January 19 2000	279.75	8.01	−3.893	−3.8189	−4.0815	31.39	24.22
February 2 2000	279.45	8.17	−4.042	−3.8464	−4.0153	32.22	24.83
February 9 2000	280.15	8.14	−4.017	−3.827	−4.0813	32	24.69
February 15 2000	280.35	8.16	−4.036	−3.884	−4.1167	32	24.67
March 31 2000	281.65	8.02	−4.154	−3.7619	−4.0837	31.34	24.16
April 4 2000	281.55	7.9	−4.069	−3.6635	−4.0947	30.82	23.8

Table 5. (*contd*.)

Date	*T* (K)	pH	pe	log (Fe^{2+})	log (Mg^{2+})	log IAP_{F1}	log IAP_{F2}
April 6 2000	281.45	7.87	−3.915	−3.7811	−4.0651	30.68	23.67
April 14 2000	281.45	7.91	−3.898	−3.7022	−4.1409	30.88	23.87
April 20 2000	281.75	7.95	−3.868	−3.8145	−4.1375	31	23.94
May 9 2000	284.95	8.03	−4.264	−3.7276	−4.084	31.36	24.17
May 22 2000	286.05	7.92	−4.144	−3.7362	−4.1214	30.78	23.74
June 5 2000	286.45	7.9	−4.199	−3.8221	−4.1383	30.52	23.53
Average	283.92	7.29	−3.388	−3.6446	−3.9923	28.14	21.78
σ	2.57	0.51	0.856	0.3321	0.1288	2.62	1.99

fougerite1: log IAP F_1 = log(Fe^{2+}) + ⅞log(Mg^{2+}) + ²⁷⁄₅loga_w + ⅗pe + ²⁷⁄₅pH; log K_{F1} = 10.4, see text
Fougerite2: log IAP F_2 = log(Fe^{2+}) + ⅘log(Mg^{2+}) + ²¹⁄₅loga_w + ⅗pe + ²¹⁄₅pH; log K_{F2} = 13.1, see text

The range of variation of mole fractions is narrow: ΔX_1 = 1/18, ΔX_2 = 1/12, ΔX_3 = 5/36. In the narrow range where green rusts are stable X_2 = 7/44, and according to our assumption, μ is minimal and can be considered as constant, so that as a first approximation, fougerite can be approximated as a solid of fixed composition (μ ≡ μ°) and the equilibrium reaction simply written in the classical way, for which it is convenient to use mole fractions:

$$[X_1Fe(OH)_2{\cdot}X_2Fe(OH)_3{\cdot}X_3Mg(OH)_2] + X_2e^- + (2X_1 + 3X_2 + 2X_3)H^+ \rightleftharpoons (X_1 + X_2)Fe^{2+} + X_3Mg^{2+} + (2X_1 + 3X_2 + 2X_3)H_2O \quad (44)$$

and to which mass-action law can be directly applied as:

$$(X_1 + X_2)\log(Fe^{2+}) + X_3\log(Mg^{2+}) + X_2pe + (2X_1 + 3X_2 + 2X_3)pH = \log K \quad (45)$$

where log K is given by:

$$\log K = -\frac{1}{(\ln 10)RT}[(X_1 + X_2)\Delta_f G^o(Fe^{2+}_{aq.}) + X_3\Delta_f G^o(Mg^{2+}_{aq.}) + (2X_1 + 3X_2 + 2X_3)\Delta_f G^o(H_2O_l) - \mu] \quad (46)$$

in which μ is the chemical potential of the solid, and can be computed from our model, using equation 31, the values of the parameters reported in Table 4 and the values of X_i determined above. The computations are made at 298.15 K and consistent with μ° (Fe^{2+}, aq.) = −91.5 kJ mol^{-1} from Bourrié *et al.* (1999), μ° (Mg^{2+}, aq.) = − 455.41 kJ mol^{-1} from Bratsch (1989).

The results obtained are μ(F1) = −812.7 kJ mol^{-1} and μ(F2) = −765.2 kJ mol^{-1}, from which one obtains, for 'fougerite1':

$$\log(Fe^{2+}) + ⅞\log(Mg^{2+}) + ²⁷⁄₅\log a_w + ⅗pe + ²⁷⁄₅pH = \log K_{F1} = 10.4 \quad (47)$$

and for 'fougerite2':

$$\log(Fe^{2+}) + ⅘\log(Mg^{2+}) + ²¹⁄₅\log a_w + ⅗pe + ²¹⁄₅pH = \log K_{F2} = 13.1 \quad (48)$$

Activities were computed, providing for formation of ion pairs and for correction of deviation of non-ideality of electrolyte solutions at the actual temperature of the samples, by using the EQUIL(T) code, as earlier (Bourrié *et al.*, 1999) for a set of 68 soil solutions sampled in Fougères from February 1999 to June 2000 (Feder, 2001). The complete set of data is given in Table 5.

Solutions are largely undersaturated with respect to all three pure end-members. For the two types of fougerite considered: log IAP_{F1} values range from 22.8 to 32.2 (av. = 28.14, σ = 2.62); log IAP_{F2} values range from 17.6 to 24.8 (av. = 21.78, σ = 2.).

The uncertainty in the values of log K obtained for the mineral must be about ± 4 kJ mol^{-1}, for 1 Fe atom in the mineral, which gives ±0.7 logarithmic units. Large supersaturations are observed for both 'fougerite1' and 'fougerite2'. The larger the Mg content in the mineral, the larger the supersaturations observed. It can thus be concluded that fougerite forms from solutions largely oversaturated, when Fe^{3+} coprecipitates with Fe^{2+} and Mg^{2+}. The presence of Mg has a very strong stabilizing effect on the mineral.

IMPLICATIONS CONCERNING THE GENESIS OF FOUGERITE, Mg AND Fe GEOCHEMISTRY

The implications for Fe and Mg geochemistry are as follows: due to its extremely small solubility, Fe(III) is absent from aqueous solution; when Fe oxides are reduced, Fe^{2+} is released in solution, in milieus where Mg^{2+} is generally present too. When oxidation occurs, Fe^{3+} precipitates with Fe^{2+} and Mg^{2+} to give rise to fougerite. The initial Fe/Mg in the mineral is fixed by the composition of the solution. Then, fougerite is oxidized progressively at constant Mg mole ratio, (path from *N* to *P*, Figure 3). When the Fe(III) mole ratio reaches its maximum X_2 = 1/3, fougerite dissolves or recrystallizes and lepidocrocite or goethite forms. The new consequence is that Mg geochemistry is involved: synthetic GR have been considered mainly with respect to their capacity to absorb anions in a first step and then to release them back to solutions. The same occurs here with Mg.

ACKNOWLEDGMENTS

We acknowledge the support of INRA, of the French ''Programme National de Recherche Sol et Erosion'' (PNSE), of the French Ministry of Education for the grant to F. Feder, and of the European Union (European Fund for Regional Development), and the help of Dr G. Klingelhöfer and Dr B. Bernhardt for the acquisition of Mössbauer *in situ* spectra. Comments by Dr S. Aja, an anonymous referee and Dr J. Amonette are gratefully acknowledged.

REFERENCES

Abdelmoula, M., Trolard, F., Bourrié, G. and Génin, J.-M.R. (1998) Evidence for the Fe(II)-Fe(III) green rust Fougerite mineral occurrence in a hydromorphic soil and its transformation with depth. *Hyperfine Interactions*, **112**, 235–238.

Altmeier, M., Metz, V., Neck, V., Müller, R. and Fanghänel, Th. (2003) Solid-liquid equilibria of $Mg(OH)_{2\ (cr)}$ and $Mg(OH)_3\ Cl{\cdot}4H_2O_{(cr)}$ in the system Mg-Na-H-OH-Cl-H_2O at 25°C. *Geochimica et Cosmochimica Acta*, **67**, 3595–3601.

Arden, T.V. (1950) The solubility products of ferrous and ferrosic hydroxides. *Journal of the Chemical Society*, 882–885.

Bernal, J.D., Dasgupta, D.R. and Mackay, A.L. (1959) The oxides and hydroxides of iron and their structural interrelationships. *Clay Minerals Bulletin*, **24**, 882–885.

Bourrié, G. (1983) Rôle des composés amorphes dans le contrôle de la composition chimique des solutions du sol. *Science du Sol*, **3-4**, 195–204.

Bourrié, G., Trolard, F., Génin, J.-M.R., Jaffrezic, A., Maître, V. and Abdelmoula, M. (1999) Iron control by equilibria between hydroxy-Green Rusts and solutions in hydromorphic soils. *Geochimica et Cosmochimica Acta*, **63**, 3417–3427.

Bratsch, S.G. (1989) Standard electrode potentials and temperature coefficients in water at 298.15 K. *Journal of Physical and Chemical Reference Data*, **18**, 1–21.

Davies, P.K. and Navrotsky, A. (1983) Quantitative correlations of deviations from ideality in binary and pseudobinary solid solutions. *Journal of Solid State Chemistry*, **46**, 1–22.

Détournay, J., De Miranda, L., Dérié, R. and Ghodsi, M. (1975) The region of stability of green rust II in the electrochemical E-pH equilibrium diagram of iron in sulphate medium. *Corrosion Science*, **15**, 295–306.

Drissi, S.H., Refait, Ph. and Génin, J.-M.R. (1994) The oxidation of $Fe(OH)_2$ in the presence of carbonate ions: structure of carbonate green rust one. *Hyperfine Interactions*, **90**, 395–400.

Drissi, S.H., Refait, Ph., Abdelmoula, M. and Génin, J.-M.R. (1995) Preparation and thermodynamic properties of Fe(II)-Fe(III) hydroxide-carbonate (green rust one), Pourbaix diagram of iron in carbonate-containing aqueous media. *Corrosion Science*, **37**, 2025–2041.

Feder, F. (2001) Dynamique des processus d'oxydo-réduction dans les sols hydromorphes – monitoring in situ de la solution du sol et des phases solides ferrifères. Thèse, Université d'Aix-Marseille III, Aix-en-Provence, France, 200 pp.

Génin, J.-M.R., Olowe, A.A., Refait, Ph. and Simon, L. (1996a) On the stoichiometry and Pourbaix diagram of Fe(II)–Fe(III) hydroxy-sulphate or sulphate containing green rust 2; an electrochemical and Mössbauer spectroscopy study. *Corrosion Science*, **38**, 1751–1762.

Génin, J.-M.R., Simon, L. and Refait, Ph. (1996b) Existence of sulphite-containing green rust one. Pp. 51–54 in: *Proceedings ICAME 95* (I. Ortalli, editor). SIF, Bologna, Italy.

Génin, J.-M.R., Abdelmoula, M., Refait, Ph. and Simon, L. (1998a) Comparison of the Green Rust Two lamellar double hydroxide class with the Green Rust One pyroaurite class: Fe(II)-Fe(III) sulphate and selenate hydroxides. *Hyperfine Interactions*, **(C), 3**, 313–316.

Génin, J.-M.R., Bourrié, G., Trolard, F., Abdelmoula, M., Jaffrezic, A., Refait, Ph., Maître, V., Humbert, B. and Herbillon, A. (1998b) Thermodynamic equilibria in aqueous suspensions of synthetic and natural Fe(II)-Fe(III) Green Rusts: occurrences of the mineral in hydromorphic soils. *Environmental Science and Technology*, **32**, 1058–1068.

Génin, J.-M.R., Refait, Ph., Bourrié, G., Abdelmoula, M. and Trolard, F. 2001 Structure and stability of the Fe(II)-Fe(III) green rust ''fougerite'' mineral and its potential for reducing pollutants in soil solutions. *Applied Geochemistry*, **16**, 559–570.

Girard, A. and Chaudron, G. (1935) Sur la constitution de la rouille. *Comptes-Rendus de l'Académie des Sciences, Paris*, **200**, 127–129.

Hansen, H.C.B. (1989) Composition, stabilisation and light absorption of Fe(II)-Fe(III) hydroxycarbonate (green rust). *Clay Minerals*, **24**, 663–669.

Hansen, H.C.B. and Taylor, R.M. (1991) Formation of synthetic analogues of double metal-hydroxy carbonate minerals under controlled pH conditions: II. The synthesis of desautelsite. *Clay Minerals*, **26**, 507–525.

Hashimoto, K. and Misawa, T. (1973) The solubility of γFeOOH in perchloric acid at 15 °C. *Corrosion Science*, **13**, 229–231.

Jolivet, J.P. (1994) *De la solution à l'oxyde — Condensation des cations en solution aqueuse – Chimie de surface des oxydes*. InterEditions / CNRS Editions, Paris, 387 pp.

Koritnig, S. and Susse, P. (1975) Meixnerit, $Mg_6Al_2(OH)_{18}{\cdot}4H_2O$, ein neues Magnesium-Aluminium-Hydroxid-Mineral. *Tschermaks Mineralogische Petrologische Mitteilungen*, **22**, 79–87.

Mascolo, G. and Marino, O. (1980) A new synthesis and characterization of magnesium-aluminium hydroxides. *Mineralogical Magazine*, **43**, 619–621.

Murad, E. and Taylor, R.M. (1984) The Mössbauer spectra of hydroxycarbonate green rusts. *Clay Minerals*, **19**, 77–83.

Olowe, A.A. and Génin, J.-M.R. (1991) The mechanism of oxidation of Fe(II) hydroxide in sulphated aqueous media: importance of the initial ratio of the reactants. *Corrosion Science*, **32**, 965–984.

Ponnamperuma, F.N., Tianco, E.M. and Loy, T. (1967) Redox equilibria in flooded soils: I. The iron hydroxide system. *Soil Science*, **103**, 374–382.

Prigogine, I. and Defay, R. (1946) *Thermodynamique chimique conformément aux méthodes de Gibbs et De Donder*. Dunod, Paris, tome I, 348 pp., tome II, 430 pp.

Refait, Ph., Abdelmoula, M. and Génin, J.-M.R. (1998a) Mechanisms of formation and structure of green rust one in aqueous corrosion of iron in the presence of chloride ions. *Corrosion Science*, **40**, 1547–1560.

Refait, Ph., Abdelmoula, M., Trolard, F., Génin, J.-M.R., Ehrhardt, J.-J. and Bourrié, G. (2001) Mössbauer and XAS study of a green rust mineral; the partial substitution of Fe^{2+} by Mg^{2+}. *American Mineralogist*, **86**, 731–739.

Refait, Ph., Bon, C., Simon, L., Bourrié, G., Trolard, F., Bessière, J. and Génin, J.-M.R. (1999) Chemical composition and Gibbs standard free energy of formation of Fe(II)-Fe(III) hydroxysulphate green rust and Fe(II) hydroxide. *Clay Minerals*, **34**, 499–510.

Refait, Ph., Charton, A. and Génin, J.-M.R. (1998b) Identification, composition, thermodynamic and structural properties of a pyroaurite-like iron(II)-iron(III) hydroxy-oxalate Green Rust. *European Journal of Solid State Inorganic Chemistry*, **35**, 655–666.

Refait, Ph. and Génin, J.-M.R. (1993) The oxidation of Ni(II)-Fe(II) hydroxides in chloride-containing aqueous media. *Corrosion Science*, **34**, 2059–2070.

Refait, Ph., Simon, L., Louis, C. and Génin, J.-M.R. (2000) Reduction of SeO_4^{2-} anions and anoxic formation of iron(II)-iron(III) hydroxy-selenate green rust. *Environmental Science and Technology*, **34**, 819–825.

Roussel, H., Briois, V., Elkaim, E., de Roy, A. and Besse, J.P. (2000) Cationic order and structure of [Zn-Cr-Cl] and [Cu-Cr-Cl] layered double hydroxides: a XRD and EXAFS study. *Journal of Physical Chemistry*, **B25**, 5915–5953.

Shannon, R.D. (1976) Revised effective ionic radii and systematic studies of interatomic distances in halides and chalcogenides. *Acta Crystallographica*, **A32**, 751–767.

Simon, L., François, M., Refait, Ph., Renaudin, G., Lelaurain, M. and Génin, J.-M.R. (2003) Structure of the Fe(II-III) layered double hydroxysulphate green rust two from Rietveld analysis. *Solid State Sciences*, **5**, 327–334.

Simon, L., Refait, Ph. and Génin, J.-M.R. (1998) Transformation of Fe(II)-Fe(III) hydroxysulphite into hydroxysulphate Green Rusts. *Hyperfine Interactions*, **112**, 217–220.

Stampfl, P.P. (1969) Ein basisches Eisen-II-III-Karbonat in Rost. *Corrosion Science*, **9**, 185–187.

Taylor, R.M. (1981) Color in soils and sediments. A review. In: "International Clay Conference 1981" (H. Van Olphen ed.), Developments in Sedimentology, **35**, p. 749–761, Elsevier, Amsterdam.

Taylor, R.M. and MacKenzie, R.M. (1980) The influence of aluminum on iron oxides. VI. The formation of Fe(II)-Al(III) hydroxy-chlorides, -sulfates, and -carbonates as new members of the pyroaurite group and their significance in soils. *Clays and Clay Minerals*, **28**, 179–187.

Trolard, F., Abdelmoula, M., Bourrié, G., Humbert, B. and Génin, J.-M.R. (1996) Mise en évidence d'un constituant de type ''rouilles vertes'' dans les sols hydromorphes - Proposition de l'existence d'un nouveau minéral : la ''fougérite''. *Comptes-Rendus de l'Académie des Sciences, Paris*, **323, IIa**, 1015–1022.

Trolard, F., Génin, J.-M.R., Abdelmoula, M., Bourrié, G., Humbert, B. and Herbillon, A. (1997) Identification of a green rust mineral in a reductomorphic soil by Mössbauer and Raman spectroscopies. *Geochimica et Cosmochimica Acta*, **61**, 1107–1111.

Vucelic, M., Jones, W. and Moggridge, G.D. (1997) Cation ordering in synthetic layered double hydroxides. *Clays and Clay Minerals*, **45**, 803–813.

Vysotskii, G.N. (1905) Gley. *Pochvovedeniye*, **4**, 291–327. (original paper in Russian). (1999) Gley. An abridged version of Vysotskii (1905) on the 257th Anniversary of the Russian Academy of Sciences. *Eurasian Soil Science*, **32**, 1063–1068.

Wagman, D.D., Evans, W.H., Parker, V.B., Schumm, R.H., Halow, L., Bailey, S.M., Churney, K.L. and Nuttall, R.L. (1982) The NBS Tables of chemical thermodynamic properties. Selected values for inorganic and C1 and C2 organic substances in SI units. *Journal of Physical and Chemical Reference Data*, **Supplement nº2**, 11.

(*Received 23 January 2003; revised 6 January 2004; Ms. 753; A.E. James E. Amonette*)

Science of the Total Environment 511 (2015) 238–248

Contents lists available at ScienceDirect

Science of the Total Environment

journal homepage: www.elsevier.com/locate/scitotenv

Repeated pig manure applications modify nitrate and chloride competition and fluxes in a Nitisol

Frédéric Feder [a,b,*], Vincent Bochu [a,c], Antoine Findeling [d], Emmanuel Doelsch [d]

[a] CIRAD, UPR Recyclage et risque, F-97408 Saint Denis, Réunion, France
[b] CIRAD, UPR Recyclage et risque, 18524 Dakar, Sénégal
[c] Chambre d'agriculture de Champagne-Ardenne, France
[d] CIRAD, UPR Recyclage et risque, F-34398 Montpellier, France

HIGHLIGHTS

- Pig manure nitrification modified nitrate and chloride adsorption and transfer.
- Retardation factors differed for the two pig manure applications.
- Nitrates were available for a shorter time for crops.
- Nitrate leaching below the root depth may be greater with pig manure application.

ARTICLE INFO

Article history:
Received 13 September 2014
Received in revised form 18 December 2014
Accepted 18 December 2014
Available online xxxx

Editor: Charlotte Poschenrieder

Keywords:
Variable-charge soil
Nitisol
Nitrate
Transfer
Pig manure
Nitrification

ABSTRACT

Solute transport was studied in a variable-charge soil (Nitisol) with two following pig manure applications. There were three identical soil columns (diameter = 37.5 cm; soil depth = 85 cm) equipped with TDR probes and tensiometers, one of which served as an untreated control. Dispersivities inferred using the CXTFIT 2.1 code presented inverse patterns with depth for nitrate and chloride breakthrough curves, while the normalized intensities had the same patterns with depth for both applications. For nitrates, the retardation factors steadily decreased with depth from 4.85 and 3.57 at 17 cm depth to 2.1 and 1.86 PV (pore volume) at 85 cm depth for each column, respectively. For chlorides, the retardation factor increased linearly with depth, from 1.05 at 17 cm depth to 1.76 and 1.86 PV at 85 cm depth. After the first application, the mean difference between nitrate and chloride retardation factors was 3.8 PV at 17 cm depth and it regularly decreased to 0.34 PV at 85 cm depth. For the second application, the mean difference was 2.52 PV at 17 cm depth and it regularly decreased to 0 PV at 85 cm depth. The kinetics of nitrate production by the pig manure nitrification process modified the pH, the ionic strength of the soil solution and then the anionic exchange capacity. This could explain the high nitrate retardation factors until 55 cm depth and the difference between nitrate and chloride retardation factors. The earlier chloride adsorption at anionic exchange sites, combined with a selectivity coefficient to the detriment of nitrates, counterbalanced the delay in nitrate production due to the kinetic mineralisation of pig manure. Nitrate fluxes then caught up with the chloride fluxes at the outlet.

1. Introduction

Tropical and subtropical soils are affected by long intense weathering (Van Wambeke, 1992), including Nitisols which are found on about 200 million ha worldwide, especially in tropical Africa (IUSS Working Group WRB, 2007). They are more productive than other tropical soils, mainly due to some good chemical and physical properties, including a stable soil structure and some deep and porous sola. These soils are thus often intensively cultivated (Warren and Kihanda, 2001). Organic and mineral fertilizers are necessary to maintain the soil fertility, but the application of such compounds represents a significant risk of environmental pollution (Cahn et al., 1993; Legros et al., 2013). Field experiments are often conducted to measure leaching of pollutants, such as nitrates, below the root depth. Indeed, when this depth is exceeded, nitrates can generally not be used by crops and could contribute to groundwater pollution (Wassenaar et al., 2014).

The mineralogy of Nitisols is dominated by iron and aluminium oxides, as well as by kaolinite and (meta)-halloysite (Parfitt, 1978; Van Wambeke, 1992). Consequently, they have positive charges on amphoteric mineral surfaces and develop an appreciable anionic exchange

* Corresponding author at: CIRAD, UPR Recyclage et risque, F-97408 Saint Denis, Réunion, France.
E-mail address: v.bochu@champagrica.fr (V. Bochu).

http://dx.doi.org/10.1016/j.scitotenv.2014.12.059
0048-9697/

capacity (AEC). Possible chemical reactions that could explain anion adsorption can take place in the outer sphere and/or diffuse layers of soil particles. These charges balance (in equivalent amounts) the positive surface charges of soil particles (Qafoku et al., 2000). Their sum represents counter-ion charges or the anion exchange capacity in soil. Like other variable-charge soils (Ferralsols, etc.), they have specific anion adsorption properties. The order of competitive adsorption at anion exchange sites is phosphates > sulphates > chlorides > nitrates (Parfitt, 1978; Katou et al., 1996). These authors also suggest that native phosphates and sulphates are strongly adsorbed (specific adsorption), while nitrate and chloride adsorption is nonspecific and largely due to the increase in total anion adsorption and not to the desorption of other species. Nitrate adsorption in several soils is completely reversible, indicating a simple electrostatic retention mechanism, i.e. salt adsorption (Toner et al., 1989; Bellini et al., 1996).

Katou et al. (1996) identified a major difficulty regarding the study of solute transport in these soils—the pH and ionic strength of the soil solution modifies adsorption on solid phases and then the equilibrium between the chemical composition of the soil solution and the adsorbed phase. Different salts ($CaCl_2$, KNO_3, etc.) are commonly used to study and explain these anion retention mechanisms in laboratory experiments and to monitor anion transport (Wong et al., 1990; Bellini et al., 1996; Vogeler et al., 1998). The physicochemical (pH, ionic strength, organic matter contents, etc.) and hydrodynamic conditions are thus maintained constant. Very few studies, especially in situ studies, have dealt with the dynamics of anions resulting from organic waste spreading (Cahn et al., 1993; Warren and Kihanda, 2001; Feder and Findeling, 2007). Among the studied anions, nitrate dynamics have been assessed because of the groundwater contamination potential in case of inappropriate agricultural practices (Payet et al., 2009; Wassenaar et al., 2014). Nitrates are studied for their environmental impact, while chlorides are studied simultaneously because they are not agricultural inputs and could be used as inert tracers.

The kinetics of organic matter mineralization and ammonium nitrification induce a lag between nitrate production and its leaching in the soil and other chemical species contained in the same organic matter (Paul and Clark, 1989; De Boer and Kowalchuk, 2001; Feder and Findeling, 2007). This lag could induce specific and original physicochemical conditions that could modify nitrate and chloride competition and fluxes in these soils. Furthermore, these physicochemical conditions are more representative of field conditions than laboratory studies in which nitrate and chloride salts are used.

This study was aimed at assessing whether repeated applications of nitrates produced by pig manure mineralization, and hence asynchronous with chloride leaching, changed the competition between nitrates and chlorides for adsorption in a variable-charge soil, as well as the leaching hazard of nitrates. Our study focused on: (i) the impact of kinetic nitrification of pig manure on nitrate production and leaching, and (ii) the lag in the nitrate and chloride breakthrough curves, and their retention in the soil. The strategy involved conducting laboratory studies to accurately control water and solute fluxes and to circumvent the natural variability in soil properties. The experimental design adopted for this purpose consisted of three instrumented soil columns. The columns were assembled so as to simulate in situ hydraulic properties. Two columns were amended with pig manure and the remaining column was used as the untreated control. The columns were maintained under controlled climatic conditions. Pig manure was chosen for its high nitrogen concentrations and its common use as nitrogen and organic fertilizer.

2. Materials and methods

2.1. Study site at La Mare research station in Réunion

Réunion is a French island located 800 km east of Madagascar in the southern Indian Ocean region. The main peak of this recent volcanic island (Piton des Neiges, 3070 m above sea level) emerged 3 million years ago. The La Mare research station is located on the northern slope of Piton des Neiges at 60 m above sea level (55°53 E; 20°89 S). Mean annual rainfall at the station is 2000 mm, with a mean annual temperature of 25 °C. Table 1 gives selected physical and chemical characteristics of the soil. It was classified as a Nitisol (Feder, 2013), including: (i) a surface A horizon (0–45 cm), and (ii) a nitic B horizon (45–150 cm).

2.2. Soil analysis

Pedological, agronomical and mineralogical analyses were performed on soil samples. The initial soil analyses were performed on samples collected in situ from the 0–15, 15–30, 30–45, 45–60, and 60–85 cm layers. The final soil analyses (at the end of the study) were

Table 1
Physical and chemical characteristics of the studied soil and pig manure.

		A horizon			B horizon		Pig manure
Depth	cm	0–15	15–30	30–45	45–60	60–80	
pH (H_2O)		5.80	5.95	5.88	6.50	6.77	7.67
pH (KCl)		4.72	4.88	4.85	5.64	5.87	
C (org.)	$g \cdot kg^{-1}$	18.3	20.7	15.5	8.5	5.2	356
N (tot.)	$g \cdot kg^{-1}$	1.19	1.21	1.13	1.13	1.15	63.4
$N–NH_4$	$mg \cdot kg^{-1}$	15.73	21.25	12.17	7.53	4.87	2800
$N–NO_3$	$mg \cdot kg^{-1}$	1.86	3.15	0.88	0.95	0.64	6
Cl^-	$g \cdot kg^{-1}$						19
AEC	$mol_{(-)} \cdot kg^{-1}$		0.0054		0.0090		
CEC	$mol_{(+)} \cdot kg^{-1}$	0.1963	0.2041	0.1809	0.1655	0.1574	
Base Sat.	%	42.49	50.76	43.54	49.24	58.91	
Fe (DCB)	$g \cdot kg^{-1}$	9.52	9.47	9.53	8.27	7.39	
Al (DCB)	$g \cdot kg^{-1}$	91.81	92.95	91.95	92.25	86.84	
Si (DCB)	$g \cdot kg^{-1}$	3.39	3.69	3.39	3.39	3.40	
Fe (ox.)	$g \cdot kg^{-1}$	3.81	3.63	3.89	3.77	4.13	
Al (ox.)	$g \cdot kg^{-1}$	8.41	8.60	8.44	8.45	9.95	
Si (ox.)	$g \cdot kg^{-1}$	0.87	0.85	0.93	1.12	1.40	
Clay	%	74.13	71.74	72.25	67.27	56.76	
Fine silts	%	19.92	21.03	22.07	26.12	32.75	
Coarse silts	%	2.13	2.83	2.38	3.40	4.84	
Fine sands	%	1.78	2.18	1.73	1.93	3.06	
Coarse sand	%	2.04	2.22	1.56	1.30	2.59	
Bulk density	$kg \cdot dm^{-3}$	1.18 (0.01)[a]	1.11 (0.1)	1.17 (0.03)	1.20 (0.03)	1.31 (0.02)	1.078
Dry matter	$g \cdot kg^{-1}$						83.5

[a] The standard deviation is in brackets.

performed on samples collected in soil columns at the following depths: 0–5, 5–10, 10–15, 15–30, 30–45, 45–60, and 60–85 cm. The pH (water) and pH (KCl) of the initial and final soils were measured according to the NF ISO 10390 standard at a soil/water volume ratio of 1:5. Total C and total N of the soil samples were analysed by dry combustion with an element analyser (Thermoquest NC2100 Soil). The content of mineral forms of N (NH_4 and NO_3) in the soil samples was measured in solution after KCl (1 M) extraction at a soil/water volume ratio of 1:5 and assayed by continuous flow colorimetry (Alliance Instruments). We measured the cation exchange capacity (CEC) by the ammonium acetate method at pH 7. The AEC of the initial soil was measured on samples collected at 30 cm (surface horizon) and 60 cm (nitic horizon) depths using the method described by Gillman and Sumpter (1986). We used the recommended analytical procedures (IUSS Working Group WRB, 2007) to measure Al, Si and Fe elements extracted by oxalate and dithionite-citrate-bicarbonate (DCB). Extractable Al, Si and Fe were assayed by inductively coupled plasma-atomic emission spectrometry (ICP-AES, Varian Vista spectrometer equipped with a coupled-charge detector device). All samples were analysed for particle-size distribution analysis by the pipette method using an automated analyser (Texsol 24B instrument) and according to the standard procedure applied to all soils: samples were treated with H_2O_2 to remove organic matter, dispersed with a sodium hexametaphosphate solution, and mechanically shaken (Alary et al., 2013). Coarse sand and fine sand fractions were obtained by sieving; clay, fine silt and coarse silt fractions were obtained by pipetting. The mineralogy of this soil was similar for both horizons. Powder diffraction (XRD) was performed with a Philips PW 3710 diffractometer with Bragg–Brentano geometry. We found four iron oxides (magnetite, hematite, maghemite, and goethite), titanium–iron oxides (ilmenite), aluminium oxyhydroxide (gibbsite) and silicates (halloysite, kaolinite, quartz and feldspath). Bulk densities were measured with three 100 cm^3 samples of undisturbed soil collected in the field at three different depths for the A horizon and at two depths for the B horizon (IUSS Working Group WRB, 2007). The saturated hydraulic conductivity K_s ($m \cdot s^{-1}$) was measured in the field using a permeameter ring (0.4 m diameter) at the soil surface.

2.3. Soil column assembly

Soil columns were assembled to reproduce in situ conditions. We assembled three identical soil columns, i.e. C1, C2, and C3, in a 0.375 m diameter × 1 m long PVC tube (Fig. 1). The bottom of each column was closed with a plexiglass plate that was slightly sloped (1 cm) to channel drained water towards the outlet. The A horizon consisted of three distinct soil layers (0–15, 15–30 and 30–45 cm) in order to take slight differences in organic matter contents and bulk densities into account. The B horizon was assembled with two distinct soil layers (45–60 and 60–85 cm) in all three columns. Soil was collected at the La Mare research station and roughly sieved (5 mm mesh) without drying to reduce sieving artefacts and to preserve the soil microstructure. The five layers were assembled in C1, C2 and C3 columns, while maintaining the soil bulk densities measured in situ. C1 and C2 were used to assess the impact of pig manure amendment of the soil, while C3 was the untreated control. Soil in the C1, C2 and C3 columns had not been previously cropped, thus avoiding bias from crop cover and enabling us to focus solely on evaluating nitrate and chloride leaching risks.

The pore volume (PV) was calculated for the 0–17, 0–30, 0–55 and 0–85 cm layers using the equation:

$$PV = 1 - \frac{BD}{PD}$$

with BD ($kg \cdot dm^{-3}$) corresponding to the bulk density measured in situ and PD ($kg \cdot dm^{-3}$) corresponding to the particle density estimated at 2.7 $kg \cdot dm^{-3}$ for this soil. The hypothesis that the entire water content was involved in water flow was checked in the Results and discussion section (Table 2).

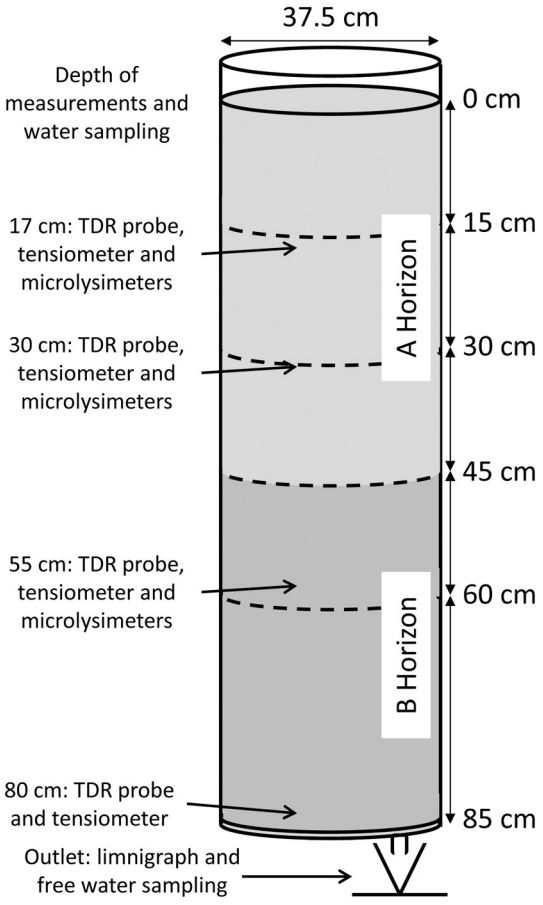

Fig. 1. Schematic diagram of the column showing vertical position of water sampling (microlysimeter) and monitoring devices (TDR probes and tensiometers).

2.4. Hydrodynamic measurements and transport parameters

Each column was equipped with instruments to monitor the volumetric water contents and fluxes. Time domain reflectometry (TDR) probes (CS616, Campbell Scientific) and microtensiometers (Sdec, France) were set at 17, 30, 55 and 80 cm depth in the three soil columns to measure volumetric water contents θ ($m^3 \cdot m^{-3}$) and matrix potentials of soil water, respectively. Tipping bucket rain gauges (ARG100, Campbell Scientific) were placed at the outlet of each column and used as limnigraphs to assess drainage flow continuously. All of these instruments were connected to a datalogger (CR10X-2 M, Campbell Scientific) with measurements recorded at 10 min intervals. We placed a tray near the soil columns to estimate the extent of evaporation from C1, C2 and C3 via gravimetric measurements.

Table 2
Experimental parameters for the three columns once steady flow was reached.

Depth (cm)	Volumetric water contents θ			Darcy velocity q		
	C1	C2	C3	C1	C2	C3
	($m^3 \cdot m^{-3}$)			($m \cdot s^{-1}$)		
17	0.47	0.49	0.48	1.0×10^{-6}	1.2×10^{-6}	1.8×10^{-6}
30	0.51	0.48	0.48	2.6×10^{-6}	4.5×10^{-6}	3.4×10^{-6}
55	0.56	0.56	0.55	2.2×10^{-6}	$3. \times 8\ 10^{-6}$	2.2×10^{-6}
80	0.57	0.58	0.57	2.0×10^{-6}	$3.7 \times 8\ 10^{-6}$	2.2×10^{-6}

The Darcy velocity q ($m \cdot s^{-1}$) was calculated using Darcy's law:

$$q = K_s \cdot S \cdot \frac{H_{z2} - H_{z1}}{z2 - z1}$$

with K_s ($m \cdot s^{-1}$) representing the saturated hydraulic conductivity, S (m^2) the surface of the column, and H (m) the total potential of water in the soil measured using microtensiometers at the different depths z (m).

Drainage flow across each horizon was calculated on the basis of the mass conservation law:

$$Dr = WA - Ev - WSa - \Delta WR$$

with Dr (m) representing the drainage, WA (m) the water application, Ev (m) the evaporation, WSa (m) the water sampling, and Δ WR (m) the variation in the volumetric water content of soil measured by TDR probes.

Transport parameters (dispersivity λ (m) and retardation factor R (pore volume)) were determined using the CXTFIT 2.1 code (Toride et al., 1995). The dispersivity λ (m) was calculated using the following equation:

$$\lambda = \frac{D}{\nu}$$

with D being the coefficient of dispersion ($m^2 \cdot s^{-1}$) used in CXTFIT 2.1 code,with $\nu = \frac{q}{\theta}$ where q is the Darcy velocity ($m \cdot s^{-1}$) and θ is the volumetric water content ($m^3 \cdot m^{-3}$).

R is the retardation factor of a chemical species relative to a non-reactive species. For non-reactive ions, the centre of gravity of a breakthrough curve should be at one pore volume for the corresponding depth after the centre of gravity of the input application ($R = 1$). With some constant bulk density ρ ($kg \cdot dm^{-3}$) and volumetric water content θ ($m^3 \cdot m^{-3}$) values, the higher retardation factor corresponded to anionic or cationic retention in the soil defined by the distribution coefficient K_D ($dm^3 \cdot kg^{-1}$). R is thus defined by:

$$R = 1 + K_D \frac{\rho}{\theta}.$$

Nitrate and chloride concentrations were normalized by reference to the input concentration, while volumes were normalized by reference to the pore volume of the considered layer or the whole column. Experimental chloride concentrations (C) were normalized by reference to the input concentration (C_0) of pig manure. To normalize the total concentrations of mineral nitrogen ($N_{min.}$) by reference to the input concentration, we considered that nitrification of ammonium from pig manure was rapid at the beginning of the experiment and complete. Consequently, we finally only considered the nitrate form of mineral nitrogen. This hypothesis is checked in the Results and discussion section.

2.5. Water and manure inputs

Water and pig manure applications were representative of typical environmental conditions in Réunion. The columns were initially irrigated regularly for 48 days in order to homogenize the soil chemical profiles and to enable pore restructuring, thus limiting sieving artefacts: 2000 mm corresponding to 4.15 PV. We then began measurements and water sampling on day 0. On days 11 (corresponding to 0.9 PV) and 72 (corresponding to 4.45 PV), 0.735 kg of pig manure (Table 1) was applied on the surface of C1 and C2, followed by 0.29 dm^3 of water, while the C3 control remained untreated. This pig manure dosage was calculated to be equivalent to the application of 370 $m^3 \cdot ha^{-1}$ containing 6.34 $g \cdot kg^{-1}$ of the total mineral nitrogen, which is a typical maximum for manure spreading practices in Réunion (Payet et al., 2009; Legros et al., 2013). The C3 control received 0.9 dm^3 of water, which was equivalent to the amount of moisture contained in the manure dose and the water addition. After manure amendment, C1, C2, and C3 were irrigated with identical amounts of water twice a week for 4 months. Each column received 22.09 dm^3 of water weekly, corresponding to 200 mm or 0.415 PV. Thus, 3300 mm of water was added to reproduce field conditions over a 1.5 year period and two well separated manure amendment applications were carried out.

2.6. Soil solution analysis

The soil solution was regularly sampled and analysed. The soil solution was sampled at 17, 30 and 55 cm depth with small zero-tension microlysimeters inserted when the columns were assembled. These microlysimeters were made by covering an open PVC bottle (1.5 cm diameter), without cap, with an inert cloth. This inert cloth had a very fine mesh and prevented soil particles from penetrating into the bottle. This was certified by the clarity of the water samples collected. The leached water accumulated gradually in the bottle and was extracted regularly after each irrigation using a teflon capillary positioned at the bottom of the bottle and out of the column. The top of these microlysimeters corresponded to the sampling depth. Four microlysimeters were placed at each depth in the three columns to collect sufficient quantities of leachate. At the outlet (85 cm depth), drained water was cumulated after each irrigation. A mean sample of irrigation water was collected each week by mixing, in equivalent amounts, two samples. All soil solution samples were filtered at 0.45 μm and divided into three aliquots. Right after sampling, the first untreated aliquot was used for the physicochemical analyses: pH, oxido-reduction potential, electric conductivity, and dissolved oxygen. The pH was measured with an ISFET electrode (Senstron, Hot-line). The oxido-reduction potential was measured with a platinum electrode against a standard Ag/AgCl electrode with temperature correction. Electric conductivity was measured with a standard conductivity cell (WTW, TetraCon 325), and the temperature was corrected to 25 °C. Dissolved oxygen was measured with a Clark-type electrode (WTW, FDO 925). The second aliquot was acidified with HNO_3 (suprapure) to quantify chlorides using ICP-AES spectrometry (Varian Vista). The third aliquot was used to quantify nitrate and ammonium by continuous flux colorimetry (Alliance Instruments). The last two aliquots were maintained at 4 °C before analysis. An aliquot of water was collected before each application and analysed along with the soil solution.

2.7. Pig manure analysis

Table 1 gives the physical and chemical characteristics of pig manure, which came from a small farrow-to-finish swine production farm with a herd of around 10 sows. The manure pH and electric conductivity measurements were obtained in the same way and with the same instrumentation as for the soil solutions. Nitrate and ammonium were measured immediately by continuous flux colorimetry (Alliance Instruments). Total C and total N were determined by the Dumas method using an element analyser (Thermoquest NC2100 Soil). Chlorides were assayed on the soluble fraction, after 0.45 μm filtration, by ICP-AES spectrometry (Varian Vista).

2.8. Statistical analysis

Transport parameters (dispersivity, intensity and retardation factor), determined using the CXTFIT 2.1 code, were estimated using the

Fig. 2. Experimental points and modelling of nitrate (left) and chloride (right) breakthrough curves at 17, 30, 55 and 85 cm depths for C1 and C2 columns according to the applied water (pore volume) for the whole column; arrows correspond to pig manure applications.

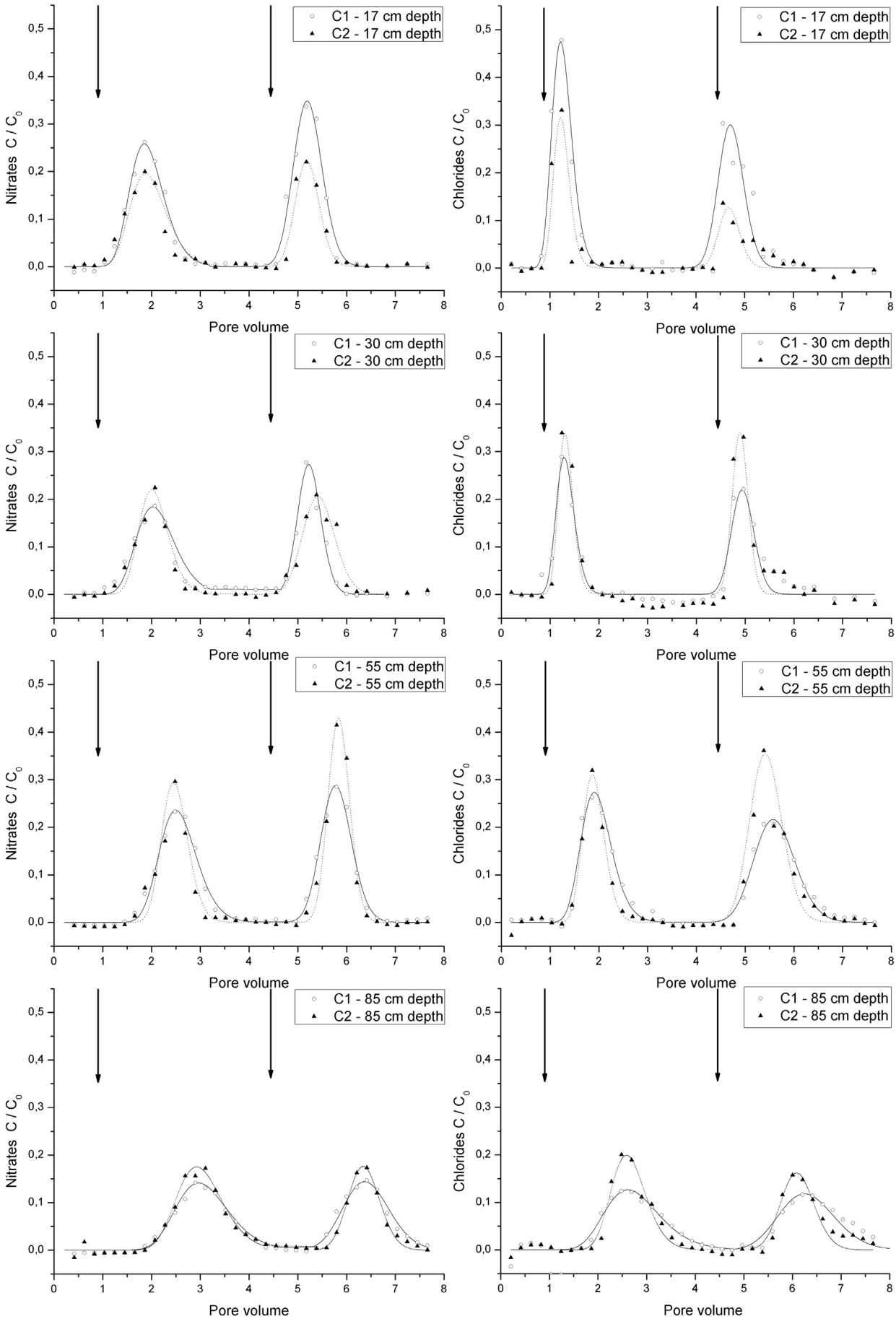
C1 - 17 cm depth
C2 - 17 cm depth
Nitrates C / C0
Chlorides C / C0
Pore volume
C1 - 30 cm depth
C2 - 30 cm depth
C1 - 55 cm depth
C2 - 55 cm depth
C1 - 85 cm depth
C2 - 85 cm depth

nonlinear least squares method. For each CXTFIT 2.1 simulation, the code provided a coefficient of determination (R^2) of observed (experimental data) versus predicted regression and the mean squared error (MSE). The confidence intervals, mean and standard deviation for data obtained in the column experiments were calculated with OriginPro 8.0 software using the Student t-test at the 95% confidence level.

3. Results and discussion

3.1. Hydrodynamic patterns of soil columns and flux modelling

We checked whether the experimental setup could closely reproduce flows that occur in field soil by calculating the Darcy velocity, the hydraulic conductivity and by measuring the volumetric water contents and the total water potential in the soil. For each irrigation, once the saturated steady flow was reached, the volumetric water contents (Table 2) measured by TDR probes were similar, at a given depth, for the three columns throughout the measurement period and indicated almost saturated volumetric soil moisture contents θ ($m^3 \cdot m^{-3}$). Differences between the three columns were minor ($\Delta\theta < 0.03\ m^3 \cdot m^{-3}$) and close to the measurement error. For each column, the drainage flow and Darcy velocity at four depths (17, 30, 55 and 80 cm) were calculated from the mass conservation and Darcy's laws. The hydraulic conductivity was then deduced from Darcy's law for the same duration at the same depths. These calculations gave very close values for the three columns and were in line with the saturated hydraulic conductivity measured in situ with a permeameter ring at saturation: $3.6 \times 10^{-6}\ m \cdot s^{-1}$. The hydraulic properties of the three columns were similar and close to those of in situ soil. The three soil columns could thus accurately replicate the hydrodynamic behaviour of in situ soil.

The transport of nitrates and chlorides in repacked soil columns should be described by an equilibrium convection–dispersion equation. Molecular diffusion was neglected in relation to dispersion; according to Toride et al. (1995), this hypothesis was valid for high Darcy velocities, as in our study (Table 2). The mobile–immobile model was not used in our study. Several studies have shown that simulations with the mobile–immobile model were rather better than without it (Vogeler et al., 1998). However, it required estimation of several other model parameters for only a slight improvement in the simulation. Seyfried and Rao (1987) obtained better simulation under 0 or 0.1 kPa tension and with asymmetric breakthrough curves, but not under tensions higher than 0.1 kPa with quite symmetric breakthrough curves like ours. After each pig manure application, C1 and C2 breakthrough curves for nitrates and chlorides were fitted with CXTFIT 2.1 to deduce and compare the dispersivity, the normalized C/C_0 intensity, and the retardation factor of each curve (Fig. 2). Our fitted curves were symmetrical, so the deterministic linear equilibrium adsorption model for the convection–dispersion equation could thus be used suitably to define transport parameters for nitrates and chlorides (Toride et al., 1995). The breakthrough curve for C3, i.e. the untreated control, was not presented because the C/C_0 ratio was never significantly different from the C1 and C2 baselines outside of the nitrate and chloride peak. The pore volume on the x-axis in Fig. 2 was always calculated for the whole column (0–85 cm depth) to compare the progression of the breakthrough curves at the different depths. Differences between the predicted breakthrough curves obtained with CXTFIT 2.1 and the experimental data were always negligible (Fig. 2). This was supported by MSE and the coefficient of determination (R^2) for each simulation of the observed versus predicted regression (Table 3). The nitrate and chloride breakthrough curves were symmetrical and presented Gaussian shapes, which indicated that these solute transfers occurred under physical and chemical equilibrium. The deterministic equilibrium convection–dispersion equation could thus be used to calculate transport parameters.

Table 3
Coefficient of determination (R^2) for each simulation of observed versus predicted regression and the mean squared error (MSE).

			Nitrates		Chlorides	
	Depth (cm)	Application	R^2	MSE × 10^3	R^2	MSE × 10^3
Column 1	17	1	0.95	0.44	0.99	0.08
		2	0.91	1.36	0.74	0.39
	30	1	0.72	7.59	0.97	0.24
		2	0.97	0.19	0.71	0.44
	55	1	0.97	0.22	0.99	0.10
		2	0.97	0.32	0.99	0.05
	85	1	0.97	0.08	0.87	0.45
		2	0.87	0.38	0.90	0.12
Column 2	17	1	0.91	0.44	0.98	0.14
		2	0.98	0.09	0.81	0.36
	30	1	0.94	0.31	0.71	0.66
		2	0.93	0.37	0.93	0.79
	55	1	0.93	0.55	0.99	0.11
		2	0.98	0.41	0.97	0.39
	85	1	0.98	0.11	0.97	0.15
		2	0.92	0.28	0.96	0.13

3.2. Characteristics of the nitrate and chloride breakthrough curves

The dispersivities presented an inverse pattern with depth for nitrates and chlorides. The dispersivities obtained with CXTFIT 2.1 and inferred from the nitrate breakthrough curves decreased from 8.48 and 8.79 mm at 17 cm, respectively, for the first and second applications, to 3.33 and 2.62 mm at 85 cm depth (Table 4). These nitrate dispersivity values were similar after the first and second applications for all depths. For chlorides, the dispersivities inferred from the breakthrough curves respectively increased from 0.69 and 3.1 mm at 17 cm depth for the first and second applications to 4.28 and 4.55 mm at 85 cm depth. However, at 17, 30 and 55 cm depth, respectively, the chloride dispersivities were significantly lower after the first application (0.69, 0.71 and 4.55 mm), than after the second (3.1, 1.1 and 9.35 mm). Furthermore, the nitrate dispersivity breakthrough curves were significantly (t-test < 0.05) higher at 17 and 30 cm depths than the curves plotted for chlorides, and they were lower at 55 and 85 cm depths.

The normalized C/C_0 intensities of the nitrate and chloride breakthrough curves showed the same pattern with depth for both applications (Table 4). The normalized C/C_0 intensities of the nitrate breakthrough curves presented a slight increase from 0.23 and 0.28 at 17 cm depth to 0.29 and 0.36 at 55 cm depth. At 85 cm depth, the normalized C/C_0 intensities were significantly lower (t-test < 0.05), with a value of 0.16 for both applications and good reproducibility (0.02 standard deviation). The normalized C/C_0 intensities of the chloride breakthrough curves showed a similar pattern as compared to nitrates. Indeed, at 17 cm depth, the normalized C/C_0 intensities of chlorides were slightly different for the first and second applications (0.4 and 0.22). However, at 30 and 55 cm depth, the normalized C/C_0 intensities were similar, with a value of around 0.3 and then it decreased significantly to 0.17 and 0.14 at 85 cm depth. Furthermore, at 55 and 85 cm depth, all the normalized C/C_0 intensities were statistically similar (t-test < 0.05) for nitrates and chlorides.

The nitrification kinetics influenced the pattern of the dispersivities and the normalized C/C_0 intensities for nitrates and chlorides until 55 cm depth. The normalized C/C_0 intensities were closely related to the dispersivity (Toride et al., 1995) and decreased (logically) with depth, as observed in other studies (Feder and Findeling, 2007). Dispersivity depended on various physical factors (Vanderborght et al., 2001) such as the water flow conditions (transient or steady state), the soil structure, the soil rebuild in the column (undisturbed soil or not), and the porosity. Moreover, the dispersion coefficient was not very sensitive (Tang et al., 2009). Our average dispersivity values inferred from the nitrate and chloride breakthrough curves were similar

Table 4
Average normalized C/C_0 intensities and dispersivities inferred from the nitrate and chloride breakthrough curves at four depths, for the first and the second pig manure applications, for the two C1 and C2 columns.

Depth (cm)	Normalized C/C_0 intensities				Dispersivities (mm)			
	Nitrate breakthrough curves		Chloride breakthrough curves		Nitrate breakthrough curves		Chloride breakthrough curves	
	First application	Second application	First application	Second application	First application	Second application	First application	Second application
17	0.23 (0.03)[a]	0.28 (0.04)	0.40 (0.06)	0.22 (0.07)	8.48 (0.06)	8.79 (0.07)	0.69 (0.04)	3.10 (0.02)
30	0.21 (0.01)	0.25 (0.02)	0.31 (0.02)	0.28 (0.04)	6.77 (0.24)	6.25 (0.05)	0.71 (0.02)	1.10 (0.05)
55	0.29 (0.01)	0.36 (0.05)	0.30 (0.02)	0.29 (0.06)	2.26 (0.08)	2.29 (0.09)	4.55 (0.15)	9.35 (0.05)
85	0.16 (0.02)	0.16 (0.02)	0.17 (0.03)	0.14 (0.01)	3.33 (0.04)	2.62 (0.09)	4.28 (0.18)	4.55 (0.17)

[a] The standard deviation is in brackets.

to those noted in other studies with repacked soil (Magesan et al., 2003; Vanderborght and Vereecken, 2007). This could be explained by the similar methodology and the homogeneity of the repacked soils in the column. Our average dispersivity values were an order of magnitude lower than reported in several studies with intact soil columns (Magesan et al., 2003; Prado et al., 2011). The dispersivity was generally independent of the Darcy velocity and lower for well-structured soils like ours than for weakly structured soils (Vogeler et al., 1998; Magesan et al., 2003; Vanderborght and Vereecken, 2007). The dispersivities inferred from the chloride breakthrough curves increased with depth, as observed in many studies (Vogeler et al., 1998; Vanderborght and Vereecken, 2007). In contrast, the dispersivities inferred from the nitrate breakthrough curves decreased until 55 cm depth and became statistically similar to the chloride dispersivities at 55 and 85 cm depths. This unexpected pattern could thus be explained by these kinetics of nitrate production via the nitrification process near the surface; the time step of the nitrate pulse input was delayed and longer. This effect was mitigated with depth until it disappeared at 55 and 85 cm depths.

3.3. Impact of pig manure nitrification on the soil solution

The fast and almost complete pig manure nitrification process was confirmed in the soil solution by the acidification, the low ammonium concentration and the high nitrate concentration. Mineralisation of pig manure, like other organic amendments, enhanced acidification in soil because the nitrification process produced nitrates and protons from ammonium (Paul and Clark, 1989; De Boer and Kowalchuk, 2001; Goss et al., 2013). After 28 days, the mineralized carbon rate of pig manure on this Nitisol ranged from 30 to 33% of organic carbon added (Doelsch et al., 2010). The ammonium concentrations in the soil solution were always low (0.02 to 0.1 $mg \cdot l^{-1}$) at all sampling depths and were not different between the C3 untreated column and the C1 and C2 amended columns (Fig. 3). At 17, 30, and 55 cm depths, the soil

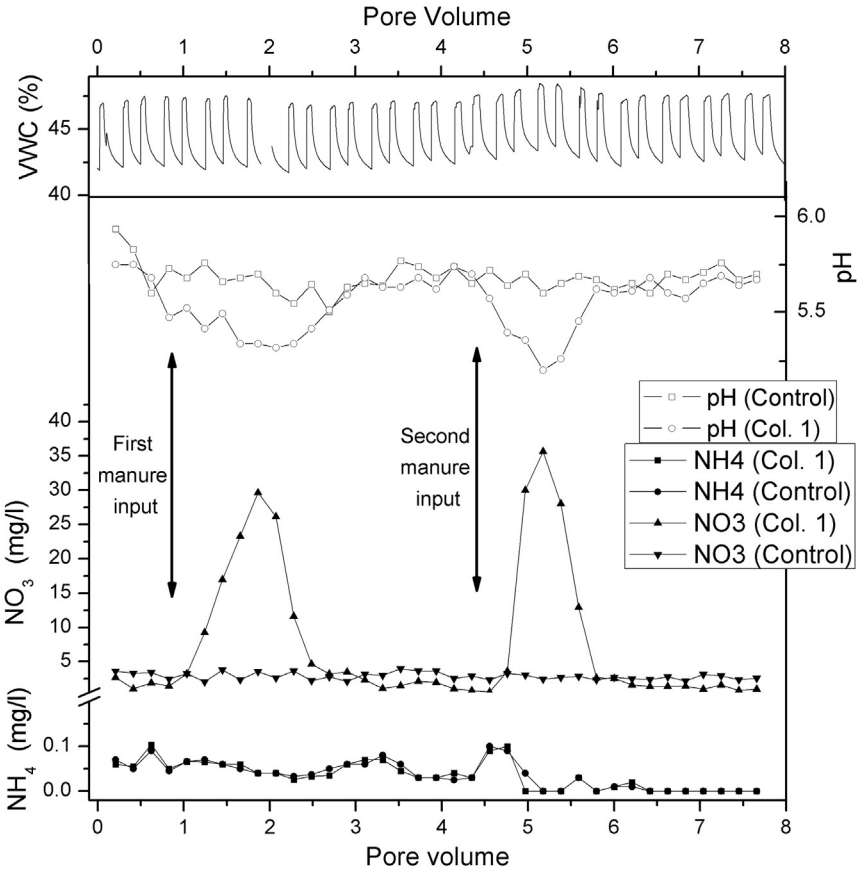

Fig. 3. At 17 cm depth for column 1 and the control column, concomitant variations in pH, and nitrate and ammonium concentrations (mg/l). On the upper part, the volumetric water content (in %) of the column 1 at 17 cm depth.

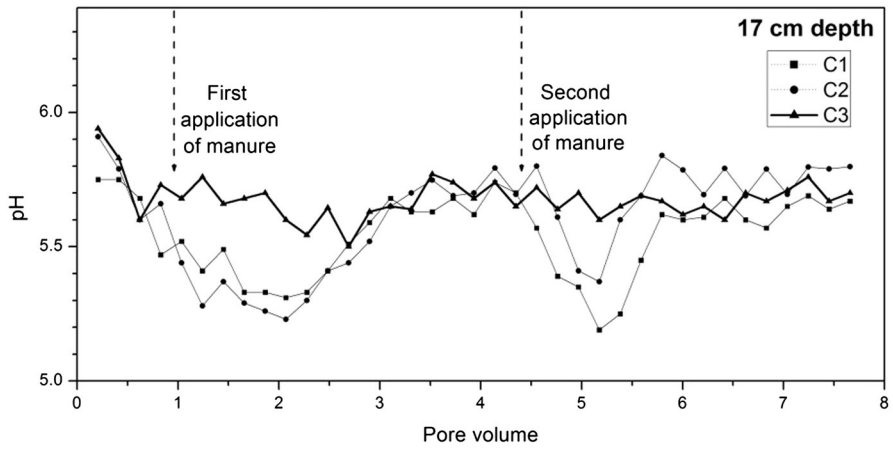
17 cm depth
C1
C2
C3
First application of manure
Second application of manure
pH
Pore volume

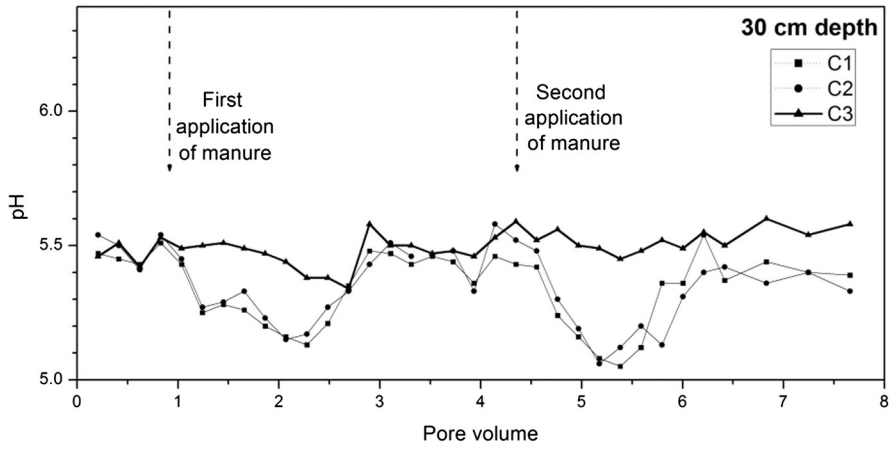
30 cm depth
C1
C2
C3
First application of manure
Second application of manure
pH
Pore volume

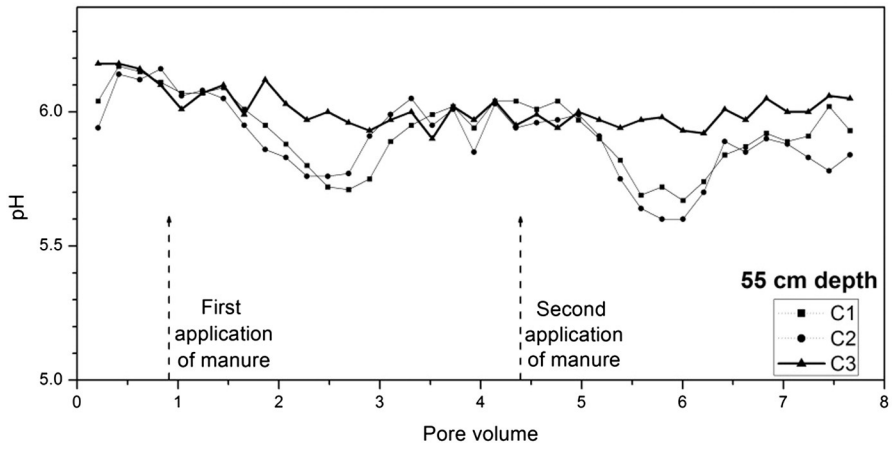
55 cm depth
C1
C2
C3
First application of manure
Second application of manure
pH
Pore volume

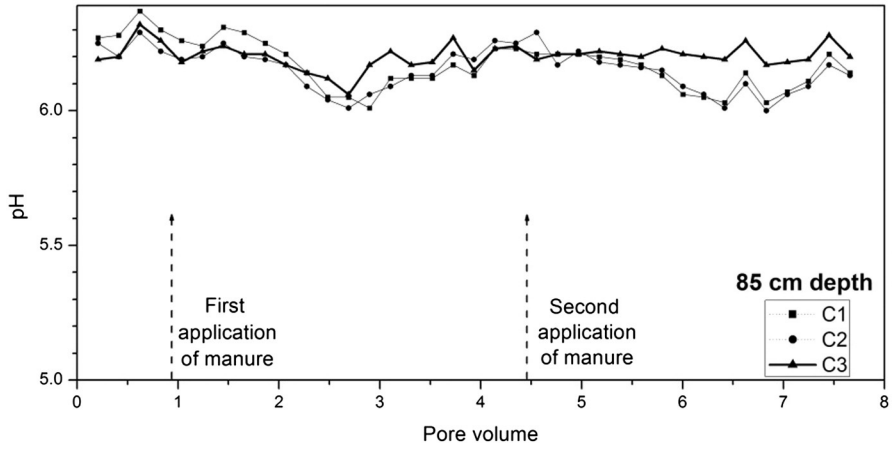
85 cm depth
C1
C2
C3
First application of manure
Second application of manure
pH
Pore volume

solution pH measured in the C1 and C2 amended columns decreased quickly from 0.2 to 0.5 units, by comparison to the C3 untreated column, after the first and the second pig manure applications, when there was a pore volume of 1.5 (Fig. 4). At 85 cm depth, the soil solution pH in C1 and C2 amended columns were not significantly different from the C3 untreated column after the first application. This acidification of the soil solution following nitrification has already been observed (Cooper, 1975; Paul and Clark, 1989; Feder and Findeling, 2007). The nitrification process generated acidification and also nitrates. The nitrate concentration in pig manure (6 mg·kg^{-1}) was insignificant by comparison with the concentration in the soil solution and the ammonium concentration in the pig manure (28,00 mg·kg^{-1}). All nitrates measured in soil solutions at the different depths came only from the pig manure nitrification process. Indeed, nitrate production via the natural mineralisation of soil organic matter should be negligible as compared to nitrate production via pig manure mineralisation during the same several day period (Cooper, 1975; Bengtsson et al., 2003; Payet et al., 2009). This was confirmed by the findings for the C3 untreated column, which showed the same baseline values for nitrate concentrations as the amended columns outside the nitrate breakthrough curves, and by the nitrate and ammonium concentrations extracted by KCl in the soils of the C1 and C2 amended columns at the end of the experiment. The pig manure nitrification process was clearly fast and almost complete in the ideal conditions of our study (Bengtsson et al., 2003; Paul and Clark, 1989): constant temperature of 25 °C, soil pH below 6, and alternating wetting–drying sequences in the surface horizon.

3.4. Retardation factors for nitrates and chlorides at the different depths

Retardation factors inferred from the breakthrough curves were significantly different for nitrates and chlorides at the outlet after the first application but not after the second. At 17, 30 and 55 cm depths, nitrate and chloride retardation factors were always statistically different (t-test < 0.05) for both applications (Fig. 5). At the outlet (85 cm depth), the mean retardation factor values for nitrates were 2.1 PV and 1.86 PV, respectively, after the first and the second applications, while they were 1.76 PV and 1.86 PV for chlorides. These retardation factors for nitrate and chloride breakthrough curves were thus significantly different (t-test < 0.05) at the outlet after the first pig manure application but not after the second. Furthermore, the retardation factors were always different for nitrates at all depths between the first and the second applications. The retardation factors for chlorides were similar for both applications, except at 30 cm depth (1.03 and 1.29, respectively after the first and the second applications).

The kinetics of nitrate production by the nitrification process and the AEC explained the high nitrate retardation factors until 55 cm depth. Several reference soil groups are able to retain anions because they have positive surface charges on their constituent minerals; these charges are either permanent or variable with pH, e.g. in highly developed soils (nitisols, ferralsols, etc.) or andosols. The presence of this AEC was the main reason to explain the retardation factors of greater than 1 for anions (Parfitt, 1978; Wong et al., 1990). However, our retardation factors for nitrates at 17 cm depth were significantly higher than in other studies. For 30 acid variable-charge subsoils like ours but collected in southeastern USA and other subtropical and tropical areas, Qafoku et al. (2000) measured retardation factors from 0.9 to 3.12 pore volumes. On an Andosol, Prado et al. (2011) measured some nitrate and bromide retardation factors from 1.5 to 2.3 pore volumes, with some ranging from 1.16 to 1.61 pore volume for nitrates and chlorides on packed and intact soil columns. At 17 cm depth, our retardation factors were 4.85 and 3.57 pore volumes after the first and the second pig manure application, respectively. The soil AEC could not solely explain these differences because our values were never significantly higher than those of other studies (Table 1). Furthermore, the differences in affinity to adsorption sites between monovalent anions, such as bromides, nitrates and chlorides, were not sufficient to explain the differences in our retardation factors (Parfitt, 1978; Katou et al., 1996). Pig manure mineralisation had to be taken into account in our study. Indeed, the nitrification process was described by first order kinetics by Mary et al. (1998), but it was dependent on many local factors such as soil humidity, temperature or soil microbiology (Bengtsson et al., 2003). The shapes of our nitrate breakthrough curves were always symmetrical (Fig. 2), which means that nitrates produced by the nitrification process corresponded mainly to a well-defined pulse input, like chlorides from the pig manure. In the conditions of our experimentation, an asymetric breakthrough curve would have revealed a physical or chemical nonequilibrium process (fluxes, adsorption). The retardation factors of the nitrate breakthrough curves at 17 cm depth were thus directly related to the time step of this pulse input and its application time. The nitrification process induced a time lag in nitrate production, and then the arrival time was shifted at 17 cm depth and deeper in the soil columns. This time lag was greater at shallow depth and the retardation factor was thus higher near the surface. The time lag gradually diminished with depth and was no longer detected beyond 55 cm depth.

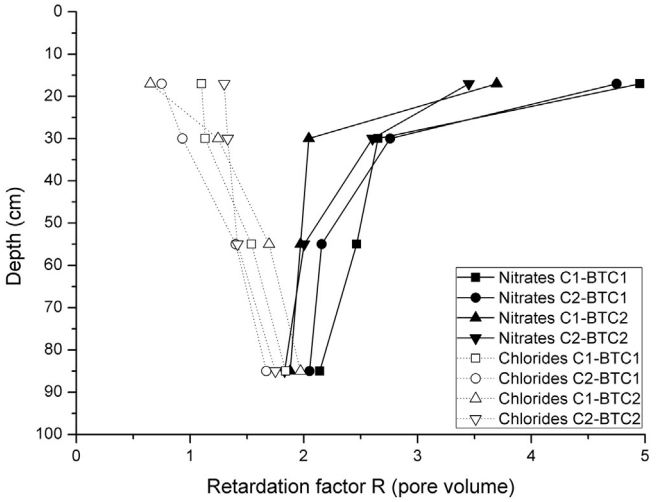

Fig. 5. Nitrate and chloride retardation factors for the C1 and C2 columns and for the first (BTC1) and the second (BTC2) pig manure applications at 17, 30, 55 and 85 cm depths. Pore volume was calculated specifically for each depth.

Pig manure nitrification modified the chemistry of the soil solution and thus the competition for anion adsorption. In our experiment, the nitrification process induced acidification of the soil solution until 55 cm depth, while the ionic strength of pig manure leaching was lower until the nitrates were produced. The increased ionic strength was directly correlated with the increase in major chemical species in solution, especially nitrates. Qafoku et al. (2000) demonstrated that anion adsorption increased when the soil pH or leaching solution concentration decreased. Katou et al. (1996) reported that the adsorption of monovalent anions such as chlorides and nitrates was directly correlated with the ionic strength of the soil solution. In our study, however, pig manure nitrification induced a delay in nitrate production and acidification. In the soil solution, the pH decreased while the ionic strength increased simultaneously with time—both of these effects were antagonistic regarding the modification of anionic adsorption. Our soil columns were then saturated at first by chloride fluxes followed by nitrates, but with some differences in pH and ionic strength; the competition for adsorption between chlorides and nitrates was not

Fig. 4. pH of the soil solution at 17, 30, 55 and 85 cm depths for C1 and C2 columns amended with pig manure, while the C3 column was the untreated control. Arrows correspond to both pig manure applications according to the applied water (pore volume) for the whole column.

synchronous. Moreover, Toner et al. (1989) and Bellini et al. (1996) showed that anion adsorption on variable-charge soils was completely reversible, indicating electrostatic retention. For Katou et al. (1996), nitrate ions have a smaller affinity to adsorption sites as chlorides and show greater penetration in the presence of chlorides i.e. higher nitrate fluxes. These modifications in the chemistry of the soil solution explained the high nitrate retardation factors and the marked decrease until the outlet, where the nitrate fluxes caught up with the chloride fluxes. Although nitrates were produced with a delay because of pig manure nitrification and, although soil has an affinity for nitrate adsorption like chlorides, nitrate fluxes caught up to the chloride fluxes at the outlet.

The AEC and kinetics of the nitrification process explained the difference in retardation factors for nitrates and chlorides until 55 cm depth. The soil solution at 17 and 30 cm depths was sampled in the A horizon, with an AEC of 0.0054 $mol_{(-)} \cdot kg^{-1}$, while the soil solution sampled at 55 and 85 cm depths corresponded to the B horizon, with an AEC of 0.009 $mol_{(-)} \cdot kg^{-1}$ (Table 1). The linear increase with depth of the chloride retardation factors could simply be explained by the higher AEC in the deeper soil horizon because the nitrification process produced nitrates but did not affect chloride production. Indeed, several studies have demonstrated the close correlation between the retardation factor for an anion and the AEC (Parfitt, 1978; Bellini et al., 1996; Qafoku et al., 2000). However, the nitrate retardation factors presented an inverse pattern and the nitrate and chloride retardation factors differed markedly near the surface and decreased until the outlet. The time step of the pulse input for nitrates was then delayed and longer than for chlorides, which induced a significant difference for the retardation factors. This difference decreased when the time lag diminished with depth and with the modification in the chemistry of soil solution, as in our columns beyond 55 cm depth. At the outlet, the nitrate and chloride retardation factors were similar and their differences were negligible because competitive adsorption on the soil between these anions counterbalanced the nitrification process.

Retardation factors inferred from the breakthrough curves increased linearly with depth for chlorides and decreased with depth for nitrates, but linearly only from 30 to 85 cm depth. To compare the retardation factors for the different sampling depths, we calculated the total pore volume for each corresponding depth: 0–17, 0–30, 0–55 and 0–85 cm. To facilitate the comparison of the first (BTC1) and second (BTC2) pig manure applications, these lag values were corrected for each application by subtracting 0.9 and 4.45 pore volumes, which respectively corresponded to the exact time of the first and second pig manure applications. Fig. 5 presents these retardation factors for the nitrate and chloride breakthrough curves as a function of the soil depth for the two amended columns (C1 and C2) and after both pig manure applications. For chlorides, the retardation factor increased linearly with depth, from 1.05 PV at 17 cm depth to 1.76 and 1.86 PV at 85 cm depth (mean slope = 0.0125; mean intercept = 0.769; R^2 ranged from 0.9 to 0.97). For nitrates, the retardation factors decreased continuously with depth, from 4.85 and 3.57 at 17 cm depth to 2.1 and 1.86 PV at 85 cm depth. This decrease was linear only from 30 cm to 85 cm depth (mean slope = −0.0097; mean intercept = 2.761; R^2 ranged from 0.82 to 0.99). The absence of chemical transformation and the constant increase in chloride adsorption in soil explained the linear increase with depth of the retardation factor for chlorides. On the contrary, the non-linear decrease with depth of the retardation factor for nitrates could be explained by several factors. First, on the surface, the nitrification process induced a delay in nitrate production, which explained the higher retardation factor at 17 cm depth. Secondly, the linear decrease in the retardation factor from 30 to 85 cm depth corresponded to a constant decrease in nitrate adsorption in soil jointly with the increase in chloride adsorption. As previously presented, the main reason was the modification in the chemistry of the soil solution and the higher affinity of chlorides for the soil.

Table 5
Mean difference between nitrate and chloride retardation factors after the first and second pig manure applications. Pore volume was calculated specifically for each depth.

Depth (cm)	Difference between the retardation factors (nitrates–chlorides)			
	First application		Second application	
17	3.80	(0.15)[a]	2.52	(0.27)
30	1.67	(0.14)	1.04	(0.32)
55	0.84	(0.22)	0.43	(0.14)
85	0.34	(0.12)	0.00	(0.13)

[a] The standard deviation is in brackets.

3.5. Differences between the two pig manure applications

Differences between the retardation factors for nitrates and chlorides decreased regularly with depth and were also significantly different between the first and second applications. Table 5 presents the mean differences between nitrate and chloride retardation factors for both columns after the first and second pig manure applications at all sampling depths. After the first application, the mean difference was 3.8 PV at 17 cm depth and decreased regularly to 0.34 PV at 85 cm depth. For the second application, the mean difference was 2.52 PV at 17 cm depth and decreased regularly to 0 PV at 85 cm depth. For each pig manure application, the differences in nitrate and chloride retardation factors were significantly (t-test < 0.05) higher near the surface at 17 cm depth than at the outlet at 85 cm depth and they were higher for the first than for the second applications. The first application of pig manure increased the microbial numbers and activities; repeated application of organic amendment improved soil biological functions (Diacono and Montemurro, 2010). Moreover, soil drying and rewetting stimulated these microbial communities (Bengtsson et al., 2003). Nitrification of the second pig manure application was then enhanced and the nitrate retardation factor was lower than for the first application (Fig. 5). This effect did not impact the chlorides, i.e. the differences in nitrate and chloride retardation factors were then also lower for the second pig manure application (Table 5).

Differences between the two pig manure applications induced differences in anion adsorption. Nitrate retardation factors for the second pig manure application were significantly lower than for the first application at all depths. The nitrification process was faster for the second application—this effect was previously observed after several organic amendment applications (Diacono and Montemurro, 2010) which stimulated microbial activity (Paul and Clark, 1989). Acidification of the soil solution and nitrates produced by the nitrification process thus occurred earlier after the second pig manure application. Moreover, the chloride dispersivity was significantly higher at 17, 30 and 55 cm depths after the second application. These modifications in the nitrification kinetics induced some modifications in pH and in the ionic strength of the soil solution, and thus in the adsorption and competition between anions (Katou et al., 1996; Qafoku et al., 2000), as observed for the first application. The differences in the nitrate and chloride retardation factors were also lower for the second than for the first application.

3.6. Environmental and agronomical impacts

Nitrates are available for a shorter time for crops and leached amounts may be greater when provided with pig manure. When soils are amended with pig manure, the nitrification process induces a delayed effect on nitrate production (Mary et al., 1998; De Boer and Kowalchuk, 2001). In the early days after manure input, nitrate contents are still very low in the soil and crops use little (Payet et al., 2009) regardless of soil types. For soils without anionic retention that were amended with pig manure, nitrates were found to begin leaching as soon as drainage occurred (Toner et al., 1989). The presence of other anions, except chloride, brought simultaneously with the amendment or

present in the soil solution, did not modify the interaction of nitrates with the soil solid phase and therefore did not change the nitrate fluxes. However, in soils with AEC and with similar water fluxes, crops can theoretically take up nitrates longer because they can be sorbed on soil particles (Parfitt, 1978; Warren and Kihanda, 2001; Payet et al., 2009). However, in these soils, our results showed that the transfer of nitrates from manure increased with depth due to the partition coefficient between nitrates and chlorides (Katou et al., 1996) and to the nitrification of manure, which delayed the nitrate input. Thus, for nitrates derived from manure mineralization, the first consequence was that they were available for a shorter time for crops on these soils than they would have been if they were already in nitrate form. Correspondingly, nitrate leaching below the root depth may be greater with these amendments for similar water flow and adsorption capacities. This result was counter-intuitive because the mineralization of organic matter induced a slower and more constant supply of elements to the soil. However, this kinetic effect was counterbalanced by the earlier adsorption of chlorides at anionic exchange sites combined with a selectivity coefficient to the detriment of nitrates.

4. Conclusions

After pig manure amendment in a Nitisol, nitrate transfers were highly influenced by the mineralization of this application and the kinetics of ammonium nitrification. In this study, we noted that this pig manure nitrification modified the pH and ionic strength of the soil solution. These chemical modifications induced significant differences in nitrate and chloride adsorptions and transfers until 85 cm depth. Nitrate and chloride breakthrough curves were asynchronous, but the chloride retardation factors increased linearly with depth, while those of nitrates decreased. Then the nitrate fluxes caught up with the chloride fluxes at the outlet of the columns. The earlier chloride adsorption at anionic exchange sites, combined with a selectivity coefficient to the detriment of nitrates, counterbalanced the delay in nitrate production due to the kinetic mineralisation of pig manure.

These original physicochemical conditions are more representative of field conditions. Moreover, nitrate and chloride transfers were also significantly different between the first and the second applications. Repeated application of pig manure improved the soil biological functions and enhanced nitrification and nitrate production but did not affect chlorides.

Organic fertilizers such as pig manure are attractive due to their capacity to gradually supply nutrients; nitrates should be retained on variable-charge soils and available longer for crops. The agronomical and environmental impacts included greater nitrate leaching below the root depth, while nitrates were also available to crops for a shorter time. These unexpected results should be taken into account to accurately assess the crop nutrition and the nitrate leaching risk in these soils.

Acknowledgements

This work was financially supported by ADEME under project no. 0475C0013 and the Region of Réunion and the European Agricultural Guidance and Guarantee Fund (EAGGF). The authors thank G. Moussard for his contribution to this study and the plant, soil and water analysis laboratory staff for efficient assistance ("Analyses" support unit 49, CIRAD).

References

Alary, K., Babre, D., Caner, L., Feder, F., Szwarc, M., Naudan, M., Bourgeon, G., 2013. Pretreatment of soil samples rich in short-range-order minerals before particle-size analysis by the pipette method. Pedosphere 23 (1), 20–28.

Bellini, G., Sumner, M.E., Radcliffe, D.E., Qafoku, N.P., 1996. Anion transport through columns of highly weathered acid soil: adsorption and retardation. Soil Sci. Soc. Am. J. 60, 132–137.

Bengtsson, G., Bengtson, P., Mansson, K.F., 2003. Gross nitrogen mineralization-, immobilization-, and nitrification rates as a function of soil C/N ratio and microbial activity. Soil Biol. Biochem. 35, 143–154.

Cahn, M.D., Bouldin, D.R., Cravo, M.S., Bowen, W.T., 1993. Cation and nitrate leaching in an Oxisol of the Brazilian Amazon. Agron. J. 85 (2), 334–340.

Cooper, J.E., 1975. Nitrification in soils incubated with pig slurry. Soil Biol. Biochem. 7, 119–124.

De Boer, W., Kowalchuk, G.A., 2001. Nitrification in acid soils: micro-organisms and mechanisms. Soil Biol. Biochem. 33, 853–866.

Diacono, M., Montemurro, F., 2010. Long-term effects of organic amendments on soil fertility. A review. Agron. Sustain. Dev. 30, 401–422.

Doelsch, E., Masion, A., Moussard, G., Chevassus-Rosset, C., Wojciechowicz, O., 2010. Impact of pig slurry and green waste compost application on heavy metal exchangeable fractions in tropical soils. Geoderma 155 (3–4), 390–400.

Feder, F., Findeling, A., 2007. Retention and leaching of nitrate and chloride in an andic soil after pig manure amendment. Eur. J. Soil Sci. 58, 393–404.

Feder, F., 2013. Soil map update: procedure and problems encountered for the island of Réunion. Catena 110, 215–224.

Gillman, G.P., Sumpter, E.A., 1986. Modification to the compulsive exchange method for measuring exchange characteristics of soils. Soil Res. 24 (1), 61–66.

Goss, M.J., Tubeileh, A., Goorahoo, D., 2013. A review of the use of organic amendments and the risk to human health. In: Sparks, D.L. (Ed.), Advances in Agronomy. Academic Press, Elsevier Inc., pp. 275–380.

IUSS Working Group WRB, 2007. World reference base for soil resources 2006, first update 2007. World Soil Resources Reports No. 103FAO, Rome.

Katou, H., Clothier, B.E., Green, S.R., 1996. Anion transport involving competitive adsorption during transient water flow in an Andisol. Soil Sci. Soc. Am. J. 60, 1368–1375.

Legros, S., Doelsch, E., Feder, F., Moussard, G., Sansoulet, J., Gaudet, J.-P., Rigaud, S., Basile Doelsch, I., Saint Macary, H., Bottero, J.-Y., 2013. Fate and behaviour of Cu and Zn from pig slurry spreading in a tropical water–soil–plant system. Agric. Ecosyst. Environ. 164, 70–79.

Magesan, G.N., Vogeler, I., Clothier, B.E., Green, S.R., Lee, R., 2003. Solute movement through an allophanic soil. J. Environ. Qual. 32 (6), 2325–2333.

Mary, B., Recous, S., Robin, D., 1998. A model for calculating nitrogen fluxes in soil using ^{15}N tracing. Soil Biol. Biochem. 30 (14), 1963–1979.

Paul, E.A., Clark, F.E., 1989. Soil Microbiology and Biochemistry. Academic Press, San Diego.

Payet, N., Findeling, A., Chopart, J.L., Feder, F., Nicolini, E., Saint Macary, H., Vauclin, M., 2009. Modelling the fate of nitrogen following pig slurry application on a tropical cropped acid soil on the island of Réunion (France). Agric. Ecosyst. Environ. 134, 218–233.

Parfitt, R.L., 1978. Anion adsorption by soils and soil materials. Adv. Agron. 30 (1).

Prado, B., Duwig, C., Etchevers, J., Gaudet, J.-P., Vauclin, M., 2011. Nitrate fate in a Mexican Andosol: is it affected by preferential flow? Agric. Water Manag. 98 (9), 1441–1450.

Qafoku, N.P., Sumner, M.E., Radcliffe, D.E., 2000. Anion transport in columns of variable charge subsoils: nitrate and chloride. J. Environ. Qual. 29 (2), 484–493.

Seyfried, M.S., Rao, P.S.C., 1987. Solute transport in undisturbed columns of an aggregated tropical soil: preferential flow effects. Soil Sci. Soc. Am. J. 51, 1434–1444.

Tang, G., Mayes, M.A., Parker, J.C., Yin, X.L., Watson, D.B., Jardine, P.M., 2009. Improving parameter estimation for column experiments by multi-model evaluation and comparison. J. Hydrol. 376 (3–4), 567–578.

Toner, C.V., Sparks, D.L., Carski, T.H., 1989. Anion exchange chemistry of middle Atlantic soils: charge properties and nitrate retention kinetics. Soil Sci. Soc. Am. J. 53, 1061–1067.

Toride, N., Leij, F.J., Genuchten, M.Th., 1995. The CXTFIT code for estimating transport parameters from laboratory or field tracer experiments. Version 2.0. Research Report No. 137. U. S. Salinity Laboratory, USDA, ARS, Riverside, CA.

Vanderborght, J., Vanclooster, M., Timmerman, A., Seuntjens, P., Mallants, D., Kim, D.-J., Jacques, D., Hubrechts, L., Gonzales, C., Feyen, J., Diels, J., Deckers, J., 2001. Overview of inert tracer experiments in key Belgian soil types: relation between transport and soil morphological and hydraulic properties. Water Resour. Res. 37, 2873–2888.

Vanderborght, J., Vereecken, H., 2007. Review of dispersivities for transport modeling in soils. Vadose Zone J. 6, 29–52.

Van Wambeke, A., 1992. Soils of the Tropics: Properties and Appraisal. McGraw Hill.

Vogeler, I., Scotter, D.R., Clothier, B.E., Tillman, R.W., 1998. Anion transport through intact soil columns during intermittent unsaturated flow. Soil Tillage Res. 45 (1), 147–160.

Warren, G.P., Kihanda, F.M., 2001. Nitrate leaching and adsorption in a Kenyan nitisol. Soil Use Manag. 17 (4), 222–228.

Wassenaar, T., Doelsch, E., Feder, F., Guerrin, F., Paillat, J.-M., Thuriès, L., Saint Macary, H., 2014. Returning Organic Residues to Agricultural Land (RORAL) — fuelling the Follow the Technology approach. Agric. Syst. 124, 60–69.

Wong, M.T.F., Hughes, R., Rowell, D.L., 1990. Retarded leaching of nitrate in acid soils from the tropics. Measurement of the effective anion exchange capacity. J. Soil Sci. 41, 655–663.

European Journal of Soil Science, April 2007, **58,** 393–404 doi: 10.1111/j.1365-2389.2006.00885.x

Retention and leaching of nitrate and chloride in an andic soil after pig manure amendment

F. FEDER[a] & A. FINDELING[b]

[a]*CIRAD (centre de coopération internationale en recherche agronomique pour le développement), research unit ''Environmental Risks of Recycling'', station de la Bretagne, BP 20, F-97408 Saint-Denis messagerie Cedex, Réunion, and* [b]*CIRAD (centre de coopération internationale en recherche agronomique pour le développement), research unit ''Environmental Risks of Recycling'', TA 70/01 - Avenue Agropolis, F-34398 Montpellier Cedex 5, France*

Summary

In Réunion, crop fields are commonly amended with nitrogen-rich pig manure, which is currently a major source of groundwater pollution. We constructed three large andic soil columns in the laboratory to study the impacts of pig manure amendment on (i) global organic carbon and nitrogen decay in the soil, (ii) nitrate and chloride retention in the soil, and (iii) lags in nitrate and chloride breakthrough. One untreated column served as a control, while the two others were amended with pig manure. Over a 15-month period, the three columns received water applications that matched rainfall under the climatic conditions of Réunion. Carbon and nitrogen balances were determined. The soil moisture regimes and soil-solution compositions were monitored (at 7.5, 15, 35 and 100 cm depth) to determine carbon and nitrogen transformations and NO_3^- and Cl^- transfers. The soil organic matter mineralization rate was low, i.e. 5.1 mg C-CO_2 day^{-1} kg^{-1} soil in the A horizon and 4.2 mg C-CO_2 day^{-1} kg^{-1} soil in the andic B horizon. The rate was higher in the manure-amended columns, suggesting a priming effect. Rapid manure nitrification led to acidification of the surface soil solution. Nitrate and Cl^- flux patterns differed at the column outlet and their interactions with the soil exchange capacity differed in the two soil horizons. Leaching fluxes highlighted an interaction between anions and soil solid phases—a lag of 1.5 to 2.5 pore volumes was observed in the breakthrough curves. About 85% (at 30–40 and 90–100 cm depth) of mineral nitrogen was adsorbed on soil solids. These results highlighted the specific properties of andic soils under tropical conditions and the complexity of assessing nitrate contamination of groundwater after pig manure amendment.

Résumé

Sur l'île de la Réunion, les épandages de lisiers de porc, très riches en azote sont courants et induisent actuellement des risques élevés de pollution. Pour étudier les impacts de ces apports de lisier, trois larges colonnes d'un cambisol andique ont été reconstituées au laboratoire. Les objectifs de ce travail sont (i) de mesurer les taux de minéralisation du carbone et de l'azote dans le sol amendé par un lisier, (ii) d'évaluer la rétention des nitrates et des chlorures et (iii) d'analyser les différences dans les courbes de percée de ces deux anions. Une colonne a servi de témoin, les deux autres ont reçu un apport de lisier. Pendant quinze mois, sur les trois colonnes, les apports d'eau ont simulé les conditions pluviométriques de l'île. Des bilans de carbone et d'azote ont été réalisés entre le début et la fin de l'expérimentation. Le régime hydrique et la composition de la solution du sol ont été suivi à plusieurs profondeurs (7.5, 15, 35 et 100 cm) afin de déterminer les transformations du carbone et de l'azote et les transferts de NO_3^- et Cl^-. Les taux de minéralisation de la matière organique du sol sont faibles : 5,1 mg de C-CO_2 d^{-1} kg^{-1} sol dans l'horizon A et 4,2 mg de C-CO_2 d^{-1} kg^{-1} sol dans l'horizon B andique. Dans les colonnes ayant reçues le lisier ce taux est supérieur au témoin, suggérant un «priming effect». La rapide nitrification du lisier a entraîné une acidification de la solution du sol dans les horizons de surface. Les flux de NO_3^- et de Cl^- à l'exutoire des colonnes ont présenté des comportements distincts ; l'interaction de chacun des anions avec la capacité d'échange anionique du sol diffère selon les deux horizons de sols. Les interactions

Correspondence: F. Feder. E-mail: frederic.feder@cirad.fr
Received 30 May 2006; revised version accepted 30 October 2006

entre la solution du sol et la phase solide entraîne un retard des courbes de percée de NO_3^- et de Cl^- qui atteint 1,5 à 2,5 volumes de pores. 84,7 % (à 30–40 cm) et 85.1 % (à 90–100 cm) de l'azote minéral a été adsorbé sur la phase solide du sol. Ces résultats montrent le comportement atypique des sols andiques après un épandage de lisiers de porc dans un contexte tropical et la difficulté d'estimer les risques de pollution des nappes suite à la lixiviation de NO_3^-.

Introduction

Management of organic waste, especially pig manure, from livestock farms is a major challenge on the island of Réunion. Nitrogen (N) volumes derived from organic waste were estimated at 2325 t year^{-1}, with about 17% of the island (43 692 ha) devoted to agriculture, but the distribution of these wastes was found to be highly imbalanced (Aubry *et al*., 2006). Livestock manure is commonly recycled by spreading it on crop fields, but the area that can be amended in this way is limited in island environments and problems of nitrate (NO_3^-) pollution of groundwater may arise (Payet, 2005). In Réunion, andic soils cover about 70% of the arable land area and organic matter (OM) is mainly applied on this type of soil.

Little is known about the impact of organic amendment on Andosols (Dahlgren *et al*., 2004). Mineralization of organic matter and subsequent solute transfers are complicated to study due to the atypical physicochemical properties of Andosols (Shoji *et al*., 1993). Morvan *et al*. (2003) showed that mineralization rates of organic amendments were low in Andosols. Complexes formed with OM and poorly crystallized minerals (allophanes, imogolites...) have a protective effect on OM biodegradation in these soils (Aran *et al*., 2001; Boudot, 1992; Huygens *et al*., 2005; Legay & Schaefer, 1984). Also, the microstructure of Andosol surface horizons is an adverse factor for enzymatic reactions with organic N compounds (Saito, 1990). Interactions between solutes and the solid phase of a soil with a marked anionic exchange capacity (AEC) were addressed by Madeira *et al*. (2003). They showed that AEC is generally greater in the B horizon than in the A horizon, and they also found that AEC increases with the oxalate-extractable Fe and Al contents and decreases with the soil organic matter content. The AEC can induce anion retention and cause a lag in the breakthrough curves for soilborne anions, as demonstrated by Ryan *et al*. (2001) and Katou *et al*. (1996). Lehman *et al*. (2004) highlighted the adsorption of large quantities of NO_3^- (300–400 g N kg^{-1} soil) on a soil. They emphasized the importance of nitrogen retention in determining the potential of nitrate contamination of groundwater.

This study was aimed at assessing leaching hazard in an andic soil after pig manure amendment, by quantifying: (i) global organic carbon and nitrogen decay in the soil, (ii) lags in nitrate and chloride breakthrough curves, and (iii) nitrate and chloride retention in the soil. The strategy adopted was to work in laboratory conditions to control water and solute fluxes accurately and to circumvent the natural variability of soil properties. The experimental layout designed for this purpose consisted of three instrumented soil columns. The columns were constructed so as to simulate *in situ* hydraulic properties and realistic mineralization rates. Two columns were amended with pig manure and the remaining column was used as the untreated reference. The columns were maintained under controlled climatic conditions.

Materials and Methods

Study site at the Colimaçons research station in Réunion

Réunion is an island located 700 km east of Madagascar in the southern Indian Ocean region. The main peak of this relatively recent volcanic island (Piton des Neiges, 3070 m ASL) emerged 3 million years ago. The Colimaçons research station is located on the western slope of Piton des Neiges at 800 m ASL (21°07′47S; 55°18′19E). Mean annual rainfall at the station is 1600 mm, with a mean annual temperature of 19°C.

Soil studied

The soil studied at the Colimaçons research station was located in the middle of a toposequence in which Andosols prevail (Feder *et al*., 2006). Table 1 gives the physicochemical characteristics of this soil. It was classified as an andic Cambisol, which included: (i) a surface A horizon (0–40 cm) altered to a shallow depth (< 50 cm) by anthropedogenic processes, and (ii) an andic B horizon (40–200 cm). Triplicate 100 cm^3 samples of undisturbed soil were collected in the field (0–5, 5–10, 10–20 ... 90–100 and 100–110 cm) for physical analysis. The saturated hydraulic conductivity K_s (m s^{-1}) of the soil samples was measured using a permeameter. Gravimetric analyses were conducted to determine the soil bulk density.

Soil column construction

We constructed three identical soil columns, i.e. C1, C2, and C3, in a 0.375 m dia. × 1 m long PVC tube. The bottom of each column was closed with a plexiglass plate that was slightly sloped so as to channel drained water towards the outlet. The A horizon was constructed with two distinct soil layers (0–20 and 20–40 cm) in order to take slight differences in OM contents and bulk densities into account. The B horizon was the 40–100 cm layer in all three columns. Soil was collected at the Colimaçons research station, roughly sieved (5 mm mesh) without drying. The three layers were constructed in columns C1, C2 and C3, while maintaining the soil bulk densities measured *in situ*. Columns C1 and C2 were used to assess the impact of manure amendment of the soil, while C3

Table 1 Physicochemical characteristics and organic matter content of the initial soil

		A horizon		B horizon
		0–20 cm	20–40 cm	40–100 cm
Bulk density	/kg dm^{-3}	0.90	0.80	0.85
Sat. water, content, θ_s	/m^3 m^{-3}	0.67	0.70	0.69
Water conductivity, K_s:	/m s^{-1}	2.1×10^{-5}	4.4×10^{-6}	5.5×10^{-7}
– measured *in situ*		8.2×10^{-7} for 0–100 cm		
– calculated, in the columns		4.7×10^{-7} (C1) and 4.0×10^{-7} (C3) for 0–100 cm		
Clay fraction	/g kg^{-1}	365	384	213
Soil color moist (Munsell's chart)		10 YR 3/2	10 YR 3/2	7.5 YR 5/6
pH_{Water}		5.4	5.6	6.2
pH_{KCl}		4.2	5.0	5.4
pH_{NaF}		9.4	9.8	10.0
Organic matter	/g kg^{-1}	68.6	56.0	29.7
Total C	/g kg^{-1}	39.8	32.5	17.2
Total N	/g kg^{-1}	3.79	3.09	1.51
C:N ratio		10.5	10.5	11.4
CEC	/$cmol_{(+)}$ kg^{-1}	26.94	18.57	17.27
AEC	/$cmol_{(-)}$ kg^{-1}	0.68		1.20
$Al_{ox.} + ½ Fe_{ox.}$	/%	2.3	1.8	3.7
$Si_{ox.}$	/%	0.4	0.3	1.3
$Al_{py.} / Al_{ox.}$	/%	3.05	2.15	1.3
P retention	/%	95.6	97.6	99.1

was the untreated control. The C1, C2 and C3 soils had not been cropped, thus avoiding bias from crop cover and enabling us to focus solely on evaluating NO_3^- leaching risks.

Water and manure inputs

The columns were initially irrigated from 10 June 2003 to 25 June 2003 (150 mm daily on average) in order to homogenize the soil chemical profiles and permit pore restructuring, thus limiting sieving artifacts (hydraulic properties and mineralization rates). On 2 July 2003, 2 litres of manure was applied on the surface of C1 and C2, while the C3 control remained untreated. This dosage was calculated to be equivalent to the application of 180 m^3 ha^{-1} of manure containing 218 kg of total N, which is typical of manure spreading practices in Réunion (Aubry *et al*., 2006; Payet, 2005). The C3 control received 16.3 mm of water, which was equivalent to the amount of moisture contained in the manure dose.

After manure amendment, C1, C2, and C3 were irrigated with identical amounts of water during three phases (Table 2). Phase 1 corresponded to a typical annual rainfall level, with a distribution representative of cyclone periods. Phase 2 was representative of dry climatic periods, while phase 3 was representative of wet periods.

Soil column sampling and measurement

The columns were equipped with instruments to monitor water and solute contents and fluxes. Time domain reflectometry (TDR) probes (CS616, Campbell Scientific) were set at 15, 35 and 95 cm depth to measure moisture in the three soil columns. Tipping bucket raingauges were placed at the outlet of one column per treatment, i.e. C1 and C3, and used as limnigraphs (ARG100, Campbell Scientific) to assess drainage flow. All of these instruments were connected to a datalogger (CR10X-2M, Campbell Scientific) that recorded measurements on a 10-minute basis from 1 July 2003 to 2 October 2003 (measurement period). We placed a tray near the soil columns to estimate the extent of evaporation from C1, C2 and C3 from gravimetric measurements.

The C1, C2 and C3 soil solutions were collected in duplicate from each column with Rhizon soil-solution microsamplers (Rhizosphere Research Products, The Netherlands) that were set at 7.5, 15 and 35 cm depth. These 70 ml samples were obtained by applying a partial vacuum to each microsampler a few hours after each soil column water application. From 2 July 2003 to 14 July 2003 and 6 April 2004 to 23 April 2004, the soil solution could not be sampled with the microsamplers due to the unsuitable water potential. Drainage water was, however, sampled at the column outlets after each watering.

Soil analysis

After construction of columns C1, C2 and C3, we performed initial soil analyses on samples collected from the 0–20, 20–40 and 40–100 cm layers. The final soil analyses (at the end of the

Table 2 Three water application phases for the C1, C2 and C3 soil columns during the study

	Date	Water application conditions	Total /mm
phase 1	2/7/2003 to 4/2/2004	12×10 mm d^{-1} 3/7/2003 to 14/7/2003 1×150 mm d^{-1} 15/7/2003 5×10 mm d^{-1} 16/7/2003 to 28/7/2003 1×150 mm d^{-1} 29/7/2003 1×10 mm d^{-1} 30/7/2003 20×50 mm d^{-1} 31/7/2003 to 4/2/2004	1496[a]
phase 2	5/2/2004 to 5/4/2004	(drying)	0
phase 3	6/4/2004 to 22/9/2004	67×50 mm d^{-1} 5 water applications every 2 weeks	3350
phases 1 + 2 + 3	2/7/2003 to 22/9/2004		4846

[a]C1 and C2 benefited from a 16 mm water supplement derived from the manure application on 2/7/2003. An equivalent amount of water was thus applied to C3 on the same day.

study) were performed on samples obtained at the following depths: 0–2.5, 2.5–5, 5–7.5, 7.5–10, 10–20, 20–30, …, 80–90 and 90–100 cm. Total C and total N of the initial and final soils were determined by dry combustion with an element analyser (Thermoquest NC2100 Soil). We measured the cation exchange capacity (CEC) by the ammonium acetate (pH 7) method. The pH_{water} and pH_{KCl} of the initial and final soils were measured according to the NF ISO 10390 standard at a soil/water volume ratio of 1:5. The N_{min} content of the final soil was measured in solution by KCl (1 M) extraction at a soil/water volume ratio of 1:5 and assayed by continuous flow colorimetry (Alliance Instruments). We used the procedure described by USDA-NRCS (2004) to measure (only in the initial soil) the pH_{NaF} and the elements Al, Si and Fe extracted by oxalate (M_{ox}) and pyrophosphate (M_{py}). Extractable Al, Si and Fe were assayed by inductively coupled plasma-atomic emission spectrometry (ICP-AES, Varian Vista spectrometer equipped with a coupled-charge detector device). The AEC of the initial soil was measured using the method described by Gillman & Sumpter (1986). Phosphorus retention was determined by the method of Blakemore *et al*. (1987).

Soil-solution analysis

All soil-solution samples were filtered at 0.45 μm and divided into three aliquots. Immediately after sampling, the first untreated aliquot was used for the pH and electrical conductivity (EC) analyses. The pH was measured with an ISFET electrode (Senstron, Hot-line), whilst EC was measured with a standard conductivity cell (WTW, TetraCon 325), and the temperature was corrected to 25°C. The two other aliquots were maintained at 4°C. The second aliquot was acidified with HNO_3 (suprapure) in preparation for assaying the main elements by ICP-AES spectrometry (Varian Vista). The third aliquot was used to quantify $N\text{-}NO_3^-$ and $N\text{-}NH_4^+$ by continuous flux colorimetry (Alliance Instruments).

A mean water sample from the top of the column was obtained by cumulation of 5-ml aliquots that were collected systematically at each water application. The soil-solution analysis procedure was also used to analyse three of these mean water samples during the study.

Manure analysis

Table 3 gives the physical and chemical characteristics of the manure, which came from a small farrow-to-finish swine production farm with a herd of around 10 sows. The manure pH and EC measurements were done in the same way and with the same instrumentation as for the soil solutions. The $N\text{-}NH_4^+$ contents were measured immediately using Quantofix test sticks. Total C and total N were determined by the Dumas method with an element analyser (Thermoquest NC2100 Soil). Chloride was assayed on the soluble fraction, after 0.45 μm filtration, by ICP-AES spectrometry (Varian Vista). Following manure amendment of C1 and C2, the C contents corresponded to 1.5% of the initial contents in the A horizon and the N contents corresponded to 2.3% of the initial contents.

Results

Hydraulic patterns of the columns

We checked whether the experimental setup would closely reproduce flows that occur in field soil by calculating the hydraulic

Table 3 Physicochemical characteristics and composition of pig manure and water applied to the soil columns (means shown for water)

		Pig manure	Water
Dry matter	/g kg^{-1}	52.5	–
Density	/kg dm^{-3}	1.01	1.00
pH		7.6	7.6
EC	/mS cm^{-1}	14.2	0.09
Total C	/g l^{-1}	18.0	–
Total N	/g l^{-1}	2.47	–
C:N ratio		7.29	–
$[NO_3^-]$	/g l^{-1} ($N\text{-}NO_3^-$)	0.00	3.43×10^{-1}
$[NH_4^+]$	/g l^{-1} ($N\text{-}NH_4^+$)	1.70	5.70×10^{-2}
$[Cl^-]$	/g l^{-1}	1.40	3.93×10^{-3}

conductivity of the reconstructed soil and the soil moisture regimes of the three soil columns from 2 July 2003 to 2 October 2003. Our conclusions were: (i) the hydraulic properties of C1, C2 and C3 were close to those of *in situ* soil (Table 1), and (ii) C1, C2 and C3 had similar soil moisture regimes (Figure 1). These soil columns could thus accurately replicate the behaviour of *in situ* soil and C1, C2 and C3 could be legitimately compared. Moreover, the drainage flow estimations—which in turn were used to assess solute leaching fluxes—were reliable since the water budget terms were efficiently controlled.

Hydraulic conductivity. The saturated hydraulic conductivity was calculated for the whole columns by Darcy's law on the basis of a hypothetical saturated flow regime. This calculation gave very close values for C1 and C3, i.e. $K_s = 4.7 \times 10^{-7}$ m s^{-1} for C1 and 4.0×10^{-7} m s^{-1} for C3. These calculations were in line with the *in situ* measurements recorded with a permeameter at saturation, where the B horizon (40–100 cm) was found to hamper hydraulic conductivity to the greatest extent (Table 1).

Soil water content. The soil moisture regimes were similar for C1, C2 and C3 throughout the measurement period (Figure 1). The TDR probes indicated almost saturated volumetric soil moisture contents, θ (m^3 m^{-3}). Differences between C1, C2 and C3 were minor ($\Delta\ \theta < 0.03$ m^3 m^{-3}) and close to the measurement error. Moisture contents paralleled the water application patterns. The variations were greatest on the surface where the wetting and drying cycles were most marked. The total soil water content of each column remained close to saturation (around 690 mm). Total soil water content variations ranged from 30 to 50 mm, for a relative deviation of less than 7%.

Water budget and drainage. Drainage flow was calculated on the basis of the mass conservation law applied to water in the soil columns:

$$\Delta\ W_R = W_A - E_V - W_{SA} - D_R \qquad (1)$$

with $\Delta\ W_R$ representing the variation in the total soil water content (mm), W_A is water application (mm), E_V evaporation (mm), W_{SA} water sampling (mm), and D_R drainage (mm).

The applied water volumes (W_A) are given in Table 2. The water sample (W_{SA}) quantity was 0.6 mm per water application. Evaporation (E_V) was estimated to be 0.8 mm day^{-1}. We also checked the consistency of the $\Delta\ W_R$ calculation by comparing the calculated drainage flow rate with rates measured by the limnigraphs throughout the measurement period (Figure 2) and found that the difference between the calculated and measured drainages was consistent with the water-loss fraction. Figure 2 shows that these water losses were moderate, i.e. the mean loss for C1 and C3 was 27 mm throughout the measurement period (4% of the cumulative drainage). The peaks noted at 150-mm water application (15 and 29 July 2003) were due to a poor TDR-probe estimation of total soil water

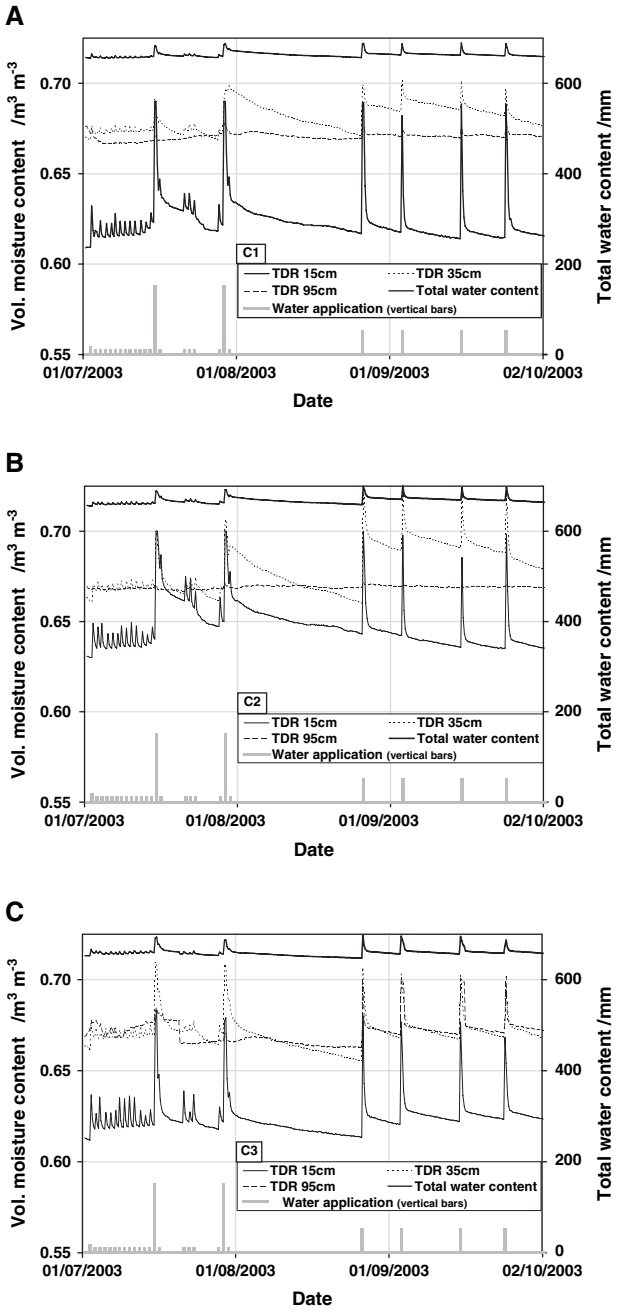

Figure 1 Variations in volumetric soil moisture content and total water content in C1, C2 and C3.

contents since the probes did not take into account the water layer that temporarily formed on the soil surface.

Drainage flow rates were calculated during the 1 July 2003 to 2 October 2003 period on the basis of the mass conservation law. After 2 October 2003, we considered that total soil water content variations were negligible. This hypothesis was confirmed by the drainage measurements (Figure 2). The water budget terms for C1, C2 and C3 were very similar for all experiments conducted from 1 July 2003 to 22 September 2004. For a total application of

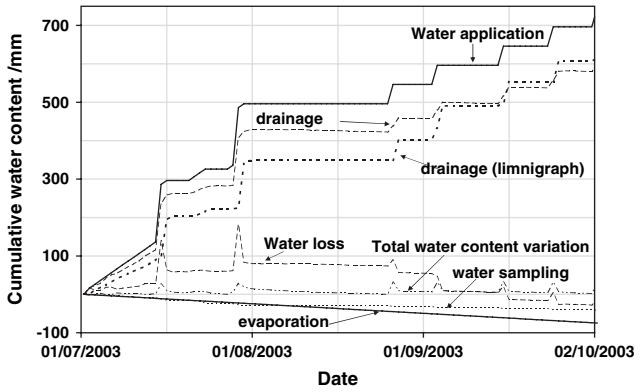

Figure 2 Verification of the water budget throughout the measurement period (results shown for C1).

4846 mm, the columns drained 4390 mm of water on average (91% of the applied amount), while 100 mm (2% of the applied amount) was sampled and evaporation accounted for 360 mm (7% of the applied amount).

Organic carbon and nitrogen dynamics

Mineralization conditions. We checked whether the experimental setup would reproduce realistic soil mineralization conditions by considering the untreated C3 column. The average mineralization rate was calculated in the A horizon of C3 from total C and N contents (Table 4), which provided a mineralization rate of 5.0 mg C-CO_2 day^{-1} kg^{-1} soil. This value was in line with the results of Morvan *et al.* (2003), who measured a mineralization rate of 5.1 mg C-CO_2 day^{-1} kg^{-1} soil on average in the A horizon of the same soil. We considered that mineral nitrogen production in the columns was thus representative of *in situ* conditions.

Organic carbon and nitrogen decay in the soil. Total C and N variation patterns indicated that there were substantial losses from C1, C2 and C3, i.e. 10.9% (for C3) and 11.6% (mean for C1 and C2) loss of the initial C content and 4.3% (for C3) and 7.1% (mean for C1 and C2) loss of the initial N content.

The total C loss was similar in A and B horizons of C3, i.e. 10.8 and 11%. Total C losses from the A horizon of C1 and C2 were greater in comparison to C3: 186.8 –147.8 = 39 g more (absolute value), which was close to the 36 g provided by the manure application (Table 4).

In the A horizon of C3, the net total N loss was almost nil (3.7×10^{-3} g N kg^{-1} soil). In the B horizon of C3, the total N loss was similar to that of total C (10.8% of the initial amount). Total N losses from the A horizon of C1 and C2 were greater and more significant than those noted in C3 (0.21 g N kg^{-1} soil). The absolute deviation between these losses and those of C3 (0.206 g of total N kg^{-1} soil, i.e. 7.75 g for the A horizon) was greater than the quantity derived from the manure (4.94 g of total N). However, total N losses from the B horizon of C1 and C2 were less for C3.

Table 4 Total carbon and nitrogen contents in the control soil column and the two manure-amended columns at the beginning (2 July 2003) and end (22 November 2004) of the study

Soil horizon		A		B	
Depth /cm		0–40		40–100	
Mass of dry soil /kg		37.56		56.38	
		Carbon	Nitrogen	Carbon	Nitrogen
All columns					
Initial content	/g kg^{-1} soil	36.36	3.46	17.20	1.51
Control column: C3					
Final content	/g kg^{-1} soil	32.43	3.46	15.31	1.35
Losses	/g kg^{-1} soil	3.93	0.00	1.89	0.16
	/%	10.8	0	11.0	10.8
Manure-amended columns[a]: C1 & C2					
Pig manure	/g	36.0	4.94	/	/
Final content	/g kg^{-1} soil	32.35	3.38	15.63	1.37
Losses	/g kg^{-1} soil	4.97	0.21	1.57	0.14
	/%	13.3	5.8	9.1	9.1

[a]Average values are presented because the differences between C1 and C2 were very small.

Solute transfer in soil

Mineral nitrogen. Nitrification was not limited since NH_4^+ concentrations in the soil solution of the three columns were always very small. Consequently, we only considered the NO_3^- form of mineral nitrogen (N_{min}). In C1 (and C2, results not shown), the NO_3^- concentration increased to more than 6 mM $litre^{-1}$ and the solution pH dropped by around one pH unit during the first months of the study (Figure 3). This behaviour could be explained by the nitrification of NH_4^+ derived from the manure, which only affected the surface layer of the A horizon in C1 and C2. The effects of this nitrification were no longer seen when more than 600 mm of water was applied, i.e. the NO_3^- and pH values merged in C1, C2 and C3 (Figure 3).

The N_{min} concentrations in the soil solution of C1, C2 and C3 were compared at 15, 35 and 100 cm depth on the basis of quantities of water applied (Figure 4). During phase 1 (0–1500 mm), the breakthrough curves differed markedly at the three depths in C1 and C2. At 15 cm, the peak concentration (6 mM $litre^{-1}$) was reached after a water application of around 500 mm. At 35 cm, the peak concentration was similar but reached after a water application of 600 to 650 mm. At 100 cm (column outlet depth), breakthrough occurred after 1100 to 1350 mm of water application, with a much broader spread due to the dispersiveness of the porous soil medium and the peak N_{min} concentration of 2.3 mM $litre^{-1}$. For C3, we did not observe any breakthrough and the N_{min} concentrations were always around 0.5 mM $litre^{-1}$.

During phase 2 (drying), no drainage was noted. During phase 3 (1550–4850 mm), we observed a second N_{min} breakthrough at 100 cm depth (at the outlet) in C1, C2 and C3 (Figure 4). This

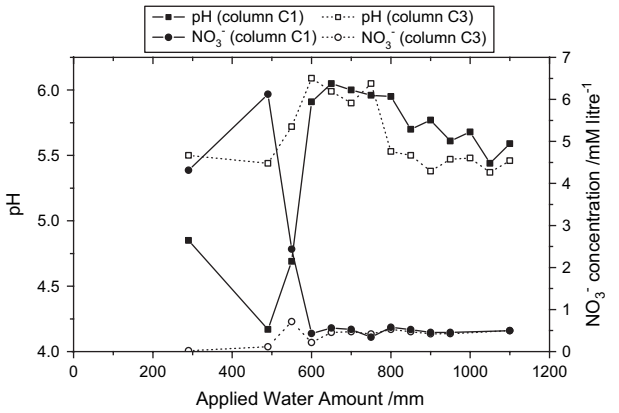

Figure 3 Variations in pH and nitrate concentration at 7.5 cm soil depth in C1 and C3.

occurred when the NO_3^- concentrations had dropped to very small values (0.2 mM litre^{-1}). For each column, the concentration began peaking at 2850 mm water application and reached its apex at around 3000 mm. The three maxima were less than the breakthrough curve peaks noted during the first 3 months of the study. At 15 and 35 cm depth, the peaks were more spread out than during phase 1 and the intensity was less. We could not monitor the greatest NO_3^- concentrations—that were likely reached between 1550 and 1850 mm water application—since the soil solution could not be sampled at these depths. We did detect an elution tail at 35 cm depth, as shown by a decrease in NO_3^- concentration from 1850 to 2500 mm water application.

At 15, 35 and 100 cm depth, we calculated quantities of N leached on the basis of calculated water flows and N_{min} concentrations occasionally measured in the soil solution (Figure 5). During water application phase 1 (0–1500 mm), 4.1 to 4.6 g of N_{min} was leached from the 0–15 cm soil layer in C1 and C2, respectively, and 1.1 g in C3. This difference was close to the total quantity of NH_4^+ derived from the 2 litres of manure (3.4 g), which was quickly nitrified and leached. At 35-cm depth in C1 and C2, smaller quantities of N were leached (2.9 and 3 g), however these quantities still differed markedly from the quantity leached in C3 (1.3 g). At 100 cm depth (at the outlet) in C1, C2 and C3, much smaller quantities of N were leached (1.5 g for C1 and C2 and 0.4 g for C3).

Water flows were negligible and no significant leaching occurred during phase 2. During phase 3 (1550–4850 mm), in C1, C2 and C3 at 100 cm depth, we detected a leaching flux rate

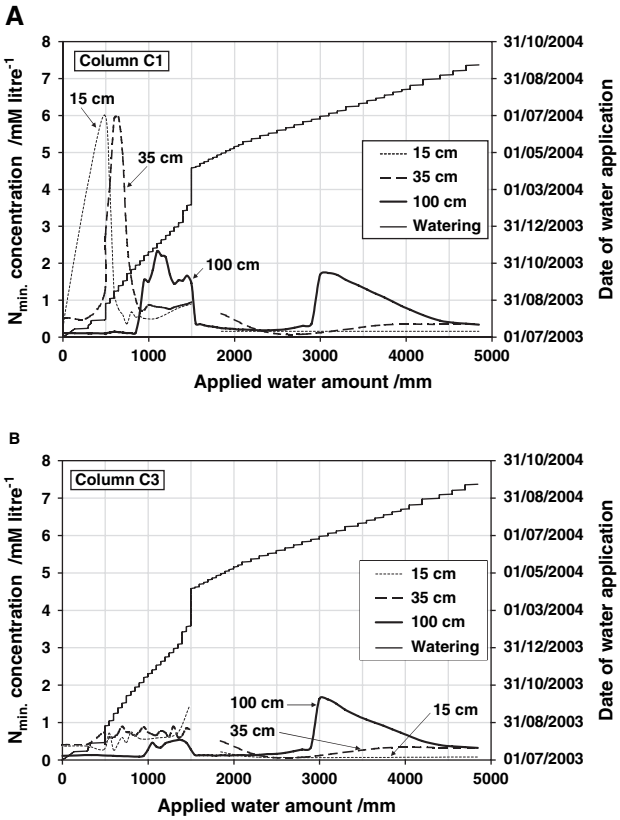

Figure 4 Variations in mineral N_{min} patterns according to water applications at 15, 35 and 100 cm soil depth in C1 and C3. N_{min} concentrations in C2 (not shown) were similar to patterns in C1.

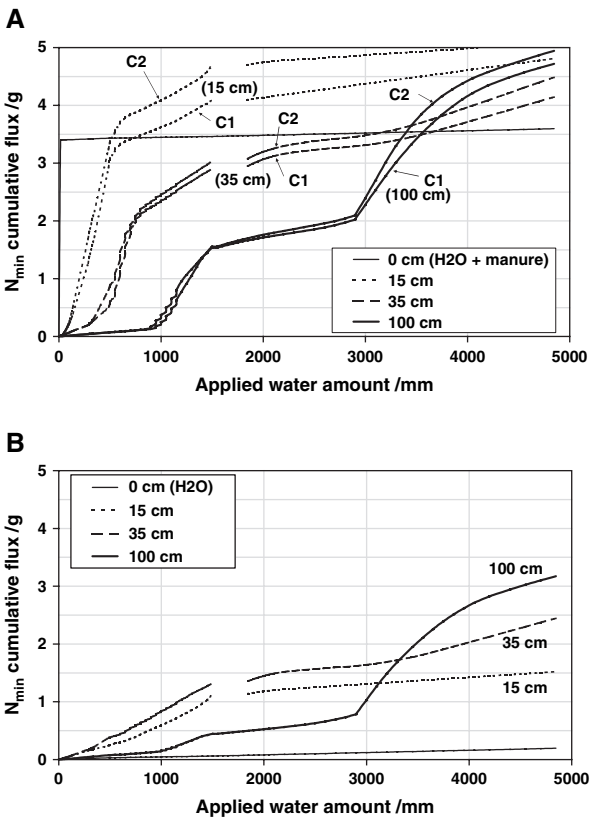

Figure 5 Cumulated mineral N_{min} fluxes according to applied water volumes calculated at 15, 35 and 100 cm soil depth (a) for amended columns C1 and C2 and (b) for untreated column C3.

that fitted the last N breakthrough curve. The quantity of N_{min} leached only at the outlet during this phase was 3.2 and 3.4 g for C1 and C2 (69% of the total amount leached) and 2.7 g for C3 (84% of the total amount leached). At 15- and 35-cm depth, leached quantities of N_{min} were likely less than at 100-cm depth (part of the leached N_{min} could not be measured at 15 and 35 cm in the 1500 to 1850 mm water application range).

Chloride. We estimated leached quantities of Cl^- by the same method as that used for N_{min} (Figure 6). In C1 and C2, massive input of Cl^- from the manure induced substantial leaching flux rates at all soil depths. At 15-cm depth, all Cl^- derived from the water and manure applications was thus leached (4.8 g for C2). However, the leaching flux rates noted at 35 cm indicated that 15.7% of the input Cl^- had been adsorbed in the 15–35 cm soil layer. The cumulative flux observed at 35 cm was also recorded at 100 cm (at the outlet). In C3, the Cl^- leaching flux rates observed at 15-cm depth corresponded to the amount applied at the top of the column. However, at the same times at 35 cm and at the outlet, we detected a slight leaching pulse (0.85 g) in C1 and C2. This phenomenon was not detected at 15 cm, likely because of the single sampling on 15 July 2003.

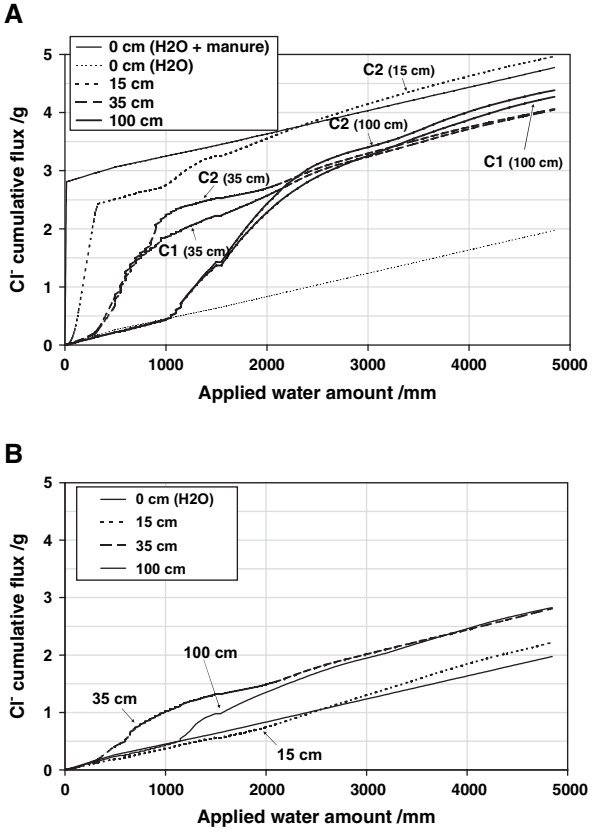

Figure 6 Cumulated Cl^- fluxes according to applied water volumes calculated at 15, 35 and 100 cm soil depth (a) for amended columns C1 and C2 (data not available for C1 at 15 cm) and (b) for untreated column C3.

Interactions between nitrate and chloride anions and the soil

We analysed soil-solute interactions by comparing the volume of water required for solute percolation to the soil pore volume (*PV*) in the 0–35, 35–100 and 0–100 cm soil layers. The *PV* was calculated for each layer (Table 5) according to the soil volumetric water content at saturation (Table 1) and based on the hypothesis that all soil moisture was involved in water flow. Water volumes involved at peak leaching flux, which were deduced from the instantaneous leaching flux curves, were considered as representative of the solute percolation volumes (Figure 7). The ratio between the solute percolation volume and *PV* was used to assess the lag in solute detection and thus the extent of the soil-solute interaction in each soil layer.

Figure 7 shows that there was great reproducibility between C1 and C2 with respect to mineral nitrogen and chloride fluxes. At 35 cm depth, the very clearcut leaching peaks were reached earlier for Cl^- (at 496 mm water application) than for NO_3^- (at 596 mm). At 100 cm (at the outlet), the less distinct peaks occurred between 1196 and 1346 mm water application. A slight column effect was noted, but there were no significant differences between the two solutes. Throughout the C1 and C2 soil columns (0–100 cm), the transfer kinetics were similar for Cl^- and NO_3^- and 1.86 *PV*s were required to leach these anions (Table 5). However, the A horizon was more reactive: at 35 cm, Cl^- peaked at 2.08 *PV* and NO_3^- peaked at 2.50 *PV*, whereas NO_3^- and Cl^- were transported from 35 to 100 cm respectively with 1.5 and 1.7 *PV* (Table 5).

We quantified N_{min} adsorbed by the soil at the end of the study at the bottom of the A horizon (30–40 cm) and B horizon (90–100 cm). Adsorbed N_{min} was calculated by the difference between total soil N_{min} (KCl extraction) and soil-solution N_{min} at 35 and 100 cm depth (Figure 4). Table 6 gives the mean adsorbed N_{min} values obtained for C1, C2 and C3. These results highlight that 84.7 and 85.1% of N_{min} was in an adsorbed form and only 15.3 and 14.9% was in solution in the 30–40 and 90–100 cm soil layers, respectively.

Discussion

Organic carbon and nitrogen decay in the soil

In the A horizon of C1 and C2, carbon loss was greater than in the C3 control, i.e. 13.3 vs. 10.8% (Table 4). This suggests that

Table 5 Analysis of interactions between nitrate and chloride anions and the soil

Soil layer /cm		0–35	35–100	0–100
Pore volume, *PV*	/mm	239	446.3	685
NO_3^- percolation volume	/mm	596	675.0	1271
Ratio		2.5	1.5	1.9
Cl^- percolation volume	/mm	496	775.0	1271
Ratio		2.1	1.7	1.9

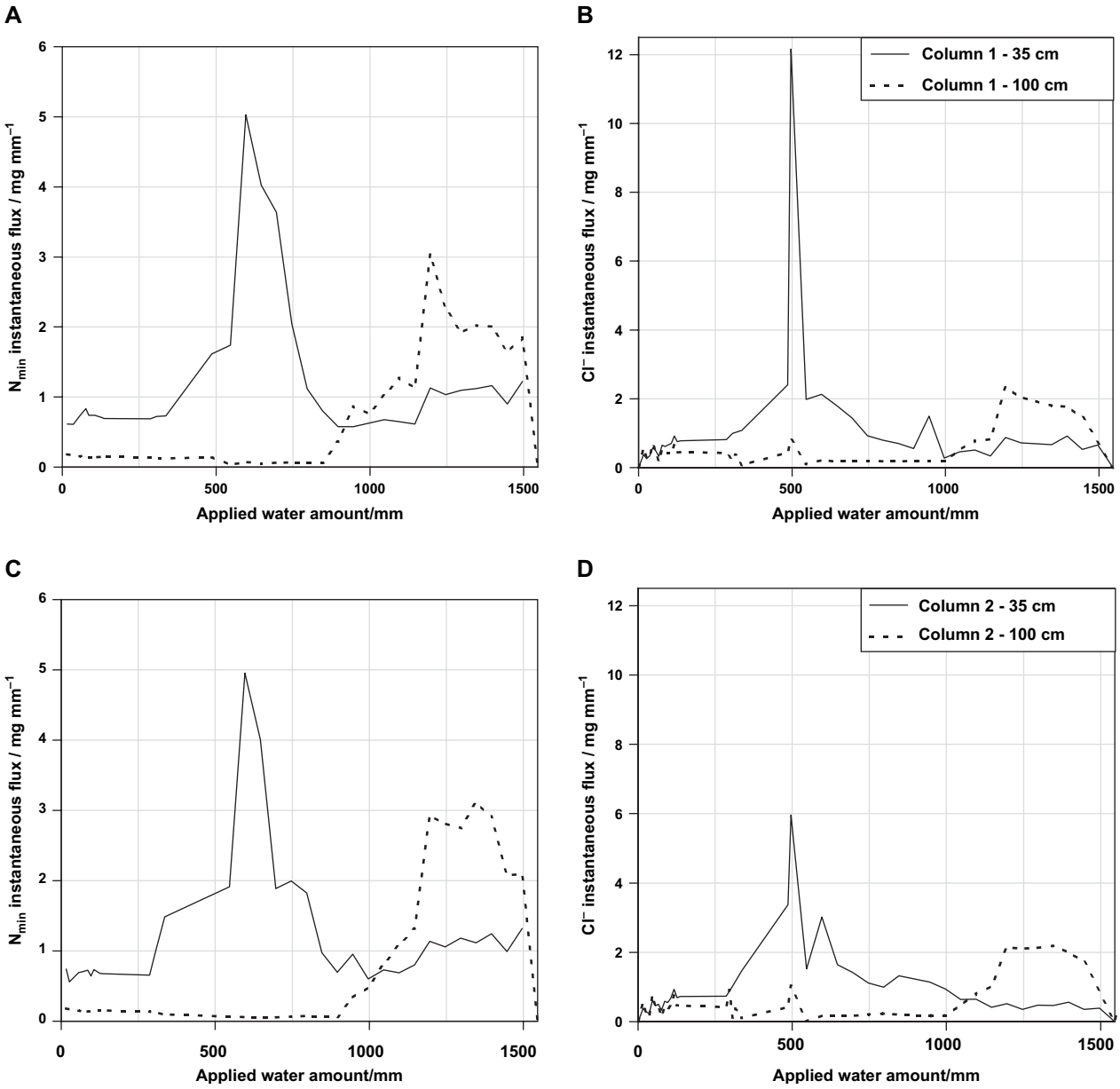

Figure 7 Instantaneous mineral N and Cl^- fluxes according to applied water volumes calculated at 35 and 100 cm soil depth for C1 and C2.

most of the manure C had been mineralised and that a small fraction had been humified. A priming effect (Fontaine *et al*., 2003) also increased soil OM mineralization in the presence of exogeneous OM, which stimulates microbial activity (Paul & Clark, 1989; Trinsoutrot *et al*., 2000). Carbon loss in the B horizon of C1 and C2 was less than in C3. This could be explained by greater C assimilation by microorganisms whose available N_{min} resources were boosted by the manure input. Aran *et al*. (2001), Legay & Schaefer (1984) and Boudot (1992) also demonstrated that OM-mineral complexes formed are greatly resistant to biodegradation in Andosols. These mainly nitrogenous insoluble organic compounds are known to occur in large quantities and are persistent (Boudot *et al*., 1988; Wang *et al*., 2001).

Manure nitrification was rapid and intense during phase 1 (Figure 3). Large NO_3^- concentrations were detected in the soil solution of C1 and C2. Manure nitrification was associated with acidification of the soil solution at 7.5 cm depth. Drainage water acidification has already been noted after nitrogen fertilisation (Bergkvist & Folkeson, 1992) and in conjunction with natural OM mineralization (Nilsson *et al*., 1988). Nitrification had slowed down after 40 days since at that point we did not note any difference with respect to C3. All of the very mineralizable manure fraction had thus been transformed.

Table 6 Estimation of mean mineral nitrogen adsorbed and in the soil solution at the end of the study (standard deviation in brackets)

Soil layer /cm		30–40		90–100	
Total $N_{min.}$	/mg	242	(6)	238	(23)
Solute $N_{min.}$	/mg l^{-1}	5	(1)	5	(1)
	/mg	37	(5)	35	(2)
	/%	15.3	(1.9)	14.9	(2.3)
Adsorbed $N_{min.}$	/mg kg^{-1} soil	23	(1)	22	(3)
	/mg	205	(8)	203	(25)
	/%	84.7	(1.9)	85.1	(2.3)

Leaching fluxes of nitrate and chloride

Columns C1, C2 and C3 lost 4.7, 4.9 and 3.2 g N_{min}, respectively, after 4850 mm water application (Figure 5). These quantities were much greater than those supplied by the water applications (0.2 g). Columns C1 and C2 thus leached 1.5 and 1.7 g more N_{min} than C3. This difference was much less than the quantity of N derived from the manure, which was 4.9 g total N, including 3.4 g N_{min}. This indicates that N_{min} interacted with the soil and soil-borne microorganisms. Measured total N losses (Table 4) could only be partially explained by N_{min} leaching, and other factors of the N cycle also contributed to these losses. However, the chemical features of the soil solution (dissolved oxygen and redox potential, data not shown) and the hydric conditions were not favourable for denitrification. Thus, N_{min} was probably partially immobilised by soil microorganisms to ensure their metabolic activity (Mary *et al*., 1996).

At 100 cm, the breakthrough curves were asymmetrical for C1, C2 and C3 during phase 3 (Figure 4) — from the beginning of the peak to the maximum required 150 mm of water, whereas from the peak back to the baseline required another 1500 mm. The fact that C1, C2 and C3 had the same behaviour indicates that the observed N_{min} pattern was not related to the manure input. In the A horizon, maintenance of unsaturated moisture conditions in the soil during phase 2 stimulated the aerobic activity of microorganisms responsible for soil OM mineralization. This activity prompted an increase in N_{min} content. In the B horizon, the saturated conditions and the smaller OM contents did not induce recharge, as indicated by the NO_3^- concentrations at 100-cm depth at the onset of phase 3 (Figure 4). The N_{min} concentrations were found to be distributed in the upper part of the soil profile, and N_{min} transport thus led to a differently shaped breakthrough curve as compared to that of a concentration pulse at the soil surface. Overlap of N-transport peaks for each elementary soil layer could account for this broad breakthrough curve. Deeper layers produced sharper peaks that quickly reached the outlet.

Retention of nitrate and chloride

Retention of NO_3^- and Cl^- varied according to the constituents present in each horizon. The Cl^- and NO_3^- breakthrough curves differed at 35 cm soil depth. For these two elements, the lags were 2.1 and 2.5 pore volumes (*PV*), respectively, but this trend reversed between 35 and 100 cm, i.e. 1.7 and 1.5 *PV*. On a soil column scale (0–100 cm), lag differences between these two anions were not detectable due to mutual compensation (1.9 *PV*). These values are in agreement with those of many studies conducted on soils of different charges (Wong *et al*., 1990; Bellini *et al*., 1996; Katou *et al*., 1996). However, the respective impacts of constituents responsible for positive charges have not yet been clearly delineated. Bellini *et al*. (1996) and Katou *et al*. (1996) used $CaCl_2$ and $Ca(NO_3)_2$ in their experiments to study lags in the transfer of these anions through packed soil columns. They highlighted the influence of the ionic strength of the soil solution and anion concentrations. According to Katou *et al*. (1996), adsorption sites have a lesser affinity for NO_3^- than for Cl^-. Toner *et al*. (1989) found that NO_3^- adsorption was completely reversible and explained this by a simple electrostatic retention mechanism. Hence, there is great competition for anion adsorption in soil and this phenomenon is dependent on several factors. In the surface horizon of our soil, the Al_{py}/Al_{ox} ratio was twice as high as in the 40–100 cm horizon (Table 1). This trend was reversed for the $Al_{ox} + ½\ Fe_{ox}$ term. The NO_3^- retention was thus greater than Cl^- retention when OM and organomineral complexes prevailed over poorly crystallized minerals.

The soil-solute interaction was confirmed by the great adsorption capacity of the two soil layers: about 23 and 22 mg N kg^{-1} soil was adsorbed in A and B horizons, respectively. These quantities correspond to 24.1% of the AEC for the A horizon and 13.1% for the B horizon (Table 1). This proportion was greater than that found by Ryan *et al*. (2001), who estimated that less than 10% of the AEC was occupied by nitrate in an Andosol in coffee plantations. By extrapolating these quantities to the whole column, we obtained a retention capacity of 2.1 ± 0.2 g N per soil column, i.e. 190 ± 17 kg N ha^{-1}, which is close to the results reported by Lehmann *et al*. (2004) and Ryan *et al*. (2001).

Conclusion

The objective of this study was to assess the leaching hazard in an andic soil after pig manure amendment. We developed a laboratory setup to control water and solute fluxes in the soil during a 15-month experiment. The latter was conducted with mineralization rates and a hydric regime representative of the *in situ* conditions. Total C and N of the soil decreased by 11% and 4%, respectively, without amendment. Carbon and N decay was greater for amended soil (12% and 7%, respectively), due to the addition of easily decomposable organic matter. Rapid nitrification produced large quantities of nitrate, especially in amended soils during the first irrigation phase. Nitrate leaching reached about 4.9 g N in amended soil versus 3.2 g N in untreated soil. The difference was far less than the manure nitrogen input but was probably not due to denitrification. Leaching fluxes highlighted an interaction between anions and

soil solid phases—a lag of 1.5 to 2.5 pore volumes (*PV*) was observed in the breakthrough curves. This interaction was stronger in the A horizon (> 2 *PV*) than in the B horizon (< 1.7 *PV*), and was anion specific—nitrate was more retained than chloride when organomineral complexes prevailed over poorly-crystallized minerals. Nitrate adsorption was estimated at around 22 mg N kg^{-1} soil which, when extrapolated to the plot scale, corresponded to substantial amounts (190 kg N ha^{-1}). Leaching of this retained nitrate could be delayed but still represents a risk in the long run, since adsorption is a reversible process. A similar study that takes variability of soil properties and interactions with crops into account is being carried out to assess this risk in the field.

Acknowledgements

The authors thank L. Calichiama, J.-M. Bégue and G. Moussard for their contributions to this study and the plant, soil and water analysis laboratory staff for their efficient assistance (''Analyses'' support unit 49, CIRAD). We are also very grateful to C. Fovet-Rabot, M. Wopereis and H. Saint Macary for their critical comments on the article. This study was funded by the Region of Réunion and the European Agricultural Guidance and Guarantee Fund, EAGGF (Fonds européen d'orientation et de garantie agricole, FEOGA).

References

Aran, D., Gury, M. & Jeanroy E. 2001. Organo-metallic complexes in an Andosol: a comparative study with a Cambisol and Podzol. *Geoderma*, **99,** 65–79.

Aubry, C., Paillat, J.-M. & Guerrin, F. 2006. A conceptual representation of animal waste management at the farm scale. The case of the Reunion Island. *Agricultural Systems*, **88,** 294–315.

Bellini, G., Sumner, M.E. Radcliffe, D.E. & Qafoku, N.P. 1996. Anion transport through columns of highly weathered acid soil: Adsorption and retardation. *Soil Science Society of America Journal*, **60,** 132–137.

Bergkvist, B.O. & Folkeson, L. 1992. Soil acidification and element fluxes of a Fagus sylvatica forest as influenced by simulated nitrogen deposition. *Water, Air and Soil Pollution*, **65,** 111–133.

Blakemore, L.C., Searle, R.L. & Daly, B.K. 1987. *Methods for chemical analysis of soils*. New Zealand Soil Bureau Science. Report 80. New Zealand Society of Soil Science, Lower Hutt.

Boudot, J.P. 1992. Relative efficiency of complexed aluminium, non-crystalline Al hydroxide, allophane and imogolite in retarding the biodegradation of citric acid. *Geoderma*, **52,** 29–39.

Boudot, J.P., Brahim, A.B.H. & Chone, T. 1988. Internal nitrogen cycling in two humic-rich acidic soils. *Geoderma*, **42,** 245–260.

Dahlgren, R.A., Nanzyo, M. & Saigusa, M. 2004. Volcanic soils: an overview and new perspectives. In: *Volcanic soil resources in Europe*. (eds H. Oskarsson & O. Arnalds), pp 119–120. Abstracts of COST Action 622 Final Meeting, June 2004, Akureyri-Egilsstadir, Iceland. Rala Report, No. 214, Agricultural Reseach Institute, Reykjavik.

Feder, F., Olivier, R., Alary, K. & Bourgeon, G. 2006. *Characterisation of a soil catena on the western slope of the Piton des Neiges volcano (la Réunion)*. Proceedings of 18th World Congress of Soil Science, July 9–15, 2006. Philadelphia, PA, USA. CD-ROM.

Fontaine, S., Mariotti, A. & Abbadie, L. 2003. The priming effect of organic matter: a question of microbial competition? *Soil Biology & Biochemistry*, **35,** 837–843.

Gillman, G.P. & Sumpter, E.A. 1986. Modification to the compulsive exchange method for measuring exchange characteristics of soils. *Australian Journal of Soil Research*, **24,** 61–66.

Huygens, D., Boeckx, P., Van Cleemput, O., Godoy, R. & Oyarzun, C. 2005. Aggregate structure and stability linked to carbon dynamics in a south Chilean Andisol. *Biogeosciences Discussions*, **2,** 203–238.

Katou, H., Clothier, B.E. & Green, S.R. 1996. Anion transport involving competitive adsorption during transient water flow in an andisol. *Soil Science Society of America Journal*, **60,** 1368–1375.

Legay, B. & Schaefer, R. 1984. Modalities of the energy-flow in different tropical soils, as related to their mineralization capacity of organic carbon and to the type of clay. II: The degradation of various substrates. *Zentralblatt fur Mikrobiologie*, **139,** 389–400.

Lehmann, J., Lilienfein, J., Rebel, K., do Carmo Lima, S. & Wilcke, W. 2004. Subsoil retention of organic and inorganic nitrogen in a Brazilian savanna Oxisol. *Soil Use and Management*, **20,** 163–172.

Madeira, M., Auxtero, E. & Sousa, E. 2003. Cation and anion exchange properties of andisols from the Azores, Portugal, as determined by the compulsive exchange and the ammonium acetate methods. *Geoderma*, **117,** 225–241.

Mary, B., Recous, S., Darwis, D. & Robin, D. 1996. Interactions between decomposition of plant residues and nitrogen cycling in soil. *Plant and Soil*, **181,** 71–82.

Morvan, T., Chabalier, P.F., Saint-Macary, H. & Paillat, J.-M. 2003. Biotransformations résultant de l'apport de produits organiques sur des sols de la Réunion : acquisitions de références. In: *Modélisation des flux de biomasse et des transferts de fertilité – cas de la gestion des effluents d'élevage à l'île de la Réunion*. (eds F. Guerrin & J.-M. Paillat). Review of the research of ATP 99/60. Seminar proceedings, 19–20 June 2002, Montpellier, France. CIRAD, conferences, CD-ROM.

Nilsson, S.I., Berdén, M. & Popovic, B. 1988. Experimental work related to nitrogen deposition, nitrification and soil acidification – A case study. *Environmental Pollution*, **54,** 233–248.

Paul, E.A. & Clark, F.E. 1989. *Soil Microbiology and Biochemistry*. Academic Press, San Diego.

Payet, N. 2005. *Impact des apports de lisier sur un sol cultivé de la Réunion: étude expérimentale et modélisation des flux d'eau et de nitrate dans la zone non saturée*. (Impact of pig effluent spreading on a cultivated soil of Réunion: experimental study and water and nitrate flux modelling in the vadose zone). Doctoral dissertation, Université de la Réunion, Saint-Denis, Réunion.

Ryan, M.C., Graham, J.R. & Rudolph, D.L. 2001. Contrasting nitrate adsorption in andisols of two coffee plantations in Costa Rica. *Journal of Environmental Quality*, **30,** 1848–1852.

Saito, M. 1990. Nitrogen mineralization parameters and its availability indices of soils in Tohuku district, their relationship. *Japanese Journal of Soil Science and Plant Nutrition*, **61,** 265–272. In Japanese with English abstract.

Shoji, S., Nanzyo, M. & Dahlgren, R.A. 1993. *Volcanic ash soils: genesis, properties and utilization*. *Developments in Soil Science*, **21**. Elsevier, Amsterdam.

Toner, C.V., Sparks, D.L. & Carski, T.H. 1989. Anion exchange chemistry of Middle Atlantic soils: charge properties and nitrate retention kinetics. *Soil Science Society of America Journal*, **53,** 1061–1067.

Trinsoutrot, I., Recous, S., Bentz, B., Linères, M., Chéneby, D. & Nicolardot, B. 2000. Biochemical quality of crop residues and carbon and nitrogen mineralization kinetics under nonlimiting nitrogen conditions. *Soil Science Society of America Journal*, **64,** 918–926.

USDA-NRCS. 2004. *Soil Survey Laboratory Methods Manual*. Soil survey investigations report, 42, version 4.0, November 2004. (ed. R. Burt), USDA-NRCS, Lincoln, Nebraska.

Wang, W.J., Smith, C.J., Chalk, P.M. & Chen, D. 2001. Evaluating chemical and physical indices of nitrogen mineralization capacity with an unequivocal reference. *Soil Science Society of America Journal*, **65,** 368–376.

Wong, M.T.F., Hughes, R. & Rowell, D.L. 1990. Retarded leaching of nitrate in acid soils from the tropics: measurement of the effective anion exchange capacity. *Journal of Soil Science*, **41,** 655–663.

Agriculture, Ecosystems and Environment 134 (2009) 218–233

Contents lists available at ScienceDirect

Agriculture, Ecosystems and Environment

journal homepage: www.elsevier.com/locate/agee

Modelling the fate of nitrogen following pig slurry application on a tropical cropped acid soil on the island of Réunion (France)

Nicolas Payet [a,b], Antoine Findeling [c], Jean-Louis Chopart [d], Frédéric Feder [a], Eric Nicolini [b], Hervé Saint Macary [c,*], Michel Vauclin [e]

[a] CIRAD, UPR Recyclage et Risque, F-97408 Saint-Denis, La Réunion, France
[b] LSTUR, Laboratoire des Sciences de la Terre de l'Université de la Réunion, 15 av. René Cassin, BP 7151, F-97715, Saint-Denis Messagerie Cedex 9, La Réunion, France
[c] CIRAD, UPR Recyclage et Risque, F-34398 Montpellier, France
[d] CIRAD, UPR Systèmes de Culture Annuels, F-97410 Saint-Pierre, La Réunion, France
[e] LTHE, UMR 5564 (CNRS, INPG, IRD, UJF), BP 53, F-38041 Grenoble Cedex 9, France

ARTICLE INFO

Article history:
Received 25 November 2008
Received in revised form 19 May 2009
Accepted 7 July 2009
Available online 11 August 2009

Keywords:
Pig slurry
Maize
Andic soil
Field experiment
WAVE model

ABSTRACT

A comprehensive field study was conducted to determine the fate of nitrogen in pig (*Sus scrofa*) slurry applied to an acid tropical andic soil of Réunion with the aim of estimating drainage and nitrogen leaching below the root zone. Water movement and nitrate dynamics were monitored during two successive cropping seasons on a plot (PSP) treated with liquid manure, with an input of 264 kg N ha^{-1} the first year and 185 kg N ha^{-1} the second year, in comparison to levels recorded in a unfertilized control plot (CP). The field was cropped with rainfed maize (*Zea mays* L.) The process-based WAVE field-scale model was used to simulate water flow and nitrogen transport in the unsaturated zone and highlight the main processes controlling water and N fate. A calibration procedure was performed one year, while the prediction capability of the model was assessed during another cropping year. A sensitivity analysis was performed to address some critical parameters.

Due to the high hydraulic conductivities measured in this andic soil, the drainage risk became high when the rain intensity was above 30 mm d^{-1} and the soil humidity was close to saturation. The time between the first slurry application on PSP and the nitrate onset in the drainage water at 135 cm depth (about 15 months) was attributed to nitrate adsorption on the soil particles (the retardation factor was estimated at 2.6 in the surface layer and 1.5 in deeper layers) and to the fact that the water stored in the 0–135 cm soil layer was slowly displaced. The nitrate migrated in this andic soil at rate of about 50 mm per 100 mm of infiltrated water.

The main features of the experimental values of state variables (water content, water pressure head, NO_3^- concentration, natural mineralization and nitrification of the pig slurry ammonium at different depths and dates) as well as the water fluxes across boundaries were generally correctly reproduced by WAVE for both plots. The calibrated modelled budget error arising from net mineralization was +15 and +9 kg N ha^{-1} for CP and PSP, respectively. For the model evaluation, it was estimated at −9 and −13 kg N ha^{-1}, respectively, which was considered as very acceptable.

WAVE required refinements in some processes and parameters but was still found to be robust enough to work in conditions for which it was not primarily designed.

1. Introduction

For many years and in many regions around the world, farmers in areas with high swine and poultry production have disposed of liquid manure wastes (i.e. pig slurry, dairy effluent) by spreading them on crop fields thanks to their fertilizer function. Manures are an important source of nutrients for crops but may represent a significant environmental pollution risk. Consequently, it is essential to gain insight into manure nutrient behaviour so as to be able to efficiently manage the application practices and thus enhance the cost-effectiveness of crop production while minimizing the adverse impacts on water and soil quality.

In Réunion, pig slurry production reached 180,000 T in 2007 (DAF and CIRAD, 2007). This high amount was to be applied on limited areas (20,000 ha), but with a potential risk of contaminat-

Abbreviations: CP, control plot; DAS, day after sowing; PSP, pig slurry plot; TDR, time domain reflectometry; WAVE, Water and Agrochemicals in the Vadose Environment model.

* Corresponding author at: CIRAD, Avenue Agropolis, TA B – 78/01, 34398 Montpellier Cedex 5, France. Tel.: +33 4 67 61 71 02; fax: +33 4 67 61 71 48.
E-mail address: herve.saint_macary@cirad.fr (H. Saint Macary).

0167-8809/$ – see front matter © 2009 Elsevier B.V. All rights reserved.
doi:10.1016/j.agee.2009.07.004

ing soils and water with excessive nitrogen, phosphorus or trace elements. This paper deals only with nitrogen since there is growing concern in public and regulatory agencies on possible nitrate contamination of groundwater resources and downstream lagoons on this island. In addition, the European Union Directive 91/676 obliges all Member States to assess the nitrate concentration and trophic status of their water resources in order to detect pollution and to launch Action Programmes to, for instance, optimise nitrogen fertilization efficiency in the most vulnerable zones.

A number of studies showed that adequate pig slurry applications can help to generate satisfactory crop yields, while totally or partially offsetting the need for mineral fertilizer applications (i.e. Brechin and McDonald, 1994; Cameron et al., 1995; Petersen, 1996; Zebarth et al., 1996; Jensen et al., 2000; Daudén and Quilez, 2004). On the other hand, several authors reported results which showed that there is an increased risk of nitrate leaching when liquid manure is applied to soils in large amounts or with inappropriate agronomic techniques (i.e. Nielsen and Jensen, 1990; Cameron et al., 1995; Beckwith et al., 1998, 2002; Jensen et al., 2000; Harter et al., 2002; Sanchez-Pérez et al., 2003; Thomsen, 2005; Mantovi et al., 2006). It has also been observed that in fields in which pig slurry is applied at adequate rates, there is less or equivalent nitrate leaching as compared to fields in which mineral fertilizers are applied (i.e. Beauchamp, 1986; Carey et al., 1997; Diez et al., 2001).

Extensive research on the use of pig slurry as fertilizer has been carried out in temperate (i.e. northern Europe, North America, New Zealand) and Mediterranean (i.e. Italy, Spain) regions. Studies in tropical regions are much scarcer despite the high growth of livestock production and the increased recognition that on-farm nutrient recycling is essential to avoid off-site environmental degradation.

In this setting, the island of Réunion has some unique features. It has a humid tropical climate with world daily and yearly precipitation records. Soils originating from volcanic materials generally have high clay and silt contents and have an aggregated structure with high porosity and hydraulic conductivity values. Combined with high rainfall intensities, greater water and possibly leaching fluxes below the root zone than in temperate regions may be expected (Hodnett and Tomasella, 2002; Bernard et al., 2005). In addition, increased rates of nitrification, denitrification and organic matter decomposition can occur due to higher air and soil temperature, with smaller seasonal variations than in temperate areas.

Mechanistic models are powerful tools that can be used to reproduce real systems as they are based on physical, chemical and biological processes. However, most of them (Addiscott and Wagenet, 1985; Wagenet and Hutson, 1989; Brusseau and Rao, 1990; Simunek and Suarez, 1993; Vanclooster et al., 1994; Jarvis, 1994; Eckersten et al., 1996; Simunek et al., 1999 among others) were initially developed and evaluated under temperate climate conditions. According to Thorsen et al. (1998), a model generally cannot be validated, but must be tested under all conditions for which it will be used, i.e. for different climate, soil, crop and agronomic practices.

The goal of this study was threefold: (i) to gain further insight into the processes which govern the fate of nitrogen in the unsaturated zone after application of pig slurry on a tropical and andic soil cropped with maize, (ii) to model these processes in that context by comparing 2 years of field data with simulations of the mechanistic WAVE model (Vanclooster et al., 1994), and (iii) to estimate the potential risk of nitrate leaching below the root zone in conditions for which the model was not originally designed and tested.

2. Materials and methods

2.1. Field experiment

The study was conducted on the western side of the island of Réunion at the experimental site of Colimaçons (21°7′S, 55°18′E, 780 m *ASL*) during the southern summers (November to March) of 2003–2004 and 2004–2005. The climate is tropical with a hot humid season between December and April, and a dry season between May and November. The mean annual rainfall and potential evapotranspiration levels are 1600 and 800 mm, respectively, with a mean annual temperature of 19 °C with variation of 2 °C around this value. During the study period of each year, the mean daily temperature slowly increased from 19.5 °C at sowing date to 21 °C at harvest time.

The soil is in the middle of a toposequence in which Andosols (IUSS Working Group WRB, 2006) prevail. According to Feder and Findeling (2007), it is classified as a desaturated andic Cambisol, which includes: (i) a surface A horizon (0–40 cm), with a pH_{water} below 6, and (ii) an andic B horizon (40–220 cm) characterized by a pH_{water} between 6 and 6.6 and by lower organic matter content and dry bulk density than in the first horizon. At the Colimaçons site, the interface between horizons A and B was found to be at 30 cm, thus highlighting the depth of layers for subsequent measurements and modelling. The main physicochemical properties of this soil are given in Table 1. The subsoil consists of altered fissured and fractured rocks (Payet, 2005). The aquifer is located several hundreds of meters below the surface (Join and Coudray, 1993), so there is a very thick unsaturated zone.

A field that had been in fallow since 1983 was selected. An unfertilized maize–oat rotation was set up in 2002–2003 in order to reduce soil nitrogen storage prior to the experiment. In 2003, the field was split into two parts: one 620 m^2 plot (PSP) was fertilized yearly with pig (*Sus scrofa*) slurry from a nearby piggery, and another 570 m^2 control plot (CP) was left unfertilized. The field was cropped with rainfed maize (*Zea mays*, local open-pollinated variety) adapted to a tropical climate. It was sown in rows by dibbling three grains every 50 cm with interrows of 1 m. Due to losses during germination the final density corresponded to about 50,000 plants ha^{-1}. The total cycle duration (between sowing and maturity) was about 120–130 days, which is shorter than commonly encountered in colder regions. Before sowing the maize crop, pig slurry was applied on the surface of PSP at a rate of approximately 65 m^3 ha^{-1} through a fire hose nozzle. It was immediately incorporated into the surface soil layer (0–10 cm) by

Table 1
Selected physicochemical properties of the investigated soil.

Soil layer (cm)	ρ_d (g cm^{-3})	pH (H_2O)	pH (KCl)	C tot. (g kg^{-1})	N tot. (g kg^{-1})	CEC ($cmol_{(+)}$ kg^{-1})	Al(ox.) + 1/2 Fe(ox.) (%)
0–10	0.9	5.1	4.4	47.7	4.91	8.71	2.3
10–30	0.8	5.7	5.2	24.9	2.68	10.9	1.8
30–100	0.85	6.2	5.8	11.3	1.25	8.7	3.7
100–200	0.8	6.5	6.2	11.4	0.91	8.7	4.1

ρ_d: Soil dry bulk density; pH (H_2O): pH of soil water extract; pH(KCl): pH of soil KCl extract; C tot. and N tot.: total carbon and total nitrogen; CEC: cation exchange capacity (acetate method); Al(ox.) and Fe(ox.): Al and Fe of oxalate extraction.

Table 2
Main physicochemical characteristics of pig slurry applied in 2003 and 2004.

	2003		2004	
	Mean	SD	Mean	SD
Dry matter, DM (g kg^{-1} of fresh matter)	32.7	7.6	12.7	1.2
Density (kg L^{-1})	–	–	1.01	0.03
Total OM (% of DM)	66.1	4.8	43.2	3.3
Total C (% of DM)	37.3	2.0	26.3	1.6
Total N (% of DM)	12	2.5	23	1.2
C/N of OM	28	–	10	–
$N\text{-}NH_4^+$ (% of DM)	9.05	2.06	20.4	2.00
pH_{water}	7.6	0.06	7.8	0

SD = standard deviation for three measurements.

chiselling in order to minimize ammonium loss by volatilization. Table 2 gives the main physicochemical properties of pig slurry applied in 2003 and 2004. A summary of the main agricultural practices and the climate characteristics is given in Table 3 for the two cropping seasons. Weeds were regularly controlled by spot application of glyphosate and 2,4-D. Both plots were cropped with unfertilized oats between the two successive maize cycles.

Each plot was equipped in order to monitor the soil water and nitrogen dynamics. Volumetric water content profiles (θ) were measured by time domain reflectometry (TDR) probes (CS 616 Campbell Scientific) horizontally buried in pits at depths of 15 cm, 30 cm and every 30 cm down to 240 cm. They were connected to a data logger (Campbell CR 10X-2 M) to obtain one measurement every 20 min. Due to the specific characteristics of the volcanic soil (Miyamoto et al., 2001) each probe was duly calibrated in the laboratory on repacked field soil samples. Soil water pressure head (h) was measured by tensiometers installed vertically from the surface at the same depths as the TDR probes. Measurements were manually obtained two to three times per week by a tensimeter device (SDEC® SMS2500S). Soil temperature was measured at 10, 30 and 200 cm depths by thermocouples and stored on the datalogger every 20 min. The soil solution was sampled by suction porous cups installed vertically at five depths (20, 45, 75, 135, 175 cm). Samples were collected after a depression of—70 hPa had been applied for about 24 h by a vacuum pump. They were kept at 4 °C before chemical analysis. Nitrate concentrations were measured by ionic chromatography (Dionex DX 100). Ammonium concentrations in the soil solution were not measured. The N concentration in the soil profile in each treatment was recorded (four replicates per plot) every 2 weeks. Samples were taken with an auger at different depths: 0–10 cm, 10–30 cm, and every 30 cm down to 210 cm. At each depth, the four samples were mixed and nitrate and ammonium concentrations were determined in the 1:3 soil extract (1 h shaking) with 1 M KCl solution by continuous flux colorimetry (Alliance Instruments).

Each treatment was also equipped with a runoff plot (3 m long, 1 m wide) bordered by a thin steel sheet driven a few centimeters into the soil. Collected water was measured by an automatic device (one measurement every 20 min) installed downstream in a small pit. On-site rainfall was automatically recorded by a tipping bucket connected to a data logger (one measurement every 10 s). Daily Penman-Monteith potential evapotranspiration (PET) values were calculated from solar radiation, wind speed, air temperature and humidity routinely measured at a meteorological station located in the same field.

Soil water retention curves, $h(\theta)$, were experimentally determined by correlating water pressure heads and volumetric water contents measured at the same depths and times. Field values were complemented by laboratory pressure plate measurements up to—1.5×10^4 hPa. The Van Genuchten closed-form equation (Van Genuchten, 1980) was fitted to the experimental values. Soil hydraulic conductivity curves, $K(\theta)$, were obtained at different depths by performing a classical internal drainage test (Vachaud et al., 1978). Values close to saturation were determined at the surface and at two depths (135 and 220 cm) by using the tension disk infiltrometer method described in Vauclin and Chopart (1992). The Brooks and Corey (1964) equation was fitted to the measured values.

The leaf area index (LAI) of maize was classically determined from the leaf sizes measured by sampling 10 plants per treatment at two dates after sowing in 2004 (62 and 74 DAS) and 20 plants in 2005 (36 and 58 DAS). The geometrical characteristics of the root system (root length density, total root length and root front depth, mean distance between roots) were determined at different maize phenological stages by the trench-profile method (Böhm, 1976; Vepraskas and Hoyt, 1988). The model developed by Chopart and Siband (1999) was used to calculate these characteristics from counts of numbers of living roots on a grid placed on walls of pits dug perpendicular to the rows. The corresponding LAI and root front depth (L_r) values for the PSP and CP are given in Table 4 for the two maize cycles. For the estimation of plant growth and final yield, five 3 m^2-areas of each plot were harvested at different dates. The sampled aboveground fresh biomass was weighed and oven dried at 80 °C for 48 h to obtain the dry matter mass (Table 3). The total nitrogen concentration was determined using the standard Kjeldahl analysis. Samples were collected only at 100 DAS in 2003–2004 and at 36, 58, 77 and 100 DAS in 2004–2005.

2.1.1. Experimental estimation of soil water budget

For each plot, the soil water budget components were calculated from the mass conservation law between the surface and a control depth (z_d = 135 cm) which corresponded more or less to the maximum depth of the root front measured at harvest in both plots (Table 4). This leads to:

$$\Delta S = R - \mathrm{RN} - \mathrm{AET} - D \quad (1)$$

where ΔS is the variation in soil water storage between two dates separated by Δt, R is the rain amount, RN is the surface runoff, AET is the actual evapotranspiration and D is the drainage at z_d. All values are expressed in mm of water.

ΔS in the soil profile was calculated from the volumetric water content, θ ($cm^3\ cm^{-3}$), measured by TDR probes. R and RN were recorded in the field. Drainage losses below z_d were estimated by

Table 3
Summary of agricultural practices carried out in the 2003–2004 and 2004–2005 cropping seasons. Each year, maize was harvested about 120 days after sowing.

Year	Treatment	Application date of pig slurry	Sowing date	Application rate of pig slurry ($m^3\ ha^{-1}$)	Nitrogen application rate (kg ha^{-1})	Rain between sowing and harvest (mm)	Total dry matter (T ha^{-1})
2003–2004	Pig slurry plot	29 Oct. 03	20 Nov. 03	67	264	720	13.6 (2.1)
	Control plot	–	20 Nov. 03		–	720	8.5 (1.8)
2004–2005	Pig slurry plot	20 Nov. 04	6 Dec. 04	64	185	1066	12.4 (1.9)
	Control plot	–	6 Dec. 04		–	1066	8.6 (1.6)

Numbers in brackets are standard deviations for five measurements.

Table 4
Leaf area index (LAI), crop coefficient (K_c), root front depth (L_r) and N uptake (N_{upt}) by crop measured at different dates on both treatments during the 2003–2004 and 2004–2005 cropping seasons.

Year	DAS	Pig slurry plot				Control plot			
		LAI	K_c	L_r (m)	N_{upt} (kg ha^{-1})	LAI	K_c	L_r (m)	N_{upt} (kg ha^{-1})
2003–2004	43	–	0.75	0.56	–	–	0.71	0.32	–
	62	2.38 (0.51)	0.95	0.77	–	1.34 (0.53)	0.9	0.43	–
	74	2.65 (0.73)	1.05	0.99	–	1.82 (0.46)	1	1.03	–
	100	–	1.2	1.4	183	–	1.14	1.42	102
2004–2005	10	–	0.5	–	0	–	0.48	–	0
	36	0.47 (0.17)	0.7	0.52	99	0.31 (0.19)	0.65	0.28	69
	58	2.39 (0.68)	0.95	0.79	144	1.90 (0.63)	0.9	0.45	71
	77	–	1.05	0.97	154	–	1	1.01	91
	100	–	1.2	1.4	168	–	1.14	1.42	94

Numbers in brackets are standard deviations of 10 and 20 measurements of LAI, respectively. DAS is day after sowing.

Darcy's law:

$$D = -\frac{K(\theta)\,\mathrm{d}H}{\mathrm{d}z\,\Delta t} \quad (2)$$

where $K(\theta)$ is the unsaturated hydraulic conductivity (mm h^{-1}) measured at z_d. H is the hydraulic head (cm of water) defined as $h - z$, where z (cm) is the depth positively oriented downward, with the origin taken at the soil surface. The hydraulic head gradient at z_d was calculated from tensiometer readings at z = 120 and 150 cm. The actual evapotranspiration (AET) was thus obtained from Eq. (1), with all the other terms being known.

2.1.2. Experimental estimation of nitrogen budget

For the PSP treatment, the mineral nitrogen budget was calculated by using the mass conservation law between the soil surface and z_d:

$$\Delta N_{min} = N_{appl} + N_{net\,min} - N_{upt} - N_{leach} \quad (3)$$

where ΔN_{min} is the variation in soil total mineral nitrogen (NO_3^- and NH_4^+) storage between two dates separated by Δt, N_{appl} is the amount of applied inorganic nitrogen by pig slurry, $N_{net\ min}$ is the net mineralization of soil and manure organic nitrogen during Δt, N_{upt} is the nitrogen crop uptake, and N_{leach} is the amount of nitrate leached below z_d, upwards water fluxes being considered negligible in our conditions. All the terms are expressed in kg N ha^{-1}. Note that gaseous losses were neglected in Eq. (3).

Equation (3) was also applied to the control plot with N_{appl} = 0 and only soil organic nitrogen was concerned in the mineralization process.

ΔN_{min} was calculated from total nitrogen concentrations measured on soil samples taken at different depths and dates. N_{upt} was calculated from the plant total N concentration between the same dates. The amount of nitrate leached below z_d was estimated by:

$$N_{leach} = 10 C_r D \quad (4)$$

where C_r, expressed here in g L^{-1}, is the resident nitrate concentration of the soil solution extracted by porous cups at z_d and D (mm of water) is given by Eq. (2). Note that Eq. (4) assumes that dispersive transport is negligible as compared to convective transport.

Consequently, Eq. (3) calculates the net mineralization, $N_{net\ min}$, with all other terms being known.

It was assumed that nitrogen input from rain was negligible since winds in the vicinity of the experimental site come during most of the time from sea, which is very close to the field station.

2.2. Modelling

2.2.1. Modelling description and conditions

The process-based WAVE model (Vanclooster et al., 1994) describes the one-dimensional vertical transport and transformations of matter (water and agrochemicals) and energy in the soil-crop continuum. It combines the SWATNIT model (Vereecken et al., 1991), that integrates the SWATRER model (Feddes et al., 1978), a nitrogen module based on the SOILN approach (Bergström et al., 1991), a heat and solute transport model based on LEACHN (Wagenet and Hutson, 1989) and the crop growth SUCROS model (van Keulen et al., 1982; Spitters et al., 1988). A very detailed description of the model was given by their developers (Vanclooster et al., 1994, 1995), and more recently by Duwig et al. (2003). It should be mentioned that since our field experiments did not provide the necessary data to use the SUCROS module, the plant growth was forced by the observed time variations in the LAI, the crop coefficient (K_c) and root density profiles.

For both treatments, WAVE was applied to a 0–200 cm soil profile divided into four layers (0–10, 10–30, 30–100 and 100–200 cm). Each layer was defined according to observed soil properties (Table 1) and was assumed to be homogeneous. The model was forced at the soil surface by daily rainfall and PET values. The upper boundary condition for infiltrated water was either flux or pressure head type depending on the rainfall intensity as compared to the soil infiltrability. The free drainage condition was set at the bottom of the soil profile (z = 200 cm). The air temperature was measured at the soil surface. The soil temperature at z = 200 cm was considered constant in time and set at 24 °C. For the PSP treatment, quantities of organic and mineral nitrogen in pig slurry were measured at the surface. The organic fraction was included in the manure pool of the 0–10 cm soil layer, and the mineral fraction (NH_4^+) was incorporated into the first 10-cm depth. For the CP treatment, zero flux was set at the surface for both organic and mineral N. For both treatments, a zero concentration gradient was set at the bottom of the simulated flow domain for NO_3^- and NH_4^+ solutes.

Measured values of soil volumetric water content and solute concentration in the profile as well as C and N concentrations in the different organic matter pools (see below) were entered as initial conditions of every simulation run. The initial soil temperature profile was provided by thermocouple measurements.

Water, heat and solute equations of WAVE were solved by using a finite difference technique with a regular node spacing of 0.5 cm and a variable time step ranging from a few seconds for fast processes, such as transport phenomena and solute transformations during rainfall, to 1 day for slower processes such as evapotranspiration.

Table 5
Overview of the most important model parameters and summary of the way they were acquired.

	Model parameter	Values			Sensitivity analysis
		Prescribed	Measured	Calibrated	
Water	θ_r	0			n/a
	θ_s		Field + lab.		n/a
	α_d; n		Field + lab.	100–200 cm	(+)
	K_s; η		Field	0–10 cm	(+)
	S_{max} (0); $\gamma(h)$	0.03 d^{-1}; (a)			(+); n/a
	L_r		Field (Table 4)		n/a
	RDENS (0)		0.6 cm cm^{-3}		n/a
	α_{rdens}		4×10^{-2} cm^{-1}		n/a
	RORAD	2.2×10^{-2} cm			n/a
	D_0	10^{-3} m			n/a
	$CanStor_{max}$	0.5 mm d^{-1}			(+)
	LAI, K_c		field (Table 4)		(+); (+)
Heat	$C^*(\theta)$; $\kappa(\theta)$	(b)	ρ_d (Table 1)		n/a
Solute	λ		Laboratory		(+)
	D_0	12×10^{-5} m^2 d^{-1}			n/a
	a; b	10^{-2}, 10			n/a
	K_d (NO_3^-)		Laboratory	4 soil layers	(+)
	K_d (NH_4^+)			4 soil layers	(+)
	RNMAXP	170 kg N ha^{-1}			n/a
N-transformations	f_e; f_h	0.5; 0.15			(+); (+)
	K_{nit}	0.1 d^{-1}			(+)
	K_{denit}; K_{volat}; K_{lit}	0; 0; 0			n/a
	K_{man}			4 soil layers	+
	K_{hum}			4 soil layers	+

Parameters submitted to a sensitivity analysis are indicated by (+). All the symbols are defined along the text.
(a) Feddes et al., 1978; (b) de Vries (1952).

2.2.2. Model parameters

The most important WAVE parameters are summarized in Table 5 along with the way they were obtained.

2.2.2.1. Soil water flow and related maize crop parameters. Measured soil water pressure head versus volumetric water content and hydraulic conductivity versus water content were readily fitted by van Genuchten (1980) linked by Burdine (1953) equation and Brooks and Corey (1964) expression. However, preliminary WAVE simulations showed the need to calibrate some of these parameters (see below). The resulting values are given in Table 6 for the four layers. Crop coefficient, K_c, as a function of the maize phenological stages, was taken from values given by Doorenbos and Pruitt (1977) forced on field measurements obtained at some selected dates (Table 4). Since no actual amount of rainfall (R) intercepted by the canopy data for maize was found in the literature, a $CanStor_{max}$ value of 0.5 mm d^{-1} given by Rutter and Morton (1977) for small trees was used.

The actual crop water uptake rate, $S(h, z)$, proposed by Feddes et al. (1978) was used and its related critical pressure heads of the $\gamma(h)$ function were assigned to the values cited by Hupet et al. (2003) for maize. The maximum root water uptake $S_{max}(z)$ (Feddes et al., 1978) was described by an exponential decay function for depth which was determined from observed root length density profiles. For both treatments, the decay coefficient was estimated at 0.03 d^{-1}. Average root radius (RORAD), root length density at the soil surface ($RDENS_0$), and its decay coefficient with depth (α_{rdens}) were set at 2.2×10^{-2} cm, 0.60 cm cm^{-3} and 4×10^{-2} cm^{-1}, respectively. The mean distance between the soil solution and the root surface was set at $D_0 = 10^{-3}$ m. Maximum nitrogen uptake by maize (RNMAXP) was set at 170 kg N ha^{-1}. On the PSP, the observed time course of the root front depth, L_r, was found to be highly linear at a growing rate of 1.4 cm d^{-1} from the end of germination (7 DAS) to 100 DAS where it reached 140-cm depth (Table 4). On the CP, the temporal development of the root front was more erratic with a slower growth rate (0.90 cm d^{-1}) than in the PSP for the first 50 DAS, with a faster rate between 50 and 70 DAS, so the front reached a maximum depth equivalent to that of the PSP at 100 DAS (Table 4). More details can be found in Chopart et al. (2007).

2.2.2.2. Heat transfer parameters. Soil volumetric heat capacity, $C^*(\theta)$, and thermal conductivity, $\kappa(\theta)$, as function of the soil bulk dry density ρ_d (Table 1) and volumetric water content θ were calculated according to the de Vries equations (1952) encapsulated in WAVE.

2.2.2.3. Solute movement and nitrogen cycle parameters. The diffusion coefficient D_0 and its related parameters a and b were set at $D_0 = 12 \times 10^{-5}$ m^2 d^{-1}, $a = 0.001$ and $b = 10.0$, respectively (Olsen

Table 6
Summary of some selected soil parameters used in the WAVE model.

Soil layer (cm)	ρ_d (Mg m^{-3})	θ_r (m^3 m^{-3})	θ_s (m^3 m^{-3})	α_d (mm^{-1})	n	K_s (mm h^{-1})	η	λ (mm)	K_d [NO_3^-] (L kg^{-1})	K_d [NH_4^+] (L kg^{-1})
0–10	0.97	0	0.64	2.7	2.12	45[a]	0.49[a]	10	1.11[a]	2[a]
10–30	0.83	0	0.65	2.6	2.09	78	0.67	10	1.11[a]	2[a]
30–100	0.82	0	0.67	0.9	2.08	283	0.04	30	0.50[a]	0[a]
100–200	0.76	0	0.72	2.0[a]	2.04[a]	283	0.02	30	0.30[a]	0[a]

ρ_d: dry soil bulk density; θ_r, θ_s, α_d, and n: parameters of the van Genuchten equation; K_s and η: parameters of the Brooks and Corey equation; λ: dispersivity length; K_d [NO_3^-] and K_d [NH_4^+]: partition coefficients for nitrate and ammonium, respectively.
[a] Calibrated values.

and Kemper, 1968 cited in Vanclooster et al., 1994). Dispersivity lengths, λ, were obtained in the laboratory from measured breakthrough curves of a solution of KCl percolating into repacked soil columns. They were estimated at 10 mm for the first two top layers (0–10 and 10–30 cm) and at 30 mm for the other two deeper layers (Payet, 2005). These values are similar to those obtained by Duwig et al. (1999) for a ferralitic-allitic tropical soil and fall within the range reported by Ramos and Carbonel (1991) for repacked soils. Laboratory experiments carried out on both batch reactor and column with soil repacked at the same bulk density as in the field showed that NO_3^- was significantly adsorbed in this andic soil. Experimental values were adequately represented by linear isotherms of adsorption (Payet, 2005). However, the first WAVE simulation runs showed that the corresponding solute distribution coefficient (K_d) values were not fully satisfying with respect to properly representing the *in situ* nitrate transport. Consequently, they were calibrated by fitting the model to the experimental field data (see below). The resulting values are given in Table 6 for the four soil layers. They led to retardation factors ($RF = 1 + \rho_d K_d/\theta$) of about 2.8, 2.6, 1.7 and 1.4, respectively, from top to bottom. The calibrated K_d [NO_3^-] values appeared to be similar to those given by Kinjo and Pratt (1971) and Maeda et al. (2003) for different andic soils of comparable acidity, but higher than estimates reported by Duwig et al. (2003) for a tropical oxidic ferralitic soil that also presented anionic retention.

Ammonium was also considered to be reactive with the soil particles. K_d [NH_4^+] was estimated at 2×10^{-3} m^3 kg^{-1} for the 0–10 and 10–30 cm soil layers, and at 0 for the two other ones by fitting the model to the experimental data (see below). The retardation factors for the first two top layers (RF = 4.2 and 3.9, respectively) were significantly higher than those for nitrate. This means that NH_4^+ transport would likely be more delayed than NO_3^- and obviously more than the water flow. Calibrated K_d [NH_4^+] values (Table 6) were close to those suggested by Vereecken et al. (1991), but higher than those reported by Ducheyne et al. (2001) for most soils in Belgium, ranging from silt to clay.

Some of the *N* turnover parameters were taken from literature values given in the WAVE user's manual (Vanclooster et al., 1994). The C turnover efficiency f_e was set at 0.5 for a well aerated soil, and the humification constant f_h was set at 0.15. For the control plot, the total soil organic matter was represented only by the humus pool because all the shoots of the previous oat crop were hand removed. This led to consider negligible the litter degradation rate K_{lit}. For the pig slurry plot, the total soil organic matter was represented by the humus and slurry pools. Since no detailed study on the fate of organic matter was carried out, the decomposition rates were obtained by the best fit between WAVE outputs and field data (see below). For both plots, the humus decomposition rates (K_{hum}) were retained at 9×10^{-5}, 6×10^{-5} d^{-1} for the first two layers (0–10 cm and 10–30 cm), and 0 for the deeper layers. The decomposition rate of manure (K_{man}) for the PSP treatment was 0.02 d^{-1} for the same two top layers, and 0 for the deeper ones. NH_4^+ nitrification was described by a high constant ($K_{nit} = 0.1$ d^{-1}) since ammonium was observed to disappear rapidly in the 0–30 cm horizon. The denitrification constant K_{denit} was assumed to be 0. Volatilization rate, K_{volat}, was also set at 0 because pig slurry was applied in the absence of wind and immediately incorporated into the surface layer. In addition, it was thought that the initial soil and pig slurry pH values (Tables 1 and 2, respectively) led to a mean value of under pH 7 for which volatilization can be neglected (Stevenson, 1982). The C/N ratio of the soil organic matter was calculated as the mean between the C/N value given by Bradbury et al. (1993) for microbial biomass in arable soils (C/N = 6.7) and the measured organic matter at the soil surface (C/N = 9.3). The resulting value (C/N = 8.0) falls well within the range of data reported in the literature (Dendooven, 1990).

2.3. Modelling strategy

The model had to be calibrated due to the lack of knowledge of some parameters and/or uncertainties in their experimental determinations. This was achieved step by step to account for interactions between organic matter transformations and transport processes. First, the water flow sub-model was calibrated on both plots. Then, parameters for solute transport and nitrogen transformation were calibrated using control plot data. Finally, data collected on the pig slurry plot allowed calibration of the manure decomposition rate. A summary of some selected parameters is given in Table 6. The calibration procedure was based on the assumption that transport and transformation parameters did not vary between both plots. It was performed on the 2004–2005 field measurements since that year presented the most complete dataset.

Assessment of parameter sensitivity prior to any model calibration is of paramount importance, as efforts should normally be concentrated on parameters for which the simulation model is most sensitive. In the present work, a sensitivity analysis was carried out empirically to evaluate the impact of parameter uncertainties on model outputs.

The results obtained by WAVE with the set of calibrated parameters (P_{opt}) were considered as the control solution Y_{opt} for the sensitivity analysis. The model was subsequently run many times for different input parameter values. For each evaluation, the output Y was compared to Y_{opt} and the results were expressed in terms of the relative error $y = (Y - Y_{opt})/Y_{opt}$ which arises from the relative uncertainty $x = (P - P_{opt})/P_{opt}$ introduced to parameter P. These are listed in Table 5. Note that since only one parameter was changed at once (with the others kept unchanged), it was not possible to study correlated effects on the parameter sensitivity. This analysis was mainly focused on drainage and nitrate leaching losses below the root zone.

The prediction capacity of WAVE was subsequently evaluated on the 2003–2004 data, by not changing the parameter values from the model calibration. For both the calibration and validation stages, a trial and error method was adopted, using statistical and graphical criteria for evaluating the model performance. The Nash efficiency coefficient, EF (Nash and Sutcliffe, 1970), the normalized root mean square error, NRMSE, and the coefficient of residual mass, CRM (Loague and Green, 1991) were used to express the goodness of fit between simulated and observed values. EF, NRMSE and CRM should be as close as possible to 1, 0, and 0, respectively. Negative EF values mean that the mean measurement value is a better estimate of the measurements than the model. Since WAVE is a mechanistic-based model, we considered that it was important to not only consider fluxes across the soil profile boundaries (actual evapotranspiration and runoff at the surface, drainage and nitrate leaching losses below the root zone), but also to look at the internal state variables (temporal variations in soil water content, soil water pressure head, NH_4^+ and NO_3^- concentration at different depths) in the comparison between simulated and observed values.

3. Results and discussion

3.1. Agricultural practices and crop development

Table 2 shows that there was high yearly variability in the physicochemical characteristics of slurries, as also mentioned by Leirós et al. (1983) or Sánchez and González (2005). The slurry spread in 2003 was richer in nitrogen than that applied in 2004. In 2004, 89% of the pig slurry nitrogen content was in the form of ammonium, as compared to 75% in 2003. Different C/N values in 2003 and 2004 could reflect more or less important nitrogen

immobilization (Morvan et al., 1996). The maize crop in the PSP had a higher LAI than in the CP in 2004 and 2005 (Table 4). However, the values were relatively low as compared to those generally noted in temperate regions. This could mainly be attributed to the low solar radiation during the cropping cycles. At harvest, the total dry matter (Table 3) in the PSP was 60% higher than in the CP in 2004 and 44% higher in 2005. Pig slurry application substantially improved maize shoot biomass development. Nitrogen uptake by the maize crop was higher both years in the PSP and could have been linked to the application of high amounts of mineral and organic nitrogen. In 2004, a 264 kg N ha^{-1} application resulted in an 81 kg N increase in N uptake by the maize crop, and in 2005 a 185 kg N ha^{-1} application resulted in an 74 kg N increase. On this basis, a mineral fertiliser equivalent (MFE) was calculated for the pig slurry and ranged from 30.7 to 40%, whereas MFE values for pig slurry mentioned by several authors (Chabalier et al., 2006; Sorensen and Eriksen, 2009) ranged from 60 to 100%. Although our experiment was not designed to assess MFE in optimal conditions, it can be assumed that the values obtained were lower than usually obtained.

3.2. Water flow

Daily rainfall and potential evapotranspiration values for the two cropping seasons are displayed in Figs. 1 and 2, which also show examples of the time course of volumetric water content and water pressure heads measured at two depths (15 and 150 cm) for each treatment. Cumulative values of the soil water balance components as a function of time are presented in Fig. 3 for both maize cycles and plots. Values between sowing and harvest are given in Table 7.

Rainfall in 2003–2004 was 720 mm and 1041 mm in 2004–2005. In the 2004–2005 cropping season, eight rainstorms exceeded 50 mm d^{-1} and only three in 2003–2004. No cyclones affected the island during the two study periods.

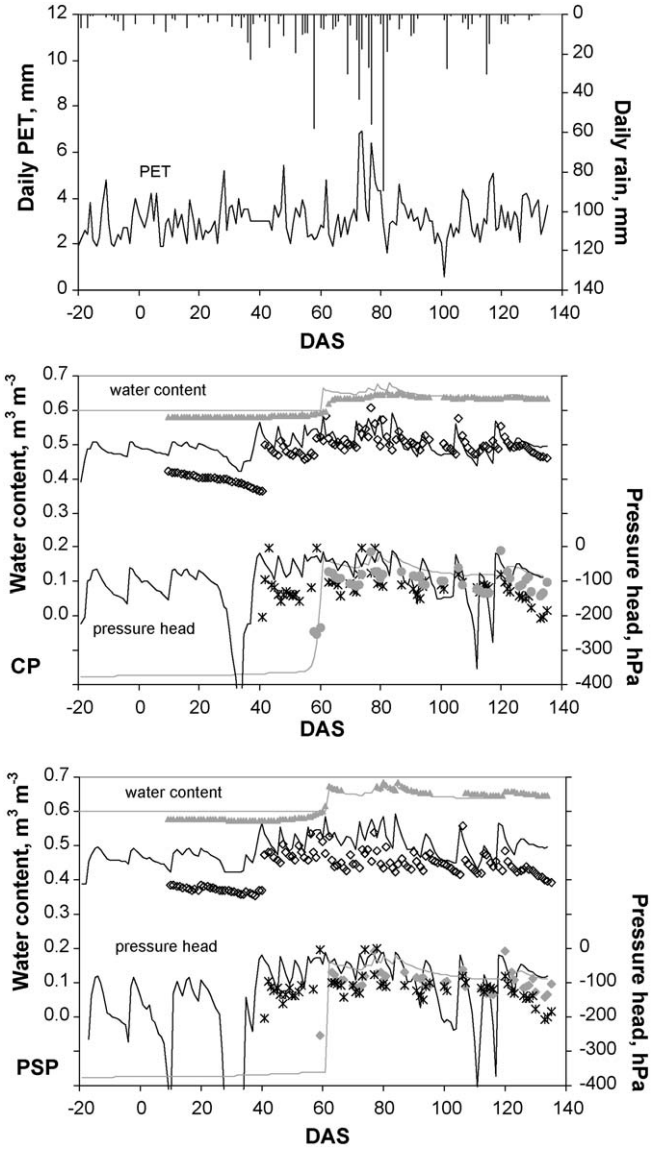

Fig. 1. Measured (symbols) and simulated (continuous lines) soil volumetric water content and water pressure head at 15 cm (in grey) and 150 cm (in black) depths of both treatments for the 2003–2004 year (model validation). Daily values of precipitation (R) and potential evaporation (PET) are also reported. Maize was sown on 20 November (DAS = 0) and pig slurry was applied on the PSP on 29 October 2003.

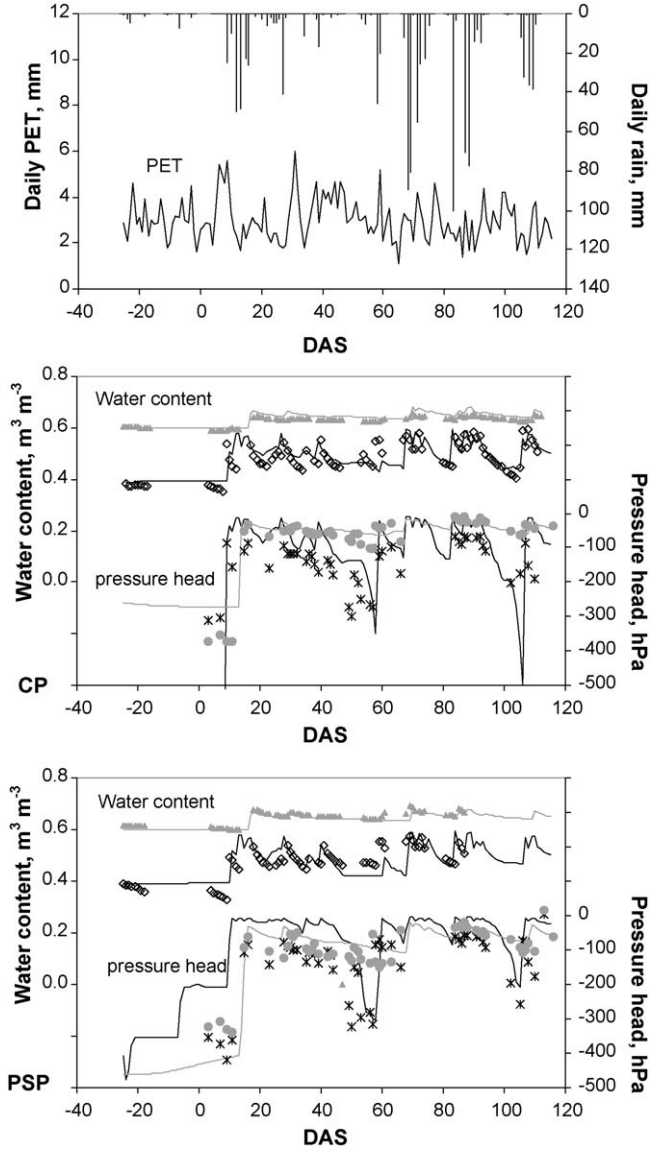

Fig. 2. Measured (symbols) and simulated (continuous lines) soil volumetric water content and water pressure head at 15 cm (in grey) and 150 cm (in black) depths of both treatments for the 2004–2005 year (model calibration). Daily precipitation (R) and potential evaporation (PET) values are also reported. Maize was sown on 6 December (DAS = 0) and pig slurry was applied on the PSP treatment on 20 November 2004.

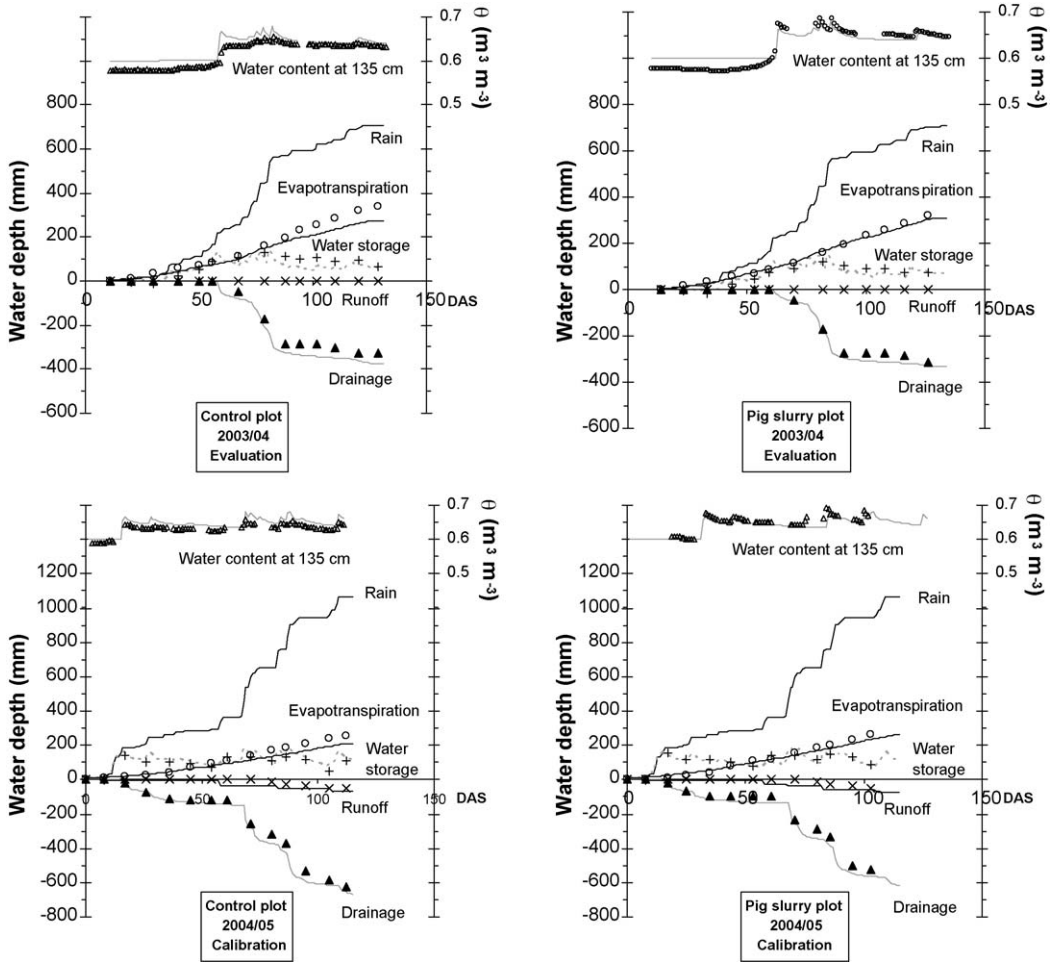

Fig. 3. Measured (symbols) and simulated (continuous or dotted lines) cumulative soil water balance component values during the 2003–2004 (model evaluation) and 2004–2005 (model calibration) cropping seasons for both treatments. DAS is day after sowing.

Table 7
Measured and simulated cumulative soil water balance component values between maize sowing and harvest in both treatments and for the two cropping seasons.

Rainy season	Treatment		ΔS between 0 and 135 cm	AET	Drainage at 135 cm	Surface runoff
2003–2004	Control plot	Measured	68	312	329	0
		Simulated	58	276	375	0
2003–2004	Pig slurry plot	Measured	72	319	318	0
		Simulated	69	308	332	0
2004–2005	Control plot	Measured	134	257	625	50
		Simulated	127	213	657	69
2004–2005	Pig slurry plot	Measured	140	285	591	50
		Simulated	128	257	607	74

ΔS and AET are the soil water storage variation and actual evapotranspiration, respectively. Values are in mm.

For both treatments, while the TDR probe and tensiometers set up at 15 cm depth reacted to almost every rain event, responses at 150 cm depth were only sensitive to rain intensities higher than 30 mm d^{-1}. For both plots and years, drainage began to occur when the soil water storage reached field capacity, corresponding to about 100 mm excess water in the 0–135 cm soil layer (which then contains 850 mm). Thereafter, all rain events higher than 30 mm d^{-1} led to drainage at 135 cm depth. About 320 mm in 2003–2004 and 610 mm in 2004–2005 were drained beyond the root zone (Table 7), which corresponded to 45 and 57% of the rain quantities, respectively. Note that drainage loss of the PSP was slightly lower than that of the CP (by 3% in 2003–2004 and 5.5% in 2004–2005). In terms of dynamics, drainage was very fast when the soil water content was close to saturation: approximately 30% of any substantial rain was drained beyond the root zone within 24 h. This was attributed to the high hydraulic conductivity of this soil (Table 6) and corroborates results obtained in other andic soils by Shoji et al. (1993), Fontes et al. (2004) and Cattan et al. (2006). This high hydraulic conductivity also explains that very little runoff was observed in spite of the very high rain intensities. In 2003–2004, no runoff was measured on either of the plots and only 50 mm (4% of the total precipitation) was recorded in 2004–2005. Runoff occurred during very heavy rains. For instance, at 83 DAS, 12 mm was measured for a rain event of 85 mm h^{-1}, i.e. a much higher intensity than the saturated hydraulic conductivity (45 mm h^{-1}) of the soil surface (Table 6). For both cropping seasons, in both plots, cumulative actual evapotranspiration (AET) values were close to maximum (more than 90%), indicating that

water was not a limiting factor. AET in PSP was slightly higher (by about 2% in 2003–2004 and 10% in 2004–2005) than in the CP (Table 7). This is in line with drainage loss results and with the better growth of maize on PSP, as confirmed by the higher dry matter yield on this plot (Table 3).

3.2.1. Model calibration and sensitivity analysis

The first WAVE simulation runs showed that some of the input parameters required calibration, although they were experimentally obtained. This was achieved through a trial and error approach to define the objective function, as the differences between simulated and observed time series of water contents and water pressure heads at 15, 30, 60, 90, 120, 150, and 180 cm depth for the 2004–2005 cropping period. Table 6 gives the calibrated values of the saturated hydraulic conductivity (K_s) and of the shape factor (η) (Brooks and Corey, 1964) for the superficial soil layer (0–10 cm), and of n and the scale factor (α_d) (van Genuchten, 1980) for the 100–200 cm soil layer. The corresponding simulated results are reported in Fig. 2 for water contents and water pressure heads at 15 and 150 cm depths and in Fig. 3 for the soil water budget components. Statistics are given in Table 8 for h and θ at different depths.

For both treatments, Fig. 2 shows that the time course of the experimental water content and water pressure head values were fairly reproduced by the model. However, the statistics for h and θ (Table 8) differed depending on the criteria used. For instance, based on CRM values, WAVE tended to slightly underestimate (resp. overestimate) the observed water content values in the pig slurry treatment (resp. control treatment). At some depths, the two other criteria indicated a very satisfactory representation of the measured water contents (i.e. EF = 0.97 and NRMSE = 13.4% at z = 120 cm, or EF = 0.71 and NRMSE = 6% at z = 150 cm for PSP; EF = 0.92 and NRMSE = 3.4% at z = 60 cm, or EF = 0.84 and NRMSE = 3.1% at z = 90 cm for CP). At other depths, (i.e. z = 30, 90 and 180 cm for PSP; z = 15, 120 and 180 cm for CP), the EF values indicated a poor restitution of the measured water contents by WAVE, while the NRMSE values were still very acceptable (except at z = 180 cm for PSP). The water pressure head results were not as accurately reproduced by the calibrated model for both treatments, especially for the surface layers, when the discrepancies were measured according to the NRMSE statistics, and via the EF statistics for the deeper layers. Apart from the fact that there were fewer measurements than for the water contents, it may also have been due to the nonlinear shape of the water retention curve with increasing sensitivity of h to θ uncertainties as the water pressure head decreased. Similar behaviour was also reported by Duwig et al., 2003. Moreover, detailed assessment of the h time series (Fig. 2) showed that the greatest discrepancies between the observed and simulated values occurred when the soil was relatively dry, and corresponded to a range of water pressure heads

Table 8
Statistics of EF, NRMSE and CRM between observed and simulated values at different depths for the WAVE calibration and validation.

H	Control plot						Pig slurry plot					
	2003–2004[a]			2004–2005[b]			2003–2004[a]			2004–2005[b]		
	EF	NRMSE	CRM	EF	NRMSE	CRM	EF	NRMSE	CRM	EF	NRMSE	CRM
	N = 52			N = 48			N = 52			N = 48		
15 cm	<0	−78.5	−19.1	0.89	−121.5	0.7	<0	−111.7	11.5	0.71	−159.6	−26.0
30 cm	<0	−47.9	−6.2	0.84	−153.4	15.4	<0	−31.7	3.5	0.85	−172.9	34.3
60 cm	0.77	−32.1	−9.0	<0	−39.6	−6.3	<0	−88.1	14.1	0.98	−379.3	51.5
90 cm	0.85	−29.4	−6.9	<0	−50.4	−9.0	<0	−72.8	7.4	<0	−37.4	−6.8
120 cm	0.86	−31.5	−1.6	<0	−41.3	−6.1	0.84	−32.6	−13.7	0.38	−85.2	−3.9
150 cm	–	–	–	–	–	–	<0	−205.2	39.9	<0	−42.2	−3.8
180 cm	–	–	–	–	–	–	0.94	−22.3	−4.6	0.32	−79.9	−5.4
θ	Control plot						Pig slurry plot					
	2003–2004[a]			2004–2005[b]			2003–2004[a]			2004–2005[b]		
	EF	NRMSE	CRM	EF	NRMSE	CRM	EF	NRMSE	CRM	EF	NRMSE	CRM
	N = 125			N = 85			N = 125			N = 85		
15 cm	0.31	11.5	7.0	<0	13.5	6.1	0.42	10.5	0.0	0.75	21.8	7.2
30 cm	0.35	6.2	−5.5	0.73	16.3	−11.1	0.55	9.1	4.4	<0	12.6	−14.3
60 cm	0.76	4.0	2.6	0.92	18.3	−11.1	<0	8.8	−7.1	0.14	7.8	−14.1
90 cm	0.68	5.8	4.0	0.84	13.1	−8.3	0.35	6.7	7.0	<0	5.4	−2.3
120 cm	0.49	5.7	4.9	<0	3.8	−2.1	<0	5.4	−5.4	0.97	13.4	−2.5
150 cm	0.63	2.8	2.9	0.544	9.4	6.2	0.80	2.9	1.3	0.71	6.0	6.3
180 cm	0.86	1.7	−1.1	<0	1.8	0.7	0.86	1.7	0.1	0.02	55.8	0.7
C	Control plot						Pig slurry plot					
	2003–2004[a]			2004–2005[b]			2003–2004[a]			2004–2005[b]		
	EF	NRMSE	CRM	EF	NRMSE	CRM	EF	NRMSE	CRM	EF	NRMSE	CRM
	N = 9			N = 9			N = 9			N = 9		
0–10 cm	<0	113.1	−5.3	0.30	63.3	−3.3	0.82	48.3	−1.2	0.39	77.0	−3.8
10–30 cm	<0	108.9	−1.5	0.63	38.2	1.1	0.01	86.9	−0.1	0.65	54.5	3.2
30–60 cm	<0	192.1	7.0	0.10	43.2	−0.3	<0	67.1	−2.8	0.11	44.6	−1.9
60–90 cm	<0	208.7	5.4	0.57	33.9	1.4	0.40	40.8	−3.1	<0	41.7	1.5
90–120 cm	0.41	93.3	−0.6	0.76	27.1	−1.3	<0	80.9	−6.6	0.62	25.0	1.1
120–150 cm	<0	91.9	0.3	<0	62.2	−3.9	<0	128.5	−7.6	0.65	29.6	0.2
150–180 cm	0.28	61.6	1.1	<0	69.4	−5.1	<0	113.1	−7.3	<0	54.1	−0.8

NRMSE and CRM are expressed in %. N is the number of observations.
[a] Model validation.
[b] Model calibration.

within which the tensiometers may not have efficiently functioned (below about -5 to -6×10^2 hPa).

The time course of the observed cumulative values of the soil water budget components was reasonably well simulated by the calibrated model, as seen in Fig. 3 for both plots, with a slight overestimation of experimental values of drainage losses from sowing to harvest and underestimation of water storage variations (Table 7). Estimates of actual evapotranspiration were more drastically underestimated for the control (17%) and pig slurry (9.8%) treatments. Nevertheless, these discrepancies, which mainly occurred at the end of the cropping season (Fig. 3), could still be considered acceptable when considering that the experimental AET values were indirectly obtained from the closure of the soil water budget (Eq. (1)). All of these differences resulted in a relatively poor simulation of the measured runoff volumes, which were overestimated by 31% and 48% for the CP and PSP treatments, respectively. Note, however, that the calibrated K_s and η values for the 0–10 cm soil layer allowed a faithful reproduction of the observed runoff onset time on both plots.

Fig. 4 presents the relative errors (y) of the cumulative drainage losses at z_d = 135 cm as a function of the following input parameter relative uncertainties (x): K_c, LAI, S_{max}, $CanStor_{max}$, K_s and η. The model calculations were performed using the 2004–2005 meteorological data. The responses of WAVE to these uncertainties were nonlinear and nonsymmetric. For instance, underestimation of K_c led to higher error in drainage than that resulting from an equivalent overestimation of the same parameter. Among the parameters which were considered, K_c, K_s, η (and to a lesser extent S_{max}) were the ones which more affected the drainage. As reported by Duwig et al. (2003) for maize growing in wet tropical conditions, cumulative drainage simulated by WAVE was also very sensitive to K_c, while this is one of the most difficult parameters to accurately determine. Similar trends were obtained by Chopart and Vauclin (1990) for upland rice in Côte d'Ivoire, as well as by Hupet et al. (2003) who found that K_c was the third most sensitive parameter, after θ_s and n, for maize cultivated in a medium–fine soil (K_s = 50 mm d^{-1}). Drainage was not very sensitive to LAI and $CanStor_{max}$, at least in their variation range. The influence of parameters α_d and n, describing the water retention curve for the 100–200 cm soil layer with respect to drainage loss was found to be negligible (results not shown). Drainage was not very sensitive to the saturated hydraulic conductivity (K_s) of the surface layer, as long as it remained higher than a critical value for allowing water to infiltrate into the soil. On the other hand, the cumulative drainage at the base of the soil was very sensitive to scale parameter η. However, it was not necessary to make it vary in such proportions during the model calibration. The influence of parameters α_d and n, describing the water retention curve for the 100–200 cm soil layer with respect to drainage loss was found negligible (results not shown).

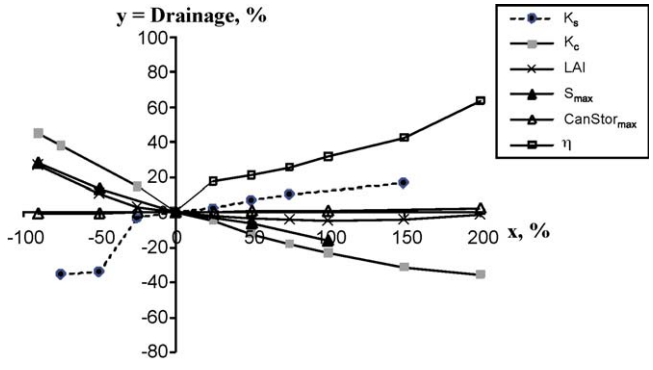

Fig. 4. Relative sensitivity of the simulated cumulative drainage losses at 135 cm depth to relative changes (y-axis) in the model input parameters (x-axis): crop coefficient (K_c), leaf area index (LAI), maximum crop water uptake (S_{max}), maximum amount of rainfall intercepted by canopy ($CanStor_{max}$) and hydraulic properties (K_s, η) of the 0–10 cm soil layer (mean values between the control and pig slurry plots).

3.2.2. Model evaluation

WAVE was evaluated on data collected during the 2003–2004 cropping season, which was a much drier season than 2004–2005, and the calibrated parameters were unchanged. Table 8 shows that the water content measurements at all depths were very well reproduced on the control plot (EF ranged from 0.31 to 0.86, with a mean of 0.58, NRMSE was under 11.5%, and the CRM values were close to 0). On the PSP, the measurements were not as accurately simulated by the model. However, the agreement was still very acceptable on the basis of all the statistics, except for EF at two depths (60 and 120 cm). On the other hand, for both plots, measured water pressure heads (Fig. 1) were poorly reproduced, with most of the EF values being negative, especially in the first soil layers (Table 8). These poor values are due to the fact that the $h(\theta)$ curve was calibrated for high water contents encountered during the wet season 2004–2005 (Fig. 2), while the soil was still dry at the beginning of the 2003–2004 maize cycle. This may explain the marked discrepancies between the measured and predicted pressure heads. However, since one of the study objectives was to determine water and nitrate flows during the wet season, i.e. when the soil was close to saturation, poor reproduction of pressure heads by WAVE when the soil water contents were low was not considered to be a major drawback.

Fig. 3 shows that the water balance components were well predicted by WAVE for both treatments, with a slight drainage overestimation of 9.7% and 4.4% for the control and pig slurry plots, respectively (Table 7), and an AET underestimation of 11.5% for CP and 3.4% for PSP. In agreement with the observations, no runoff was predicted by the model.

3.3. Nitrogen

Time courses of mineral nitrogen (ammonium and nitrate) quantities measured in the first two soil layers (0–10 cm and 10–30 cm) are presented in Fig. 5 for both treatments and seasons. The resident nitrate concentration in the soil solution, measured at z_d = 135 cm as function of time, as well as the nitrogen budget components are plotted in Fig. 6. Table 9 gives the cumulative values of all terms of the nitrogen balance between pig slurry application and harvest dates. Note that the first measurements were obtained before the pig slurry application and maize sowing dates of each year. This explains the negative DAS values on the x-axis in Figs. 5 and 6. Fig. 7 shows the soil mineral nitrogen concentration profiles measured in both treatments at three dates per cropping season (a few days before slurry spreading, about 30 days and 120 days afterwards).

On the control plot and for both years, the increase in N storage measured in the 0–10 cm and 10–30 cm layers up to 50 kg N ha^{-1} the first 50 DAS (Fig. 5) corresponded to natural soil mineralization since no fertilization was applied. This mineralization occurred when the soil was humid and the temperature high, which are favourable conditions for soil organic matter degradation. For andic soils of Mexico with very similar annual temperature and precipitation conditions, Salinas-Garcia et al. (2001, 2002) reported potential nitrogen mineralization rates ranging from 2.4 to 11.5 kg N ha^{-1} per day, i.e. even higher than the value obtained here (about 1 kg N ha^{-1} per day).

In the deeper layers of CP, the soil nitrogen contents remained very low during the two maize cycles (Fig. 7). This was confirmed by the nitrate concentrations in the soil solution, which were close to 0 at z_d = 135 cm (Fig. 6). Consequently, insignificant nitrate leaching under the root zone was observed (Table 9) during the

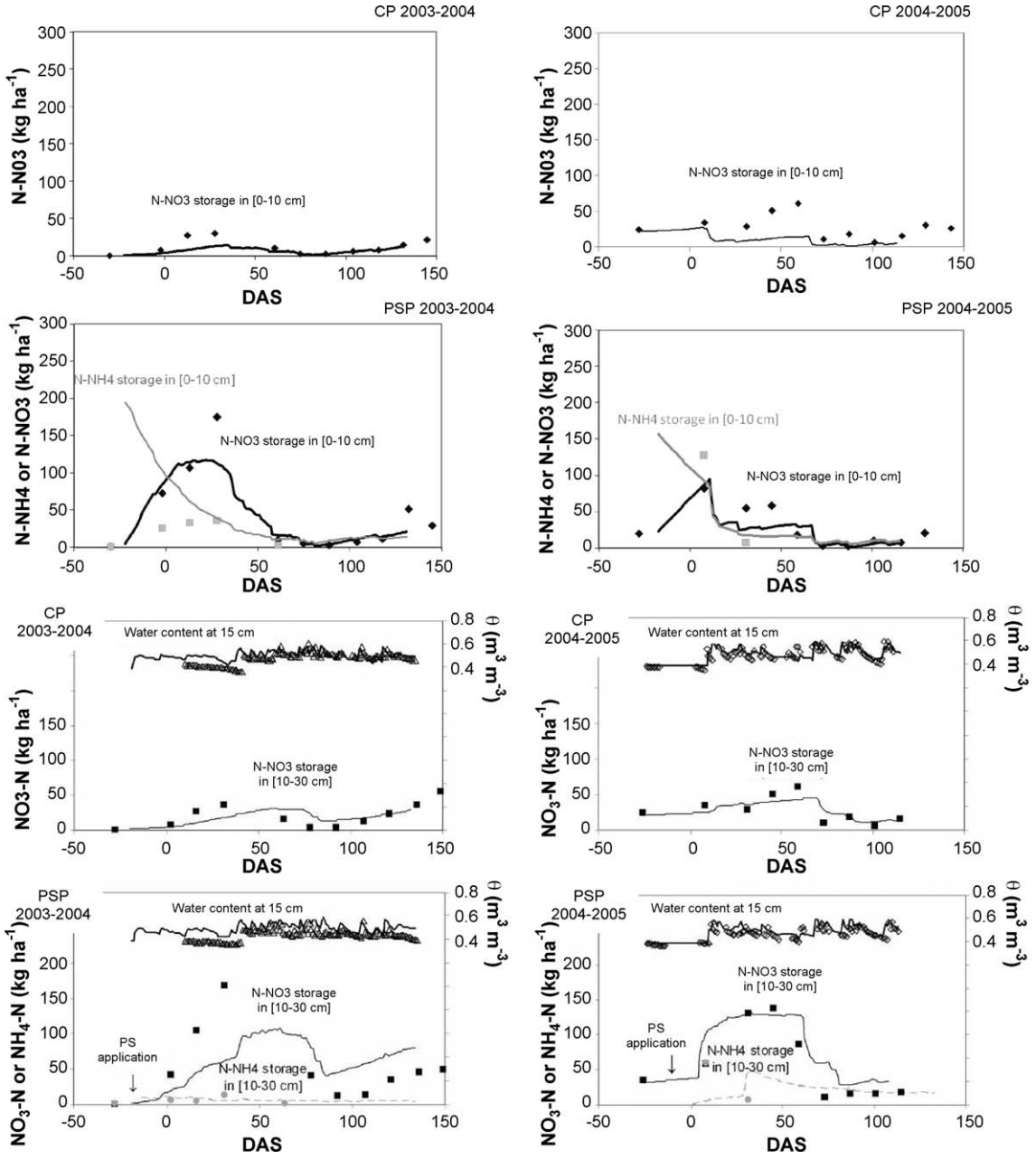

Fig. 5. Measured (symbols) and simulated (continuous or dotted lines) values of the amount of N-NO_3 and N-NH_4 stored in the [0–10 cm] (high) and [10–30 cm] (bottom) soil layers of the control (CP) and pig slurry (PSP) treatments during the 2003–2004 (model evaluation) and 2004–2005 (model calibration) cropping seasons. Time course of volumetric water content at 15 cm is also plotted. DAS is day after sowing.

two years (2 and 5 kg N ha^{-1} in 2003–2004 and 2004–2005, respectively), while drainage losses (Table 7) were estimated at 329 and 625 mm, respectively. In 2004–2005, the increase in soil nitrate observed in the 50–100 cm layer between 8 and 114 DAS (Fig. 7) was attributed to the nitrates produced by mineralization of soil organic matter in the superficial layers (Fig. 5) which were leached to deep horizons by heavy rains (635 mm) between 50 and 90 DAS (Fig. 2).

On the PSP, the increase in soil nitrate which occurred at the same time as on the CP (Fig. 5) was much more greater (+150 kg N ha^{-1}) and corresponded to two processes: (i) nitrification of the pig slurry ammonium and (ii) natural mineralization of the organic matter contained in both the soil and the pig slurry. According to Morvan (1999) and Morvan et al. (1997), nitrification processes after a pig slurry application on soil can last 3 weeks, whereas pig slurry organic matter mineralization ends after about 10 days. These values are in agreement with our results. In 2003–2004, a significant amount of mineral nitrogen was displaced from the surface to the 40–80 cm soil layer (Fig. 7). However, a very small amount of leaching (6 kg N ha^{-1}) was observed at z_d = 135 cm at the end of the cropping season (Table 9), although 264 kg N ha^{-1} was applied on that plot (Table 3) and 318 mm of water were drained beyond the root zone (Table 7). This clearly illustrated the retention of nitrate by the soil. Before the second pig slurry spreading in the 2004–2005 cropping season, the nitrate distribution with depth was comparable to that measured at the end of the 2003–2004 maize cycle, where most nitrates were located between 40 and 100 cm (Fig. 7). During the 2004–2005 cropping season, they migrated beyond the root zone due to heavy rainfall. Between 60 and 120 DAS, the resident concentration in the soil solution at z_d = 135 cm increased from 8 to 50 mg $N\text{-}NO_3^-$ L^{-1} (Fig. 6) while the drainage losses were 591 mm (Table 7). This led

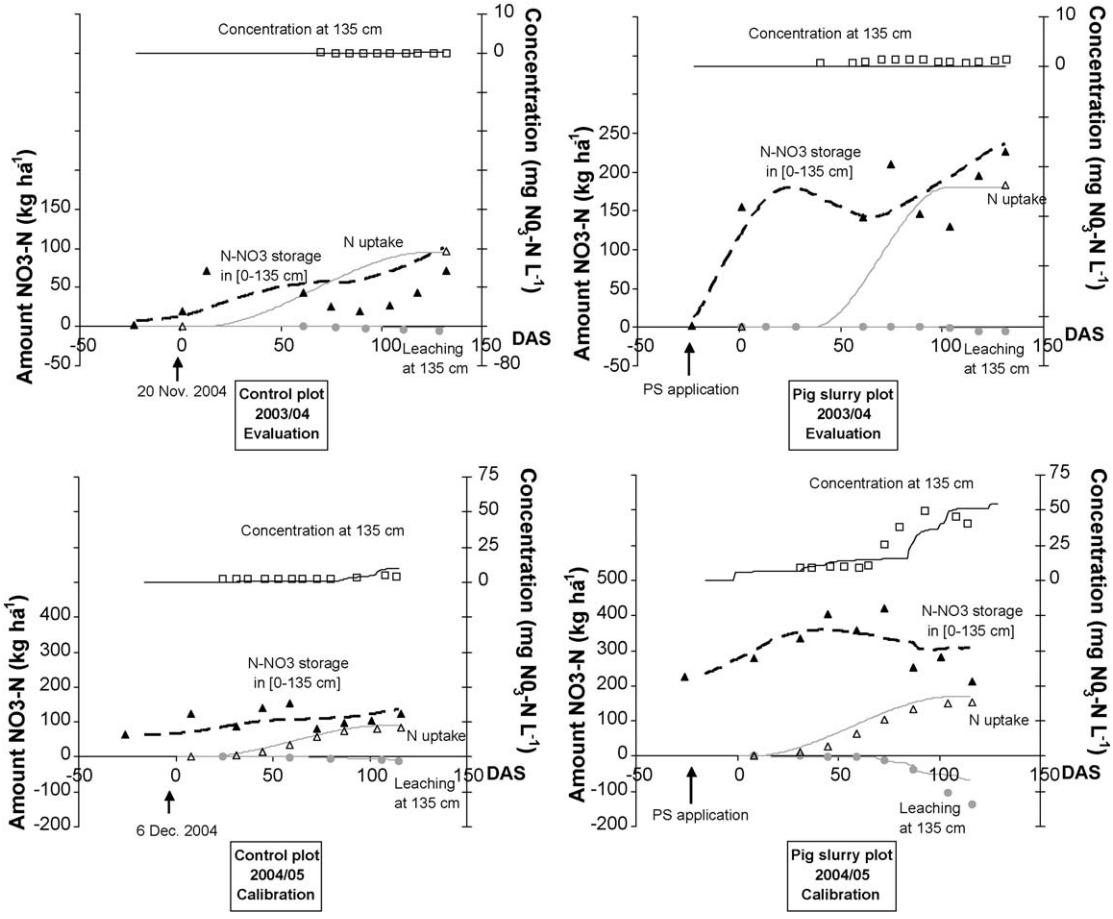

Fig. 6. Measured (symbols) and simulated (continuous or dotted lines) cumulative nitrogen balance component values during the 2003–2004 (model evaluation) and 2004–2005 (model calibration) cropping seasons for both treatments. Time course of the resident nitrate concentration is also plotted. DAS is day after sowing.

Table 9
Measured and simulated components of the nitrogen balance between pig slurry application and harvest dates for both CP and PSP.

Treatment		$\Delta(NH_4\text{-N})$ (kg N ha^{-1})	$\Delta(NO_3\text{-N})$ (kg N ha^{-1})	ΔN ($NH_4 + NO_3$) (kg N ha^{-1})	N_{appl} (kg N ha^{-1})	N_{uptake} (kg N ha^{-1})	N_{leach} (kg N ha^{-1})	$N_{net\ min}$ (kg N ha^{-1})
Evaluation (2003–2004)								
Control plot	Measured	–	99	99	0	102	2	203[a]
	Simulated	27	93	120	0	95	2	226 (−9)
Pig slurry plot	Measured	–	224	224	194[b]	183	6	219[a]
	Simulated	20	225	245	194[b]	180	2	246 (−13)
Calibration (2004–2005)								
Control plot	Measured	–	60	60	0	94	5	159[a]
	Simulated	24	74	98	0	89	8	180 (+15)
Pig slurry plot	Measured	–	56	56	157[c]	168	109	176[a]
	Simulated	31	80	111	157[c]	170	68	183 (+9)

Numbers in brackets are the budget error modelling defined as: $\varepsilon = \Delta N = (N_{harvest} - N_{in}) - (N_{appl} + N_{net\ min}) + N_{upt} + N_{leach}$, where N_{in} is the soil nitrogen storage just before the date of PSP application.

[a] Estimated from closure of the nitrogen budget by neglecting soil NH_4^+ storage at harvest.

[b] About 74% of total nitrogen content in PSP.

[c] About 85% of total nitrogen content in PSP (to account for total mineral N only).

to nitrate losses of 109 kg N ha^{-1} beyond the root zone (Table 9), which corresponded to about 60% of the total nitrogen of pig slurry ammonium applied in 2004. Thus, the first significant nitrate losses were observed more than 15 months after the first slurry spreading. During that period, 924 mm of water drained beyond the root zone (Table 7) which was slightly higher than the soil water storage of the 0–135 cm layer. Note that the onset of nitrate flux at z_d = 135 cm was delayed by about 2.2-fold as compared to that of the water flux (Fig. 7). This is very consistent with the retardation factor values (ranging from 2.8 in the 0–10 cm soil layer to 1.38 in the 100–200 cm layer) estimated from K_d determinations. This means that the nitrate migrated in the soil at a rate of about 45–50 mm per 100 mm of infiltrated water. These values are in agreement with those reported by Ogawa (1984) and Shoji et al. (1986) for andic soils in Japan. For soils without anionic retention that were also amended by pig slurry fertilization, nitrate begins leaching beyond the root zone as soon as drainage occurs (i.e. Daudén and Quilez, 2004; Basso and Ritchie, 2005).

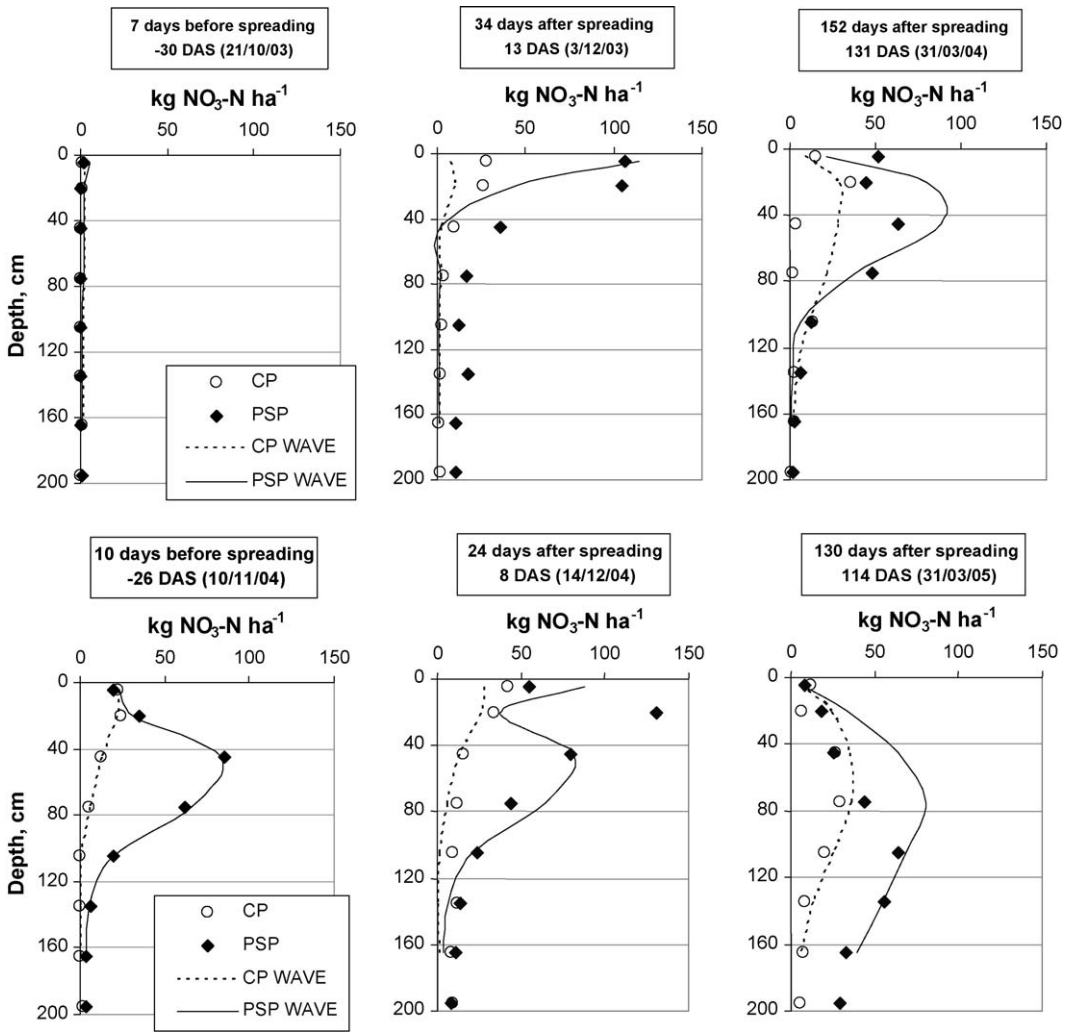

Fig. 7. Measured (symbols) and simulated (continuous or dotted lines) soil nitrate-nitrogen content profiles at selected dates of the control (CP) and pig slurry (PSP) treatments during the 2003–2004 (model validation) and 2004–2005 (model calibration) cropping seasons. DAS is day after sowing.

For both years, nitrate uptake by maize was about 80% higher on the pig slurry plot than on the control plot (Fig. 6), which largely explained the higher measured dry matter yields (Table 3). It also indicates that nitrogen was a limiting factor for maize growth in the CP treatment.

3.3.1. Model calibration and sensitivity analysis

The model was calibrated by minimizing the differences between simulated and observed time series of soil nitrate concentration at different depths (0–10, 10–30, 30–60, 60–90, 90–120, 120–150, and 150–180 cm) for the 2004–2005 cropping season. The best results were obtained by the set of parameters given in the solute and nitrogen cycle section. Special attention was paid to those which were not measured (K_d [NH_4^+], K_{nit}, K_{hum}, K_{man}), as well as for K_d [NO_3^-] and λ [NO_3^-] which were obtained through laboratory experiments.

For both treatments, the corresponding statistics (Table 8) for EF and CRM (mean values of 0.47 and −1%, respectively) were very satisfactory, except at two depths of each plot (below 120 for CP, at 60–90 and 150–180 cm for PSP). The NRMSE values were high because of the small number of observations ($N = 9$). The good statistical indicator for the superficial soil layer on the pig slurry plot suggested that WAVE satisfactorily simulated the substantial nitrate increase about 10 days after spreading (Fig. 5) as a result of the proper calibration of the nitrification coefficient (K_{nit}). The decay constant for the manure pool (K_{man}) was found to be close to the value given by Ducheyne et al. (2001) for a Belgium fluvisol, also amended by pig slurry applied to a maize crop. However, this coefficient was not very high in our case because the amount of pig slurry organic matter was small both years (see Table 2).

For both treatments, Figs. 5 and 6 show that the main features of the experimental values of the N–NO_3^- and N–NH_4^+ stored in the 0–30 cm soil layer (Fig. 5) and throughout the entire profile were faithfully reproduced by the model (Fig. 6). There was quite good agreement between the measured and simulated values of the nitrogen balance components: the budget modelling error due to the net mineralization was + 15 and +9 kg N ha^{-1} for the control and pig slurry plots, respectively (Table 9). Note that the nitrogen spatial variability was not measured in the field and it could partly explain the marked observed variations in nitrate storage (Netto et al., 1999).

Modelling of the different terms of nitrogen budget with a denitrification rate K_{denit} of 0.1 d^{-1} (according to Ducheyne et al., 2001) was tested. The results, not shown here, led to losses of about 20 kg N ha^{-1} for a 4-month period, in close agreement with the results of Hénault and Germon (1995) and Sánchez et al. (2000). Therefore, the balance error due to ignoring the denitrification process was considered to be rather low.

The time course of nitrogen crop uptake (N_{upt}) was also correctly simulated (Table 4 and Fig. 6). However, after 100 DAS, nitrate leaching of the pig slurry plot was underestimated by the

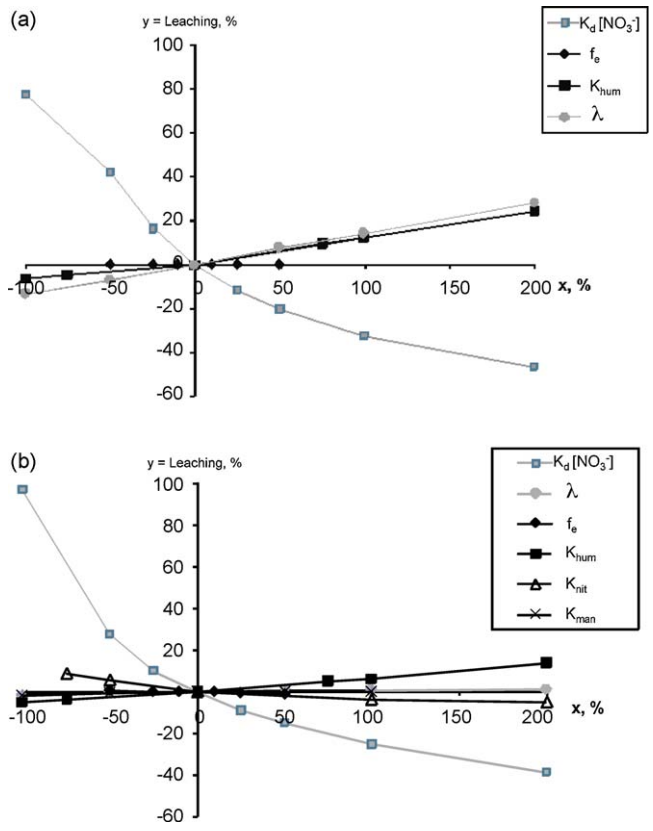

Fig. 8. Sensitivity of the simulated cumulative nitrate leached at 135 cm depth of the control (a) and pig slurry (b) plots relative to changes (y-axis) in the model input parameters (x-axis): humification coefficient (f_e), rates of humus mineralization (K_{hum}), manure degradation (K_{man}), nitrification (K_{nit}), nitrate partition coefficient (K_d) and dispersivity length (λ).

model, although the measured and calculated nitrogen contents in the soil solution were in close agreement (Fig. 6). The difference could be explained by the fact that the existence of an immobile water compartment was not taken into account in the WAVE options. This assumption is probably more relevant in the case of the abundant precipitations encountered during the 2004–2005 cropping season.

As for water flow, the model calibration was completed by performing a sensitivity analysis for nitrate. This was conducted on the 2004–2005 data without changing the calibrated parameters. Fig. 8 presents the relative errors (y) of the cumulative nitrate leaching at z_d = 135 cm as function of the following input parameter uncertainties (x): f_e, f_h, K_{hum}, K_d [NO_3^-] and λ [NO_3^-] for both treatments, as well as K_{nit} and K_{man} for the pig slurry plot. K_d [NO_3^-] was by far the most sensitive parameter. For example, a 100% increase in its value decreased the leaching by nearly 30%, thus confirming that an accurate estimate of K_d was required to obtain a good prediction of the nitrate concentration in the studied andic soil. The model was also sensitive to the humus decomposition rates (K_{hum}), at least in the CP. Increasing this parameter by one order of magnitude led to an increase of about 25% in nitrate leaching. The sensitivity of the dispersivity was quite low, except when small amounts of nitrate were leached, as was the case in the control plot. Leaching was slightly sensitive to K_{nit} and almost insensitive to the other parameters, namely f_e, K_{man}, f_h and K_d [NH_4^+] (the last two are not shown in Fig. 8), within their order of magnitude variation range.

3.3.2. Model evaluation

The model was evaluated on the basis of 2003–2004 season data with the parameters calibrated on the 2004–2005 season. Note that the WAVE prediction capacity was evaluated with less measured data than those which were available for its calibration. Based on the statistical indicators (Table 8), the observed internal state variable values would appear to be poorly predicted by the model, with negative efficiencies at almost all depths and high NRMSE values. However, the results should be considered in the light of the mean CRM values (about 1% for CP, and −4% for PSP), which were very close to those obtained from the calibration (−1% for both plots). Moreover, on the pig slurry plot, nitrate content patterns in the 0–10 cm soil layer (Figs. 5 and 7) were satisfactorily predicted (EF = 0.82), indicating that the nitrification coefficient was properly estimated. On the control plot, the deviation was more marked in the first meter of the soil profile (NRMSE ranged from 108 to 208% in the 0–90 cm layer and from 61 to 93% below). This could be explained by the fact that the measured nitrate contents were stable in the deeper layers, while they presented high temporal variations in the more superficial soil layers due to an increase in mineralization–nitrification processes. Lastly, a close agreement was observed between the measured and predicted nitrogen balance component values for both treatments (Table 9): the budget modelling error due to net mineralization was − 9 and − 13 kg N ha^{-1} for the control and pig slurry plots, respectively. Moreover, WAVE was able to faithfully reproduce the quasi absence of nitrate leaching under the root zone on both plots.

4. Conclusion

Field experiments were carried out to assess the risk of drainage and nitrate leaching below the root zone after pig slurry application on an acid tropical andic soil. The experimental results showed that the drainage risk was high when the rain intensity was higher than 30 mm d^{-1} and the soil humidity was close to saturation. The high hydraulic conductivities measured in this andic soil (282 mm h^{-1}) resulted in substantial drainage below the root zone within one day. Although 720 mm of water was drained during the first rainy season, no nitrate leaching was observed in CP nor in PSP. In the second rainy season, 100 kg of N ha^{-1} (about 60% of pig slurry ammonium applied in 2004) was leached beyond the root zone in PSP, whereas nitrate leaching was almost negligible in CP. The 15 month delay observed between the first pig slurry application in 2003 and the nitrate onset in the drainage water at 135 cm depth was explained by nitrate adsorption on the soil particles and by the fact that the water stored in the 0–135 cm soil layer was fully displaced only after the accumulation of 990 mm of rainfall. The nitrate front progression rate in this soil was estimated at about 45–50 mm per 100 mm of infiltrated water. This slow rate delayed nitrate leaching but could not prevent eventual groundwater pollution.

The WAVE model was able to correctly reproduce the water and nitrogen state variables (except the water pressure head, which was poorly estimated in both plots for both years), the fluxes across the boundaries (actual evapotranspiration, runoff, drainage, crop uptake and leaching) and the resulting budget terms.

The stepwise calibration–validation approach used was efficient for assessing the performance of the different model components and finally WAVE was found to be robust enough to work in tropical conditions and could therefore be used for further studies involving long-term evaluation of the impact of agricultural practices on the environment. Moreover, the sensitivity analysis highlighted that parameters K_c, K_s, η, K_d [NO_3^-], K_{hum} had to be accurately estimated to efficiently simulate the water and nitrogen fate in the studied agrosystem.

This work also suggested some improvements for the model. Accounting for denitrification and mineralization processes in humid tropical conditions and for rich organic matter soil would improve the nitrogen budget. Furthermore, a better representation

of the andic soil hydraulics (particularly the mobile–immobile water behaviour) would probably improve the water flux and, in turn, nitrate leaching predictions. In addition, the WAVE prediction capacity could be increased by taking crop growth processes in interaction with climate, fertilization and soil variables into account.

In terms of practical recommendations for agricultural practices, it should be mentioned that the rates of pig slurry application in this experiment were substantially higher than those generally applied by farmers in Réunion. Leaching values should therefore not be considered as representative of the actual situation on the island.

This study showed that the nitrate adsorption in an andic soil can significantly delay nitrate leaching. Consequently, nitrates remained in the soil profile for a longer time than observed in other soils. We recommend agricultural practices that allow for the removal of this nitrate pool. Crops having permanently active and deep root systems such as forage grass or sugarcane should therefore be preferred over shallow rooting annual crops.

It would be important to conduct complementary experiments to check that the rather low MFE of pig slurry is correct, since this value is used to calculate optimal rates of pig slurry application by farmers. This would require experiments comparing several rates of application of slurry and a plot design allowing to evaluate the standard error on the determination of MFE.

Finally, the results of this work can be used to enhance mineralization and leaching simulation, and to design and monitor cropping systems, in order to manage slurry application and limit leaching and subsequent pollution risks. For this purpose, the experiment described in this paper will be pursued to gather datasets on a long-term basis for assessing soil, water and solute time patterns as well as taking the impact of climatic variations into account.

Acknowledgements

This research was funded by CIRAD, the "Conseil Régional de La Réunion" and the "Département de La Réunion", European Community FEOGA Fund and also DIREN. The first author is very grateful to the "Conseil Régional de La Réunion" for providing him with a doctoral fellowship. The last author acknowledges CIRAD and the University of La Réunion for inviting him to be involved in the research.

References

Addiscott, T.M., Wagenet, R.J., 1985. Concepts of solute leaching in soils: a review of modelling approaches. J. Soil Sci. 36, 411–424.

Basso, B., Ritchie, J.T., 2005. Impact of compost, manure and inorganic fertilizer on nitrate leaching and yield for a 6-year maize-alfa rotation in Michigan. Agric. Ecosyst. Environ. 108, 329–341.

Beauchamp, E.G., 1986. Availability of nitrogen from three manures to corn in the field. Can. J. Soil Sci. 66, 713–720.

Beckwith, C.P., Cooper, J., Smith, K.A., Shepherd, M.A., 1998. Nitrate leaching loss following application of organic manures to sandy soils in arable cropping. I: effects of application time, manure type, overwinter crop cover and nitrification inhibition. Soil Use Manage. 14, 123–130.

Beckwith, C.P., Chalmers, A.G., Jackson, D.R., Smith, K.A., 2002. Nitrate leaching following autumn and winter application of animal manures to grassland. Soil Use Manage. 18, 428–434.

Bergström, L., Johnsson, H., Totensen, G., 1991. Simulation of the nitrogen dynamics using the SOILN model. Fert. Res. 27, 181–188.

Bernard, H., Chabalier, P.F., Chopart, J.L., Legube, B., Vauclin, M., 2005. Assessment of herbicide leaching risk in two tropical soils of Reunion Island (France). J. Env. Qual. 34, 534–543.

Böhm, W., 1976. *In situ* estimation of root length at natural soil profiles. J. Agric. Camb. 87, 365–368.

Bradbury, N.J., Whitmore, A.P., Hart, P.B.S., Jankinson, D.S., 1993. Modeling the fate of nitrogen in crop and soil in the years following application of 15N-labelled fertilizer to winter wheat. J. Agric. Sci. 121, 363–379.

Brechin, J., McDonald, G.K., 1994. Effect of form and rate of pig manure on the growth, nutrient uptake and yield of barley (*cv*.Galleon). Aust. J. Exp. Agr. 34, 505–510.

Brooks, R.H., Corey, A.T., 1964. Hydraulic Properties of Porous Media. Hydrology Paper No. 3, Colorado State University, Fort Collins, CO.

Brusseau, M.L., Rao, P.S., 1990. Modelling solute transport in structured soils: a review. Geoderma 46, 169–192.

Burdine, N.T., 1953. Relative permeability calculation from size distributions data. Trans. AIME 198, 71–78.

Cameron, K.C., Rate, A.W., Carey, P.L., Smith, N.P., 1995. Fate of nitrogen in pig effluent applied to a shallow stony pasture soil. J. Agric. Res. 38, 533–542.

Carey, P.L., Rate, A.W., Cameron, K.C., 1997. Fate of nitrogen in pig slurry applied to a New Zealand pasture soil. Aust. J. Soil Res. 35, 941–959.

Cattan, P., Cabidoche, Y.M., Lacas, J.G., Voltz, M., 2006. Effects of tillage and mulching on runoff under banana (*Musa* spp.) on a tropical Andosol. Soil Till. Res. 35–51, doi:10.1016/j.still.2005.02.002.

Chabalier, P.F., Van de Kerchove, V., Saint Macary, H., 2006. Guide de la fertilisation organique à La Réunion. CIRAD, Chambre d'Agriculture Réunion, Saint Denis, 302 pp.

Chopart, J.L., Vauclin, M., 1990. Water balance estimation model: field test and sensitivity analysis. Soil Sci. Soc. Am. J. 54, 1377–1384.

Chopart, J.L., Siband, P., 1999. Development and validation of a model to describe root length density of maize from root counts on soil profiles. Plant Soil 214, 61–74.

Chopart, J.L., Payet, N., Saint Macary, H., Vauclin, M., 2007. Is maize root growth affected by pig slurry application on a tropical acid soil? PlantRoot 1, 75–84. doi:10.3117/plantroot.1.75.

DAF (Direction de l'Agriculture et de la Forêt), CIRAD (Centre de coopération Internationale en Recherche Agronomique pour le Développement), 2007. Atlas des matières organiques issues des activités d'élevage et d'assainissement urbain à la Réunion, DAF Réunion, CIRAD, Saint Denis, La Réunion, 70 pp.

Daudén, A., Quilez, D., 2004. Pig slurry versus mineral fertilization on corn yield and nitrate leaching in a Mediterranean irrigated environment. Eur. J. Agron. 21, 7–19.

Dendooven, L., 1990. Nitrogen Mineralization and Nitrogen Cycling. Dissertationes de Agricultura, Nr. 191, Faculteit der Landbouwwetenschappen, Katholieke University, Leuven, 180 pp.

de Vries, D.A., 1952. The Thermal Conductivity of Soil. Meded, Lanbouwhogesschool, Wageningen, Netherlands.

Diez, J.A., de la Torre, A.I., Cartagena, M.C., Carballo, M., Vallejo, A., Mũnoz, M.C., 2001. Evaluation of the application of pig slurry to an experimental crop using agronomic and ecotoxicological approaches. J. Env. Qual. 30, 2165–2172.

Doorenbos, J., Pruitt, W.O., 1977. Crop Water Requirements. FAO Irrigation and Drainage Paper No. 24. Rome, Italy, 193 pp.

Ducheyne, S., Schadeck, N., Vanongeval, L., Vandendriessche, H., Feyen, J., 2001. Assessment of the parameters of a mechanistic soil-crop-nitrogen simulation model using historic data of experimental field sites in Belgium. Agric. Water Manage. 51, 53–78.

Duwig, C., Becquer, T., Clothier, B.E., Vauclin, M., 1999. A simple dynamic method to estimate anion retention in an unsaturated soil. C. R. Acad. Sci. (Earth and Planetary Sci.) 328, 759–764.

Duwig, C., Normand, B., Vauclin, M., Vachaud, G., Green, S.R., Becquer, T., 2003. Evaluation of the WAVE model for predicting nitrate leaching for two contrasted soil and climate conditions. Vadose Zone J. 2, 76–89.

Eckersten, H., Jansson, P.E., Johnsson, H., 1996. SOILN Model. User's Manual, 3rd Ed., Com. 96:1, Swedish University of Agricultural Sciences, Dept. of Soil Sciences, Uppsala, Sweden.

Feddes, R.A., Kowalik, P.J., Zaradny, H., 1978. Simulation of Field Water Use and Crop Yield. Simulation Monograph Pudoc, Wageningen, Netherlands, 189 pp.

Feder, F., Findeling, A., 2007. Retention and leaching of nitrate and chloride in an andic soil after pig manure amendment. Eur. J. Soil Sci. 58, 393–404, doi:10.1111/j.1365-2389.2006.00885.x.

Fontes, J.C., Gonçalves, M.C., Pereira, L.S., 2004. Andosols of Terceira Azores: measurement and significance of soil hydraulic properties. Catena 56, 145–154.

Harter, T., Davis, H., Mathews, M.C., Meyer, R.D., 2002. Shallow groundwater quality on dairy farms with irrigated forage crops. J. Contam. Hydrol. 55, 287–315.

Hénault, C., Germon, J.C., 1995. Quantification de la dénitrification et des émissions de protoxyde d'azote (N_2O) par les sols. Agron. 15, 321–355.

Hodnett, M.G., Tomasella, J., 2002. Marked difference between van Genuchten soil water-retention parameters for temperate and tropical soil: a new water retention prod-transfer function developed for tropical soil. Geoderma 108, 155–180.

Hupet, F., Lambot, S., Feddes, R.A., van Dam, J.C., Vanclooster, M., 2003. Estimation of root water uptake parameters by inverse modelling with soil water content data. Water Resour. Res. 39, 1312. doi:1029/2003WR002046.

IUSS Working Group WRB, 2006. World Reference Base for Soil Resources 2006. World Soil Resources Reports No. 103. FAO, Rome.

Jarvis, N.J., 1994. The MACRO model (version 3.1). Technical Description and Sample Simulations. Reports and Dissertation 19. Swedish University of Agricultural Sciences, Dept. of Soil Sciences, Uppsala, Sweden.

Jensen, L.S., Petersen, I.S., Nielsen, N.E., 2000. Turnover and fate of 15N-labelled cattle slurry ammonium-N applied in autumn to winter wheat. Eur. J. Agron. 12, 23–35.

Join, J.L., Coudray, J., 1993. Caractérisation géostructurale des émergences et typologie des nappes d'altitude en milieu volcanique insulaire (Ile de La Réunion). Geodyn. Acta 6, 243–254.

Kinjo, T., Pratt, P.F., 1971. Nitrate adsorption. I: in some acid soils of Mexico and South America. Soil Sci. Soc. Am. Proc. 35, 722–725.
Leirós, M.C., Villar, M.C., Cabaneiro, A., Carballas, T., Diaz-Fieros, F., Gil, F., Gómez, C., 1983. Caracterización y valor fertilizante de los pig slurry de vacuño en Galicia. An. Edafol. y Agrobiol. 42, 753–768.
Loague, K., Green, R.E., 1991. Statistical and graphical methods for evaluating solute transport models: Overview and applications. J. Contam. Hydrol. 7, 51–73.
Maeda, M., Zhao, B., Ozaki, Y., Yoneyama, T., 2003. Nitrate leaching in an andosol treated with different types of fertilizers. Environ. Poll. 121, 225–241.
Mantovi, P., Fumagalli, L., Beretta, G.P., Guermandi, M., 2006. Nitrate leaching through the unsaturated zone following pig slurry applications. J. Hydrol. 316, 195–212.
Miyamoto, T., Kobayashi, R., Annaka, T., Chikushi, J., 2001. Applicability of multiple length TDR probes to measure water distributions in an andosol under different tillage systems in Japan. Soil Till. Res. 60, 91–99.
Morvan, T., Leterme, P., Mary, B., 1996. Quantification par marquage isotopique 15N des flux d'azote consécutifs à un épandage d'automne de lisier de porc sur triticale. Agron. 16, 541–552.
Morvan, T., Leterme, P., Arsene, G.G., Mary, B., 1997. Nitrogen transformation after the spreading of pig slurry on bare soil and ryegrass using ^{15}N-labelled ammonium. Eur. J. Agron. 7, 181–188.
Morvan, T., 1999. Quantification et modélisation des flux d'azote résultant de l'épandage de lisier. Ph.D. dissertation, University of Paris VI (in french), 157 pp.
Nash, J.E., Sutcliffe, J.V., 1970. River flow forecasting through conceptual models. J. Hydrol. 10, 282–290.
Netto, A.M., Pieritz, R.A., Gaudet, J.P., 1999. Field study on the local variability of soil water content and solute concentration. J. Hydrol. 215, 23–37.
Nielsen, N.E., Jensen, H.E., 1990. Nitrate leaching from loamy soils as affected by crop rotation and nitrogen fertilizer application. Fert. Res. 26, 197–207.
Ogawa, Y., 1984. Effect of leached fertilizers from the volcanic ash soil upland fields on the fresh water environment and its control. Jap. J. Soil Plant Nutr. 55, 195–196.
Olsen, S.R., Kemper, W.D., 1968. Movement of nutrients to plant roots. Adv. Agron. 20, 91–151.
Payet, N., 2005. Impact des apports de lisier sur un sol cultivé de La Réunion: Etude expérimentale et modélisation des flux d'eau et de nitrate dans la zone non saturée. Ph.D. dissertation. University of La Réunion, France (in French with English summary), 239 pp.
Petersen, J., 1996. Fertilization of spring barley by combination of pig slurry and mineral nitrogen fertilizer. J. Agric. Sci. 127, 151–159.
Ramos, C., Carbonel, E.A., 1991. Nitrate leaching and soil moisture prediction with the LEACHN model. Fertilizer Res. 27, 171–180.
Rutter, A.J., Morton, A.J., 1977. A predictive model of rainfall interception in forests. J. Appl. Ecol. 14, 567–588.
Salinas-Garcia, J.R., Báez-González, A.D., Tiscareno-Lopez, M., Rosales-Robles, E., 2001. Residue renoval and tillage interaction effects on soil properties under rain-fed corn production in Central Mexico. Soil Till. Res. 59, 67–79.
Salinas-Garcia, J.R., Velásquez-Garcia, J., de, J., Gallardo-Valdez, M., Diaz-Mederos, P., Caballero-Hernández, F., Tapia-Vargas, L.M., Rosales-Robles, E., 2002. Tillage effects on microbial biomass and nutrient distribution in soils under rain-fed corn production in Central Mexico. Soil Till. Res. 66, 143–152.
Sánchez, M., Mosquera-Corral, A., Méndez, R., Lema, J.M., 2000. Simple methods for the determination of the denitrifying of sludges. Bioresour. Technol. 75, 1–6.
Sánchez, M., González, J.L., 2005. The fertilizer value of pig slurry. I: values depending on the type of operation. Bioresour. Technol. 96, 1117–1123.
Sanchez-Pérez, J.M., Antiguedad, I., Arrate, I., Garcia-Linares, C., Morell, I., 2003. The influence of nitrate leaching through unsaturated soil on groundwater pollution in agricultural area of the Basque country: a case study. Sci. Total Environ. 317, 173–187.
Shoji, S., Nanzyo, M., Dahlgren, R.A., 1993. Volcanic Ash Soils: Genesis, Properties and Utilization. Developments in Soil Science, 21, Elsevier, Amsterdam, Netherlands.
Shoji, S., Saigusa, M., Goto, J., 1986. Acidity of subsoils of andisols and nitrogen uptake and growth of sorghum. Jap. Soil Plant Nutr. 57, 264–271 in Japanese.
Simunek, J., Suarez, D.L., 1993. The UNSATCHEM_2D code for simulating two-dimensional variability-saturated water flow, heat transport, carbon dioxide transport and solute transport with major ion equilibrium and kinetic chemistry. Version 1.1. Research Rep. 128. US Salinity Laboratory, USDA, ARS, Riverside, CA.
Simunek, J., Sejna, M., van Genuchten, M.T.h., 1999. The HYDRUS-2D Software Package for Simulating the One-dimensional Movement of Water, Heat and Multiple Solutes in Variably-saturated Media. IGWMC-TPS 53, Version 2.0. Int. Ground Water Modeling Center, Colorado School of Mining, Golden, CO.
Sorensen, P., Eriksen, J., 2009. Effects of slurry acidification with sulphuric acid combined with aeration on the turnover and plant availability of nitrogen. Agric. Ecosyst. Environ. 131, 240–246.
Spitters, C.J.T., van Keulen, H., van Kraailingen, D.W.G., 1988. A simple but universal crop growth simulation model, SUCROS 87. In: Rabbinge, R., et al. (Eds.), Simulation and Systems Management in Crop Protection, Pudoc, Wageningen, Netherlands.
Stevenson, F.J., 1982. Origin and distribution of nitrogen in soil. In: Stevenson, F.J. (Ed.), Nitrogen in Agricultural Soils, Agronomy Monograph 22, ASA-CSSA, SSSA, Madison, WI, 1022 pp.
Thomsen, I.K., 2005. Nitrate leaching under spring barley is influenced by the presence of a ryegrass catch crop: results from a lysimeter experiment. Agric. Ecosyst. Environ. 11, 21–29.
Thorsen, M., Jorgensen, P.R., Felding, G., Jacobsen, O.H., Spliid, N.H., Refsgaard, J.C., 1998. Evaluation of a stepwise procedure for comparative validation of pesticide leaching models. J. Environ. Qual. 27, 1183–1193.
Vachaud, G., Dancette, C., Sonko, S., Thony, J.L., 1978. Méthodes de caractérisation hydrodynamique *in situ* d'un sol non saturé. Application à deux types de sol du Sénégal en vue de la détermination du bilan hydrique. Ann. Agron. 29, 1–36.
Vanclooster, M., Viaene, P., Diels, J., Christianens, K., 1994. WAVE: A Mathematical Model for Simulating Water and Agrochemicals in the Soil and Vadose Environment. Release 2.0, References and User's Manual. Institute for Land and Water Management. Katholieke Universiteit, Leuven.
Vanclooster, M., Viaene, P., Diels, J., Feyen, J., 1995. A determistic evaluation analysis applied to an integrated soil-crop model. Ecol. Model. 81, 83–95.
van Genuchten, M.Th., 1980. A closed-form equation for predicting the hydraulic conductivity of unsaturated soils. Soil Sci. Soc. Am. J. 44, 892–898.
van Keulen, H., Penning de Vries, F.W.T., Drees, E.M., 1982. A summary model for crop growth. In: Penning de Vries, F.W.T., Van Laar, H.H. (Eds.), Simulation of Crop Growth and Crop Production, Pudoc, Wageningen, Netherlands, pp. 87–98.
Vauclin, M., Chopart, J.L., 1992. L'infiltrométrie multi-disques pour la détermination in situ des caractéristiques hydrodynamiques de la surface d'un sol gravillonnaire de la Côte-d'Ivoire. Agron. Trop. 46, 259–271.
Vepraskas, M.J., Hoyt, G.D., 1988. Comparison of the trench-profile and core methods for evaluating root distribution in tillage studies. Agron. J. 80, 166–172.
Vereecken, H., Vanclooster, M., Swerts, M., Diels, J., 1991. Simulating water and nitrogen behaviour in soil cropped with winter wheat. Fert. Res. 27, 233–243.
Wagenet, R.J., Hutson, J.L., 1989. Leaching Estimation and Chemistry Model (LEACHN).Version 2. Dept. of Agron., Cornell Univ., Ithaca, NY.
Zebarth, B.J., Paul, J.W., Schmidt, O., McDougall, R., 1996. Influence of the time and rate of liquid-manure application on yield and nitrogen utilization of silage corn in South Coastal British Columbia. Can. J. Soil Sci. 76, 153–164.

Pedosphere **23**(1): 20–28, 2013
ISSN 1002-0160/CN 32-1315/P

Published by Elsevier B.V. and Science Press

PEDOSPHERE

www.elsevier.com/locate/pedosphere

Pretreatment of Soil Samples Rich in Short-Range-Order Minerals Before Particle-Size Analysis by the Pipette Method*[1]

K. ALARY[1], D. BABRE[1], L. CANER[2], F. FEDER[3,4,*2], M. SZWARC[1], M. NAUDAN[1] and G. BOURGEON[5]

[1] *CIRAD, US Analyse, F-34 398 Montpellier (France)*
[2] *Université de Poitiers, IC2MP-HydrASA UMR 7285, F-86 022 Poitiers (France)*
[3] *CIRAD, UPR Recyclage et risque, 18 524 Dakar (Sénégal)*
[4] *CIRAD, UPR Recyclage et risque, F-97 408 Saint-Denis La Réunion (France)*
[5] *CIRAD, UPR Recyclage et risque, F-34 398 Montpellier (France)*

(Received April 18, 2012; revised October 28, 2012)

ABSTRACT

The possibilities of combining the dissolution of short-range-order minerals (SROMs) like allophane and imogolite, by ammonium oxalate and a particle size distribution analysis performed by the pipette method were investigated by tests on a soil sample from Reunion, a volcanic island located in the Indian Ocean, having a large SROMs content. The need to work with moist soil samples was again emphasized because the microaggregates formed during air-drying are resistant to the reagent. The SROM content increased, but irregularly, with the number of dissolutions by ammonium oxalate: 334 and 470 mg g^{-1} of SROMs were dissolved after one and three dissolutions respectively. Six successive dissolutions with ammonium oxalate on the same soil sample showed that 89% of the sum of oxides extracted by the 6 dissolutions were extracted by the first dissolution (mean 304 mg g^{-1}). A compromise needs to be found between the total removal of SROMs by large quantities of ammonium oxalate and the preservation of clay minerals, which were unexpectedly dissolved by this reagent. These tests enabled a description of the clay assemblage of the soil (gibbsite, smectite, and traces of kaolinite) in an area where such information was lacking due to the difficulties encountered in recuperation of the clay fraction.

Key Words: allophane, Andosols, clay content, mineralogy

Citation: Alary, K., Babre, D., Caner, L., Feder, F., Szwarc, M., Naudan, M. and Bourgeon, G. 2013. Pretreatment of soil samples rich in short-range-order minerals before particle-size analysis by the pipette method. *Pedosphere*. **23**(1): 20–28.

INTRODUCTION

During the soil survey of the western slope of the Piton des Neiges volcano on Reunion, a volcanic island located in the Indian Ocean, we had to characterize different types of soils developed on lavas, and organized in catenas. From 2 000 m a.s.l. down to the sea level, a typical catena on Reunion comprises Podzols, Andosols, Umbrisols, Alisols, Phaeozems and several subgroups of Cambisols (IUSS Working Group WRB, 2007; Feder and Findeling, 2007; Feder and Bourgeon, 2009). A common characteristic of all these soils, even when they do not key out as Andosols, is that they contain considerable amounts of ammonium oxalate extractable Fe and Al, indicating organically bound Fe and Al, noncrystalline hydrous oxides of Fe and Al, allophane, and/or amorphous aluminosilicates. These components will be designated hereafter as short-range-order minerals (SROMs); and they often prevent soil dispersion before the particle size distribution analysis (PSDA).

In fact, since the definition of Andepts given in the 7th Approximation (Soil Survey Staff, 1960), PSDA of these soils rich in allophane, volcanic ash or both is known to be very difficult, even impossible, to carry out. This is due to formation of aggregates by flocculation occurring during the course of the analysis and irreversible alteration of the physical properties of these soils when they are dried. With the recent developments in soil classification systems, such as World Reference Base for Soil Resources (WRB) (IUSS Working Group WRB, 2007) and Soil Taxonomy (Soil Survey Staff, 1999), PSDA is not required to identify and classify Andosols (Andisols). Notwithstanding, it is sometimes required for soils containing large amounts of SROMs in at least three cases:

*[1]Supported by the Center for International Cooperation in Agronomic Research for Development, the French Ministry of Overseas Departments and Territories, the European Agricultural Guidance and Guarantee Fund, and the Regional Direction of Environment, France.
*[2]Corresponding author. E-mail: frederic.feder@cirad.fr.

i) When stratifications in the parent material need to be studied (Buurman *et al.*, 1997).

ii) When the clay fraction has to be collected for mineralogical characterization. In the study area, clay mineralogical investigations were scanty. Zebrowski (1975) concluded from X-ray diffraction (XRD) patterns and thermogravimetric curves obtained on the powdered fine earth of several samples that phyllosilicates were absent above 900 m a.s.l. in the toposequence he analysed. He identified only amorphous material in the whole soil profile and gibbsite at depth. More recently, Basile-Doelsch *et al.* (2005) studied the mineralogy of an Andic Podzol located at 1 720 m a.s.l., on the western slope of the Piton des Neiges, using non-destructive spectroscopy methods (XRD, Fourier transform infrared (FTIR) and nuclear magnetic resonance (NMR) of Si and Al); and they did not identify phyllosilicates but short-range-order proto-imogolite, and allophane. In the study, gibbsite was also identified in amounts increasing with depth; and opal, attributed to phytoliths, was present in the E horizon.

iii) If soils, which do not key out as Andosols despite the presence of SROMs, have to be classified in other groups. On Reunion, this is the case for soils located just below the lower boundary of Andosols (*i.e.*, about 900 m a.s.l.) which are still rich in SROMs but have bulk density values above 0.9 g cm^{-3}, the upper limit for andic properties (Payet *et al.*, 2009). They are therefore particularly difficult to classify because the identification of an argic horizon is not easy in the absence of reliable PSDA results and relies solely on the appreciation of field textures.

Fifty years after recognition of the difficulties encountered while performing PSDA on soils rich in SROMs, there is no commonly accepted procedure and the situation is even quite confusing. From a perusal of recent literature in soil science, three positions can be identified among scientists:

i) The problem is simply ignored, samples are air-dried and the analytical procedure used for non-andic soil material is applied for Andosol samples (Briggs *et al.*, 2006).

ii) The problem is known and, either the interpretations are based solely on field textures, without the backing of analytical results (Iamarino and Terribile, 2008), or the samples are air-dried before a conventional analysis by the pipette method, the accuracy of results is discussed (Delvaux *et al.*, 1989; Fontes *et al.*, 2004) and the underestimation of the clay content is sometimes assessed (*e.g.*, Fehér *et al.*, 2007).

iii) The drying of samples is avoided before analysis and moist samples are pre-treated (sonication, dissolution with citrate-bicarbonate-dithionite or ammonium oxalate, *etc.*) to prevent flocculation and ensure a better dispersion during analysis by the pipette method (Nieuwenhuyse *et al.*, 2000) or using a laser diffraction particle size analyzer (Buurman *et al.*, 1997, 2004).

In France, in the event of incomplete dispersion, a pretreatment with 2 mol L^{-1} HCl recommended to destroy the so-called organo-mineral cements is included in PSDA procedure (NF X 31-107 method) (AFNOR, 2004) to ensure complete dispersion. In the soil laboratory of CIRAD (Centre de Coopération Internationale en Recherche Agronomique pour le Développement), this HCl pretreatment has sometimes been applied to Andosol samples when the sum of fractions obtained after a routine PSDA was far from 1 000 mg for 1 g of soil and the results were generally improved (*i.e.*, the sum of fractions was closer to 1 000 mg). We were nevertheless aware that this procedure was not specifically designed for the analysis of this type of soil material and that, in addition to SROMs, clay minerals and iron oxides can also be destroyed by the acid. In his detailed study of a soil toposequence on Reunion, Zebrowski (1975) also indicated that a pretreatment with 2% HCl (approximately 0.66 mol L^{-1}) is necessary to ensure the dispersion of samples from soils located above 650 m a.s.l. To improve our PSDA method for SROM-rich samples, it was decided to adapt the dissolution procedure using ammonium oxalate (van Lagen, 1996; Buurman *et al.*, 1997, 2004) to the pipette method. Dissolution quality was assessed using both the PSDA results and those of the XRD analysis of clay fraction. In parallel, and using the same criteria, the effects of HCl pretreatment were evaluated. The aim of this paper was to describe these different tests, the difficulties encountered, and to propose a procedure for soil laboratories having standard pipette equipment.

MATERIALS AND METHODS

Soil

After a general characterization of the main soils in the study area involving routine analyses, we selected the third horizon of an Andosol containing a large amount of SROMs (referred to as R-JGR-F16 profile in the CIRAD soil profiles database for Reunion), for which mineralogical investigations were considered essential due to the scarcity of information on clay minerals. Furthermore, as this soil is one of the richest in SROMs, if the tests proved successful, the method could be applied to all samples with variable amounts

of SROMs.

The R-JGR-F16 soil profile was excavated in 2006 on the western slope of the Piton des Neiges volcano on Reunion during the regional soil survey already mentioned. It was located at 1 450 m a.s.l., 21° 10′ 23″ S and 55° 21′ 07″ E in a large cartographic unit of Andosols developed on thick explosive ash falls (15 000–40 000 years BP) of trachytic-basaltic composition (Raunet, 1991) which have covered older lavas. In that particular location, the mean annual rainfall and the mean annual temperature are 1 800 mm and 16 °C, respectively. These conditions correspond to an udic soil moisture regime and an isothermic soil temperature regime. The soil exhibited strong andic properties and keyed out as a Hydric Silandic Andosol (IUSS Working Group WRB, 2007). Selected physical and chemical characteristics of the soil samples analysed for the purpose of the survey are grouped in Tables I and II.

Si_o and Al_o (subscript o refer to oxalate selective dissolution) contents increased by 20- and 10-fold, respectively, from the first to the third horizon, whereas the Al_{py}/Al_o (subscript py refer to pyrophosphate selective dissolution) ratio decreased from 0.89 to 0.14, where Al_{py} was extracted with sodium pyrophosphate, as described by Blakemore *et al.* (1987). The incorporation of Al into Al-humus complexes in the first and second horizons might have resulted in an anti-allophanic effect (Shoji *et al.*, 1993). This is consistent with the allophane content C_{Allo} estimated according to the following formula proposed by Parfitt (1986):

$$C_{Allo} = a Si_a \quad (1)$$

where a takes different values from 5 to 16 depending on the value of $[(Al_o - Al_{py})/Si_o]$, and formula proposed by Mizota and van Reeuwijk (1989):

$$C_{Allo} = 100 Si_o / \{-5.1[(Al_o - Al_{py})/Si_o] + 23.4\} \quad (2)$$

For safety reasons, the pit opened during the soil survey was closed after the survey and a second pit was opened up a few metres away, to avoid the disturbed

TABLE I

Selected characteristics of soils in the different horizons of the profile R-JGR-F16[a)]

Horizon	Depth	Munsell colour	TOC[b)]	pH			P ret[d)]	Bulk density[e)]	CEC[f)]	SEB[g)]
				H_2O	KCl	NaF[c)]				
	cm		mg g^{-1}				%	g cm^{-3}	— $cmol_c$ kg^{-1} —	
H1	0–20	5 YR 3/2	92.8	5.1	4.3	8.4	89.16	0.81	36.09	4.83
H2	20–35	7.5 YR 4/4	80.1	5.0	4.4	9.2	98.47	0.50	39.29	2.06
H3	35–65	10 YR 3/2	62.6	5.0	5.0	9.2	99.33	0.51	95.27	0.61
H4	65–80	5 YR 4/4	75.4	5.3	5.2	9.0	99.67	0.40	85.37	0.36
H5	80–100	10 YR 3/3	69.1	4.9	5.2	10.0	99.59	0.56	85.87	0.35
H6	100–115	7.5 YR 4/4	68.2	4.8	5.3	10.0	99.60	0.58	79.87	0.25
H7	115–140	10 YR 3/3	60.3	4.8	5.5	10.1	99.79	0.63	84.87	0.24

[a)]All the analyses, with the exception of bulk density measurements, were made on air-dried fine earth (< 2 mm); [b)]Total organic carbon; [c)]Soil pH measured in 1 mol L^{-1} NaF according to USDA-NRCS (2004); [d)]Retention of phosphorus measured according to Blakemore *et al.* (1987); [e)]Bulk density measured using 100 cm^3 steel cylinders in three replicates; [f)]Cation exchange capacity; [g)]Sum of exchangeable bases measured after extraction with 1 mol L^{-1} ammonium acetate at pH 7.

TABLE II

Soil Si, Fe and Al contents measured by selective extractions[a)] and the allophane content estimated according to two formulas: (A) proposed by Parfitt (1986) and (B) by Mizota and van Reeuwijk (1989) for the different horizons of the profile R-JGR-F16

Horizon	Depth	Si_o	Fe_o	Al_o	$Al_o + 1/2Fe_o$	Fe_d	Al_d	Fe_{py}	Al_{py}	Al_{py}/Al_o	Allophane	
											A	B
	cm	mg g^{-1}										
H1	0–20	1.2	42.3	6.5	27.6	62.1	6.8	45.0	5.8	0.89	6.1	6.0
H2	20–35	3.6	86.2	25.0	68.1	122.3	21.8	93.3	20.7	0.83	18.0	20.7
H3	35–65	23.3	15.6	71.6	79.4	73.7	43.2	4.3	10.2	0.14	233.0	233.9
H4	65–80	19.6	31.6	69.3	85.1	119.8	57.4	7.5	12.1	0.17	235.2	230.0
H5	80–100	19.9	28.4	67.6	81.8	108.5	54.1	4.8	10.5	0.16	239.6	226.3
H6	100–115	13.8	54.8	56.6	84.0	161.3	57.0	14.0	12.1	0.21	165.8	198.1
H7	115–140	22.7	17.4	72.1	80.8	90.1	57.4	2.9	9.9	0.14	226.5	240.9

[a)]Subscripts o, d and py refer to oxalate, dithionite, and pyrophosphate selective dissolutions, respectively.

soil, for the purpose of the particle size analysis tests presented here. A bulk sample (8 kg) was taken from the third horizon (35–65 cm), then sent to the CIRAD soil laboratory located in Montpellier, France, under field moisture conditions (150% on a dry basis) in sealed plastic bags. Once received in Montpellier, the sample was kept moist and stored under cold conditions (4 °C).

Sample preparation and sub-sampling

Approximately half of the field-moist soil material received in the laboratory was gently passed through the round holes (2 mm) of a sieve using a rubber stopper, the unsieved part of the sample remained stored at 4 °C. Two stages of sub-sampling were necessary before analyses.

For the first stage of sub-sampling, all the sieved material was quickly spread over a plastic tray and manually divided into 40 sub-equal areas; eight subsamples were prepared by mixing the soil of five different areas, randomly chosen and fully collected on the tray. Seven of these subsamples were placed in hermetically sealed plastic containers and kept in a refrigerator, and the last sub-sample was dried at room temperature up to constant weight. The quality of this stage of sub-sampling was assessed later by comparing the results of PSDA obtained on soil taken from two containers.

The different sub-samples needed for the different PSDA tests in 6 replicates were obtained after a second stage of sub-sampling on a smaller quantity of soil taken from a given container.

SROMs dissolution pretreatments

SROMs were dissolved using either 2 mol L^{-1} HCl according to the Association francaise de Normalisation (AFNOR) recommendation (AFNOR, 2004), or a buffered ammonium oxalate solution in the dark (Blakemore *et al.*, 1987; van Lagen, 1996). 2 mol L^{-1} HCl is recommended by AFNOR (2004) as a reagent that can be used to dissolve organo-mineral cements without excluding the use of other reagents, such as oxalate solutions or oxalic acid, for particular types of soil. This method was recently used in our laboratory for some Andosol samples and it was interesting to evaluate this method. Five grams of moist soil (AFNOR procedure concerns air-dried soil) were mixed with 300 mL of 2 mol L^{-1} HCl, then heated at 70 °C for 1 h. After cooling, the supernatant was collected in a 1 L flask for the analyses of dissolved elements. The sample was then rinsed twice with 300 mL of deionized water, the supernatants were added to the flask and the volume was adjusted to 1 L with deionized water. Fe, Al and Si contents were measured in an aliquot of the extract by using Varian, Inc. Vista-PRO inductively coupled plasma-optical emission spectrophotometry (ICP-OES; simultaneous with axial torch); and calibration was done using certified reference solutions of Fe, Al and Si.

For ammonium oxalate dissolutions, opinions differ regarding the soil:solution ratio, the pH and the concentration of the reagent. For routine selective dissolutions, The United States Department of Agriculture (USDA) recommends mixing 0.5 g of air-dried soil with 15 mL of 0.2 mol L^{-1} ammonium oxalate reagent buffered at pH 3.0 (USDA-NRCS, 2004). Fe, Al and Si extracted with ammonium oxalate are identified with the subscript o (*i.e.*, Fe_o, Al_o, and Si_o). In the case of samples containing large quantities of Al_o, USDA recommends decreasing the soil:solution ratio to 1:100 and increasing the concentration of the reagent to 0.275 mol L^{-1} with a pH buffered at 3.25. For the Al_o-rich samples, van Lagen (1996) also recommends a soil:solution ratio of 1:100 but without any change in the ammonium oxalate concentration and pH. In all these recommendations, in the case of samples containing large quantities of Al_o, the general idea is to increase the quantity of ammonium oxalate compared to that used for routine measurements. For samples of Andosols from Costa Rica containing large amounts of allophane (up to 39%), Buurman *et al.* (1997) considered that two extractions using the soil:solution ratio of 1:100, as recommended by van Lagen (1996), were necessary to destroy microaggregates of fine silt size.

In our study, a compromise was made between what is used for a routine selective dissolution and the 1:100 ratio recommended by USDA and van Lagen, with a soil:extractant ratio corresponding to 4 g air-dried soil in 250 mL of ammonium oxalate solution. To obtain this ratio, 10 g of < 2 mm moist soil (corresponding to approximately 4 g of air-dried soil), weighed to the nearest mg were mixed once with 125 mL of 0.2 mol L^{-1} ammonium oxalate reagent buffered at pH 3.0. The mixture was placed in a 175 mL centrifuge tube, wrapped with aluminium paper to ensure darkness, and shaken for 4 h on a rotary end-over-end shaker (30 r min^{-1}). After centrifugation, the supernatant was collected in a 1 L volumetric flask labelled with the number of the replicate. These operations were repeated a second time to obtain the chosen soil:extractant ratio, then the sample was rinsed with distilled water; and after centrifugation, the supernatant was added to the flask, and the volume ad-

justed to 1 L with deionized water. Fe, Al and Si contents were measured in an aliquot of the extract by ICP-OES similarly to what was indicated above for the HCl pretreatment.

As the soil:extractant ratio was less than 1:100, the relevance of several successive dissolutions was evaluated in order to obtain the complete dissolution of SROMs, and a kinetics curve was plotted.

The efficiency of the ammonium oxalate treatment was also tested on air-dried samples to check the irreversibility of physical modifications due to drying. To summarize, the AFNOR method (dissolution of cements using 2 mol L^{-1} HCl) was compared to a new, and probably more specific method (dissolution of SROMs using the ammonium oxalate reagent) for which adjustments were investigated, including number of dissolutions, moist or dried sample.

PSDA procedure and complementary analysis

After the SROM dissolution pretreatments, PSDA was performed with at least six replicates, using an automated analyser (Texsol 24B instrument equipped with 0.5 L cylinders) and following the standard procedure (NF X 31-107 method; AFNOR, 2004) applied to all soils: samples were treated with 35% H_2O_2 at ambient temperature, then heated on a hot plate at 70 °C, to remove organic matter, dispersed with a sodium hexametaphosphate solution, and mechanically shaken. The coarse and fine sand fractions were obtained by wet sieving; the clay, the fine and coarse silt fractions by pipetting in the cylinder. The sum of all fractions, including soil moisture and organic carbon, was calculated. Only results corresponding to a sum within the range 950–1 070 mg for 1 g of soil (*i.e.*, 95%–107%) were retained.

In addition to the PSDA tests, the moisture content of field-moist soil was measured in six replicates. The organic matter content was measured by burning at 850 °C in an elementary analyser (Thermoquest NC analyser, EA 1112 model) in six replicates using air-dried, sieved and crushed to < 200 µm soil.

After performing PSDA, clays were separated from sand and silt through successive dispersion and gravity sedimentation operations following the principles of Stoke's Law. Clays of the different replicates of each treatment were collected together, flocculated with $MgCl_2$, then rinsed until free of chloride and dried at room temperature for mineralogical studies using X-ray diffraction and infrared spectroscopy. XRD patterns of clay fractions were obtained on oriented preparations after different treatments and recorded on a Panalytical Xpert Pro diffractometer (Cu Kα radiation) on zero-background silicon wafers from 2.5° to 35° 2θ with steps of 0.017° 2θ and a counting time per step of 200 s (converted from scanning mode) to obtain a reliable signal. FTIR spectra of clay fractions were recorded on KBr disks dried at 110 °C from 4 000 to 400 cm^{-1} using a Nicolet 510-FTIR continuously purged with dry CO_2-depleted air.

Statistical analysis

The Origin Pro 8 software package (Originlab Corporation, Northampton, USA) was used for the basic statistics. For each set of data obtained after dissolution procedures, mean, standard error (SE) and coefficient of variation (CV) have been calculated. The CV, defined as the ratio of the standard deviation to the mean and expressed in percentage, quantifies the experimental repeatability.

RESULTS AND DISCUSSION

Effect of pretreatments on the mineralogy of samples

The X-ray diffraction patterns (data not shown) obtained on the powdered fine earth of the third horizon without any pretreatment indicated the presence of quartz, magnetite (or titanomagnetite), ilmenite, traces of amphibole (tremolite) and gibbsite. In the same area, gibbsite had already been identified by Zebrowski (1975) after HCl pretreatment but he did not give any indication regarding the primary minerals. Fourier transform infrared (FTIR) spectroscopy was also performed on a raw sample; the pattern obtained also confirmed the abundance of SROMs and the presence of poorly crystallised kaolinitic minerals (proto-kaolinite/proto-halloysite) and poorly crystallised gibbsite (Fig. 1).

On the clay fraction, comparison between untreated and treated samples (Fig. 1) showed that the different reagents eliminated the short-range-order minerals (wide band at about 1 000 cm^{-1}). The bands at 3 690, 3 620, 3 527, 3 451 and 3 390 cm^{-1} revealed the presence of kaolinitic minerals (kaolinite or halloysite) and gibbsite with poor crystallinity. These minerals are "relatively concentrated" in the treated samples but they are however hardly detected by X-ray diffraction due to their poor crystallinity.

PSDA of a moist sample pretreated with 2 mol L^{-1} HCl

This pretreatment is recommended by AFNOR (2004) without restriction regarding the types of soil

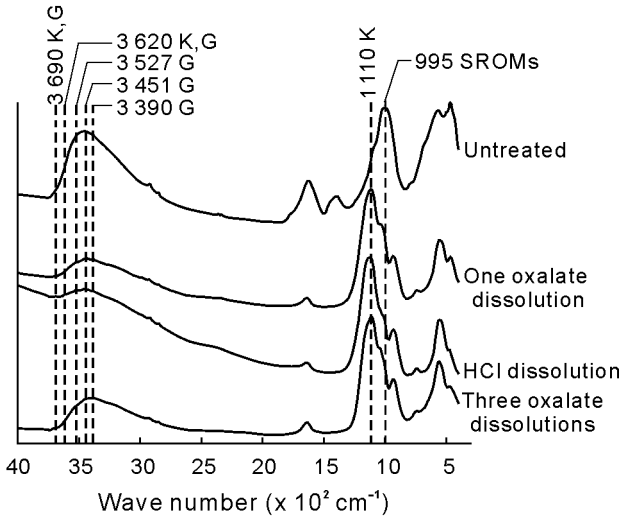

Fig. 1 Fourier transform infrared (FTIR) spectra obtained on soil (untreated) and clay fractions collected after different treatments. G = gibbsite; K = kaolinitic minerals; SROMs = short-range-order minerals (*i.e.*, allophane or imogolite).

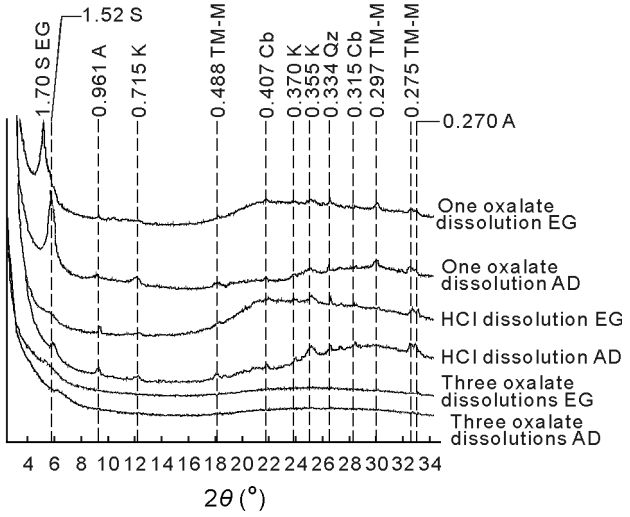

Fig. 2 X-ray diffraction patterns on oriented preparation of clay fractions obtained after different treatments recorded in air-dried state at room temperature (AD) and following solvation with vapour ethylene glycol at 60 °C (EG). S = smectite (in air dried state); S EG = smectite (following ethylene glycol solvation); A = amphibole (tremolite); K = kaolinite; TM-M = titanomagnetite and magnetite; Cb = cristobalite; Qz = quartz.

involved. The fact that a field-moist sample was used instead of a dry sample decreased the soil:reagent ratio compared to what is recommended and possibly amplified the effect of HCl (Table III).

TABLE III

Particle size distribution analysis on field-moist samples pretreated with 2 mol L^{-1} HCl ($n = 6$)

Replicate No.	Organo-mineral cements[a)]	Clay	Fine silt	Coarse silt	Fine sand	Coarse sand
	mg g^{-1} dry mineral matter					
01	476	207	252	38	15	12
02	456	193	222	57	20	52
03	446	226	253	47	20	8
04	492	274	152	54	17	11
05	449	151	340	36	16	9
06	449	257	187	59	18	30
Mean	461	218	234	48	18	20
SE[b)]	19	45	65	10	2	18
CV[c)] (%)	4	20	28	21	11	90

[a)] Corresponding to the sum of dissolved Al, Fe and Si expressed as oxides; [b)] Standard error; [c)] Coefficient of variation.

Two mol L^{-1} HCl dissolved approximately 461 mg of organo-mineral cements per gram of mineral soil, *i.e.*, nearly half of the sample. After this pretreatment, the clay content was 220 mg g^{-1}. The X-ray diffraction patterns obtained on the clay-fraction of the soil sample pretreated with 2 mol L^{-1} HCl (Fig. 2) showed few clay minerals and, more importantly, that this pretreatment induced an alteration of the smectite denoted by a broadening of the peaks at 1.52 nm in the air-dried state, and 1.70 nm following solvation with ethylene glycol.

Kinetics of SROM dissolution by ammonium oxalate on moist samples

The kinetics of SROM obtained from six successive dissolutions with 0.2 mol L^{-1} ammonium oxalate on the same moist soil sample are illustrated in Fig. 3 where the points represent means of the six replicates (expressed as the sum of Si, Al and Fe oxides). In detail, these kinetics showed that 89% of the sum of oxides extracted by the 6 dissolutions were extracted by the first dissolution (mean 304 mg g^{-1}), 5.4% were extracted during the second dissolution and approximately 1.5% by each of the following; the kinetics reached steady dynamics after the second dissolution. With the sam-

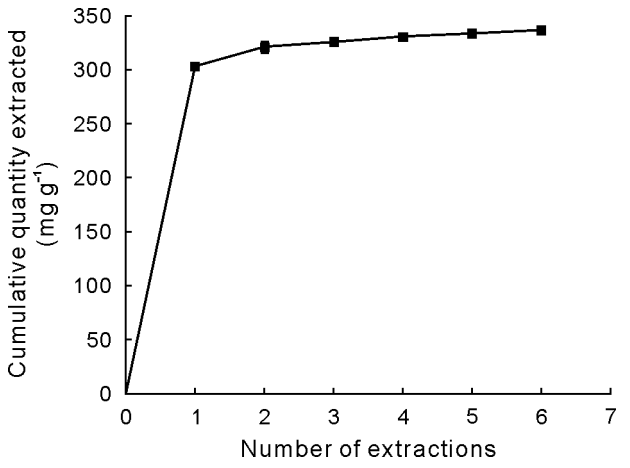

Fig. 3 Kinetics of SROM (short-range-order mineral) dissolution by 0.2 mol L^{-1} ammonium oxalate.

ple used for the tests, SROM extraction appeared to be complete after two or three dissolutions; three dissolutions corresponded to 4 g of dry soil treated with 750 mL of 0.2 mol L^{-1} ammonium oxalate solution (*i.e.*, a soil:solution ratio significantly lower than the 1:100 suggested by USDA-NRCS, 2004).

PSDA on a moist sample after one oxalate dissolution

In Table IV the results from PSDA on field-moist samples after one ammonium oxalate dissolution showed good repeatability, better than after HCl pre-treatment.

TABLE IV

Particle size distribution analysis on field-moist samples after one ammonium oxalate dissolution ($n = 6$)

Replicate No.	Ammonium oxalate extract[a)]	Clay	Fine silt	Coarse silt	Fine sand	Coarse sand
	mg g^{-1} dry mineral matter					
01	335	274	279	59	28	24
02	330	258	277	83	28	25
03	338	257	321	39	28	17
04	323	272	252	88	28	37
05	337	263	286	59	30	24
06	342	245	267	82	27	36
Mean	334	262	280	68	28	27
SE[b)]	7	11	23	19	1	8
CV[c)] (%)	2	4	8	28	4	29

[a)] Corresponding to the sum of dissolved Al, Fe and Si expressed as oxides; [b)] Standard error; [c)] Coefficient of variation.

There was nevertheless a noticeable difference between the SROM content found here (mean 334 mg g^{-1}) and the allophane content estimated using the formula of Parfitt (233 mg g^{-1}, Table II). This difference can be explained by at least two reasons that i) more ammonium oxalate solution was used here, for the PSDA tests, than during the routine characterization of the profile, and the kinetics study illustrated the fact that SROM dissolution depends on the quantity of reagent used; and ii) the Parfitt formula is designed to estimate only allophane and not all the products potentially dissolved by the ammonium oxalate solution.

Further information was provided by X-ray diffraction (XRD patterns labelled "one oxalate dissolution", Fig. 2). The different peaks were attributed to clay minerals (smectite with a peak at 1.52 nm in air-dried state, displaced to 1.70 after solvation with ethylene glycol, and kaolinite), quartz, amphibole, traces of gibbsite. The X-ray scattering domain between 20° and 32° 2θ was interpreted as being produced by the remaining amorphous material mixed with clay (cf. kinetics results). These results tallied with the FTIR spectra showing the abundance of poorly crystallised silicates (Fig. 1).

PSDA on a moist sample after three oxalate dissolutions

For this test, PSDA after three oxalate dissolutions, two sets of six sub-samples taken from two different containers were used to evaluate the first stage of sub-sampling carried out immediately after sieving. In Table V, the mean values were very close for the two sets and illustrated the good quality of the first stage of sub-sampling.

A comparison of the PSDA results grouped in Tables IV and V and the kinetics study indicated that the SROM content increased, but irregularly, with the number of dissolutions by ammonium oxalate: 334 and 470 mg g^{-1} of SROMs were dissolved after one and three dissolutions respectively, but "only" 331 mg g^{-1} at the end of the kinetics (*i.e.*, after 6 dissolutions); and that the clay content sharply decreased between one and three dissolutions; which was not really expected but was probably the consequence of a partial dissolution of clay minerals by the oxalate ammonium reagent. At the same time, the fine silt content unexpectedly increased (from 280 to 362 mg g^{-1}) while the coarse silt, fine sand, and coarse sand contents remained the same.

Further information was again provided by the interpretation of FTIR spectra and X-ray diffraction patterns. Two clay samples were analysed: the first was collected from the five replicates taken from container 3, and the second from the six replicates taken from container 8. XRD and FTIR results were rather similar for both samples; those obtained from the clay sample of container 3 were selected for Figs. 1 and 2 and labelled "three oxalate dissolutions". The peaks corresponding to smectite appear less defined compared to those observed after only one dissolution. The repeated extractions partially dissolved the clay fraction, as shown by the PSDA results, and probably affected the crystallinity of the remaining clay minerals. The X-ray scattering domain between 20° and 32° 2θ, previously attributed to remaining SROMs, disappeared as expected. FTIR spectra (Fig. 1) showed that ammonium oxalate dissolved the SROMs and "concentrated" proto-kaolinite and proto-gibbsite, which are identified by their specific bands in Fig. 1. However, their absence on X-ray diffraction patterns (Fig. 2) was furthermore related to their low amounts and low crystallinity.

After these tests carried out on moist soil samples, doubt existed on the need to perform several oxalate

TABLE V

Particle size distribution analysis on field-moist samples after three ammonium oxalate dissolutions ($n = 5$ or 6)

Container No.	Replicate No.	Ammonium oxalate extract[a)]	Clay	Fine silt	Coarse silt	Fine sand	Coarse sand
		mg g^{-1} dry mineral matter					
3[b)]	01	481	28	372	59	31	28
	02	465	53	368	56	32	26
	03	458	64	354	67	29	29
	04	489	61	347	49	27	27
	05	431	62	405	48	31	23
	Mean	465	54	369	56	30	27
8	01	476	53	362	53	29	26
	02	451	56	371	56	39	27
	03	486	75	324	55	32	29
	04	476	61	366	48	33	27
	05	479	53	358	50	33	27
	06	482	42	353	60	33	30
	Mean	475	55	356	54	33	28
General mean		470	54	362	55	32	27
SE[c)]		18	12	20	6	3	2
CV[d)] (%)		4	22	6	11	9	7

[a)]Corresponding to the sum of dissolved Al, Fe and Si expressed as oxides; [b)]The results for the replicate 06 of container 3 had to be discarded because the total sum of components was too low (950 mg g^{-1}) and the clay content was negative (−15 mg g^{-1}); [c)]Standard error; [d)]Coefficient of variation.

ammonium extractions in order to completely remove SROMs before PSDA. Repeated extractions, even if they are in limited number, can partly destroy clay minerals. As regards the PSDA results, repeated extractions profoundly changed the estimates of the contents for the three finer fractions (SROMs, clay and fine silt) without changing the content of the three coarser fractions (coarse silt, fine and coarse sand). The increase in fine silt content while the contents of coarser fractions remained the same did not correspond to the general hypothesis of microaggregate destruction provoked by the dissolving reagent but, on the contrary, to a recombination (aggregation) of finer particles. After three ammonium oxalate dissolutions, the PSDA results indicated artefacts.

PSDA of an air-dried sample after three oxalate dissolutions

The PSDA results of an air-dried sample after three oxalate dissolutions are grouped in Table VI and showed that SROMs were incompletely and irregularly dissolved (between 144 and 306 mg g^{-1}); and consequently, the results of the PSDA were very variable between the 6 replicates for each particle size fraction.

The physical transformation of the soil material induced by air-drying was therefore not retrograded by the ammonium oxalate reagent, and part of the SROMs became inaccessible to the reagent, despite the duration of the treatment. The pretreatment with ammonium oxalate therefore appeared not to be relevant for air-dried samples.

TABLE VI

Particle size distribution analysis on air-dried samples pretreated with ammonium oxalate at pH 3.0 ($n = 6$)

Replicate No.	Ammonium oxalate extract[a)]	Clay	Fine silt	Coarse silt	Fine sand	Coarse sand
	mg g^{-1} dry mineral matter					
01	144	3	182	83	138	450
02	292	64	273	114	50	207
03	301	67	213	177	54	189
04	306	81	198	164	50	201
05	296	37	229	159	59	220
06	300	1	360	56	59	224
Mean	273	42	243	126	68	248
SE[b)]	19	34	65	49	34	100
CV[c)] (%)	7	81	27	39	50	40

[a)]Corresponding to the sum of dissolved Al, Fe and Si expressed as oxides; [b)]Standard error; [c)]Coefficient of variation.

CONCLUSIONS

To ensure correct sample dispersion before PSDA by the pipette method, a single SROM extraction using ammonium oxalate buffered at pH 3.0 appeared to be a good compromise, as had already been established for the laser method. The various tests presented here furthermore illustrated i) that the reagent could have partly dissolved clay minerals, such as smectite, and ii) that the PSDA results ultimately depended on the

number of ammonium oxalate dissolutions performed. These points were not fully investigated during the pretreatment tests for PSDA using the laser method. A procedure combining one ammonium oxalate dissolution and the standard pipette method for PSDA will give consistent results for andic and non-andic soils during a soil survey, avoiding discrepancies in the results due to the use of different PSDA methods. It would also enable the use of standard pipette equipment available in most soil laboratories. Furthermore, collection and mineralogical studies of the clay fraction would be made possible. In the case presented here, smectite and kaolinite were identified at moderate depth in a Hydric Silandic Andosol located at 1 450 m on the western slope of the Piton des Neiges on Reunion. This is an original and unexpected result because previous studies in the same area, but on different soils, had concluded that phyllosilicate clay-size minerals did not occur. If used in other geographical areas where soils rich in SROMs occur, it is expected that this procedure will help in studying their clay assemblage and produce substantial improvements in the mineralogical knowledge of these soils.

From a practical viewpoint, the cost of this combined procedure was evaluated at twice that of a standard particle size analysis; it cannot be qualified as a "relatively cheap" method, unlike the laser diffraction grain-sizing method. For this reason its use will probably be restricted to a limited number of samples, mostly in the framework of pedogenetic studies.

REFERENCES

Association Francaise de Normalisation (AFNOR). 2004. PSDA procedure (NF X31-107). *In* AFNOR (ed.) Soil Quality Evaluation Methods for Chemical Analysis (in French). Saint-Denis La Plaine, France. Vol. 1. pp. 21–40.

Basile-Doelsch, I., Amundson, R., Stone, W. E. E., Masiello, C. A., Bottero, J. Y., Colin, F., Masin, F., Borschneck, D. and Meunier, J. D. 2005. Mineralogical control of organic carbon dynamics in a volcanic ash soil on La Réunion. *Eur. J. Soil Sci.* **56**: 689–703.

Blakemore, L. C., Searle, P. L. and Daly, B. K. 1987. Methods for Chemical Analysis of Soils. New Zealand Bureau Scientific Report 80. New Zealand Soil Bureau, Lower Hutt.

Briggs, C. A. D., Busacca, A. J. and McDaniel, P. A. 2006. Pedogenic processes and soil-landscape relationships in North Cascades National Park, Washington. *Geoderma.* **137**: 192–204.

Buurman, P., de Boer, K. and Pape, Th. 1997. Laser diffraction grain-size characteristics of Andisols in perhumid Costa Rica: the aggregate size of allophane. *Geoderma.* **78**: 71–91.

Buurman, P., García Rodeja, E., Martínez Cortizas, A. and van Doesburg, J. D. J. 2004. Stratification of parent material in European volcanic and related soils studied by laser-diffraction grain-sizing and chemical analysis. *Catena.* **56**: 127–144.

Delvaux, B., Herbillon, A. J. and Vielvoye, L. 1989. Characterization of a weathering sequence of soils derived from volcanic ash in Cameroon. Taxonomic, mineralogical and agronomic implications. *Geoderma.* **45**: 375–388.

Feder, F. and Bourgeon, G. 2009. Updating the soil map of Réunion island: Methodology and problems to be overcome. *Étude et Gestion des Sols* (in French). **16**: 85–99.

Feder, F. and Findeling, A. 2007. Retention and leaching of nitrate and chloride in an andic soil after pig manure amendment. *Eur. J. Soil Sci.* **58**: 393–404.

Fehér, O., Langohr, R., Füleky, Gy. and Jakab, S. 2007. Late Glacial-Holocene genesis of Andosols from the Seaca-Tătarca (South Gurghiu Mountains, Romania). *Eur. J. Soil Sci.* **58**: 405–418.

Fontes, J. C., Gonçalves, M. C. and Pereira, L. S. 2004. Andosols of Terceira, Azores: measurement and significance of soil hydraulic properties. *Catena.* **56**: 145–154.

Iamarino, M. and Terribile, F. 2008. The importance of andic soils in mountain ecosystems: a pedological investigation in Italy. *Eur. J. Soil Sci.* **59**: 1284–1292.

IUSS Working Group WRB. 2007. World Reference Base for Soil Resources 2006. First update 2007. World Soil Resources Report No. 103. FAO, Rome.

Mizota, C. and van Reeuwijk, L. P. 1989. Clay Mineralogy and Chemistry of Soils Formed in Volcanic Material in Diverse Climatic Regions. Soil Monograph 2. ISRIC, Wageningen.

Nieuwenhuyse, A., Verburg, P. S. J. and Jongmans, A. G. 2000. Mineralogy of a soil chronosequence on andesitic lava in humid tropical Costa Rica. *Geoderma.* **98**: 61–82.

Parfitt, R. L. 1986. Towards Understanding Soil Mineralogy. III. Notes on Allophane. New Zealand Soil Bureau Laboratory Report CM 10.

Payet, N., Findeling, A., Chopart, J. L., Feder, F., Nicolini, E., Saint Macary, H. and Vauclin, M. 2009. Modelling the fate of nitrogen following pig slurry application on a tropical cropped acid soil on the island of Réunion (France). *Agr. Ecosyst. Environ.* **134**: 218–233.

Raunet, M. 1991. Physical Characteristics and Soils of Réunion Island (in French). Cirad, Montpellier, France.

Shoji, S., Nanzyo, M. and Dahlgren, R. A. 1993. Volcanic Ash Soils: Genesis, Properties and Utilization. Developments in Soil Science 21. Elsevier, Amsterdam.

Soil Survey Staff. 1960. Soil Classification: A Comprehensive System. 7th Approximation. Soil Conservation Service, U.S. Department of Agriculture. U.S. Govt. Printing Office, Washington, D.C.

Soil Survey Staff. 1999. Soil Taxonomy. 2nd Edition. USDA Handbook No. 36. U.S. Govt. Printing Office, Washington, D.C.

United States Department of Agriculture Natural Resources Conservation Service (USDA-NRCS). 2004. Soil Survey Laboratory Methods Manual. Soil Survey Investigations Report No. 42. Soil Survey Investigations, USDA-NRCS, Lincoln, Nebraska.

Van Lagen, B. 1996. Soil analysis. *In* Buurman, P., van Lagen, B. and Velthorst, E. J. (eds.) Manual for Soil and Water Analysis. Backhuys Publishers, Leiden. pp. 1–120.

Zebrowski, C. 1975. Study of a climatic sequence of soils of Réunion Island. *Cah. ORSTOM Pédol.* (in French). **13**: 255–278.

Catena 110 (2013) 215–224

Contents lists available at SciVerse ScienceDirect

Catena

journal homepage: www.elsevier.com/locate/catena

Soil map update: Procedure and problems encountered for the island of Réunion

Frédéric Feder *

CIRAD, UPR Recyclage et Risque, Dakar, Sénégal

ARTICLE INFO

Article history:
Received 7 February 2012
Received in revised form 13 June 2013
Accepted 20 June 2013

Keywords:
Updating
WRB
CPCS
Tropical soils
Ferrallitic soils
Andosols

ABSTRACT

Many soil maps were drawn up after World War II with different soil classifications that have significantly evolved since. Updating such old maps with a new version or a new classification system is always complex: (i) we do not always possess all the original information; (ii) the criteria for determining references are often different, and (iii) on the most accurate scales, correlations come up against the complexity and specificities of each classification system. On Reunion, a volcanic tropical island in the Indian Ocean, we undertook a comprehensive overview of the old existing soil studies. This article describes (i) the procedure used to update the soil maps and the toposequence acquired with the old French *Commission de Pédologie et de Cartographie des Sols* (CPCS) classification system, without any new information, using the World Reference Base for soil resources (WRB); (ii) the construction of a new soil map drawn up with completely new information, and (iii) a comparison of these two approaches. At elevations below 350 m asl (above sea level), without any new pedological information, we updated Brown ferruginous soils, Reddish-brown ferrallitic soils, and Fersialitic soils into Haplic Nitisols (Humic, Eutric). The acquisition of new data showed that this update was incorrect because not all the diagnostic criteria of the Nitic horizons were met. The correct diagnostic horizons were a Mollic horizon when the thickness was 25 cm or more, or a Cambic horizon. Leptic Phaeozems and Leptic Cambisols were then the correct Reference Soil Group (RSG). At elevations from 350 to 900 m asl, without any new information, Brown and Reddish-brown ferrallitic soils, Andic ferrallitic soils, and Brown and Andic brown soils were updated into Haplic Nitisols (Humic, Dystric) and Andic Umbrisols (Humic). The acquisition of new data showed that this update was incorrect because Andic properties and the diagnostic criteria of the Nitic horizons were not met. Over 900 m asl, Pozols were correctly updated, as were the Andosols except from 900 to 1050 m asl where not all the Andic properties were met. Without any new information, incorrect updates were observed for both the determination of RSG and the qualifiers. Despite the field descriptions, the lack of any analytical determinations on the old soil studies was a source of updating errors for the more developed soils formerly qualified as ferrallitic. In order to update limits for Andic properties and Andosols, the systematic use of analytical determinations has to be considered for updating old soil maps, as the diagnostic criteria are more restrictive than in the past.

1. Introduction

Many soil surveys were undertaken after World War II in tropical and developing countries to assess land productivity and sustainability on different scales (D'Hoore, 1964; Eswaran et al., 1997). In sub-Saharan Africa for example, such maps were mostly established using one of the three major soil classifications at that time. The French classification, called the CPCS (*Commission de Pédologie et de Cartographie des sols*; CPCS, 1967), was used for historical reasons in the 1970s in Burkina Faso, Benin, Togo, Senegal, and also in Ivory Coast and Chad. The American classification, Soil Taxonomy, published by the Soil Survey Staff (USDA-SCS, 1975) was used in Cameroon and in Mali. The Legend of the Soil Map of the World published by FAO and UNESCO (FAO, 1974) was used in Nigeria, Ghana, and Liberia. These three classification systems were then improved through both technical developments and changes in soil science concepts (Bockheima et al., 2005; Kellogg, 1974; Mermut and Eswaran, 2001). The CPCS was significantly overhauled to obtain the *Référentiel Pédologique* (Baize and Girard, 1995) with two major innovations: (i) the new system was not a hierarchical classification like the CPCS, but a typological classification; (ii) the object of the study was the catena which can be subdivided into horizons according to vertical or lateral sequences (Baize, 1993). A new version was recently published (Baize and Girard, 2009). The Legend of the Soil Map of the World (FAO, 1974) evolved into a real classification system (FAO, 1998) and many improvements were added at later dates (IUSS Working Group WRB, 2007) while a new edition of the Soil Taxonomy was also published (Soil Survey Staff, 1998).

* Tel.: +221 774165640.
E-mail address: frederic.feder@cirad.fr.

0341-8162/$ – see front matter © 2013 Elsevier B.V. All rights reserved.
http://dx.doi.org/10.1016/j.catena.2013.06.019

There are various and multiple reasons for updating old soil maps depending on the situations. The old soil science classifications were based on concepts that are no longer considered relevant (Mermut and Eswaran, 2001). Current consideration of our ecosystems has greatly evolved and soils in particular are recognized as playing a major role in many environmental services. However, we do not always have the necessary information (descriptions, analyses, etc.) for assessing such services and quantifying their role.

Re-interpreting old maps or updating them with a new version or another classification system can be tricky and often complex, for three main reasons. Firstly, it is sometimes difficult to gain access to all the data and additional information needed to re-interpret them, especially for the oldest studies (georeferencing, methods used, accuracy, etc.). Secondly, the criteria for determining references are not necessarily the same, or their threshold values have changed (pH, base saturation rate, soil horizon colors, etc.). Thirdly, often depending on the scale used to draw up the map, the updating problems differ. Indeed, on scales of between 1:1,000,000 and 1:250,000, correlations exist between several major soil groups in the different soil classifications because there are similarities, notably for analytical and descriptive characteristics. However, on larger more precise scales (1:100,000 or even 1:25,000), establishing correlations comes up against the complexity of the highly localized case studies, and against the subtleties and specificities of each classification system.

In Reunion, a volcanic tropical island in the Indian Ocean (Fig. 1), we undertook a comprehensive overview of existing soil studies in order to assess the role played by soils in retaining and transferring nitrates to the aquifers (Feder and Findeling, 2007; Payet et al., 2009). In fact, many properties (anion exchange capacity, variable charge with pH, hydraulic conductivity, etc.) influence pollutant transfers through tropical soils (Legros et al., 2013). These properties, which are highly dependent on the soil type, can be obtained or deduced from recent soil maps and are not always present on the old maps. Our analysis of the different sources of pedological information for the western zone of Reunion showed that the soil data were insufficient to update the existing old maps (Feder and Bourgeon, 2009).

This article presents: (i) a summary attempt to update the existing pedological information, a priori, without any new information; (ii) the results of new soil mapping; and (iii) a comparative analysis of the previous two results to show the possibilities and limitations of updating soil maps with or without new pedological information.

2. Materials and methods

2.1. Description of the island of Reunion and the study sector

The tropical island of Reunion (2512 km^2; an estimated population of 821,136 in 2010 according to the French statistics institute, INSEE) is located in the Indian Ocean 800 km east of Madagascar (Fig. 1). Reunion is composed of two volcanoes, the *Piton des Neiges* (3069 m asl (above sea level)) to the northwest, which has been dormant for 12,000 years, and the *Piton de la Fournaise* (2631 m asl) to the southeast, a recent volcano that is still active (Bussière, 1958). The existence of these two volcanoes explains the extreme geographical variability of the climate. Annual rainfall increases from 600 mm on the west coast to 8000 mm on the east coast. Temperatures are correlated with altitude and range from an average of 24 °C at sea level to 10 °C at the highest points.

The region on the western slope of the *Piton des Neiges*, which receives little rainfall in its lower section as it is "leeward" has seen considerable agricultural expansion linked to the development of irrigation over the last ten years or so. Our study sector covered 428 km^2 of that region, amounting to 17% of the total land area of the island (center: 21° 00′ S–55° 20′ E; Fig. 1) with a coastline bordered by a coral reef. This sector exhibits a strong climatic gradient in line with altitude, with the average temperature falling 0.7 °C every 100 m in elevation. The coastal climate, with average temperatures of 24 °C and 800 mm year^{-1}, contrasts quite strongly with that of the highest point in the region (2203 m asl), at 10 °C and 1700 mm year^{-1}.

On the western slope of the *Piton des Neiges*, volcanic rocks were initially dated by Bussière (1957, 1958) at between 5 and 2 Ma BP (Before Present) and he did not report any ash overlay. McDougall (1971) reduced that age, indicating an age of between 250,000 and 210,000 years BP for the same rock formations. In the western zone of the island, the most recent data from Gillot and Nativel (1982) led to a distinction between:

(i) the olivine basalts (series of oceanites over 340,000 years BP),
(ii) the so-called "pintade" basalts due to the white plagioclase crystals that contrast with the gray paste (hawaiites dating back to around 340,000 to 250,000 years BP), and
(iii) the sodic basalts (mugearites dated between 250,000 and 70,000 years BP).

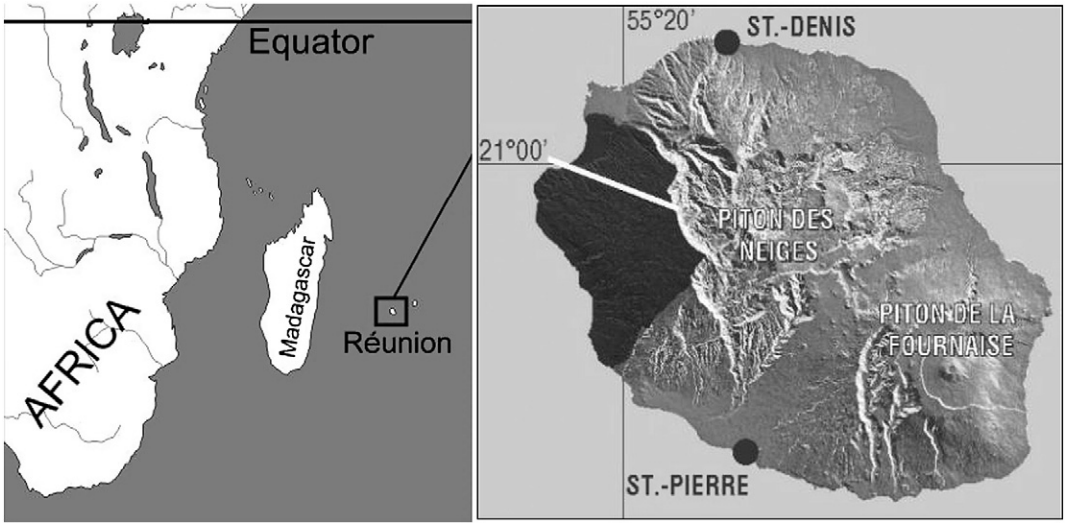

Fig. 1. Location of the island of Reunion (on left) and of the study zone (in dark gray) on the western slope of the *Piton des Neiges* ancient volcanic landmass. The Zebrowski (1975) toposequence in the study zone, between the bay of Saint-Paul and the crest of the *Cirque de Mafate* is shown by a continuous white line.

2.2. Nature and location of soil samples and observations for the new soil map

The new soil survey in the 428 km^2 study area involved digging 78 pits, taking one or more soil samples (depending on the depth, to 1.25 m maximum) with an auger at 175 places (Fig. 2) and almost 200 further localized observations (not presented in Fig. 2). Each of the 78 reference pits underwent a full pedological description and sampling. The accuracy and reliability of the description and analytical results enabled the full characterization of all soil horizons to a depth of 125 cm (FAO, 2006; Schoeneberger et al., 2002). Complete soil analyses were carried out for each horizon in the pits and the results are presented in the following "Laboratory soil analyses" section. The 175 augerings were carried out to increase the density of sampling points, in order to define certain limits between units. The location of the 175 augerings, and the analyses carried out on them, were chosen as the compilation of the soil map progressed. We carried out a pedological description or partial analyses (color, texture, exchangeable base contents, etc.) on the 200 additional observations (roadside pits, etc.).

2.3. Spatial resolution and cartographic representation

The new map was drafted for publication on a scale of 1:100,000. Soil maps call for a number of observations that are proportional to the desired final representation scale. For instance, for a map published at a scale of 1:100,000, several authors (FAO, 1990; Legros, 1996) recommend from 0.5 to 4 observations per km^2. This observation density primarily depends on the prior knowledge of the terrain and its complexity. In our case, we carried out around 450 observations for 428 km^2 (pits, augerings, and additional observations) and we used additional sources of information (geological map, aerial photographs, and old soil maps). The observation point density was therefore high and the accuracy of our map on a scale of 1:100,000 was in line with recommendations (FAO, 1990; Legros, 1996).

The new map is primarily based on pedological and geomorphological elements. Tracing of the outlines of the cartographic units followed the geomorphological outlines identified by aerial photography based on the work by Raunet (1991a). We also used recent DTM data (Digital Terrain Model) and geological maps. These cartographic units were drawn to correspond to a pedolandscape, thereby jointly including pedological and geomorphological elements. By construction, a pedolandscape unit can group several soil typological units. Correlatively, it is theoretically possible for a soil typological unit to be found in several pedolandscape units. However, that will remain exceptional, especially in the presence of the climatic and topographical gradients that are so strongly expressed in Reunion. A pedolandscape unit might be essentially composed of just a single soil typological unit. In addition, the contour lines were traced every 200 m.

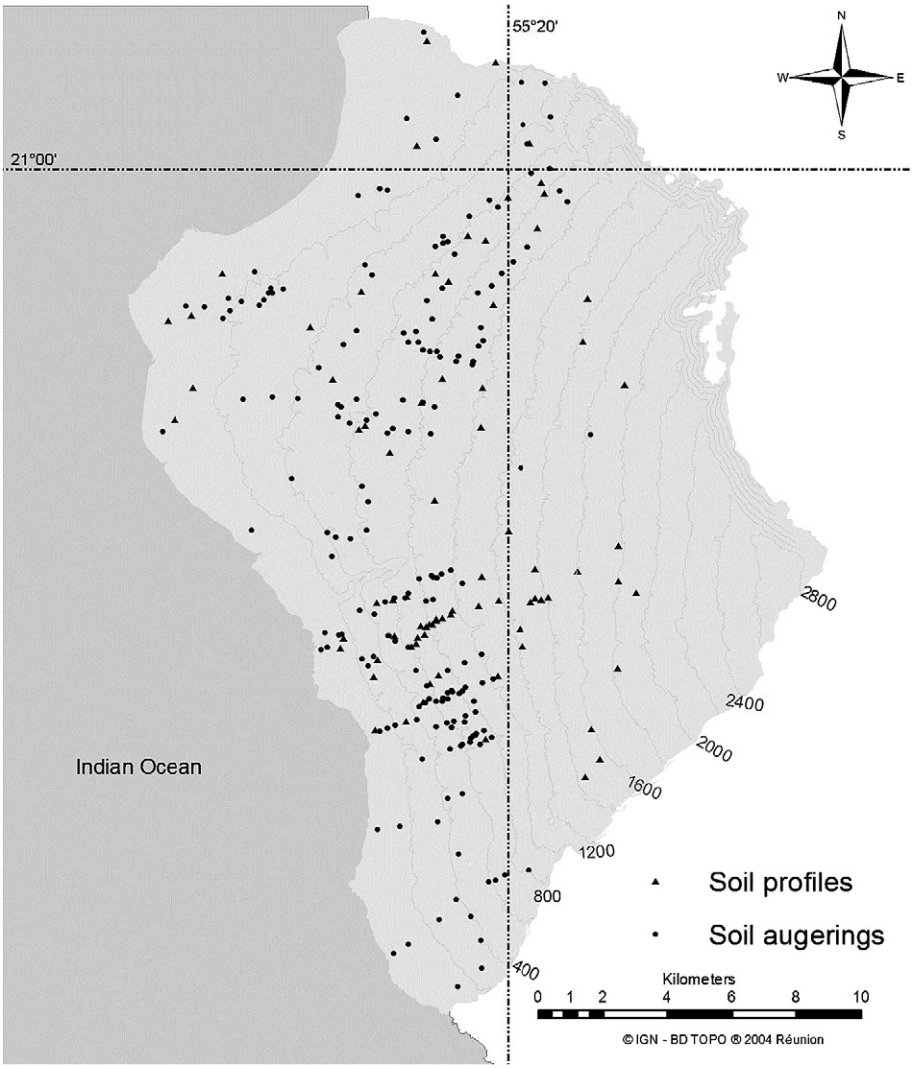

Fig. 2. Location of the soil profiles (triangles) and augerings (circles) on island of Reunion.

2.4. Choice of pedological reference framework

The modern and international classification system of the World Reference Base (WRB) was the natural choice when drawing up the new map (IUSS Working Group WRB, 2007). WRB proved to be well suited to our objectives and we considered that it guaranteed the reproducibility and a degree of longevity for our interpretations. We followed strict principles (georeferenced sampling, quality approach for conditioning, storage, follow-up of samples, and their analyses, etc.) and up-to-date international standards for the description of soils (FAO, 2006).

2.5. Laboratory soil analyses

For each horizon, a soil sample was taken for analysis and the bulk density was measured. Bulk density was measured with cylinders of known volume (NF X31–501, AFNOR 1999), weighed wet then dried in an oven at 105 °C to measure their moisture content at the time of sampling. The mean of three replicates was used for each horizon. The soil sample for laboratory analyses was air-dried, crushed, and sieved with a 2 mm round-holed sieve (NF ISO 11464 X31–412, AFNOR 1999).

The first set of analyses was carried out at the CIRAD laboratory in Saint-Denis de la Réunion (ISO 9001 certified): pH_{water}, pH_{KCl}, electrical conductivity (NF ISO 10390 X31-117, AFNOR 1999), pH_{NaF} (4C1a1a1a-b1 protocol, Soil Survey Staff, 2004).

The second set of analyses was carried out by the CIRAD soil analysis laboratory in Montpellier (ISO 9001 certified). Organic carbon rates and total nitrogen levels were measured on an elemental analyzer (Thermoquest NC2001 Soil). The cation exchange capacity (CEC) and exchangeable base contents were measured using 1 M ammonium acetate buffered at pH 7. Exchange acidity was measured after extraction with KCl 1 M. The phosphate retention percentage was measured by the Blakemore method (4D8a1a-b1 protocol, Soil Survey Staff, 2004). The quantities of iron, aluminum, and silicon extracted by selective dilutions in ammonium oxalate at pH 3 were quantified by ICP-OES (Varian Vista equipped with a CCD detector) and recorded as Fe(o), Al(o), and Si(o), respectively. The "oxalfe" index (Van Wambeke, 1991) corresponds, as a percentage, to the quantity of Al(o) + 1/2 Fe(o). These values can also be used to calculate the quantity of allophane (Allo) present in the different horizons using several formulas; one of the simplest, Allo = 7.14 Si(o), was proposed by Parfitt and Wilson (1985). The quantities of iron, aluminum, and silicon extracted by selective dissolutions with CBD (citrate–bicarbonate–dithionite) were also quantified by ICP-OES (Varian Vista equipped with a CCD detector) and recorded as Fe(d), Al(d), and Si(d), respectively. The optical density of the oxalate extract was measured (4G2a2a1 protocol, Soil Survey Staff, 2004) to be used as an indicator of the podzolization process. Particle size analysis in five fractions was carried out by the pipette method after the destruction of organic matter by oxygenated water and dispersal by sodium hexametaphosphate (NF X 31–107 method, AFNOR, 2004). Dispersal was sometimes improved by ultrasound treatment (Vibracell 75041 instrument, AGTT-00366 at 750 W, equipped with a 13 mm probe and used at 75% of its power). The existence of poorly crystallized mineral phases (allophane, imogolite) in a large proportion of the soils hindered the particle size analyses. This problem limited the study, hindering the identification of clay accumulation horizons (horizons called Argic in the WRB) and groups of soils that are conditioned by the existence of those horizons. This recurring problem for Andosols and more generally for soils with Andic properties (Alary et al., 2013) also hindered attribution of the textural suffix qualifiers Clayic or Siltic, which could only be done on the basis of tactile impressions in the field, without cross-checking with the particle size analysis results.

3. Results and discussion

3.1. Updating existing pedological information without any new data

The soils in the western part of the island of Reunion have been studied on various scales by three different authors since 1960. The zone on the western slope of the *Piton des Neiges* was first studied by Riquier (1960a, 1960b: map and booklet). Zebrowski (1975) studied a toposequence between Saint-Paul and the crest of the *Cirque de Mafate* (indicated by a continuous white line in Fig. 1). Raunet (1988) produced a morphopedological map on a scale of 1:50,000 and some morphopedological maps of the west coast on a scale of 1:10,000 (1989, and partially 1991a). These three authors agreed in recognizing that the soils are distributed in an altitudinal sequence of major genetic types. From one author to the next, there are some large variations in the way they assess the distribution of soils in the western zone of the island and the terminology they use to describe them. For each of the three main domains (separated by altitude), we first summarized the available information before updating it without any new data.

3.1.1. Domain of Ferrallitic soils (0–350 to 400 m asl)

The most pedologically developed soils, i.e. all the soils for Riquier (1960b) and only those located near the bottom of the sequence for Zebrowski (1975) and Raunet (1988), are Ferrallitic soils as defined in the 1960s in the old French CPCS classification (Aubert and Ségalen, 1966; CPCS, 1967). These Ferrallitic soils were defined by extensive or even complete alteration of primary minerals and the formation of secondary minerals such as kaolinite, aluminum hydroxides, and iron oxy-hydroxides. These neoformations were verified by mineralogical techniques and assessed by calculating the Ki ratio (silica/aluminum) from the results of a triacid analysis (sulfuric, nitric, and hydrochloric acids).

The extent and meaning of the Ferrallitic soils differed depending on the author, though they used the same classification system. Riquier (1960b) qualified all soils with Ki values remaining well below 2 as Ferrallitic and an increasing degree of ferrallitization in line with the height above sea level, without any mineralogical analyses. Thus, Brown ferruginous soils were identified at low elevations from 0 to 200 m while Reddish-brown Ferrallitic soils were identified at elevations from 200 to 400 m. This genesis of thick, highly weathered Ferrallitic soils was compatible with the rock dating reported by Bussières (1957, 1958). For Zebrowski (1975), in the lower part of his sequence (at 350 m), a Ferrallitic soil always had a low Ki, $0.8 \leq Ki \leq 2.0$ and no reaction to the pH_{NaF} test. Interpretation of the Ki ratio values obtained from triacid analysis was well adapted to characterize secondary minerals in soils developed on gneissic rocks but failed when applied to soils derived from other types of rocks because primary minerals were partly dissolved (Claisse, 1968; Pédro, 1966). This probably occurred for Reunion soils and led Riquier (1960b) and Zebrowski (1975) to Ki interpretations that can be considered as erroneous today. Raunet (1988, 1989) reduced the extent of the Ferrallitic soils because (i) he did not use Ki ratio values, and (ii) the last dating of the rocks was incompatible with ferrallitization over a substantial thickness. He only represented Ferrallitic soils to the north and south of our study zone, on the most ancient rock outcrops of Reunion volcanism (olivine basalts of the oceanite series more than 340,000 years BP). For Raunet (1989, 1991a), Brown ferruginous soils and Fersiallitic soils were differentiated at mid-altitude (<350 m) depending on whether they were located on flows corresponding to hawaiites (dated around 340,000 to 250,000 years BP) or flows corresponding to mugearites (dated around 250,000 to 70,000 years BP). The maps by Raunet (1988, 1989, 1991a) provided some new morphopedological information. He also recognized soils with some Vertic properties located in some concave colluvial zones at the bottom of the slope.

Reinterpretation of existing data did not always make it possible to strictly identify an RSG in this altitude range. Pedological descriptions by Riquier (1960b), Zebrowski (1975), and Raunet (1988, 1989, 1991a) clearly show no Argic, Ferralic, Plinthic or Petroplinthic horizons, thus excluding the following typical tropical soils: Alisols, Acrisols, Luvisols, Lixisols, Plinthosols, and Ferralsols. The particle size analysis and CEC values were compatible with Nitic horizons. However, it is not possible to identify Nitic horizons in the absence of measured quantities of active iron extractable by acid oxalate (pH 3), free iron extractable by citrate–bicarbonate–dithionite, and water-dispersible clay to the total clay ratio. Moreover, the observations and analyses did not contradict the diagnostic criteria of Cambic, Mollic, or Umbric horizons, with less clear properties than the Nitic horizon. Lastly, the age of the geological materials and the local conditions of hydrolytic alteration steered our updating of the different Ferrallitic soils of Riquier (1960b), Zebrowski (1975), and Raunet (1988, 1991b), towards Haplic Nitisols with Nitic diagnostic horizons. In addition, with the available information, we defined two qualifier suffixes: Humic and Eutric. Soils with Vertic properties were only observed by Raunet (1989, 1991a). With his descriptions, we assigned these soils unequivocally to the Haplic Vertisols with two qualifiers: Humic and Hypereutric. Nevertheless, their small areas may restrict their cartographic representation at scales of between 1:100,000 and 1:1,000,000.

The current concept of ferrallitization, inherited from the lateritization concept (Van Wambeke, 1991), has disappeared from modern classification systems, at the same time as the triacid analysis (used to calculate Ki ratio) has disappeared from the laboratory. For Aubert (1966), the classification was too largely based: (i) on the mineralogical traits of the mid- or deep horizons, and (ii) on some original material of the soil, often acquired a very distant time ago. The exchange capacity or degree of saturation of the absorbing complex was too rarely used, if at all.

3.1.2. Intermediate domain of Brown and Andic soils (from 350 to 400–900 m asl)

In this domain, all the authors acknowledged a major but gradual change in soil properties and at lesser degrees of alteration when compared to the lower altitudes. From 400 to 700 m asl, Riquier (1960a) distinguished Reddish-brown ferrallitic soils and, up to 900 m asl, Brown ferrallitic soils that were less weathered, thicker, less acid, and richer in organic matter. From 350 to 650 m asl, Zebrowski (1975) identified Ferrallitic soils ($0.8 \leq Ki \leq 2.0$) with no reaction to the pH_{NaF} test and with a clay texture. From 650 to 900 m asl, he identified Andic ferrallitic soils with a very weak reaction to the pH_{NaF} test and a loamy texture. Zebrowski (1975) indicated the existence of gibbsite from 650 m to 900 m asl, and phyllitic minerals composed of halloysite and metahalloysite below an elevation of 650 m asl. From 350 to 700 m asl, Raunet (1988) identified Brown soils and, from 450 to 700 m asl, Andic brown soil. He found mostly Andosols from 700 m upwards but he brought down locally the lower elevation limit for these Andosols to 550 m asl.

The difficulty in reinterpreting data at elevations from 350 to 900 m asl mainly lies in defining the Andic properties of the soils used by each author. Indeed, Riquier (1960b) found Brown ferrallitic soils between Reddish-brown ferrallitic soils (400 to 700 m asl) and Beige ferrallitic soils (beyond 900 m asl), but he did not have any methods at the time to identify the existence of poorly crystallized substances that are typical of Andic soils. Zebrowski (1975) and Raunet (1991b) used the pH_{NaF} test but with a different interpretation. Zebrowski (1975) considered the development of the red color in 20 s as being characteristic of an Andosol and the occurrence of a pink color after 2 min as indicating Andic properties. Raunet (1991b) considered that soils rich in amorphous substances displayed a large increase in pH after 2 min as defined by Fieldes and Perrott (1966). In addition, only Raunet (1991b) used the high phosphate retention percentage as an Andic criterion and he also used extractions with acid oxalate to quantify the poorly crystallized substances of Andic soils. However, for these two parameters, he did not apply precise thresholds and extended the limit of the soils with Andic properties towards lower elevations (down to 450 m).

Updating this information on Andic properties cannot be strict because not all the diagnostic criteria were measured by these authors (aluminum and iron extractible by acid oxalate, bulk density, and phosphate retention percentage). The field descriptions and partial analyses of the three authors lead us to set a lower limit to Andic properties around 500 m asl. As for the lower elevations, the diagnostic horizon is neither Argic, Ferralic, Plinthic, nor Petroplinthic. From 350 to 500 m asl, the CEC and particle size analyses are strong criteria for assigning these soils to the Nitisols: 50 to 60% clay for Riquier, 58 to 73% for Zebrowski, and 50 to 52% for Raunet. From 500 and 900 m asl, the determination of the diagnostic horizon is different because of this same particle size criterion. All the authors identified a loamy texture in situ. The particle size analyses undertaken showed clay contents of 15 to 35% (Riquier), 11 to 11.2% (Zebrowski), and 22 to 35% (Raunet). Despite high heterogeneity, these particle size data no longer make it possible to diagnose a Nitic horizon. Moreover, the soil structure, strong but not massive, the Munsell colors, with a chroma of 3 or less, an organic carbon content always higher than 20 g kg^{-1}, and a base saturation of less than 50% suggest to us an Umbric diagnostic horizon. In addition, Andic properties were always present and the Andic qualifier could be added.

3.1.3. Domain of Andosols and Podzols (above 900 m asl)

Andosols (or Beige ferrallitic soils for Riquier (1960b)) and some mascareignite-bearing soils or some Podzols have always been recognized above 900 m asl. The soils called Beige ferrallitic soils by Riquier (1960a,b) were subsequently qualified as Andosols and he already recognized some phytolith-bearing soils. In 1960, the parent rock was assumed to be uniformly ancient and knowledge of soils formed over volcanic ash was still very much in its infancy. Andepts were recognized as a sub-order of little developed soils created for soils comprising at least 60% allophanes, while pointing out that "measures of allophane percentages are very rough" (USDA, 1960). Zebrowski (1975) recognized Andosols, notably through the pH_{NaF} test but he did not propose any intermediate soil between Ferrallitic soils and Andosols. Starting from an elevation of 900 m, Andosols were characterized by a strong reaction to the pH_{NaF} test, but displaying a very low Ki ratio (well below 1) and these soils were found up to 1500 m, an altitude at which he identified Podzols. Zebrowski (1975) thus identified the zone where podzolization was taking place, by revealing a major redistribution of fulvic acids. Raunet (1988, 1991b) observed, from 700 to 1200 m asl, some Chromic, non-perhydrated desaturated Andosols, some perhydrated desaturated Andosols (from 1200 to 1800 m), and some Vitric Andosols (above 1800 m). Raunet (1991b) did not indicate Podzols from 1600 to 1800 m above sea level, but a sub-category of desaturated mascareignite-bearing Andosols (phytoliths). He thus opted for the establishment of a material comprising phytoliths rather than the mechanism of organic matter distribution within the profile. At elevations over 900 m asl, the pedological information of the three authors converged towards unambiguous updating. Andic diagnostic properties were not defined with the same criteria as we would use today. However, all the descriptions and analyses carried out by the three authors converged to update the Beige ferrallitic soils of Riquier (1960a,b) and Andosols of Zebrowski (1975) and Raunet (1991b) as Andosols. The Vitric, Hydric, and Dystric qualifiers can be added at different altitudes with Raunet's information. The mascareignite-bearing soils of Riquier (1960a,b) and Raunet (1991b) and Podzols of Zebrowski (1975) can be updated as Podzols because all the diagnostic criteria of a Spodic horizon are met. The qualifier Andic can be added to be coherent with the recognition of Andic properties.

3.2. New cartography of the western part of Reunion

3.2.1. Analytical characteristics of the main soil types encountered

The observations and analyses of the 78 reference pits and the augerings led to the identification of 30 soil types. They were attached

to 11 reference soil groups (RSGs) of the WRB (IUSS Working Group WRB, 2007), which were subsequently subdivided using 9 prefixes used alone or combined. Twenty-six soil types were found to have developed directly over the volcanic parent rocks in place, distributed from the top to the bottom of the slope; the 7 RSGs to which they were attached were Andosols, Podzols, Umbrisols, Alisols, Cambisols, Phaeozems, and Vertisols. The main pedological and physico-chemical characteristics of the 7 soil types are presented in Table 1. These 7 soil types covered the largest areas in this study zone and they were also the most relevant for explaining the pedogenic evolution on the slope. Four soil types corresponding to 4 RSGs were recognized as being independent of the altitude and the volcanic parent rock: Fluvisols, Arenosols, Gleysols, and Leptosols.

Soils displaying Andic properties were identified in the zones located highest up the slope. In fact, Table 1 presents the four characteristics used to diagnose the Andic properties of a horizon: bulk density, phosphate retention percentage, organic carbon rate, and the "oxalfe" index. All the Andosols and the other soils displaying Andic properties were identified in high altitude environments (Silandic and Vitric Andosols (Dystric)), high hummocky basaltic plateaux (Andic Podzols and Silandic Andosols (Dystric)), and mid-altitude basaltic plateaux with an undulating topography (Andic Cambisols (Humic, Dystric) and Andic Umbrisols (Humic)). The pH_{NaF} in Table 1 was used as an andosolization indicator by Zebrowski (1975) and Raunet (1989, 1991b). Thus, on the basis of this criterion, the Haplic Cambisol at 830 m was "closer" to the Andic characteristic than the Andic Cambisol located at 1064 m; this disagrees with two of the three criteria defining Andic properties.

All the Andosols exhibited the Silandic property and most of them the Hydric property. All the Andic horizons sampled were qualified as Silandic as the Si(o) was always over 0.6%, reaching as much as 3.49%. Allophanes and similar minerals dominated; for a typical Andosol, the quantities of allophane, calculated by Parfitt and Wilson's formula (1985), varied from 114.2 g kg^{-1} in the surface horizon to 178.5 g kg^{-1} at a depth of 1 m. The Hydric property was acknowledged for 60% of the Andosols identified. The geographical distribution was not uniform, though most of the Hydric Andosols were found at the highest altitudes.

Podzols were formed from Andosols. The Andic Podzols were all characterized by an Albic horizon over a Spodic horizon. One or more horizons with Andic properties were always recognized at depth under the Albic and Spodic horizons. Identification of the podzolization process through the migration of organic matter from an Albic horizon to a Spodic horizon was confirmed by measuring the optical density of the oxalate extract at a 430 nm wavelength.

Most of the analytical parameters displayed a monotonous evolution in line with altitude. The organic carbon, total nitrogen, CEC, pH_{NaF}, phosphate retention percentage, "oxalfe" index, Si(o), and Al(d) parameters increased with altitude. Conversely, the pH_{water}, pH_{KCl}, base saturation rate, and bulk density parameters decreased with the increase in altitude. Only the sub-surface horizons of the Podzols (Albic and Spodic horizons) disturbed the monotony for the phosphate retention percentage, pH_{NaF}, and Si(o) parameters. These parameters were used to assess the transfer of Nitrates (Feder et al., 2008).

3.2.2. Compilation of the pedolandscape map and its legend

In the cartographic representation of the study zone, we identified four major altitude zones and fourteen pedolandscapes corresponding to as many cartographic units (Fig. 3). The four main altitude zones

Table 1
Andic properties and general characteristics of 7 selected pedons covering the largest areas of the western part of Reunion.

Horizons	pH	pH	$C_{org.}$	$N_{tot.}$	CEC[a]	BS [b]	Color	B.D. [c]	P ret.[d]	Oxalfe [e]	pH	Si(o)	Fe(d)	Al(d)	Si(d)
	Water	KCl	g kg^{-1}	g kg^{-1}	cmol kg^{-1}	%	Munsell	g cm^{-3}	%	%	NaF	g kg^{-1}	g kg^{-1}	g kg^{-1}	g kg^{-1}
Andic Podzol (1630 m asl[f]; 21° 7′2.04″ S–55° 21′7.17″ E)															
0–5/20 cm	4.5	3.6	144	10.8	45.2	5	7,5 YR 3/4	n.d.	65	2.4	7.7	3	34	9	6
5/10–10/30 cm	4.4	3.3	67	4.0	23.8	4	2,5 YR 5/1	0.39	30	0.5	7.4	1	12	2	10
10/30–20/30 cm	4.3	3.5	141	9.9	52.3	3	5 YR 3/2	n.d.	77	3.0	7.8	2	52	10	6
20/30–70 cm	4.7	4.6	103	5.3	53.5	1	10 YR 4/4	0.44	95	9.3	10.9	24	71	56	9
70–135 cm	5.1	5.3	19	1.2	26.9	1	10 YR 4/6	0.85	94	7.8	10.4	25	112	55	19
Silandic Andosol (Dystric) (1110 m asl; 21° 7′35.66″ S–55° 19′6.38″ E)															
0–7/15 cm	6.3	5.3	139	11.4	57.5	30	7,5 YR 3/2	0.58	96	8.1	10.7	16	85	45	5
7/15–40/50 cm	5.9	5.4	66	3.7	42.8	9	10 YR 4/4	0.75	94	9.0	10.8	21	107	57	9
40/50–130/140 cm	5.4	5.8	16	1.0	22.2	3	7,5 YR 4/4	0.77	94	7.1	10.5	25	124	56	18
Andic Cambisol (Humic, Dystric) (1064 m asl; 21° 8′48.03″ S–55° 19′18.93″ E)															
0–35 cm	5.1	4.5	40	4.4	36.1	24	10 YR 3/4	1.09	84	2.8	9.2	5	76	24	7
35–95 cm	5.7	5.2	11	0.9	28.6	18	7,5 YR 4/3	0.70	90	2.0	8.2	3	91	19	5
95–135 cm	5.3	4.7	8	0.6	35.7	11	10 YR 4/3	0.72	97	2.5	9.1	7	99	29	11
Haplic Cambisol (Humic, Dystric) (830 m asl; 21° 7′45.17″ S–55° 18′31.48″ E)															
0–40 cm	5.4	4.7	31	3	28.1	19	7,5 YR 4/3	1.06	80	3.5	9.7	7	94	34	9
40–75 cm	6.0	5.0	29	3.3	25	34	7,5 YR 4/4	0.80	77	2.9	9.2	5	93	28	7
75–215 cm	6.0	5.6	12	1.1	24	19	7,5 YR 4/4	0.78	93	3.8	10.0	10	106	41	12
Haplic Umbrisol (Humic) (640 m asl; 21° 1′20.87″ S–55° 19′14.16″ E)															
0–30 cm	5.2	4.8	31	3.1	26.0	29	10 YR 3/2	1.18	67	1.0	8.5	1	75	16	3
30–80 cm	5.3	4.8	25	2.7	25.8	28	7,5 YR 3/2	1.10	80	1.2	8.6	1	81	17	3
80–150 cm	5.7	6.7	6	0.6	24.2	31	10 YR 3/3	1.00	87	1.1	9.2	2	83	16	3
Leptic Phaeozem (Eutric) (262 m asl; 21° 8′41.05″ S–55° 17′21.60″ E)															
0–50 cm	6.9	6.0	25	2.4	22.7	85	7,5 YR 3/2	1.30	42	0.7	8.2	2	61	5	5
Leptic Cambisol (Humic, Eutric) (131 m asl; 21° 7′57.98″ S–55° 16′54.76″ E)															
0–15 cm	6.6	5.3	20	1.6	26.1	85	5 YR 3/4	1.27	31	0.5	8.1	1	59	4	5
15–40 cm	7.2	5.8	4	0.4	36.3	76	2,5 YR 3/4	1.32	50	0.7	9.1	2	65	4	6
40–85 cm	7.1	5.6	2	0.2	36.5	75	2,5 YR 3/6	1.42	47	0.7	8.9	2	51	4	9

[a] Cation exchange capacity.
[b] Base saturation.
[c] Bulk density.
[d] Phosphate retention percentage (Blakemore procedure).
[e] Oxalfe index = Al(o) + 1/2 Fe(o).
[f] Above sea level; n.d. not determined.

from top to bottom of the slope, based on geomorphological observations, were: high altitude environments, high hummocky basaltic plateaux, mid-altitude basaltic plateaux with an undulating topography, and low basaltic plateaux with an undulating topography. Each of these major zones consisted of one or more pedolandscapes. This grouping was based on geographical proximity within a geomorphological whole and a certain uniformity of use or development of soil types. Ten cartographic units (CU 1 to CU 10) were distributed along the four major altitude zones adopted, from top to bottom of the slope, and four units were independent from this altitudinal gradient (CU 11 to CU 14). Several pedolandscape units were only formed by a single soil typological unit: CU 2 and CU 9 for the elevation-dependent zones and all the units independent from this altitudinal gradient. A well developed soil type corresponded to each altitude range, which was generally associated with an incompletely developed type of soil (Cambisol) displaying the same pedogenic tendency.

The pedogenic processes were correlated with the altitude gradient. The high hummocky basaltic plateaux were marked by andosolization down to 900 m asl. Under forest from 1600 to 1800 m podzolization was superimposed, facilitated by the existence of a layer of phytoliths from non-current bamboo vegetation (*Nastus borbonicus*) as shown by Alarcon (1995). Below 900 m asl, pedogenesis has not been long and marked enough to have formed typically tropical soils. Accordingly, we found Umbrisols, Phaeozems, and Cambisols, young and moderately developed soils, at those elevations.

3.3. Comparison of two types of updating approach

At the lower elevations, under 500 m asl, Haplic Phaeozems (Dystric), Leptic Phaeozems (Eutric), and Leptic Cambisols were poorly updated into Haplic Nitisols (Humic, Eutric). All the field descriptive criteria (texture, structure, Munsell colors) of a Nitic diagnostic horizon were met. The CEC value and the presence of kaolinite and halloysite (Zebrowski, 1975) were thus in line with the additional characteristics of a Nitic horizon defined in the WRB. Quantities of active iron extractable by acid oxalate (pH 3), and free iron extractable by citrate–dithionite were compatible with the diagnostic criteria of a Nitic horizon, while the water-dispersible clay to the total clay ratio was not; this parameter reflects the degree of soil alteration. The surface diagnostic horizons were thus a Mollic horizon and the RSG was a Phaeozem (Table 2). When the thickness was not sufficient, the subsurface diagnostic horizon was thus a Cambic horizon and the RSG was a Cambisol (Table 2). Both these RSGs, at these altitudes, therefore displayed a shorter and less intense pedogenesis than the majority of typical tropical soils. However, Nitisols have been observed in the northwest of Reunion (La Mare, Sainte-Marie) over identical parent rocks, though subjected to more intense hydrolytic alteration. The properties of the soils in the west of Reunion therefore resemble these Nitisols, though without meeting all the diagnostic criteria due to a less marked pedogenesis.

In comparison with other studies in similar ecosystems, the intensity and duration of tropical pedogenesis on the island of Reunion have therefore been overestimated. None of the authors identified Reddish-brown halloysite-bearing soils, yet they were reported in numerous other studies on tropical soils developed over volcanic material (Albrecht et al., 1992; Colmet-Daage et al., 1967, 1970, 1973), or simply Brown soils with the clay fraction seemingly dominated by halloysite, as in Ecuador (Winckell et al., 1991). With similar climatic conditions, soils from the Hawaiian archipelago do not show a chronotoposequence (Deenik and McClellan, 2007). The youngest island (Hawaii, about 500,000 years BP) does not show Oxisols or

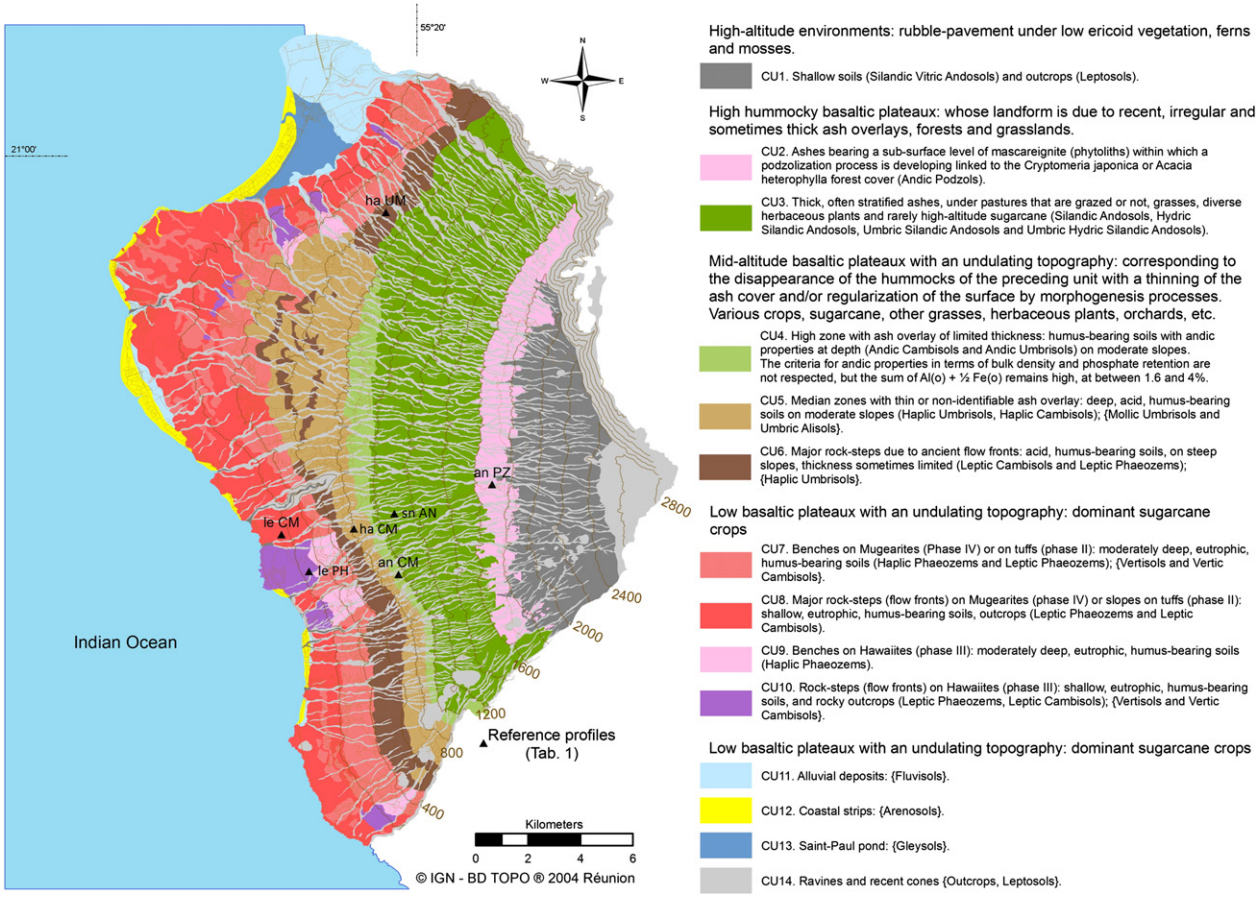

Fig. 3. New soil map and its legend for the study zone in the western region of Reunion. For each cartographic unit (CU) or pedolandscape unit, the most common soil taxonomic units are indicated in brackets and the least represented or those deduced from earlier studies are indicated in curly brackets.

Table 2
Synthetic comparison of the pedological studies undertaken in the study area and our two types of updating approach.

Altitude (m)	Riquier (1960a; 1960b)	Zebrowski (1975)	Raunet (1988, 1991b)	This study (2013) without new data	This study (2013) with new data
1850 and +	Organic beige ferrallitic soils; Mascareignite-bearing soils; Organic Lithosols	Podzols (type IV)	Vitric Andosols; outcrops	Vitric Andosols	Vitric Andosols (Dystric)
1800–1850 1750–1800 1700–1750			Desaturated mascareignite bearing Andosols	Andic Podzols	Andic Podzols
1650–1700 1600–1650					
1550–1600 1500–1550	Beige ferrallitic soils	Andosols (type III)	Perhydrated desaturated Andosols	Hydric Andosols (Dystric)	Silandic Andosols (Dystric)
1450–1500 1400–1450 1350–1400 1300–1350 1250–1300 1200–1250					
1150–1200 1100–1150 1050–1100			Desaturated Andosols	Andosols (Dystric)	
1000–1050					Silandic Andosols (Dystric); Andic Umbrisols (Humic); Andic Cambisols (Humic, Dystric)
950–1000 900–950					
850–900 800–850	Brown ferrallitic soils; Reddish-brown ferrallitic soils	Andic ferrallitic soils (type II)		Andic Umbrisols (Humic)	Haplic Umbrisols (Humic); Haplic Cambisols (Humic, Dystric)
750–800 700–750 650–700 600–650			Andic brown soils		
550–600 500–550		Ferrallitic soils (type I)			
450–500 400–450			Brown soils; outcrops	Haplic Nitisols (Humic, Dystric)	Haplic Phaeozem (Dystric); Leptic Cambisols (Humic, Dystric)
350–400 300–350	Reddish-brown ferrallitic soils	(no data)	Brown ferruginous soils; Fersialitic soils	Haplic Nitisols (Humic, Eutric); outcrops	Leptic Phaeozems (Eutric); Leptic Cambisols (Humic, Eutric); outcrops
250–300 200–250					
150–200 100–150	Brown ferruginous soils; Lithosols				
50–100				Haplic Vertisols (Humic, Hypereutric); Haplic Nitisols (Humic, Eutric); outcrops	Haplic Vertisols (Humic, Hypereutric); Leptic Cambisols (Humic, Eutric); outcrops
0–50			Vertic soils; outcrops		

Ultisols, unlike the other older islands (up to 5,000,000 years BP). The pedogenesis therefore applies to materials of different ages (corresponding to the different islands in the archipelago) that are more contrasting than in Reunion.

At intermediate elevations, from 500 to 900 m asl, Haplic Umbrisols (Humic) and Haplic Cambisols (Humic, Dystric) were poorly updated into Andic Umbrisols (Humic). In fact, the Andic prefix was attributed though not all the diagnostic criteria were met. The creation of several analytical criteria (bulk density, "oxalfe" index and phosphate retention percentage) in new systems of soil classifications has substantially limited the impact of field descriptions in defining Andic properties. However, the Umbric diagnostic horizon has been properly identified. Haplic Cambisols (Humic, Dystric) corresponded to soils with the same properties, except for the thickness of the diagnostic surface horizon, which was not sufficient.

From 900 to 1050 m asl, several soils with Andic properties were poorly interpreted as Andosols. All the analytical criteria of Andic properties were met (Andic prefix for Umbrisols) except the thickness or the beginning of Andic layers within 25 cm of the soil surface. Moreover, several soils at the lower altitudes (about 900 m asl) did not display all the Andic diagnostic criteria and have thus been classed as Haplic Cambisols (Humic, Dystric). These differences come from a stricter definition of Andic properties in new soil classification systems. In addition, Hydric properties were not always observed and the Hydric prefix could not be applied to all the Andosols over 1250 m asl. Conversely, the Silandic prefix could be applied to all the Andosols over 1050 m asl using the analysis results for silicon extractable by oxalate at pH 3.

Correlation problems were observed for the determination of both the RSG and the qualifiers. The soils in the western zone of Reunion do not exhibit a sufficient degree of alteration to be classed as Nitisols, unlike other soils developed over rocks of identical age and characteristics as those in the northeast of the island (La Mare, Sainte-Marie). The water-dispersible clay to total clay ratio was not compatible with the diagnostic criteria of a Nitic horizon; only the determination of this parameter in the laboratory would have made it possible to avoid poor updating as the field descriptions for all the other parameters

pointed to a Nitic diagnostic horizon. Likewise, the diagnostic criteria for Andic properties need to be measured in the laboratory to avoid poor updating, both for the Andic prefix and for determining Andosols. In the case of Reunion, further analysis is therefore essential to avoid poor updating. In other similar situations, updating as Nitisols, without further analyses, would have been alright if the pedogenesis had been greater. However, in order to define precise and reliable limits for Andic properties and Andosols, systematic use of analytical determinations needs to be considered when updating old soil maps.

3.4. Conclusion

The age of the studies is not the decisive factor in the updating difficulty. The latest and most complete study prior to ours (Raunet, 1988, 1991b) with its Andosols descending as far as 700 m asl and its Andic brown soils between 500 and 700 m, seems more difficult to update than the oldest study (Riquier, 1960a,b). Between the two, the study by Zebrowski (1975), which is more satisfactory in some ways since it offers a good Andosol limit and the correct identification of Podzols, only involved a toposequence and only began above 350 m asl. While it is accepted that the Beige ferrallitic soils reported by Riquier (1960a) are in fact Andosols that were not identified for historical reasons, the "Podzols–Andosols–other soils" succession is acknowledged by all.

When comparing our study with these old studies in our project zone, we found that there did not exist any one-to-one correlation between two of these studies. The use of the WRB led to some real progress, as the prefixes and suffixes proposed were more suitable for the description of these soils than the previously used classification (CPCS). The CPCS did not make it possible to account for such a distribution of soils without "inventing" sub-groups based on personal definitions. Soil Taxonomy did not offer the same facilities: for example, the sub-orders of the Inceptisols (poorly developed soils in that system) were identified by the pedoclimate and not by the, as yet, little marked pedogenesis. Updating would not have been easier using the new French classification, a follow-on from the CPCS used in earlier studies. The old studies we analyzed here came well before the publication of the 1995 version (Baize and Girard, 1995), followed by the 2008 version (Baize and Girard, 2009) of the *Référentiel Pédologique Français* (RPF), which itself followed on from the CPCS classification. As regard correlations between the CPCS and the RPF, Baize and Girard (2009) specified that there was no one-to-one correlation, as the principles of the two systems were not identical. In addition, it was only in the last RPF version (2008) that new sections dealing with solums of intertropical zones (Ferrallitisols, Oxydisols, Nitosols, and Ferruginosols) were introduced. The authors pointed out that this was a first draft which would no doubt merit in-depth revision once tried and tested by its users. Use of the RPF can raise similar difficulties to those encountered by Zebrowski in 1975 for two reasons: (i) the RPF does not impose any true hierarchy in the criteria adopted, and (ii) mineralogy is still deduced from Ki ratio values.

Over the last fifty years the progress made in our knowledge and classification of soils developed over volcanic materials in the Tropics, and progress made in assessing the age of volcanic events, are two factors that explain the rapid obsolescence of old soil maps, such as those we analyzed for the island of Reunion. Our approach, and the conclusions drawn from our comparison of the old studies, can be usefully applied in other situations, when updating other soil maps, be it in tropical or temperate surroundings.

Acknowledgments

This study received funding from the Ministry of Overseas France, from the *Direction Régionale de l'Environnement* of the island of Reunion, and, from the EAGGF (European Agricultural Guidance and Guarantee Fund). The authors thank the members of the "Recycling and Risk" research unit (CIRAD) for their contributions: Romain Olivier, Jean-Guillaume Robin, Didier Baret, Olivier Salmacis; the team from the "Water, soil, and plant analysis" service unit (CIRAD) for the care and patience in carrying out the soil analyses, Cécile Fovet-Rabot and Peter Biggins for their critical comments on the article and the English revision.

References

AFNOR, 1999. Qualité des sols. Recueil de normes françaises, 4e édition. Paris-La Défense. 2 volumes 566 et 408 pages.
Alarcon, C., 1995. Cycle biogéochimique du silicium en environnement tropical : application à l'étude des sols à mascareignite de l'île de la Réunion. (PhD thesis) Aix-Marseille III University.
Alary, K., Babre, D., Caner, L., Feder, F., Szwarc, M., Naudan, M., Bourgeon, G., 2013. A modified pipette method for particle-size analysis of soil samples rich in short-range-order minerals. Pedosphere 23 (1), 20–28. http://dx.doi.org/10.1016/S1002-0160(12)60076-9.
Albrecht, A., Brossard, M., Chotte, J.-L., Feller, C., 1992. Les stocks organiques des principaux sols cultivés de la Martinique (Petites Antilles). Cahiers ORSTOM, série Pédologie 27 (1), 23–36.
Association Française de Normalisation (AFNOR), 2004. PSDA procedure (NF X31-107). Soil Quality Evaluation Methods for Chemical Analysis (in French). In: AFNOR (Ed.), vol. 1. Saint-Denis La Plaine, France, pp. 21–40.
Aubert, G., 1966. Observations sur la classification des sols ferrallitiques. Cahiers ORSTOM, série Pédologie 4 (4), 89–90.
Aubert, G., Ségalen, P., 1966. Projet de classification des sols ferrallitiques. Cahiers ORSTOM, série Pédologie 4 (4), 97–112.
Baize, D., 1993. Place of horizons in the new french "Référentiel Pédologique". Catena 20, 383–394.
Baize, D., Girard, M.-C., 1995. Référentiel pédologique. Les principaux sols d'Europe. Collection Techniques et Pratiques, INRA Edition, Paris.
Baize, D., Girard, M.-C., 2009. Référentiel pédologique 2008. Édition Quae. 978-2-7592-0185-3 (406 pp.).
Bockheima, J.G., Gennadiyevb, A.N., Hammer, R.D., Tandarichd, J.P., 2005. Historical development of key concepts in pedology. Geoderma 124, 23–36.
Bussière, P., 1957. Carte géologique. Île de la Réunion au 1:100 000. Tirage provisoire. Service géologique de Madagascar et service de la carte géologique de France.
Bussière, P., 1958. Étude géologique de l'île de la Réunion. Travaux du bureau géologique, 84. Service Géologique, Tananarive (64 pp.).
Claisse, G., 1968. Étude expérimentale de l'analyse aux trois acides : comportement du quartz pur à l'attaque triacide. Cahiers ORSTOM, série Pédologie 6 (2), 129–149.
Colmet-Daage, F., Cucalon, F., Delaune, M., Gautheyrou, J., Gautheyrou, M., Moreau, B., 1967. Caractéristiques de quelques sols d'Équateur dérivés de cendres volcaniques: première partie. Essai de caractérisation des sols des régions tropicales humides. Cahiers ORSTOM, série Pédologie 5 (1), 3–38.
Colmet-Daage, F., de Kimpe, C., Delaune, M., Gautheyrou, J., Gautheyrou, M., Sieffermann, G., Fusil, G., 1970. Caractéristiques de quelques sols dérivés de cendres volcaniques de la côte pacifique du Nicaragua. Cahiers ORSTOM, série Pédologie 8 (2), 113–172.
Colmet-Daage, F., Gautheyrou, J., Gautheyrou, M., de Kimpe, C., 1973. Étude des sols à allophane dérivés de matériaux volcaniques des Antilles et d'Amérique latine à l'aide de techniques de dissolution différentielle. Cahiers ORSTOM, série Pédologie 11 (2), 97–120.
CPCS, 1967. Classification des sols. École Nationale Supérieure Agronomique, Grignon, France (87 pp.).
D'Hoore, J.L., 1964. Soil map of Africa (Scale 1 to 5,000,000). Joint projet no. 11, commission for technical cooperation in Africa, Lagos.
Deenik, J., McClellan, A.T., 2007. Soils of Hawaii. Soil and Crop Management (SCM-20, sept. 2007) (12 pp.).
Eswaran, H., Almaraz, R., van den Berg, E., Reich, P., 1997. An assessment of the soil resources of Africa in relation to productivity. Geoderma 77 (1), 1–18.
FAO, 1974. The Legend of the Soil Map of the World, vol. 1. Unesco, Paris.
FAO, 1990. Études et prospections pédologiques en vue de l'irrigation. Bulletin pédologique de la FAO, no 42. FAO, Rome (192 pp.).
FAO, 1998. World reference base for soil resources, by ISSS–ISRIC–FAO. World Soil Resources Report No. 84. (Rome).
FAO, 2006. Guidelines for Soil Description, 4th edition. (Rome).
Feder, F., Findeling, A., 2007. Retention and leaching of nitrate and chloride in an andic soil after pig manure amendment. European Journal of Soil Science 58, 393–404. http://dx.doi.org/10.1111/j.1365-2389.2006.00885.x.
Feder, F., Bourgeon, G., 2009. Mise à jour de la carte des sols de la Réunion: démarche suivie et problèmes rencontrés. Étude et gestion des sols 16 (2), 85–99.
Feder, F., Robin, J.-G., Bourgeon, G., 2008. Cartography of groundwater vulnerability to pollutants transfer in Western part of La Reunion Island. IWRA, Proceedings of the XIII World Water Congress, 1–4 September 2008, Montpellier, France.
Fieldes, M., Perrott, K.W., 1966. Nature of allophane in soils. III. Rapid field and laboratory test for allophane. New Zealand Journal of Science 9, 623–629.
Gillot, P.Y., Nativel, P., 1982. K.Ar chronology of the ultimate activity of Piton des Neiges volcano, Reunion Island, Indian Ocean. Journal of Volcanology and Geothermal Research 13, 131–146.

IUSS Working Group WRB, 2007. World reference base for soil resources 2006, first update 2007. World Soil Resources Reports No. 103. FAO, Rome.
Kellogg, C.E., 1974. Soil genesis, classification, and cartography: 1924–1974. Geoderma 12 (4), 347–362.
Legros, J.-P., 1996. Cartographies des sols. De l'analyse spatiale à la gestion des territoires. Presses Polytechniques et Universitaires Romandes (321 pp.).
Legros, S., Doelsch, E., Feder, F., Moussard, G., Sansoulet, J., Gaudet, J.-P., Rigaud, S., Basile Doelsch, I., Saint Macary, H., Bottero, J.-Y., 2013. Fate and behaviour of Cu and Zn from pig slurry spreading in a tropical water–soil–plant system. Agriculture, Ecosystems and Environment 164, 70–79. http://dx.doi.org/10.1016/j.agee.2012.09.008.
McDougall, I., 1971. The geochronology and evolution of the young volcanic island of Réunion, Indian Ocean. Geochimica et Cosmochimica Acta 35 (3), 261–288.
Mermut, A.R., Eswaran, H., 2001. Some major developments in soil science since the mid-1960s. Geoderma 100, 403–426.
Parfitt, R.L., Wilson, A.D., 1985. Estimation of allophane and halloysite in three sequences of volcanic soils, New Zealand. Volcanic Soils, Weathering and Landscape Relationships of Soils on Tephra and Basalt. In: Caldas, E.F., Yaalon, D.H. (Eds.), Catena supplement, 7, pp. 1–8.
Payet, N., Findeling, A., Chopart, J.-L., Feder, F., Nicolini, E., Saint Macary, H., Vauclin, M., 2009. Modelling the fate of nitrogen following pig slurry application on a tropical cropped acid soil on the island of Reunion (France). Agriculture, Ecosystems and Environment 134, 218–233. http://dx.doi.org/10.1016/j.agee.2009.07.004.
Pédro, G., 1966. Intérêt géochimique et signification minéralogique du paramètre moléculaire Ki = SiO_2/Al_2O_3 dans l'étude des latérites et bauxites. Bulletin du Groupe Français des Argiles 18 (13), 19–31.
Raunet, M., 1988. Département de la Réunion. Carte morpho-pédologique au 1:50 000 en quatre feuilles. Cirad-Irat et région Réunion.
Raunet, M., 1989. Littoral ouest — Rivière des Galets à ravine du Cap. Carte morpho-pédologique. Aptitudes à l'irrigation au 1:10 000 en cinq feuilles. Cirad-Irat et conseil général de la Réunion.
Raunet, M., 1991. Périmètres du bras de Cilaos et du bras de la Plaine. Carte morpho-pédologique. Aptitudes à l'irrigation au 1:10 000 en six feuilles. Cirad-Irat et conseil général de la Réunion.
Raunet, M., 1991b. Le milieu physique et les sols de l'île de la Réunion. Cirad (438 pp.).
Riquier, J., 1960a. Carte pédologique de reconnaissance des grands groupes de sols de la Réunion au 1:100 000. Communauté – Office de la Recherche Scientifique et Technique Outre–Mer - Institut de Recherche Scientifique de Madagascar, Tananarive.
Riquier, J., 1960b. Notices sur les cartes pédologiques de reconnaissance. Île de la Réunion. Publications de l'institut de Recherche Scientifique de Madagascar, Tananarive-Tsimbazaza (72 pp.).
Schoeneberger, P.J., Wysocki, D.A., Benham, E.C., Broderson, W.D. (Eds.), 2002. Field Book for Describing and Sampling Soils, Version 2.0. Natural Resources Conservation Service, National Soil Survey Center, Lincoln, NE.
Soil Survey Staff, 1998. Keys to Soil Taxonomy, 8th edition. USDA-NRCS.
Soil Survey Staff, 2004. Soil survey laboratory methods manual. Soil Survey Investigations Reports, No 42, Version 4.0. USDA-NRCS.
USDA, 1960. Soil Classification, a Comprehensive System, 7th Approximation. Soil Conservation Service, USDA (265 pp.).
USDA-SCS, 1975. Soil taxonomy: a basic system of soil classification for making and interpreting soil surveys. U.S. Dept. of Agric. Handb. 436.U.S. Govt. Print. Off., Washington, DC (754 pp.).
Van Wambeke, A., 1991. Soils of the Tropics. Properties and Appraisal. McGraw-Hill, New York (343 pp.).
Winckell, A., Zebrowski, C., Delaune, M., 1991. Évolution du modelé quaternaire et des formations superficielles dans les Andes de l'Équateur: 2. Quelques aspects de l'histoire paléogéographique quaternaire. Géodynamique 6 (2), 119–139.
Zebrowski, C., 1975. Étude d'une climatoséquence dans l'île de la Réunion. Cahiers ORSTOM, série Pédologie 13 (3–4), 255–278.

Agriculture, Ecosystems and Environment 164 (2013) 70–79

Contents lists available at SciVerse ScienceDirect

Agriculture, Ecosystems and Environment

journal homepage: www.elsevier.com/locate/agee

Fate and behaviour of Cu and Zn from pig slurry spreading in a tropical water–soil–plant system

S. Legros[a], E. Doelsch[b,*], F. Feder[a], G. Moussard[a], J. Sansoulet[a], J.-P. Gaudet[c], S. Rigaud[d], I. Basile Doelsch[d], H. Saint Macary[b], J.-Y. Bottero[d]

[a] CIRAD, UPR Recyclage et risque, F-97408 Saint-Denis, Réunion, France
[b] CIRAD, UPR Recyclage et risque, F-34398 Montpellier, France
[c] UJF-Grenoble 1, CNRS, IRD, Grenoble-INP, LTHE UMR 5564, BP 53, F-38041 Grenoble Cedex 9, France
[d] Aix-Marseille Univ, CNRS, IRD, CEREGE UMR 7330, F-13545 Aix en Provence Cedex 4, France

ARTICLE INFO

Article history:
Received 4 February 2012
Received in revised form 27 August 2012
Accepted 10 September 2012

Keywords:
Swine manure
Trace element
Recycling
Organic waste
HYDRUS-1D

ABSTRACT

Pig slurry is commonly spread on crop fields as a means of managing this agricultural waste product. However, this practice has an impact on the environment, e.g. increasing soil copper (Cu) and zinc (Zn) concentrations. Many studies have assessed the fate of these elements, but some questions remain, especially with respect to tropical agrosystems which have yet to be studied in depth. The aim of this study was to determine the fate of Cu and Zn from pig slurry spreading while also focusing on describing the dynamics of these elements in a tropical system and accounting for the three compartments of the water–soil–plant system. We observed that all of the Zn accumulated within the 20–60 cm soil layer. Although the uncertainty calculated for these results was high, these findings were confirmed by the absence of uptake by the plant cover and of leaching via water flows. This pattern for Zn in a tropical setting differed from findings generally reported in temperate areas. The Zn accumulation mechanism in tropical soil seems to be a reversible sorption phenomenon, suggesting the possibility of long-term Zn leaching. The Cu mass derived from pig slurry spreading was stored in the 0–20 cm soil layer. This result obtained in a tropical environment was similar to that noted in temperate areas. This could be explained by Cu speciation in the pig slurry (insoluble copper sulfide), and was therefore relatively independent of the soil–climate system.

1. Introduction

World pig production has increased by 42% over the last 40 years (1970–2009), reaching 941 million animals in 2009 (FAOSTAT-*faostat.fao.org*). Substantial pig slurry production is a direct impact of this intensive pig production, with single pigs generating 2–20 l/day of slurry (Levasseur, 1998).

Pig slurry spreading in crop fields has been common practice for several decades (L'Herroux et al., 1997; Martinez and Peu, 2000). Chemical fertilization can be partially replaced by pig slurry, which has high nitrogen, phosphorus and potassium concentrations. However, this practice may also have negative environmental impacts, including contamination of groundwater by nitrates (Peu et al., 2007; Payet et al., 2009, 2010) or phosphate (Smith et al., 2004).

The presence of trace elements in slurries has been documented for many years (e.g. Atkinson et al., 1954) especially copper (Cu) and zinc (Zn), which occur in high quantities (Nicholson et al., 1999; Sanchez and Gonzalez, 2005; Moral et al., 2008). Both of these elements are added to livestock feed on account of their growth factor (Cu) and antibiotic (Zn) properties (Jondreville et al., 2003). During pig slurry spreading, Cu and Zn may be released in the environment and could be toxic to animals and plants (Alloway, 1995; Kabala and Singh, 2001). After spreading, Cu and Zn can contaminate plants (Singh and Agrawal, 2007), but Cu and Zn uptake by plants varies depending on the crop, i.e. no uptake noted for maize (*Zea mays*), alfalfa (*Medicago sativa*) or sugar beet (*Beta vulgaris*) (Mantovi et al., 2003), whereas 1.4% uptake of Cu and 4% of Zn have been reported for Indiangrass (*Sorghastrum nutans*) (McLaughlin et al., 2004). Massive input of Cu and Zn following pig slurry spreading is also responsible for the contamination of water resources by leaching, ultimately with an impact on the groundwater (Xue et al., 2000; Aldrich et al., 2002; Xue et al., 2003; Hao et al., 2008). However, most authors describe a significant increase in soil Cu and Zn concentrations following pig slurry spreading (Martinez and Peu, 2000; Mantovi et al., 2003; Novak et al., 2004; Gräber et al., 2005; Lipoth and Schoenau, 2007).

The above mentioned studies were all conducted in temperate soil–climate conditions. To our knowledge, no studies have assessed the impact of pig slurry spreading on tropical soils with

* Corresponding author. Tel.: +33 04 42 97 17 75; fax: +33 04 42 97 15 59.
E-mail address: doelsch@cirad.fr (E. Doelsch).

0167-8809/$ – see front matter © 2012 Elsevier B.V. All rights reserved.
http://dx.doi.org/10.1016/j.agee.2012.09.008

respect to trace elements (Cu and Zn). And the results obtained to date in temperate soil–climate conditions cannot be applied to tropical environments with different soils, crops and climatic conditions. The conditions that prevail in tropical regions may, however, be hazardous, especially due to heavy rainfall.

The aim of this study was to determine the behaviour of Cu and Zn following pig slurry spreading by taking three points into account: (i) the pedological and climatic conditions in the tropical environment, (ii) the monitored Cu and Zn concentrations in the three compartments of the water–soil–plant system following pig slurry spreading, and (iii) an in-depth examination of uncertainty during the different experiments in order to assess the mass balance for Cu and Zn derived from slurry spreading in the water–soil–plant system.

2. Materials and methods

2.1. Site description

This study was carried out on the island of Réunion (Indian Ocean, 55°18′E–21°07′S), in the Colimaçons research station, which is located at 780 m asl. The annual mean rainfall is 1250 mm during two seasons: a dry season (May–October), during which the rainfall (210 mm) is lower than the potential evapotranspiration (PET) (460 mm), and a rainy season (November–April), when the rainfall (1040 mm) is higher than the PET (550 mm). Cyclones only occur during the rainy season (Chopart and Mézino, 2003). At Colimaçons, Feder and Findeling (2007) classified the soil as an Andic Cambisol (WRB, 2006). It has two horizons: a surface horizon A (0–40 cm) which has been altered by human activity at a shallow depth (<50 cm), and an Andic horizon B (40–200 cm). *Stenotaphrum dimidiatum* grass was selected as plant cover because pig slurry spreading on a grass-covered soil is representative of farming practices in this region of Réunion, and also because this grass has a creeping root system, which reduces the risk that the roots could have an effect on soil solution sampling at 60 cm depth.

2.2. Field experiment

The study was conducted on a 1200 m^2 experimental plot. The plot was divided in two sub-plots: no pig slurry was spread on the first one (control plot), whereas there were five slurry applications on the second one (pig slurry plot). The area of the control plot was 537 m^2 and the pig slurry plot was 589 m^2. Three pig slurry applications (PSo) were carried out over the 2002–2005 period. A pig slurry volume of 71 m^3 ha^{-1} was spread in 2003, 68 m^3 ha^{-1} was spread in 2004 and 69 m^3 ha^{-1} in 2005. Then 163 m^3 ha^{-1} of pig slurry was spread the 14 and 15 November 2006 and again the 4 and 5 July 2007. The volume of slurry spread per application was between 68 and 163 m^3 ha^{-1} y^{-1}, which corresponds to the mean level for pig slurry spreading on crop fields in France (Coppenet et al., 1993).

The test plot was equipped to monitor soil water and solute flows (Fig. 1). A meteorological station that is part of the Météo France network was located less than 100 m from the crop plot. This meteorological station provides PET readings with 1 measurement per day. Rainfall was recorded with a tipping-bucket rain gauge (Campbell ARG 100; Campbell Scientific, Antony, France) set up close to the test plot. The measurement frequency was 1 measurement h^{-1}.

Measurement sites R_C and R_{PS} included a rectangular 3 m^2 plot for measuring runoff. Runoff water accumulates in a can equipped with a bottom-mounted pressure sensor. This pressure sensor measures the water pressure and, after calibration, the runoff water volume per surface unit can then be determined with a frequency of 1 measurement h^{-1}.

Measurement sites T_{C1}, T_{C2}, T_{PS1} and T_{PS2} were equipped with two time domain reflectometry (TDR) probes (Campbell CS616; Campbell Scientific, Antony, France) set at 30 cm and 60 cm depth and two automatic tensiometers (SDEC STCP 850; SDEC, Reignac sur Indre, France) set at 45 cm and 75 cm depth (Fig. 1). The TDR probes, tensiometers and pressure sensors in the runoff plot were calibrated beforehand and linked to a datalogger (Campbell CR10X-2M via AM16/32 multiplexers; Campbell Scientific, Antony, France) so as to be able to perform automatic measurements. The TDR probes permit to measure the volumetric water content θ (m^3 m^{-3}) with a frequency of 1 measurement h^{-1}. The tensiometers permit to measure the Water pressure head h (cm) with a frequency of 1 measurement h^{-1}.

The data acquisition timing is shown in Fig. 2. Hereafter, the time at which the data was collected is labelled with a day code, with day 1 being 1 November 2006. Following pig slurry spreading (PS1, days 15–16), data were collected over the following 4 months of the rainy season (R1, days 32–149). Pig slurry spreading (PS2, days 248–249) was carried out and data were collected during the rainy season (R2, days 250–352).

Due to time schedule management, the R2 rainy season was actually an artificial rainy season that was simulated by artificial watering. The watering conditions were calculated to simulate the mean recorded precipitation over a 20 year period for the four most rainy months, i.e. 736 mm total precipitation. This involved two monthly watering treatments ranging from 46 to 112 mm during the four R2 months.

2.3. Sampling and analysis

2.3.1. Pig slurry sampling and analysis

During each spreading, a composite pig slurry sample (representing a mixture of 10 samples collected during spreading) was collected. The samples were stored at 4 °C prior to analysis.

The dry matter content was determined along with the total nitrogen (Kjeldahl nitrogen) and organic carbon (C_{org}) contents. C_{org} was determined using the NF ISO 10694 standard procedure. The assay was performed by dry combustion on a THERMOQUEST CN 2100 (Thermo Fisher Scientific, Villebon sur Yvette, France) elemental analyser (gas chromatography measurement). The analyser was calibrated with a pure organic compound (glycine).

Pig slurry has an organic matter concentration of over 5%, so sample dissolution was performed by acid digestion using the NF X31-147 standard procedure. 0.2 g of slurry was calcined at 500 °C and then dissolved in a mixture of nitric, perchloric and hydrofluoric acid until dry. The mineral (P, K, Na, Ca, Mg, Al, Ni, Cu and Zn) contents were determined with an inductively coupled plasma-optical emission spectrometer (ICP-OES Vista-PRO, Varian Inc.; Agilent, France). Certified reference samples were analyzed in the same way at a rate of one per 20 samples. The uncertainty was estimated at ±10%.

2.3.2. Soil sampling and analysis

Soil samples (Ss) were collected on the control plot and the pig slurry plot (Fig. 1). The test plot was divided into 5 m × 5 m squares. Soil samples were extracted from the 0–20 cm, 20–40 cm and 40–60 cm soil layers at the centre of each square using an auger. Overall, 108 samples were collected (21 within each soil layer for the pig slurry plot and 15 for the control plot).

The samples were dried at ambient temperature, ground and dried for 24 h at 105 °C, to measure the dry mass. The samples were then beaded (PANalytical benchtop MiniFuse 2 system; PANalytical, Limeil, France), which minimizes matrix effects during analysis. Total concentrations of Si, Al, Fe, Mn, Mg, Ca, Na, K, Ti, Cr, Cu, Ni,

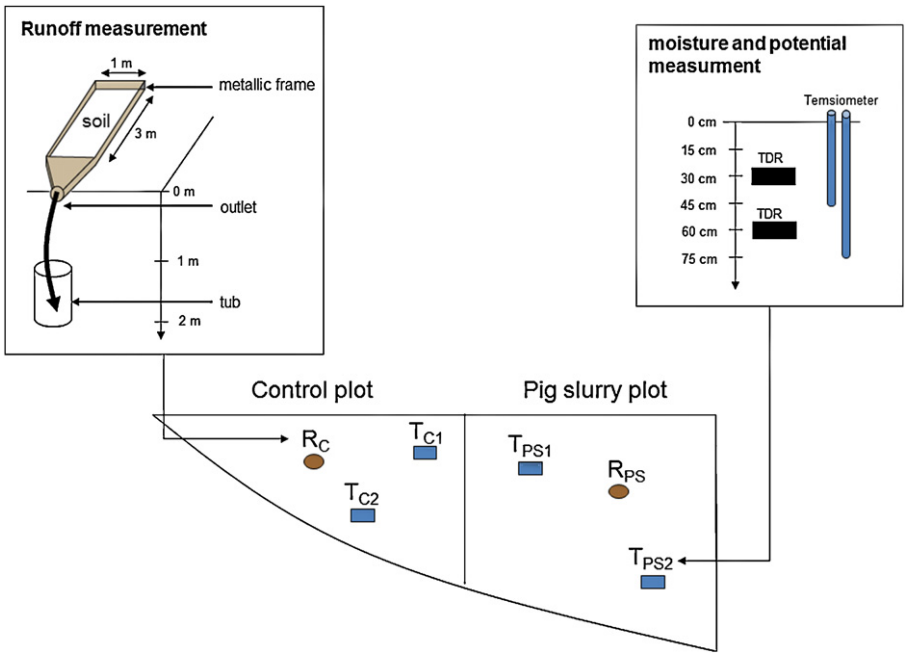

Fig. 1. Top view of the situation and instrumentation of the measurement sites on the test plots: RC and RPS were sites with runoff plots on the control plot and the pig slurry plot, respectively; TC1 and TC2 were sites equipped with tensiometers and TDR on the control plot; and TPS1 and TPS2 were sites equipped with tensiometers and TDR on the pig slurry plot.

Pb and Zn were analyzed by X-ray fluorescence (PANalytical Axios PW4400; PANalytical, Limeil, France). Calibration and uncertainty determination were carried out using standard international soil and rock materials (Chinese standard soils and geochemical reference materials from Service d'Analyse des Roches et des Minéraux (SARM)). The uncertainty was less than 10%.

2.3.3. Plant sampling and analysis

S. dimidiatum grass samples (Vs) were collected in the control plot and pig slurry plot. Six samples were randomly collected per plot. The sampling involved collecting all plants (stems and leaves) growing within a 1 m^2 area. The plants were then washed with pure water and dried at 60 °C for 24 h to measure the dry mass. They were then calcined at 500 °C and the ash was dissolved in 6 N HCl. These solutions were then analyzed by ICP-OES to determine the Cu and Zn concentrations. The uncertainty was estimated to be ±10%.

2.3.4. Soil solution extraction

Soil samples were collected weekly at 60 cm depth using an auger during the R1 and R2 rainy seasons. The soil solution was then extracted using a procedure adapted from Keller (1995). Geotextile was placed at the bottom of punctured centrifuge tubes. Each tube was filled with 50 g of fresh soil and then placed in adapters and centrifuged at 6000 × *g* for 60 min (Eppendorf 5810-R centrifuge). The soil solution was collected at the bottom of the adapters. The procedure was repeated until 32 ml of soil solution was obtained.

These solutions were stored in sealed containers to prevent air contact. They were then filtered at 0.2 μm (Sartorius Minisart high flow syringe filters with a polyethersulfone membrane) and acidified in concentrated nitric acid (Fischer nitric acid 70%, trace metal analysis grade) in order to avoid oxide precipitation. Ca, Mg, K, Na, Fe, Al, Mn, Si, Cu and Zn concentrations were analyzed by ICP-MS (Varian Vista).

2.4. Mass balance

2.4.1. Calculation of Cu and Zn inputs from pig slurry

The element quantity *Q* (Cu or Zn) derived from pig slurry spreading was calculated using Eq. (1):

$$Q = \frac{1}{10,000} \times \frac{\mathrm{Vps} \times \mathrm{dps} \times \mathrm{Mps_s} \times [E]}{S} \quad (1)$$

where *Q* (kg ha^{-1}) is the element quantity (Cu or Zn) derived from pig slurry spreading, Vps (dm^3) is the volume of pig slurry spread, dps (kg dm^{-3}) is the pig slurry density, $\mathrm{Mps_s}$ (%) is the percentage of dry mass in the pig slurry, [*E*] is the element concentration (Cu or Zn) in the pig slurry (mg kg^{-1} of M_s) and *S* is the area of the pig slurry plot (m^2).

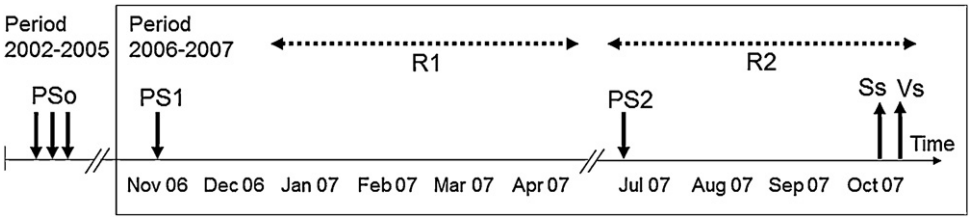

Fig. 2. Diagram of the data acquisition timing. PSo = pig slurry spreading before the period of data acquisition; PS1 = first pig slurry spreading of the data acquisition period; R1 = first rainy season; R2 = second rainy season; PS2 = second pig slurry spreading of the data acquisition period; Ss = soil sampling; Vs = plant sampling.

2.4.2. Calculation of the exogenous Cu and Zn mass in soil

Cu and Zn were from two sources: (i) Cu and Zn occur naturally in the soil (pedogeochemical background) and (ii) Cu and Zn were derived from pig slurry spreading. The mass M (kg ha^{-1}) of Cu and Zn from this second source was calculated for each of the studied soil layers (0–20, 20–40 and 40–60 cm) with the following equation:

$$M = \frac{1}{10,000} \times \mathrm{Sls_s} \times \mathrm{ds} \times \mathrm{Ms_s} \times ([E]_{\mathrm{PS}} - [E]_{\mathrm{GB}}) \quad (2a)$$

where M is the exogenous mass of the element (Cu or Zn) (kg ha^{-1}), ds is the soil density (kg dm^{-3}), $\mathrm{Sls_s}$ is the thickness of the studied soil layer (always equal to 0.2 m), $\mathrm{Ms_s}$ is the percentage of dry mass in the soil (%), $[E]_{PS}$ (mg kg^{-1}) is the concentration of the element (Cu or Zn) measured in the pig slurry plot, and $[E]_{GB}$ (mg kg^{-1}) is the concentration of element E that occurs naturally in the pig slurry plot.

Each term of this equation was measured in the field, except $[E]_{\mathrm{GB}}$, which is the element concentration (Cu or Zn) of the pedogeochemical background of the pig slurry plot. This concentration was not determined when the experiment was set up. $[E]_{\mathrm{GB}}$ was approximated: (i) according to the Cu and Zn concentration in the control plot, (ii) using the typological method (Baize, 1997; Dère et al., 2006). The typological method is based on the fact that in natural conditions there is a linear relationship between the concentration of major soil elements (Al or Fe) and trace metal concentrations (Cu, Zn, etc.) of the pedogeochemical background. The following equations were used:

$$[\mathrm{Cu}]_{\mathrm{GB}} = a[\mathrm{Al}] + b \quad (2b)$$

$$[\mathrm{Zn}]_{\mathrm{GB}} = c[\mathrm{Al}] + d \quad (2c)$$

For each soil layer, parameters a, b, c and d were determined by linear regression from the Cu, Zn and Al concentrations measured in 15 soil samples collected in the control plot. Eqs. (2b) and (2c) were then used to calculate the Cu and Zn concentrations of the pedogeochemical background of the pig slurry plot from Al concentrations measured in 26 soil samples collected in the pig slurry plot.

2.4.3. Calculation of the Cu and Zn mass taken up by plants

We calculated the element mass (Cu or Zn) taken up by plants (P in kg ha^{-1}) derived from pig slurry spreading with the following equation:

$$P = \frac{1}{100} \times \mathrm{Mv_S} \times ([E]_{\mathrm{VPS}} - [E]_{\mathrm{VC}}) \quad (3)$$

where $\mathrm{Mv_S}$ is the dry mass of the plants (kg m^{-2}), $[E]_{\mathrm{VPS}}$ (mg kg^{-1}) is the element concentration (Cu or Zn) measured in plants in the pig slurry plot, and $[E]_{\mathrm{VC}}$ (mg kg^{-1}) is the element concentration (Cu or Zn) measured in plants in the control plot.

2.4.4. Calculation of the flow of Cu and Zn leached to 60 cm

The quantity of Cu and Zn leached to 60 cm depth (L in kg ha^{-1}) was calculated with the following equation:

$$L = \frac{1}{100,000} \left[\int_{t_1}^{t_2} q_m(z_0, t) \times c_m(z_0, t) dt \right] \quad (4)$$

where $c_m(z_0, t)$ is the Cu and Zn concentration in the solution at 60 cm depth at time t (μg dm^{-3}) and $q_m(z_0, t)$ is the water leached to 60 cm depth at time t (dm^{-3} m^{-2}), provided that the dispersion before convection is neglected in the flow equation.

$c_m(z_0, t)$ was measured in soil solutions collected weekly at 60 cm depth. The water flux $q_m(z_0, t)$ was not measured and was modelled with HYDRUS 1D software. HYDRUS-1D is a hydrodynamic modelling programme that is based on the assumption of water flow described by Richards' equation.

$$\frac{\partial \theta}{\partial t} = \frac{\partial}{\partial z} \left\{ k(\theta) \left(\frac{\partial h(\theta)}{\partial z} - 1 \right) \right\} - \Gamma(z, t) \quad (5)$$

where θ is the water content (m^3 m^{-3}), $K(\theta)$ is the soil hydraulic conductivity (m s^{-1}), $h(\theta)$ is the soil water pressure head (m), Γ (m^3 m^{-3} s^{-1}) is the root water extraction rate at depth z and time t.

The Van-Genuchten functions (van Genuchten, 1980) were chosen for this study.

$$\theta(h) = \begin{cases} \theta_r + \dfrac{\theta_s - \theta_r}{\left[1 + |\alpha h|^n\right]^m} & \text{if} \quad h < 0 \\ \theta_s & \text{if} \quad h \geq 0 \end{cases} \quad (6a)$$

$$K(\theta) = K_s \times \left(\frac{\theta - \theta_r}{\theta_s - \theta_r} \right) \times \left[\left(1 - \left(\frac{\theta - \theta_r}{\theta_s - \theta_r} \right)^{l/m} \right)^m \right]^2 \quad (6b)$$

$$m = 1 - \frac{1}{n} \quad \text{if} \quad n > 1 \quad (6c)$$

where θ_r and θ_s are the residual water content and water content at saturation, respectively (m^3 m^{-3}), K_s is the hydraulic conductivity at saturation (mm h^{-1}), α, n, m and l are form parameters.

HYDRUS-1D numerically solves Richards' equation for water flows in one dimension (Simunek et al., 1998) using the retention $h(\theta)$ and conductivity $K(\theta)$ functions with appropriate initial and boundary conditions.

A domain representing a soil column must be defined to be able to simulate soil water flows with HYDRUS-1D. Here the domain consisted of two compartments representing the two soil horizons. Compartment 1 (0–40 cm) and compartment 2 (40–100 cm). The finite element grid consisted of a total of 101 nodes. The hydrodynamic characteristics differed for the two horizons. The initial time step was 0.1 days, the minimum 0.01 days, and the maximum 2 days.

The initial pressure head profile was set at values similar to the tensiometric data measured in situ and increasing with depth. The conditions at the upper limit were rainfall and daily potential evapotranspiration (PET) measured at the weather station. PET was considered equal to the evapotranspiration (ET) because the plant cover was a grass. Indeed, grasses have a crop coefficient (K_c) very close to 1. The lower boundary condition was free drainage.

The saturated hydraulic conductivity (K_s) of the Colimaçons soil was measured in situ using the double-ring method (Reynolds et al., 2002). The moisture at saturation (θ_s) was set at the maximum moisture value measured for the two combined rainy seasons.

We assessed the performances of the model using the Willmott coefficient (d), as defined by the following equation (Willmott, 1981, 1982):

$$d = 1 - \left[\frac{\sum_{i=1}^{n} m_i - S_i}{\sum_{i=1}^{n} (|S_i - \bar{m}| + |m_i - \bar{m}|)^2} \right] \quad (7)$$

where n is the number of available values, m_i is the ist measured value, $\bar{m}$ is the mean of the measured values, and S_i is the ist simulated value.

The Willmott coefficient (d) is a dimensionless coefficient between 0 and 1. When the measured values were well reproduced by the model, it was equal to 1. d is used in many different fields (Chahinan, 2004; Sogbedji et al., 2006; Zhang et al., 2007) to measure the nonsystematic uncertainty that quantifies the

Table 1
Physical and chemical characteristic of the spread pig slurry, with PSo for the three pig slurry applications carried out over the 2002–2005 period, PS1 for the pig slurry spread the 14 and 15 November 2006 and PS2 for the pig slurry spread the 4 and 5 July 2007.

Pig slurry	PSo			PS1		PS2		Mean	SD
Date	2003	2004	2005	2006	2006	2007	2007		
Density (kg m^{-3})	1015	1041	1067	1041	1041	1006	1006	1031	21
Dry matter (g kg^{-1} bm)	32.7	12.7	51.7	25	54	8.6	11	28.0	17.6
pH	7.6	7.8	n.d.	8.3	7.9	7.7	7.7	7.8	0.2
C_{org} (g kg^{-1} bm)	373	263	n.d.	276	327	288	319	308	37
N_{tot} (g kg^{-1} dm)	120	230	n.d.	165	89.8	235	169	168	53
P (g kg^{-1} dm)	35.6	25.4	n.d.	31.3	33	21.8	29.4	29.4	4.6
K (g kg^{-1} dm)	78.6	220	n.d.	143	68.9	177	137	138	53
Na (g kg^{-1} dm)	n.d.	n.d.	n.d.	18.3	9.0	33.5	26.3	21.8	10.6
Ca (g kg^{-1} dm)	19.5	7.9	16.1	13.4	21.1	16.3	18.4	16.1	4.1
Mg (g kg^{-1} dm)	17.9	8.1	12.3	11.2	17	6.86	12.2	12.2	3.8
Al (g kg^{-1} dm)	n.d.	n.d.	n.d.	0.70	0.67	0.36	1.99	0.9	0.6
Fe (g kg^{-1} dm)	n.d.	n.d.	n.d.	1.54	1.57	0.75	2.76	1.6	0.8
Cu (mg kg^{-1} dm)	n.d.	n.d.	342	371	434	271	575	399	103
Zn (mg kg^{-1} dm)	n.d.	n.d.	593	659	782	348	792	635	162
Ni (mg kg^{-1} dm)	n.d.	n.d.	n.d.	19.1	12.2	n.d.	n.d.	15.7	4.9

C_{tot} = total carbon, N_{tot} = total nitrogen, bm = raw matter, dm = dry matter, n.d. = not determined.

measurement accuracy and the systematic uncertainty (Zhang et al., 2007).

For each rainy season, the water balance was defined as:

$$R = D + R_{off} + E + \Delta S \quad (8)$$

where R is the cumulative rain during the rainy season period, D is the cumulative drainage during the rainy season period, R_{off} is the cumulative run off during the rainy season period, E is the cumulative evapotranspiration during the rainy season period of available values, and ΔS is the water storage variation during the rainy season.

2.5. Uncertainty calculations

For each measured variable, the uncertainty was taken as being equal to the standard deviation σ of the measurements. We used the following equations for propagation of uncertainty.

The uncertainty of a sum or difference was equal to the sum of uncertainties:

$$\Delta(A+B) = \Delta(A-B) = \Delta A + \Delta B \quad (9)$$

The relative uncertainty of a product or quotient was the sum of relative uncertainties:

$$\text{For } C = A \times B \text{ or, } C = \frac{A}{B} \text{ we have : } \frac{\Delta C}{C} = \frac{\Delta A}{A} + \frac{\Delta B}{B} \quad (10)$$

3. Results

3.1. Cu and Zn in pig slurry

Pig slurry is a mixture of pig wastes (urine and faecal matter). The characteristics of the spread pig slurry considered in this study are given in Table 1. This slurry was characterized by a low dry matter content, ranging from 8.6 to 54 g kg^{-1}. It had a pH of around 8, high plant nutrient contents (N, P and K), as well as high Ca, Na, Mg and Cl concentrations.

The Fe and Al concentrations ranged from 0.75 to 2.76 g kg^{-1} and 0.36 to 1.99 g kg^{-1}, respectively. These concentrations were very low with respect to the Fe and Al concentrations naturally present in the Colimaçons soil, which ranged from 156 to 159 g kg^{-1} and 160 to 179 g kg^{-1}, respectively (Table 4).

The Cu and Zn concentrations of the spread pig slurry ranged from 271 to 575 mg kg^{-1} for Cu and 348 to 792 mg kg^{-1} for Zn.

The quantity Q of Cu and Zn derived from spreading was estimated with Eq. (1) according to the quantity of slurry applied and the slurry concentration measurements (Table 1). The uncertainty for Q (calculated using Eqs. (9) and (10) and the values in Table 1) was 108% for Cu and Zn, and hence $Q_{Cu} = 6 \pm 6$ kg ha^{-1} and $Q_{Zn} = 10 \pm 11$ kg ha^{-1} for all of the slurry applications.

3.2. Cu and Zn in the plant compartment

The Cu and Zn concentrations in the plant cover are shown in Table 2. For Zn, no significant difference was measured between the pig slurry plot (47 ± 13.9 mg kg^{-1}) and the control plot (39 ± 9.1 mg kg^{-1}). The Cu concentration in plants sampled in the pig slurry plot (10 ± 1.4 mg kg^{-1}) was significantly higher at the 5% level (Student's t-test) than that in the control plot (7 ± 1.7 mg kg^{-1}).

The Cu mass taken up by plants (P_{Cu}) that could be explained by pig slurry spreading was calculated using Eq. (3) according to the dry mass of *S. dimidiatum* grass measured in the plots (3.15 ± 0.37 kg ha^{-1}) and the Cu concentrations (Table 2). $P_{Cu} = 0.005 \pm 0.006$ kg ha^{-1}. P_{Zn} was considered as nil since there was no significant difference between Zn concentrations in the plants in both plots.

3.3. Cu and Zn in the water compartment

Cu and Zn flows at 60 cm depth were calculated on the basis of Cu and Zn concentrations in the soil solution and water flows at 60 cm depth (Eq. (4)). Water flows were modelled with HYDRUS 1D using the parameters given in Table 3.

The high K_s measured between 40 and 100 cm is consistent with classical Andosol values (Sansoulet et al., 2008). Parameters α and n (shape parameters from Van Genuchten's equations $K(\theta)$ and $h(\theta)$) were optimized by reverse simulation with the moisture (θ) and water potential (h) parameters measured on the T_{C1} site over a 17 days period (days 92–115). The model very accurately reproduced the θ and h data, with an R^2 of 0.97 and a 0.5% water balance uncertainty.

Table 2
Cu and Zn concentrations in the *S. dimidiatum* grass in the control plot and the pig slurry plot.

	Cu (mg kg^{-1})	Zn (mg kg^{-1})
Control plot	7 ± 1.7a*	39 ± 9.1a
Pig slurry plot	10 ± 1.4b	47 ± 13.9a

* ±Standard deviation; values followed by different letters in the same column are significantly different at the 5% level (Student's t-test).

Table 3
Hydrodynamic parameters used for the HYDRUS-1D simulations.

Horizon	Depth (cm)	K_s (mm h^{-1})	θ_r (m^{-3} m^{-3})	θ_s (m^{-3} m^{-3})	α	n	l
A	0–40	158	0	0.71	2.58	1.15	0.5
B	40–100	202	0	0.71	1.02	1.07	0.5

Then we evaluated the capability of HYDRUS-1D (using the previously calculated α and n) to reproduce θ and h measured on the sites T_{C1}, T_{C2}, T_{PS1} and T_{PS2} throughout the month of March (day 121–150). The Willmott coefficient (d) was between 0.51 and 0.92 for θ and between 0.67 and 0.97 for h. For R2, the assessment concerned the month of August (days 273–304). Coefficient d ranged from 0.48 to 0.88 for θ and from 0.56 to 0.96 for h.

The cumulative drainage, rain, and PET for the R1 and R2 rainy seasons calculated by HYDRUS-1D are shown in Fig. 3. For R1, cumulated rainfall was 0.826 m, cumulated PET was 0.364 m, cumulated drainage was 0.483 m and runoff was nil. The variation in the groundwater storage was negligible (−0.02 m). The water balance showed a slight excess of +0.001 m, which represents 0.12% of the cumulated rainfall. For R2, the cumulated rainfall was 0.737 m, cumulated PET was 0.229 m, cumulated drainage was 0.472 m and runoff was also nil. The variation in the groundwater storage was +0.03 m. There was an excess of +0.005 m in the water supply, representing 0.67% of the cumulated rainfall.

In summary, for R1 and R2, the water fluxes were very satisfactorily simulated, with less than 1% uncertainty. R1 was very dry and the few rain events recorded did not induce any drainage until day 105, because they were balanced by the PET. Then, there was a very heavy rainy period, notably with a cyclone occurring at day 116–118, which induced most of the drainage for the season. These results underline the difference between tropical and temperate systems. First the average rainfall is higher in tropical systems but most importantly there can be very intense rain storms (cyclones) over very limited period of time. During R2, almost every rain event induced drainage. Indeed for R2, the rain storms are artificial watering treatments that were calculated in order to induce drainage.

No runoff was measured in the field (runoff plot), in agreement with the zero runoff simulated by the model. In the model, this is due to water fluxes at the upper limit that were always lower than the K_s of the 0–20 cm soil layer.

Time-course variations in Cu and Zn concentrations in the soil solution sampled at 60 cm depth are shown in Fig. 4. In the control plot, Cu concentrations in the soil solution ranged from 2.69 to 33.7 μg dm^{-3}, while Zn concentrations were from 63.8 to 827 μg dm^{-3}. In the pig slurry plot, the concentrations were very similar and ranged from 2.76 to 49.3 μg dm^{-3} for Cu and from 50.7 to 889 μg dm^{-3} for Zn. The concentration patterns in the soil solution were very similar for the two plots (with or without pig slurry spreading), and this was particularly notable for Zn during the R1 rainy season (Fig. 4c).

Table 4
Soil characteristics of control plot.

	A horizon		B horizon
Depth (cm)	0–20	20–40	40–100
Bulk density (kg dm^{-3})	0.90 ± 0.06*	0.80 ± 0.03	0.85 ± 0.02
pH	5.4	5.6	6.2
Dry matter (% bm)	76 ± 6	70 ± 4	64 ± 6
C_{org} (% dm)	4.16 ± 0.83	2.11 ± 0.13	1.74 ± 0.03
Fe (g kg^{-1} dm)	156 ± 1	157 ± 2	159 ± 1
Al (g kg^{-1} dm)	160 ± 6	169 ± 7	179 ± 4
Cu (mg kg^{-1} dm)	66 ± 6	66 ± 15	55 ± 17
Zn (mg kg^{-1} dm)	229 ± 12	218 ± 11	210 ± 10
Ni (mg kg^{-1} dm)	101 ± 4	100 ± 7	92 ± 8

* ±Standard deviation; n = 3 for density, dry matter and C_{org}; n = 17 for Fe, Al, Cu, Zn, and Ni; bm = raw matter, dm = dry matter.

Cumulated Cu and Zn flows during R1 and R2 are given in Fig. 5. For R1, no flow was observed up to day 111, and rainfall was especially low during this period. For Cu, there was no significant difference between the cumulated flows (Eq. (4)) in the two plots during the two rainy seasons: $L_{\text{Cu-pig slurry plot}} = 0.14$ kg ha^{-1} and $L_{\text{Cu-control plot}} = 0.16$ kg ha^{-1} for R1 (Fig. 5a) and $L_{\text{Cu-pig slurry plot}} = 0.14$ kg ha^{-1} and $L_{\text{Cu-control plot}} = 0.15$ kg ha^{-1} for R2. For Zn, we also did not note any significant difference between cumulated flows in the two plots (with and without pig slurry spreading) and for the two rainy seasons (Fig. 5c and d).

3.4. Cu and Zn in the soil compartment

The bulk density of the Colimaçons soil was low (0.8–0.9) and the pH was relatively acidic (5.4–6.2, Table 4). This soil had a high organic matter content, with an organic carbon (C_{org}) concentration ranging from 4.2% at the surface to 1.7% at deeper layers. The Colimaçons soil had naturally high levels of Ni (92–101 mg kg^{-1}), Cu (55–66 mg kg^{-1}) and Zn (210–229 mg kg^{-1}).

The Cu and Zn concentrations in the pig slurry plot measured after pig slurry spreading were significantly higher than those measured in the control plot in the three soil layers (Table 5).

Exogenous Cu and Zn masses calculated on the basis of concentrations measured on the plots (Table 5, Eq. (2a)) were $M_{Cu} = 40 \pm 20$ kg ha^{-1} and $M_{Zn} = 57 \pm 12$ kg ha^{-1}. These levels were significantly higher than the quantities of Cu and Zn derived from all of the pig slurry applications and determined on the basis of Cu and Zn from pig slurry: $Q_{Cu} = 6 \pm 6$ kg ha^{-1} and $Q_{Zn} = 10 \pm 11$ kg ha^{-1}. This overestimation seems to indicate that the Cu and Zn concentrations in the control plot were unsuitable for accurately assessing the pedogeochemical background of the pig slurry plot.

The pedogeochemical background of the pig slurry plot was therefore estimated using the typological technique, with Al taken as the major element. Fig. 6 shows the relationships between Cu, Zn and Al, which enabled us to calculate Cu and Zn concentrations of the pedogeochemical background ($[Cu]_{GB}$ and $[Zn]_{GB}$, respectively, with GB for pedoGeochemical Background) in the pig slurry plot in the 0–20, 20–40 and 40–60 cm soil layers (Table 6, referred to as pig slurry GB). Cu and Zn concentrations in the pig slurry GB (Table 6) were significantly higher than those of the control plot (Table 5), thus confirming the difference in GB between the two plots, despite being located in the same vicinity.

The Cu concentration in the 0–20 cm soil layer in the pig slurry plot was significantly higher than concentrations of the pedogeochemical background. However, no significant differences in Cu

Table 5
Cu and Zn concentrations measured in the control and pig slurry plots.

Depth (cm)	Plot	Cu (mg kg^{-1})	Zn (mg kg^{-1})
0–20	Control	66 ± 7a*	229 ± 12a
	Pig slurry	75 ± 5b	235 ± 12b
20–40	Control	66 ± 15a	218 ± 12a
	Pig slurry	79 ± 7b	238 ± 15b
40–60	Control	55 ± 17a	210 ± 8a
	Pig slurry	76 ± 10b	241 ± 14b

* ±Standard deviation; values followed by different letters in the same column are significantly different at the 5% level (Student's t-test) for two samplings.

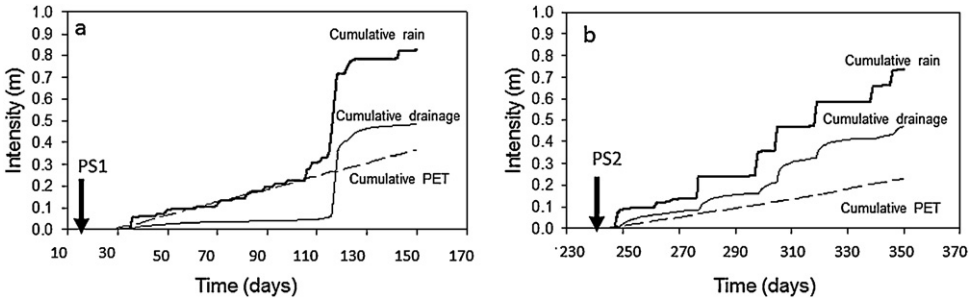

Fig. 3. Cumulative water balance components intensities; Cumulative rain (bold line), cumulative drainage (solid line) and cumulative PET (dashed line) for the (a) R1 season and (b) the R2 season.

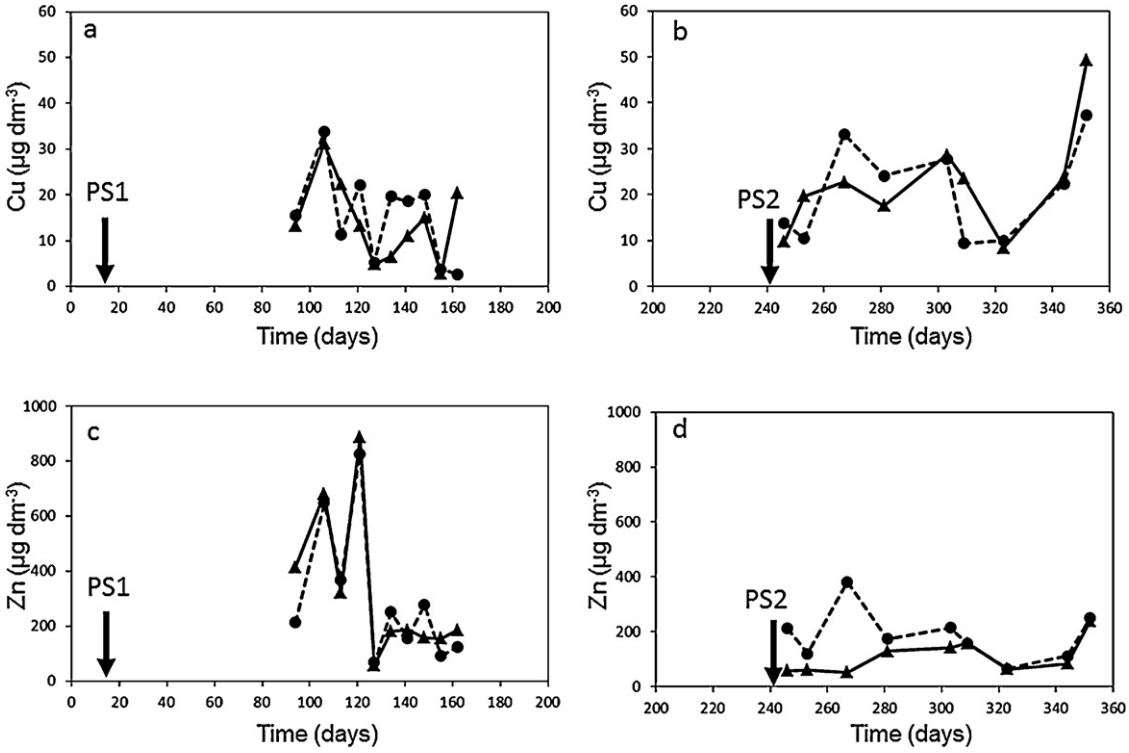

Fig. 4. Cu and Zn concentrations in the soil solution at 60 cm depth for the control plot (dashed lines) and the pig slurry plot (solid lines) (a) Cu for R1, (b) Cu for R2, (c) Zn for R1, and (d) Zn for R2.

concentration were noted in the 20–40 and 40–60 cm soil layers. In contrast, Zn concentrations in the pig slurry plot were significantly higher than concentrations of the pedogeochemical background for the 20–40 and 40–60 cm soil layers, but there was no significant difference for the 0–20 cm layer. Only soil layers showing significant differences in Cu and Zn concentration were taken into account in the mass balance calculation. Exogenous Cu and Zn masses calculated on the basis of the concentrations given in Table 6 (Eq. (2a)) were $M_{Cub} = 6 \pm 3.3\ kg\ ha^{-1}$ and $M_{Znb} = 33 \pm 16.2\ kg\ ha^{-1}$. These levels are close to the quantities of Cu and Zn derived from all of the pig slurry applications ($Q_{Cu} = 6 \pm 6\ kg\ ha^{-1}$ and $Q_{Zn} = 10 \pm 11\ kg\ ha^{-1}$), indicating enhancement of the mass balance. It could thus be considered that, to the nearest uncertainty, all of the Cu accumulated between 0 and 20 cm depth, whereas all of the Zn accumulated in the 20–60 cm layer.

Table 6
Cu and Zn concentrations in pig slurry plots, a pedogeochemical background levels (GB).

Depth (cm)	Plot	Cu (mg kg^{-1})	Zn (mg kg^{-1})
0–20	Pig slurry	75 ± 5a**	235 ± 12a
	Pig slurry GB*	71 ± 3.7b	237 ± 6.9a
20–40	Pig slurry	79 ± 7a	238 ± 15a
	Pig slurry GB	75 ± 16.9a	226 ± 15.4b
40–60	Pig slurry	76 ± 10a	241 ± 14a
	Pig slurry GB	82 ± 35.4a	224 ± 15.7b

* GB = Pedogeochemical background.
** ±Standard deviation; values followed by different letters in the same column are significantly different at the 5% level (Student's *t*-test) for two samplings.

4. Discussion

4.1. Cu and Zn in the pig slurry

The applied pig slurry had high Cu and Zn concentrations, in line with concentrations reported in the literature (Nicholson et al., 1999; Levasseur, 2002; Sanchez and Gonzalez, 2005). Cu and Zn occurred in high quantities in the pig slurry as compared, for instance, to Ni with a concentration of around 15 mg kg^{-1}. These high concentrations could be explained by Cu and Zn supplements

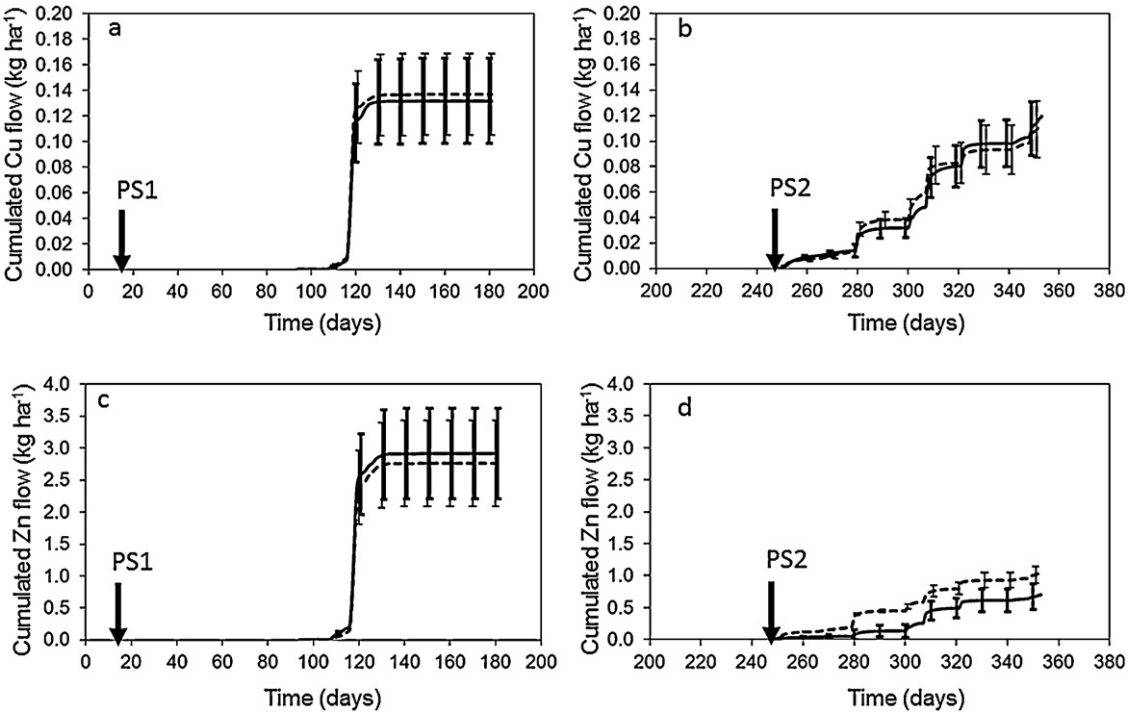

Fig. 5. Cumulated Cu and Zn flows determined at 60 cm depth in the control plot (dashed line) and pig slurry plot (bold line): (a) Cu for R1, (b) Cu for R2, (c) Zn for R1, and (d) Zn for R2. Vertical bars are calculated errors.

in pig feed (Jondreville et al., 2003). All of the pig slurry applications represented inputs of $Q_{Cu} = 6 \pm 6\,kg\,ha^{-1}$ and $Q_{Zn} = 10 \pm 11\,kg\,ha^{-1}$. The high uncertainty noted with respect to Q could mainly be explained by the high variability in dry matter rates (±63%, Table 1) and the Cu and Zn concentrations in the spread pig slurry (±25.5%, Table 1).

4.2. Cu and Zn in the plant compartment

The uptake of pig slurry derived Cu ($P_{Cu} = 0.005\,kg\,ha^{-1}$) by the plant cover (*S. dimidiatum*) was documented, but no Zn uptake was noted. This finding is surprising since the bioavailability of Zn is generally higher than that of Cu (Mantovi et al., 2003; Wen et al., 2007; Collin and Doelsch, 2010). Zn uptake by plants was possibly masked by the variability in the Zn concentration available for the plant cover in the pig slurry plot ($\sigma = 9.1$ and $13.9\,mg\,kg^{-1}$ for Zn as compared to $\sigma = 1.7$ and $1.4\,mg\,kg^{-1}$ for Cu in the control plot and pig slurry plot, respectively, Table 2). Moreover, the Cu mass taken up by plants was negligible ($P_{Cu} = 0.005\,kg\,ha^{-1}$) in comparison to the quantity of Cu supplied by the pig slurry applications ($Q_{Cu} = 6 \pm 6\,kg\,ha^{-1}$). This is in line with previously published results. Indeed, Cu and Zn uptake by plants has already been observed, but here it only represented a very small proportion of the quantity of Cu and Zn supplied by pig slurry spreading (Novak et al., 2004; Lipoth and Schoenau, 2007).

4.3. Cu and Zn in the water compartment

The mean Cu and Zn concentrations in the soil solution in the control plot (18 and 244 $\mu g\,dm^{-3}$, respectively) were comparable to those measured by Hao et al. (2008), i.e. 30 $\mu g\,dm^{-3}$ for Cu and 250 $\mu g\,dm^{-3}$ for Zn, in a Luvisol in China (soil that had received no external inputs). These results show that the high Cu and Zn in the Andic Cambisol studied here (65 and 220 $mg\,kg^{-1}$) had no direct impact on the Cu and Zn concentration in the soil solution. There was no significant difference between the control plot and the pig slurry plot for R1 and R2 with respect to the Cu and Zn flows calculated at 60 cm depth. The existing Cu and Zn flows could thus be considered as natural and uninfluenced by pig slurry spreading. Martinez and Peu (2000) came to the same conclusion in a study on soil in a temperate region—they only noted a nonsignificant increase (less than 0.1%) in Cu and Zn flows following pig slurry spreading.

4.4. Cu and Zn in the soil compartment

The Colimaçons soil had naturally high trace elements levels (Ni, Cu and Zn), which could be explained by the pedogeochemical background in Réunion, which is a volcanic island (Doelsch et al., 2006).

The exogenous Cu mass in the 0–20 cm soil layer was $M_{Cu} = 6 \pm 3.3\,kg\,ha^{-1}$, which corresponds to the Cu mass derived from pig slurry spreading ($Q_{Cu} = 6 \pm 6\,kg\,ha^{-1}$). The Cu from the pig slurry thus all accumulated in the 0–20 cm soil layer, which is similar to previous findings in other soil types (e.g. Kastanozem or Chernozem) under temperate climatic conditions (Novak et al., 2004; Gräber et al., 2005; Lipoth and Schoenau, 2007). Moreover, this finding is perfectly in line with our recent description of Cu speciation in pig slurry (Legros et al., 2010a). In this latter study, we used a multitechnique approach in pig slurry and demonstrated that Cu was mainly in sulfide form (Cu_2S) with a Cu(I) oxidation state. We put forward the hypothesis that the solubility of copper sulfide from pig slurry would be very low in soil, even in aerobic conditions, when the soil pH is over 4.5. Cu accumulation at the soil surface resulting from intensive pig slurry spreading (observed here) could therefore be explained by the very low solubility of Cu_2S.

The exogenous mass of Zn at 20–60 cm depth ($M_{Zn} = 33\,kg\,ha^{-1} \pm 16.2\,kg\,ha^{-1}$) was higher than that supplied by the pig slurry ($Q_{Zn} = 10 \pm 11\,kg\,ha^{-1}$). However, considering the uncertainty, the exogenous Zn mass ranged from 17 to 50 $kg\,ha^{-1}$, an interval that overlaps that of the Zn input from the pig slurry

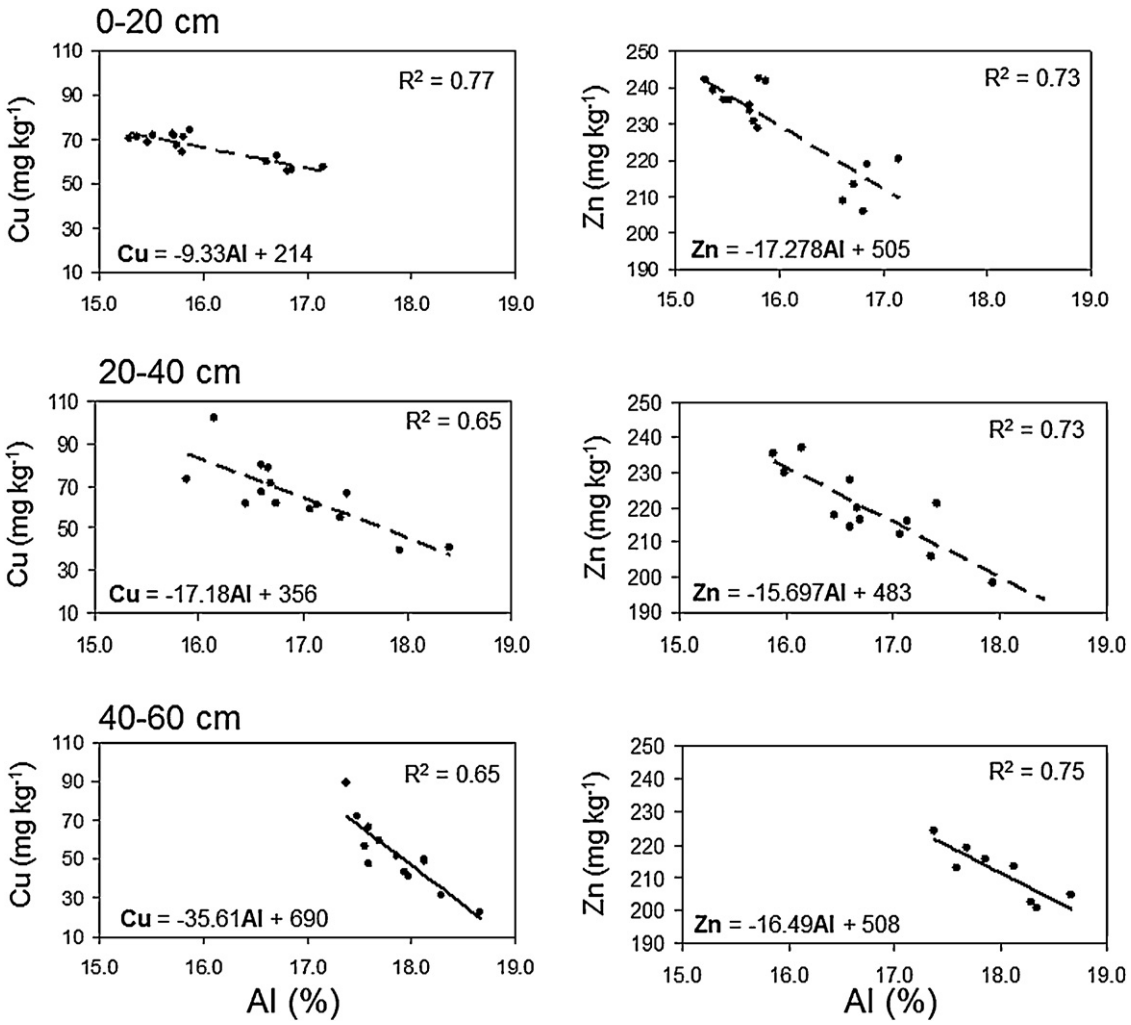

Fig. 6. Relationship between Al and Cu or Zn in the control plot soil for the 0–20, 20–40 and 40–60 cm soil layers.

(0–21 kg ha^{-1}). It can thus be concluded that all of the Zn accumulated in the 20–60 cm soil layer. This is a surprising result with respect to previous findings obtained under temperate climatic conditions. For instance, Martinez and Peu (2000) studied the impact of intensive pig slurry spreading on a brown soil with a sandy silty texture under a temperate climate. They noted an increase in the soil Zn concentration between 0 and 60 cm depth. In their study, however, the 0–20 cm soil layer showed the greatest increase in Zn concentration. Similarly, in the study of Lipoth and Schoenau (2007), where they spread pig slurry on a black Chernozem soil in temperate conditions, an increase in Zn concentration was also noted in the 0–18 cm soil layer.

However, despite the high uncertainty concerning the Zn mass balance, the accumulation of this element in the soil was confirmed by the lack of uptake by plants and the flow at 60 cm depth. Moreover, these results are in line with our characterization of Zn speciation in pig slurry (Legros et al., 2010b). In this latter study, zinc speciation within pig slurry revealed the presence of three main components: 49% Zn bound to organic matter, 37% amorphous Zn hydroxides and 14% sphalerite. These three forms were shown to be soluble under aerobic conditions and within the pH 5–8 range, which corresponds to the pH measured in many soils (Pourbaix, 1963; Robert et al., 1988; Adams and Martin, 1994; Stanton et al., 2008). The mechanism of Zn accumulation was thus sorption on the soil. We put forward two hypotheses: (i) the characteristics of the 0–20 cm soil layer differed from those of the 20–40 and 40–60 cm layers and did not enable Zn sorption. This hypothesis was supported by the high C_{org} concentration at 0–20 cm depth even when the two layers are in the same horizon. (ii) Zn sorption by the Andic Cambisol was reversible and water flows gradually carried Zn to deeper soil layers. This Zn transfer was relatively slow since Zn was still present in the 20–60 cm soil layer after 5 years of pig slurry spreading. This, nevertheless, indicates that long-term Zn leaching could take place with a risk of impact on water resources.

5. Conclusion

In this study, we assessed the impact of 5 years of pig slurry spreading on a water–soil–plant system: an Andic Cambisol under *S. dimidiatum* grass cover. It was found that the Cu and Zn mass derived from pig slurry spreading was not taken up by the plant cover, nor was it leached beyond the 0–60 cm soil layer. These results obtained in a tropical system were very similar to previous findings in temperate systems.

The Cu mass derived from pig slurry spreading was stored in the 0–20 cm soil layer, which was attributed to the very low solubility of Cu_2S (the form in which Cu occurs in pig slurry). In contrast, the Zn mass supplied by pig slurry spreading was stored in the 20–60 cm soil layer. This result obtained in a tropical system differs from previous findings in temperate systems. This could have been due to a reversible Zn sorption mechanism in the studied Andic Cambisol.

We thus conclude that Cu accumulation in soil was the result of its highly insoluble form in pig slurry, and seemed to be relatively independent of the studied water–soil–plant system. On the other hand, Zn accumulation in soil was controlled by sorption mechanisms and thus depended on the studied water–soil–plant system.

Acknowledgments

This work was financially supported by ADEME under project no. 0475C0013, the European Community (FEOGA) and the French Réunion Region.

References

Adams, F., Martin, J.B., 1994. Liming Effect on Nitrogen Use and Efficiency. American Society of Agronomy, Madison, United States of America.
Aldrich, A.P., Kistler, D., Sigg, L., 2002. Speciation of Cu and Zn in drainage water from agricultural soils. Environ. Sci. Technol. 36, 4824–4830.
Alloway, B.J., 1995. Heavy Metals in Soils, 2nd ed. Blackie Academic & Professional, Glasgow.
Atkinson, H.J., Giles, G.R., Desjardins, J.G., 1954. Trace element content of farmyard manure. Can. J. Agric. Sci. 34, 76–80.
Baize, D., 1997. Teneurs totales en éléments traces métalliques dans les sols (France). INRA ed., Paris, p. 408.
Chahinan, N., 2004. Paramétrisation multi-critère et multi-échelle d'un modèle hydrologique spatialisé de crue en milieu agricole. Université de Montpellier II, p. 264.
Chopart, J.L., Mézino, M., 2003. Caractéristiques des précipitations et des risques d'excès d'eau dans l'environnement du poste météorologique des Colimaçons (moyenne altitude dans l'Ouest de l'île de la Réunion). rapport CIRAD, Saint-Denis, p. 12.
Collin, B., Doelsch, E., 2010. Impact of high natural soilborne heavy metal concentrations on the mobility and phytoavailability of these elements for sugarcane. Geoderma 159, 452–458.
Coppenet, M., Golven, J., Simon, J.C., Le Corre, L., Le Roy, M., 1993. Evolution chimique des sols en exploitations d'élevage intensif: exemple du finistère. Agronomie 13, 77–83.
Dère, C., Lamy, I., van Oort, F., Baize, D., Cornu, S., 2006. Reconstitution des apports en éléments traces métalliques et bilan de leur migration dans un Luvisol sableux soumis à 100 ans d'irrigation massive par des eaux usées brutes. C. R. Geosci. 338, 565–573.
Doelsch, E., Van de Kerchove, V., Saint Macary, H., 2006. Heavy metal content in soils of Reunion (Indian Ocean). Geoderma 134, 119–134.
Feder, F., Findeling, A., 2007. Retention and leaching of nitrate and chloride in an andic soil after pig manure amendment. Eur. J. Soil Sci. 58, 393–404.
Gräber, I., Hansen, J.F., Olesen, S.E., Petersen, J., Ostergraard, H.S., Krogh, L., 2005. Accumulation of copper and zinc in danish agricultural soils in intensive pig production areas. Dan. J. Geogr. 105, 15–22.
Hao, X.-Z., Zhou, D.-M., Chen, H.-M., Dong, Y.-H., 2008. Leaching of copper and zinc in a garden soil receiving poultry and livestock manures from intensive farming. Pedosphere 18, 69–76.
Jondreville, C., Revy, P.S., Dourmad, J.Y., 2003. Dietary means to better control the environmental impact of copper and zinc by pigs from weaning to slaughter. Livest. Prod. Sci. 84, 147–156.
Kabala, C., Singh, B.R., 2001. Fractionation and mobility of copper, lead, and zinc in soil profiles in the vicinity of a copper smelter. J. Environ. Qual. 30, 485–492.
Keller, C., 1995. Application of centrifuging to heavy metals studies in soil solution. Commun. Soil Sci. Plan. 26, 1621–1636.
L'Herroux, L., Le Roux, S., Appriou, P., Martinez, J., 1997. Behevoir of metals following intensive pig slurry applications to a natural field traitement process in Britany (France). Environ. Pollut. 97, 119–130.
Legros, S., Chaurand, P., Rose, J., Masion, A., Briois, V., Ferrasse, J.-H., SaintMacary, H., Bottero, J.-Y., Doelsch, E., 2010a. Investigation of copper speciation in pig slurry by a multitechnique approach. Environ. Sci. Technol. 44, 6926–6932.
Legros, S., Doeslch, E., Masion, A., Rose, J., Proux, O., Hazemann, J.L., SaintMacary, H., Bottero, J.Y., 2010b. Combining size fractionation, scanning electron microscopy and X-ray absorption spectroscopy to probe Zn speciation in pig slurry. J. Environ. Qual. 39, 1–10.
Levasseur, 2002. Composition chimique détaillée des aliments et des lisiers de porc. Techni-Porc 25, 19–25.
Levasseur, P., 1998. Composition et volume de lisier produit par le porc: données bibliographiques. Techni-Porc 21 (4), 17–24.
Lipoth, S.L., Schoenau, J.J., 2007. Copper, zinc, and cadmium accumulation in two prairie soils and crops as influenced by repeated applications of manure. J. Plant Nutr. Soil Sci. 170, 378–386.
Mantovi, P., Bonazzi, G., Maestri, E., Marmiroli, N., 2003. Accumulation of copper and zinc from liquid manure in agricultural soils and crop plants. Plant Soil 250, 249–257.
Martinez, J., Peu, P., 2000. Nutrient fluxes from a soil treatment process for pig slurry. Soil Use Manage. 16, 100–107.
McLaughlin, M.R., Fairbrother, T.E., Rowe, D.E., 2004. Nutrient uptake by warm-season perennial grasses in a swine effluent spray field. Agron. J. 96, 484–493.
Moral, R., Perez-Murcia, M.D., Perez-Espinosa, A., Moreno-Caselles, J., Paredes, C., Rufete, B., 2008. Salinity, organic content, micronutrients and heavy metals in pig slurries from South-eastern Spain. Waste Manage. 28, 367–371.
Nicholson, F.A., Chambers, B.J., Williams, J.R., Unwin, R.J., 1999. Heavy metal contents of livestock feeds and animal manures in England and Wales. Bioresour. Technol. 70, 23–31.
Novak, J.M., Watts, D.W., Stone, K.C., 2004. Copper and zinc accumulation, profile distribution, and crop removal in coastal plain soils receiving long-term, intensive applications of swine manure. Trans. ASAE 47, 1513–1522.
Payet, N., Findeling, A., Chopart, J.L., Feder, F., Nicolini, E., Saint Macary, H., Vauclin, M., 2009. Modelling the fate of nitrogen following pig slurry application on a tropical cropped acid soil on the island of Reunion (France). Agric. Ecosyst. Environ. 134, 218–233.
Payet, N., Nicolini, E., Rogers, K., Saint Macary, H., Vauclin, M., 2010. Evidence of soil pollution by nitrates derived from pig effluent using O-18 and N-15 isotope analyses. Agron. Sustain. Dev. 30, 743–751.
Peu, P., Birgand, F., Martinez, J., 2007. Long term fate of slurry derived nitrogen in soil: a case study with a macro-lysimeter experiment having received high loads of pig slurry (Solepur). Bioresour. Technol. 98, 3228–3234.
Pourbaix, M., 1963. Atlas d'équilibres électrochimiques. Gauthier-Villars, Paris.
Reynolds, W.D., Elrick, D.E., Youngs, E.G., Amoozegar, A., Booltink, H.W.G., 2002. Saturated and field-saturated water flow parameters. In: Dane, J.H., Topp, G.C. (Eds.), Methods of Soil Analysis, Part 4—Physical Methods. Soil Science Society of America Inc., Madison, WI, USA, pp. 797–878.
Robert, C.W., Melvin, J.A., Beyer, W.H., 1988. Handbook of Chemistry & Physics. CRC Press, Boca Raton, FL.
Sanchez, M., Gonzalez, J.L., 2005. The fertilizer value of pig slurry. I. Values depending on the type of operation. Bioresour. Technol. 96, 1117–1123.
Sansoulet, J., Cabidoche, Y.M., Cattan, P., Ruy, S., Simunek, J., 2008. Spatially distributed water fluxes in an andisol under banana plants: experiments and three-dimensional modeling. Vadose Zone J. 7, 819–829.
Simunek, J., Wendroth, O., van Genuchten, M.T., 1998. Parameter analysis of the evaporation method for determining soil hydraulic properties. Soil Sci. Soc. Am. J. 62, 894–905.
Singh, R.P., Agrawal, M., 2007. Effects of sewage sludge amendment on heavy metal accumulation and consequent responses of *Beta vulgaris* plants. Chemosphere 67, 2229–2240.
Smith, D.R., Moore Jr., P.A., Maxwell, C.V., Haggard, B.E., Daniel, T.C., 2004. Reducing phosphorus runoff from swine manure with dietary phytase and aluminum Chloride. J. Environ. Qual. 33, 1048–1054.
Sogbedji, J.M., van Es, H.M., Melkonian, J.J., Schindelbeck, R.R., 2006. Evaluation of the PNM model for simulating drain flow nitrate-N concentration under manure-fertilized maize. Plant Soil 282, 343–360.
Stanton, M.R., Gemery-Hill, P.A., Shanks Iii, W.C., Taylor, C.D., 2008. Rates of zinc and trace metal release from dissolving sphalerite at pH 2.0–4.0. Appl. Geochem. 23, 136–147.
van Genuchten, M.T., 1980. A closed-form equation for predicting the hydraulic conductivity of unsaturated soils. Soil Sci. Soc. Am. J. 44, 892–898.
Wen, C.G., Chen, T.H., Hsu, F.H., Lu, C.H., Lin, J.B., Chang, C.H., Chang, S.P., Lee, C.S., 2007. A high loading overland flow system: impacts on soil characteristics, grass constituents, yields and nutrient removal. Chemosphere 67, 1588–1600.
Willmott, C.J., 1981. On the validation of models. Phys. Geogr. 2, 184–194.
Willmott, C.J., 1982. Some comments on the validation of model performance. Bull. Am. Meteorol. Soc. 63, 1309–1313.
WRB, 2006. World Reference Base for Soil Resources. FAO, Rome.
Xue, H., Nhat, P.H., Gächter, R., Hooda, P.S., 2003. The transport of Cu and Zn from agricultural soils to surface water in a small catchment. Adv. Environ. Res. 8, 69–76.
Xue, H., Sigg, L., Gachter, R., 2000. Transport of Cu, Zn and Cd in a small agricultural catchment. Water Res. 34, 2558–2568.
Zhang, L., Wylie, B., Loveland, T., Fosnight, E., Tieszen, L.L., Ji, L., Gilmanov, T., 2007. Evaluation and comparison of gross primary production estimates for the Northern Great Plains grasslands. Remote Sens. Environ. 106, 173–189.